Final Report

Title: Temperature Effects in Match-cast segmental Bridge Construction
FDOT Contract Number: BDV31-977-132

Submitted to

The Florida Department of Transportation Research Center
605 Suwannee Street, MS 30 Tallahassee, FL 32399

c/o William Potter, P.E.
State Structures Design Engineer
Structures Research Center

Submitted by:

Alvaro Rafael Mendoza Grisales
Dr. Kyle A. Riding (kyle.riding@essie.ufl.edu) (Principal Investigator)
Dr. Gary Consolazio (Co Principal Investigator)
Dr. Trey Hamilton (Co Principal Investigator)
Engineering School of Sustainable Infrastructure and Environment
University of Florida
Gainesville, Florida 32611

February 2023

Department of Civil Engineering

Engineering School of Sustainable Infrastructure and Environment

College of Engineering

Disclaimer

The opinions, findings, and conclusions expressed in this publication are those of the authors and not necessarily those of the State of Florida Department of Transportation or the U.S. Department of Transportation.

Approximate Conversions to SI Units (from FHWA)

Symbol	When You Know	Multiply By	To Find	Symbol
Length				
in	inches	25.4	millimeters	mm
ft	feet	0.305	meters	m
yd	yards	0.914	meters	m
mi	miles	1.61	kilometers	km
Area				
in²	square inches	645.2	square millimeters	mm²
ft²	square feet	0.093	square meters	m²
yd²	square yard	0.836	square meters	m²
mi²	square miles	2.59	square kilometers	km²
Volume				
fl oz	fluid ounces	29.57	milliliters	mL
gal	gallons	3.785	liters	L
ft³	cubic feet	0.028	cubic meters	m³
yd³	cubic yards	0.765	cubic meters	m³
NOTE: volumes greater than 1000 L shall be shown in m³				
Mass				
oz	ounces	28.35	grams	g
lb	pounds	0.454	kilograms	kg
Temperature (exact degrees)				
°F	Fahrenheit	5 (F-32)/9 or (F-32)/1.8	Celsius	°C
Illumination				
fc	foot-candles	10.76	lux	lx
fl	foot-Lamberts	3.426	candela/m²	cd/m²
Force and Pressure or Stress				
lbf	pound-force	4.45	newtons	N
lbf/in²	pound-force per square inch	6.89	kilopascals	kPa

TECHNICAL REPORT DOCUMENTATION

1. Report No.	2. Government Accession No.	3. Recipient's Catalog No.
4. Title and Subtitle Temperature Effects in Match-cast segmental Bridge Construction		5. Report Date February 2023
		6. Performing Organization Code
7. Author(s) Alvaro Rafael Mendoza Grisales, Kyle A. Riding, Gary Consolazio, Trey Hamilton		8. Performing Organization Report No.
9. Performing Organization Name and Address Department of Civil and Coastal Engineering Engineering School of Sustainable Infrastructure & Environment University of Florida 365 Weil Hall P.O. Box 116580 Gainesville, FL 32611-6580		10. Work Unit No.
		11. Contract or Grant No. BDV31-977-132
12. Sponsoring Agency Name and Address Florida Department of Transportation 605 Suwannee Street, MS 30 Tallahassee, FL 32399		13. Type of Report and Period Covered Final Report May 2020-February 2023
		14. Sponsoring Agency Code
15. Supplementary Notes – N/A		

16. Abstract

Precast segmental bridge construction has provided a versatile, efficient, and cost-effective method for constructing bridges. Bowing distortion issues can however occur during segment fabrication, causing segments to have slightly different lengths in the center than outside edges. This occurs when the match-cast segment bows as a result of the heating of the face in contact with the hydrating concrete of the newly cast segment. A simulation matrix of 157 member geometry, materials, and construction factor combinations that explored the variables believed to be the most influential on bowing distortion was developed. The ability of the finite element software used for modeling, b4cast (ConTech Analysis ApS), the finite element software used for modeling in this project, to predict temperatures of hydrating concrete members was confirmed by comparison with a concrete physical model instrumented for temperature. The ability of an analytical expression to predict the bowing distortion of the concrete members studied from the thermal gradient developed in the match-cast segment was confirmed; however, the utility of this method is limited because it requires the temperature development to be known. A decision tree was developed to classify risk of bowing distortion in the construction process. A regression model was also developed that relates the member geometry, materials, and construction variables to the bowing distortion calculated. Analysis of the simulation results showed that segments with a width-to-length ratio lower than six had a low risk of excessive bowing distortion. They also showed that use of low heat of hydration mixes and low coefficient of thermal expansion aggregates can reduce the bowing distortion generated in the match-cast segments. Recommendations on methods to mitigate bowing distortion in match-cast segmental construction are given.

17. Key Word Segmental Bridge Construction, Heat of Hydration, Bowing Distortion		18. Distribution Statement No restrictions.	
19. Security Classif. (of this report) Unclassified.		20. Security Classif. (of this page) Unclassified.	21. No. of Pages 497	22. Price

ACKNOWLEDGEMENTS

EXECUTIVE SUMMARY

E.1 Background

Precast segmental bridge construction has provided a versatile, efficient, and cost-effective method for constructing bridges. Bowing distortion, however, can occur during segment fabrication, causing segments to have slightly different lengths in the center than along the outside edges. This can occur when the match-cast segment bows due to the development of a temporary thermal gradient that is the result of heating of the face in contact with the hydrating concrete of the newly cast segment. The newly cast segment acquires the bowed shape of the match-cast segment and locks in the bowed shape on the exposed edge when it hardens. The opposite edge of the newly cast segment remains fixed against the formwork and does not bow, resulting in a slightly longer segment near the edges than along the centerline.

It has been documented that in spans using epoxied joints, this bowed shape has the potential to accumulate as the temporary prestressing between segments is applied, reaching the point where the accumulated gap is difficult to close with the temporary prestressing [1,2]. Studies using analytical modeling have also shown that bowing-induced gaps between segments with dry joints may prevent the development of compressive stresses that are adequate to meet the minimum required levels specified for prestressed concrete [3]. A limit of 0.03 in. for bowing distortion per individual segment or 0.5 in. cumulative bowing distortion in a span has been proposed based on field observations for epoxied joints [2].

Review of the literature identified an analytical expression derived from beam theory to predict the bowing distortion of segments; the expression was validated with field measurements of temperatures and bowing distortions taken on the San Antonio Y project [1]. Several studies on the subject also mentioned segment geometry, mix design, ambient condition (ambient temperature, wind velocity), and curing as the most influential variables affecting bowing distortion [1–4]. Current FDOT specification 452-6.7.1 [5] suggests that bowing can be mitigated by using curing blankets or other approved curing systems to minimize the effects of differential temperature between segments. The present research was conducted to provide a better understanding of the effects that important casting variables have on the development of bowing and to document possible mitigation methods and suggest circumstances in which mitigation is required.

E.2 Research Objectives

The objectives for this project were:

- Develop best practices that can be used to mitigate transverse bowing distortion of match-cast segmental bridge segments during production.
- Identify bridge segment geometries that have an elevated risk of bowing and may require mitigation.
- Determine which practical curing-related mitigation measures are effective in reducing bowing distortion.

E.3 Main Findings

Based on the analytical modeling conducted for this research, the project findings can be summarized as follows:

- Segments with a width-to-length ratio lower than six had a reduced risk of problematic bowing distortion over 0.03 in. for an individual segment.
- The use of low heat of hydration mixes reduced the bowing distortion generated in the match-cast segments.
- The use of low coefficient of thermal expansion aggregates, yielding low coefficient of thermal expansion concrete, was found to be effective in reducing bowing distortion.
- Applying insulation tarps to both segments, while the newly cast segment is hydrating, was found to be detrimental. Insulating in this way increases the bowing distortion effect as it causes the newly cast concrete to heat up faster and achieve steeper thermal gradients during curing.
- The cooling effect of lower ambient temperatures or wind lowers bowing distortion. Such sources of cooling reduce the maximum hydration temperature reached in the concrete in the newly cast segment.
- Steam curing applied to both segments increased bowing distortion as it causes the concrete in the newly cast segment to reach higher temperatures as it hydrates.

E.4 Recommendations

Based upon the findings from this study, the following recommendations are made:

- The analytical expression proposed by Roberts-Wollmann et al. [1] can be used to estimate the bowing distortion of a match-cast segment with geometries similar to the Florida Bridge geometries studied in this project. This method requires the concrete temperature development to be known, limiting the utility of this method for estimating the bowing distortion.
- A decision tree was proposed that considers important variables such as member geometry, material properties, and construction conditions to classify the risk that bowing distortion will exceed 0.03 in. [2] during fabrication. Projects that have a predicted bowing distortion exceeding this value are deemed to have high bowing risk. For cases classified as having low bowing risk as determined by the decision tree, no further analysis is necessary. For cases classified as high-risk, however, two options are recommended. One is that the contractor constructs a full-scale mockup and measure temperatures for use in the Roberts-Wollmann expression. The other is to require that a numerical temperature simulation of the segment fabrication process be conducted and that temperatures from such a simulation be used in the Roberts-Wollmann expression. The bowing distortion thus calculated should be below 0.03 in. per segment. If not, then the contractor must design and implement mitigation measures unless it can be demonstrated that the cumulative gap produced will not exceed 0.5 in.
- A predictive expression developed by linear regression of temperatures, generated in this study through numerical simulations, can also be used to estimate expected bowing distortion for the given conditions. A 0.03 in. single segment limit, or 0.5 in. accumulated bowing distortion in a span, should be used with this approach to avoid mitigation measures.

- Mitigation measures when the predicted bowing exceeds 0.03 in. may be used to keep the match-cast segment warm and to prevent hydrating concrete in the newly cast segment from heating up to a problematic level. Possible mitigation measures include the following:
    - The match-cast segment can be cured and protected with insulation prior to and during the time in contact with the newly cast segment. Insulation should not be used on the newly cast segment. Such insulation will increase in temperatures developed in the newly cast concrete and also in the adjacent match-cast concrete, thus increasing bowing in the match-cast member. The new concrete member should still be cured to prevent moisture loss from the concrete to the environment. An example of this type of wet curing would be placing wet burlap and plastic over the new concrete.
    - During Florida summer conditions, night placement of concrete can be implemented. The lower ambient temperatures associated with night placement can help to reduce concrete temperatures developed during curing and thus reduce bowing distortion.
    - During Florida winter conditions, the match-cast segment should be insulated before the newly cast concrete is placed to keep the match-cast segment warm to reduce thermal gradients that may develop during the new segment curing.
    - Mitigation of bowing distortion can be achieved if steam curing or high ambient temperature conditions are applied only to the match-cast segment. High temperatures applied to the newly cast segment will be detrimental in that they will cause the concrete to reach higher temperatures and thus may cause an increase in bowing distortion.

E.5 Future work

The following should be considered for future work:

- Geometric mitigation for segments in the short line match-cast segment process should be further explored. The influence that increasing the segment top slab thickness has on bowing distortion should be explored. The influence of the location of the junction of the web and top slab could also be investigated to determine if there is an optimal location to reduce bowing distortion.
- The only complete and available field measured data with temperatures and corresponding bowing distortion measurements in segments in the short line match-casting method are those provided in Roberts et al. [1]. Future work should thus be carried out to collect additional field measurements of temperature and bowing distortions during segment fabrication with the short line match-casting method. Such data would help further validate numerical simulation models and could provide new insights into methods for mitigating bowing deformations.

TABLE OF CONTENTS

LIST OF FIGURES

xii

LIST OF TABLES

1 Introduction

1.1 Background

Precast segmental bridge construction has provided a versatile, efficient, and cost-effective method for constructing bridges. Bowing distortion, however, can occur during segment fabrication, causing segments to have slightly different lengths in the center than along the outside edges. This can occur when the match-cast segment bows due to the development of a temporary thermal gradient that is the result of heating of the face in contact with the hydrating concrete of the newly cast segment. The newly cast segment acquires the bowed shape of the match-cast segment and locks in the bowed shape on the exposed edge when it hardens. The opposite edge of the newly cast segment remains fixed against the formwork and does not bow, resulting in a slightly longer segment near the edges than along the centerline.

It has been documented that in spans using epoxied joints, this bowed shape has the potential to accumulate as the temporary prestressing between segments is applied, reaching the point where the accumulated gap is difficult to close with the temporary prestressing [1], [2]. Studies using analytical modeling have also shown that bowing-induced gaps between segments with dry joints may prevent the development of compressive stresses that are adequate to meet the minimum required levels specified for prestressed concrete [3]. A limit of 0.03 in. for bowing distortion per individual segment or 0.5 in. cumulative bowing distortion in a span has been proposed based on field observations for epoxied joints [2].

Review of the literature identified an analytical expression derived from beam theory to predict the bowing distortion of segments; the expression was validated with field measurements of temperatures and bowing distortions taken on the San Antonio Y project [1]. Several studies on the subject also mentioned segment geometry, mix design, ambient condition (ambient temperature, wind velocity), and curing as the most influential variables affecting bowing distortion [1]–[4]. Current FDOT specification 452-6.7.1 [5] suggests that bowing can be mitigated by using curing blankets or other approved curing systems to minimize the effects of differential temperature between segments. The present research was conducted to provide a better understanding of the effects that important casting variables have on the development of bowing, and to document possible mitigation methods and suggest circumstances in which mitigation is required.

1.2 Research Objectives

The 3 objectives for this project were:

- Develop best practices that can be used to mitigate transverse bowing distortion of match-cast segmental bridge segments during production.
- Identify bridge segment geometries that have an elevated risk of bowing and may require mitigation.
- Determine which practical curing-related mitigation measures are effective in reducing bowing distortion.

1.3 Research Approach

To accomplish the research objectives of this project, 157 thermo-mechanical finite element simulations representing the precast segmental bridges short line match-casting process were developed in the finite element software b4cast following a testing matrix that explored typical Florida construction conditions. The finite element software ability to simulate concrete temperatures was validated by comparing temperatures measured in a physical model with simulated results.

2 Literature Review

2.1 Introduction

Match-cast segmental bridge construction was first conceived by Jean M. Muller [6] and is employed globally for the variety of benefits inherent in its unique construction process. Match-cast segmental construction has significant advantages over more traditional construction methods including economical fabrication, reduced pier requirements, increased structural durability, and expedited construction processes that do not significantly hinder neighboring traffic flow [3], [7]. Generally, match-cast segmental construction is described as the process of casting one segment against another; however, it can be further subdivided into short-line and long-line match-casting.

The short-line casting method employs one fixed and one removable bulkhead. The first segment of the span is cast between both the fixed and removable bulkhead. Once the primary segment has cured, the removable bulkhead is replaced with the original segment, termed the "match-cast" segment in this review. The "new" segment is cast against the match-cast segment and the fixed bulkhead [8], [9]. The long-line construction method operates similarly; however, all segments are cast in a single line for a single span length without repositioning [8]. This is accomplished using a moveable bulkhead. By employing match-cast segmental construction, proper aligning of shear keys is ensured.

Although match-cast segmental construction possesses a number of advantages over more traditional bridge erection methods, thermal gradients that develop during the curing process can cause unintended distortion of the segment. As the new segment cures, it releases large amounts of heat from the heat of hydration of the cementitious materials. The heat generated during curing flows outward from the new segment and into the side of the match-cast segment serving as a removable bulkhead as shown in Figure 1 [2]. The differing temperatures on each side of the match-cast segment causes a thermal gradient. As the adjacent side of the match-cast segment heats, it expands, potentially inducing significant bowing distortion [3], [4]. Upon cooling, the old match-cast segment will return to its undistorted geometry after it cools back to ambient temperature [1] while the new match-cast segment will harden in the distorted shape [7]. Thus, the new segment will possess one distorted side and one side that has been correctly formed by the fixed bulkhead.
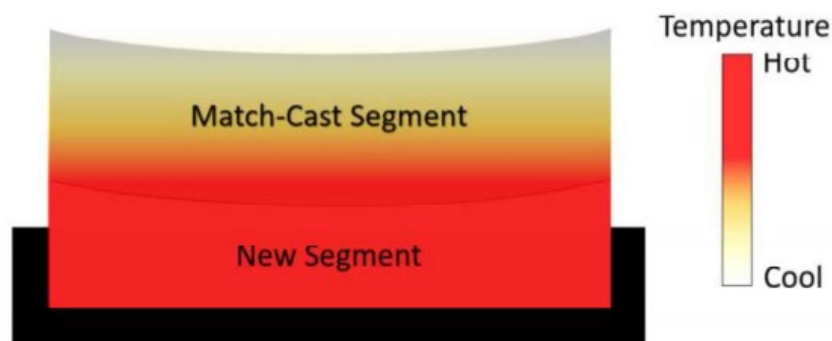
Figure 1: Bowing distortion caused by the heat of hydration in the new segment [2]

The gap resulting from segments that have set in a distorted geometry, as seen in Figure 2, can significantly reduce durability and load bearing capacity of the structure [3]. Additional issues during epoxy and post-tensioning operations can cause uneven stress distributions, potentially reducing the service life of the structure [1], [2], [7]. Furthermore, the cumulative effect of all the individual gaps has the potential to be substantial, possibly forming a large final gap during construction [1], [3].
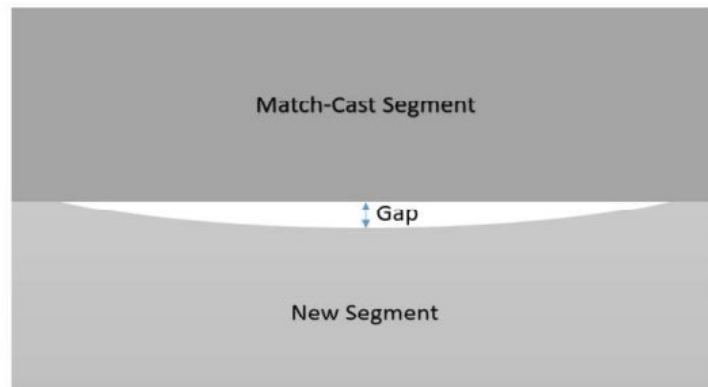
Figure 2: Resultant gap forming along the centerline between the two segments [2]

It has been documented in literature that bowing distortion of a match-cast segment is controlled by its thermal gradient curve [3], [7]. By reducing the thermal gradient, bowing distortion risk is lowered [2]. This literature review discusses contributing factors that influence bowing distortion risk in segmental construction; consider mitigation measures that may reduce thermal bowing distortion in match-cast segments; and address fundamentals of modeling concrete segment thermal behavior during the period of time when the concrete transitions from a fluid to a solid.

2.2 Contributing Factors

Factors contributing to segment bowing distortion can include any physical, environmental, or chemical variables that have the potential to influence thermal gradient development and associated hardening and stress relaxation during fabrication. Factors include environmental conditions, the coefficient of thermal expansion, setting time, modulus of elasticity development, heat of hydration development, thermal diffusivity, and geometric considerations.

2.2.1. Environmental Conditions

Environmental factors including wind, ambient temperature, and solar radiation contribute to the development of a thermal gradient during the match-cast process. Because of the effect they have on the concrete temperature development, these factors must be considered to determine whether mitigation measures are required.

The presence of wind accelerates thermal gradient formation in match-cast segmental construction [3]. As concrete hydrates, interior temperatures increase significantly while surface temperatures remain cooler [10]. Surface temperatures are notably lower due to forced convection and heat dissipation into the environment. Temperature differentials between the surface and internal portions of early-age concrete can cause deformations or tensile stresses

[10]. Although there is no suggestion in literature that wind influences bowing potential in the new segment, it does affect the concrete temperature development and indirectly member bowing during curing. Wind aids in cooling all external surfaces of the match-cast segment while the new segment warms the match-cast segment on one face via conductive heat transfer. Broadly, wind could exaggerate thermal gradient development through convective heat transfer in both the new and match-cast segments. Quantitatively, research suggests an 8% increase in overall gap due to wind velocity upon erection of superstructure components [7].To combat the effect of wind on bowing distortion, mitigation methods like curing blankets, plastic sheeting, and other insulative materials can be employed; these materials rely on their low convection coefficients to reduce heat transfer and give more uniform heating of the match-cast segment. Additionally, shielding concrete by means of tenting can prevent increased convective heat transfer by shielding segments from wind gusts.

Thermal gradient and thermal stress development are influenced by disparities between concrete temperature and the ambient temperature [11]. While wind influences thermal gradient development through forced convection. Increased levels of convection are associated with heightened gap measurements upon superstructure erection. A study by Rombach found that a drop of 10.8°F (6°C or K) in ambient temperature resulted in a 19% change in maximum segment gap [7].

To avoid the increased gap size associated with convection, it is advantageous to begin placing the concrete when the ambient temperature is rising [3]. Consideration must also be given to the season in which casting is taking place to reduce temperature differentials between segment and environment [1], [12]. Warmer seasons intrinsically possess warmer ambient temperatures, thereby changing thermal gradient development. Thus, casting during warmer seasons in the morning while temperatures are rising is optimal. If project stipulations inhibit optimal casting procedures, mitigation measures including thermal insulation can be employed to facilitate semi-adiabatic conditions.

Along with wind and ambient temperature, solar radiation is a factor in determining whether mitigation measures are required. Solar radiation influences both seasonal and daily temperature gradients in concrete structures [13]. Solar radiation intensity fluctuates between seasons and can differ significantly between summer and winter. Furthermore, solar radiation differs depending on the time of day due to angle of incidence variations per hour. Although temperature gradients formed by solar radiation are typically considered undesirable, harnessing the sun to support heat generation in segmental construction provides distinctive benefits at no additional cost to the project budget. To combat this, solar radiation can be utilized as a natural heat source. Engineers may position the free face of the match-cast segment toward the sun, warming it, thus aiding in reducing temperature differentials resulting from the heat of hydration generated in the new segment [1]–[3].

2.2.2. Coefficient of Thermal Expansion

The coefficient of thermal expansion (CTE) relates the change in temperature of a material to its associated change in physical dimensions [3], [14]. To mitigate bowing risk during match-cast segmental fabrication, it is advantageous to control how a concrete mix will respond to variations in temperature. Logically, bowing distortion of a segment decreases as its CTE is reduced

because the match-cast segment will not expand as much in response to the heat of hydration in the new segment. Thermal expansions and contractions of concrete are highly variable and depend chiefly on aggregate characteristics and secondarily on moisture content [15]. However, additional aspects of concrete mix design including cement paste characteristics and concrete age influence the CTE of a section [16].

While the concrete CTE is a composite of those of the individual constituent materials, aggregate forms the largest portion of a concrete mix by volume and therefore highly influences the overall material CTE [17]. Thus, assessing common aggregates for their thermal properties is crucial to comprehending thermal behaviors of the resulting segment. Research by Alungbe determined that the CTE of an aggregate is highly dependent on its composition and quality [18]. Based on his research, limestone and marble were found to have the lowest CTE values of common aggregates used in concrete mix design. Conversely, quartz had the highest CTE values. Findings by Alungbe are further supported by Browne, who found that limestone and basalt have low CTE values while chert and quartzite have heightened thermal expansion coefficients [15]. Additional research by Bonell found that concrete formed of siliceous aggregates have higher expansion coefficients than concretes form with calcareous aggregates [19]. Further, concretes formed of igneous aggregates have moderate CTE values that exist between calcareous and siliceous aggregates [19]. Because aggregates often have mixed composition or impurities present, wide variations in CTE have been measured a given aggregate type.

Moisture content of a concrete mixture also influences its CTE. Moisture content is directly correlated to water-cementitious material ratio (w/cm) at early ages. Concrete coefficient of thermal expansion has been shown to be at a maximum at moderate levels of relative humidity [20]. Maruyama et al. observed a noteworthy increase in CTE during early stages of concrete casting when the w/cm ratio was low [21]. It was determined that internal self-desiccation can occur in low w/cm cement pastes because these cements are commonly associated with reduced levels of free water content; this causes an increase in CTE [21], [22]. Increasing the w/c ratio of a concrete mixture reduces self-desiccation, reducing desaturation of pores and, thus keeping the CTE of the mixture from rising [22].

If the w/cm ratio of a concrete mix must be low to achieve desired characteristics, internal curing by superabsorbent polymers (SAP) provides additional curing water to compensate for water consumed during cement hydration [23], [24]. Utilizing SAP for internal curing promotes hydration of constituent materials while suppressing the potential for internal self-desiccation, thus reducing autogenous shrinkage and thermal expansion [23]–[25]. Additionally, internal curing via SAP inclusion eliminates CTE increase within the first few days of concrete maturation [22]. Through the first three to four days of age, SAP application ensures constant, low values of CTE [22]. The additional time afforded by SAP inclusion may significantly reduce bowing distortion by mitigating CTE rise with age. As an added benefit, superabsorbent polymers retard maximum heat flow [22]. By reducing heat flow, thermal bowing distortion in the match-cast segment is reduced.

Conflicting information has been obtained regarding the influence of w/cm on CTE development. As mentioned in this section, Maruyama found variations in CTE with w/cm fluctuations. However, various studies by Alungbe found that w/cm did not have any effect on CTE [18], [26].

The CTE of a concrete structure is further influenced by ambient relative humidity (RH). The substantial CTE evolution over the first few days of maturation is attributed to the steep decline in internal RH [22]. This maximum is 50-100% larger than the CTE of a concrete specimen under saturated conditions [20]. This is further supported by Meyers, who found that as concrete dries, CTE increases until a maximum is reached; however, upon apex, CTE decreases with further drying [27]. Additional research by Yeon et al. indicates that maximum CTE values in concrete occur at 70% to 80% RH [28]. Further, the effect of RH is larger on cement paste than concrete, supporting the notion that increasing aggregate content is an effective strategy for CTE reduction. By optimizing RH of the environment and avoiding 70% to 80% RH during curing, the CTE of a segment can be minimized, thus reducing bowing distortion potential.

Cement paste characteristics are known to influence CTE development. Cement paste is approximately 25 to 35% by volume of the concrete volume [17]. Although this percentage is less than that of aggregate, Alungbe found that the CTE of the cement paste is typically greater than any common aggregate used in concrete mix design and increases the composite concrete CTE [18]. Therefore, it is imperative to understand the thermal characteristics of the paste to minimize CTE development.

Meyers found that the CTE of a cement paste is dependent on the quantity of tricalcium silicate, C_3S [29]. Based on one year of observation, it was concluded that pastes formulated with cements high in C_3S had high expansion coefficients, while pastes with cements low in C_3S had lower expansion coefficients. Over time, however, cements with low C_3S values possessed thermal expansion coefficients similar to cements with high C_3S values [29]. Given the unique circumstances surrounding bowing in match-cast segmental construction, CTE values at early cement ages are important. Therefore, utilizing cements with low C_3S values will reduce expansion coefficients of the segments, thus reducing bowing.

Additionally, reducing cement content while increasing aggregate content when feasible can reduce the overall CTE of the segment [18]. This stems from the concept that cement paste typically possesses a higher CTE than commonly used aggregates [18]. Overall, high-quantity aggregate mixtures formed of appropriately tailored aggregate and cement types can be effective at reducing overall CTE of concrete.

In addition to cement paste, concrete age also influences the CTE of a section. In essence, as a segment ages, its CTE decreases [3]. This is quantitatively supported by Cusson et al., who found that CTE of a concrete structure decreases to a minimum value of 10.8 x 10^{-6} /°F (6 x 10^{-6} / °C) one day post set, followed by a linear increase until reaching a stable value of 14.4 x 10^{-6} /°F (8 x 10^{-6} / °C) at four days of age [30]. Cusson et al. details that high CTE values commonly found in fresh concrete can be attributed to excess unbound water, because water possesses a thermal expansion coefficient that is approximately seven times that of matured concrete [30]. Once a microstructure has formed within the concrete, the CTE rapidly decreases, establishing a lower and more stable CTE [30], [31].

2.2.3. Setting Time

The setting time of the new segment influences the likelihood of bowing distortion. Reducing the concrete setting time could be an effective strategy to mitigate bowing. It is advantageous to promote a reduction in setting time to ensure that the new match-cast segment hardens before the

members deform a significant amount. Variables that influence setting time include the cement composition, and the use of retarders, accelerators, plasticizers, and finer cement particles. W/cm may also positively influence a rapid setting time. Finally, employing methods like steam curing may increase the rate of reaction and reduce setting time, but it could lead to a lower ultimate strength [32].

Use of retarders, accelerators, and plasticizers can also influence setting time. Retarders are commonly used to delay the initial set time, allowing added time for transportation, placement, and to maintain workability. However, retarder application during match-cast segmental construction could exacerbate bowing, by allowing more time for thermal deformations to distort the segment shape before it hardens [33]. Conversely, accelerators are effective at decreasing setting time and increasing hardening rate, depending on accelerator content [34]. Additions like water-soluble inorganic salts may be employed to provide concrete with additional early-strength performance by increasing the hydration rate of C_3S [34]. Finally, plasticizers can influence setting time. Experiments conducted by Kocáb et al. found that cements containing plasticizers can exhibit significant delays in setting time compared to cement pastes that did not contain plasticizer, depending on the dosage [35]. This was evidenced by the temperature development inside the specimen and the reduced values of dynamic modulus of elasticity during the first 24 hours of aging [35].

Utilizing finer cement can aid in setting time reduction and increased hydration rates [3], [36]. As cement becomes finer, the amount of surface area exposed to react with water increases, accelerating setting time [36], [37]. However, the benefit of faster reaction is offset by a sharp increase in heat of hydration rate because increased hydration rates are associated with increased heat generation while heat dissipation remains constant [38]. The cement fineness has a larger impact on rate of heat generation and less so on total heat generation [38].

Altering the w/cm of concrete is effective at modifying hydration rates. Hydration rates are accelerated when water-binder ratio decreases [39]. Increasing hydration rates cause reduced setting times, because setting time and rate of hydration are interconnected. However, increases in hydration rate are commonly associated with substantial increases in temperature. Lu et al. determined that concrete possessing a low w/cm retains a small heat release coefficient, thus indicating a greater hydration heat release [39]. This can pose hazards to structural durability, thermal gradient development, and thermally-induced cracking. Therefore, careful consideration of w/cm can be an effective strategy to reduce setting time.

2.2.4. Modulus of Elasticity Development

The development rate and ultimate value of elastic modulus are significant considerations when employing match-cast segmental construction. Most equations used to calculate the concrete modulus of elasticity relate it to the compressive strength. ACI 318 provides an equation shown in Equation 1 that is intended to be used with concrete having a density between 90 and 160 lb/ft^3 [40]:

$$E_c = w_c^{1.5} \cdot 33\sqrt{f'_c}$$ Equation 1

Where: Ec = modulus of elasticity of concrete, psi (MPa)

                      w_c = density of concrete, lb/yd^3 (kg/m^3)

                      f'_c = compressive strength of concrete, psi (MPa)

For normal weight concrete, a more generalized modulus of elasticity expression is shown in Equation 2 [40]:

$$E_c = 57{,}000\sqrt{f'_c} \hspace{4cm} \text{Equation 2}$$

Where: E_c = modulus of elasticity of concrete, psi (MPa)

                      f'_c = compressive strength of concrete, psi (MPa)

As indicated, a high Young's modulus is commonly sought in concrete structures. When attempting to mitigate the effects of bowing distortion during segmental construction, however, the rate at which the modulus of elasticity develops is more important than the final value obtained. A rapid development of a segment's elastic modulus may aid in reducing bowing distortion levels through increased stiffness at early ages. Increased levels of stiffness and rigidity may affect any bowing distortion that develops.

The elastic modulus of concrete is known to rapidly increase between the ages of 3 and 5 hours [41]. After this period of rapid development, rate of increase in modulus of elasticity declines significantly. A host of variables that influence the modulus of elasticity of a concrete specimen have been identified, including concrete composition, aging conditions, w/cm, and the implementation of plasticizer [35], [42].

The composition of a concrete mix greatly influences its developed modulus of elasticity. For example, high strength concrete is known to rapidly increase in strength and elastic modulus when compared to other types of concrete [42]. Kocáb et al. considers concrete composition to be inclusive of variables such as type and amount of cement, grain size, quality, and type and amount of aggregate [35]. Additionally, consideration must be given to admixtures and supplementary cementitious materials (SCM) present in the mix.

Aggregate type and size influence the elastic modulus of a concrete segment. Zhao asserts that lightweight aggregates tend to have lower elastic moduli than heavier aggregates [43]. More specifically, Piasta et al. found that aggregates like quartzite and granite have reduced elastic moduli as compared to aggregates like basalt and dolomite [44]. It was determined that replacing granite aggregates with dolomitic aggregates can increase the elastic modulus from 1,450,300 psi to 2,175,500 psi (10 GPa to 15 GPa), depending on the w/c ratio employed [44]. As a further point, concrete containing gravel as coarse aggregate has a relatively high modulus of elasticity [44].

Aggregate size may further influence elastic modulus development. Ahmad et al. determined that the larger the maximum size of coarse aggregate and the coarser the associated grading, the higher the elastic modulus of the mix [45]. Fine aggregates also play a role in modulus of elasticity development of a mix. Work by Harsh et al. found that sand particles can act as a skeleton within the concrete mix, enabling a higher stiffness than the hardened cement matrix alone [46]. Under a compressive load, the sand skeleton will restrain the deformations of the concrete matrix, consequently improving elastic modulus values [46]. Given these points, a careful selection of both coarse and fine aggregates can yield significant increases in modulus of elasticity in both ordinary and high-performance concretes [44].

Employing various types of admixtures and SCMs can influence the resulting characteristics of the concrete. To begin, steel fibers may be used to improve the modulus of elasticity development of a concrete. Alsalman et al. found that a steel fiber content of 6% caused compressive strength to increase by 8-20% and elastic modulus to increase by 6-15% [47]. Although the addition of steel fibers may increase the modulus of elasticity of a concrete, its implementation is costly [47]. Therefore, steel fiber applications may be heavily reliant upon the budget of the project. Additional consideration should be given to the use of pumice and zeolite. Yıldız et al. found that increasing the amount of zeolite while decreasing pumice levels in high strength concrete had a positive influence on the modulus of elasticity of concrete at all stages of development [48]. Finally, silica fume may be useful in increasing the rate of elastic modulus development. Lee et al. found that adding silica fume to a concrete mix increased the development of the modulus of elasticity at early ages [49]. As shown, several admixtures and SCMS may be implemented to improve elastic modulus development over time.

The w/cm of a concrete mix influences its rate of elastic modulus development. Through experimentation, Kocáb et al. determined that the lower the w/cm ratio, the higher the overall value of the modulus of elasticity of a concrete specimen [35]. Although elastic modulus reached higher levels as w/cm ratio decreased, the trend and rate of change of the various cements tested was relatively constant [35]. Reduced w/cm ratios were associated with increased physical properties regardless of concrete age [44], [50].

Use of plasticizer in a cement mix influences the modulus of elasticity development during concrete early ages. Kocáb et al. found that cement pastes containing plasticizer exhibited significant delays in property development compared to cement pastes without plasticizer [35]. A reduction in elastic modulus was prevalent during the first 24 hours of age [35]. Additionally, Kocáb et al. determined that cement pastes containing plasticizer exhibited a significant reduction in rate of dynamic elastic modulus increase as compared to pastes that did not employ plasticizers [35]. Stemming from this observation, Kocáb et al. found that the lower the plasticizer amount in cement paste, the higher the elastic modulus, irrespective of the w/cm ratio of the paste [35].

The packing density of a concrete specimen affects early life development of the modulus of elasticity of a concrete section. Tests performed by Klein et al. determined that performing particle packing of the granular skeleton increased the static modulus of elasticity by an average of 21% at the age of 7 days for both concrete mixes tested [51]. This increase in elastic modulus will favor worksite productivity while reducing deformation associated with concrete demolding [51].

Aging and concrete curing conditions influence the modulus of elasticity of a concrete structure. [52]. To prevent excessive water loss, concrete may be cured under water. Kocáb et al. determined that concrete cured under water portrayed a constant increase in elastic modulus, especially during the first few days of curing [52]. For reference, concrete that was not outfitted with any curing measures depicted a smaller increase in modulus of elasticity over the first few days of curing [52]. Steam curing may also be employed to reduce water loss while maintaining optimal temperatures. Through experimentation, Oluokun found that steam curing benefited elastic modulus development within the age of 1 to 3 days [41]. Essentially, at any moment in time, the elastic modulus of a specimen cured in wet conditions will be greater than a specimen that is cured in dry conditions [49].

Further, the application of heat curing imparts a myriad of positive effects on various concrete properties including modulus of elasticity [53]. More specifically, employing temperature-matched curing results in higher development rates of modulus of elasticity during the first 24 hours of aging [54]. This form of heat curing increased the early-age elastic modulus more than sealed curing or air-dried curing [54]. Ensuring optimal curing conditions throughout the first few days of age is essential to the development of the modulus of elasticity of a concrete specimen [52].

2.2.5. Heat of Hydration

Cement hydration is an exothermic chemical reaction. Excessive heat development within a concrete member can be detrimental to its longevity and durability. In addition, heat development in the new segment can exacerbate bowing distortion. The heat generated during the hydration process in the new segment is transmitted into the match-cast segment. The side of the old match-cast segment that is closest to the new segment will warm, causing a temperature differential. The temperature differential that exists between ends of the match-cast segment encourages thermal gradient development. As the thermal gradient increases in severity, bowing distortion of the match-cast segment escalates [3], [7]. Controlling the temperature rise from the newly cast segment could aid in reducing the severity of the thermal gradient developed in the old segment, thus reducing bowing distortion. A variety of options may be employed to reduce the heat of hydration and associated degree of hydration within a concrete mix. Identified solutions include altering mix proportions, cement composition, aggregate type, structural dimensions, and environmental conditions [3].

The choice of cement and associated cement composition influences heat development during the setting process. Employing low-heat portland cement can aid in reducing the heat of hydration of a concrete, but is generally resisted by precast concrete producers because of lower strength-gain rates and productivity [55]. Low-heat portland cement possesses reduced levels of alite (C_3S) and aluminate (C_3A) [55]. These compounds possess the highest heat of hydration values per gram of the compounds commonly used in concrete [3], [56]. For example, some low heat of hydration portland cements were found to have adiabatic temperature rise 3.6 °F to 5.4 °F (2 to 3 °C) lower than general use portland cement; this reduction was achieved while lowering cracking behavior and increasing strength development properties when compared to moderate-heat concrete [57]. Cements that possess finer particles tend to react faster than coarser cements. Finer cements contain particles that possess higher surface area-to-volume ratios. Raising surface

area-to-volume ratio increases the amount of surface area of a particle that is in contact with water, facilitating a more rapid strength gain rate [56].

Supplementary cementitious materials (SCMs) are commonly used as a partial cement replacement to alter various physical or chemical attributes. For example, slags and fly ash are commonly used to reduce the heat generation in a concrete specimen [39], [56]. Generally, the reduction in temperature rise increases as replacement percentage of fly ash increases [39]. Although literature suggests that all fly ash types are known to reduce heat of hydration intensity at early ages, Class F fly ash was determined to reduce heat of hydration generation the most as measured using semi-adiabatic calorimetry [58]. Although the reduction in heat of hydration is beneficial to mitigate bowing, it also results in a reduced strength gain rate that is antithetical to productivity goals important to precast concrete producers [58], [59]. Additionally, utilizing fly ash is associated with increased setting times, which may exacerbate bowing distortion [58]. However, this setting time increase may be addressed by decreasing the w/cm and increasing cement fineness [37], [39].

Any means of cooling a concrete mixture before placing can aid in reducing the development of the heat of hydration within a segment. The addition of ice chips to the mix water, chilling aggregate, or chilling concrete by means of liquid nitrogen injection may be effective at controlling placing temperature, thus reducing temperature rise in early age concrete [36]. However, reducing placing temperature reduces the rate of hydration, thus increasing curing time [58]. This reduction in rate of hydration could be a disadvantage for precasters concerned about productivity when performing match-cast segmental construction and should be considered accordingly.

2.2.6. Thermal Diffusivity

Thermal diffusivity is a coefficient that describes the rate at which a body with a non-uniform temperature approaches equilibrium [18]. The thermal diffusivity of a material is dependent on its thermal conductivity, specific heat, and density. Thermal diffusivity is calculated using Equation 3 [60]:

$$\alpha = \frac{k}{\rho c_p} \qquad\qquad \text{Equation 3}$$

Where: α = thermal diffusivity, ft^2/h (m^2/h)

   k = thermal conductivity, BTU/(h·ft·°F) (W/(m·K))

   c_p = specific heat, BTU/(lb·°F) ((kJ/kg·K))

   ρ = density of the material, lb/ft^3 (kg/m^3)

A reduction in thermal conductivity, increase in specific heat capacity, or increase in density will reduce the overall thermal diffusivity of a section.

It is well established that higher temperatures develop in thicker portions of a concrete structure because they are insulated by surrounding concrete. Reducing the thermal diffusivity of a concrete mix decreases the ability for heat to propagate from thicker sites to outer portions of a segment. An increase in the time required for temperature equilibrium affords additional setting time to the new segment before its heat of hydration causes the match-cast segment to become distorted. Abendeh showed that decreasing the thermal diffusivity of a concrete mix will reduce the gap size after hardening from match-cast segmental construction [3].

The thermal diffusivity of a material is influenced by a host of factors, however aggregate type possesses the greatest control over the thermal diffusivity [3]. To expand on this concept, Tokuda et al. found that when coarse and fine aggregates are from the same rock type and source, the overall diffusivity of concrete tends to increase as aggregate content increases [61]. However, this relation is not necessarily valid when aggregate types differ between the coarse and fine aggregates [61]. Beyond this generalization, Bažant et al. found reduced thermal diffusivities in concretes formed with basalt aggregates and increased thermal diffusivities in concretes formed with quartz aggregates [62]. Additional research by Fintel suggests that increasing aggregate content or decreasing w/cm increases thermal diffusivity values [63]. Conversely, thermal diffusivity decreases with increases in concrete temperature [63].

Specific heat plays an integral role in the thermal diffusivity of a material. It can be defined as the amount of heat per unit mass required to change the temperature of a material by one degree [3]. In other words, increasing the specific heat of a material will increase the heat required to cause the physical temperature of the material to rise. Accordingly, increasing the specific heat of a concrete mix is advantageous when employing match-cast segmental construction. By increasing the specific heat of a concrete mix, the new segment can tolerate larger amounts of heat developed via heat of hydration before physically rising in temperature. This could reduce bowing in the match-cast segment. Additionally, the match-cast segment can tolerate more heat from the new segment before temperature differentials and associated thermal gradients encourage bowing [3].

Various characteristics including aggregate type, composition, density, and moisture content influence the specific heat capacity of a concrete mix [64]. However, it has been found that moisture content may play a more significant role in specific heat development than the other factors mentioned, especially if the concrete mix is composed of porous lightweight components [65]. Work by Whiting et al. found that the relationship between moisture content and specific heat is approximately linear for both normal and structural lightweight aggregate concretes; however, low density mixes did not exhibit the same linear relation [65]. Degree of hydration may influence specific heat development. A study conducted by De Schutter et al. found that specific heat decreases linearly with the degree of hydration of the cement mix [66].

Thermal conductivity is defined as the ratio of heat flow and temperature gradient per unit length of material [3]. Essentially, thermal conductivity indicates the resistance to heat transfer between materials. When employing match-cast segmental construction, a low thermal conductivity could reduce heat transfer to the hardened concrete, but would increase the thermal gradient between them and in the match-cast segment [3].

Numerous characteristics of a concrete mix influence its thermal conductivity. Similar to specific heat capacity, thermal conductivity depends on composition, density, and moisture content [64]. Additionally, aggregate type, porosity, w/cm, SCM use, water-reducing agent content and temperature control thermal conductivity [3], [67], [68].

To expand on the concept of aggregate type, Abendeh suggests that siliceous aggregates tend to possess higher thermal conductivities than other normal weight aggregates [3]. Employing siliceous aggregates will encourage heat transmission. Additionally, work by Ganjian found that the thermal conductivity of lightweight and normal-weight concretes is directly related to density while possessing an inversely proportional relationship to porosity and pore diameter [68]. Thus, as density decreases, thermal conductivity decreases. As porosity and pore diameter increases, thermal conductivity decreases. Abendeh suggests that reducing the concrete density can increase bowing distortion because low density concrete typically has a lower thermal conductivity [3].The thermal conductivity of water is greater than the thermal conductivity of air [62]. Air-dried concrete with a moisture content of 50% less than saturated concrete could experience a 25% drop in thermal conductivity [62]. Concrete will have plenty of free water during the first 12 hours of curing when the member deflections occur, making moisture content less of a concern for match-cast segment bowing.

2.2.7. Geometric Considerations

It is known that bowing distortion of match-cast segments is a direct result of the heat of hydration in the new segment [69]. Prior research indicates that segments possessing a high segment slenderness ratio or width-to-length (w/L) ratio as defined in Figure 3 are at increased risk for bowing distortion in response to thermal gradient development.
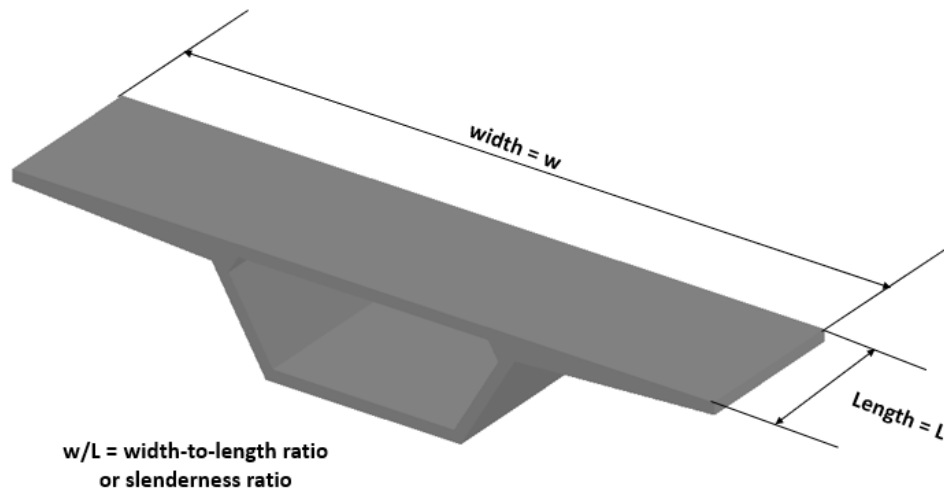
Figure 3: Width and length dimensions in match-cast segments (after Roberts-Wollmann et al, 1995) [6]

By reducing the w/L of bridge segments where feasible, bowing distortion can be mitigated without any alteration to the concrete mix design. More knowledge of the segment bowing distortion response to w/L will help fabricators determine when mitigation is necessary.

Current research does not suggest a conclusive w/L ratio at which bowing becomes problematic; however, it is known that bowing increases nonlinearly as w/L ratio increases [7]. Although universal agreement regarding optimal w/L ratio has not been identified, the following findings are noted based on a comprehensive literature review:

- Podolny discovered significant bowing in segments with w/L ratios larger than 6 [4]. This discovery was formed from practical experience and has yet to be verified through experimentation [7].
- Prescon Corporation and Roberts-Wollmann et al. encountered bowing issues in segments possessing w/L ratios larger than 9; conversely, segments with w/L ratios of less than or equal to 3 did not encounter bowing or warping during segment fabrication [2], [12].
- Figg and Muller Engineers indicate that bowing is particularly significant at large w/L ratios and is caused by improper heating during accelerated curing procedures commonly used in segmental construction [70].
- Numerical modeling combined with real-world analysis performed by Rombach et al. suggests that the slenderness ratio should be limited to 10 [7]. If slenderness ratio is not limited, additional measures such as supplementary curing procedures or modifications to concrete mix design are required for bowing mitigation.
- A guideline provided by Rombach et al. found that segments possessing w/L ratios of 10.7 bow 8 times more than segments with w/L ratios of 3, suggesting that as w/L ratio increases, thermally induced deformation increases [1], [7].

Based on the aforementioned findings, it is evident that segment dimensions influence bowing severity; however, an optimal w/L ratio has not been established. As segment slenderness ratios increase, bowing distortion likelihood increase. However, bridge designs involving large slenderness ratio segments may be unavoidable. In this case, additional curing procedures like isothermal enclosures or alterations to concrete mix design may be necessary to compensate for large w/L ratios.

2.3 Determination and Implementation of External Mitigation Measures

External mitigation measures may be employed if conditions or dimensional constraints exist that are known to encourage bowing during match-cast segmental construction. External mitigation measures including isothermal enclosures, curing blankets, plastic sheeting, and steam curing are recommended when alterations to the concrete mix design are deemed infeasible [1]–[3]. This section will explore a preliminary design and construction approach to determine whether mitigation measures are required. Next, methods of calculating deformations in match-cast segments will be discussed. Finally, a variety of external mitigation measures will be presented and discussed in detail.

2.3.1. Preliminary Design and Construction Approach

Determining the worst-case design gradient can be used as a preliminary step in determining if bowing mitigation measures are required. A design and construction approach has been proposed [2]:

1. Calculate width-to-length (w/L) ratio

     a. If the w/L ratio is less than 6, casting temperature does not warrant consideration

     b. If the w/L ratio is greater than 6, continue to step 2

2. Determine the worst-case design gradient. Design gradients have been developed for climates similar to San Antonio, TX. Thermal analysis would need to be performed for segments made in other climates.
3. Calculate segment deformation at time of concrete set
4. Calculate cumulative deformation for all segments contained within a span

     a. If maximum deformation for one segment exceeds 0.03 in. (0.8 mm), thermal gradient must be reduced

     b. If maximum cumulative deformation for all segments in a span exceeds 0.50 in. (12 mm), thermal gradient must be reduced

Application of this procedure provides a quantitative determination of appropriate design conditions that may require mitigation measures.

Abendeh and Rombach discuss allowable tolerances at the manufacturing process of the match-cast segments according to German Regulations, in which an allowable bowing distortion of 0.1 in. (2.5 mm) is specified for match-cast segments after transverse prestressing is applied [3], [71]–[73]. This bowing distortion limit value is mainly derived from practical experience, and by using it no problems have been documented, however the lack of research base for this value is a source of uncertainty that must be addressed [73]

2.3.2. Deformation Quantification

Quantifying potential deformations prior to implementing match-cast segmental construction procedures helps determine whether mitigation measures are required. Thus, calculating segment deformation is a key preliminary step when employing match-cast segmental construction. Roberts-Wollmann et al. provides several methods to calculate the bowing distortion anticipated in match-cast segments. First, a method of determining maximum segment bowing distortion observed in a match-cast segment is presented in [2]. The specified thermal gradient is used to calculate an equivalent moment using Equation 4 [2]:

$$M = E\alpha \int T(Y)b(Y)YdY \qquad\qquad \text{Equation 4}$$

Where: E = the modulus of elasticity of the concrete, ksi (MPa)

               α = the coefficient of thermal expansion of concrete, 1/°F (1/°C)

               T = temperature difference between a point at distance Y from the centroid of the section and the centroid, °F (°C)

               b = width of the section at a distance Y from the centroid of the section, in. (mm)

               Y = the distance from the centroid of the section, in. (mm)

Next, the curvature of the segment can be calculated using Equation 5 [2]:

$$\varphi = \frac{M}{EI} \qquad\qquad \text{Equation 5}$$

Where: M = moment calculated based on the above equation, lb-in. (kg-mm)

E = the modulus of elasticity of the concrete, ksi (MPa)

I = the moment of inertia of the section of interest, in.^{4} (mm^4)

Finally, the maximum bowing distortion may be calculated using values obtained from prior equations by employing Equation 6 [2]:

$$\Delta = \frac{\varphi w^2}{8} \qquad\qquad \text{Equation 6}$$

Where: φ = curvature of the segment, 1/in. (1/mm)

w = width of the segment, wing tip to wing tip, in. (mm)

Equation 6 was implemented by Roberts-Wollmann et al. to calculate the bowing distortion for various segments. Calculated values agreed well with measured deflections of instrumented segments, thus validating the analytical approach.

Beyond a general bowing distortion equation, Roberts-Wollmann et al. provided equations to estimate bowing distortions during cold and warm weather casting. For cold weather placements, Equation 7 (US customary units) and Equation 8 (metric units) aid in estimation of maximum segment bowing distortion [2]:

In. U.S. customary units:

$$\Delta = \frac{\alpha T_{max} w^2 (7.5L - 106)}{L^3} \qquad\qquad \text{Equation 7}$$

In metric units:

$$\Delta = \frac{\alpha T_{max} w^2 (191L - 68340)}{L^3} \qquad\qquad \text{Equation 8}$$

Where: Δ = calculated bowing distortion, in. (mm)

α = the coefficient of thermal expansion of concrete, 1/°F (1/°C)

T_{max} = maximum temperature differential in the segment, °F (°C)

w = width of the segment, wing tip to wing tip, in. (mm)

L = length of segment, in. (mm)

Equation 9 (US customary units) and Equation 10 (metric units) are applicable to segments that are cast during warm weather conditions [2]:

In. U.S. customary units:

$$\Delta = \frac{\alpha T_{max} w^2 (5.2L - 88)}{L^3}$$

Equation 9

In metric units:

$$\Delta = \frac{\alpha T_{max} w^2 (133L - 56720)}{L^3}$$

Equation 10

These equations can provide engineers with a preliminary understanding of how a segment is expected to deform when employing match-cast segmental construction. From this understanding, external or internal mitigation measures may be implemented if potential segment bowing distortions are calculated in excess of the allowable tolerances discussed prior.

2.3.3. Isothermal Enclosures

Thermal gradient development can be mitigated through isothermal enclosure implementation. Isothermal enclosures ensure uniform temperature distributions throughout the interior of the apparatus. Relative to ambient environmental conditions, uniform temperatures are ideal for thermal gradient reduction. If casting in the open air, the side of the match-cast segment nearest to the new segment can experience extreme heat fluctuations, while surfaces further from the new segment will be cooler, giving high thermal gradients. To mitigate heat fluctuations commonly observed in the ambient environment, Podolny suggests enclosing the new and old match-cast segments in an isothermal enclosure [4]. Heat from hydration and from an external source would heat the air around the concrete, giving more uniform temperatures throughout the old match-cast section.

Although Podolny suggests enclosing both the new and old match-cast segments in an isothermal enclosure to prevent thermal gradient development [4], Abendeh recommends enclosing segment joints to reduce heat transfer between segments [3]. However, heat transfer via conduction will still occur between the two segments, causing a thermal gradient in the match-cast segment. Determining whether full isothermal enclosure deployment or joint deployment is viable is an objective of this research effort.

2.3.4. Curing Blankets and Plastic Sheeting

Methods of thermal insulation including curing blankets and plastic sheeting are commonly used to shield concrete from otherwise unavoidable weather conditions like rain, wind, and unfavorable ambient temperatures. Employing thermal insulation is associated with many benefits including increased hydration rate, stress mitigation, and thermal gradient reduction.

Various forms of thermal insulation may be employed to cover the new segment during curing. Insulation traps heat, potentially reducing the temperature gradient through the match-cast member [33]. As temperature increases, the rate of hydration increases, producing reduced

setting times [36]. Reducing setting times may help in reducing deformations by helping the concrete harden before gradients occur.

Abendeh recommends controlling maximum temperature in early life concrete due to the increased potential for early age cracking [3]. Thermal insulation aids in stress development mitigation by reducing thermal gradients and stresses [33]. In one case studied, insulating concrete blocks with curing blankets or plastic sheeting reduces temperature differentials in models between the surface and inner portions of the block, thus reducing thermal gradients and giving a more uniform temperature distribution in the specimen [33].

Various sources support the use of thermal insulation on the match-cast segment. Abendeh [2] suggests utilizing thermal insulation such as isothermal enclosures or thermal blankets to keep the match-cast segment warm. By insulating the match-cast segment, thermal gradient development resulting from the heat of hydration generated in the new segment is minimized, reducing bowing distortion potential. Roberts further confirms this notion by suggesting that any means of warming the match-cast segment will aid in thermal gradient reduction [1]. Lastly, Podolny [4] recommends enclosing both the new and the match-cast segment to prevent longitudinal thermal gradients.

Insulating materials are applicable regardless of climate because they promote semi-adiabatic temperature development [33]; however, thermal gradients are more severe in colder climates and thus may require the implementation of additional mitigation measures. For example, thermal insulation by itself may be sufficient in warmer climates because thermal gradient development is minimal due to favorable atmospheric conditions [1], [2]. However, Abendeh suggests using insulating materials in cold, windy climates [3]. Because cooler ambient temperatures support more severe thermal gradient development due to increased temperature differentials, additional measures like steam curing or heating of aggregate may be required to ensure bowing distortion is controlled.

2.3.5. Steam Curing

Although not common in Florida, steam curing is used in cold climates as a heat treatment to accelerate strength development in concrete structures [1]–[3], [32], [74]. Steam curing may be employed in segmental construction to provide supplementary heat to the match-cast segment and maintain a more consistent thermal profile throughout the match-cast member.

Specific steam curing procedures vary depending on environmental conditions and desired material properties. The total cycle length should not exceed 18 hours, excluding the delay period [32]. Additionally, the most effective temperature range for steam curing is between 149°F and 185°F (65°C and 85°C) [32], [74]. A satisfactory steam curing cycle is as follows [32]:

1. Preheating/delay period of 2 to 5 hours
2. Heat at a rate of 71.6°F to 111.2°F (22°C to 44°C) per hour until a maximum temperature between 122 °F and 179.6°F (50°C and 82°C) has been obtained
3. Store segment at the maximum temperature
4. Utilize a cooling period to avoid thermal shock

19

Steam curing can be expensive to implement, and thus, may not be suitable for all projects [3]. In cases where cost reduction is paramount, thermal blankets or plastic sheeting can be used to provide insulation and reduce the amount of steam used, reducing developed thermal gradients while remaining cognizant of cost [3]. In addition, heating coils may be used to heat the free end of the match-cast segment, reducing overall thermal gradient development. However, steam curing is known to reduce long-term compressive strength of concrete when compared to other moist curing measures [40].

2.4   Modeling Fundamentals

In order to model the deformation in match-cast segments during curing, a study of the heat generation and transfer during the match-casting process can be done to determine the temperature distribution within the segments, the amount of energy moving into or out the segments, and the subsequent thermal stresses and deformations [75]. Thermal stress modeling involves a coupled chemo-thermo-mechanical phenomenon. Modeling can be performed by decoupling the phenomenon into two models with an interface between them. The first model describes the heat generation and transfer process in a chemo-thermal or temperature model, while the second uses the calculated temperatures to calculate the evolution of the mechanical properties of the concrete during the hydration process, including an aging model [3], [76].

2.4.1.   Temperature Modeling

Thermal modeling of concrete early-age temperature development involves a number of interdependent mechanisms that do not have closed form solutions and must be solved numerically [58]. The three main components of concrete heat transfer analysis are: the heat conduction in the concrete, the heat generation from the hydration process, and the heat exchanged at the boundary of the structural element [58], as illustrated in Figure 4 for a generic concrete member.
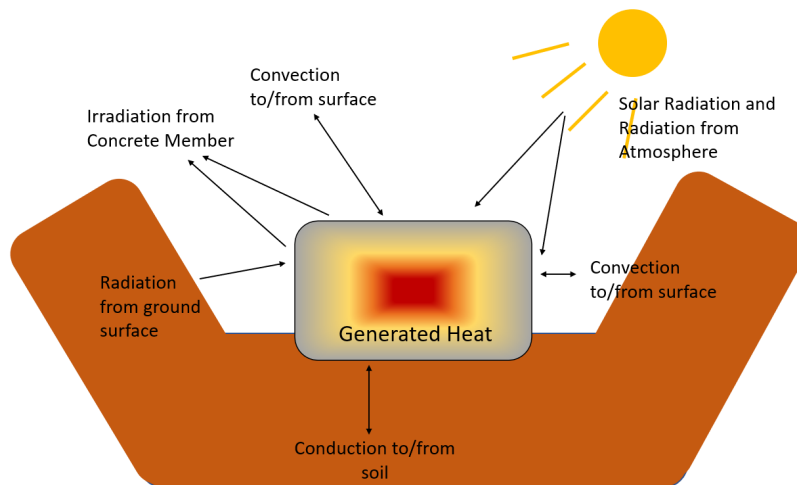
Figure 4: Heat transfer in concrete member

Heat Conduction

Thermal energy in a solid tends to flow from areas of high temperature to areas of lower temperature to even out differences between them and achieve an equilibrium. The rate at which the heat flows in a solid is a function of the thermal diffusion coefficient as discussed in section 1.2.6.

The heat diffusion equation shown in Equation 11 calculates the interaction between the heat generation and conduction [58]:

$$\frac{\partial}{\partial x}\left(k\frac{\partial T}{\partial x}\right) + \frac{\partial}{\partial y}\left(k\frac{\partial T}{\partial y}\right) + \frac{\partial}{\partial z}\left(k\frac{\partial T}{\partial z}\right) + Q_h = \rho c_p \frac{\partial T}{\partial t} \qquad \text{Equation 11}$$

Where: k = thermal conductivity, BTU/(h·ft·°F) (W/(m·K))

Q_h = heat generation term, BTU/h (W)

ρ = material density, lb/ft^3 (kg/m^3)

c_p = specific heat, BTU/(lb·°F) (kJ/(kg·K))

Equation 11 is essentially an energy balance formulation that illustrates how the conduction of heat in and out a body plus the thermal energy generation within its boundaries is equal to the change of the energy stored within the volume [77]. Using this approach, heat flux that passes through one edge of the control volume can be modeled using the conduction terms shown in Equation 11, or replaced with another term as a boundary condition.

Heat Generation

Concrete hydration is an exothermic process, represented by the term Q_h in the heat diffusion equation shown in Equation 11. The rate and magnitude of heat generation of concrete is a function of the amount of cement and pozzolan in the concrete, the fineness and compound composition of cement, admixtures used, and the temperature during hydration [38]. ACI 207.2R-07 [38] present charts with the adiabatic temperature development for concrete based on factors such as type of cement used, cement fineness, placement temperature.

While adiabatic temperature rise charts in ACI 207.2R-07 are often used to obtain the heat of hydration for temperature analysis, they do not provide accurate temperature development curves when SCM's or admixtures are included in the concrete [56]. A model has been developed to calculate heat release with time, using equivalent age maturity function concepts, apparent activation energy, and degree of hydration and total heat available, as shown in Equation 12 [37], [58];

$$Q_h(t) = H_u \cdot C_c \cdot \left(\frac{\tau}{t_e}\right)^\beta \cdot \left(\frac{\beta}{t_e}\right) \cdot \alpha_u \cdot exp\left(-\left[\frac{\tau}{t_e}\right]^\beta\right)$$
$$\cdot \frac{E}{R}\left(\frac{1}{273+T_r} - \frac{1}{273+T_c}\right) \qquad \text{Equation 12}$$

Where: t_e= concrete equivalent age at the reference temperature, h

H_u = total heat of hydration of cementitious materials at 100% hydration BTU/lb (kJ/kg)

C_c = total amount of cementitious materials, lb/yd^3 (g/m^3)

τ = hydration time parameter, h

β=hydration shape parameter (no dimensions)

α_u= ultimate degree of hydration

E= activation energy, BTU/mol (kJ/mol)

R= universal gas constant, BTU/(lb-mol·°R) (kJ/(mol·K))

T_r= reference temperature, °F (°C)

T_c= temperature of concrete, °F (°C)

In the hydration process of concrete, it has been recognized that higher ambient temperatures influence the rate of the reaction of cementitious materials [56]. The equivalent age maturity function is used to account for the effects of concrete temperature on the hydration and strength gain rates [78]. This method assumes that the concrete will reach the same ultimate degree of reaction independent of temperature history. The equivalent age maturity function calculated the equivalent curing age t_e for a specimen cured at a specific reference temperature T_r, to have the same properties as the concrete cured at temperature T_c for a period of time t, as expressed in Equation 13 by [56]:

$$t_e(T_r) = \sum_0^t e^{-\frac{E_a}{R}\left(\frac{1}{T_C}-\frac{1}{T_R}\right)} \cdot \Delta t \qquad \text{Equation 13}$$

Where: t_e= concrete equivalent age at the reference temperature, h

T_r= reference temperature, °F (K)

E_a= apparent activation energy, BTU/mol (kJ/mol)

R= universal gas constant, BTU/(lb-mol·°R) (kJ/(mol·K))

T_c= temperature of concrete, °F (K)

$\Delta t=$ time step used

The apparent activation energy is a measure of temperature sensitivity of the hydration reaction [56]. E_a is referred to as the apparent activation energy because in the cement hydration process, various interdependent chemical reactions involving the cement components take place, making this measurement of activation energy an average of the effects of the different reactions [79]. A model has been developed to estimate the apparent activation energy as a function of the cement properties as shown in Equation 14 [78]:

$$Ea = 22,100 \cdot p_{C_3A}{}^{0.30} \cdot p_{C_4AF}{}^{0.25} \cdot Blaine^{0.35} \qquad \text{Equation 14}$$

Where: pC_3A= weight ratio of C_3A in terms of total cement content

                    pC_4AF = weight ratio of C_4AF in terms of total cement content

                    $Blaine$ = Blaine value, specific surface area of cement, ft^2/lb (m^2/kg)

An expanded model to estimate apparent activation energy when SCMs and chemical admixtures are used was developed, as shown in Equation 15 [80]:

$$\begin{aligned} Ea = 41,230 &+ 1,416,000 \cdot \left[\left(p_{C_3A} + p_{C_4AF} \right) \cdot p_{Cement} \cdot p_{SO_3} \cdot p_{Cement} \right] \\ &- 347,000 \cdot p_{Na_2O_{eq}} - 19.8 \cdot Blaine + 29,600 \, p_{FA} \cdot p_{FA-CaO} \\ &+ 16,200 \cdot p_{slag} - 51,600 \cdot p_{SF} - 3,090,000 \cdot WRRET \\ &- 345,000 \cdot ACCL \end{aligned} \qquad \text{Equation 15}$$

Where: p_i= mass of i component to total cement content ratio

                    pFA = weight % of fly ash in terms of total cementitious material

                    $pFA\text{-}CaO$ = weight % of CaO in fly ash

                    $pslag$ = weight % of slag cement in terms of total cementitious material

                    p_{Na2Oeq} = weight % of Na_2O_{eq} in cement

                    $WRRET$= ASTM Type B&D water reducer/retarder, weight % solids per gram of cementitious material

                    $ACCL$= ASTM Type C calcium-nitrate-based accelerator, weight % solids per gram of cementitious material

A model has been developed to estimate the heat of hydration coefficients α_u, τ, and β used in Equation 12 [56], [58] . In order to adjust these coefficients, first the relationship between amount of heat released, total heat available in the cementitious system and degree of hydration is expressed mathematically in Equation 16 [56]:

$$\alpha(t) = \frac{H(t)}{H_u} \qquad\qquad \text{Equation 16}$$

Where: $H(t)$= cumulative heat of hydration released at time t, BTU/lb (kJ/gram)

H_u=total heat available for reaction, BTU/lb (kJ/gram)

An assumption used in modeling the heat generation with the approach in Equation 16 is that the amount of heat released is proportional to the cementitious system degree of reaction with time $\alpha(t)$.

The total heat available for reaction H_u is a direct function of the chemical components of the cementitious materials. A model to estimate this parameter based on cementitious components can be observed in Equation 17 and Equation 18 [56]:

$$H_u = H_{cem} \cdot p_{cem} + 461 \cdot p_{slag} + 1800 \cdot p_{FA-CaO} \cdot p_{FA} \qquad \text{Equation 17}$$

$$H_{cem} = 500 \cdot p_{C_3S} + 260 \cdot p_{C_2S} + 260 \cdot p_{C_3A} + 420 \cdot p_{C_4AF} + 624 \\ \cdot p_{SO_3} + 1186 \cdot p_{FreeCa} + 850 \cdot p_{MgO} \qquad \text{Equation 18}$$

The s-shaped curve formed when degree of hydration α is plotted against equivalent age t_e can be modeled using an exponential formulation as expressed in Equation 19 [37]:

$$\alpha(t_e) = \alpha_u \cdot exp\left(-\left[\frac{\tau}{t_e}\right]^{\beta}\right) \qquad\qquad \text{Equation 19}$$

The degree of hydration $\alpha(t_e)$, expressed as a function of the equivalent age instead of the actual age allows the hydration system to be modeled using any temperature history. Riding et al. presented empirical models for α_u, τ, and β developed using statistical analysis of the relation between α_u, τ, and β fits from semi-adiabatic calorimetry results and the cementitious material composition, physical properties, w/cm, and chemical admixtures used. One model was based on the composition being determined using Bogue equations and the other using X-ray diffraction with Rietveld refinement [56]. Equation 20, Equation 21 and Equation 22 show the expressions developed using X-ray diffraction with Rietveld refinement [56]:

$$\alpha_u = \frac{1.031 \cdot w/cm}{0.194 + w/cm} \\ + exp\left(-0.297 - 9.73 \cdot p_{C_4AF} \cdot p_{cem} - 325 \cdot p_{Na_2O_{eq}} \cdot p_{cem} \qquad \text{Equation 20} \\ - 8.89 \cdot p_{FA} \cdot p_{FA-CaO} - 331 \cdot WRRET - 93.8 \cdot PCHRWR\right)$$

$$\tau = exp\left(2.95 - 0.972 \cdot p_{C_3S} \cdot p_{cem} - 152 \cdot p_{Na_2O_{eq}} \cdot p_{cem} + 1.75 \cdot p_{slag} + 4.00 \\ \cdot p_{FA} \cdot p_{FA-CaO} - 11.8 \cdot ACCL + 95.1 \cdot WRRET\right) \qquad \text{Equation 21}$$

$$\beta = exp\big(-0.418 + 2.66 \cdot p_{C_3A} \cdot p_{cem} - 0.864 \cdot p_{slag} + 108 \cdot WRRET$$
$$+ 32.0 \cdot LRWR - 13.3 \cdot MRWR + 42.5 \cdot PCHRWR \qquad \text{Equation 22}$$
$$+ 11.0 \cdot NHRWR\big)$$

Where: p_i= mass of i component to total cement content ratio as determined by Rietveld analysis.

LRWR= ASTM Type A water reducer

MRWR= midrange water reducer

NHRWR= ASTM Type F naphthalene or melamine-based high-range water reducer

PCHRW= ASTM Type F polycarboxylate-based high-range water reducer

Figure 5, Figure 6 and Figure 7 illustrate the effect of the variation of each empirical fit coefficient α_u, τ, and β from Equation 19 in the s-shaped curves [80].
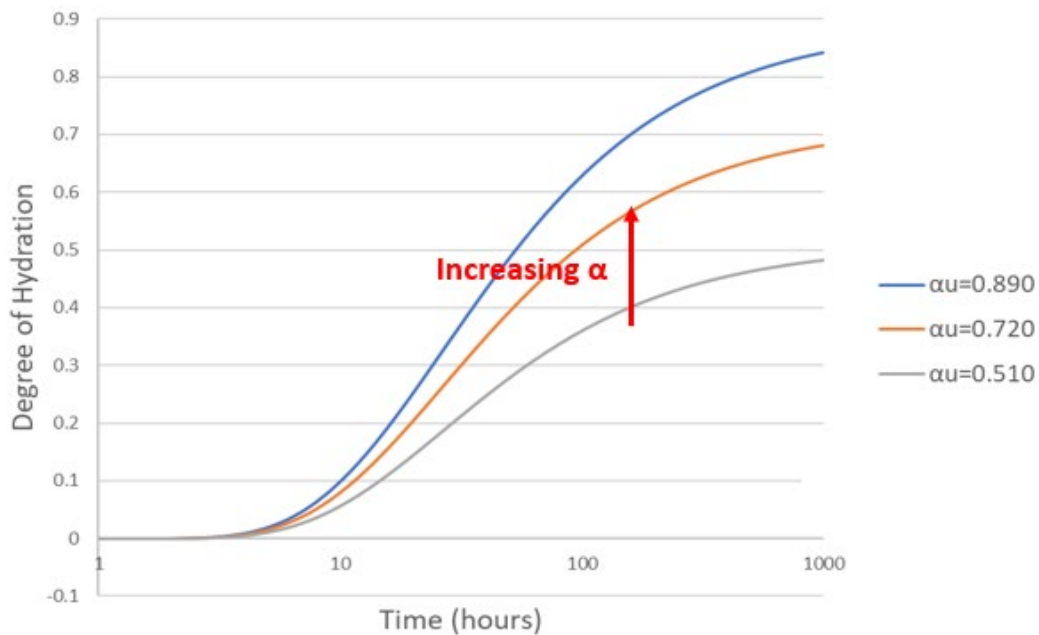
Figure 5: Change in degree of hydration curve as ultimate degree of hydration α_u changes (after Poole, 2007) [80]
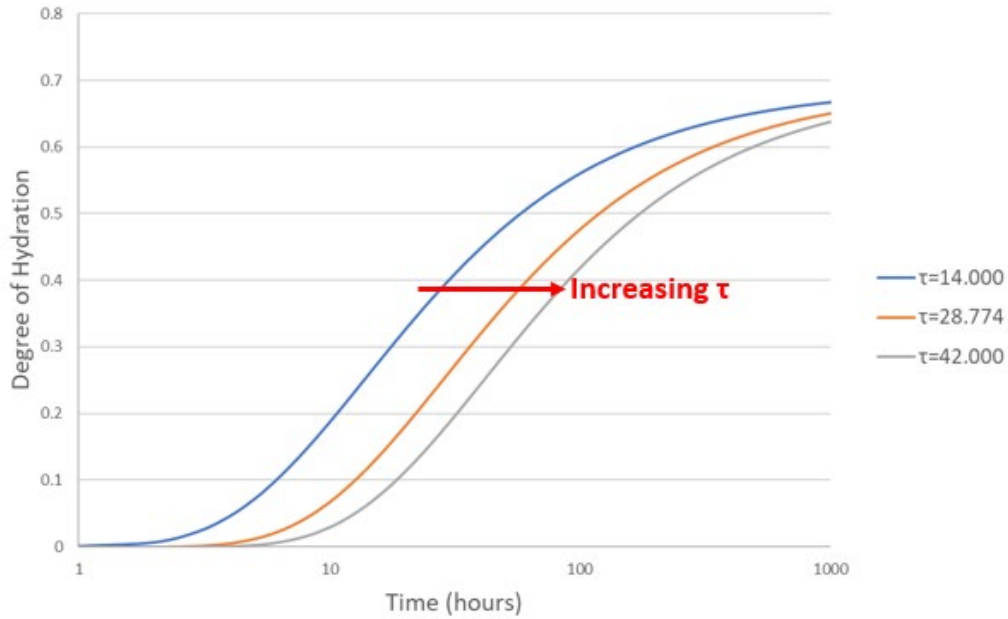
Figure 6: Change in degree of hydration curve as ultimate degree of hydration τ changes (after Poole, 2007) [80]
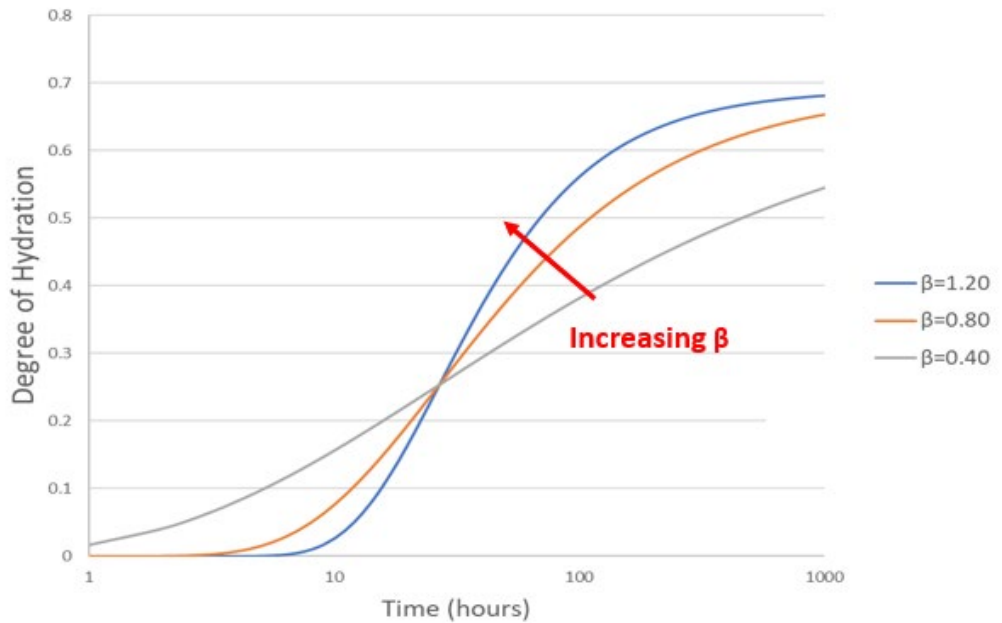
Figure 7: Change in degree of hydration curve as ultimate degree of hydration β changes (after Poole, 2007) [80]

Temperature measurements in concrete members can be used to calculate the adiabatic temperature rise. In this case, the member temperature can be simulated with the temperature rise used in the analysis changed until the measured and simulated temperatures match. Abendeh

used this approach [3], where the heat of hydration was estimated by using the temperature measurements taken in the San Antonio Y project [1] and in the Bang Na segmental bridge [3].

2.4.2. Heat Exchanged at Boundary Conditions

Boundary condition effects play a critical role in concrete member thermal models. Boundary conditions are the most complex and variable portion of the heat transfer analysis for concrete members because it is dependent on the surrounding features such as ambient conditions, formwork, curing blankets. Heat transfer at the boundary involves radiation and convection heat transfer. Both of these processes require information on the local weather conditions. It can be difficult to quantify the spatial variations in local radiation and convection conditions [81]. The heat transfer at boundary conditions can be treated as separate terms in the heat diffusion equation.

Solar Radiation

Solar radiation is the energy provided by the sun's rays to the concrete member surface and is a significant source of energy in temperature analysis. Riding et al. [81] present expressions to approximate the solar radiation that concrete members receive based on public weather data and the angles in which the concrete member receives this radiation. The surface horizontal solar radiation, E_H in BTU/ft^2 (W/m^2), which is the total amount of direct and diffuse solar radiation that would strike a horizontal surface at ground level, is a value required to perform these estimations. Equation 23 is an expression developed to estimate the surface horizontal solar radiation based on cloud cover fraction, C, and the extraterrestrial horizontal solar radiation, E_{TOA} in BTU/ft^2 (W/m^2) [81]:

$$E_H = (0.91 - (0.7 \cdot C)) \cdot E_{TOA} \qquad \text{Equation 23}$$

Atmospheric Radiation

All matter emits radiation energy. Radiation emitted from gas in the atmosphere can be a significant source of energy in temperature analysis [81]. This type of radiation must be taken into account in the energy balance at an exposed concrete surface using the expression shown in Equation 24 [81]:

$$q''_a = \sigma \varepsilon_a (T_a)^4 \qquad \text{Equation 24}$$

Where: q''_a = heat flux from the air, BTU/(h·ft^2) (W/m^2)

                 σ = Stefan-Boltzmann constant $\approx 1.714 \cdot 10^{-9}$ BTU/(hr·ft^2·°R^4) (or $5.670 \cdot 10^{-8}$ W/(m^2·K^4))

                 ε_a = emissivity of the air

                 T_a = temperature of the air, °F (K)

The emissivity of the air, $\varepsilon_{a,}$ is an estimated value that can be computed from schemes that take into account air vapor pressures and temperatures [82]. An expression presented in Equation 25 [81] which also includes the term cloud cover fraction, C, is used to calculate ε_a:

$$\varepsilon_a = C + 1.24(1 - C) \cdot \left(\frac{e_a}{T_a}\right)^{\frac{1}{7}}$$
Equation 25

The term e_a, ksi (kPa), in Equation 25 represents the partial water vapor pressure, and can be obtained using the expression in Equation 26 [81]:

$$e_a = R_h \cdot P_{ws} \cdot \left(\frac{10 \; milibar}{kpa}\right)$$
Equation 26

Where:　　　R_h = air relative humidity (%)

　　　　　　P_{ws} = saturated vapor pressure, psi (kPa)

The saturated vapor pressure P_{ws} [81] can be estimated using expressions presented by the American Society of Heating, Refrigerating and Air Conditioning Engineers (1993) based on the ambient temperature range. Equation 27 gives P_{ws} for the ambient temperature T_a between -148°F and 32°F (-100°C and 0°C), while Equation 28 gives P_{ws} for the ambient temperature T_a between 32°F and 392°F (0°C and 200°C):

$$P_{ws} = exp\left[\frac{C_1}{T_a} + C_2 + C_3 T_a + C_4 T_a^2 + C_5 T_a^3 + C_6 T_a^4 + C_7 ln(T_a)\right]$$
Equation 27

$$P_{ws} = exp\left[\frac{C_8}{T_a} + C_9 + C_{10} T_a + C_{11} T_a^2 + C_{12} T_a^3 + C_{13} ln(T_a)\right]$$
Equation 28

Where:　　　C_1 = -5.6745359 x 10^3

　　　　　　C_2 = -5.1523058 x 10^{-1}

　　　　　　C_3 = -9.677843 x 10^{-3}

　　　　　　C_4 = 6.2215701 x 10^{-7}

　　　　　　C_5 = 2.0747825 x 10^{-9}

　　　　　　C_6 = -9.484024 x 10^{-13}

　　　　　　C_7 = 4.1635019

　　　　　　C_8 = -5.8002206 x 10^3

　　　　　　C_9 = -5.516256

　　　　　　C_{10} = -4.8640239 x 10^{-2}

C_{11}= 4.1764768 x 10^{-5}

C_{12}= -1.4452093 x 10^{-8}

C_{13}= -6.5459673.

Irradiation

Concrete surfaces emit radiation. This radiation, called irradiation, has a cooling effect on the surface and must be included in the surface energy balance The Stefan-Boltzmann law applies to concrete surface irradiation as shown in Equation 29 [81]:

$$q''_c = \sigma \varepsilon_c (T_c)^4$$
Equation 29

Where: q''_c= heat lost from the concrete from the air, BTU/(h·ft^2) (W/m^2)

ε_c= emissivity of the concrete surface

T_c= temperature of the concrete surface, °F (K)

Convection

Convection is the energy transfer between a surface and a fluid moving over the surface [77]. This convective heat flux can be calculated using Newton's law of cooling in Equation 30 [81]:

$$q''_{cv} = h(T_s - T_\infty)$$
Equation 30

Wherein: q''_{cv}= convection heat flux, BTU/(h·ft^2) (W/m^2)

h= convection coefficient, BTU/(h·ft^2) (W/m^2)

T_s= surface temperature, °F (K)

T_∞ = ambient temperature °F (K)

Convection heat transfer can be divided into free convection and forced convection [81]. Natural or free convection occurs because of buoyancy forces in the fluid. When the fluid temperature changes locally, the density also changes, causing the fluid to sink or rise. Forced convection is induced by forced flows such as from fans or the wind causing more fluid molecules to interact with the solid surface and transfer energy [3]. Convection ovens are a good example of this phenomenon. Fans in the convection oven circulate the air, causing the food in the oven to heat up and cook quicker. The convection coefficient from forced and free convection, h, can be estimated according to Equation 31 [81]:

$$h = C \; x \; 0.2782 \; x \; \left[\frac{1}{T_{avg} + 17.8} \right]^{0.181} x \; |T_s$$
$$- \; T_a|^{0.266} x \; \sqrt{1 + 2.8566 \; x \; w}$$
Equation 31

Where: C = heat flow constant, 10.15 for bottom horizontal surface cooler than ambient, 20.4 for bottom horizontal surface cooler than ambient.

T_{avg} = average air film temperature, °F (°C).

w = wind speed, ft/s (m/s)

2.4.3. Aging Modeling

Thermal stress modeling of concrete members is a nonlinear problem because of its early age changing mechanical properties that include elastic modulus, strength, Poisson's ratio, coefficient of thermal expansion, and creep and stress relaxation [58]. Therefore, once the temperature development and degree of hydration is calculated for a given concrete member, the member mechanical properties can be calculated as a function of the equivalent age or degree of hydration.

Concrete Strength Development

Concrete strength is one of the most important concrete parameters, and it is important to include its development with time in any concrete member simulation. Concrete maturity methods were developed to take into account the effects of temperature history on concrete strength development with time. Two different concrete maturity methods are described in ASTM C1074 [83], the Nurse-Saul method and the equivalent age maturity method. The Nurse-Saul method, also known as the Time-Temperature Factor method, uses the integral of the time-temperature history as the maturity. It is simple, but not as accurate as the equivalent age maturity method. The equivalent age maturity function is shown in Equation 13.

There are many different equations that have been developed to relate the concrete maturity to the concrete strength. One such equation shown in Equation 32 uses an exponential relationship [84]:

$$f_c(t_e) = f_{cult} \cdot exp\left(-\left(\frac{\tau_s}{t_e}\right)^{\beta_s}\right)$$ Equation 32

Where: f'_c = compressive strength development, psi (MPa)

f'_{cult} = ultimate compressive strength parameter fit from the compressive strength tests, psi (MPa)

τ_s = fit parameter (h)

β_s = fit parameter

Another expression for the development of strength as a function of the maturity for a mean temperature of 20°C is shown in Equation 33 and Equation 34 [85]:

$$f_{cm}(t) = \beta_{cc}(t) \cdot f_{cm}$$ Equation 33

$$\beta_{cc}(t) = exp\left[s\left(1 - \sqrt{\frac{28}{t_e}}\right)\right] \qquad \text{Equation 34}$$

Where: f_{cm}(t)= mean compressive strength in age t, psi (MPa)

f_{cm}= mean compressive strength at an age of 28 days, psi (MPa)

$\beta_{cc}(t)$= function to describe development with time

t_e= concrete equivalent age at the reference temperature, h or days

Modulus of Elasticity Development

The elastic modulus development with time is a critical parameter in calculation of the match-cast concrete deformations. The low modulus during early ages allows the concrete to deform easily when the hardened concrete section deforms from thermal gradients [58]. It is known that the elastic modulus depends on the unit weight, aggregate modulus, strength, moisture condition and maturity [58]. Several models for the elastic modulus development with time have been developed and use an equation form similar to Equation 35:

$$E(t) = E_{ref} \cdot \beta(t) \qquad \text{Equation 35}$$

Where: E_{ref}=reference modulus, psi (MPa)

β =modification factor that accounts for the modulus development with time

In order to estimate $\beta(t)$, Larson [86] presents several expressions to estimate it as a function of time, time of setting and model parameters. An idealization describing the material behavior as a piece -wise linear curve in logarithm of time is shown in Equation 36. Further, a model introducing the apparent setting time, t_s, is presented in Equation 37. At last, an additional model introducing α and τ parameters is presented in Equation 38,

$$\beta(t) = \begin{cases} 0 & for\ t < t_s \\ b_1 \cdot \log\left(\frac{t}{t_s}\right) & for\ t_s \le t_0 < t_B \\ b_1 \cdot \log\left(\frac{t_B}{t_s}\right) + b_2 \cdot \log\left(\frac{t}{t_s}\right) & for\ t_B \le t < 28\ days \\ 1 & for\ t \ge 28\ days \end{cases} \qquad \text{Equation 36}$$

$$\beta(t) = \left(exp\left(s \cdot \left(1 - 1/\sqrt{\frac{t - t_s}{28 - t_s}}\right)\right)\right)^{0.5} \qquad \text{Equation 37}$$

31

$$\beta(t) = \frac{E_\infty}{E_{ref}} \cdot exp\left(-\left(\frac{\tau}{t}\right)^\alpha\right)$$ Equation 38

Where: t_s= apparent setting time, h

$b_1, b_2, \alpha, \tau, s$=model parameters

t_B= constant that represents the time of change in slope of the elastic modulus, h

E_∞= ultimate elastic modulus, psi (MPa)

Furthermore, there are other models to estimate the elastic modulus development as a function of age that could be useful in modeling the early age development of this property. Equation 39 shows an expression based in the Fib 2010 model to determine the early-age evolution of the modulus of elasticity during the first four weeks after production [85], [87]:

$$E_u(t) = E_{u,28d} \cdot \left\{exp\left[s\left(1 - \sqrt{\frac{28\ days}{t_e}}\right)\right]\right\}^{0.5}$$ Equation 39

Where: $E_u(t)$ = Modulus of elasticity at time t in days, psi (MPa)

$E_{28,d}$ = Modulus of elasticity at an age of 28 days , psi (MPa)

s = speed at which the 28-day strength is approached (dimensionless parameter)

t_e= concrete equivalent age at the reference temperature, h or days

Coefficient of Thermal Expansion Development

The CTE of the concrete is particularly important in determining how much deformation or segment bowing distortion occurs in match-cast concrete segments. The concrete CTE is known to change during the setting process and it has also been reported to increase with age [88]. The thermal expansion coefficient is dominated by the water CTE before setting. The CTE comes to a minimum near the time of final setting, as the concrete microstructures are partially formed and the concrete is still in a wet condition [88].

An expression was developed for the CTE to describe the increase in concrete CTE after setting up to an age of 3 months, assuming an initial CTE value at the final setting is shown in Equation 40 [88]:

$$\alpha_{cte}(t) = a_1 \cdot ln\left(\frac{t}{t_{fs}}\right) + b_1$$ Equation 40

Where: α_{cteh}= hardened concrete CTE, 1/°F (1/°C)

a_1, b = material constants

t = equivalent age, h or days.

t_{fs} = final setting time, h or days

Because the existing match-cast concrete segment is already hardened, use of a hardened non-varying concrete CTE should be acceptable. Equation 41 can be used to estimate the concrete CTE based on the CTE of individual concrete constituent materials:

$$\alpha_{cteh} = \frac{\alpha_{ca} \cdot V_{ca} + \alpha_{fa} \cdot V_{fa} + \alpha_p \cdot V_p}{V_{ca} + V_{fa} + V_p}$$

Equation 41

Where: α_{cteh} = coarse aggregate CTE, με/°F (με/°C)

α_{ca} = coarse aggregate CTE, με/°F (με/°C)

V_{ca} = coarse aggregate volume, ft^3 (m^3)

α_{fa} = fine aggregate CTE, με/°F (με/°C)

V_{fa} = fine aggregate volume, ft^3 (m^3)

α_p = paste CTE, με/°F (με/°C)

V_p = paste volume, ft^3 (m^3)

Autogenous Shrinkage

Shrinkage can be considered an important characteristic in early age concrete behavior. Total shrinkage, $\varepsilon_{cs}(t, t_s)$ in concrete is a product of the sum of the autogenous shrinkage, $\varepsilon_{cas}(t)$ and drying shrinkage, $\varepsilon_{cds}(t, t_s)$, as shown in Equation 42 [85]:

$$\varepsilon_{cs}(t, t_s) = \varepsilon_{cas}(t) + \varepsilon_{cds}(t, t_s)$$

Equation 42

Where: t = concrete age, h or days.

t_s = concrete age at the beginning of drying, h or days.

Drying shrinkage is defined as shrinkage resulting from loss of moisture in hardened concrete. It has been determined that for the purpose of this study, drying shrinkage can be considered negligible as it will not impact very early age concrete behavior.

Autogenous shrinkage, $\varepsilon_{cas}(t)$, is defined as a volume variation caused by two main processes, chemical shrinkage and self-desiccation [89]. Chemical shrinkage results from the difference between the specific volume of reactants and hydration products, in other words, the cement paste occupies less volume after the hydration reaction. Moreover, self-desiccation is the change in volume of the hardened concrete as a result of the development of a negative capillary pressure on the porous network related to the water consumption by the hydration reactions [89].

33

There have been various attempts to model autogenous shrinkage based on two approaches, the maturity principle and the capillary tension approach. In this context, the expressions for estimating the autogenous shrinkage given in the Fib Model Code for Structures 2010 [85] and Eurocode 2 [90] use the maturity principle and are very similar. The Fib model is shown in Equation 43, Equation 44 and Equation 45 [85]:

$$\varepsilon_{cas}(t, t_s) = \varepsilon_{cas0}(f_{cm}) \cdot \beta_{as}(t) \qquad \text{Equation 43}$$

$$\varepsilon_{cas0}(f_{cm}) = -\alpha_{as}\left(\frac{f_{cm}/10}{6 + f_{cm}/10}\right)^{2.5} \cdot 10^{-6} \qquad \text{Equation 44}$$

$$\beta_{as}(t) = 1 - \exp\left(-0.2 \cdot \sqrt{t}\right) \qquad \text{Equation 45}$$

Where: $\varepsilon_{cas0}(f_{cm})$ = notional autogenous shrinkage component, in./in. (mm/mm)

$\beta_{as}(t)$ = time function

f_{cm} = mean compressive strength at the age of 28 days, psi (MPa).

α_{as} = coefficient, dependent on the type of cement.

Subsequent studies by Grondin et al. have developed multiscale modeling of autogenous shrinkage based in a capillary tension approach. Two stages of autogenous shrinkage are recognized, first the chemical shrinkage is modeled using chemical equations of hydration and the specific volume of each phase, and then when the setting of the cement paste takes place, the shrinkage is calculated according to the evolution of the capillary pressure and the stiffness of the cement paste [89].

Creep and Stress Relaxation

Some other important parameters that must be taken into account for the concrete aging-mechanical modeling are the concrete creep and stress relaxation effects at early ages. While the same physical phenomenon is responsible for both, creep is the time-dependent deformation during a constant stress, while stress relaxation is a time-dependent decrease in stress during a constant strain [58]. The total strain at time t, $\varepsilon_c(t)$, of a concrete member uniaxially loaded at time t_0 with a constant stress $\sigma_c(t_0)$, is expressed in Equation 46 and Equation 47 [85]:

$$\varepsilon_c(t) = \varepsilon_{ci}(t_0) + \varepsilon_{cc}(t) + \varepsilon_{cs}(t) + \varepsilon_{cT}(t) \qquad \text{Equation 46}$$

$$\varepsilon_c(t) = \varepsilon_{c\sigma}(t) + \varepsilon_{cn}(t) \qquad \text{Equation 47}$$

Where: $\varepsilon_{ci}(t_0)$ = initial strain at loading, in./in. (mm/mm)

$\varepsilon_{cc}(t)$ = creep strain at time t > t_0, in./in. (mm/mm)

$\varepsilon_{cs}(t_0)$ = shrinkage strain, in./in. (mm/mm)

$\varepsilon_{cT}(t_0)$ = thermal strain, in./in. (mm/mm)

Equation 47 illustrates that the total strain at time, $\varepsilon_c(t)$, has a stress dependent strain contribution, $\varepsilon_{c\sigma}(t)$ and a stress independent strain contribution, $\varepsilon_{cn}(t)$. The stress dependent strain contribution would be the sum of the initial strain at loading $\varepsilon_{ci}(t_0)$ and the creep strain, $\varepsilon_{cc}(t)$. The stress independent strain contribution would be the sum of the shrinkage strain $\varepsilon_{cs}(t_0)$ and the thermal strain $\varepsilon_{cT}(t_0)$ [85].

Within the range of service stresses under 40% of the mean compressive strength at the age of 28 days, it can be assumed that the instantaneous strain is linearly related to stress. The creep strain can be calculated for a constant stress applied at time t_0 using the expression in Equation 48 [85]:

$$\varepsilon_{cc}(t, t_0) = \frac{\sigma_c(t_0)}{E_{ci}} \varphi(t, t_o)$$

Equation 48

Where: $\varphi(t,t_0)$= creep coefficient (dimensionless)

               $\sigma_c(t)$= constant stress applied at time t_0, psi (MPa)

               E_{ci}= modulus of elasticity at the age of 28 days, psi (MPa)

An expression for the stress dependent strain $\varepsilon_{c\sigma}(t)$ at time t is presented in Equation 49 [85]:

$$\varepsilon_{c\sigma}(t, t_0) = \sigma_c(t_0) \left[\frac{1}{E_{ci}(t_0)} + \frac{\varphi(t, t_0)}{E_{ci}} \right] = \sigma_c(t_0) J(t, t_0)$$

Equation 49

Where: $J(t,t_0)$= creep compliance, representing the total stress dependent strain per unit stress, 1/psi (1/MPa)

               $E_{ci}(t)$= modulus of elasticity at time t, psi (MPa)

The creep compliance function is used for calculating the creep response as shown in Equation 50 [91]:

$$Compliance\ J(t, t_0) = \frac{(elastic\ strain + basic\ creep + drying\ creep)}{stress}$$

Equation 50

Ultimately, it has been established that there is a stress- strain relation due to creep and relaxation effects in concrete [92] [93], expressed in Equation 51 and Equation 52 [92]:

$$\varepsilon_{c\sigma}(t) = J(t, t_0) \cdot \sigma_c(t_0)$$

Equation 51

$$\sigma_c(t_0) = R(t, t_0) \cdot \varepsilon_{c\sigma}(t)$$

Equation 52

Where: $R(t,t_0)$= relaxation function

Furthermore, a uniaxial creep law is expressed in Equation 53 [94]:

$$\varepsilon_{c\sigma}(t) - \varepsilon_{c\sigma}^0(t) = \int_0^t J(t, t_0) \, d\sigma \, (t_0)$$

<div align="right">Equation 53</div>

Where: t = time from casting concrete, h or days

$\varepsilon_{c\sigma}^0$ = prescribed stress independent inelastic strain, in./in. (mm/mm)

Many different models have been developed to relate the concrete creep compliance term with mixture proportions and concrete physical characteristics. For example, ACI 209.2R-08 [91] presents 4 accepted models that are used for this matter: the ACI209R-92 model, Bazant-Baweja B3 model, CEB MC90-99 model and GL2000 model. These models are based on concrete creep coefficients fits from ASTM C512 [95] tests performed, with many models developed from the same dataset [96]. The ACI209R-92 [91] model introduces the compliance function to estimate creep as shown in Equation 54:

$$J(t, t_0) = \frac{1 + \phi(t, t_0)}{E_{cmto}}$$

<div align="right">Equation 54</div>

Where: E_{cmto} = modulus of elasticity at the time of loading t_0, psi (MPa)

$\phi(t,t_0)$ = creep coefficient as the ratio of the creep strain to the elastic strain at the start of loading at the age t_0 (dimensionless)

The Bazant-Baweja B3 model [91] defines the compliance formulation as shown in Equation 55 to Equation 68:

$$J(t, t_0) = q_1 + C_0(t, t_0) + C_d(t, t_0, t_c)$$

<div align="right">Equation 55</div>

$$q_1 = \frac{0.6}{E_{cm28}}$$

<div align="right">Equation 56</div>

$$C_0(t, t_0) = q_2 Q(t, t_o) + q_3 \cdot ln[1 + (t - t_0)^n] + q_4 \cdot ln\left(\frac{t}{t_0}\right)$$

<div align="right">Equation 57</div>

In. U.S. customary units:

$$q_2 = 86.814 \times 10^{-6} c^{0.5} f_{cm28}^{-0.9}$$

<div align="right">Equation 58</div>

In. metric units:

$$q_2 = 185.4 \times 10^{-6} c^{0.5} f_{cm}^{-0.9}$$

<div align="right">Equation 59</div>

$$Q(t, t_o) = Q_f(t_0)\left[1 + \left(\frac{Q_f(t_0)}{Z(t, t_0)}\right)^{r(t_0)}\right]^{-1/r(t_0)}$$

<div align="right">Equation 60</div>

$$Q_f(t_0) = \left[0.086(t_0)^{\frac{2}{9}} + 1.21(t_o)^{4/9}\right]^{-1}$$ Equation 61

$$Z(t, t_o) = (t_0)^{-m} \cdot ln[1 + (t - t_o)^n]$$ Equation 62

$$r(t_0) = 1.7(t_0)^{0.12} + 8$$ Equation 63

$$q_3 = 0.29(\frac{w}{c})^4 q_2$$ Equation 64

In. U.S. customary units:

$$q_4 = 0.14 \times 10^{-6}(\frac{a}{c})^{-0.7}$$ Equation 65

In. metric units:

$$q_4 = 20.3 \times 10^{-6}(\frac{a}{c})^{-0.7}$$ Equation 66

$$C_d(t, t_o, t_c) = q_5[exp\{-8H(t)\} - exp\{-8H(t_0)\}]^2$$ Equation 67

$$q_5 = 0.757 f_{cm28}^{-1} |\varepsilon_{sh} x\ 10^6|^{-0.6}$$ Equation 68

Where: q_1 = the instantaneous strain due to unit stress.

E_{cm28} = mean modulus of elasticity of concrete at 28 days, psi. (MPa)

$C_0(t,t_0)$ = compliance function for basic creep term

q_2 = aging viscoelastic parameter

c = cement content, lb/yd^3. (kg/m^3)

f_{cm} = mean compressive strength at 28 days, psi (MPa)

$Q(t,t_0)$ = approximate binomial integral used to obtain the aging viscoelastic compliance term

t = age, h

t_0 = age when loading starts, h

m = empirical parameter, 0.5 for normal concrete

n = empirical parameter, 0.1 for normal concrete

q_3 = non-aging viscoelastic compliance parameter

w/c = water to cement ratio

$q_{4=}$ aging flow compliance parameter

$a/c=$ aggregate-cement ratio

$C_d(t,t_0)=$ compliance function for drying creep

$q_{5=}$ drying shrinkage compliance parameter

$f_{cm}=$ concrete mean compressive cylinder strength, psi (MPa)

$\varepsilon_{sh}(t,t_c)=$ shrinkage strain at concrete age t since the start of drying age t_c, in/in (mm/mm)

$H(t)$ and $H(t_0)=$ spatial averages for pore relative humidity

The CEB MC90-99 model [91] introduces the compliance function shown in Equation 69 [91]:

$$J(t,t_0) = \frac{1}{E_{cmto}} + \frac{\phi_{28}(t,t_0)}{E_{cm28}}$$

Equation 69

Where: $E_{cmto}=$ modulus of elasticity at the time of loading t_0, psi (MPa)

$E_{cmto}=$ mean modulus of elasticity at 28 days, psi (MPa)

$\phi_{28}(t,t_0)=$ 28 day creep coefficient (dimensionless)

The GL2000 model [91] introduces a compliance function influenced by and similar to the CEB MC90-99 model, seen in Equation 69, with variations in the calculation of the $\phi_{28}(t,t_0)$ term.

The creep compliance models presented in Equation 54 to Equation 69 are valid for hardened concrete moist cured for at least 1 day and loaded at the end of 1 day of curing or later [91]. Modifications have been proposed to some creep compliance models to account for the high creep during the first day of curing. For example, modifications of this nature have been introduced to the B3 model. This model was developed to provide a better fit during the first day of curing, while transitioning to have no effect on the later age compliance function that was calibrated to the RILEM experimental creep data bank [96]. This new compliance function is introduced by modifying the aging viscoelastic compliance term q2, also modifying the instantaneous strain due to unit stress q1 and omitting drying shrinkage. This is shown in Equation 70:

$$J(t,t_0) = q_1 \left[\frac{t_0}{t_0 - q_6}\right] + q_2 \left[\frac{t_0}{t_0 - q_5}\right] Q(t,t_o) \\ + q_3 \ln(1 + (t - t_o)^n) + q_4 \left(\frac{t}{t_0}\right)$$

Equation 70

Where: $q_{5=}$ new parameter modifying q_2 and represents structural setting time.

q_6= new parameter modifying q_1 and represent a factor for early age elastic behavior.

The numerical implementation of the mathematical models for creep and stress relaxation discussed in this section can be approached by two different methods, the principle of superposition and a rate type formulation of creep [92]. Both approaches involve approximating a solution for Equation 53.

The method of superposition consists in calculating a final strain value based on the stress history [92], [94]. It is performed by evaluating a stress differential $d\sigma$ for various time steps and calculating a final strain $\varepsilon_{c\sigma}(t)$ at the end of the process, as it can be seen expressed in Equation 71 [92]:

$$\varepsilon_{c\sigma}(t) = \int_0^t J(t,t_0)\, d\sigma\,(t_0) + \varepsilon_{c\sigma}^0(t) \qquad\qquad \text{Equation 71}$$

This numerical implementation provides good correlation to experimental data and provides a robust and flexible tool for various types of concrete mixes with relatively few test data to model thermal cracking and early age thermal stress measurement. [58], [86]. However, it has also been discussed that the nonlinearity nature of creep diminishes the accuracy of this numerical implementation [97]. This approach becomes computationally expensive for long time periods.

The rate type formulation of creep approach is based on the solidification theory for concrete creep and its application using a Kelvin chain model [92], [98]. It can be defined as a rheological model that consists of a series of couplings of several Kelvin units. Each of these units is composed of parallel couplings of a spring and dashpot, as can be seen in Figure 8 [92], [99]. Springs represent the elastic response when a stress is applied to a member and the dashpot represents the viscous response to it. The reasoning of this type of approach is that when a constant load is applied to the system, the strain value is the same for both the spring and the dashpot at all times. The stress is assumed initially by the dashpot and transfers it gradually to the spring to represent the viscoelastic behavior of concrete [92].
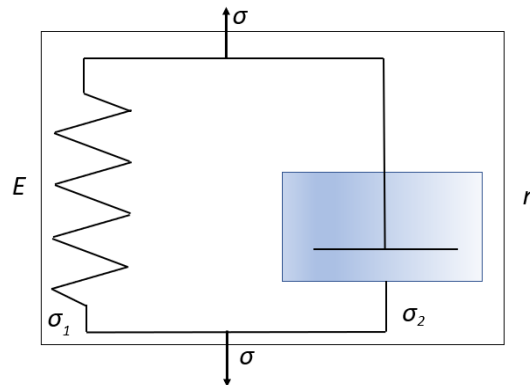
Figure 8: The Kelvin model (after Liu, 2018) [92]

Based in this idealization, Equation 72 [92] illustrates that the strain is related with the elastic nature of the spring, *E*. Equation 73 [92] illustrates that the rate of change of the strain is related to the viscous nature of the dashpot, η. Equation 74 [92] represents that the sum of the stresses assumed by the spring and the dashpot is equal to the total external stress applied.

$$\varepsilon = \frac{1}{E}\sigma_1 \qquad\qquad \text{Equation 72}$$

$$\dot{\varepsilon} = \frac{1}{\eta}\sigma_2 \qquad\qquad \text{Equation 73}$$

$$\sigma = \sigma_1 + \sigma_2 \qquad\qquad \text{Equation 74}$$

Equation 75 [92] represents a differential equation that can be established using the principles shown in Equation 72, Equation 73 and Equation 74 and is the base of the numerical implementation used to approximate the strain caused by creep. Because the idealization is composed of an N number of coupling of Kelvin units, the total strain in a system can be represented by a sum seen in Equation 76 which yields the total strain obtained based on this numerical implementation.

$$\sigma = E\varepsilon + \eta\dot{\varepsilon} \qquad\qquad \text{Equation 75}$$

$$\varepsilon = \sum_{i=1}^{N} \varepsilon_i \qquad\qquad \text{Equation 76}$$

The rate type formulation – Kelvin chain approach to model concrete creep in structures is found in common finite element software packages such as B4cast [100] or Diana FEA [101], mainly because it is more computationally efficient in comparison with the principle of superposition for large concrete structures [92].

2.4.4. Finite Element Modeling

The finite-element method (FEM) is a numerical analysis technique that has been extensively used for solving a wide range of engineering problems lately. It has the advantage of being able to model complicated geometries and boundary conditions in 3-dimensional settings to evaluate behavior of full scale structures [92].

It is possible to use a finite element modeling approach to study the bowing in match-cast segments in segmental bridge construction by integrating the temperature development of early age concrete in match-cast construction and the resulting mechanical properties in both the old segment and the new segment that induce the bowing distortion of the sections [3]. Such a finite element simulation must be able to model several processes including: the heat generation from the concrete of the new match-cast segment, the heat flux through a thermal linkage of the new segment to the old match-cast segment, the temperature field and gradients in the old match-cast segment as a result of the heat influx from the old segment and environmental conditions, the thermal deformation produced in the old segment which produces the bowing distortion and its interaction with the mechanical properties development of the old and new match-cast segments.

In finite element modeling of early age behavior of concrete, it is widely acceptable practice to calculate the fields of temperature and degree of chemical reaction first and then calculate mechanical properties of interest using the results of the thermal analysis as an input [102]. Initially, elements capable of modeling heat generation using the expressions presented in Section 1.4.1 are formulated to represent the new match-cast segment. Then, elements that provide thermal linkage are established between the new segment and the old match-cast segment.

Temperature distributions in the old match-cast segment can be modeled realistically using finite elements [103]. A typical approach using variational methods can be used to solve for the temperature values in the nodes of a meshed section as a result of the heat transfer and conduction within a body, as well as the influence of external environmental conditions in the development of heat gradients in the body [103]. As the heat generated by the new match-cast segment enters through the match-cast face, a thermal gradient will form in the old match-cast segment.

Thermal stresses and, by extension, displacements or deformations causing bowing distortions in the old match-cast segment can also be calculated using the temperature distributions obtained in the previous step. Finite element formulations based on strain energy have been developed [103] to analyze strains caused by temperature variations. These formulations include mechanical properties of concrete such as the coefficient of thermal expansion and elastic modulus and the evolution of these properties through time so as to ultimately facilitate the calculation of bowing distortion caused by temperature variations [103]. Abendeh [3] conducted a study in which a finite element model was developed to estimate the gap generated between segments from the match-casting process, achieving good results when validating the model. The finite element software package ANSYS was used, and the new match-cast segment was modeled by meshing the section with three-dimensional eight node thermal elements to model the concrete heat generation, while the concrete of the old match-cast segment was modeled by using three-dimensional eight node thermal and structural field capability solid brick elements to simulate the thermo-mechanical behavior of solid concrete [3]. Heat transfer between the segments was represented using two-node links elements, which also allowed free movement of the structural solid brick elements, ultimately representing the bowing effect [3]. Standard segmental bridge cross-sections were modelled using approximately 5000 elements for smaller sections and approximately 9000 elements for larger size sections, obtaining accurate results with these mesh resolutions [3].

Liu [92] also provides a finite element modeling approach to estimate early age concrete stress development of concrete. The software package ABAQUS was used to create eight-node linear hexahedral brick elements with three translational degrees of freedom at each node. The concrete temperature profiles obtained from the software ConcreteWorks and the CTE value of each concrete mixture were inputted in the model. The thermal strains were calculated based on the CTE and then based on the strain increment at each time step and the compliance subroutine. The stress at each time step was calculated and reported [92]. It was noted that for this particular model, an element size of 1 in. was ideal. After evaluating larger and smaller element sizes, it was concluded that the 1-in. size was optimal in terms of accuracy and the computational resources required to run the model [92]. As for the time step, it was noted that a time step of 1 hour was optimal in the same terms discussed for the mesh size.

2.5 Conclusions

This literature review presented a comprehensive overview of the match-cast segmental construction process. Although segmental construction possesses significant advantages, geometric warping is a potential downside if not managed. Bowing distortion of a segment results from thermal gradient development of the match-cast segment. This bowing distortion results in several issues including non-uniform stress distributions and gaps that need filled between joints.

A number of considerations to reduce, or completely mitigate, bowing were analyzed in this review. Potential solutions include considering environmental impacts, the coefficient of thermal expansion, setting time, modulus of elasticity development, heat of hydration, thermal diffusivity, and geometric considerations. A simplified approach to establishing if a segment is at an increased risk for bowing distortion was analyzed. This approach quantitatively determines whether mitigation measures may be required. External mitigation measures such as isothermal enclosures, curing blankets, and steam curing were also explored. Finally, the fundamentals of modeling a segment during hardening for various geometries and compositions were presented.

3 Simulation Matrix

3.1 Introduction

Match-cast segmental bridge construction is a precast concrete fabrication process where a bridge segment is cast against a preceding segment in a precast facility or yard. Segments can then be erected at a later time in the corresponding bridge spans, ensuring proper alignment of the segments when installed. [5]. Short line casting and long line casting are two possible methods that can be used to perform the fabrication process, with the short line casting method more common [3], [5]. Short line casting consists in casting all segments in the same place, using the previously cast segment to obtain a match-cast joint as the mold for one side of the new member and stationary forms used for the other sides [104].

Segmental bridge construction using the short line match-casting method is considered a fast and versatile construction type. Many bridges in the US and around the world have been constructed using it since its invention in the 1940s [3]. Engineers have identified issues related to bowing distortions of segments as a result of thermal effects due to the construction process [1], [3], [4], [104]. The high heat of hydration of the concrete in the 'new' segment induces a thermal gradient in the 'match-cast' segment, causing it to undergo bowing distortion. The bowing of the 'match-cast' segment occurs before the concrete of the 'new' segment has set, causing the 'new' segment to acquire this curvature that becomes permanent at the time of set [1]. The 'match-cast' segment returns to its original shape after cooling down, and the 'new' segment ends up with one straight and one curved side after the concrete hardens [3].

Construction and structural problems can arise from the bowing distortions of the bridge segments [1], [3]. Accumulated gaps in the joints can change the closure pour sizes, affecting the designed installation of the dead end tendon anchors in the joint [1], and in some cases they could also cause cracking in the segments [3]. Furthermore, gaps between segments generate areas of reduced compression between joints and could cause undesirable stress redistributions in bridge spans [1], [3].

Analytical and numerical approaches have been used to calculate gap sizes in segments as a result of the short line match-casting construction method [1], [3]. The equivalent moment method developed by Robert-Wollmann et al. consists in calculating the bowing distortion gap size of the 'match-cast' segment at a certain time based on the thermal gradient generated in it as a result of the contact with the 'new' segment, the width and length of the segment and the coefficient of thermal expansion of the 'match-cast' segment. Roberts-Wollmann et al. showed that the method was able to adequately estimate segment deformations in Type I and Type III segments at the San Antonio Y project in Texas [1], [2]. Furthermore, other authors have shown the ability of finite element models to simulate the short line match-casting process, validating the results with the measurements of the San Antonio Y bridge project and the Bang Na bridge in Bangkok [3], [7], [75].

This report used the information summarized in the literature review in section 2 of this report to establish a simulation test matrix containing variables that were used in finite element simulations of concrete temperatures and deformations expected in the short line match-casting method to identify critical variables and cases that cause excessive bowing distortions in

segments. The B4Cast finite element software package was used for this purpose as it is specialized software used for simulating temperatures and stresses in 3-dimensional concrete structures during hardening [105]. Special emphasis on Florida precast segmental bridge construction characteristics was used in developing the simulation test matrix. The research team used results of the simulations to formulate best practices for mitigation of segment distortion during fabrication.

3.2 Simulation Matrix Variables

The short line match-cast construction method were represented in the simulation matrix by establishing an independent set of variables and a dependent set of variables. The independent set of variables were choices selected to perform the construction of the segments and are grouped in three groups: geometry of the segments, mix design parameters, and construction conditions or properties. Dependent variables were a result of the selections made for the independent variables influencing the concrete thermal properties, mechanical properties (elastic modulus at 28 days) and the setting time.

Several options were also set for each variable to explore a reasonable range that might have an influence on the bowing distortion studied for the segments. In some cases, parameters were chosen that are outside of values that might be expected in segmental bridge construction; this ensured that enough data was generated to gain a full understanding the behavioral changes caused by the variation of the parameter.

3.2.1 Independent Variables

Geometry

The major geometric characteristic that influences the bowing distortion of segments in the short line match-casting process was identified in the literature review as the width-to-length ratio of segments [1], [3], [4], as illustrated in Figure 9. A critical width-to-length ratio of 6 has been established in the literature as the value where the gap formed by bowing distortions of segments becomes significant and mitigation measures should be applied [1], [2], [4].
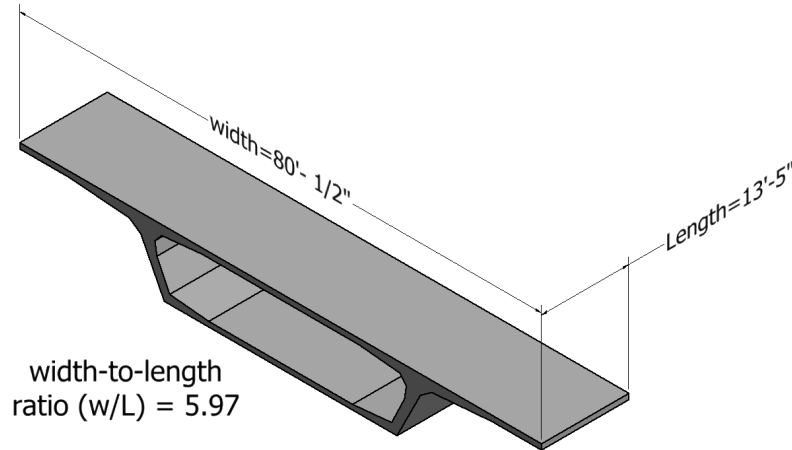
Figure 9: Florida Bridge B segment

In the San Antonio Y project in Texas, measurements of gaps formed due to the short line match-casting process were performed in two types of segments with width-to-length ratios of 9.33 and 3.0, where the segments with the higher ratios showed significantly higher gap values and caused construction issues, as opposed to the segments with lower ratios [1], [2]. Problems with excessive values for gaps generated from bowing distortions in the short line construction method were also evidenced in the Bang Na Expressway project in Bangkok, with segments of w/L ratios of 10.7 and 21.8 [3].

Width-to-length ratios of segments for precast segmental construction are a function of the need of each particular project but they can range from 2.8 to 13.8 [3], with certain exceptions as the segments with w/L ratios of 21.8 in the Bang Na Project. In the simulation matrix, 6 different Florida bridge segment geometries along with the Bang Na Pier geometry were used, as shown in Table 1. The w/L ratios for the Florida bridges considered in the simulation matrix ranged from 2.15 to 10.89, covering the range observed in the literature and also the range contained in the AASHTO-PCI-ASBI segmental box girder standards which range from 2.8 to 4.5 [106]. The Bang Na Pier geometry was added to the test matrix to represent the high end of w/L ratios that could be used.

Table 1: Bridge geometries

Bridge	Max w/L ratio
Florida Bridge A	2.15
Florida Bridge B	5.97
Florida Bridge C	10.89
Florida Bridge D	9.39
Florida Bridge E	4.09
Florida Bridge F	6.32
Bang Na Pier	21.80

Mix Design Parameters

The concrete mixes developed for this simulation matrix follow the guidelines for Class V (6500 psi) concrete as defined by FDOT Standard Specifications for Road and Bridge Construction section 346-3 [5] and FDOT Structural Design Guidelines – Structural Manual Volume I from FDOT [107]. Concrete classes IV, V, VI, and VII are all allowed for superstructures exposed to moderately and extremely aggressive environments by the mentioned specifications [5], [107]. Class V concrete mixtures were the most common class of concrete found during a review of concrete mixtures approved for use in FDOT precast segmental structures.

Type of Cement

One of the most important parameters that influence the amount of heat produced by cement hydration in concrete is the type of cement used for the mix [58]. As a result, the high temperature developed by the 'new' segment in the short line match-casting method was strongly influenced by this variable. Two values were selected for this variable to cover the desired range, one type of cement with moderate heat generation capability and another with a high heat generation capability.

The research team reviewed the database of FDOT approved concrete mixtures and found that both ASTM C150 [108]/ AASHTO M 85 [109] Type II (MH) and ASTM C595 [110]/ AASHTO M 240 [111] Type IL cements were used in precast segmental member construction. The research team selected Type II (MH) portland cement to represent a moderate heat of hydration cement. The other type of cement selected for the simulation matrix was an ASTM C150 [108]/ AASHTO M 85 [109] Type III cement, which is used for high early strength and is used frequently in the precast industry.

Total Cementitious Content

Another relevant parameter that influences the amount of heat produced by cement hydration in concrete is the amount of cement used for the mix [58]. Factors such as the need for rapid construction and concrete durability, demand the increase of the amount of cementitious materials used in a concrete mix [58]. Three values were selected for this variable to cover the desired range: a low cementitious content, a medium level cementitious content and a high cementitious content for production of class V concrete.

For extremely aggressive environments a minimum value of cementitious materials content is established by FDOT specification 346-3.5 as 600 lb/yd^3 (356 kg/m^3). [5]. Moreover, in the database of FDOT approved mixtures for precast concrete, a range from 690 lb/yd^3 (409 kg/m^3) to 920 lb/yd^3 (546 kg/m^3) of cementitious content was found for class V concrete. The total cementitious contents selected for the simulation matrix were 650 (386), 750 (445), and 950 (564) lb/yd^3 (kg/m^3).

SCM Replacement

Fly ash is a common supplementary cementitious material (SCM) used to improve durability and reduce the heat of hydration of concrete mixtures [56], [58]. FDOT specification 346-2.3 limits from 15% to 30% were established for the use of ASTM C618 Class F Fly Ash in [5] for binary

and ternary concrete mixes. The limits of allowable fly ash use, as well as the no replacement case (as a control), were included in the simulation matrix, giving cement replacement levels by mass of 0, 15, and 30%.

ASTM C1240 [112] Silica Fume is an SCM used in Florida to improve the durability of concrete mixtures, typically in ternary blends with either fly ash or slag [5], [58]. Silica fume is allowed to be used in ternary blends at a dosage of between 7 and 9% by mass replacement of cement [1]. In the simulation matrix, one case for no replacement and another for 8% silica fume used along with fly ash at dosages allowed by FDOT specification 346 Table 2 are included [5]. Ternary blends with slag cement were not considered because precast concrete producers prefer not to use mixtures with 50% or higher slag cement replacement levels because of the slow strength gain rates.

Admixtures

Precasters often use retarders in the summer in Florida to lengthen the time available for consolidation and finishing and accelerators in the winter to increase the rate of hydration and allow for daily form removal and bed turnover. These ASTM C494 [113] set-control admixtures can greatly affect the time at which the new concrete segment shape is locked in by concrete hardening, and consequently the total distortion. For the analysis of the bowing distortion problem in the short line match-cast method, the only types of chemical admixtures that were considered were the ones that influence directly the setting time of the concrete mix. Simulations were conducted without any set-control admixtures, with an accelerator, and with a retarder to cover all the possible ranges of setting times that can be generated for a concrete mix.

Water-Cement Ratio

FDOT specification 346-3.3 requires a maximum water-cementitious material ratio (w/cm) of 0.37 for class V concrete [5]. For the simulation matrix, the maximum allowable value of 0.37 was selected along with two lower w/cm ratios to determine the effects of w/cm and overall strength on distortion. A w/cm of 0.35 was selected because it is required for mixtures containing highly reactive pozzolans. A w/cm of 0.29 was also selected to represent low w/cm often used in precast construction to accelerate strength gain and bed turnover times.

Aggregates

Aggregates occupy a majority of volume in concrete mixtures, and therefore have an important influence on the thermal and mechanical characteristics of concrete, especially the modulus of elasticity [58], [114]. To reflect a range of thermal and mechanical characteristic for the numerical simulations to be performed, 3 types of typical Florida coarse aggregates were considered for the simulation matrix: porous (Brooksville) limestone, dolomitic (dense) limestone from Alabama, and siliceous gravel from Chattahoochee, Florida [114]. Siliceous gravel was selected over granite because the values for coefficient of thermal expansion and thermal conductivity of siliceous gravel are greater than the ones for granite. This gave a wider range of bowing distortion in the short line match-cast construction simulations performed [3], [58]. Additionally, an option of shale lightweight coarse aggregate [115] was selected to explore the effect of lightweight aggregate on bowing distortion in short line match-cast segmental

bridge construction. Two typical fine aggregates for Florida were selected for the simulation matrix: siliceous sand from Quincy, Florida [114] and manufactured sand (crushed limestone).

The mentioned aggregates were combined in 7 different aggregate pairs (Coarse Agg. + Fine Agg.) summarized in Table 2 that generated a set of thermal and mechanical properties that are discussed further in the dependent variables section of the report.

Table 2: Aggregates combinations

Combination #	Coarse Aggregate + Fine Aggregate
1	Porous Limestone (Brooksville) + Siliceous Sand
2	Porous Limestone (Brooksville) + Manufactured Sand (Crushed Limestone)
3	Dolomitic (Dense) Limestone (Mexico or Alabama) + Siliceous Sand
4	Dolomitic (Dense) Limestone (Mexico or Alabama) + Manufactured Sand (Crushed Limestone)
5	Siliceous Gravel + Siliceous Sand
6	Siliceous Gravel + Manufactured Sand (Crushed Limestone)
7	Lightweight Coarse Aggregate + Siliceous Sand

Environmental Conditions and Construction Properties

Ambient Temperature

The temperature development of concrete segments fabricated with the short line match-cast method is influenced by the ambient temperature through heat transfer with the environment [58], [81]. The ambient temperature is one of the parameters that defines the amount of heat flux that exits or enters a segment due to convection [3]. A set of ambient temperature curves representing a range of possible weathers in Florida were selected for the simulation matrix. Summer and winter ambient temperature curves from Miami and Tallahassee were developed from historical Florida weather information [116], as shown in Figure 10 through Figure 13.
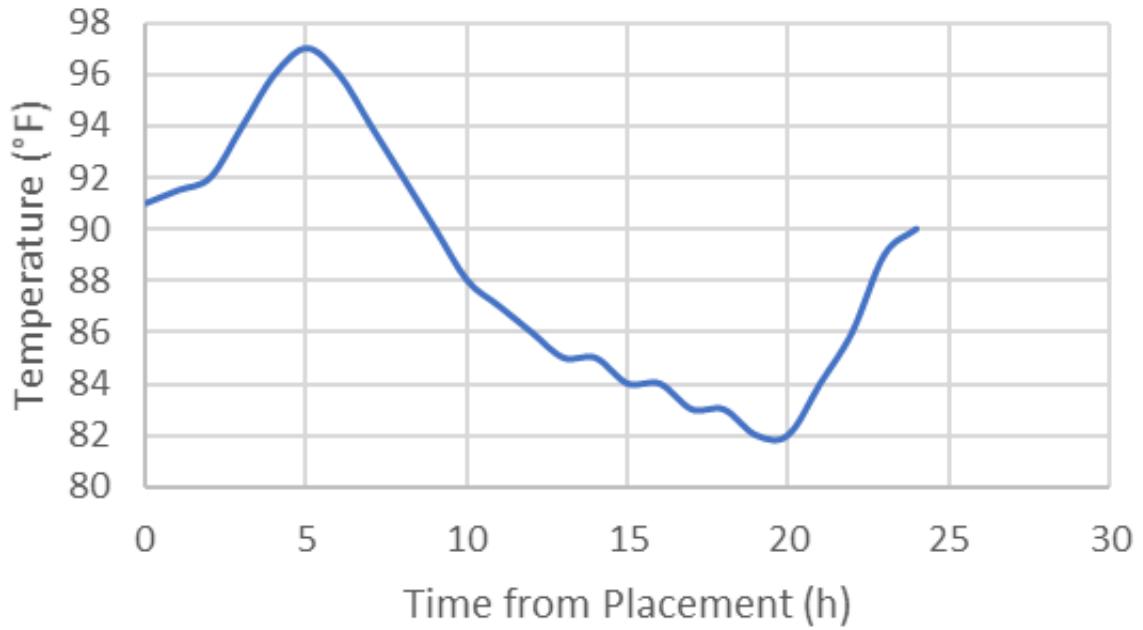
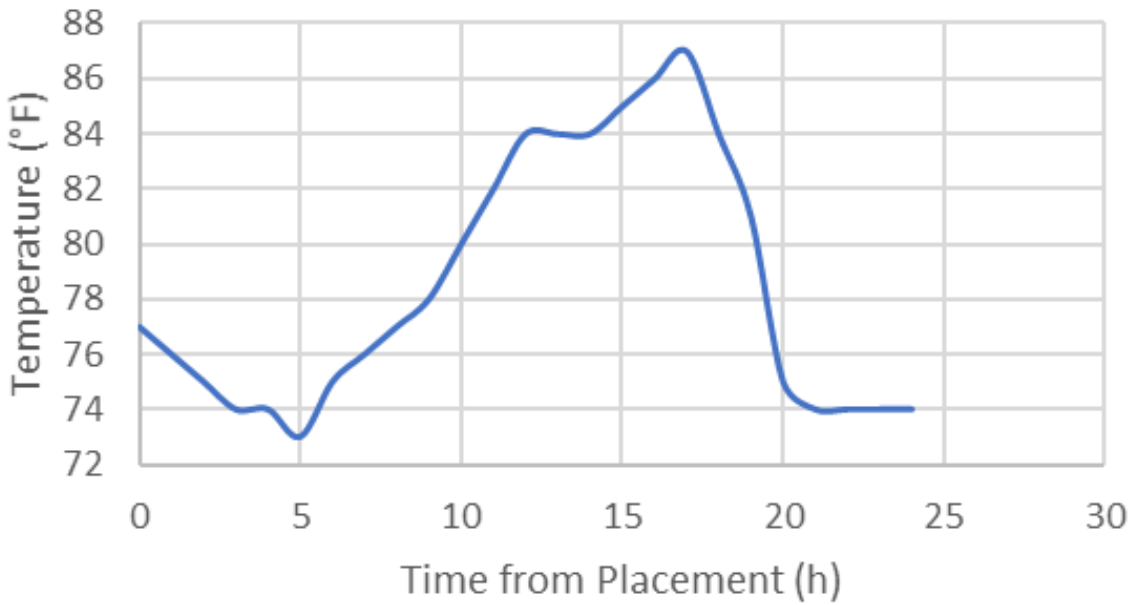Figure 10: Ambient temperature curve: Miami, summer morning placement

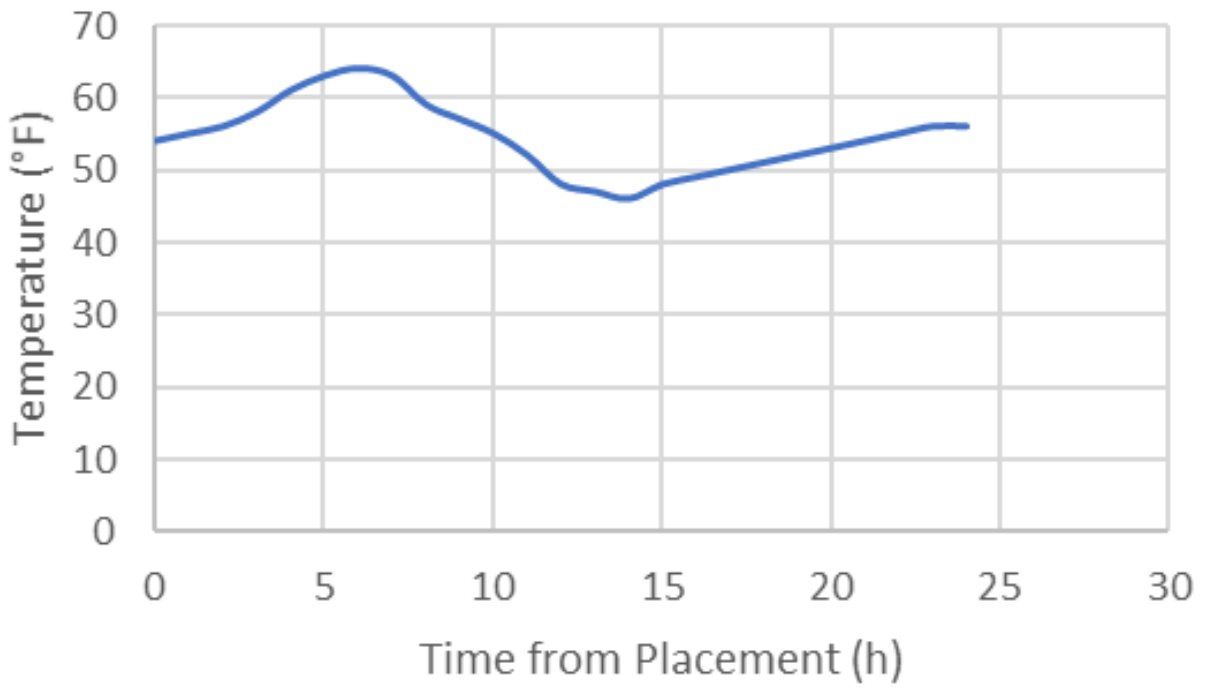Figure 11: Ambient temperature curve: Miami, summer night placement

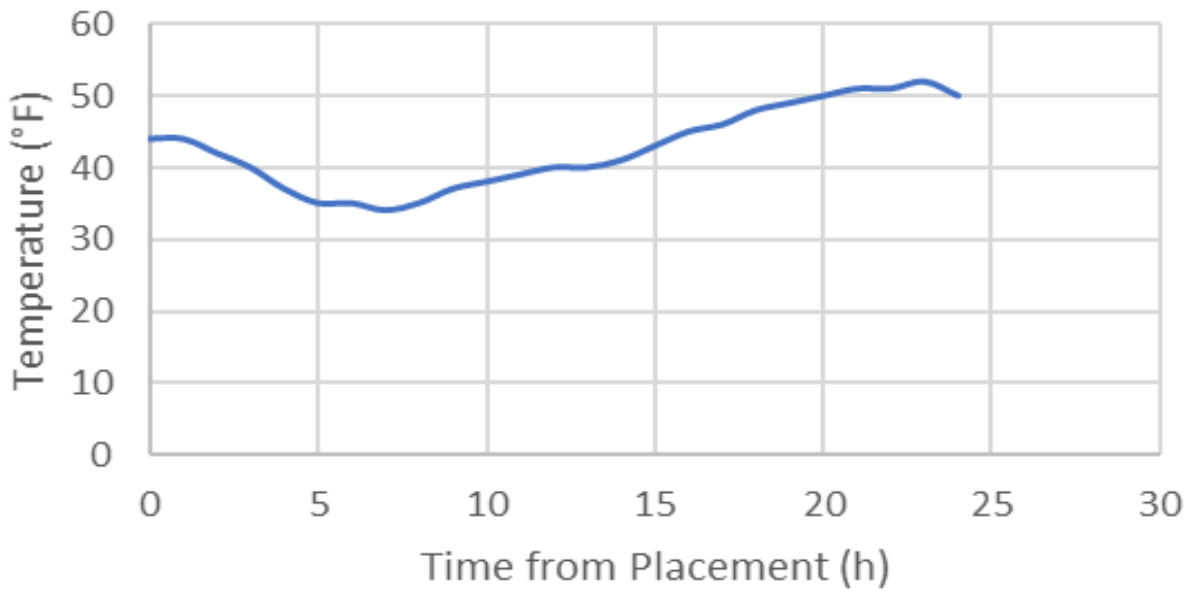Figure 12: Ambient temperature curve: Tallahassee, winter morning placement

Figure 13: Ambient temperature curve: Tallahassee, winter night placement

The ambient temperatures at placement shown from Figure 10 to Figure 13 are summarized in Table 3.

Table 3: Ambient temperatures

Condition	Ambient Temperature at
Summer, 10:00 am	91 (32.7)
Summer, 10:00 pm	77 (25)
Winter, 10:00 am placement	54 (12.2)
Winter, 6:00 pm placement	44 (6.6)

Concrete Temperature at Placement

A range of concrete temperatures at time of placement were used in the simulation matrix related to each ambient temperature at concrete placement shown in Table 3, complying with FDOT specification 346-7.5 related to hot weather concreting and specification 346-7.5 related to cold weather concreting [5]. The selected values are shown in Table 4.

Table 4: Concrete temperatures at placement

Condition	Ambient Temperature at Placement, °F (°C)	Concrete Temperature at Placement, °F (°C)
Summer, 10:00 am placement (Miami)	91 (32.7)	95(35)
Summer, 10:00 pm placement (Miami)	77 (25)	75 (23.8)
Winter, 10:00 am placement (Tallahassee)	54 (12.2)	60 (15.5)
Winter, 6:00 pm placement (Tallahassee)	44 (6.6)	50 (10)

Wind Speed

Wind speed directly impacts convective heat transfer on the surface of the exposed concrete and forms [3], [81]. FDOT specification 400-7.1.3 set limitations for concreting when weather forecasts indicate that wind speed will exceed 15 mph (24.14 km/h) at the time of concreting [5]. Wind speeds of 0, 7.5 (12.07 km/h) and 15 mph (24.14 km/h) were used in the simulations.

Insulation – Curing Method

Insulation with curing blankets or plastic sheeting is mentioned in the literature as an effective manner of preventing the development of an excessive thermal gradient in the 'old' match-cast segment, especially in cold weathers [3]. Three insulation options were selected in the simulation matrix, where plastic sheeting (tarps) as a curing technique would be the option for a high insulation level (i.e Low Thermal Conductivity material) [3], [5], [33], [117], burlap as specified in FDOT specification 452-6.7 [5] would be an intermediate insulation option, and a no insulation option in the segments was used as the control. The values can be seen in Table 5.

Table 5: Insulation: curing method

Insulation Type	Thermal Conductivity, BTU/(h·ft·°F) (W/m·°C)
None	n/a
Burlap (FDOT 925) (Thickness 1 cm = 25/64 in) [5]	0.175 (0.302)
Insulating Tarps (White Burlap Polyethylene (FDOT 925 - ASTM C171) (Thickness 1 cm = 25/64 in) [3], [5], [33], [117]	0.017 (0.03)

Formwork

The new segment fabricated in the short line match-cast construction method is supported by formwork. Besides the mechanical support, this formwork also provides a thermal boundary condition depending on the material that is used for it. The typical materials that are used for formwork in segmental bridge construction are steel and wood. The steel thermal conductivity used was 34.6 BTU/(hr·ft·°F), while a thermal conductivity of 0.081 BTU/(hr·ft·°F) was used for wood formwork [3], [77].

Isothermal Enclosures - Steam Curing

Isothermal enclosures are used in conjunction with steam curing to provide controlled ambient and moisture conditions for the hydration of concrete, and are mentioned in section 400 of FDOT specifications as accelerated curing [5]. Typical steam curing cycles have a duration of 28 hours with pre-steaming or preheating periods that range from 4 to 6 hours [5], [118]. Preheating temperatures range from 50°F to 90°F and maximum curing temperatures of cycles range from 130°F to 160°F, with the maximum heating or cooling rate of 40°F per hour [5]. Curing blankets or burlap can also be used in steam curing cycles [5].

Based on the typical steam curing durations and temperatures noted in the literature, three options for this variable were developed. First, an option of no steam curing cycle was seslected. A steam curing cycle with a maximum temperature of 130°F was selected along with a preheating temperature of 70°F. A steam curing cycle with a maximum temperature of 160°F was also selected along with a preheating temperature of 90°F. The steam curing cycle curves are shown in Figure 14 and Figure 15.
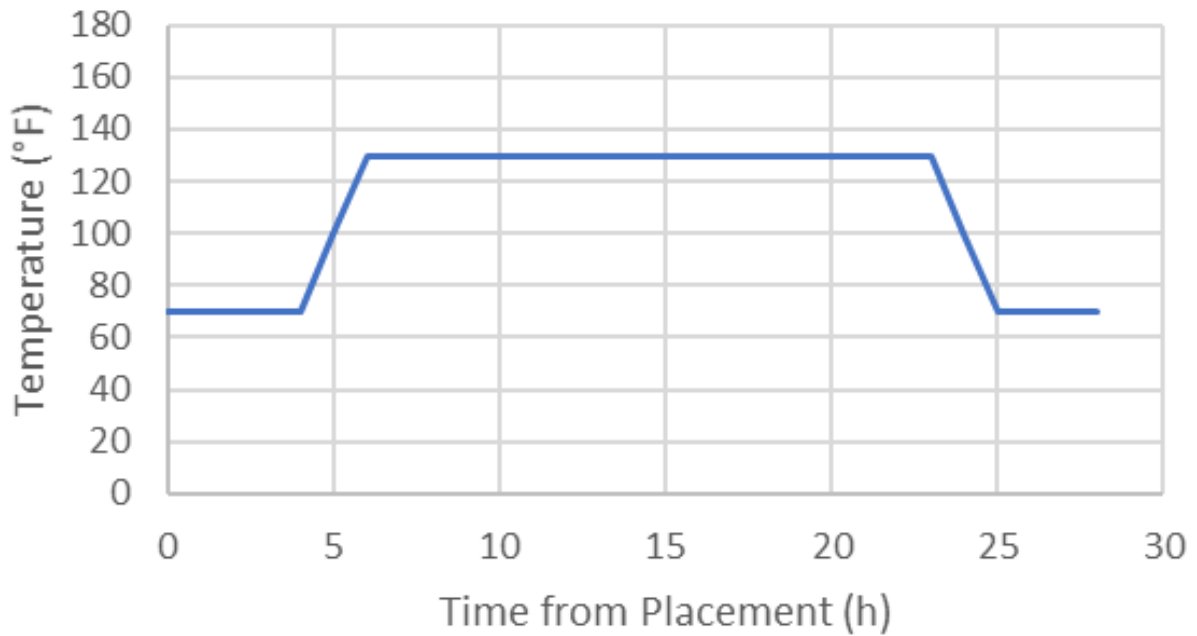
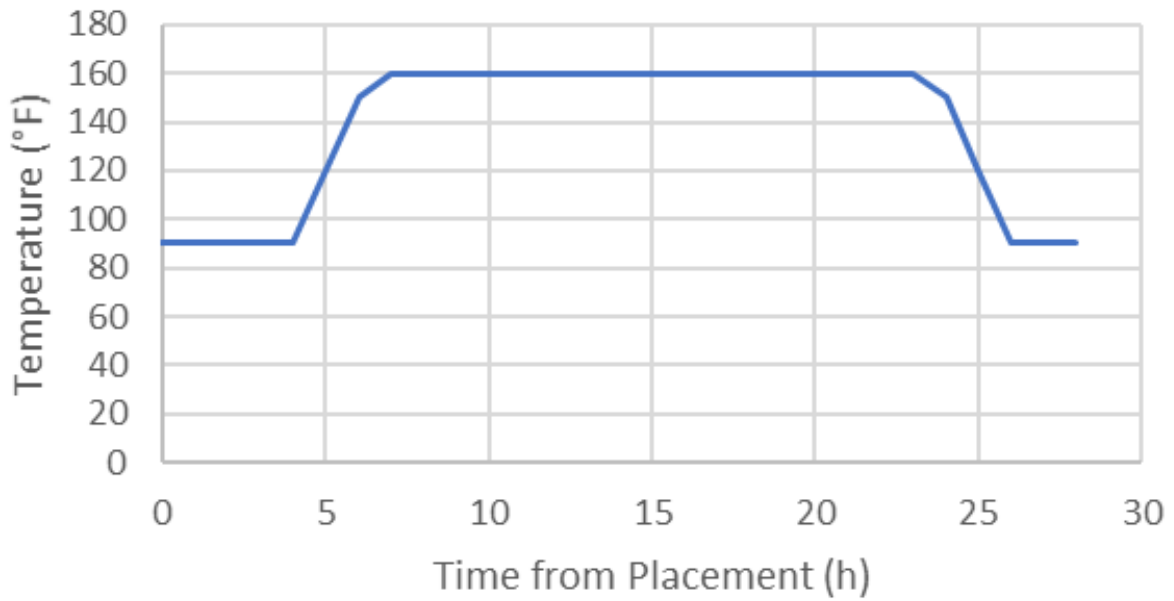Figure 14: Steam curing cycle, maximum temperature = 130°F

Figure 15: Steam curing cycle, maximum temperature = 160°F

The steam curing cycle curves shown in Figure 14 and Figure 15 are also summarized in Table 6.

Table 6: Isothermal heated enclosure: steam curing cycles

Preheating Temperature, °F (°C)	Maximum Steam Curing Cycle Temperature °F (°C)
None	None
70 (21.1)	130 (54.4)
90 (32.2)	160 (71.1)

3.2.2 Dependent Variables

The research team calculated dependent variables that serve as input when running the models in the b4Cast finite element software based on independent variables selected and discussed in section 2.1. These variables were the thermal properties of concrete, the elastic modulus at 28 days of the concrete and the setting time of the concrete. They were a function of the concrete constituent materials and mixture proportions selected.

Coefficient of Thermal Expansion

The coefficient of thermal expansion (CTE) was considered constant with time for the new segment and old match-cast segment in the simulations. The CTE value used for each model run was calculated based on the concrete constituent material CTE and volume in the mixture using Equation 77 [58].

$$\alpha_{concrete} = \frac{\alpha_{ca} \cdot V_{ca} + \alpha_{fa} \cdot V_{fa} + \alpha_p \cdot V_p}{V_{ca} + V_{fa} + V_p} \qquad \text{Equation 77}$$

Where: α_{ca}= coarse aggregate CTE, με/°F (με/°C)

V_{ca}= coarse aggregate volume, ft^3 (m^3)

α_{fa}= fine aggregate CTE, με/°F (με/°C)

V_{fa}= fine aggregate volume, ft^3 (m^3)

α_p= paste CTE, με/°F (με/°C)

V_p= paste volume, ft^3 (m^3)

Values for concrete constituent material coefficient of thermal expansion used in the calculations are summarized in Table 7. These are based on the variations in aggregate type that might be used in the segmental concrete mixtures for bridges in the State.

Table 7: Coefficients of thermal expansion

Item	Coefficient of thermal expansion value, $\mu\varepsilon$/°F ($\mu\varepsilon$/°C)
Porous Limestone (Brooksville)	1.94 (3.5) [58]
Dolomitic (Dense) Limestone	3.89 (7.00) [58]
Siliceous Gravel	6.11 (11.00) [58]
Lightweight Coarse Aggregate[†]	5.10 (9.18) [119]
Siliceous Sand	6.11 (11.00) [58]
Manufactured Sand (Crushed Limestone)	1.94 (3.50) [58]
Cementitious Paste	6.00 (10.8) [58]

[†] Value for concrete made with lightweight aggregate.

Thermal Conductivity

The thermal conductivity of the concrete was considered constant with age in the simulations, and was calculated in a similar manner as the coefficient of thermal expansion, using a weighted average by volume of each component as shown in Equation 78:

$$k_{concrete} = \frac{k_{ca} \cdot V_{ca} + k_{fa} \cdot V_{fa} + k_p \cdot V_p}{V_{ca} + V_{fa} + V_p}$$

Equation 78

Where: k_{ca}= coarse aggregate thermal conductivity, BTU/(ft·hr·°F) (W/(m·°C))

V_{ca}= coarse aggregate volume, ft^3 (m^3)

k_{fa}= fine aggregate thermal conductivity, BTU/(ft·hr·°F) (W/(m·°C))

V_{fa}= fine aggregate volume, ft^3 (m^3)

k_p= paste thermal conductivity, BTU/(ft·hr·°F) (W/(m·°C))

V_p= paste volume, ft^3 (m^3)

Values for constituent material thermal conductivity used in the calculations are summarized in Table 8.

Table 8: Material thermal conductivities

Item	Thermal Conductivity, BTU/(ft·hr·°F) (W/(m·°C))
Porous Limestone (Brooksville)	1.79 (3.1) [118]
Dolomitic (Dense) Limestone	1.90 (3.3) [118]
Siliceous Gravel	2.36 (4.1) [118]
Lightweight Coarse Aggregate[†]	1.08 (1.88) [119]
Siliceous Sand	2.36 (4.1) [118]
Manufactured Sand (Crushed Limestone)	1.79 (3.1) [118]
Cementitious Paste	0.75 (1.3) [118]

[†] Value for concrete made with lightweight aggregate.

Specific Heat

A model that uses a weighted average by weight of material with the values of each component of the concrete [58] was used to calculate the concrete specific heat. Equation 79 shows the equation used for concrete specific heat:

$$c_p = \frac{1}{\rho} \cdot (W_c \cdot \alpha \cdot c_{cef} + W_c \cdot (1 - \alpha) \cdot c_c + W_a \cdot c_a + W_w \cdot c_w) \qquad \text{Equation 79}$$

Where: c_p= specific heat of the concrete mixture, BTU/(lb·°F) (J/(kg·°C))

ρ= unit weight of concrete mixture, lb/ft^3 (kg/m^3)

W_c, W_a, W_w =amount by weight of cement, aggregate, and water, lb/ft^3 (kg/m^3)

c_c, c_a, c_w = specific heats of cement, aggregate, and water, BTU/(lb·°F) (J/(kg·°C))

c_{cef}= fictitious specific heat of the hydrated cement, BTU/(lb·°F) (J/(kg·°C)),

c_{cef}= 8.4· T_c + 339 BTU/(lb·°F) (J/(kg·°C))

α= degree of hydration, 60% is used for the old match-cast segment (24 hours old) and 5% is used for the new segment as the concrete bowing distortion occurs at early ages.

T_c = concrete reference temperature, 73.4°F (23°C)

Values for specific heat of components used in the calculations are summarized in Table 9.

Table 9: Concrete constituent material specific heat

Item	Specific Heat, BTU/(lb·°F) (J/(kg·°C))
Porous Limestone (Brooksville)	0.19 (810) [58]
Dolomitic (Dense) Limestone	0.20 (850) [58]
Siliceous Gravel	0.22 (920) [58]
Lightweight Coarse Aggregate	0.21 (879) [120]
Siliceous Sand	0.22 (920) [58]
Manufactured Sand (Crushed Limestone)	0.19 (810) [58]
Cement	0.38 (1600) [118]

† Value for concrete made with lightweight aggregate.

Concrete Physical and Mechanical Properties

Concrete Density

The concrete density is a term in the heat diffusion equation, therefore it is important to calculate it based on the materials used for each mix. The expression used to calculate the concrete density ρ_{concr} is shown in Equation 80:

$$\rho_{concr} = \sum W_i \qquad \text{Equation 80}$$

Where: W_i= weight of constituent material per cubic yard of concrete

Elastic Modulus at 28 days

An estimation of the elastic modulus of concrete at 28 days for each mix was made using Equation 81 for concrete between 90 and 160 lb/ft³ [40]:

$$E_c = w_c^{1.5} \cdot 33 \sqrt{f'_c} \qquad \text{Equation 81}$$

Where: Ec = modulus of elasticity of concrete, psi (MPa)

                w_c = density of concrete, lb/yd³ (kg/m³)

                f'_c = compressive strength of concrete, psi (MPa)

Match-cast concrete segments are often one day old when used as the form for one side of the newly-cast segment. The elastic modulus in the simulations of the match-cast segments was consequently assumed to be 60% of the 28-day concrete elastic modulus.

Setting Time

The setting time is dependent on the admixtures used for that purpose in the mix. The setting time given as equivalent age are shown in Table 10.

Table 10: Equivalent age at setting when set-control admixtures are used

#	Admixtures	Setting Time (hrs)
1	Type C Accelerating – ASTM C494	3
2	None	5
3	Type D Retarding – ASTM C494	6.5

3.2.3 Simulation Variable Permutations

Material Combinations

Three mixes were developed to provide a variation of heat generated during curing. Cementitious content was increased as fly ash content was decreased to provide higher early quantities of heat compared to lower cementitious content combined with higher fly ash content (Table 11).

Table 11: Mixes by heat generation

	Low Heat Mix	Medium Heat Mix	High Heat Mix
Type of Cement	II	III	III
Total Cementitious Content, lb/yd³ (kg/m³)	650 (385)	750 (445)	950 (563)
Fly Ash Content (%) Repl. by wt.	30	15	0
Silica Fume (%) Repl. by wt.	0	8	0
w/cm	0.37	0.35	0.29

The absolute volume method [121] was used to generate mixes with different aggregate combinations, obtaining different characteristics for the concrete thermal and mechanical properties.

From all the possible aggregate combinations listed in Table 2, 4 combinations were selected to cover a wide range of possible values for thermal properties of concrete produced with them, as shown in Table 12.

Table 12: Thermal properties from aggregate combinations

Combination #	Coarse Aggregate + Fine Aggregate	Concrete Coefficient of thermal expansion value, µε/°F (µε/°C)	Concrete Thermal Conductivity, BTU/(ft·hr·°F) (W/(m·°C))	Thermal Classification
1	Porous Limestone (Brooksville) + Siliceous Sand	4.54 – 4.55 (8.17 – 8.19)	1.502 – 1.608 (2.60 – 2.78)	Medium CTE – Medium Thermal Conductivity
2	Porous Limestone (Brooksville) + Manufactured Sand (Crushed Limestone)	3.12 – 3.40 (5.61 – 6.12)	1.352 – 1.419 (2.34 – 2.46)	Low CTE – Low Thermal Conductivity
3	Siliceous Gravel + Siliceous Sand	6.07 – 6.08 (10.926 – 10.944)	1.705 – 1.810 (2.95 – 3.13)	High CTE – High Thermal Conductivity
4	Lightweight Coarse Aggregate + Siliceous Sand	5.10 (9.18)	1.08 (1.87)	Lightweight Coarse Aggregate

Segment Material and Construction Permutations

The variables presented in section 2.1 and 2.2 were used in different combinations to formulate 160 unique permutations for a parametric study that includes the effects of segment geometry, materials, environment, and construction methods on bowing distortion. Three bridge geometries were selected to represent the range of values found in the literature and in the database received from the FDOT and are used in the majority of permutations: Florida Bridge E (w/L ratio = 4.09), Florida Bridge B (w/L ratio = 5.97) and Florida Bridge C (w/L ratio = 10.89). Twenty-seven permutations, shown in Table 13, were created to vary the heat generation and setting time properties of the concrete mixture used. The aggregate combination selected for these cases was porous limestone and siliceous sand, which result in a medium CTE and medium thermal conductivity concrete, as shown in Table 12. Placement temperature was chosen to be summer – morning placement, (Miami typical temperatures). Also, a typical wind speed of 7.5 mph is selected (medium). No isothermal heated enclosure, or steam curing was taken into account.

Table 13: Heat generation and setting time permutations

#								
#		**Key Characteristics**						
#	**Geometry**	**Heat**	**Setting Time**	**Curing -**	**Aggregate**	**Placement**	**Wind Speed**	**Isothermal**
1	w/L=4.09 (Fl. Bridge E)	Low	Medium	Burlap	Medium CTE - Medium Thermal Cond	Miami Summer - Morning	Medium	None
2	w/L=5.97 (Fl. Bridge B)							
3	w/L=10.89 (Fl. Bridge C)							
4	w/L=4.09 (Fl. Bridge E)	Low	Low	Burlap	Medium CTE - Medium Thermal Cond	Miami Summer - Morning	Medium	None
5	w/L=5.97 (Fl. Bridge B)							
6	w/L=10.89 (Fl. Bridge C)							
7	w/L=4.09 (Fl. Bridge E)	Low	High	Burlap	Medium CTE - Medium Thermal Cond	Miami Summer - Morning	Medium	None
8	w/L=5.97 (Fl. Bridge B)							
9	w/L=10.89 (Fl. Bridge C)							
10	w/L=4.09 (Fl. Bridge E)	Medium	Medium	Burlap	Medium CTE - Medium Thermal Cond	Miami Summer - Morning	Medium	None
11	w/L=5.97 (Fl. Bridge B)							
12	w/L=10.89 (Fl. Bridge C)							
13	w/L=4.09 (Fl. Bridge E)	Medium	Low	Burlap	Medium CTE - Medium Thermal Cond	Miami Summer - Morning	Medium	None
14	w/L=5.97 (Fl. Bridge B)							
15	w/L=10.89 (Fl. Bridge C)							
16	w/L=4.09 (Fl. Bridge E)	Medium	High	Burlap	Medium CTE - Medium Thermal Cond	Miami Summer - Morning	Medium	None
17	w/L=5.97 (Fl. Bridge B)							
18	w/L=10.89 (Fl. Bridge C)							
19	w/L=4.09 (Fl. Bridge E)	High	Medium	Burlap	Medium CTE - Medium Thermal Cond	Miami Summer - Morning	Medium	None
20	w/L=5.97 (Fl. Bridge B)							
21	w/L=10.89 (Fl. Bridge C)							
22	w/L=4.09 (Fl. Bridge E)	High	Low	Burlap	Medium CTE - Medium Thermal Cond	Miami Summer - Morning	Medium	None
23	w/L=5.97 (Fl. Bridge B)							
24	w/L=10.89 (Fl. Bridge C)							
25	w/L=4.09 (Fl. Bridge E)	High	High	Burlap	Medium CTE - Medium Thermal Cond	Miami Summer - Morning	Medium	None
26	w/L=5.97 (Fl. Bridge B)							
27	w/L=10.89 (Fl. Bridge C)							

Nine high setting time combinations were chosen to model with white burlap polyethylene (tarps) to determine the effects of insulation on the bowing distortion calculated, as shown in Table 14. Nine additional combinations shown in Table 15 were selected to simulate the effects of changing the aggregate combination used in the mix to the high CTE mixture. Nine additional cases were generated to examine the effects of switching the aggregate combination to the low CTE Porous Limestone and Manufactured Sand blend shown in Table 16.

Table 14: White burlap polyethylene insulation permutations

#	Geometry	Key Characteristics						
#	Geometry	Heat	Setting Time	Curing - Insulation	Aggregate	Placement Temp	Wind Speed	Isothermal Heated Enclosure
28	w/L=4.09 (Fl. Bridge E)	Low	High	White burlap polyethylene	Medium CTE - Medium Thermal Cond	Miami Summer - Morning	Medium	None
29	w/L=5.97 (Fl. Bridge B)							
30	w/L=10.89 (Fl. Bridge C)							
31	w/L=4.09 (Fl. Bridge E)	Medium	High	White burlap polyethylene	Medium CTE - Medium Thermal Cond	Miami Summer - Morning	Medium	None
32	w/L=5.97 (Fl. Bridge B)							
33	w/L=10.89 (Fl. Bridge C)							
34	w/L=4.09 (Fl. Bridge E)	High	High	White burlap polyethylene	Medium CTE - Medium Thermal Cond	Miami Summer - Morning	Medium	None
35	w/L=5.97 (Fl. Bridge B)							
36	w/L=10.89 (Fl. Bridge C)							

Table 15: High coefficient of thermal expansion mixtures

#	Geometry	Key Characteristics						
#	Geometry	Heat	Setting Time	Curing - Insulation	Aggregate	Placement Temp	Wind Speed	Isothermal Heated Enclosure
37	w/L=4.09 (Fl. Bridge E)	Low	High	Burlap	High CTE - High Thermal Cond	Miami Summer - Morning	Medium	None
38	w/L=5.97 (Fl. Bridge B)							
39	w/L=10.89 (Fl. Bridge C)							
40	w/L=4.09 (Fl. Bridge E)	Medium	High	Burlap	High CTE - High Thermal Cond	Miami Summer - Morning	Medium	None
41	w/L=5.97 (Fl. Bridge B)							
42	w/L=10.89 (Fl. Bridge C)							
43	w/L=4.09 (Fl. Bridge E)	High	High	Burlap	High CTE - High Thermal Cond	Miami Summer - Morning	Medium	None
44	w/L=5.97 (Fl. Bridge B)							
45	w/L=10.89 (Fl. Bridge C)							

Table 16: Low coefficient of thermal expansion mixtures

#	Geometry	Key Characteristics						
#	Geometry	Heat	Setting Time	Curing - Insulation	Aggregate	Placement Temp	Wind Speed	Isothermal Heated Enclosure
46	w/L=4.09 (Fl. Bridge E)	Low	High	Burlap	Low CTE – Low Thermal Cond	Miami Summer - Morning	Medium	None
47	w/L=5.97 (Fl. Bridge B)							
48	w/L=10.89 (Fl. Bridge C)							
49	w/L=4.09 (Fl. Bridge E)	Medium	High	Burlap	Low CTE – Low Thermal Cond	Miami Summer - Morning	Medium	None
50	w/L=5.97 (Fl. Bridge B)							
51	w/L=10.89 (Fl. Bridge C)							
52	w/L=4.09 (Fl. Bridge E)	High	High	Burlap	Low CTE – Low Thermal Cond	Miami Summer - Morning	Medium	None
53	w/L=5.97 (Fl. Bridge B)							
54	w/L=10.89 (Fl. Bridge C)							

Nine simulation permutations were generated to determine the effects of switching concrete placement time to a summer night placement as shown in Table 17, while nine simulation combinations were generated to determine the effects of switching the concrete placement to a winter morning placement in Tallahassee, as shown in Table 18.

Table 17: Summer nighttime placement permutations

#	Geometry	Key Characteristics						
#	Geometry	Heat	Setting Time	Curing - Insulation	Aggregate	Placement Temp	Wind Speed	Isothermal Heated Enclosure
55	w/L=4.09 (Fl. Bridge E)	Low	High	Burlap	Medium CTE - Medium Thermal Cond	Miami Summer - Night	Medium	None
56	w/L=5.97 (Fl. Bridge B)							
57	w/L=10.89 (Fl. Bridge C)							
58	w/L=4.09 (Fl. Bridge E)	Medium	High	Burlap	Medium CTE - Medium Thermal Cond	Miami Summer - Night	Medium	None
59	w/L=5.97 (Fl. Bridge B)							
60	w/L=10.89 (Fl. Bridge C)							
61	w/L=4.09 (Fl. Bridge E)	High	High	Burlap	Medium CTE - Medium Thermal Cond	Miami Summer - Night	Medium	None
62	w/L=5.97 (Fl. Bridge B)							
63	w/L=10.89 (Fl. Bridge C)							

Table 18: Winter morning placement permutations

#	Geometry	Key Characteristics						
#	Geometry	Heat	Setting Time	Curing - Insulation	Aggregate	Placement Temp	Wind Speed	Isothermal Heated Enclosure
64	w/L=4.09 (Fl. Bridge E)				Medium CTE - Medium Thermal Cond	Tallahassee Winter - Morning	Medium	None
65	w/L=5.97 (Fl. Bridge B)	Low	High	Burlap				
66	w/L=10.89 (Fl. Bridge C)							
67	w/L=4.09 (Fl. Bridge E)				Medium CTE - Medium Thermal Cond	Tallahassee Winter - Morning	Medium	None
68	w/L=5.97 (Fl. Bridge B)	Medium	High	Burlap				
69	w/L=10.89 (Fl. Bridge C)							
70	w/L=4.09 (Fl. Bridge E)				Medium CTE - Medium Thermal Cond	Tallahassee Winter - Morning	Medium	None
71	w/L=5.97 (Fl. Bridge B)	High	High	Burlap				
72	w/L=10.89 (Fl. Bridge C)							

The effects of wind speed were investigated by changing the wind speed to low (Table 19) and high (Table 20). Simulations were performed to determine any mitigating effects of using an isothermal heated enclosure at 130°F (Table 21) and 160°F (Table 22).

Table 19: Low wind speed permutations

#	Geometry	Key Characteristics						
#	Geometry	Heat	Setting Time	Curing - Insulation	Aggregate	Placement Temp	Wind Speed	Isothermal Heated Enclosure
73	w/L=4.09 (Fl. Bridge E)				Medium CTE - Medium Thermal Cond	Miami Summer - Morning	Low	None
74	w/L=5.97 (Fl. Bridge B)	Low	High	Burlap				
75	w/L=10.89 (Fl. Bridge C)							
76	w/L=4.09 (Fl. Bridge E)				Medium CTE - Medium Thermal Cond	Miami Summer - Morning	Low	None
77	w/L=5.97 (Fl. Bridge B)	Medium	High	Burlap				
78	w/L=10.89 (Fl. Bridge C)							
79	w/L=4.09 (Fl. Bridge E)				Medium CTE - Medium Thermal Cond	Miami Summer - Morning	Low	None
80	w/L=5.97 (Fl. Bridge B)	High	High	Burlap				
81	w/L=10.89 (Fl. Bridge C)							

Table 20: High wind speed permutations

#	Geometry	Key Characteristics						
#	Geometry	Heat	Setting Time	Curing - Insulation	Aggregate	Placement Temp	Wind Speed	Isothermal Heated Enclosure
82	w/L=4.09 (Fl. Bridge E)				Medium CTE - Medium Thermal Cond	Miami Summer - Morning		
83	w/L=5.97 (Fl. Bridge B)	Low	High	Burlap	Medium CTE - Medium Thermal Cond	Miami Summer - Morning	High	None
84	w/L=10.89 (Fl. Bridge C)							
85	w/L=4.09 (Fl. Bridge E)				Medium CTE - Medium Thermal Cond	Miami Summer - Morning		
86	w/L=5.97 (Fl. Bridge B)	Medium	High	Burlap	Medium CTE - Medium Thermal Cond	Miami Summer - Morning	High	None
87	w/L=10.89 (Fl. Bridge C)							
88	w/L=4.09 (Fl. Bridge E)				Medium CTE - Medium Thermal Cond	Miami Summer - Morning		
89	w/L=5.97 (Fl. Bridge B)	High	High	Burlap	Medium CTE - Medium Thermal Cond	Miami Summer - Morning	High	None
90	w/L=10.89 (Fl. Bridge C)							

Table 21: Simulation permutations with isothermal heated enclosure at 130°F

#	Geometry	Key Characteristics						
#	Geometry	Heat	Setting Time	Curing - Insulation	Aggregate	Placement Temp	Wind Speed	Isothermal Heated Enclosure
91	w/L=4.09 (Fl. Bridge E)				Medium CTE - Medium Thermal Cond			
92	w/L=5.97 (Fl. Bridge B)	Low	High	Burlap	Medium CTE - Medium Thermal Cond	N/A	N/A	130°F
93	w/L=10.89 (Fl. Bridge C)							
94	w/L=4.09 (Fl. Bridge E)				Medium CTE - Medium Thermal Cond			
95	w/L=5.97 (Fl. Bridge B)	Medium	High	Burlap	Medium CTE - Medium Thermal Cond	N/A	N/A	130°F
96	w/L=10.89 (Fl. Bridge C)							
97	w/L=4.09 (Fl. Bridge E)				Medium CTE - Medium Thermal Cond			
98	w/L=5.97 (Fl. Bridge B)	High	High	Burlap	Medium CTE - Medium Thermal Cond	N/A	N/A	130°F
99	w/L=10.89 (Fl. Bridge C)							

Table 22: Simulation permutations with isothermal heated enclosure at 160°F

#	Geometry	Key Characteristics						
#	Geometry	Heat	Setting Time	Curing - Insulation	Aggregate	Placement Temp	Wind Speed	Isothermal Heated Enclosure
100	w/L=4.09 (Fl. Bridge E)				Medium CTE - Medium Thermal Cond			
101	w/L=5.97 (Fl. Bridge B)	Low	High	Burlap	Medium CTE - Medium Thermal Cond	N/A	N/A	160°F
102	w/L=10.89 (Fl. Bridge C)				Medium CTE - Medium Thermal Cond			
103	w/L=4.09 (Fl. Bridge E)				Medium CTE - Medium Thermal Cond			
104	w/L=5.97 (Fl. Bridge B)	Medium	High	Burlap	Medium CTE - Medium Thermal Cond	N/A	N/A	160°F
105	w/L=10.89 (Fl. Bridge C)				Medium CTE - Medium Thermal Cond			
106	w/L=4.09 (Fl. Bridge E)				Medium CTE - Medium Thermal Cond			
107	w/L=5.97 (Fl. Bridge B)	High	High	Burlap	Medium CTE - Medium Thermal Cond	N/A	N/A	160°F
108	w/L=10.89 (Fl. Bridge C)				Medium CTE - Medium Thermal Cond			

The high heat generation and high setting time mix from the base case was chosen and was applied to the four additional bridge segment geometries in the test matrix as shown in Table 23: Florida Bridge A (w/L = 2.15), Florida Bridge F (w/L=5.97) and Florida Bridge D (w/L=9,39). Although it is not necessarily representative of Florida segmental bridges, the Bang Na Bridge was included to observe the effects of a really high w/L ratio value (w/L = 21.80). Additional permutations with these segment geometries were simulated with white burlap polyethylene (tarps), as shown in Table 24. Additional permutations were created to check the effect of switching to a high CTE (Table 25) and low CTE (Table 26) aggregate combination with additional geometries. The effects of switching to a summer night placement (Table 27) and winter night placement (Table 28) were also be simulated. Table 29 and Table 30 show simulation combinations designed to study the effects of low and high wind speeds, respectively. Simulations with an isothermal heated enclosure at 130°F (Table 31) and 160°F (Table 32) were used to determine mitigation method benefits.

Table 23: Additional simulation permutations that examine segment geometry

#	Geometry	Key Characteristics						
#	Geometry	Heat	Setting Time	Curing - Insulation	Aggregate	Placement Temp	Wind Speed	Isothermal Heated Enclosure
109	w/L=2.15 (Fl. Bridge A)	High	High	Burlap	Medium CTE - Medium Thermal Cond	Miami Summer - Morning	Medium	None
110	w/L=5.97 (Fl. Bridge F)							
111	w/L=9.39 (Fl. Bridge D)							
112	w/L= 21.80 (Bang Na Pier)							

Table 24: Simulation permutations that examine segment geometry and insulation

#	Geometry	Key Characteristics						
#	Geometry	Heat	Setting Time	Curing - Insulation	Aggregate	Placement Temp	Wind Speed	Isothermal Heated Enclosure
113	w/L=2.15 (Fl. Bridge A)	High	High	White Burlap Polyethylene	Medium CTE - Medium Thermal Cond	Miami Summer - Morning	Medium	None
114	w/L=5.97 (Fl. Bridge F)							
115	w/L=9.39 (Fl. Bridge D)							
116	w/L= 21.80 (Bang Na Pier)							

Table 25: Simulation permutations that examine segment geometry and high aggregate CTE

#	Geometry	Key Characteristics						
#	Geometry	Heat	Setting Time	Curing - Insulation	Aggregate	Placement Temp	Wind Speed	Isothermal Heated Enclosure
117	w/L=2.15 (Fl. Bridge A)	High	High	Burlap	High CTE - High Thermal Cond	Miami Summer - Morning	Medium	None
118	w/L=5.97 (Fl. Bridge F)							
119	w/L=9.39 (Fl. Bridge D)							
120	w/L= 21.80 (Bang Na Pier)							

Table 26: Simulation permutations that examine segment geometry and low aggregate CTE

#	Geometry	Key Characteristics						
#	Geometry	Heat	Setting Time	Curing - Insulation	Aggregate	Placement Temp	Wind Speed	Isothermal Heated Enclosure
121	w/L=2.15 (Fl. Bridge A)	High	High	Burlap	Low CTE - Low Thermal Cond	Miami Summer - Morning	Medium	None
122	w/L=5.97 (Fl. Bridge F)							
123	w/L=9.39 (Fl. Bridge D)							
124	w/L= 21.80 (Bang Na Pier)							

Table 27: Simulation permutations that examine segment geometry and summer night concrete placement

#	Geometry	Key Characteristics						
#	Geometry	Heat	Setting Time	Curing - Insulation	Aggregate	Placement Temp	Wind Speed	Isothermal Heated Enclosure
125	w/L=2.15 (Fl. Bridge A)	High	High	Burlap	Medium CTE - Medium Thermal Cond	Miami Summer - Night	Medium	None
126	w/L=5.97 (Fl. Bridge F)							
127	w/L=9.39 (Fl. Bridge D)							
128	w/L= 21.80 (Bang Na Pier)							

Table 28: Simulation permutations that examine segment geometry and winter night concrete placement

#	Geometry	Key Characteristics						
#	Geometry	Heat	Setting Time	Curing - Insulation	Aggregate	Placement Temp	Wind Speed	Isothermal Heated Enclosure
129	w/L=2.15 (Fl. Bridge A)	High	High	Burlap	Medium CTE - Medium Thermal Cond	Tallahassee Winter - Night	Medium	None
130	w/L=5.97 (Fl. Bridge F)							
131	w/L=9.39 (Fl. Bridge D)							
132	w/L= 21.80 (Bang Na Pier)							

Table 29: Simulation permutations that examine segment geometry and low wind speed

#	Geometry	Key Characteristics						
#	Geometry	Heat	Setting Time	Curing - Insulation	Aggregate	Placement Temp	Wind Speed	Isothermal Heated Enclosure
133	w/L=2.15 (Fl. Bridge A)	High	High	Burlap	Medium CTE - Medium Thermal Cond	Miami Summer - Morning	Low	None
134	w/L=5.97 (Fl. Bridge F)							
135	w/L=9.39 (Fl. Bridge D)							
136	w/L= 21.80 (Bang Na Pier)							

Table 30: Simulation permutations that examine segment geometry and high wind speed

#	Geometry	Key Characteristics						
#	Geometry	Heat	Setting Time	Curing - Insulation	Aggregate	Placement Temp	Wind Speed	Isothermal Heated Enclosure
137	w/L=2.15 (Fl. Bridge A)	High	High	Burlap	Medium CTE - Medium Thermal Cond	Miami Summer - Morning	High	None
138	w/L=5.97 (Fl. Bridge F)							
139	w/L=9.39 (Fl. Bridge D)							
140	w/L= 21.80 (Bang Na Pier)							

Table 31: Simulation permutations that examine segment geometry and an isothermal heated enclosure at 130°F

#	Geometry	Key Characteristics						
#	Geometry	Heat	Setting Time	Curing - Insulation	Aggregate	Placement Temp	Wind Speed	Isothermal Heated Enclosure
141	w/L=2.15 (Fl. Bridge A)	High	High	Burlap	Medium CTE - Medium Thermal Cond	Miami Summer - Morning	Medium	130 °F
142	w/L=5.97 (Fl. Bridge F)							
143	w/L=9.39 (Fl. Bridge D)							
144	w/L= 21.80 (Bang Na Pier)							

Table 32: Simulation permutations that examine segment geometry and an isothermal heated enclosure at 160°F

#	Geometry	Key Characteristics						
#	Geometry	Heat	Setting Time	Curing - Insulation	Aggregate	Placement Temp	Wind Speed	Isothermal Heated Enclosure
145	w/L=2.15 (Fl. Bridge A)	High	High	Burlap	Medium CTE - Medium Thermal Cond	Miami Summer - Morning	Medium	160 °F
146	w/L=5.97 (Fl. Bridge F)							
147	w/L=9.39 (Fl. Bridge D)							
148	w/L= 21.80 (Bang Na Pier)							

The effects of lightweight aggregates on concrete segment distortion during curing was simulated, as shown in Table 33.

Table 33: Lightweight coarse aggregate simulation permutations

#	Geometry	Key Characteristics						
#	Geometry	Heat	Setting Time	Curing - Insulation	Aggregate	Placement Temp	Wind Speed	Isothermal Heated Enclosure
149	w/L=4.09 (Fl. Bridge E)	Low	High	Burlap	Lightweight Coarse Aggregate + Siliceous Sand	Miami Summer - Morning	Medium	None
150	w/L=5.97 (Fl. Bridge B)							
151	w/L=10.89 (Fl. Bridge C)							
152	w/L=4.09 (Fl. Bridge E)	Medium	High	Burlap	Lightweight Coarse Aggregate + Siliceous Sand	Miami Summer - Morning	Medium	None
153	w/L=5.97 (Fl. Bridge B)							
154	w/L=10.89 (Fl. Bridge C)							
155	w/L=4.09 (Fl. Bridge E)	High	High	Burlap	Lightweight Coarse Aggregate + Siliceous Sand	Miami Summer - Morning	Medium	None
156	w/L=5.97 (Fl. Bridge B)							
157	w/L=10.89 (Fl. Bridge C)							

3.3 Summary

A simulation matrix was created to serve as an input for a parametric study of the short line match-cast segmental construction method using finite element analysis simulations; the objective is to quantify bowing distortions generated as a result of thermal and mechanical interactions between the segments. Independent and dependent variables of the matrix were established and discussed. The independent variables were established taking into account common geometries, materials, environmental conditions and construction practices in Florida for the simulations to represent the issue in Florida applicable settings. Dependent variables needed for the creation of finite element models were calculated. These variables included the thermal properties of the produced concrete such as the coefficient of thermal expansion, thermal conductivity, and specific heat. The dependent variables also included physical-mechanical properties such as elastic modulus at 28 days and the setting time of the concrete.

From the options established in the independent variables, 160 permutations were generated with the objective of exploring the impact of varying a particular independent variable in the bowing distortion issue in segments. Three different levels of heat generation, along with three different levels of thermal expansion and thermal conductivity caused by selection of aggregates were selected. Varying ambient conditions, and different curing and insulation techniques for various common Florida segmental bridge geometries were also taken into account for the simulation matrix permutations.

4 Sensitivity Analysis

4.1 Introduction

Precast segmental bridge construction has gained importance as a method to construct bridges due to its economic and logistic advantages: it can be adapted to numerous site conditions [104]. Precast segments are fabricated using a process called match-casting where a segment is cast against a previously-cast segment called the match-cast segment. The segments are cast in the order they are going to be positioned in the bridge, ensuring that they fit together when they are assembled in the structure [5], [104]. While the fabrication of the precast segments can be performed by the short line match-casting method or the long line match-casting method [5], the short line match-casting method is generally preferred [3] because of lower space requirements. In the short line match-casting method, a construction issue caused by bowing distortion of the match-cast segment when the newly cast segment is being fabricated has been documented and studied [1], [3], [104], [122]. When this happens, the new segment conforms to the deformed shape as it hardens, locking in the bowed shape. The match-cast segment returns to its original shape after it cools down [1]. This problem has caused construction issues in the past as the segments are erected and could cause structural issues [1], [3]. This research project seeks to develop best practices for the short line match-casting method applied to Florida conditions by modelling the casting process using finite element analysis to simulate the deformation during concrete member fabrication.

The software b4cast was used to model the short line match-casting method. b4cast is a finite element software package that can calculate temperatures developed in concrete members as they cure, as well as temperatures generated in other concrete members in contact with them. b4cast is also able to calculate thermal strains and stresses in concrete members as a result of the calculated concrete temperatures with time [105].

A simulation matrix developed in Task 2 provided 157 different simulation cases for segments fabricated using the short line match-cast construction method. The cases were modelled in b4cast in order to check the sensitivity of bowing distortion to changes in relevant variables during segment fabrication. A validation model compared to measured results from the San Antonio "Y" project is presented. Details of the modelling approach used and the results are given.

4.2 Finite Element Model Simulation Validation

A three-dimensional finite element model (FEM) shown in Figure 16 was developed to represent the conditions from the type III San Antonio "Y" segment. Segment temperatures developed and bowing distortion measured in the field were compared to the results obtained from the finite element model.
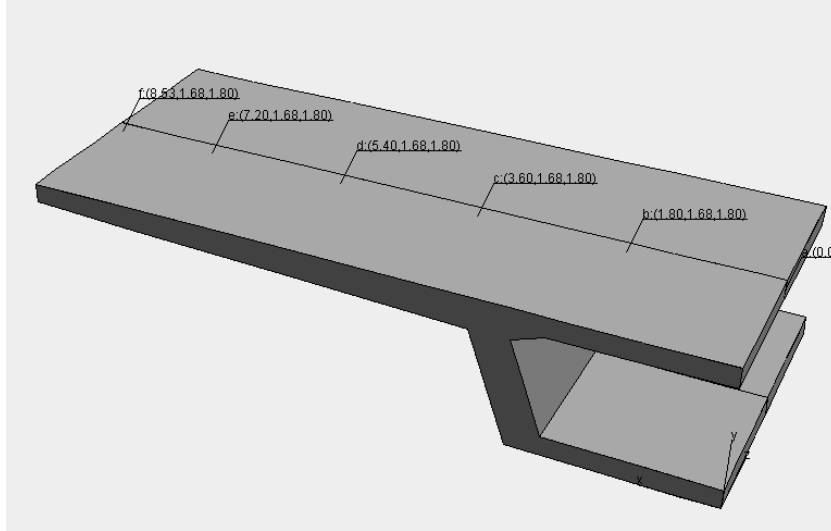
Figure 16: San Antonio "Y" model – type III segments – half symmetry view

4.2.1 San Antonio Project Description

The San Antonio "Y" Project was a six-phase construction project executed in Texas with the contract spanning from 1984 (start of construction) to 1990 (end of construction) [1]. The project took its name from the shape that the construction takes at the intersection of Interstate Highways 35 and 10 in the San Antonio area [1]. The San Antonio "Y" was made up of precast segmental box girder bridges for the elevated portions, using the "span-by-span" technique, with epoxy joints and a combination of external and internal tendons for post-tensioning [1].

Bowing distortion issues (i.e., formation of gaps between segments) were noticed in the second phase of the project during erection operations. Gaps caused by bowing were found to be difficult to close with the temporary post-tensioning, they were also very visible and also reduced the closure pour sizes for several spans [1]. Due to these issues, during the sixth and final stage of construction, field measurements were made [1], [122] to measure segment temperatures and deformations to prevent similar problems in the future. Results from this research were reported by Roberts et al. in [1], [122].

Four pairs of segments were instrumented to measure temperatures in both segments (newly-cast and match-cast) and deformations in the match-cast segment. Two pairs were type III segments, and two pairs were type I segments. The simplified half-symmetry geometry for the type III segment can be seen in Figure 17.
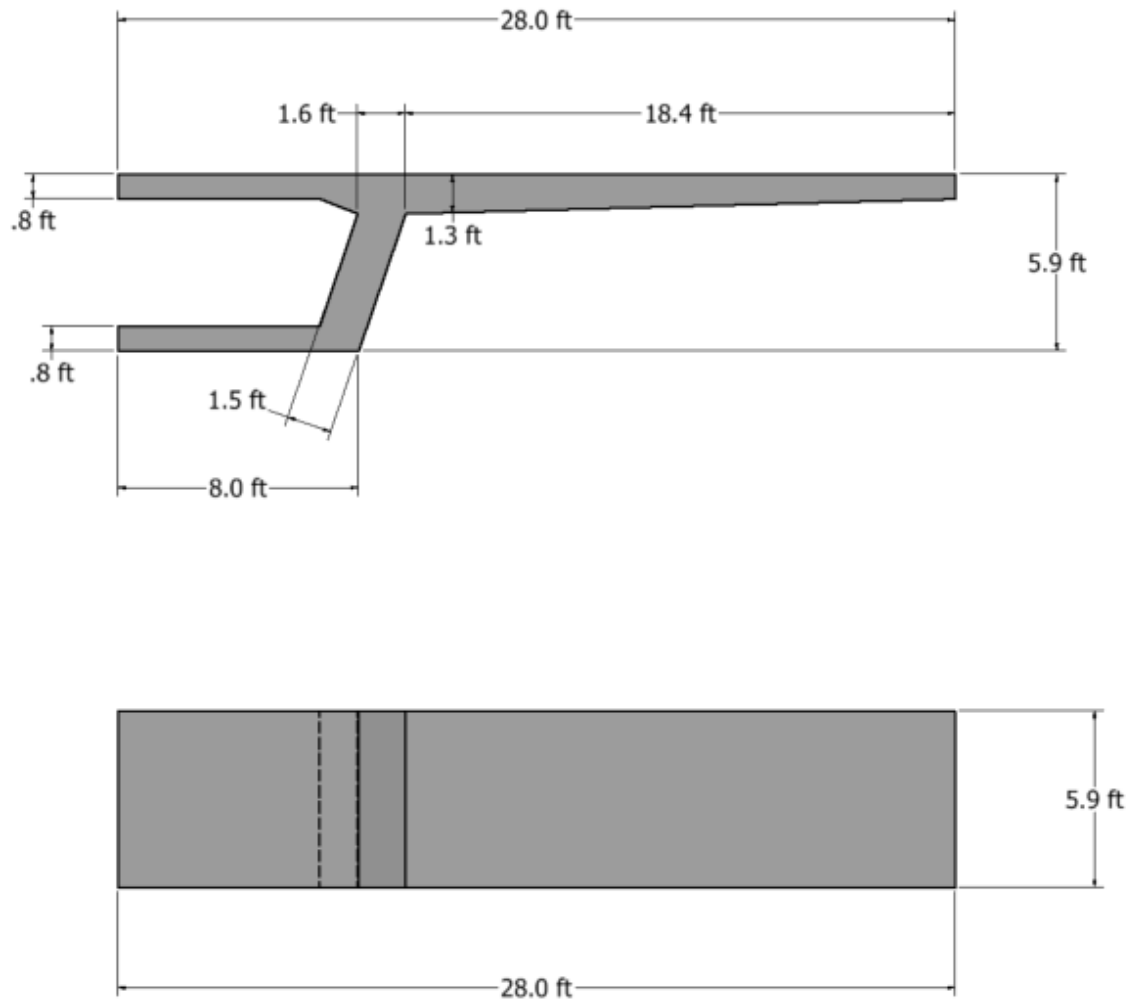
Figure 17: San Antonio "Y" model type III segment dimensions – half symmetry view

Detailed concrete temperature and deformation data for one of the studied type III segment pairs were provided in the project report by Roberts et al. [4]. Data from that segment were used to validate the simulation methodology.

4.2.2   Descriptions of Instrumentation and Measurements From San Antonio "Y" Project

For each pair of segments, two lines of eight thermocouples were installed to measure internal temperatures after placement of the concrete in the new segment [1]. One line was placed through the wing and the other line was placed through the top slab-web-wing juncture for all the studied segments [1]. The thermocouple installation locations for the type III segments are presented in Figure 18.
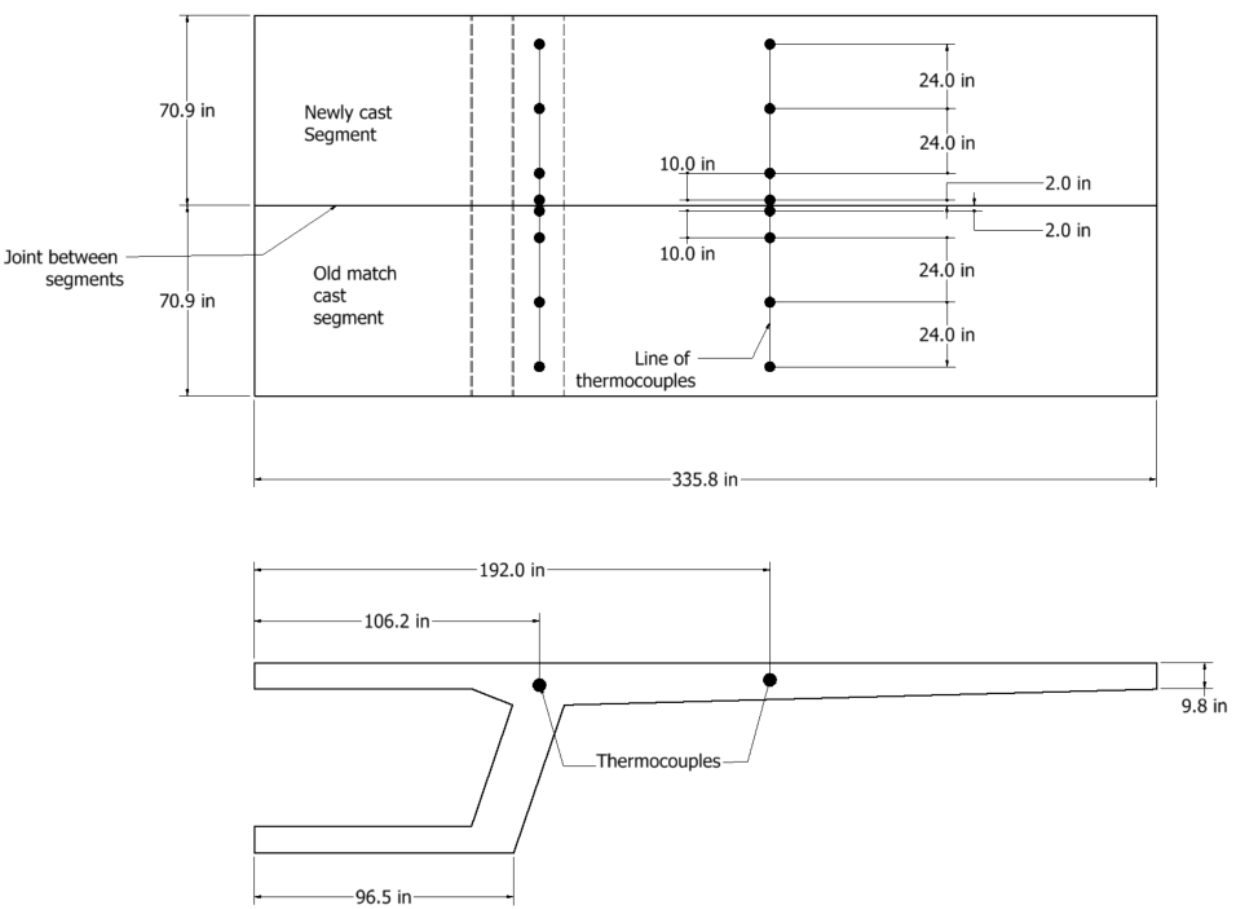
Figure 18: Thermocouple location for San Antonio "Y" segment type III. Adapted from Abendeh and Roberts et al. [1], [3], [122]

The deformation measurement system consisted of a taut piano wire passing about 1.5 in. above precision rulers embedded in the top slab of the match-cast segment, and close to the face in contact with the newly cast segment [1]. Presented results for the thermocouples located at the wing of one of the pairs of the type III segment are presented in Figure 19. Results for deformations recorded for one of the type III match-cast segments studied are presented in Figure 20.
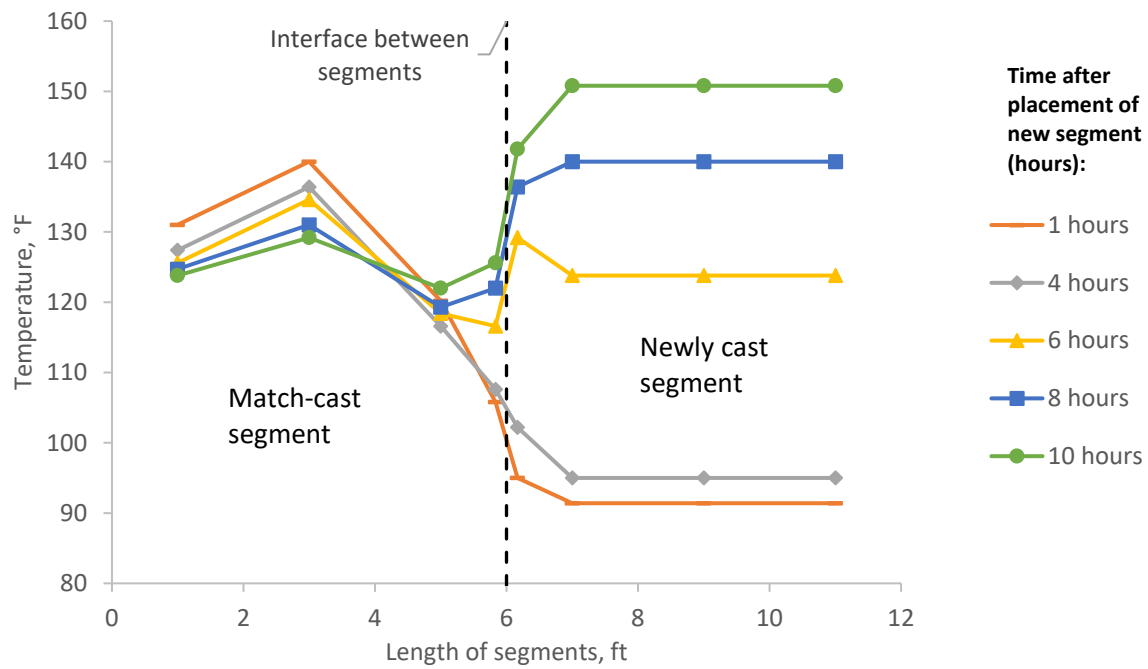
Figure 19: Concrete temperature results adapted after Roberts et al. [1], [122]
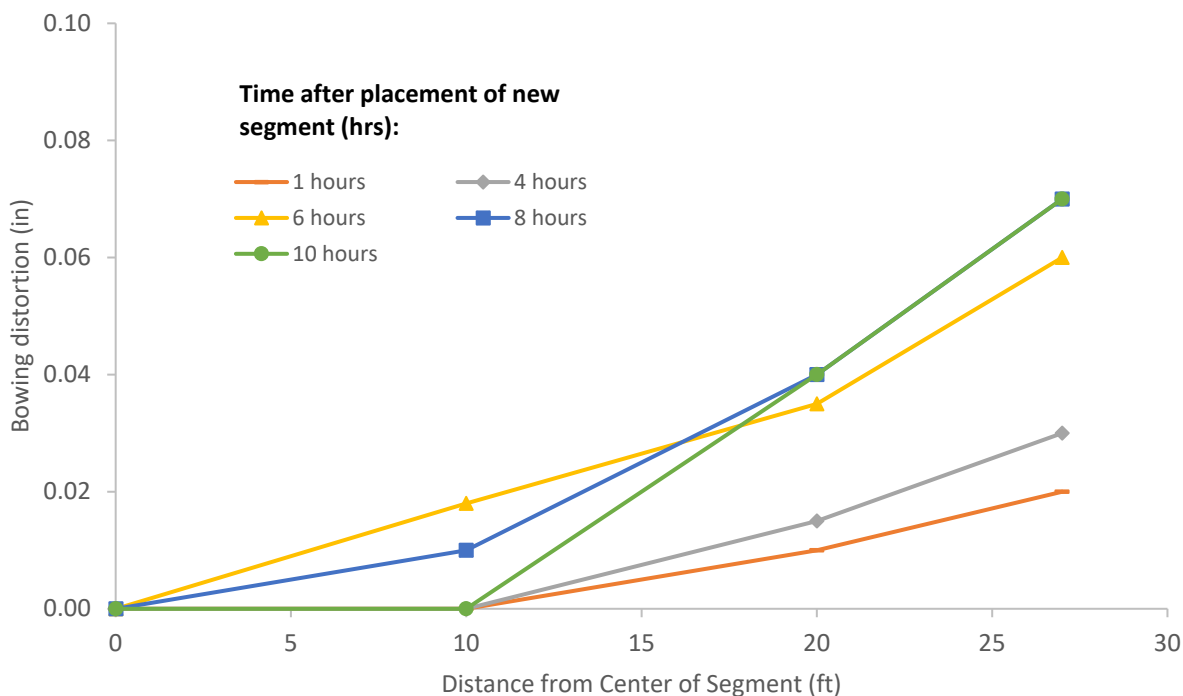
Figure 20: Deformation (bowing distortion) of match-cast segment adapted after Roberts et al. [1, 122]

4.2.3   Input Parameters for Finite Element Validation

In the validation finite element simulations, placement of the first segment was modelled and allowed to cure for 24 hrs, then placement of the second segment was modelled against the first one and allowed to cure for 24 hrs after placement, totaling 48 hrs. Bowing distortion is greatly dependent on the temperature profile of the match-cast segment [3]. This made it necessary to simulate the match-cast concrete temperatures in order to well approximate the temperature profile at the time the new concrete is placed. A period of 24 hours is a common time frame between placement of segments in the short line match-casting process and was used in this study to model the match-cast concrete temperature.

Material parameters, thermal boundary conditions, appropriate mechanical boundary conditions and mesh parameters were defined to represent the conditions in the San Antonio project. Table 34 summarizes the input parameters used.

Table 34: Concrete member modeling parameters and coefficients used to simulate the San Antonio "Y" segment bowing distortion

Model details			
Max. Mesh Size		3.15	in
Time Step		1	hrs
Placement Temperature		89.6	°F
Match-Cast Segment Time of Simulation at Casting		0	hrs
New Segment Time of Simulation at Casting		24	hrs
Concrete Properties			
Cement Content		522.59	lb/yd^3
Activation Energy, E_a		37.91	BTU/mol
Heat of Hydration Parameters			
Total Heat Development, $Q_{ult} = \alpha_u \cdot H_u$		150.80	BTU/lb
Time Parameter, τ		12.00	hrs
Curvature Parameter, β		1.57	
Concrete Density		3944.707	lb/yd^3
Concrete Specific Heat		0.27	BTU/(lb·°F)
Concrete Thermal Conductivity		1.605	BTU/(ft·h·°F)
Match-Cast Segment Elastic Modulus Dev. Parameters			
Final Value		4931.28	ksi
Time Parameter		12.420	hrs
Curvature Parameter		1.068	
New Segment Elastic Modulus Dev. Parameters			
Final Value		14.50	ksi
Time Parameter		n/a	hrs
Curvature Parameter		n/a	
Poisson Ratio		0.17	
Coefficient of Thermal Expansion		6.67	μɛ/°F
Thermal Boundary Conditions (Applied to Appropriate Faces)			
Ambient Temp	San Antonio temp curve		
Wind	No wind	0.00	mph
Formwork	Wooden formwork	0.08	BTU/(ft·h·°F)
	Thickness	0.827	in
Curing	Plastic	0.03	BTU/(ft·h·°F)
	Thickness	0.31	in

Validation Model Material Parameters

The concrete temperature at time of placement was assumed to be 89.6 °F (32 °C) based on the temperature measurements presented in [1].

The cement content was selected as 522.59 lb/yd^3 [122].

The activation energy value, E_a, was selected as 37.91 BTU/mol. The activation energy value is a parameter that depends on the chemistry of the cement used. Type III cement was assumed to be used, and for these cements values range from 28.434 BTU/mol (30000 J/mol) to 37.913

BTU/mol (40000 J/mol) according to a database seen in [56]. The Arrhenius equivalent age expression which uses the activation energy value was used to calculate the maturity of concrete at each time step for the software simulation.

The total heat development value, *Qult*, was selected as 150.8 BTU/lb (350 kJ/kg). In b4cast this value is the product of the total heat available for reaction, H_u, and the ultimate degree of hydration parameter, α_u of the cement used [123]. For type III cements the product of these variable ranges from 300 to 320 kJ/kg [56]. This is dependent on the chemistry of the cement however, so a value of 350 kJ/kg was found appropriate.

The time heat of hydration parameter, τ, was selected as 12 hours.

The curvature heat of hydration parameter, β, was selected as 1.57.

The thermal conductivity value was selected as 1.605 BTU/(ft·hr·°F) [118].

The density value was assumed to be 3945 lb/yd³. This value was taken from Abendeh [3], and it is in line with typical unit weight/density values for normal-weight concrete [124].

The specific heat value was assumed as 0.27 BTU/(lb·°F). This value was taken from Abendeh [3], and it is within the range of typical specific heat values for concrete [118].

The value of elastic modulus at 28 days (final value) for the match-cast segment was selected as 4931 ksi. This value was taken from Abendeh [3], and it is within typical elastic modulus value for concrete [124].

The time elastic modulus development parameter value for the match-cast segment was selected as 12.42 hrs. In b4cast, the development of the elastic modulus is a function of maturity, using a three-parameter exponential expression with the same form as the adiabatic heat of hydration expression that also includes a time and a curvature development parameter. The time parameter was calibrated using a nonlinear regression of maturity and elastic modulus data tested at Auburn University [125].

The curvature elastic modulus development parameter value for the match-cast segment was selected as 1.068. The curvature parameter was calibrated using a nonlinear regression of maturity and elastic modulus data tested at Auburn University [125].

The value of elastic modulus at 28 days (final value) for the new segment was selected to be a constant equal to 14.5 ksi for the time that the new segment is in the simulation. The setting of the concrete of the new segment was not modelled. Instead, the newly cast segment was idealized as a fluid for the time 24 hours to 42 hours in the simulation, free to move with the deformation (bowing distortion) that the match-cast segment acquires as a result of the thermal effects. This idealization was similar to the simulation approach for the bowing distortion adopted in [3].

The Poisson ratio value was selected to be 0.17 for both segments [118].

The coefficient of thermal expansion (CTE) value was selected as 6.67µε/°F for both segments. This value was taken from Abendeh [3], and it is within the range of typical coefficient of thermal expansion values for concrete [118].

Thermal Boundary Conditions

The ambient temperature curve was assigned to all the faces of the segments. No specific information for the time of the year when the segments were fabricated was found, so it was assumed that the fabrication of the segments was during summer time between 1990 and 1992 because the construction of the phase where the studied validation segments belonged started in 1990 and the publication of the results was in 1993 [1]. It was indicated that the placement of concrete for the newly cast segment was finished at 11:00 am [1]. Historical ambient temperature data from San Antonio was revised [126], [127] and a 100 °F ambient temperature for day-time in San Antonio was found suitable for the model. It was also assumed that the ambient temperature was constant throughout the day. For night-time ambient temperatures, a 68 °F was assigned for the first night and 77 °F was assigned for the second night. 68 °F was selected as the night ambient temperature for the night-time curing for the match-cast segment to obtain the initial temperature conditions. This was also within ranges observed for night-time temperatures in historical data [126], [127]. Ambient temperature throughout the night was also assumed constant. For the night-time temperature after the placement of the newly cast segment a 77 °F ambient temperature was assigned [126], [127]. The ambient temperature curve applied in the model is presented in Figure 21.
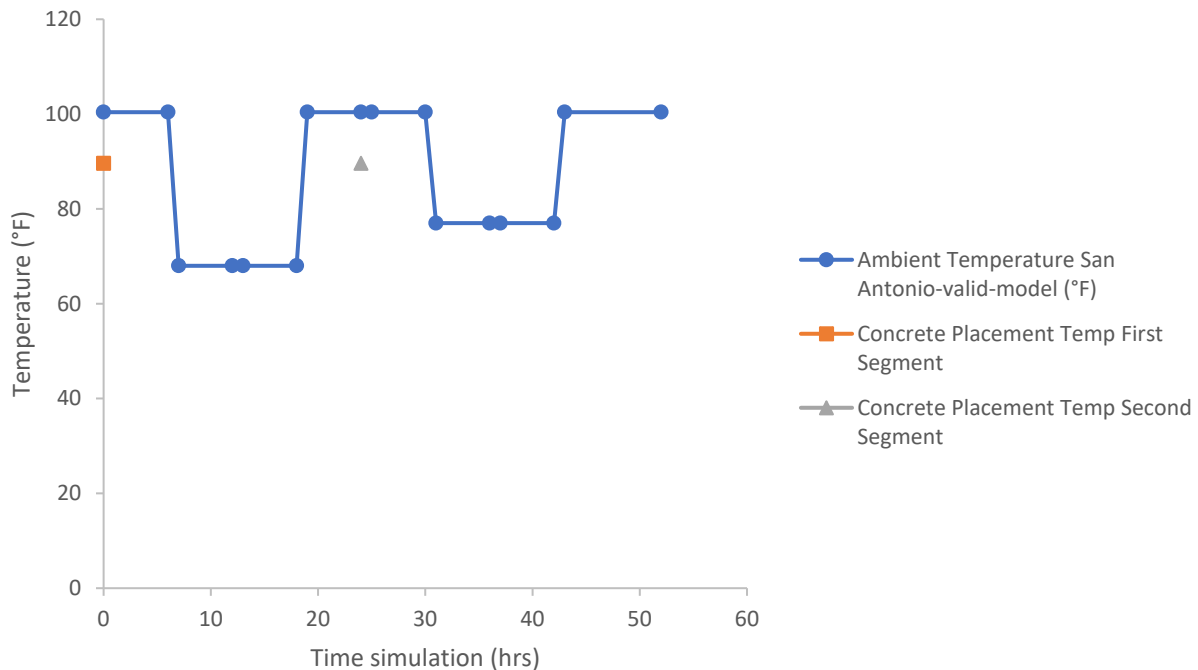
Figure 21: Ambient temperature curve San Antonio

Concrete temperatures recorded for the match-cast segment are shown in Figure 19. The concrete temperature measurements along the length of the top slab of the match-cast segment at 1 hour

after the placement of the new segment were similar to the ones recorded at the time of placement of the new segment [1]. The concrete temperature at the center of the top slab was about 140°F, the concrete temperature at the free face (face opposite to the newly cast segment) was about 130°F and at the face in contact with the newly cast segment the temperature recorded was about 115°F. This initial condition of the match-cast segment in the San Antonio project can be due to several reasons, such as ambient conditions or the remaining thermal effects from casting the match-cast segment.

For the purposes of this validation, the application of wind was used to obtain similar initial concrete temperature conditions for the match-cast segment. A wind speed of 11.2 mph was assigned from 0 to 24 hours to the face of the match-cast segment that was going to be in contact with the new segment [1], [122]. Before the new segment was placed, this assigned wind speed was within possible wind ranges given in [5]. A wind curve of 0.7 mph was also assigned from 0 to 24 hours to the free face of the match-cast segment to approximate the temperature measured in that face of the match-cast segment [1], [122]. Before the new segment was placed, this assigned wind speed was also within possible wind ranges given in [5]. After the new concrete was placed, the wind curve was assigned to be 0 mph on all faces.

A thermal conductivity value of 0.081 BTU/(ft·hrs·°F) was used to represent wooden formwork with a thickness of 0.83 in. The thermal conductivity value is typical for wood [77] and was similar to the value used in Abendeh's work [3]. The thickness value was also similar to the values used in [3] where wooden formwork thicknesses of 0.4 in. and 1.18 in. were tested. The formwork covered all the faces of the segment except the top faces of the bottom and top slabs. For the match-cast segment, the formwork was used for the first 24 hours of the simulation and then removed. For the newly cast segment, the formwork was applied from the time of placement at 24 hours in the simulation until the end of the simulation at 48 hours.

To represent curing with plastic sheets, a thermal conductivity of 0.032 BTU/(ft·hrs·°F) with a thickness of 0.32 in. were used as input values. The thermal conductivity value was similar to the value used in Abendeh's work where plastic sheets were used to represent covering as insulation Plastic sheets were tested with a lower thermal conductivity value of 0.017 BTU/(ft·hrs·°F) and a thickness 0.39 in. [3]. The value used was also within the ranges of typical plastic thermal conductivity values [128]. The insulation covered the top faces of the top and bottom slabs of the segments in the hydration process and all faces after removing formwork. In the match-cast segment, insulation covered the top faces of the top and bottom slabs from 0 hours to 24 hours. Insulation was applied at 24 hours to all the faces of the match-cast segment as indicated in [5]. In the newly cast segment, only insulation covering the top faces of the top and bottom slabs were modelled as it cured from 24 hours to 48 hours in the simulation.

Mesh Parameters

The maximum mesh size for the San Antonio model was selected so that there were at least 3 elements through the flange thickness of the top slab of the segment. Simulations with more elements through the thickness of concrete elements were performed and showed that convergence could be achieved when there were at least three elements in each direction in the flanges.

The 1-hour time step selected for the San Antonio model was also assigned to all the models studied in the simulation matrix. Convergence studies also showed that this time step was sufficiently small to limit approximation errors to an acceptable level.

The time of simulation at casting indicates the time the segment was placed in the simulation. The match-cast segment was placed at 0 hours. The curing process was modelled for 24 hours, after which the new segment placement was modelled against the match-cast segment at time 24 hours in the simulation. The simulation ran until 48 hours after the match-cast segment placement.

Mechanical boundary conditions were assigned to both segments to prevent the model from becoming unstable. Face boundary conditions and point boundary conditions were used. Symmetry of the segments was used to create half-symmetry models and reduce the computational demand of the models. Figure 22 illustrates the face mechanical boundary conditions used for both segments, restricting displacements of nodes in the perpendicular direction to these faces. Figure 23 illustrates point boundary conditions in their respective directions assigned to the model (red lines), the blue circles are generated by the software and are nodes where point boundary conditions could be assigned.
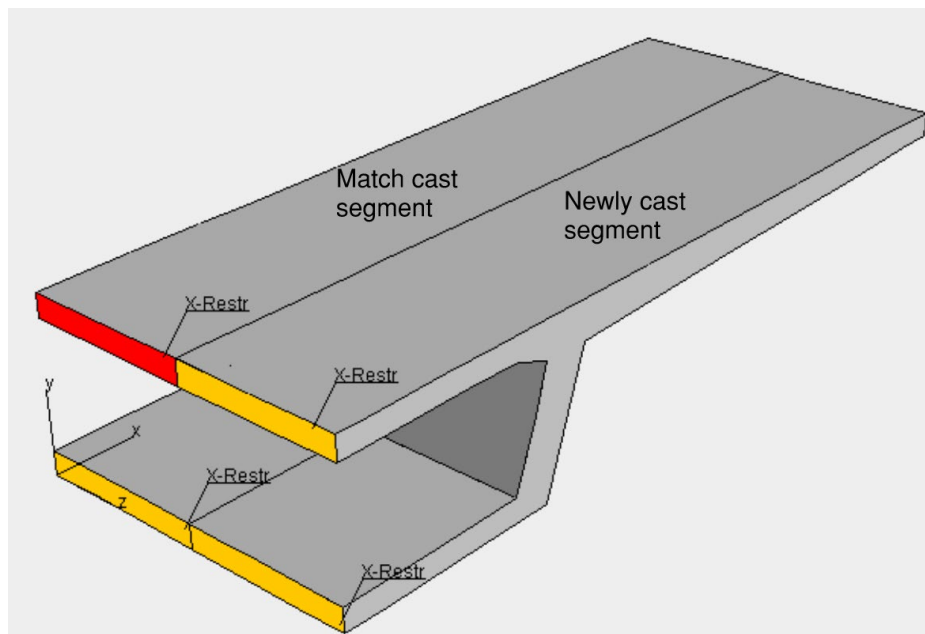
Figure 22: Fixed mechanical boundary conditions applied to faces
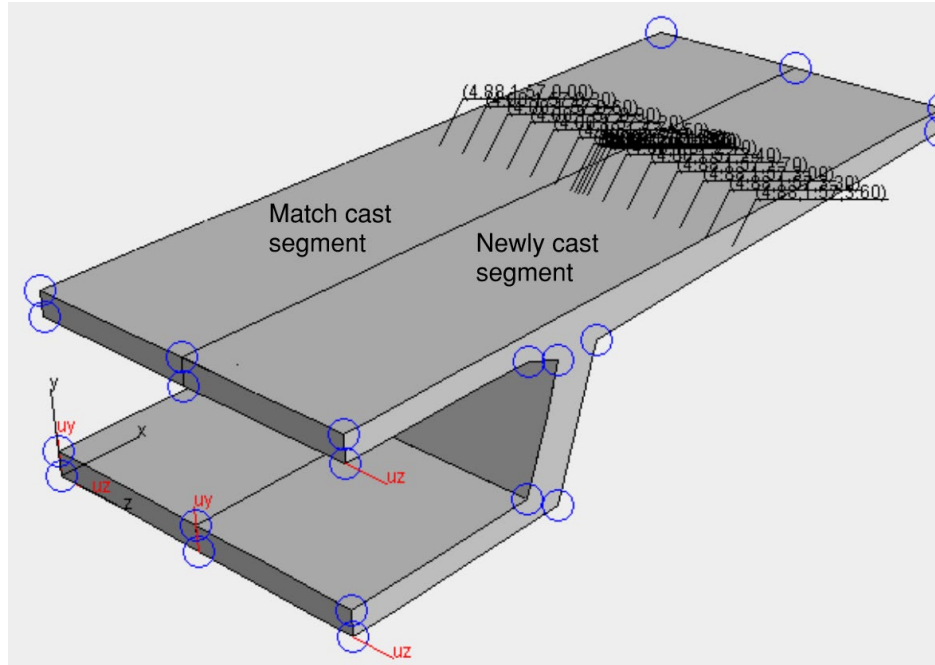
Figure 23: Fixed mechanical boundary conditions applied to points

4.2.4   Comparison of Results FEM vs. Field Measurements – Type III Segments

Concrete Temperature Results

Concrete temperatures in the San Antonio ¨Y¨ project for type III segments were simulated. Figure 24 shows the locations where concrete temperatures were extracted to examine the heat transfer across the boundary between the match cast and new segment and their temperature development. Figure 25 shows the simulated concrete temperatures at the line across the segments shown in Figure 24 for the first 10 hours after the placement of the newly cast segment. Figure 26 to Figure 29 compare the measured vs. simulated concrete temperatures from 4, 6, 8, and 10 hours after the placement of the newly cast segment.
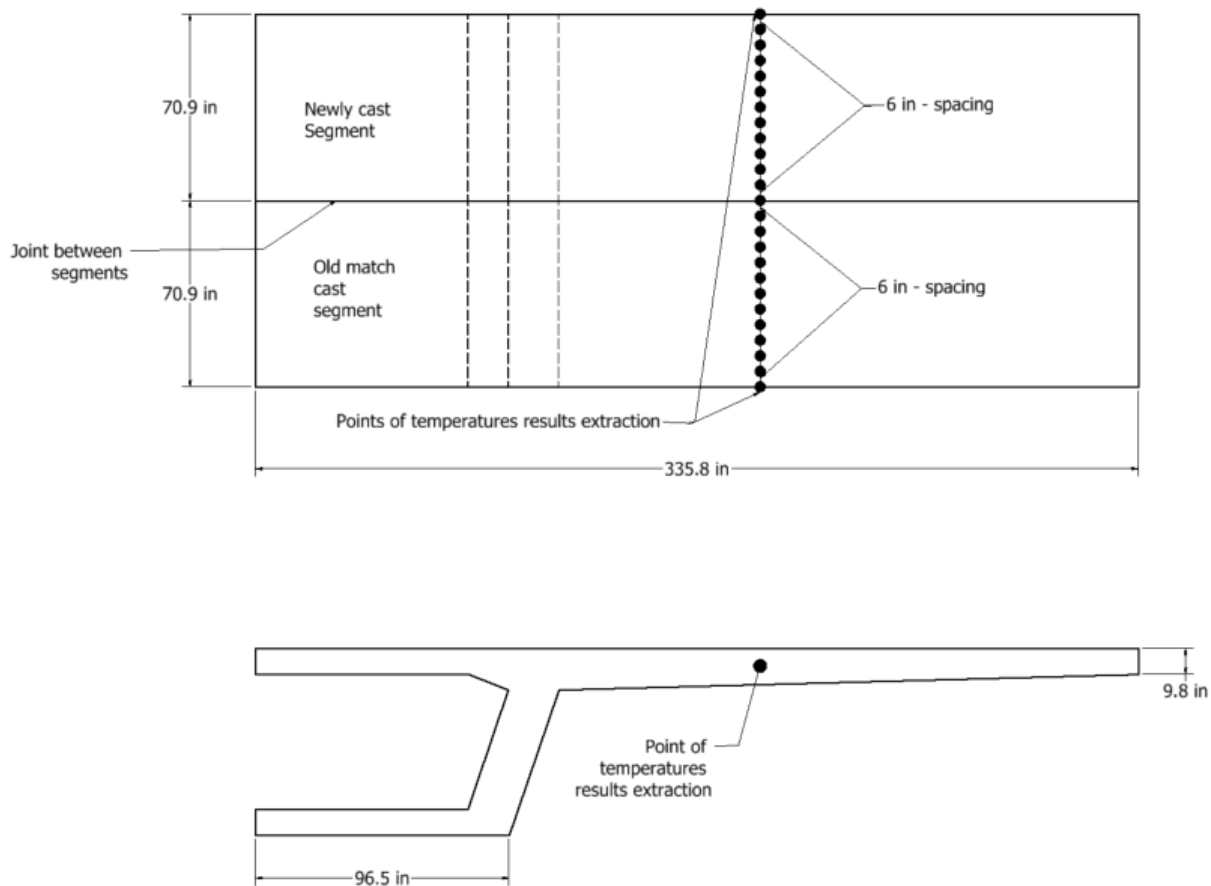
Figure 24: Location at which simulated concrete temperatures were examined
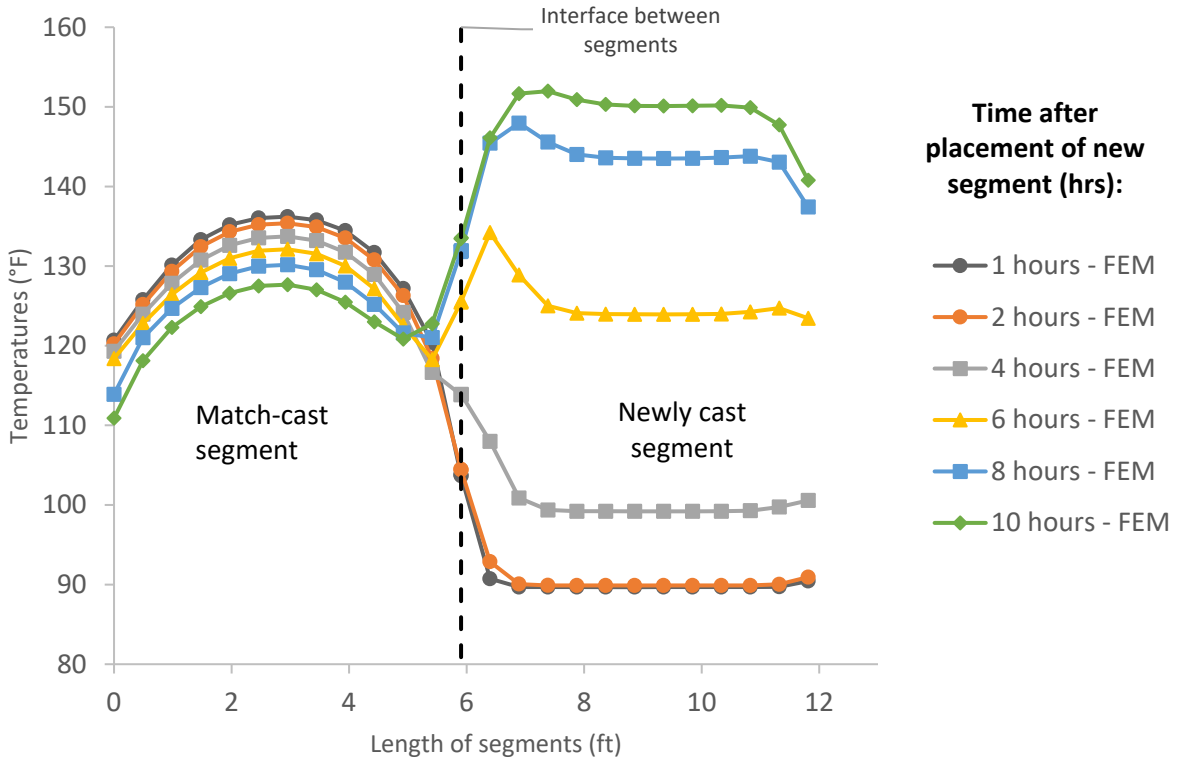
Figure 25: Time varying evolution of FEM simulated San Antonio "Y" type III segment concrete temperature profiles
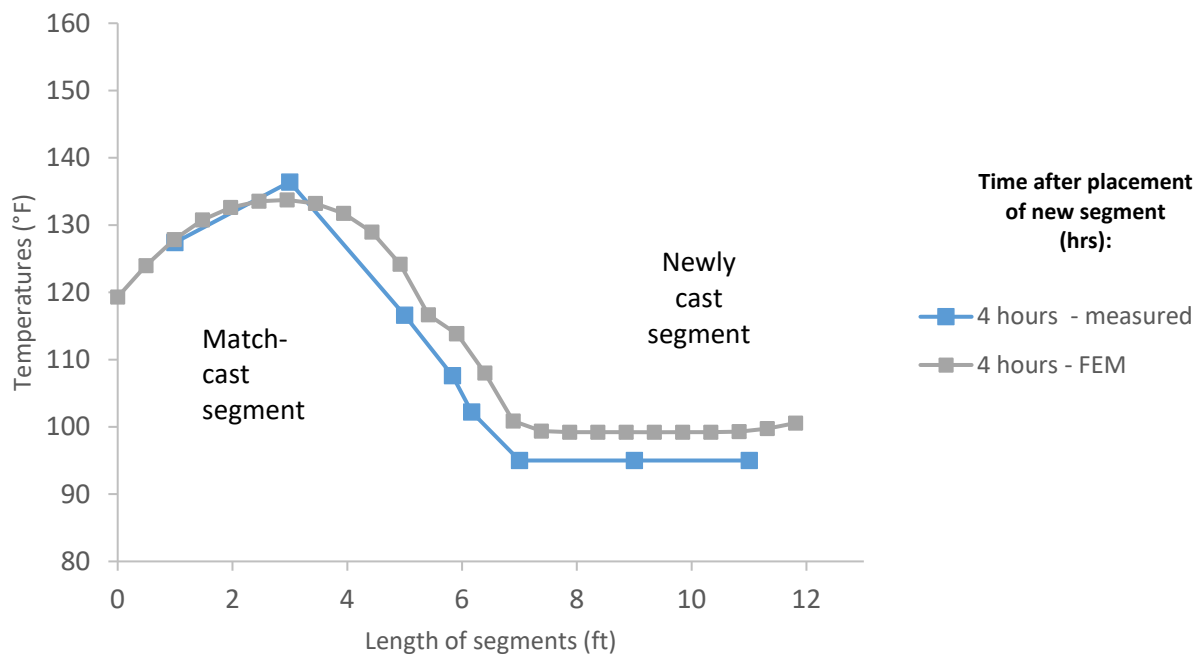
Figure 26: Measured and FEM simulated concrete temperature profiles for San Antonio "Y" type III segment at 4 hours after new concrete placement
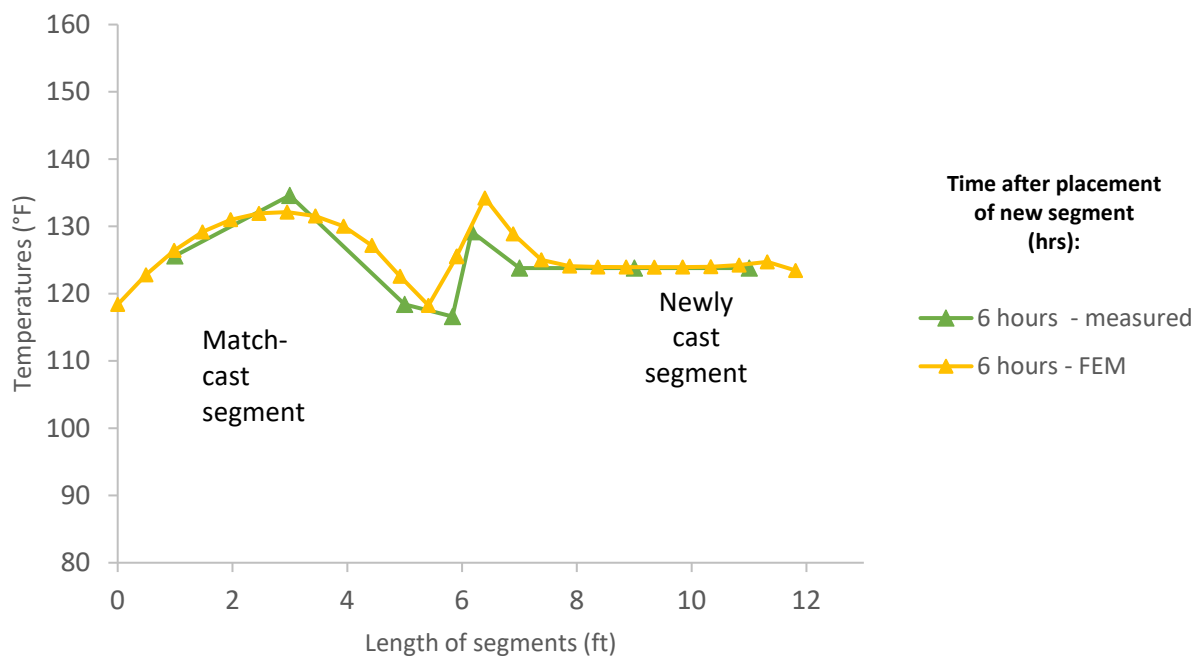
Figure 27: Measured and FEM simulated concrete temperature profiles for San Antonio "Y" type III segment at 6 hours after new concrete placement
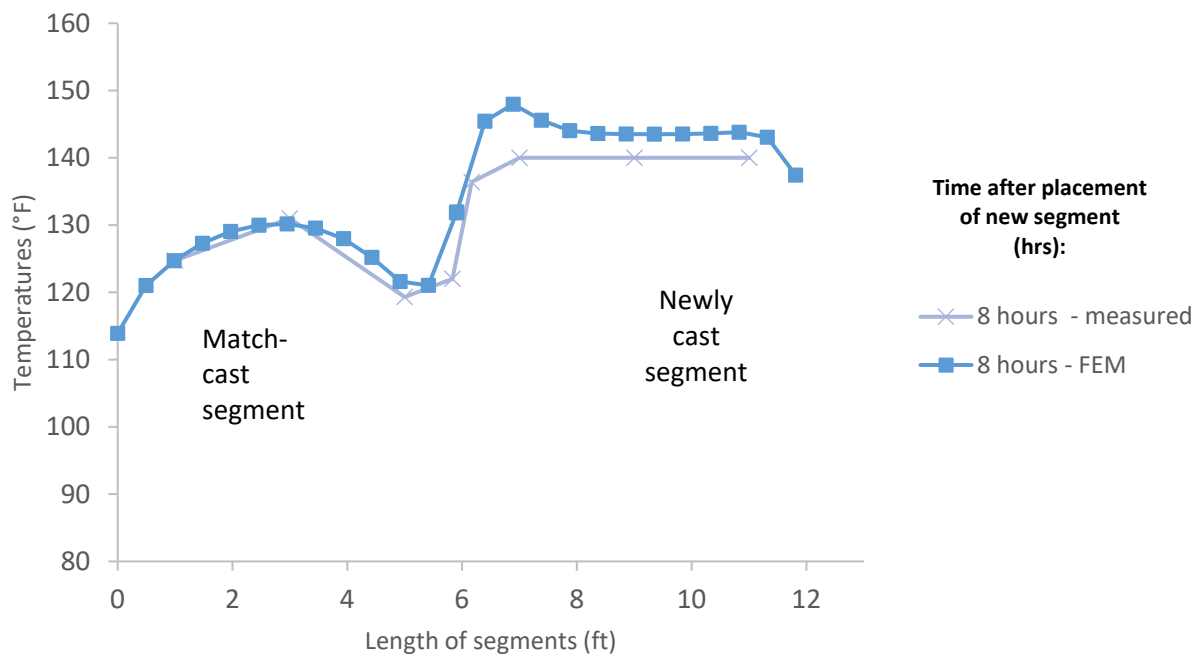
Figure 28: Measured and FEM simulated concrete temperature profiles for San Antonio "Y" type III segment at 8 hours after new concrete placement
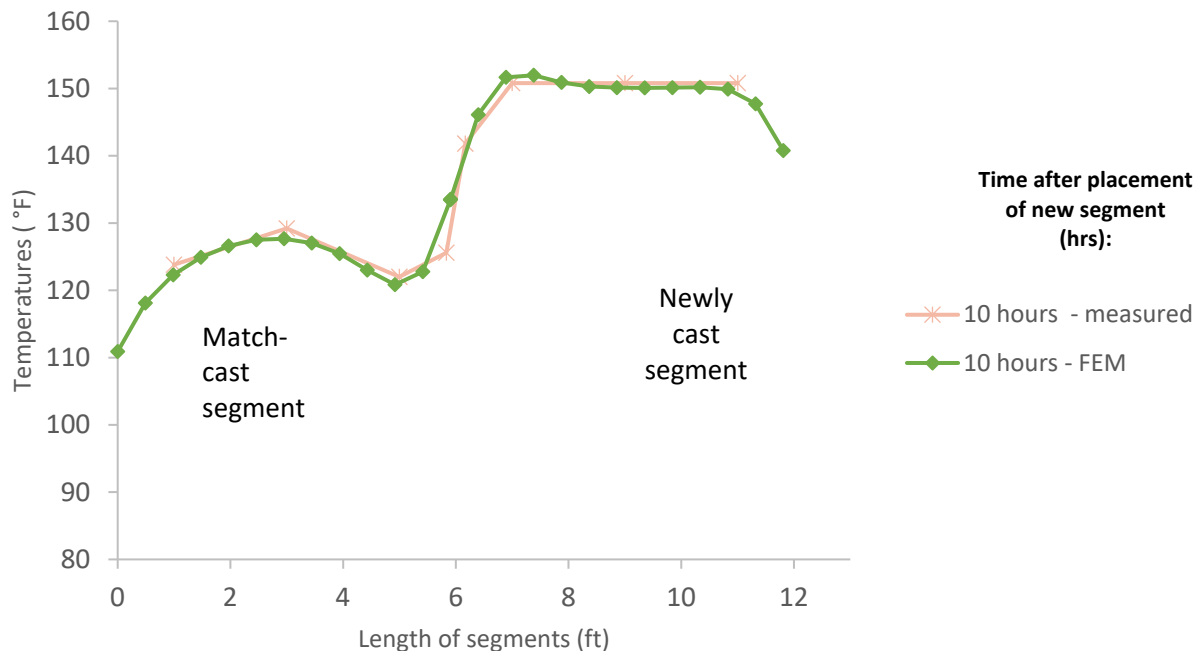
Figure 29: Measured and FEM simulated concrete temperature profiles for San Antonio "Y" type III segment at 10 hours after new concrete placement

Bowing Distortion Results

Results for nodal displacements were extracted from 6 points across the top slab of the newly cast segment at a distance 0.04 in. from the interface between the newly cast segment and the match-cast segment, as shown in Figure 30. Good agreement was seen between the field measurements of the type III segment and the FEM simulation results. Figure 31 shows a comparison of the measured results and FEM results at 8 hours after the placement of the newly cast segment. The bowing distortion results measured by Roberts et al. [1] 8 hours after placement was 0.07 in., whereas the FEM-calculated distortion was 0.043 in. Figure 32 shows a comparison of the measured results and FEM results at 10 hours after the placement of the newly cast segment. The bowing distortion measured by [1] was 0.07 in., the FEM calculated distortion was 0.063 in.
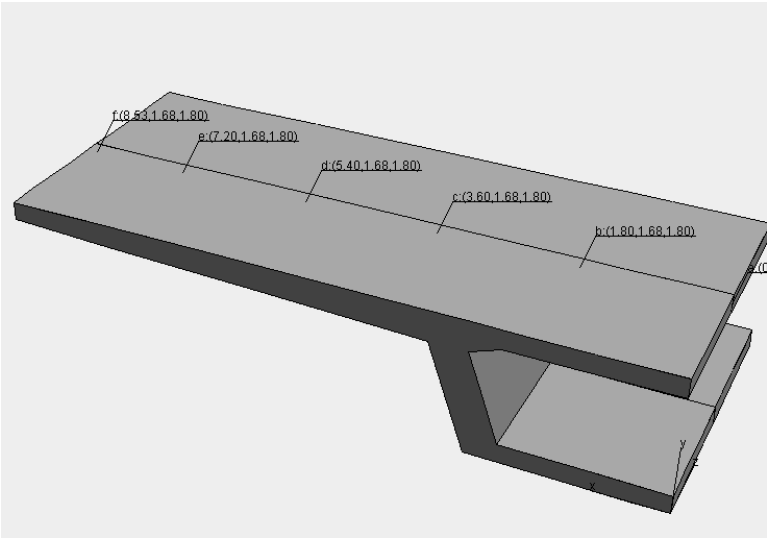
Figure 30: Locations on San Antonio "Y" structure where nodal displacements were extracted
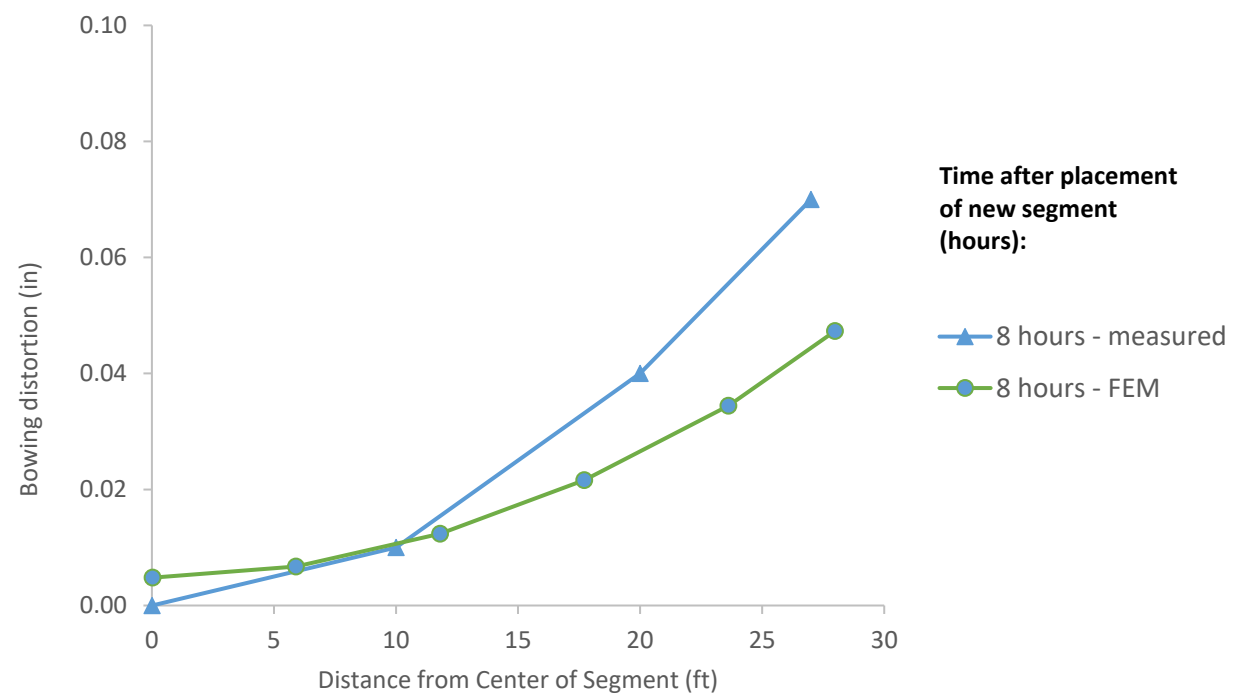
Figure 31: Measured and FEM simulated distortion for San Antonio "Y" type III segment at 8 hours after new concrete placement
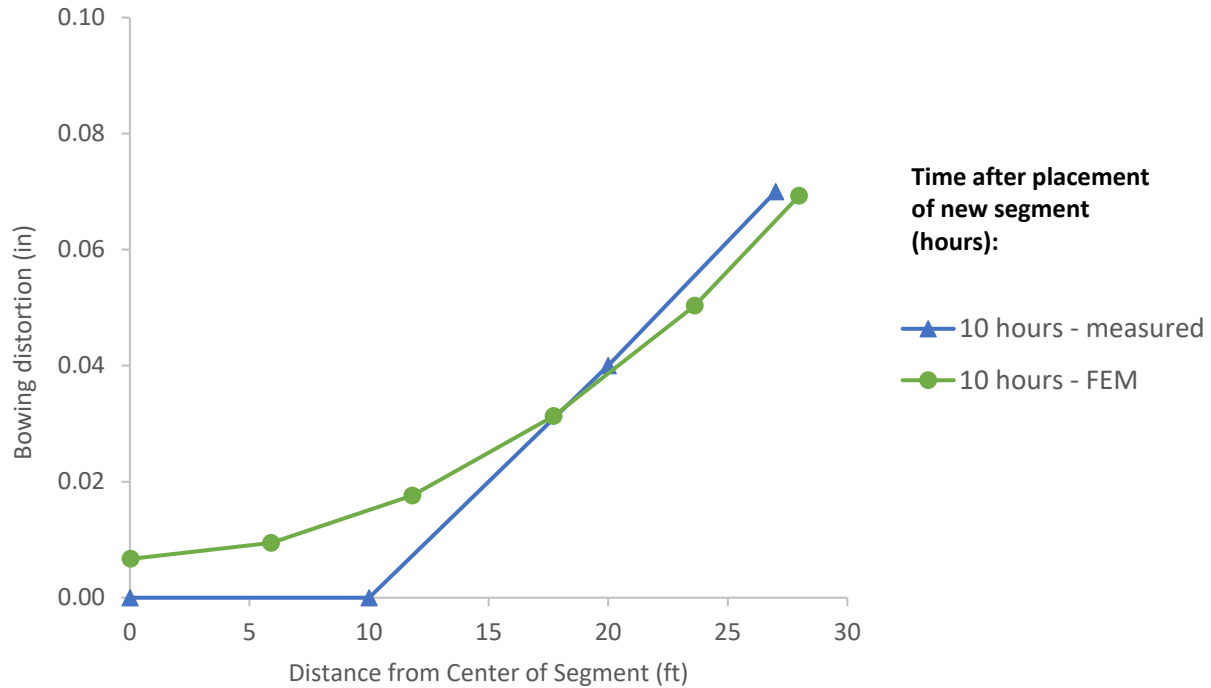
Figure 32: Measured and FEM simulated distortion for San Antonio "Y" type III segment at 10 hours after new concrete placement

Analytical Estimation of Distortions

In addition to finite element analysis, an analytical model to calculate segment distortion was also used in this study. The expressions presented in task 1 section 1.3.2 to calculate the member curvature and distortion were used as the basis for the analytical model [1], where the top slab of the segment was idealized as a beam subjected to a moment. The analytical model assumed that the top slab had a constant thickness and the elastic modulus of the concrete in the match-cast segment was constant spatially throughout segment and with time. The expression for an equivalent moment caused in the top slab of the segment by thermal effects in Equation 4 was simplified using the previously mentioned assumptions, obtaining the expression in Equation 82 [1], [3].

$$M = \alpha_t \cdot A_{t1} \cdot h \cdot E \cdot \left(\frac{l}{2} - cg_1 \right) \qquad \text{Equation 82}$$

Where: M = Equivalent thermal bending moment in top slab of segment (kip-in)

α_t = Coefficient of thermal expansion (1/ °F)

A_{t1} = Area under the curve of the gradient plot constructed from concrete temperatures in the match-cast segment from the face in contact with the newly cast segment (°F/in)

h = Thickness of top slab of the segment (in)

E = Elastic modulus of concrete of match-cast segment (ksi)

l = Length of the segment (in)

cg_l = Center of gravity of the area, At1, under the curve of the gradient plot constructed from concrete temperatures in the match-cast segment (in)

The bowing distortion experienced by the top slab of the match-cast segment was derived from the expression for maximum deflection of a simply supported beam subjected to a bending moment across its length seen in Equation 83 [1], [3], [129],

$$\Delta = \frac{M \cdot w^2}{8 \cdot E \cdot I}$$ Equation 83

Where: Δ = Bowing distortion of match-cast segment (in)

w = Width of the segment (in)

α_t = Coefficient of thermal expansion of concrete (1/ °F)

I = Moment of inertia of idealized constant thickness top slab of match-cast segment (in^4).

Substituting Equation 82 in Equation 83 and taking into account thermal effects in the free face of the match-cast segment in the same manner, the expression for bowing distortion Δ is shown in Equation 84 [1], [3]:

$$\Delta = \frac{3 \cdot w^2 \cdot \alpha_t}{2 \cdot l^3} \cdot \left[\left(A_{t1} \cdot \left(\frac{l}{2} - cg_1 \right) - \left(A_{t2} \cdot \left(\frac{l}{2} - cg_2 \right) \right) \right) \right]$$ Equation 84

Where: A_{t2} = Area under the curve of the gradient plot constructed from concrete temperatures in the match-cast segment from free face of the segment (°F/in)

cg_2 = Center of gravity of the area, A_{t2}, under the curve of the gradient plot constructed from concrete temperatures in the match-cast segment (in)

Temperature gradient plots for the match-cast segment were constructed by calculating the concrete temperature difference between the time of placement of the newly cast segment and 10 hours after its placement. The concrete temperature results obtained from the finite element model from the match-cast segment presented in were used. 10 hours was selected as a conservative time that would occur after setting and the distortion was locked in for all the segments modeled. This time was also used by Abendeh in his analysis [3]. Figure 33 illustrates the concrete temperature difference with location at 6, 8, and 10 hours after the new concrete was

placed. Table 35 shows the results obtained for this analytical distortion calculation method. Good agreement was observed between the bowing distortion obtained from the FEM models and analytical calculations based on the concrete temperatures calculated in the FEM. While this illustrates the power of the analytical model to estimate the segment distortion during curing, it still requires that the concrete temperature be measured or simulated.
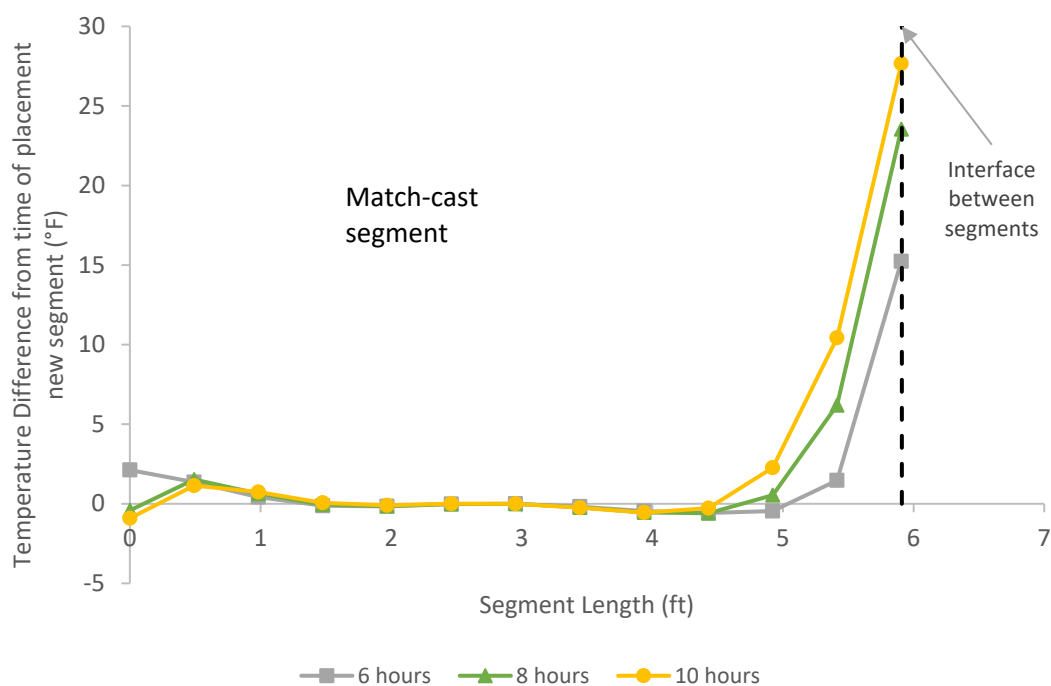
Figure 33: Concrete temperature difference from time of placement by location for the San Antonio "Y" type III match-cast segment

Table 35: Analytical vs. FEM bowing distortion results comparison

Time after new segment concrete placement	A_{t1} (°F · in)	A_{t2} (°F · in)	cg_1 (in)	cg_2 (in)	Analytical method calculated bowing distortion (in)	FEM calculate bowing distortion (in)	Difference %	Difference FEM vs. calc. (in)
6 hours	47.54	18.78	0.29	5.91	0.0141	0.0165	16%	-0.002
7 hours	77.59	6.95	1.84	5.91	0.0304	0.0296	-3%	0.001
8 hours	105.75	-3.64	2.78	5.91	0.0451	0.0425	-6%	0.003
9 hours	131.66	-5.79	3.50	5.91	0.0555	0.0534	-4%	0.002
10 hours	155.00	-8.06	4.11	5.91	0.0646	0.0626	-3%	0.002

4.3 Illustrative Example of Simulations Performed

The 157 different combinations of material, construction, and environmental variables presented in task 2 of the project were simulated in b4cast. The simulation approach was similar to the one presented in section 2 for the validation model. Appendix A gives the input parameters used for each simulation performed. Simulation 27 is described in detail as an example of the process used to simulate the segment distortion. This simulation used a cross-section with a relatively high width-to-length ratio (Florida Bridge C: w/l: 10.89); high heat of hydration concrete mixture; high setting time concrete (made with an aggregate selection that produced concrete with a medium level coefficient of thermal expansion); used burlap as the curing technique; and was placed in Miami in the summer. The geometry of this segment is shown in Figure 34. Table 36 provides details of the input parameters used in b4cast for this simulation.
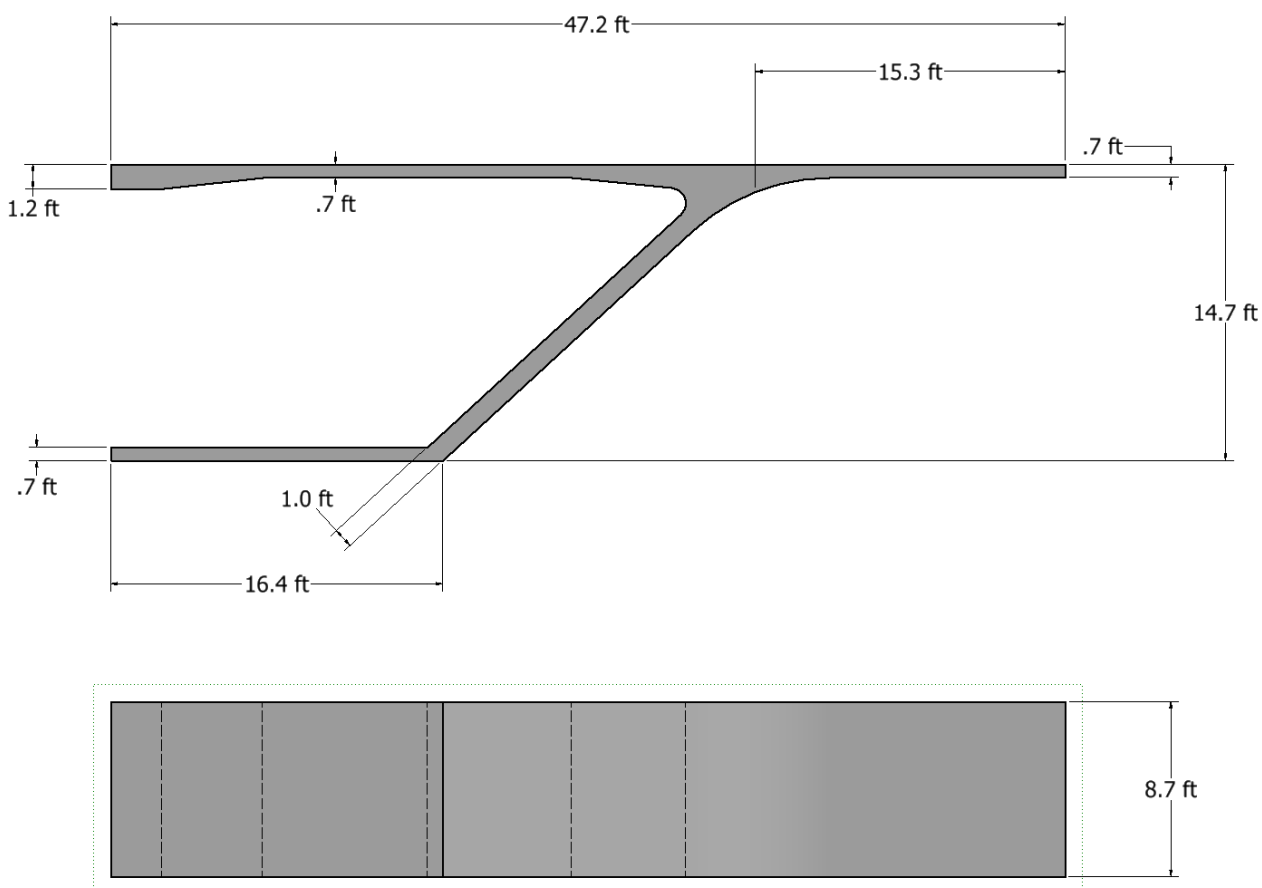
Figure 34: Florida Bridge C geometry w/l: 10.89

Table 36: Simulation inputs used for simulation 27

Model details			
Geometry		Florida Bridge C - w/l=10.89	
Max. Mesh Size		3.54	in
Time Step		1	hrs
Placement Concrete Temperature		95	°F
Match-cast segment Time of Simulation at Casting		0	hrs
New Segment Time of Simulation at Casting		24	hrs
Concrete Properties			
Cement Content		950.11	lb/yd^3
Activation Energy		28.43	BTU/mol
Heat of Hydration Parameters			
Total Heat Development, $Q_{ult} = \alpha_u \cdot H_u$		124.95	BTU/lb
Time Parameter, τ		10.50	hrs
Curvature Parameter, β		1.60	
Concrete Density		3880.948	lb/yd^3
Concrete Specific Heat		0.26	BTU/(lb·°F)
Concrete Thermal Conductivity		1.502	BTU/(ft·h·°F)
Match-cast segment Elastic Modulus Dev. Parameters			
Final Value		4584.92	ksi
Time Parameter		12.420	hrs
Curvature Parameter		1.068	
New Segment Elastic Modulus Dev. Parameters			
Final Value		14.50	ksi
Time Parameter		n/a	hrs
Curvature Parameter		n/a	
Poisson Ratio		0.17	
Coefficient of Thermal Expansion		4.54	$\mu\varepsilon$/°F
Thermal Boundary Conditions (Applied to Appropriate Faces)			
Ambient Temp	Miami - Summer - Morning - Placement		
Wind	Medium-Wind	7.50	mph
Formwork	Steel Formwork	34.60	BTU/(ft·h·°F)
	Thickness	0.118	in
Curing	Burlap	0.18	BTU/(ft·h·°F)
	Thickness	0.39	in

4.3.1   Concrete Temperature Results with Illustration Example

Calculated concrete temperatures were examined at discrete points along a line in the top slab for each simulation performed. Figure 35 shows the location of these temperature points. These points were used because Roberts et al. [1] noted that concrete temperatures recorded in the wing sections were better for using the analytical solution to calculate bowing distortion of segments.
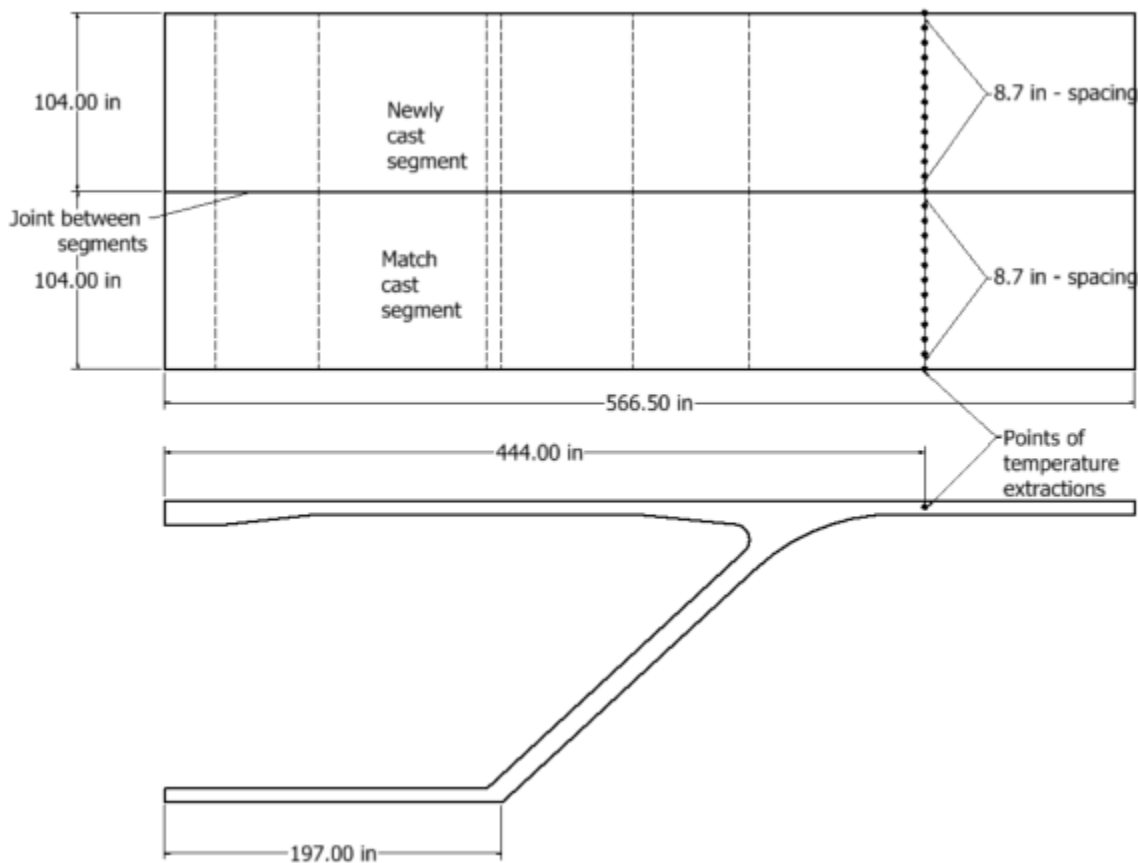
Figure 35: Locations where concrete temperatures were examined for Bridge C

Concrete temperatures at different times after placement for the new segment for simulation 27 are shown in Figure 36. In this case, the newly cast segment reached a maximum temperature due to the heat of hydration of 156°F. The match-cast segment heated up to about 123°F at the face in contact with the new segment. The free face of the match-cast segment did not change temperature much after concrete for the new segment was placed. Figure 36 shows how the concrete that was up to 2 ft from the interface was affected by the heat transferred from the newly cast segment. This temperature change at the interface in the match-cast segment was primarily responsible for the bowing distortion in the segment.
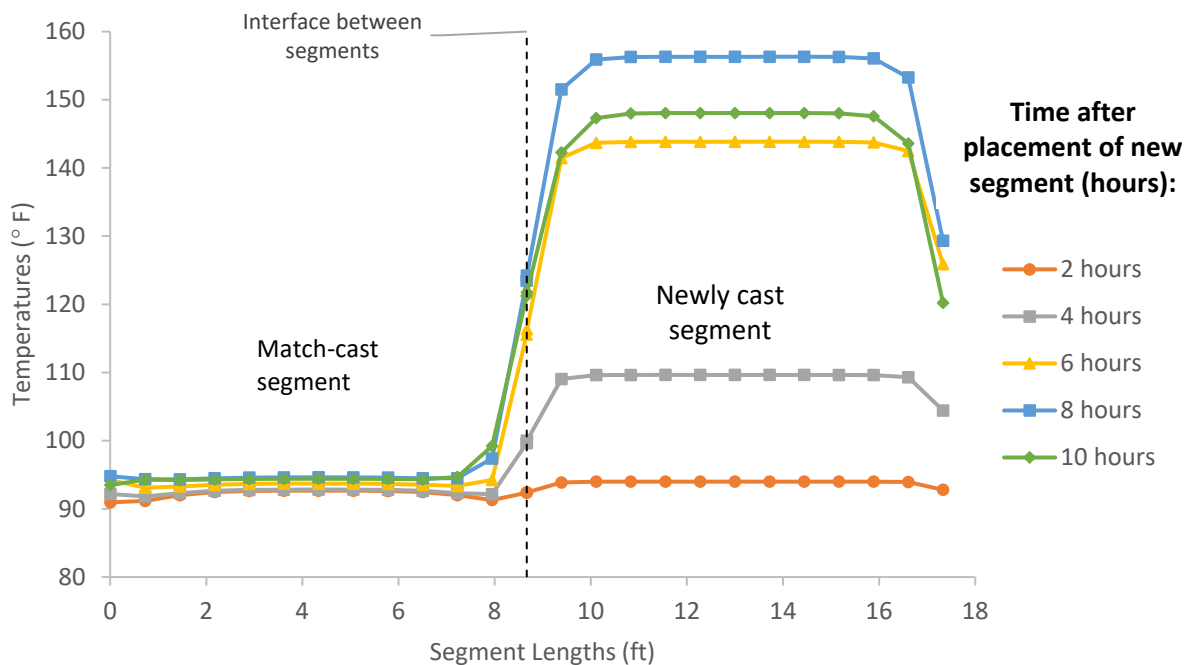
Figure 36: Simulated concrete temperature with time for simulation 27

4.3.2 Bowing Distortion Results with Illustration Example

Segment distortion was examined across the top slab of the new segment at six discrete points 0.04 in. from the interface with the match-cast segment. Figure 37 shows the location of each point examined for simulation 27. Displacement results at different times after the placement of the new segment can be seen in Figure 38. The bowing distortion values reported were taken as the difference between the point at the middle of the segment and the wing tip of the segment. The maximum distortion measured at 10 hours after placing the concrete in the new segment was 0.07 in. A bowing distortion value limit of 0.03 in. per segment was recommended to prevent the construction issues seen in [1], [122]. An accumulated bowing distortion value limit of 0.5 in. per span was recommended to prevent the construction issues seen in [1], [122]. The progression of the bowing distortion value with time for simulation 27 is shown in Figure 39.
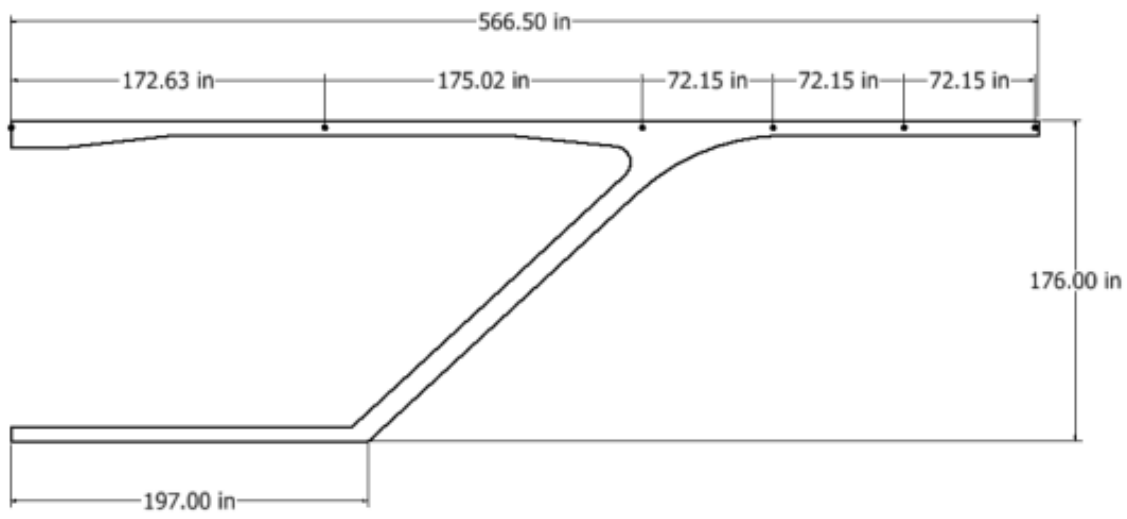
Figure 37: Locations where distortion were examined for Bridge C
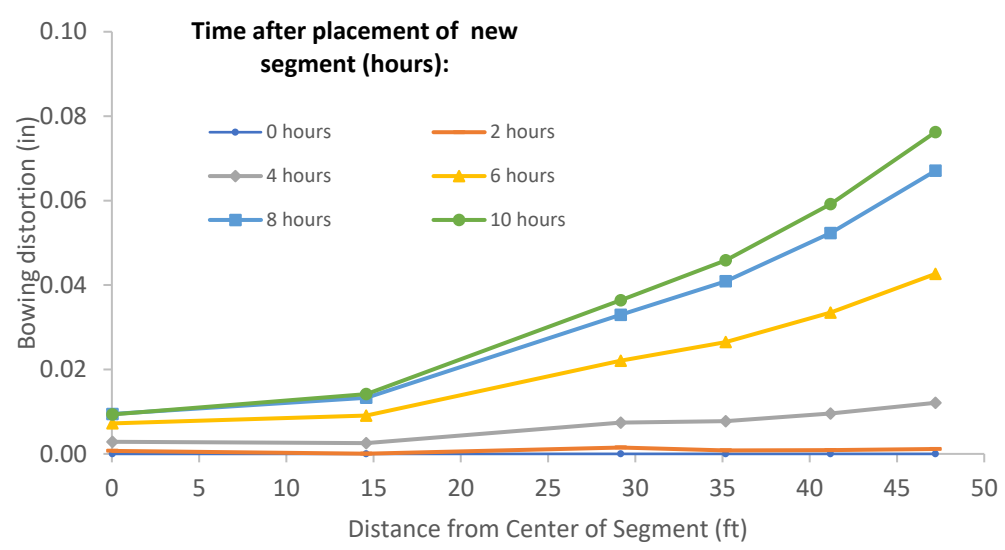
Figure 38: Distortion measured with time for simulation 27
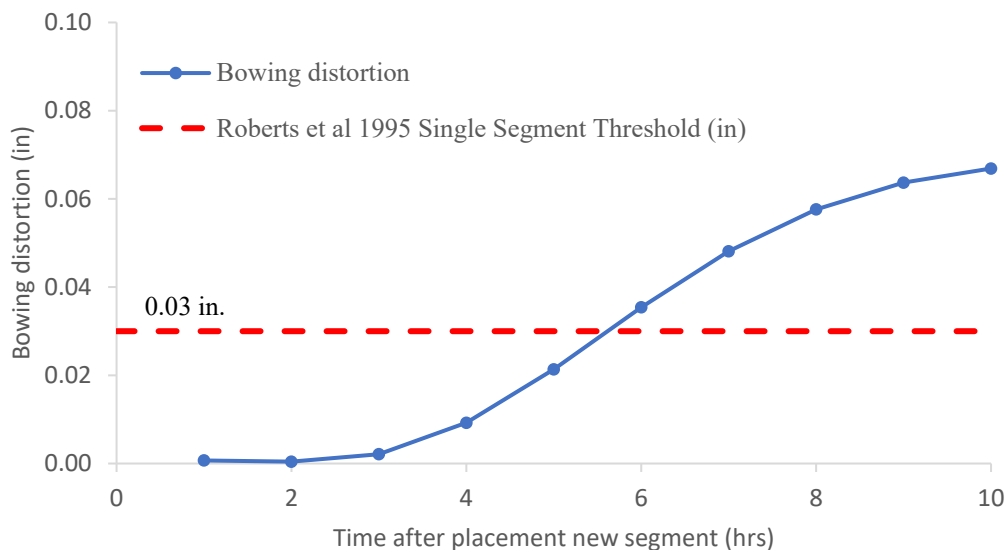
Figure 39: Bowing distortion with time for simulation 27

4.4 Sensitivity of Bowing Distortion to Changes in Each Variable

Calculated bowing distortion at 10 hours after the placement of the new segment were used to determine the segment distortion sensitivity to each input variable. The findings of the sensitivity analysis of the bowing distortion from variations in the segment geometry, concrete heat of hydration, aggregate type used, ambient temperature, wind speed, curing techniques used, and steam curing are discussed in this section.

4.4.1 Effect of Geometry

The bowing distortion of match-cast segments at 10 hours after the placement of the new segment are shown for all the cases simulated in Figure 40. It is evident that the width-to-length ratio (w/l) plays a large role in determining the bowing distortion magnitude. When the w/l was below six, large bowing distortions were not seen in the simulations. A w/l above six did not however automatically mean that the segment would have excessive distortions. Other factors discussed further in this section played a role in determining whether the distortion was excessive and would be a problem for construction. Roberts et al. [1] concluded that segments with w/l ratios of more than nine subjected to conditions similar to those in the San Antonio "Y" project were prone to experience construction issues due to the bowing distortion effects. Podolny [4] mentioned that segments with a w/l of six had a significant bowing distortion .
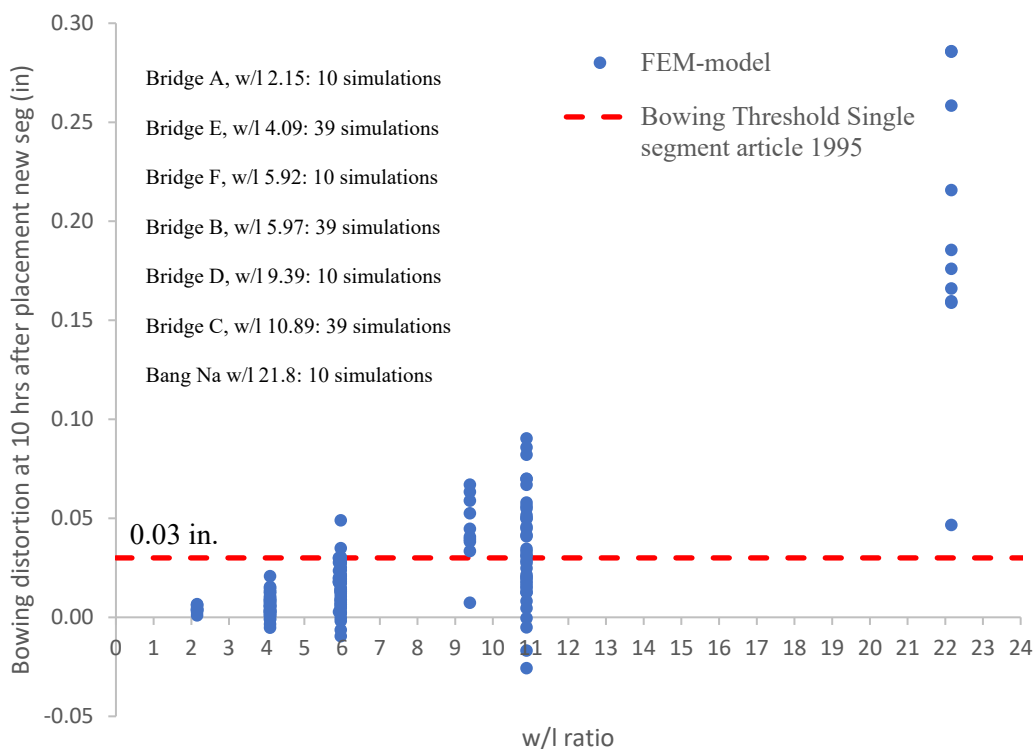
Figure 40: Bowing distortion at 10 hours for all simulations by segment w/l ratio

4.4.2   Effect of Heat of Hydration

Results of bowing distortion of match-cast segments at 10 hours after the placement of the new segment are shown in Figure 41 for the high heat of hydration and low heat of hydration mix levels. It can be seen that the low heat of hydration cases were below the bowing distortion threshold even at high w/l ratio levels for most cases. It can also be seen that most of the high heat of hydration cases are above the threshold even at high w/l ratio levels above six. The medium heat of hydration cases with w/l above six showed some cases with excessive distortion, and some with low bowing distortion. Abendeh recommended use of mixtures with low heat to avoid bowing distortion problems [3]. Our study also found that the use of lower heat of hydration mixtures resulted in lower bowing distortion values than high heat of hydration mixtures.
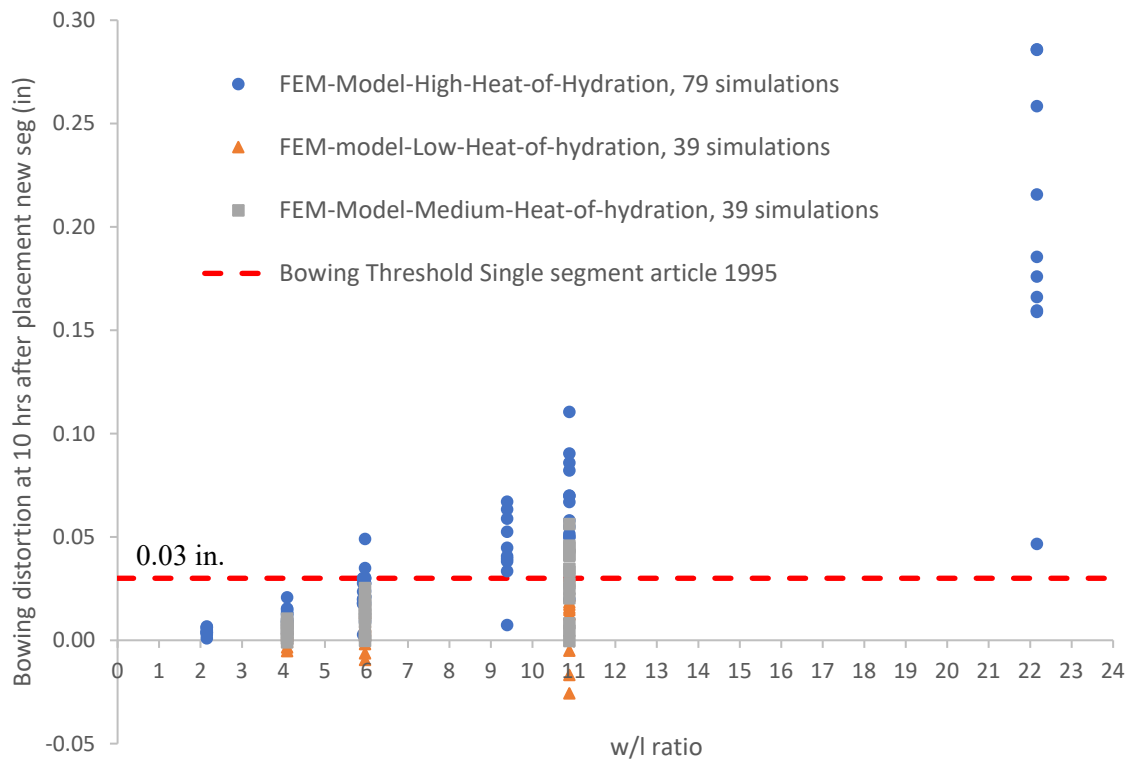
Figure 41: Bowing distortion at 10 hrs for simulations with high and low heat of hydration by segment w/l

4.4.3 Effect of Aggregate Selection – Coefficient of Thermal Expansion (CTE)

Figure 42 shows bowing distortion results for the high heat of hydration cases grouped by concrete CTE. The trend for concrete produced with a low CTE of 3.4 με/°F crossed the Roberts al. threshold at a w/l ratio level of approximately eight. The concrete produced with a medium CTE of 4.54 με/°F had higher distortion than the Roberts et al. threshold at a w/l ratio level of approximately seven. The trend for concrete produced with the high CTE of 6.07 με/°F crossed the Roberts et al. bowing distortion threshold at a w/l ratio level of approximately 6. The trendline constructed for the simulation cases that used lightweight aggregate had a different shape and showed excessive distortion above the Roberts threshold at a lower w/l ratio level, even though its coefficient of thermal expansion was lower than the highest coefficient of thermal expansion tested with normal-weight aggregate.
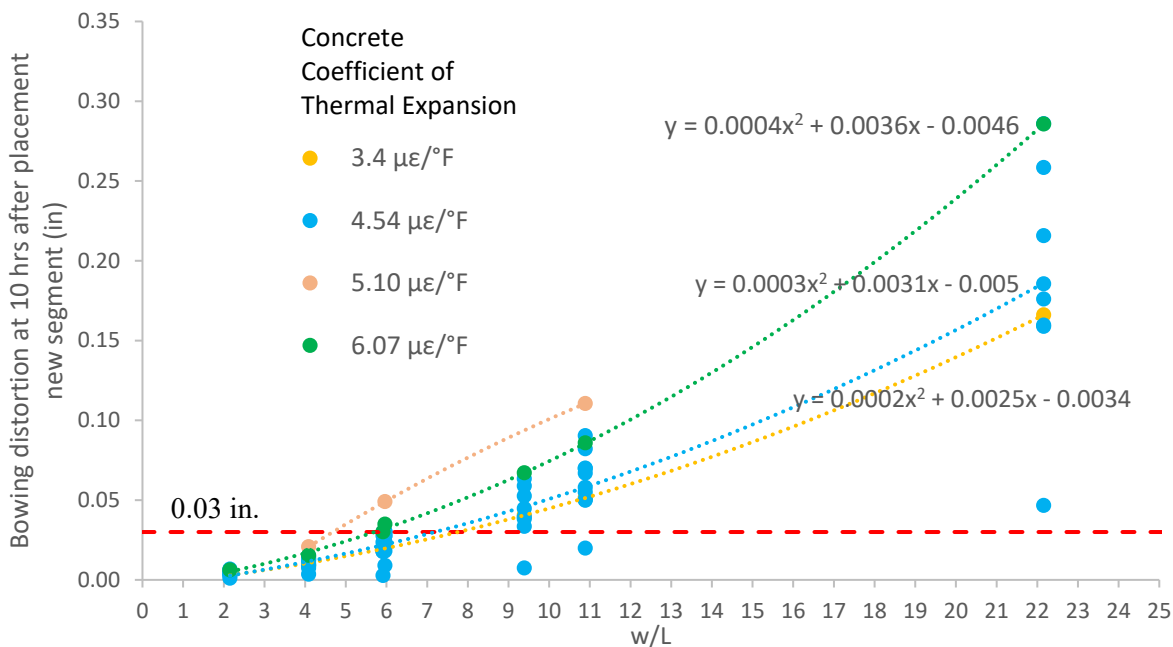
Figure 42: Bowing distortion at 10 hrs for simulations with high heat of hydration by CTE value and by segment w/l

Figure 43 shows the effect of increasing CTE of concrete produced with the bowing result for a high w/l level and high heat mix level. The increase in bowing distortion value was linearly related to the CTE as described in Equation 84. The trend of proportionality of bowing distortion to CTE was seen across geometries and across heat levels tested except for lightweight aggregate cases.
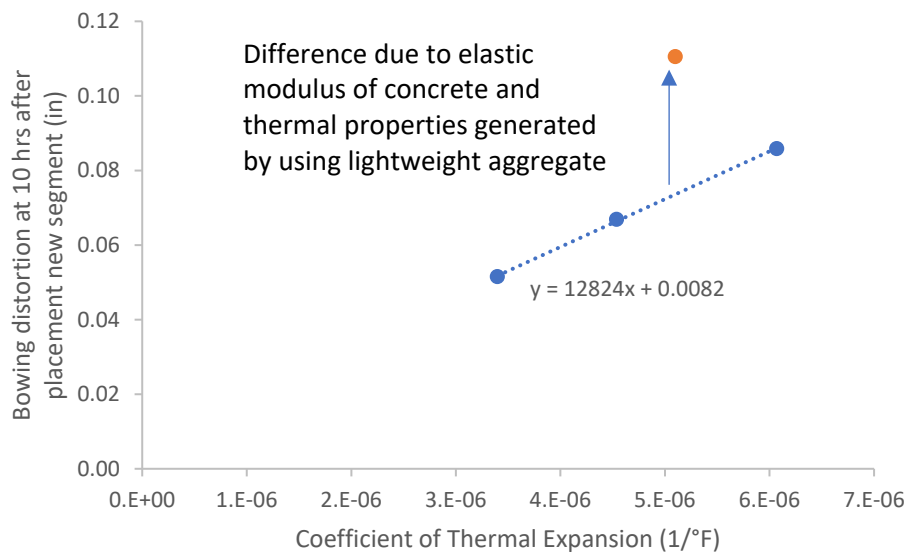
Figure 43: Simulated bowing distortion for Bridge C with a w/l ratio of 10.89, high heat of hydration and setting time

The thermal diffusivity varies with the aggregate selection, but this was not a controlling parameter when setting up the simulation matrix. Figure 44 shows for the high w/l ratio and high heat of hydration case the thermal diffusivity produced against the bowing distortion result. This trend of the bowing increasing linearly with the increase in the thermal diffusivity of the concrete is consistent at the high heat of hydration level tested across different geometries. At medium and lower heat levels simulated and shown in Figure 45, the trend of the bowing distortion value increasing linearly with the thermal diffusivity of the concrete was not seen, however. It is likely that the combination of thermal diffusivity and coefficient of thermal expansion of the lightweight aggregate were responsible for the different behavior.
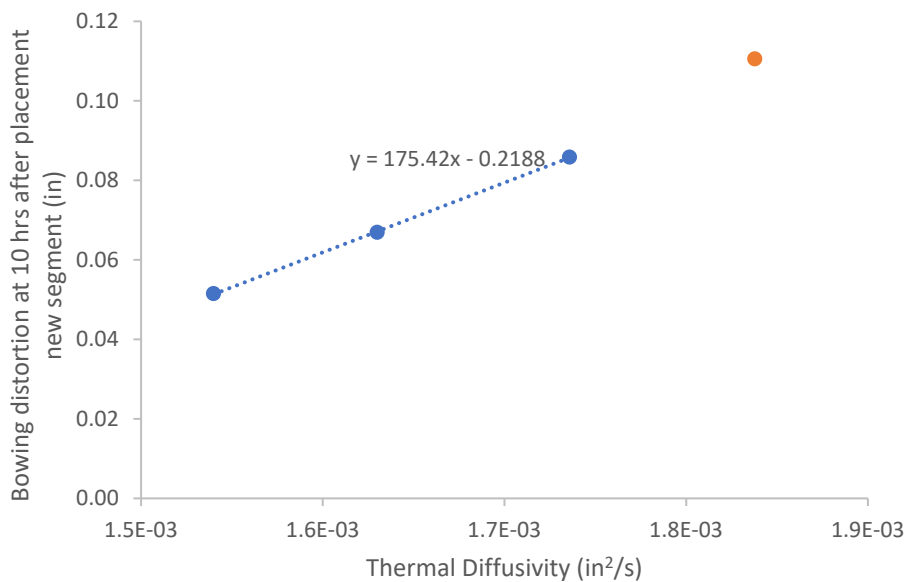
Figure 44: Simulated bowing distortion plotted against the thermal diffusivity for Bridge C with a w/l ratio of 10.89, high heat of hydration and setting time
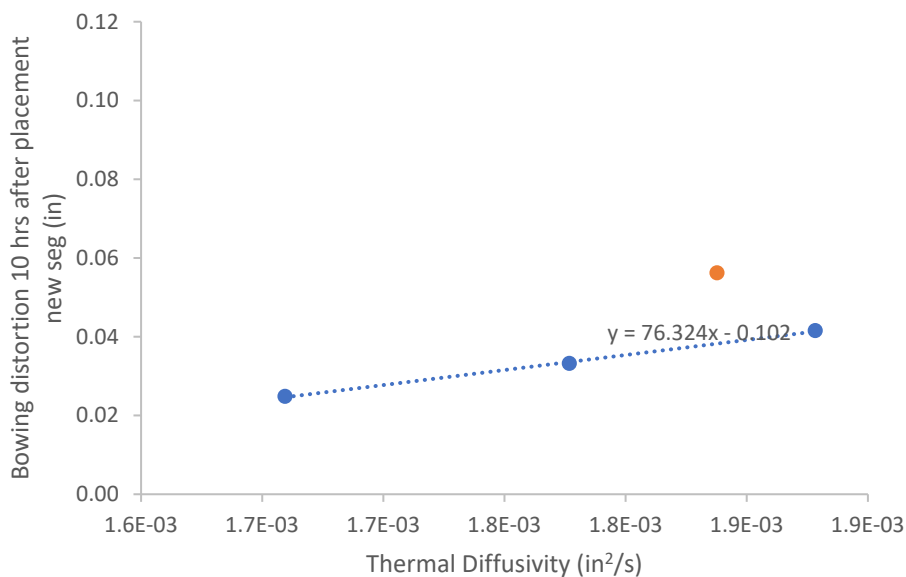
Figure 45: Simulated bowing distortion plotted against the thermal diffusivity for Bridge C with a w/l ratio of 10.89, medium heat of hydration and setting time

4.4.4 Effect of Ambient Temperatures

To analyze the influence of the ambient temperature on the bowing distortion, the sum of the ambient temperature at placement and the concrete placement temperature was plotted against the bowing results for each geometry. In Figure 46, results for Bridge C (w/l: 10.89) with the high heat and high setting time are shown. The bowing distortion increased as the sum of the concrete placement temperature plus the ambient temperature at time of placement increased. This trend was seen across the geometries tested and the heat levels simulated.
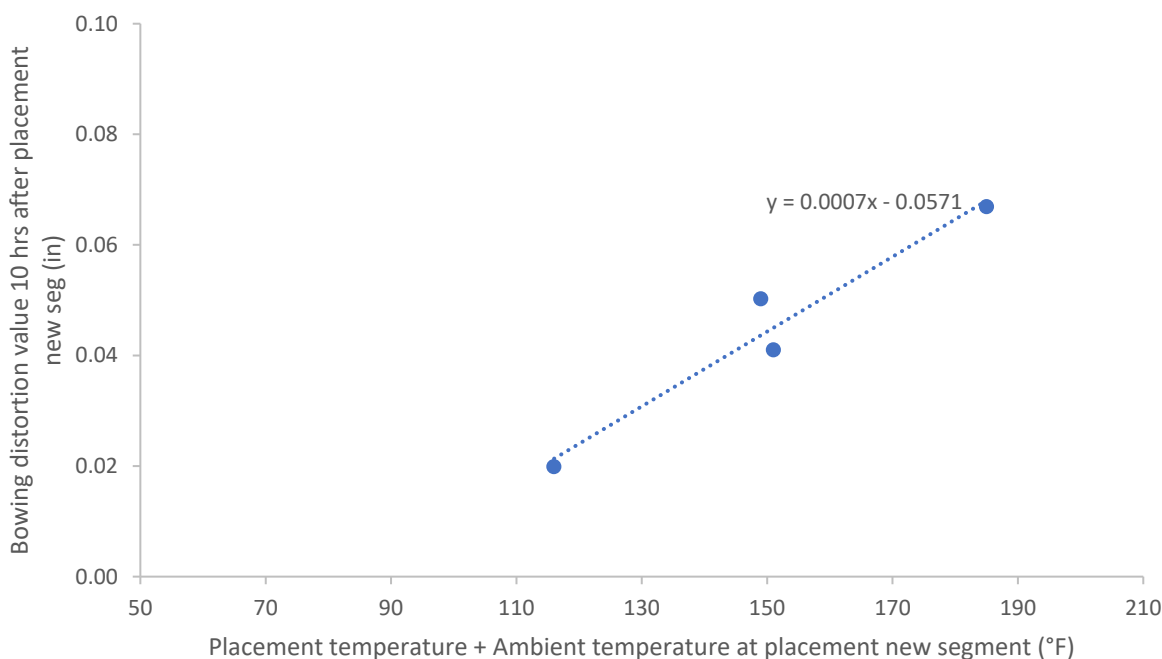
Figure 46: Simulated bowing distortion plotted against the sum of the concrete placement temperature and ambient temperature at placement for Bridge C with a w/l ratio of 10.89, high heat of hydration and setting time

4.4.5 Effect of Wind

To analyze the influence of the ambient temperature on the bowing distortion, wind speed was plotted against the bowing distortion results for each geometry. Figure 47 shows results for the high heat of hydration and high setting time concrete mixtures. The bowing distortion decreased as the wind speed increased because the cooling effect of the wind in the newly cast segments prevented them from reaching higher temperatures as they hydrated and outweighed the detrimental effect that the wind induced in the match-cast segments for the various bridge geometries observed.
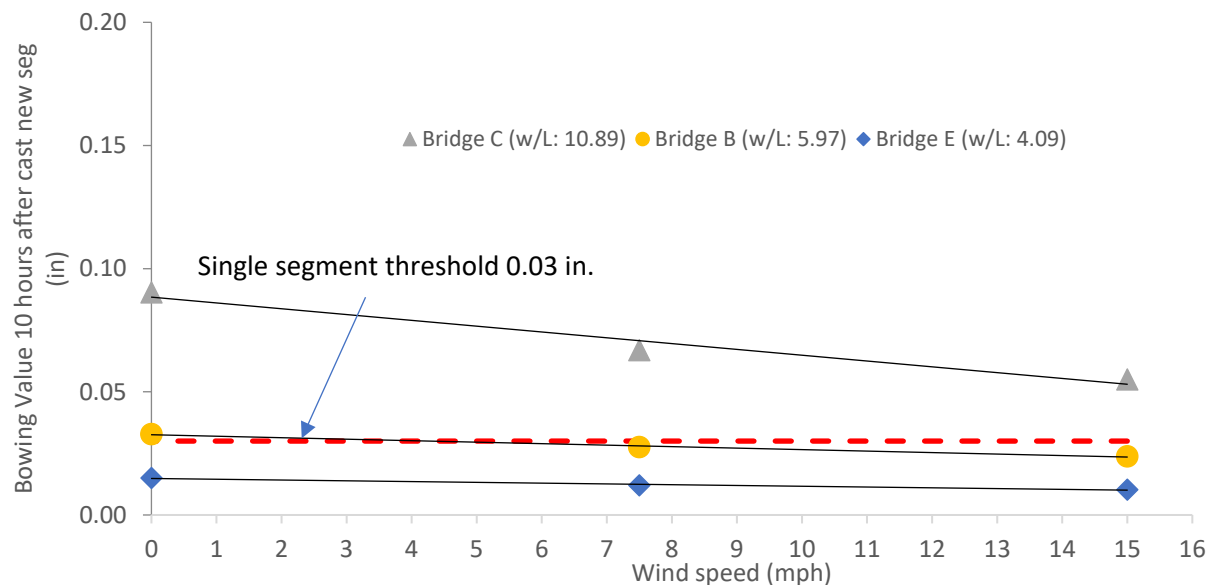
Figure 47: Simulated bowing distortion plotted against the wind speed for Bridge B (w/l: 5.97), Bridge C (w/l: 10.89), and Bridge E (w/l: 4.09), high heat of hydration and setting time

4.4.6   Effect of Insulation

Figure 48 shows the effect of using insulation to cover the segments during the match-casting process for several geometries using different levels of heat of hydration for the mixes. It was found that using the same level of insulation for both segments in the match-casting process could be detrimental for the bowing distortion problem. Using insulation to cover the match-cast segment while the newly cast segment cures has been documented as beneficial due to the fact that it prevents the concrete from cooling down on its free face, which can make the bowing distortion issue worse [1], [3], [5], [104]. However, results from this study showed that using the same level-material of insulation in the newly cast segment as it hydrates outweighs the beneficial effect that the insulation could have in the match-cast segment to prevent the bowing distortion, mainly when using high heat of hydration mixes, because it causes the concrete in the newly cast segment to reach higher temperatures. This effect influenced the bowing distortion more than the beneficial insulating effect in the match-cast segment. This was suggested as a possibility by Abendeh [3] but it was not modelled.
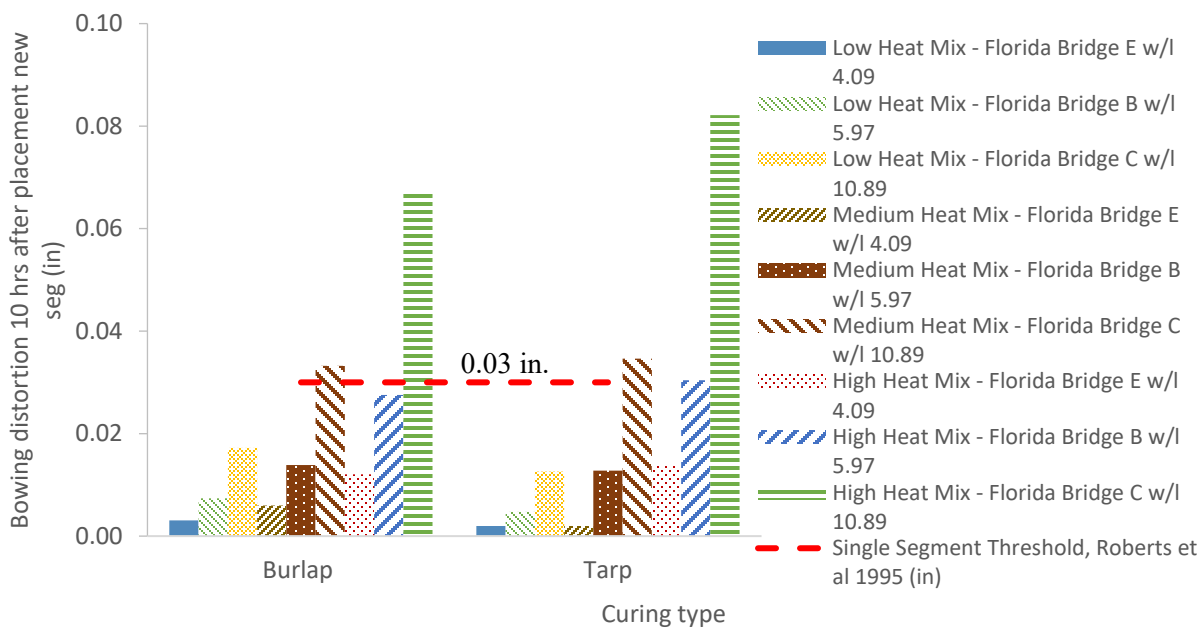
Figure 48: Effect of use of insulation for various cases

4.4.7 Effect of Steam Curing

Figure 49 shows the effect of using steam curing cycles in the match-casting process on the bowing distortion using the winter cases as control cases. Keeping the match-cast segment warm was mentioned as a method to reduce the bowing distortion problem [104]. However, this study found that for typical Florida winter conditions, steam curing cycles increased the temperatures reached by the newly cast segments and caused the bowing distortion to increase. These higher temperature increases outweighed the beneficial effects that the steam curing cycles had on the match-cast segment. The application of 160°F cycles to the match-casting process resulted in less bowing distortion in the match-cast segment because of the greater warming effect that it had in the match-cast segment. The influence of the application of the 130°F and 160°F steam curing cycles on the maximum temperatures reached in the newly cast segments were similar.
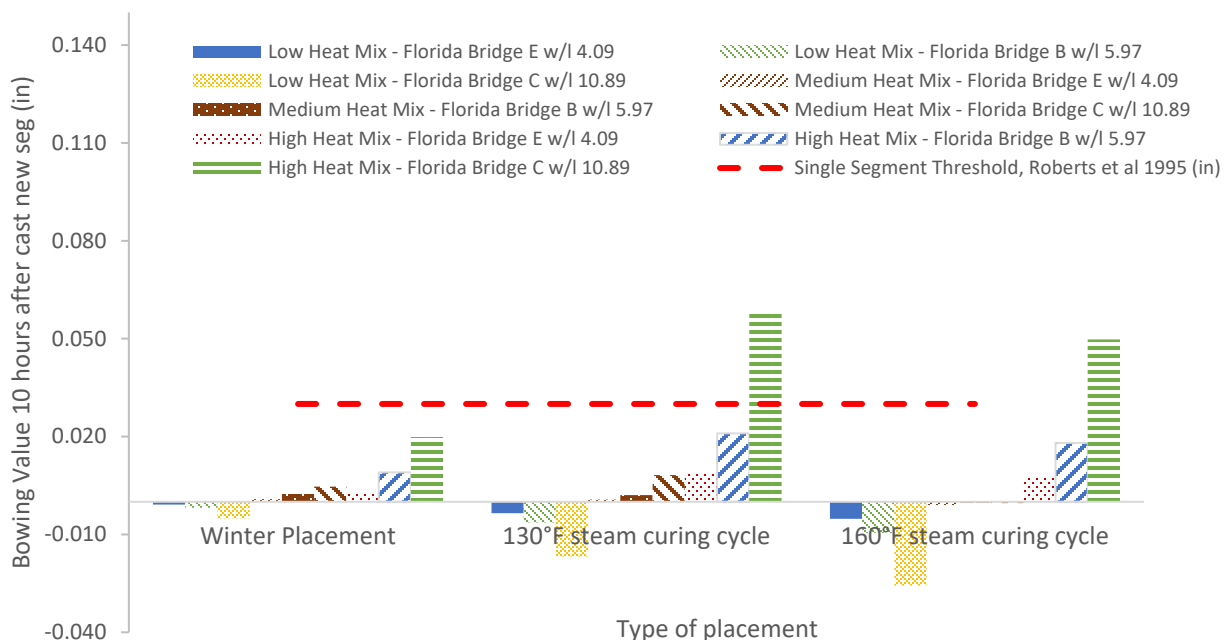
Figure 49: Effect of use of steam curing for various cases

4.5 Summary of Results

Bowing distortion during curing for bridge segments made with the short line match-cast method were simulated using different material and construction method combinations using finite elements methods. The sensitivity of the bowing distortion value locked in the newly cast segment due to changes in member geometry, concrete heat of hydration, aggregate type, weather conditions, curing techniques and steam curing application were studied. Among these parameters, member w/l and material properties were found to have the greatest influence on segment distortion. Thermal boundary conditions applied to the segments such as ambient temperatures, wind speed conditions, curing method used, and steam curing presented mixed results and had less of an impact on the bowing distortion. Segments with a w/l lower than six had a low risk of excessive bowing distortion in the simulations. The results showed that the use of low heat of hydration mixes can reduce the bowing distortion generated in the match-cast segment, but this is not always possible due to construction productivity needs. Using a combination of aggregates that produce a low CTE concrete was found to be one means of reducing bowing distortion. A decrease in the concrete placement temperature can reduce the bowing distortion risk. The placement temperature of the concrete added to the ambient temperature at the time of concrete placement temperature correlated with the bowing distortion, all other factors being equal. High wind speeds provided a cooling effect in the newly cast segment, causing a small reduction in the thermal gradient in the match-cast segment and the bowing distortion. Insulating materials used for curing the newly cast segment were found to increase the bowing distortion in the match-cast segment, using non-insulating materials for curing the newly cast segment reduced the bowing distortion in the match-cast segment. The effect that steam curing had in the mitigation of bowing distortion for winter cases in Florida could be detrimental, depending on the concrete mixture used.

5 Laboratory Temperature Validation Testing

5.1 Introduction

The construction of segmental post-tensioned concrete box girder bridges is important in Florida and the U.S. It has provided bridge designers and contractors a fast and versatile bridge solution for urban transportation needs as well as rivers and valley crossings [1], [2]. The two types of construction methods used to fabricate precast box girders are the long line casting and the short line casting method [3], with the short line casting method preferred because of its advantages in terms of space and formwork requirements [1], [2]. Although both methods use the match-casting process, a potential problem has been identified in certain cases in the short line casting method. The high heat of hydration of the new segment can induce a thermal gradient along the length of the previously cast segment that causes the segment to bow away from the new segment before the newly cast concrete has set. When the concrete in the new segment sets, it acquires the curvature of the match-cast segment at that moment, producing segments with the side that was in contact with the bulkhead straight and the side that was in contact with the previously cast segment curved [1], [2]. The match-cast segment returns to its original shape after the induced thermal gradient has cooled down [2]. This permanent curvature on one of the faces of the segments has caused construction problems [1] and could also cause structural issues in some cases [2].

As part of this research effort to develop best practices that can be used to mitigate the bowing distortion of match-cast segmental bridge segments during production, several construction scenarios are modeled using the finite element (FE) software package b4cast. b4cast is a finite element software that is able to simulate temperatures of concrete members during hardening [4]. It is also able to simulate the temperature of concrete members that are in contact with other hardening concrete members.

As a validation of the software's ability to predict concrete member temperatures, a physical model consisting of two slabs, placed one week from each other with contact on one of their faces was made. Temperature instrumentation was installed in both slabs and the measured results are compared with a corresponding model defined in b4Cast. Good agreement was observed between the results measured and the results from the finite element model.

5.2 Materials

5.2.1 Mix Components

ASTM C150 [5] Type I/II, No. 89 Florida oolitic limestone, silica sand and ADVA Cast 600 admixture were used in the concrete mixture. The cement oxide composition measured by x-ray fluorescence (XRF) is presented in Table 37 [7]. The cement phase composition calculated from x-ray diffraction with Rietveld refinement according to ASTM C1365 [8] is shown in Table 38.

Table 37: Cement oxide composition

Cement Type I/II X-Ray Fluorescence	
Compound	**wt%**
SiO_2	21.0%
TiO_2	0.2%
Al_2O_3	5.1%
Fe_2O_3	3.3%
MnO	0.1%
MgO	0.7%
CaO	66.7%
Na_2O	0.10%
K_2O	0.24%
P_2O_5	0.15%
LOI	3.0%

Table 38: Cement phase composition

Cement Type I/II Composition	
Phase	**%**
Alite	49.9%
Belite	18.3%
Aluminate	9.7%
Ferrite	10.3%
Anhydrite	0.5%
Bassanite	0.0%
Gypsum	5.2%
Arcanite	0.9%
Calcite	4.0%
Free Lime	0.8%
MgO	0.3%
Quartz	0.0%

No. 89 Florida oolitic limestone obtained from the FDOT materials research center in Gainesville was used as the coarse aggregate for the mix. Specific gravity and absorption for coarse aggregate were tested according to ASTM C127 [9], as shown in Table 39. Silica sand also obtained from the FDOT materials research center in Gainesville was used as the fine aggregate for the mix. The specific gravity and absorption for the natural silica sand used as fine aggregate was tested as per ASTM C128 [10], as shown in Table 39.

Table 39: Aggregate properties

Property	No. 89 Limestone	Silica Sand
Specific Gravity	2.44	2.60
Absorption (%)	5.75	0.08

5.2.2 Concrete Mixture Design

The concrete mix design used for the temperature validation testing is shown in Table 40.

Table 40: Mix design

Mix Design	
Material	**Quantity**
Cement (lb/yd^3)	725
Water (lb/yd^3)	254
Fine Agg. (lb/yd^3)	1201
Coarse Agg. (lb/yd^3)	1680
Admixture ADVA (oz)	19.85 oz

5.3 Methodology

5.3.1 Slab Construction

A concrete specimen was fabricated in two parts to simulate match-cast construction and instrumented to measure the temperature development in each half while curing the second section. Each half of the slab was 2 ft x 4 ft x 10 in, as seen in Figure 50. The first half (slab 1) was cast a week before the second half (slab 2), with full contact on one face. This was done to mimic the short line match-cast construction process where heat is transferred from the newly placed concrete to the previously placed concrete by conduction across the joint-interface.
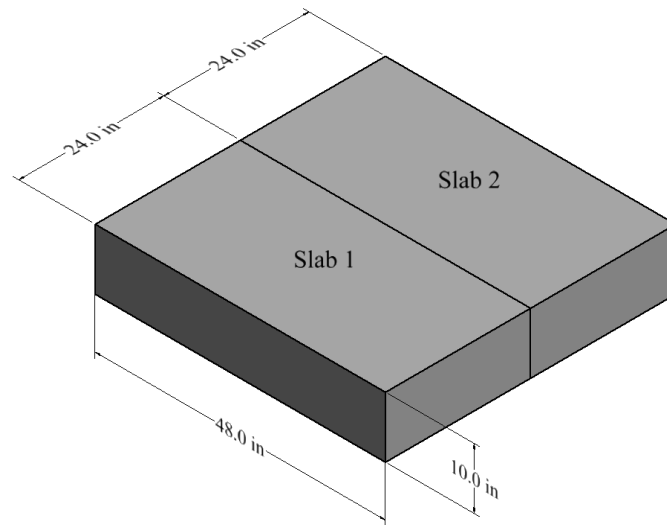
Figure 50: Slab specimens dimensions

Melamine boards 5/8 in. thick were used to construct the concrete formwork. A temporary divider board was installed for the placement of the first slab, then removed for the placement of the second slab the week after. The thermocouples were held in place by attaching them to a 5/8 in. diameter fiberglass rod passing through the middle of the slabs, as can be seen in Figure 51.

Figure 51: Formwork for slabs construction

Each specimen half required a concrete volume of 6.67 ft^3. Two batches were needed for each half because the available concrete mixer in the laboratory had a maximum capacity of 6 ft^3. For the first slab two 4.6 ft^3 concrete batches were made and for the second half two 4.4 ft^3 were made. The volume for the first slab was higher to accommodate test samples. Figure 52 shows the first slab shortly after concrete placement. The slab was cured with plastic to reduce the evaporation rate from the concrete. While there are many potential curing methods that could be used on the concrete, only one was used in this experiment and was judged sufficient to determine the validity of the b4cast software.

Figure 52: Concrete specimen after placement of the first half

5.3.2 Slabs Temperature Measurement

Each slab had thermocouples installed for temperature measurement. Slab 1 had 8 thermocouples installed along its longitudinal length connected to an 8-channel Omega Daqpro-5300 datalogger. Slab 2 had 7 thermocouples installed along its longitudinal length connected to an 8-channel PicoLog TC-08 datalogger. The 8th channel in the PicoLog datalogger was used to measure the room temperature for use as an input in the finite element model of the slabs. Diagrams of thermocouple placement are shown in Figure 53 (plan view) and Figure 54 (elevation view).
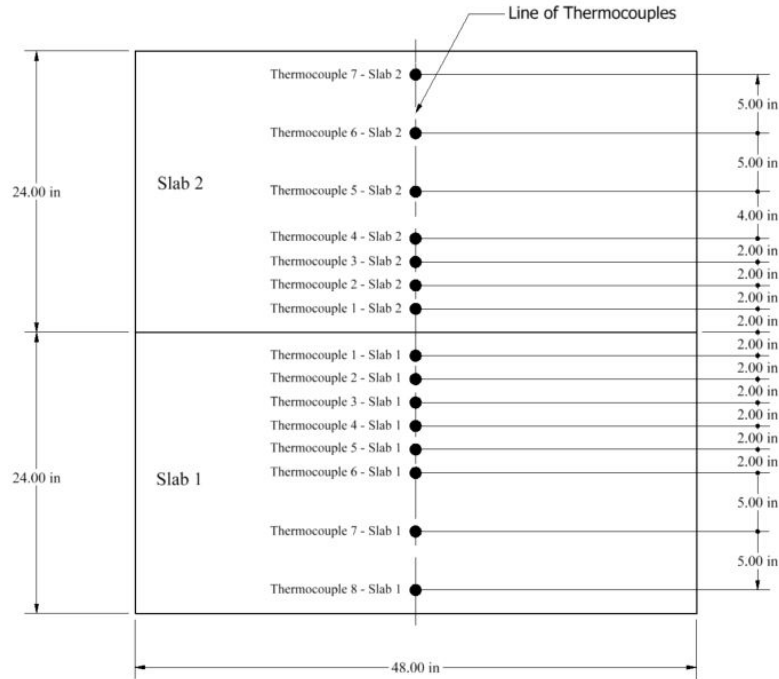
Figure 53: Plan view of thermocouple setup
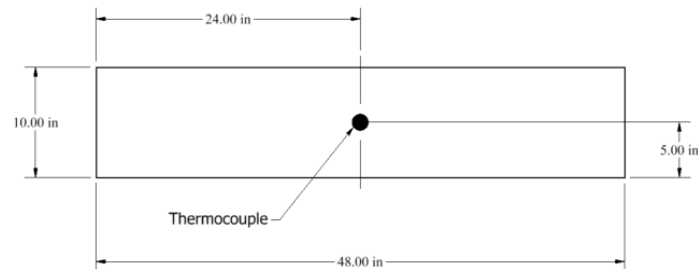
Figure 54: Elevation view of thermocouple setup

5.3.3 Concrete Heat of Hydration Parameters Estimation

b4cast uses a three-parameter exponential degree of hydration model similar to that described by Riding et al. [11] to describe the hydration development of concrete [12], as shown in Equation 85:

$$Q(t_e) = \alpha_u \cdot H_u \cdot exp\left[-\left(\frac{\tau}{t_e}\right)^{\beta}\right]$$ Equation 85

Where: Q = adiabatic heat of hydration.

   α_u = ultimate degree of hydration parameter.

H_u= total heat available for reaction (BTU/lb).

τ= hydration time parameter (hr).

t_e= concrete equivalent age at the reference temperature -68ºF (20ºC)- (hr).

β= hydration slope parameter.

The equivalent age function selected to use in b4cast is the Arrhenius equivalent age expression [11], [12], presented in Equation 13. To simulate the heat of hydration development of the concrete mix in b4cast, the hydration properties of the mix are obtained by calculating the parameters H_u, E_a, α_u, τ and β. These parameters are calculated using models found in Riding et al. [11] and Schindler & Folliard [13] along with the cement X-ray fluorescence shown in Table 37 and the cement phase information seen in Table 38. The total heat available for reaction, H_u was calculated using the models presented in Equation 17 and Equation 18 [13]. The apparent activation energy of the mix, E_a, was also calculated using a mechanistic-empirical model presented in Equation 15 [11]. The ultimate degree of hydration parameter, α_u, was calculated using the model presented in Equation 20 [11]. The hydration slope parameter, β, was calculated using the model presented in Equation 22 [11]. The hydration time parameter, τ, was calculated using the model presented in Equation 21 [11]. The heat of hydration parameters calculated for the concrete used in this study are presented in Table 41:

Table 41: Concrete heat of hydration parameters

Heat of Hydration Parameter	Value
Hydration Slope Parameter, β -Curvature Parameter-	1.058
Hydration Time Parameter, τ (hr)	16.579
Ultimate Degree of Hydration, α_u	0.724

5.3.4   Finite Element Software Details

b4cast is a finite element software package that is able to simulate temperatures, displacements and stresses in 3-dimensional concrete structures during hardening [4]. In this report, only the temperature simulation capabilities of the software are tested. Tetrahedral elements capable of modeling constant, linear, or parabolic variations of temperature (within each element) are used to simulate the slabs [4]. The finite element mesh representing the laboratory slabs is shown in Figure 55.
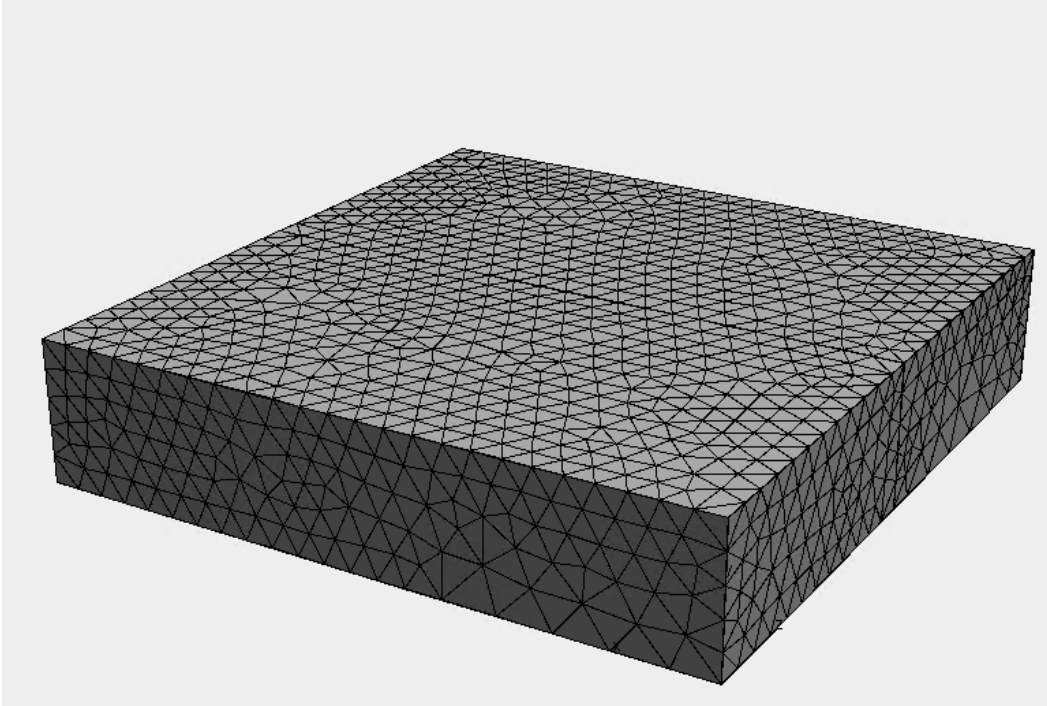
Figure 55: Meshed slabs in b4cast

The slab temperatures were simulated for 165 hr after the placement of the concrete of slab 2. The temperature of slab 1 was uniform throughout before slab 2 was placed and the concrete heat of hydration in slab 1 was negligible at that point, therefore heat of hydration properties were not assigned to slab 1.

The parameters used in the definition of the finite element model are provided in Table 42.

Table 42: Input parameters in the finite element model

Parameter	Slab 1	Slab 2
Initial Temperature (°F)	71.006	73.508
Maximum Element Mesh Size (in)	1.969	1.969
Apparent Activation Energy Value (BTU/mol)	32.263	32.263
Cement Content (lb/yd^3)	n/a	725.000
Hydration Slope Parameter, β -Curvature Parameter-	n/a	1.058
Hydration Time Parameter, τ (hr)	n/a	16.579
Ultimate Degree of Hydration, α_u	n/a	0.724
Total Heat Available for Reaction, H_u (BTU/lb)	n/a	195.005
Total Heat Development Value ($\alpha_u \cdot H_u$) (BTU/lb)	n/a	141.183
Concrete Density (lb/yd^3)	3852.865	3853.945
Concrete Specific Heat (Heat Capacity) (BTU/(lb·°F))	0.202	0.202
Concrete Thermal Conductivity (BTU/(ft·hr·°F))	1.570	1.570
Time Step (hr)	1.000	1.000
Formwork -shield- (BTU/(ft·hr·°F)) -applied to appropriate faces-	Wood - 0.081	Wood - 0.081
Convection Temperature (°F) -applied to all faces-	Measured temperature	Measured temperature
Wind Speed (mph) -applied to all faces-	0	0

Description of the Parameters:

Initial Temperature: For slab 1, the average temperature from all thermocouples read approximately 3 hr before the slab 2 placement was used as the initial temperature. That average value of 70.742 ºF was rounded to 71ºF in the simulation.

For slab 2, the concrete placement temperature used in the simulation was 73.5 ºF.

Maximum Element Size: The maximum element size chosen for meshing of both slabs was 1.969 in (0.05 m). Simulations with smaller maximum element sizes of 1.66 in. (0.04 m) and 1.42 in. (0.036 m) were also analyzed. Those temperature results were similar to that of the larger mesh size used, confirming that a maximum element mesh size of 1.969 in. was adequate.

Activation Energy: The apparent activation energy was calculated using Equation 15.

Hydration – Parameters: The hydration parameters were not applicable for slab 1 because the heat generation was considered negligible after 1 week of curing. For slab 2, the values used for the hydration parameters α_u, τ, and β are shown in Table 42. For slab 2, the value used for the total heat available for reaction H_u was calculated using Equation 17 and Equation 18. In b4Cast, the product of the parameters α_u and H_u is input as the total heat development value, Q_{total} [12].

Concrete Density: For each slab, the average of the batch unit weight measurements was chosen as the input value for the density in the software.

Concrete Specific Heat: The same specific heat value was assigned to both slabs in the simulations. This value was obtained by using the content percentage of coarse and fine aggregate in the mix and using typical specific heat values for them. The oolitic limestone specific heat value was chosen to be 0.19 (BTU/(lb·°F)) [15], while the silica sand specific heat was chosen to be 0.22 (BTU/(lb·°F)) [2], [15].

Concrete Thermal Conductivity: The same value was assigned for thermal conductivity for both slabs. A typical value for concrete of 1.57 (BTU/(ft·hr·°F)) [16] was selected for use in the model.

Formwork Application: Melamine boards with 0.75-in. thickness were used as formwork. Thermal conductivity for wood ranges from 0.081 to 0.105 (BTU/(ft·hr·°F)) [17]. A value of 0.081(BTU/(ft·hr·°F)) was chosen for the formwork in the simulations.

Convection Temperature: Room temperature was measured after placement of slab 2, as shown Figure 56. These measured temperatures were input as a convection temperature curve in contact with all the exposed faces of the concrete slabs.
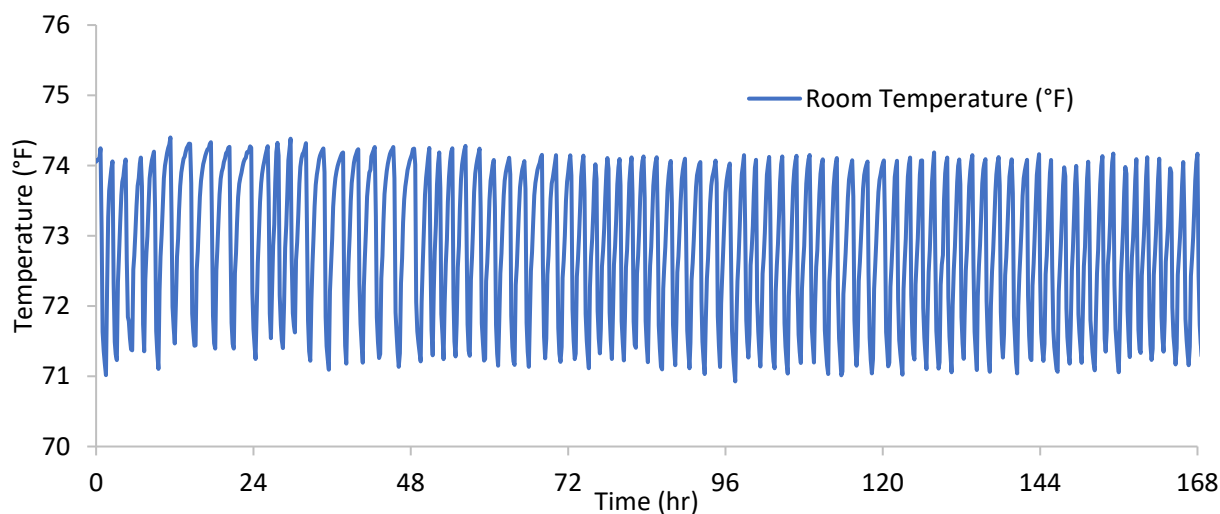
Figure 56: Measured room temperature

Wind: Wind speed was assigned in the simulation to be 0 mph to all the faces in the model because the slabs were indoors.

Time Step Chosen: The time step chosen for the simulation was 1 hr. Temperature results from 0.75 hr and 0.5 hr time steps were similar to those with a 1 hr time step, so it was determined that a 1 hr time step was appropriate.

5.4 Experimental Results

5.4.1 Concrete Testing Results

Table 43 shows the concrete fresh properties. Concrete strengths were measured according to ASTM C39 [18] at 28 days, with the average results for each slab shown in Table 44.

Table 43: Measured fresh concrete properties

Fresh Concrete Properties				
Test	Slab 1 - Batch 1	Slab 1 - Batch 2	Slab 2 - Batch 1	Slab 2 - Batch 2
Slump (in)	1.00	2.75	1.00	1.50
Placement Temperature (ºF)	75.00	75.00	75.00	76.00
Unit Weight (lb/ft^3)	143.04	142.32	143.00	142.44
Air Content, %	2.80%	3.50%	3.60%	3.50%

Table 44: Concrete tested 28-day compressive strength

Concrete 28-day strength		
Test	Slab 1	Slab 2
Strength (psi)	8290	8570

5.4.2 Results (Measured data vs. Finite Element)

Figure 57 through Figure 71 show the simulated and measured concrete temperatures for each thermocouple used in the slabs. In these figures, the initial time (t = 0 hr) indicate the moment when slab 2 was cast. Slab 1 was 7 days old at this initial time (t = 0 hr). Results for thermocouple 1 in slab 1 and thermocouple 2 in slab 2 are not presented as the data recorded by those sensors was out of the range of measurements and was deemed unreliable.
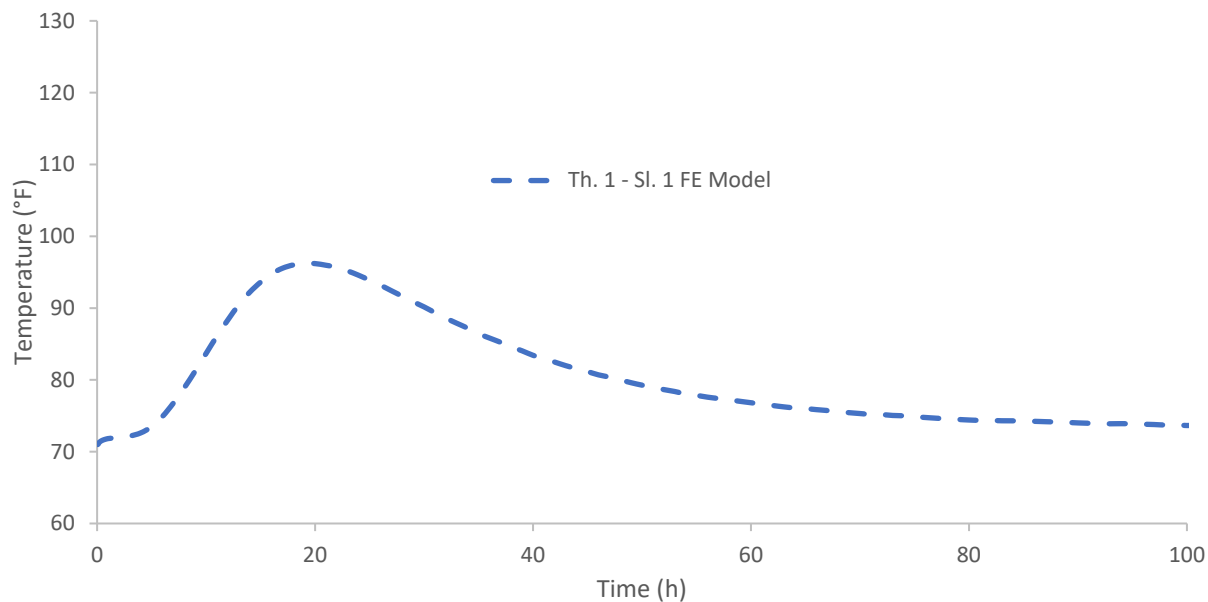
Figure 57: Thermocouple 1 - slab 1 - FE results
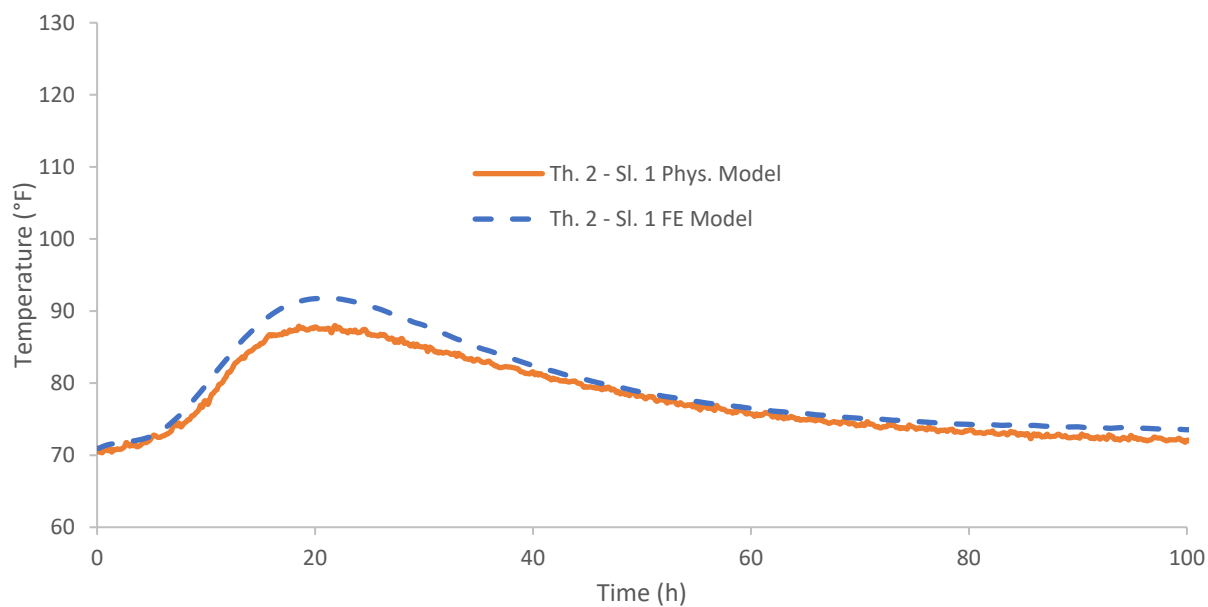
Figure 58: Thermocouple 2 - slab 1 - comparison of measured temperatures vs. FE results
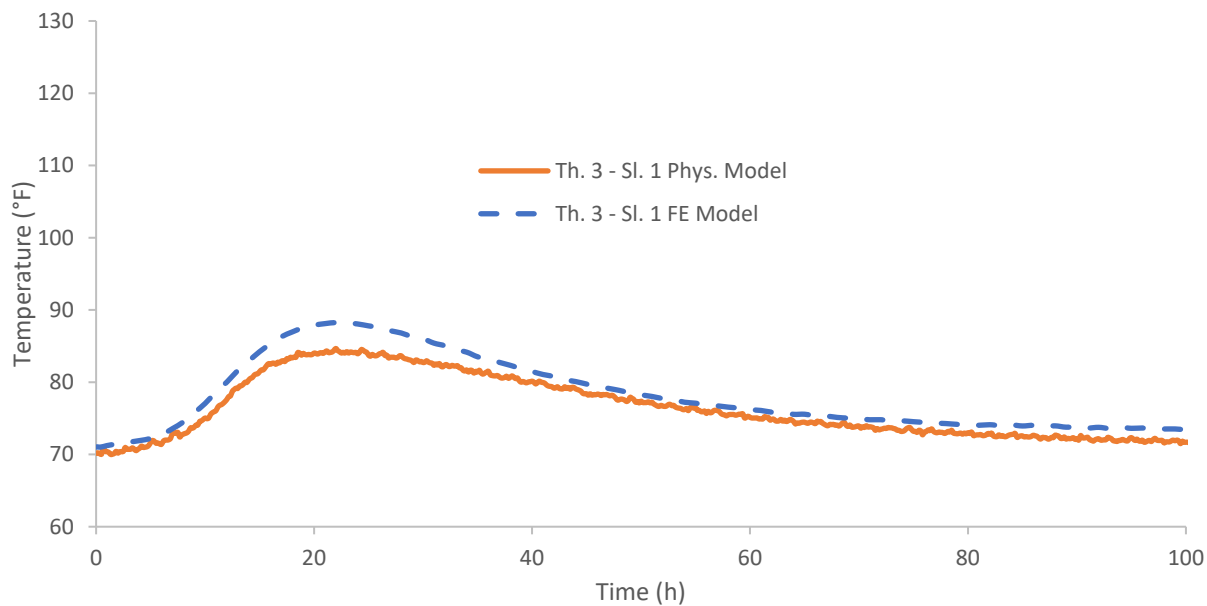
Figure 59: Thermocouple 3 - slab 1 - comparison of measured temperatures vs. FE results
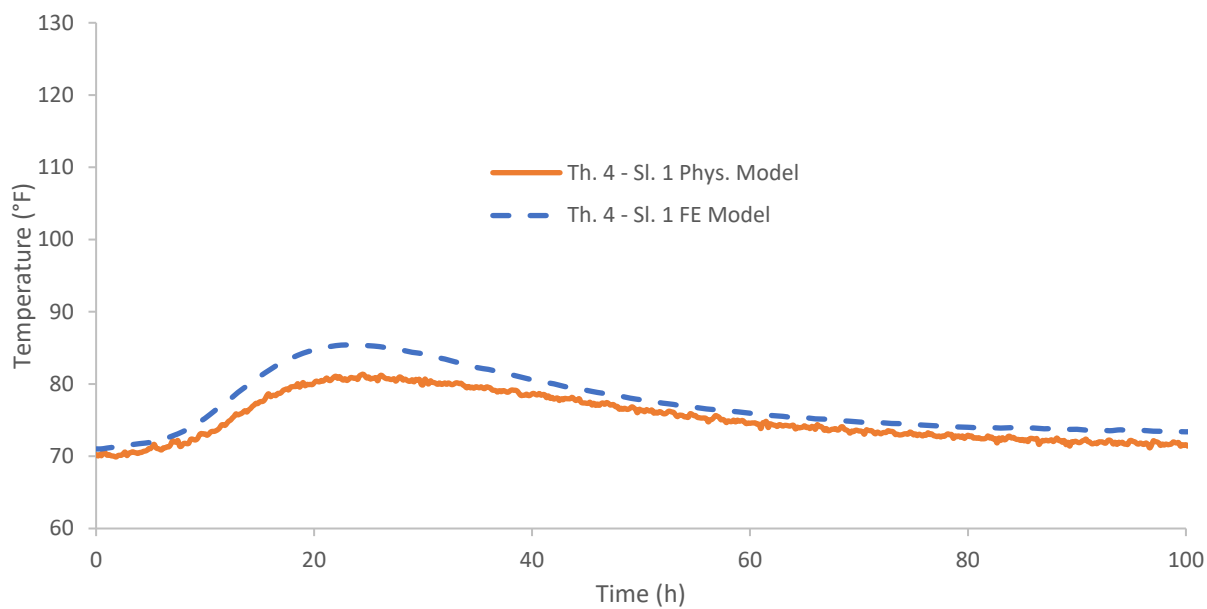
Figure 60: Thermocouple 4 - slab 1 - comparison of measured temperatures vs. FE results
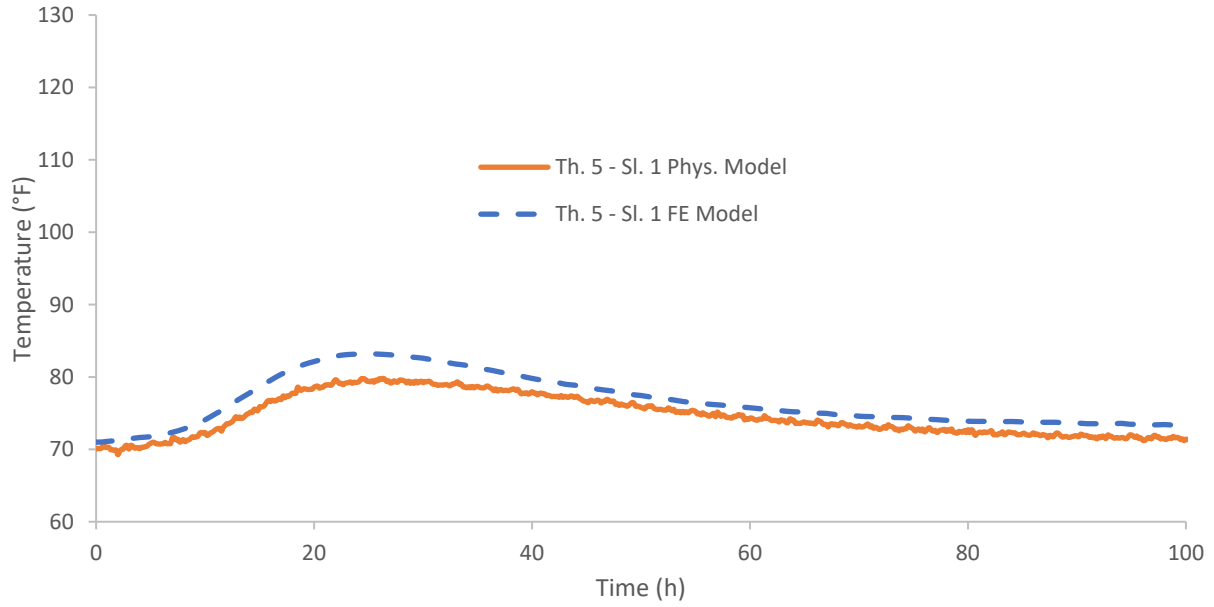
Figure 61: Thermocouple 5 - slab 1 - comparison of measured temperatures vs. FE results
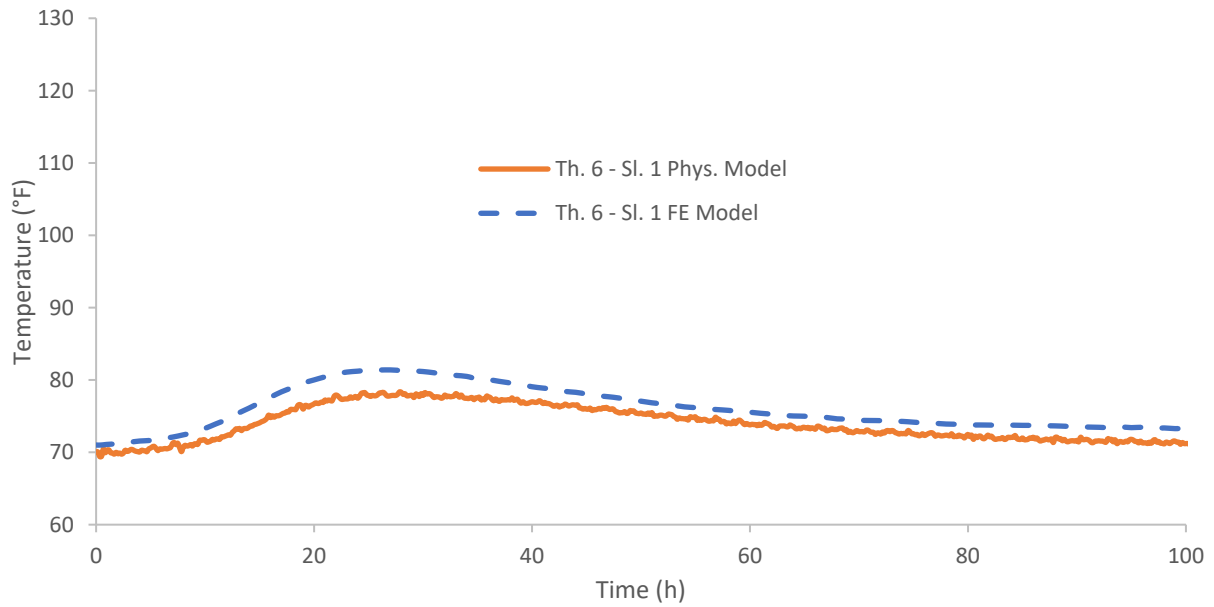
Figure 62: Thermocouple 6 - slab 1 - comparison of measured temperatures vs. FE results
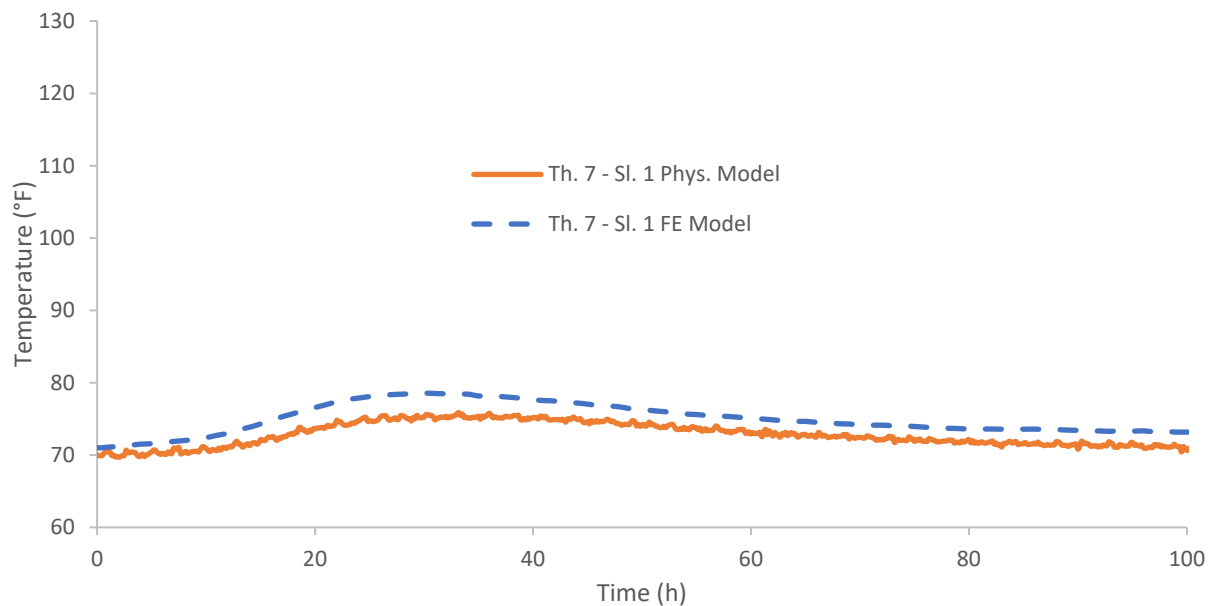
Figure 63: Thermocouple 7 - slab 1 - comparison of measured temperatures vs. FE results
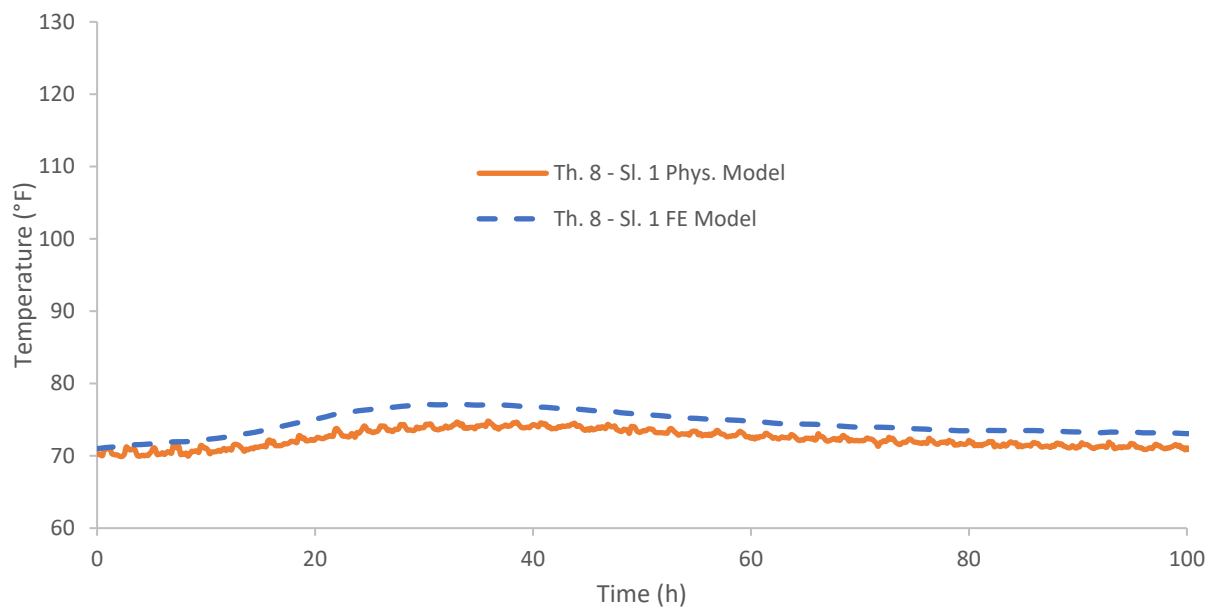
Figure 64: Thermocouple 8 - slab 1 - comparison of measured temperatures vs. FE results
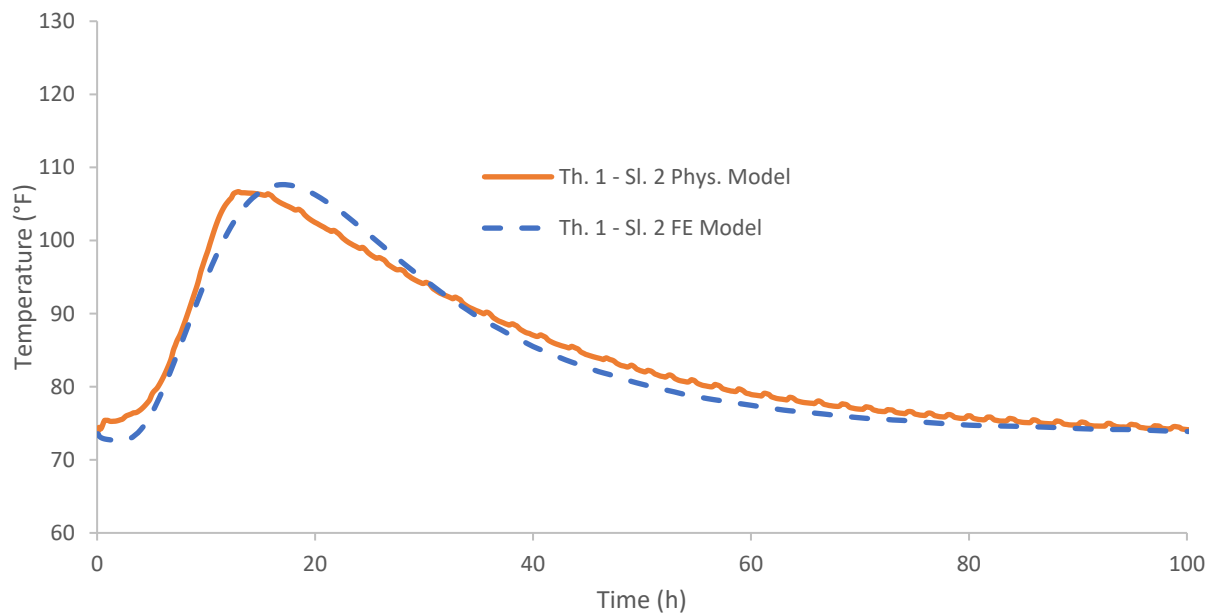
Figure 65: Thermocouple 1 - slab 2 - comparison of measured temperatures vs. FE results
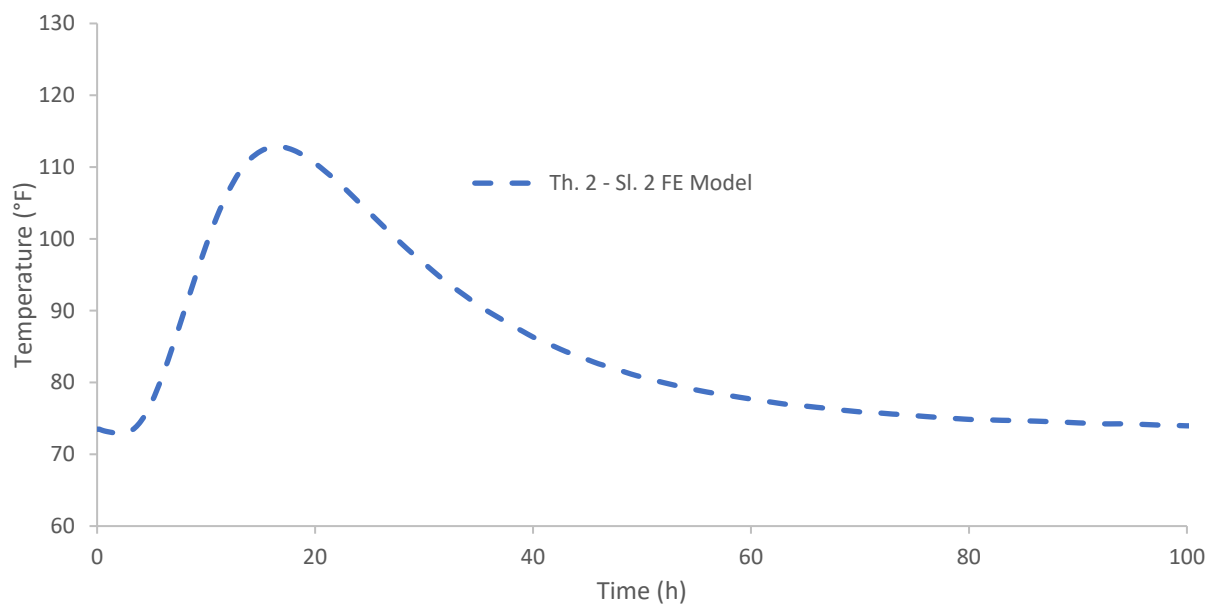
Figure 66: Thermocouple 2 - slab 2 - FE results
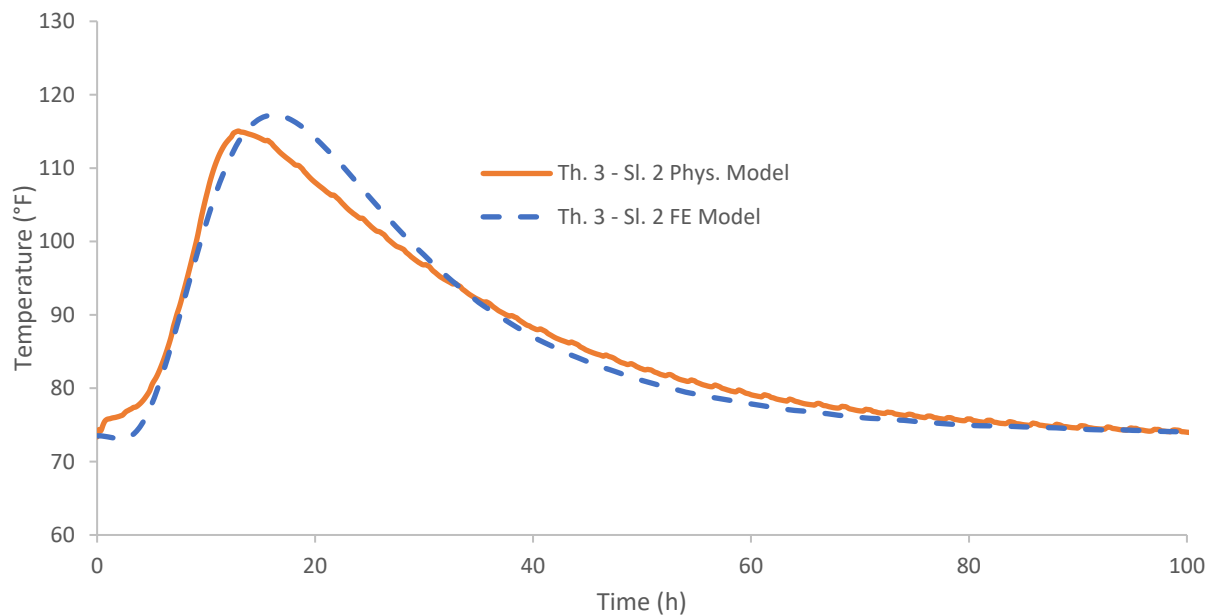
Figure 67: Thermocouple 3 - slab 2 - comparison of measured temperatures vs. FE results
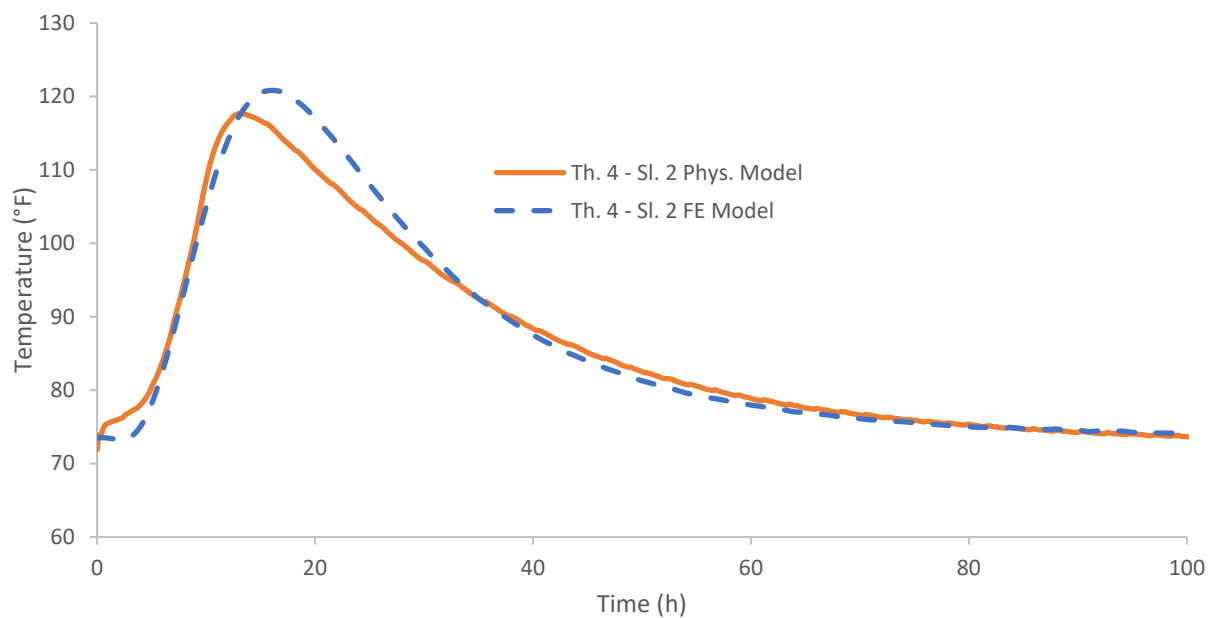
Figure 68: Thermocouple 4 - slab 2 - comparison of measured temperatures vs. FE results
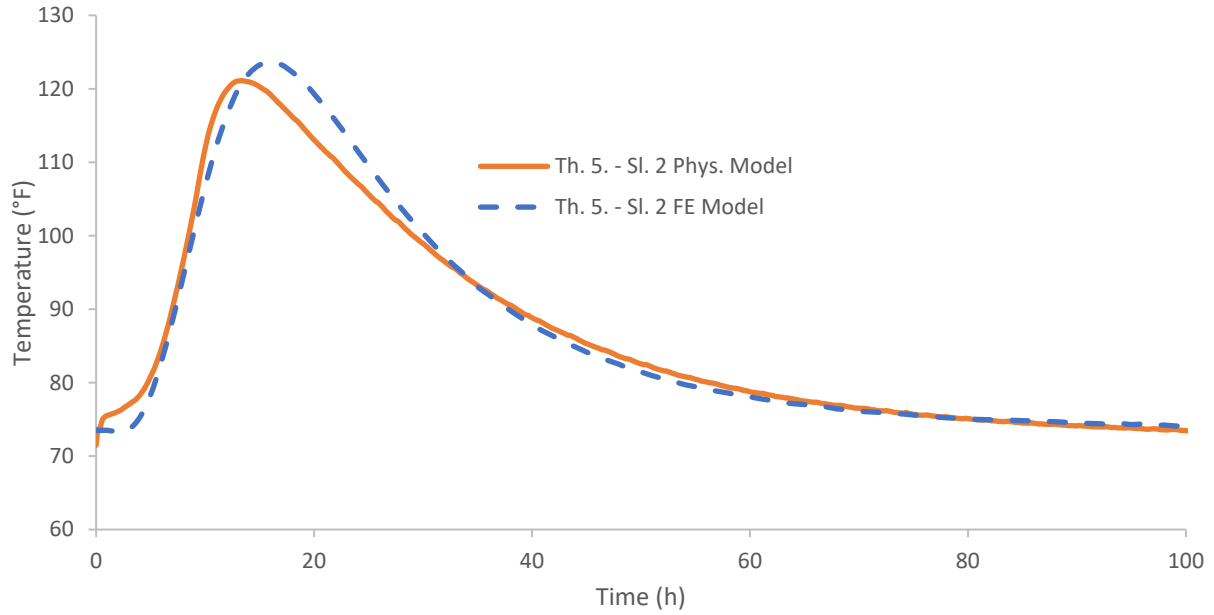
Figure 69: Thermocouple 5 - slab 2 - comparison of measured temperatures vs. FE results
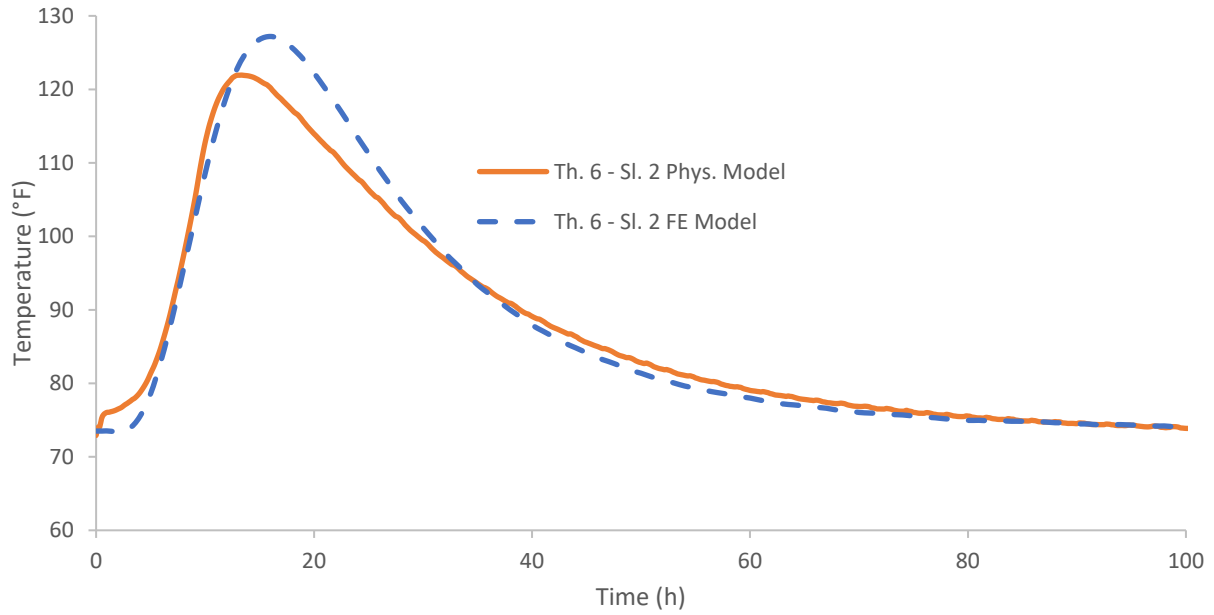
Figure 70: Thermocouple 6 - slab 2 - comparison of measured temperatures vs. FE results
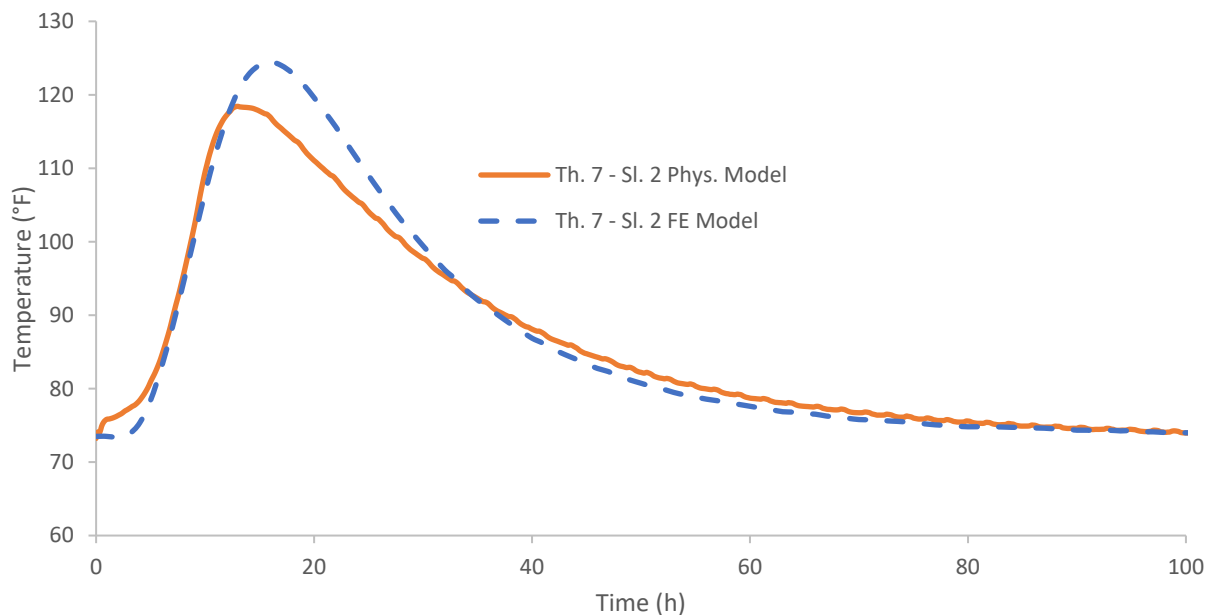
Figure 71: Thermocouple 7 - slab 2 - comparison of measured temperatures vs. FE results

Table 45 and Table 46 provide summaries of the average temperature differences and maximum temperature differences between the measured temperatures and the modelled temperatures for the first 30 hr after casting of second slab for slab 1 and slab 2, respectively.

Table 45: Slab 1 results summary

Thermocouple	Average Difference Between Laboratory Measurements and FE model (°F) – First 30 hr after casting second slab-	Maximum Difference Between Laboratory Measurements and FE model (°F) – First 30 hr after casting second slab-
Thermocouple 2 - Slab 1	2.54	4.50
Thermocouple 3 - Slab 1	2.59	4.12
Thermocouple 4 - Slab 1	3.02	4.92
Thermocouple 5 - Slab 1	2.56	3.91
Thermocouple 6 - Slab 1	2.50	3.74
Thermocouple 7 - Slab 1	2.25	3.51
Thermocouple 8 - Slab 1	2.01	3.47

Table 46: Slab 2 results summary

Thermocouple	Average Difference Between Laboratory Measurements and FE model (°F)– First 30 hr after casting second slab-	Maximum Difference Between Laboratory Measurements and FE model (°F) – First 30 hr after casting second slab-
Thermocouple 1 - Slab 2	2.39	4.29
Thermocouple 3 - Slab 2	3.21	6.07
Thermocouple 4 - Slab 2	3.56	6.98
Thermocouple 5 - Slab 2	3.49	6.29
Thermocouple 6 - Slab 2	4.19	8.49
Thermocouple 7 - Slab 2	4.11	8.86

Temperatures along the length of the slab, at different points in time after casting the second slab, were quantified for both the laboratory slab and the finite element model. Good agreement in temperature distributions was observed. Results for the laboratory slab are presented in Figure 72 and results for the finite element model are provided in Figure 73.
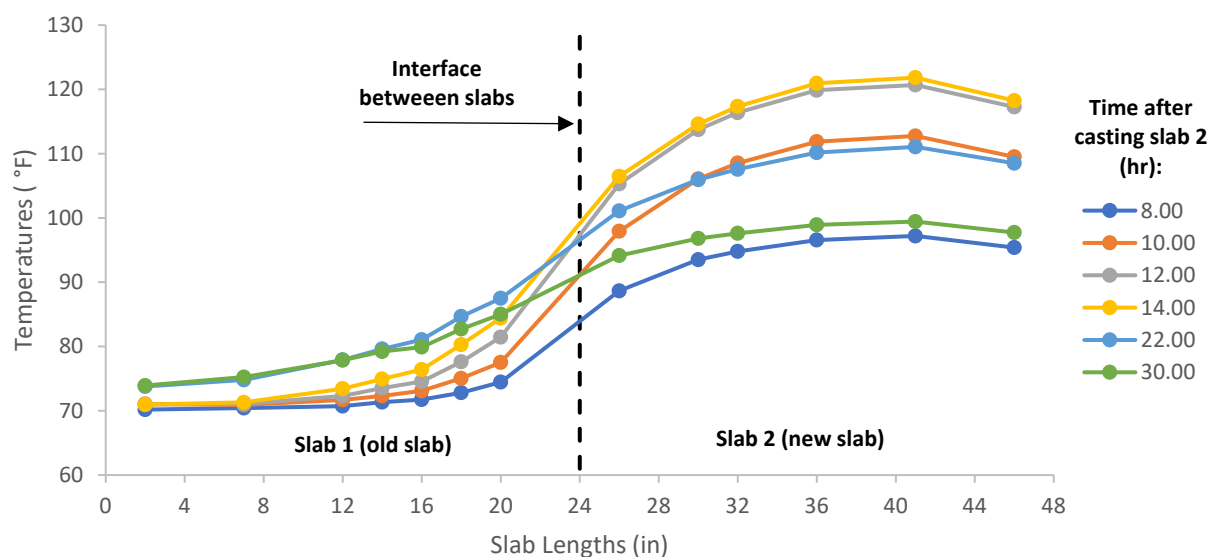
Figure 72: Temperature results measured in the laboratory
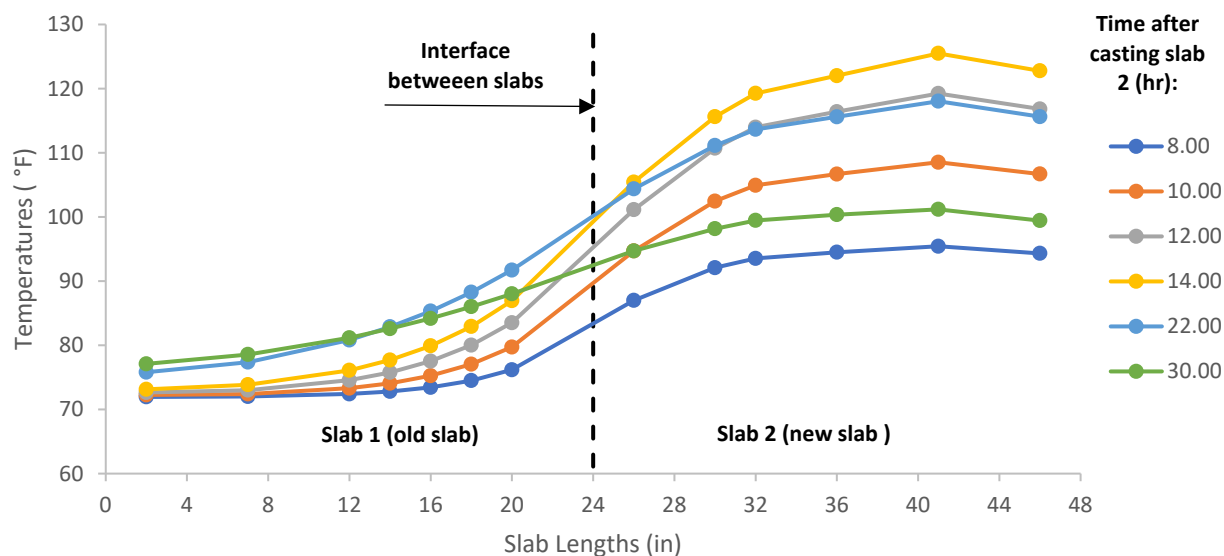
Figure 73: Temperature results from finite element simulation

5.5 Discussion of Results and Conclusions

Two separate concrete slabs with contact at a common transverse interface were cast one week apart and instrumented longitudinally for temperature measurement. This configuration was used as a simplified representation of the short line match-casting segment construction method in precast segmental bridge construction.

The finite element software package b4cast was used to build a model representing the conditions of the specimens constructed. Temperature results were extracted at corresponding positions in the laboratory slab and FE model to validate the capability of b4cast to model temperatures developed along the lengths of the hydrating concrete slab and a previously cast slab.

In slab 1, good agreement between measured temperatures and modeled temperatures was observed for all thermocouples. The bowing distortion issue that has been documented in the short line match-casting segment construction method is induced by a temperature gradient that develops mainly from 0 to 1 ft of the face of the top slab of the previously cast segment that is in contact with the newly cast segment [1], [2]. Results in slab 1 in this range, thermocouples 2 to 6, have a maximum average difference between measured vs. modeled results of 3.02ºF and a maximum difference of 4.92ºF in the first 30 hr after casting the second slab, both in thermocouple 4 at 8 inches from the interface. This is considered to be in good agreement if compared with the validation model presented by Abendeh [2]. In that study, the thermal gradient induced in the match-cast segment at 10 hr after casting of the new segment in the San Antonio Y project exhibited a temperature increase of the match-cast segment of 27.7 ºF at the interface, 9.1 ºF at 6 inches from the interface, and 2.4 ºF at 12 inches from the interface.

In slab 2, good agreement was also observed between measured and modeled temperatures. The maximum average difference between the measured temperatures and modeled temperatures in

the first 30 hr after the placement of the second slab was 4.19 ºF, recorded at thermocouple 6 at 17 inches withing the interface between slabs. Likewise, the maximum difference between the measured temperatures and the modeled temperatures was 8.86 ºF, recorded by thermocouple 7 at 22 inches from the interface between slabs. Thermocouples 6 and 7 in slab 2 were the closest ones to the free face of the slab so differences at these locations could have been caused by an increased heat loss occurring in this area in the laboratory slab. The observed level of agreement between laboratory and simulation was considered good because the maximum temperature increase caused by hydration of the slab was approximately 45 ºF, resulting in a low difference as a percentage of the temperature increase.

b4cast was able to predict the temperature distribution along the length of both slabs, modeling well the heat of hydration and temperature distributions in slab 2 and the temperature distributions in slab 1 as a product of being in contact with slab 2. b4cast is therefore found to be suitable to model the short line match-cast construction process.

6 Segment Distortion Control Best Practices

6.1 Introduction

Currently the only requirement in the Florida Department of Transportation (FDOT) Standard Specifications for Road and Bridge Construction to prevent or mitigate bowing distortion is found in section 452-6.7 and is to cover the newly cast and match-cast segments with curing blankets to minimize the differential temperature between segments [1]. Roberts-Wollmann et al. [2] reported that in one case the accumulated bowing distortion from multiple segments caused an increase in the span length of 2.8 in. This produced difficulties to form the joint and with installation of tendon anchors in the joint.

Roberts-Wollmann et al. [3] proposed a fabrication bowing distortion limit of 0.03 in. for single segments with epoxied joints and an accumulated bowing distortion limit in a span of 0.5 in. to prevent difficulties in closing gaps caused by bowing distortion effects with temporary post-tensioning and to prevent closure pour size reductions. Using an example 12-segment bridge span (width of segment/length of segment ratio (w/l) of 3), Abendeh [4] showed, through finite element modeling, that bowing distortions of 0.06 in. per segment had compressive stresses immediately after loading lower than 0.2 ksi. The 0.2 ksi compressive stresses across dry joints is required by AASHTO specifications [5]. However, the model also showed that at time t=100 days the gaps closed and complied with the minimum required compressive stresses across joints. Abendeh [4] also showed that bowing distortions of 0.11 in. in every segment of a 16-segment span (w/l ratio of 10.7) prevented the span from reaching the 0.2 ksi minimum compressive stresses that is required across joints immediately after loading required by AASHTO specifications [5]. For this case, after 100 days, the gaps did not close and did not comply with the minimum required compressive stress across joints. However, at time t=∞ the gaps closed and complied with the minimum compressive stresses across joints per specifications.

In this study the 0.03 in. single segment threshold proposed by Roberts-Wollmann et al. [2] was used to evaluate mitigation measures.

6.2 Effectiveness of Roberts-Wollmann et al. [2] Analytical Expression

The expression developed by Roberts-Wollmann et al. [2] presented in Equation 86 was used to calculate the bowing distortion in the match-cast segment as a function of time.

$$\Delta = \frac{3 \cdot w^2 \cdot \alpha_t}{2 \cdot l^3} \cdot \left[\left(A_{t1} \cdot \left(\frac{l}{2} - cg_1 \right) - \left(A_{t2} \cdot \left(\frac{l}{2} - cg_2 \right) \right) \right) \right] \qquad \text{Equation 86}$$

Where: Δ = Bowing distortion of match-cast segment (in)

w = Width of the segment (in)

α_t = Coefficient of thermal expansion of concrete (1/ °F)

l = Length of the segment (in)

A_{t1} =Area under the curve of the gradient plot constructed from concrete temperatures in the match-cast segment from the face in contact with the newly cast segment (°F/in)

cg_1 = Distance from the face in contact with the newly cast segment to center of gravity of the area, A_{t1} (in)

A_{t2} = Area under the curve of the gradient plot constructed from concrete temperatures in the match-cast segment from free face of the segment (°F/in)

cg_2 = Distance from the free face of match-cast segment to center of gravity of the area, A_{t2} (in)

Equation 86 worked well in terms of predicting the bowing distortion in the match-cast segment when FE-based temperatures extracted from about 1/3 of the distance from the top slab-web-wing junction to the tip of the wings (See Figure 74) were used in Equation 86 [2], [3].
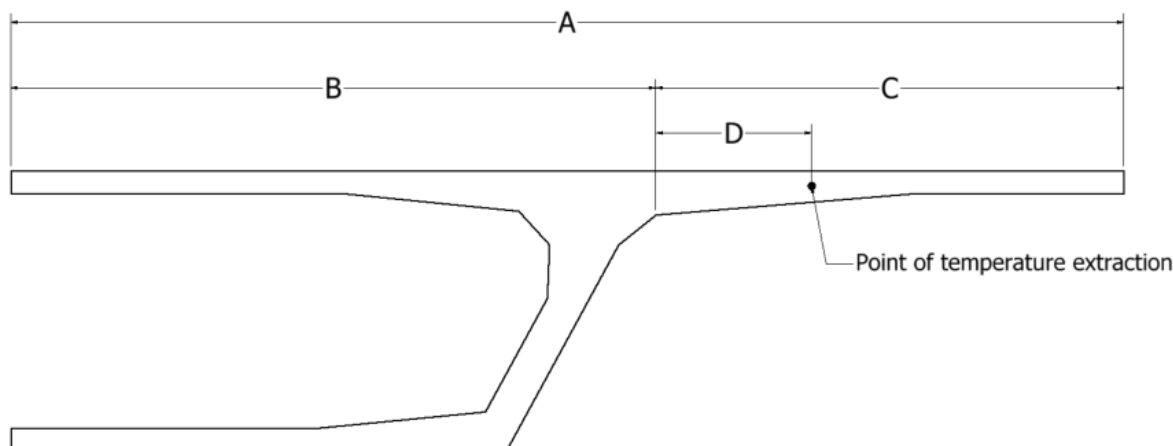
Figure 74: Bridge B example of point where to extract temperatures

The analytical expression, Equation 86, was used in 41 simulations selected to compare the deformations against those simulated using finite elements. Of the 41 simulations selected for comparison, 26 were for Bridge C (w/l 10.89), six were for Bridge B (w/l 5.97), four were for Bridge E (w/l 4.09), four were for Bridge F (w/l 5.92), and two were for Bridge D (w/l 9.39). Good agreement was observed for the deformations calculated for every hour from 2 hr to 10 hr after the placement of the new segment, as shown in Figure 75.
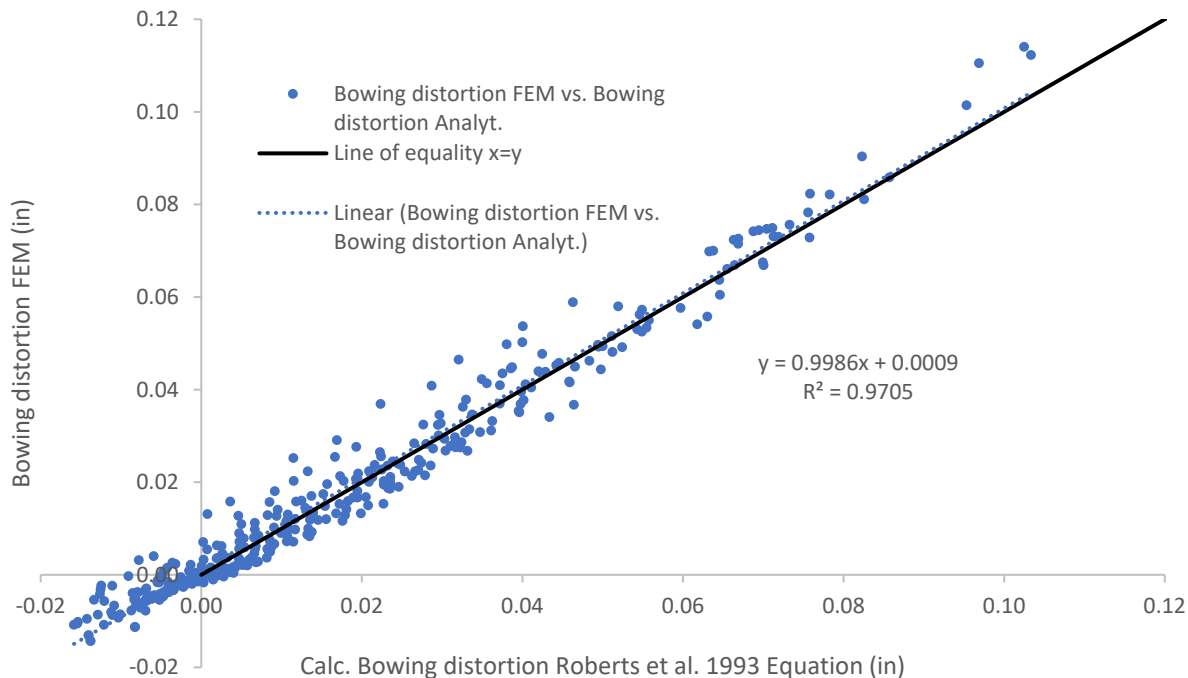
Figure 75: Bowing distortion for 41 different bridge segment conditions calculated using Equation 86 vs. finite elements for every from hour from 2 hr to 10 hr after concrete placement

Roberts et al. (1993) tested the ability of Equation 86 to predict bowing distortion against measured temperature data. Measured bowing distortions for several segment sections, which had similar top slab geometries, were found to be in good agreement with Equation 86.

In the present study, good agreement was observed for the 41 simulations across the different geometries, which indicates that Equation 86 can be used to identify cases where there could be excessive bowing distortion of segments. The difficulty of using Equation 86 lies in that fact that an appropriate thermal gradient for the match-cast segment must be developed for each specific project. Developing the thermal gradient data would typically require either performing a temperature simulation of the bridge segment during fabrication or constructing a physical mockup and measuring the temperature gradient. Neither of these approaches is practical during the bidding process.

6.3 Mitigation Decision Tree

To address the challenges of applying Equation 86, a decision tree (Figure 76) was developed, based on 157 simulations performed, to aid in determining the risk of excessive bowing distortion. Appendix A gives details of each simulation case considered. A 0.03 in. limit on per segment bowing distortion (at 10 hrs after placement of the new cast segment) was adopted as the critical limit in the development of the risk factors classifications [3], [4]. The decision tree classifies the segment based on a series of risk factors. Depending on the segment geometry, construction method, and materials used, the segments are classified as: 1) low risk, where no

further mitigation is needed, or 2) potential risk. For potential risk cases, further risk factors will need to be considered, or thermal analysis or additional mitigation will be needed.

Equivalent Cement Content (pcy)= Cement + 0.5 Fash+0.8 Cash+ 1.2Silica Fume+Slag
Lightweight concrete should be evaluated for bowing
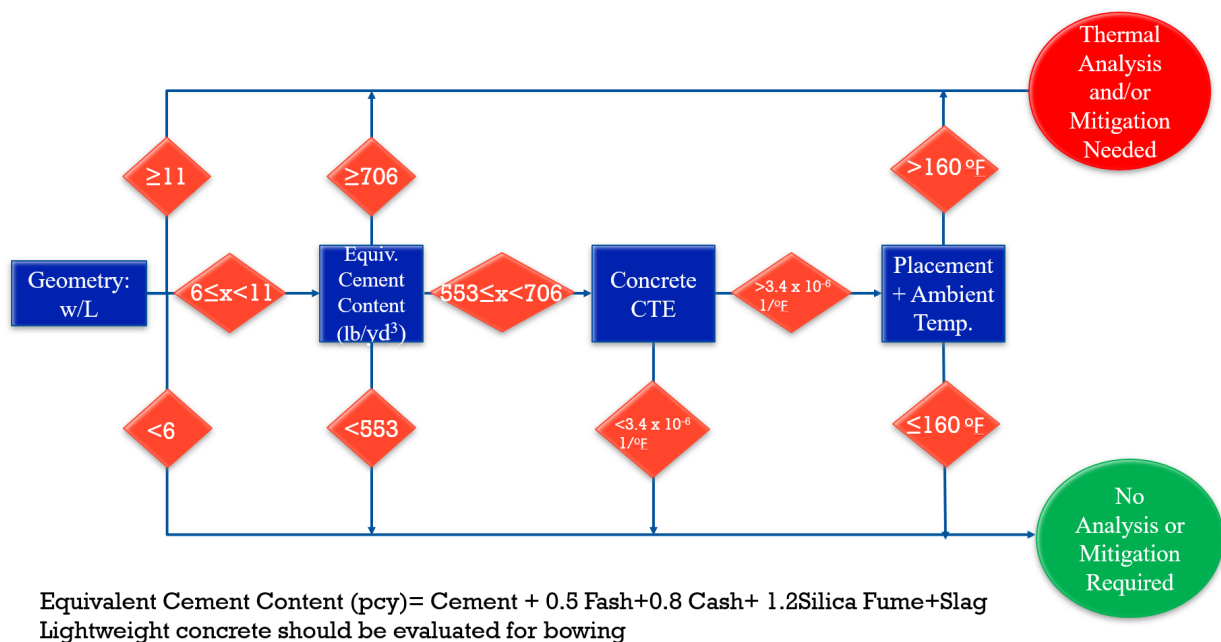
Figure 76: Mitigation decision tree

The application of the developed decision tree is illustrated with the 157 FE-simulations performed, showing how each simulation would be classified. The simulated bowing distortion and the risk classification are then compared.

Geometry:

Below w/l=6, 98 cases out of the 157 simulations performed had w/l less than 6.

49 of the 98 cases belong to Bridge F and Bridge B, which are segments that are very close to the 6 w/l limit with 5.92 and 5.97 respectively. It must be noted that the data set showed that for segments with w/l close to 6, the use of lightweight aggregates and high CTE aggregate combinations, in conjunction with high heat mixes, can cause the match-cast segments to surpass the acceptable bowing distortion limit. For this reason, the decision tree is not recommended for use with lightweight aggregate.

Between w/l= 6 to 11, 49 cases out of the 157 simulations performed were classified as needing further information for classification.

Above w/l= 11, 10 cases out of the 157 simulations performed had w/l greater than 11. For these cases, it is recommended to execute a thermal model simulating the two segments in contact to assess whether the bowing distortion in a single segment is limited to 0.03 in. or an accumulated bowing distortion in the span is limited to 0.5 in. [3] or apply additional mitigation.

The larger the width-to-length (w/l) ratio, the higher the risk for segments developing bowing distortions that are larger than the 0.03 in. single segment limit. Close to the 11 limit, low heat of hydration mixes were found to be effective in keeping the single segment bowing distortion smaller than the 0.03 in. threshold, and therefore should be considered. Low concrete placement temperatures were also found to be effective in preventing the hydrating concrete from inducing higher bowing distortions in the match-cast segments. Keeping the match-cast segment warm and preventing the new hydrating segment from heating up excessively is also a good approach to mitigating bowing distortions. It is beneficial to cure/insulate the match-cast segment (at least the top slab) in the hours previous to and during contact with the newly cast segment. The newly cast segment should be cured with a curing material with a lower R-value (resistance to heat conduction per unit thickness, with higher values representing higher insulation) [130] than the match-cast segment.

It is recommended that for modeling, the new segment hydration be modeled with the highest possible ambient temperature conditions expected for the given construction setting (more than one model might be required if fabrication of segments will extend across different seasons i.e., summer to winter). The thermal gradient generated in the match-cast segment at 10 hrs after casting of the new segment should be used with Equation 86 to estimate bowing distortion of top slabs of match-cast segments [2]. This is a conservative approach that considers the effect of higher ambient temperatures on the temperature reached by the hydrating concrete, and the detrimental cooling effect of the ambient temperatures in the match-cast segment.

Equivalent Cement Content:

The equivalent cement content (ECC) expression given in ACI 207.1 [6] and shown in Equation 87 is used for the risk factors classification related to mix design and the ability of a particular mix to produce heat.

$$ECC = Cement + 0.5\ FAsh + 0.8CAsh + 1.2SFMK + Factor \cdot Slag \qquad \text{Equation 87}$$

Where:

$Cement$ = Portland cement in the mix (lb/yd^3)

$FAsh$ = Class F fly ash (lb/yd^3)

$CAsh$ = Class C fly ash (lb/yd^3)

$SFMK$ = Silica fume or metakaolin (lb/yd^3)

$Slag$ = Slag cement (lb/yd^3)

$Factor$ = Variable that depends on the percentage of Portland cement being replaced by slag cement. 1.0 to 1.1 for 0 to 20% replacement, 1.0 for 20% to 45% replacement, 0.9 for 45% to 65% replacement and 0.8 for 65% to 80% replacement.

Equation 87 is used to approximate the heat contribution of supplementary cementitious materials (SCMs) in the mix design used. While the original equation was developed for Type I/II cement, this equation was still found to be useful to estimate the concrete heat potential for classifying risk.

Below 553 lb/yd^3 Equivalent Cement Content, 13 simulations out of 49 cases which had a w/l between 6 to 11 also had an equivalent cement content lower than 553 lb/yd^3 [6]. These cases would not need additional analysis or require mitigation. Lightweight concrete was excluded from the analysis. Two cases classified under this low risk factor slightly surpass the threshold. Simulation 6 has a lower ECC but uses an accelerating admixture which causes the concrete in the new segment to reach higher temperatures during curing. The bowing distortion for this case is 0.031 in. (slightly larger than the 0.03 in. limit) at 10 hr. after placement of the new segment. Simulation 151 has a lower ECC but uses lightweight aggregate. Bowing distortion for this case is 0.030 in. at 10 hr. after placement of the new segment.

Between 553 lb/yd^3 and 706 lb/yd^3 Equivalent Cement Content, 13 of the 49 cases which that had a w/l between 6 to 11 also had an equivalent cement content between 553 lb/yd^3 and 706 lb/yd^3 [6]. To classify the risk of these cases, more risk factors must be used in the decision tree to classify the risk.

Above 706 lb/yd^3 Equivalent Cement Content, 23 of the 49 cases, which had a w/l between 6 to 11, also had an equivalent cement content above 705 lb/yd^3 [6]. For these cases, it is recommended to execute a thermal model to assess whether the bowing distortion in a single segment is limited to 0.03 in. or an accumulated bowing distortion in the span is limited to 0.5 in. [3], or apply additional mitigation.

Concrete Coefficient of Thermal Expansion:

Below 3.4 με/°F Concrete CTE: 1 simulation out of the 13 simulations with a w/l between 6 and 11, and and an equivalent cement content between 553 lb/yd^3 and 706 lb/yd^3 had a CTE below 3.4×10^{-6} 1/°F and was classified as not requiring mitigation. That is simulation 51 with Bridge C (w/l 10.89) that used a low CTE aggregate selection. Use of low CTE concrete aids in reducing bowing distortion, as in simulation 51 where it was found to reduce the bowing distortion of the match-cast segment by 0.01 in compared to simulation 33 that used a medium CTE concrete with a CTE of 4.54×10^{-6} 1/°F.

Above 3.4 με/°F Concrete CTE: 12 simulations out of the 13 simulations with a w/l between 6 to 11, and an equivalent cement content between 553 lb/yd^3 and 706 lb/yd^3 had a CTE above CTE 3.4 με/°F. To classify the risk of these cases, more risk factors must be used in the decision tree to classify the risk.

Placement + Ambient Temperature at Time of Placement:

Below 160°F Placement + Ambient Temperature at Time of Placement: From the 12 cases that had a w/l ratio between 6 and 11, an equivalent cement content between 553 lb/yd^3 and 706 lb/yd^3, and a CTE above 3.4 με/°F, 2 simulations had a placement + ambient temperature at time of placement below 160°F and were classified as not requiring further mitigation. These were simulations 60 and 69. Both simulations were for bridge type C (w/l 10.89), and in both cases the

bowing distortion in the match-cast segment was below the 0.03 in. threshold. Case 60 was a night placement and case 69 was a winter placement where the effect of the cool ambient temperature and the low concrete placement temperature were able to prevent the newly cast segment from heating up enough to cause an excessive bowing distortion in the match-cast segment.

Above 160°F Placement + Ambient Temperature at Time of Placement: 10 out of the 12 cases that had a w/l ratio between 6 and 11, an equivalent cement content between 553 lb/yd^3 and 706 lb/yd^3, and a CTE above 3.4 µε/°F, had a placement + ambient temperature at time of placement above 160°F. These cases would need either a thermal analysis to ensure that the threshold is not surpassed, or additional mitigation measurements.

Figure 77 summarizes the number of simulations that fell into each category in the flow chart.
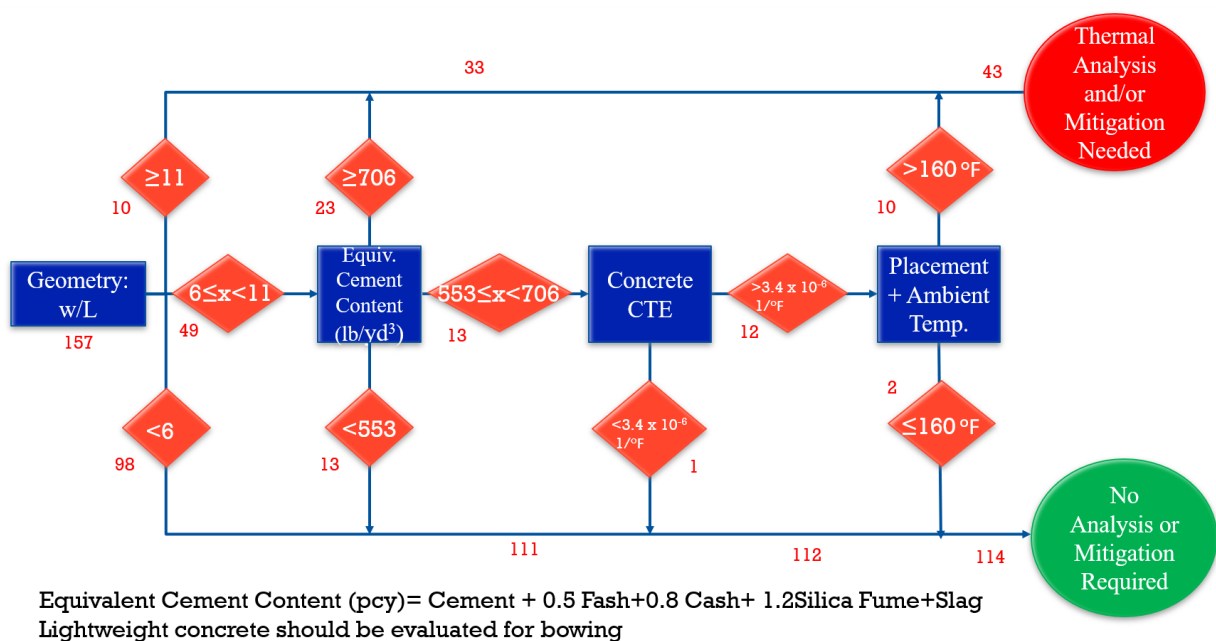
Figure 77: Decision tree used with the cases studied

Special curing techniques such as use of insulating materials for curing, use of steam curing and strategic selection of specific time of the day are sometimes used to decrease the bowing distortion risk [2]–[4], [7]. The use of insulating materials for curing of segments that are in contact with each other was evaluated in this study. Simulations showed that using insulation to keep the match-cast segment warm, while it is in contact with the newly cast segment, is beneficial and can help prevent excessive bowing distortion. The simulations also indicated that applying curing insulation to the new segment actually increases the bowing distortion in the match-cast segment because the insulation promotes heat retention and heat transfer to the match-cast segment. Currently, FDOT specification 452-6.7 [1] requires curing blankets or other approved equivalent system for both segments to minimize the effects of differential temperatures between the segments.

Steam curing is another mitigation measure described in literature [2]–[4] and mentioned in FDOT specification 452-6.7.2 [1] to be used to achieve required initial concrete strengths to remove forms, apply prestress forces, and move or handle segments. This specification also states that when steam curing is part of the fabrication process of segments, both segments must be exposed to the same curing environment (temperature and humidity) [1]. Simulations show that in cases where steam curing cycles are applied to both segments, the effect of the higher temperatures in the hydrating concrete causes the bowing distortion magnitude to increase as compared to comparable cases where the segments are exposed to low ambient temperature placements. If the purpose of the steam curing is to mitigate bowing distortion only, steam curing should only be applied to the match-cast segment and prevent the steam from heating with the newly cast segment. If the steam curing is used for increasing the speed of segment fabrication cycles, and the segments have a w/l larger than 6, segment construction should not involve the use of mixes with high cementitious content.

Placing concrete for a new segment in the morning when the ambient temperature starts to rise has been suggested to be the ideal time to decrease the thermal gradient induced in the match-cast segment [2]–[4]. This is partially correct as the warming effect of increasing ambient temperatures is beneficial to the match-cast segment. However, simulation results indicate that the effect of the lower ambient temperatures, in conjunction with lower concrete placement temperatures, can reduce bowing distortions up to 0.02 in. at 10 hrs after placement of the new segment. If placement of concrete with lower ambient temperatures is combined with insulation of the match-cast segment, reductions in bowing distortion could be expected.

6.4 Regression Model Applied to Simulation Results

A linear regression model was developed to estimate the bowing distortion of a match-cast segment at 10 hrs after casting of the new segment. The model was developed using the R software package.

Bowing distortion at 10 hrs after placement of the new segment obtained from finite element modeling were taken as the response variable of the regression model. The explanatory variables for the regression fit were: the width of the segment, the length of the segment, the equivalent OPC content, the density of the concrete, the thermal conductivity of the concrete, the coefficient of thermal expansion of the concrete and the elastic modulus value of the concrete at 28 days. Using results from the 157 simulations, the following regression model was made to estimate the bowing distortion at 10 hrs Δ_{10} (in.) (Equation 88):

$$\Delta_{10} = 14.116 + 2.337 \cdot 10^{-8} \cdot w^2 + 19654.95 \cdot \frac{1}{l^3} + 0.000108 \cdot OPC_{eq}$$
$$- 0.0111 \cdot \rho - 0.1606 \cdot k_c - 12134.92 \cdot CTE + 0.00627 \cdot E_{28} \quad \text{Equation 88}$$

Where: w= width of the segment (in)

          l= length of the segment (in)

OPC_{eq}=Equivalent cement content calculated with Equation 87 (lb/yd^3)

ρ= Density of concrete (lb/yd^3)

k_c=Thermal conductivity of concrete (BTU/(ft·h·°F))

CTE=Coefficient of thermal expansion of concrete (1/°F)

E_{28}=Elastic modulus of concrete at 28 days (ksi)

The predicted bowing distortion value for each case was then compared with the bowing distortion computed by the corresponding finite element model for each case. Results for the 157 simulations comparison can be seen in Figure 78.
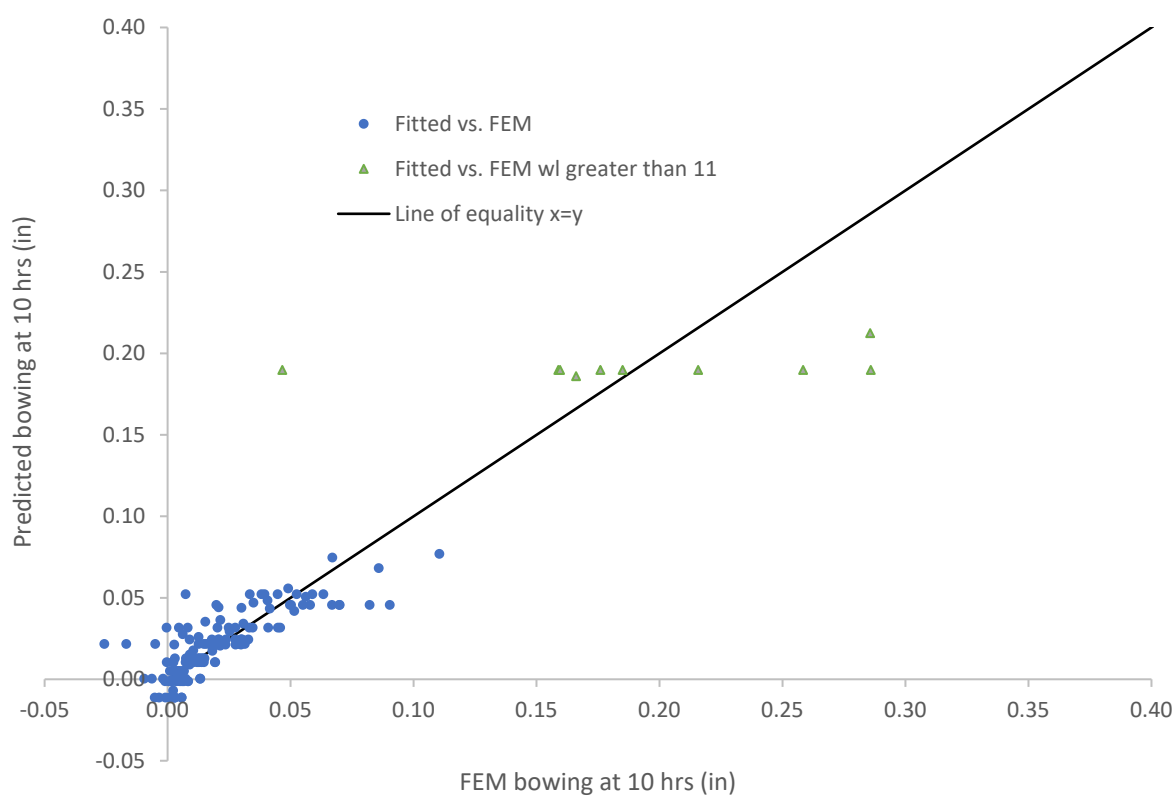
Figure 78: FEM bowing distortion at 10 hr vs. predicted bowing distortion at 10 hr

The model worked well for cases of segments with w/l ratio below 11. Most of the outliers belong to the Bang Na segment geometry (high w/l). It is recommended that this equation only be used for segments with a w/l below 11.

6.5 Summary of Recommendations

An analytical expression developed by Roberts et al. [1] was evaluated using typical Florida bridge geometries contemplated in the simulation matrix. Good agreement was observed by using Equation 1 with FE-simulated temperatures extracted at every hour of the simulation from 2 to 10 hr. The difficulty remains in being able to obtain the temperature profile developed in the match-cast segment that induces the bowing distortion without the need to perform a finite element simulation.

In the case of a segmental bridge construction case with a construction setting that falls in the "Thermal Analysis and or Mitigation Needed" classification of the decision tree proposed in Figure 76, a thermal simulation of the short line construction process with the two segments in contact using a finite element software package could be performed. Temperatures developed in the wings of the segments can be obtained from the simulation, the thermal gradient in the match-cast segment after 10 hrs of placement of the new segment could be calculated, and the analytical expression developed in Roberts et al. [1] can be used to evaluate if the bowing distortion could be excessive. The simulation performed should at a minimum meet the following:

- The simulation to estimate the temperature profile developed in the hydrating segment and the match-cast segment should simulate the heat of hydration development of concrete ideally using the three parameter exponential degree of hydration expression [56] or other equivalent function where the heat of hydration produced is a function of the maturity of concrete. The use of the equivalent age maturity function is recommended [56],[83].

- The effect of the application of different materials on the exposed faces of the concrete that would represent either formwork or curing materials covering the concrete in both the new hydrating segment and match-cast segment should be simulated when the materials are used. The layer should be defined by its thickness and the thermal conductivity of the material. The software used should have the capability of removing or adding these layers at different points of the simulation.

- The software must be able to simulate the application of ambient temperature curves on the exposed faces of the concrete.

- The software must be able to simulate the application of wind/ convective cooling on the exposed faces of the concrete.

- The software must have the capability to calculate temperatures at the nodes of the meshed geometries of the segments by means of finite elements at different times after the placement of the new segment 10 hrs after construction.

If bowing distortions are also be obtained from finite element simulations, the finite element software package used should have these minimum capabilities:

- The software must have a coupled thermo-mechanical solver.

- Depending on the assumptions in the simulation, proper mechanical boundary conditions must be assigned to the segments. It may be appropriate to idealize the newly cast segment was idealized as unhardened concrete (i.e constant low elastic modulus) from its placement moment until the end of the simulation for it not to interfere in the bowing distortion effect of the match-cast segment, and the correspondent mechanical boundary conditions can be applied to this idealization.

- The software must be able to simulate the development of the elastic modulus in the match-cast segment (first cast segment) as a function of maturity of concrete.

Roberts et al. [1],[2] suggested using a 0.03-in. bowing distortion limit for single segments and 0.5-in. cumulative distortion in a span to avoid using mitigation measures. A decision tree risk evaluation approach was developed based on the results observed in the sensitivity analysis. Width-to-length ratio (w/l), equivalent cement content, concrete CTE, and concrete placement temperature plus ambient temperature at placement were selected as criteria for the decision tree, along with specific classification thresholds to enable identification of cases where bowing distortion exceeds the 0.03-in. single segment bowing distortion limit proposed in [2]. One hundred fourteen cases out of the 157 cases studied were classified as not having a risk of developing excessive bowing distortion. Forty-three cases were identified as having risks for developing excessive bowing distortion (more than 0.03-in. single segment threshold). Recommendations for preferable curing practices were given where the match-cast segment benefits from insulation in the hours previous and while being in contact with the newly cast segment, whereas the newly cast segment should be cured with less insulating material to prevent it from heating up too much while the new concrete hydrates. If steam curing is applied, it should preferably be applied only to the match-cast segment if the objective is solely to prevent excessive bowing. If steam curing is applied to aid in rapid strength gain of the hydrating concrete, the curing should also be applied to the match-cast segment. It is possible that the extra temperature gain of the hydrating concrete caused by the steam curing may cause additional bowing distortion in the match-cast segment.

Simulations showed that the effect of lower ambient temperatures and the low concrete placement temperature have a generally beneficial effect in the match-cast process. Night placements along with insulation of the match-cast segment could be good mitigation measures in these critical cases. Thermal modeling along with the use of Equation 86 [1],[2] could also be an option to more precisely gauge risk and new mitigation measures when the w/l and mix designs fall in the critical levels of the decision tree.

A predictive equation based on values that can be obtained or estimated prior to initiating the fabrication of the segments was also developed. The predictive equation worked well for typical Florida geometries. It did not work well for the Bang Na geometry which involves a very high w/l ratio that is not typical of Florida bridge construction.

7 Conclusions and Recommendations

7.1 Conclusions

A review of the literature related to the bowing distortion problem in short line match-cast segmental construction was performed. Based in the literature review, a simulation matrix of 157-member geometry, materials, and construction factor combinations that explored the variables believed to be the most influential on bowing distortion was developed. The ability of the finite element software used for modeling, b4cast, to predict temperatures of hydrating concrete members was confirmed by comparison with a concrete physical model instrumented for temperature. The ability of an analytical expression to predict the bowing distortion of the concrete members studied from the thermal gradient developed in the match-cast segment was confirmed, however the utility of this method is limited because it requires the temperature development to be known. A decision tree was developed to classify risk of bowing distortion in the construction process. A regression model was also developed that relates the member geometry, materials, and construction variables to the bowing distortion calculated.

An analysis of the simulation results showed the following:

- Segments with a w/l ratio lower than six had a reduced risk of problematic bowing distortion over 0.03 in. for an individual segment.
- The use of low heat of hydration mixes reduced the bowing distortion generated in the match-cast segments.
- The use of low coefficient of thermal expansion aggregates yielding low coefficient of thermal expansion concrete was found to be effective in reducing bowing distortion.
- Applying insulation tarps to both segments, while the newly cast segment is hydrating, was found to be detrimental. Insulating in this way increases the bowing distortion effect as it causes the newly cast concrete to heat up faster and achieve steeper thermal gradients during curing.
- The cooling effect of lower ambient temperatures or wind lowers bowing distortion. Such sources of cooling reduce the maximum hydration temperature reached in the concrete in the newly cast segment.
- Steam curing applied to both segments increased bowing distortion as it causes the concrete in the newly cast segment to reach higher temperatures as it hydrates.

7.2 Recommendations

The analytical expression proposed by Roberts-Wollmann et al. [1] can be used to estimate the bowing distortion of a match-cast segment with geometries similar to the Florida Bridge geometries studied in this project. This method requires the concrete temperature development to be known, limiting the utility of this method for estimating the bowing distortion.

A decision tree was proposed that considers important variables such as member geometry, material properties, and construction conditions to classify the risk that bowing distortion will exceed 0.03 in. [2] during fabrication. Projects that have a predicted bowing distortion exceeding this value are deemed to have high bowing risk. For cases classified as having low

bowing risk, as determined by the decision tree, no further analysis is necessary. For cases classified as high-risk, however, two options are recommended. One is that the contractor constructs a full-scale mockup and measure temperatures for use in the Roberts-Wollmann expression. The other is to require that a numerical temperature simulation of the segment fabrication process be conducted and that temperatures from such a simulation be used in the Roberts-Wollmann expression. The bowing distortion thus calculated should be below 0.03 in. per segment. If not, then the contractor must design and implement mitigation measures unless it can be demonstrated that the cumulative gap produced will not exceed 0.5 in.

A predictive expression developed by linear regression of temperatures, generated in this study through numerical simulations, can also be used to estimate expected bowing distortion for the given conditions. A 0.03 in. single segment limit, or 0.5 in. accumulated bowing distortion in a span, should be used with this approach to avoid mitigation measures.

Mitigation measures when the predicted bowing exceeds 0.03 in. may be used to keep the match-cast segment warm and to prevent hydrating concrete in the newly cast segment from heating up to a problematic level. Possible mitigation measures include the following:

- The match-cast segment can be cured/protected with insulation prior to and during the time in contact with the newly cast segment. Insulation should not be used on the newly cast segment. Such insulation will increase in temperatures developed in the newly cast concrete and also in the adjacent match-cast concrete, thus increasing bowing in the match-cast member. The new concrete member should still be cured to prevent moisture loss from the concrete to the environment. An example of this type of wet curing would be placing wet burlap and plastic over the new concrete.
- During Florida summer conditions, night placement of concrete can be implemented. The lower ambient temperatures associated with night placement can help to reduce concrete temperatures developed during curing and thus reduce bowing distortion.
- During Florida winter conditions, the match-cast segment should be insulated before the newly cast concrete is placed to keep the match-cast segment warm to reduce thermal gradients that may develop during the new segment curing.
- Mitigation of bowing distortion can be achieved if steam curing or high ambient temperature conditions are applied only to the match-cast segment. High temperatures applied to the newly cast segment will be detrimental in that they will cause the concrete to reach higher temperatures and thus may cause an increase in bowing distortion.

7.3 Future Research

Two items have been identified for future research:

- Geometric mitigation for segments in the short line match-cast segment process should be further explored. The influence that increasing the segment top slab thickness has on bowing distortion should be explored. The influence of the location of the junction of the web and top slab could also be investigated to determine if there is an optimal location to reduce bowing distortion.
- The only complete/available field measured data with temperatures and corresponding bowing distortion measurements in segments in the short line match-casting method are

those provided in Roberts et al. [1]. Future work should thus be carried out to collect additional field measurements of temperature and bowing distortions during segment fabrication with the short line match-casting method. Such data would help further validate numerical simulation models and could provide new insights into methods for mitigating bowing deformations.

8 References

[1] C. L. Roberts, J. E. Breen, and M. E. Kreger, *Measurement Based Revisions for Segmental Bridge Design and Construction Criteria*, TxDOT REport 1234-3F, Austin, TX, 1993.

[2] C. L. Roberts-Wollmann, J. E. Breen, and M. E. Kreger, "Temperature Induced Deformations in Match-cast segments," *PCI Journal*, vol. 40, no. 4, pp. 62–71, 1995.

[3] R. Abendeh, *Temperature Induced Deformations in Match-Cast Segments and their Effects on Precast Segmental Bridges*, Doctoral Thesis, Technical University of Hamburg-Harburg, Hamburg, Germany, 2006.

[4] W. Podolny, "The Cause of Cracking in Post-Tensioned Concrete Box Girder Bridges and Retrofit Procedures," PCI Journal, vol. 30, no. 2, pp. 82-139, 1985. [Online]. Available: https://www.pci.org/PCI_Docs/Design_Resources/Guides_and_manuals/references/bridge _design_manual/JL-85-March-April_The_Cause_of_Cracking_in_Post-Tensioned_Concrete_Box_Girder_Bridges_and_Retrofit_Procedures.pdf.

[5] Florida Department of Transportation (FDOT), *Standard Specifications for Road and Bridge Construction 2021*. Tallahassee, 2021.

[6] D. M. Tassin, "Jean M. Muller: Bridge Engineer," PCI Journal, vol. 51, no. 2, pp. 88-101, 2006.

[7] G. A. Rombach and R. Abendeh, "Bow-shaped segments in precast segmental bridges," *Eng. Struct.*, vol. 30, no. 6, pp. 1711–1719, Jun. 2008, doi: 10.1016/j.engstruct.2007.11.012.

[8] Florida Department of Transportation, *Florida Department of Transportation Standard Specifications for Road and Bridge Construction*, July 2018., no. July. Tallahassee: FDOT, 2018.

[9] K. Kumar, K. S. Nathan, K. Varghese, and K. Ananthanarayanan, "Automated Geometry Control of Precast Segmental Bridges," The 25th International Symposium on Automation and Robotics in Construction, June 26-29, pp. 88-94, Jun. 2008, doi: 10.22260/ISARC2008/0015.

[10] H. Abeka, S. Agyeman, and M. Adom-Asamoah, "Thermal effect of mass concrete structures in the tropics: Experimental, modelling and parametric studies," *Cogent Eng.*, vol. 4, no. 1, pp. 1–18, Jan. 2017, doi: 10.1080/23311916.2016.1278297.

[11] M. Q. Saeed, "Experimental Investigation and Modeling the Heat of Hydration in Mass Concrete Structures," Doctoral Thesis, King Fahd University of Petroleum & Minerals, Dhahran, Saudi Arabia, 2013.

[12] Prescon Corporation, *Segment Monitoring Test Report*, San Antonio, 1988.

[13] A. Saetta, R. Scotta, and R. Vitaliani, "Stress Analysis of Concrete Structures Subjected to Variable Thermal Loads," *J. Struct. Eng.*, vol. 121, no. 3, pp. 446–457, Mar. 1995, doi: 10.1061/(ASCE)0733-9445(1995)121:3(446).

[14]   FHWA, "Portland Cement Concrete Pavements Research," *Federal Highway Administration*. Mar. 2016, Accessed: Jul. 19, 2020. [Online]. Available: https://www.fhwa.dot.gov/publications/research/infrastructure/pavements/pccp/thermal.cfm.

[15]   R. D. Browne, "Thermal Movement of Concrete," in *The Journal of the Concrete Society (London)*, 6th ed., vol. 6, no. 10, London: London: Concrete Society, 1972, 1972, pp. 51–53.

[16]   L. Grybosky, "Thermal Expansion and Contraction." Accessed: Jul. 13, 2020. [Online]. Available: https://www.engr.psu.edu/ce/courses/ce584/concrete/library/cracking/thermalexpansioncontraction/thermalexpcontr.htm.

[17]   Portland Cement Association, "PCA: Concrete Basics." Nov. 2001, Accessed: Jul. 19, 2020. [Online]. Available: http://www.portcement.org/cb/concretebasics_concretebasics.asp.

[18]   G. D. Alungbe, "Coefficient of Thermal and Moisture Expansion of Concrete Used in Florida," University of Florida, Gainesville, 1989.

[19]   D. Bonell and F. Harper, "The Thermal Expansion of Concrete Engineering Research (Summary of the Report Published by the Building Research Station)," *J. Inst. Civ. Eng.*, vol. 33, no. 4, pp. 320–330, Feb. 1950, doi: 10.1680/ijoti.1950.12917.

[20]   A. Mateos, J. Harvey, J. Bolander, R. Wu, J. Paniagua, and F. Paniagua, "Field evaluation of the impact of environmental conditions on concrete moisture-related shrinkage and coefficient of thermal expansion," *Constr. Build. Mater.*, vol. 225, pp. 348–357, Nov. 2019, doi: 10.1016/j.conbuildmat.2019.07.131.

[21]   I. Maruyama, A. Teramoto, and G. Igarashi, "Strain and thermal expansion coefficients of various cement pastes during hydration at early ages," *Mater. Struct.*, vol. 47, no. 1–2, pp. 27–37, Mar. 2014, doi: 10.1617/s11527-013-0042-4.

[22]   M. Wyrzykowski and P. Lura, "Controlling the coefficient of thermal expansion of cementitious materials - A new application for superabsorbent polymers," *Cem. Concr. Compos.*, vol. 35, no. 1, pp. 49–58, Jan. 2013, doi: 10.1016/j.cemconcomp.2012.08.010.

[23]   O. M. Jensen and P. F. Hansen, "Water-entrained cement-based materials I. Principles and theoretical background," *Cem. Concr. Res.*, vol. 31, pp. 647–654, Jan. 2001, [Online]. Available: https://reader.elsevier.com/reader/sd/pii/S000888460100463X?token=9796EF3C875B7373214E46F5104F701667FA6B108842CFE6CC7CEE688AB7AD5AB5E7698B3FDA979B7D798BFC559BD9BF.

[24]   O. M. Jensen and P. F. Hansen, "Water-entrained cement-based materials II. Experimental observations," *Cem. Concr. Res.*, vol. 32, pp. 973–978, Jan. 2002, [Online]. Available: https://reader.elsevier.com/reader/sd/pii/S0008884602007378?token=5CBC0CDE52065A32B978B6A126CC20746C981BD8DF4C92AB919B361C3CEE66F9084B01EE91D726D01BCE84FBA1599BAF.

[25]   P. Lura, O. M. Jensen, and S. I. Igarashi, "Experimental observation of internal water curing

of concrete," *Mater. Struct. Constr.*, vol. 40, no. 2, pp. 211–220, Mar. 2007, doi: 10.1617/s11527-006-9132-x.

[26] G. D. Alungbe, M. Tia, and D. G. Bloomquist, "Effects of Aggregate, Water/Cement Ratio, and Curing on the Coefficient of Linear Thermal Expansion of Concrete," Transportation Research Record, vol. 1335, pp. 44-51.

[27] S. L. Meyers, "How temperature and moisture changes may affect the durability of concrete," *Rock Prod.*, vol. 54, no. 8, pp. 153–162, 1951, [Online]. Available: https://www.scopus.com/record/display.uri?eid=2-s2.0-33845757867&origin=inward&txGid=8ccd5dc2eb57f98a84e76fa145a39fbd.

[28] J. H. Yeon, S. Choi, and M. C. Won, "Effect of relative humidity on coefficient of thermal expansion of hardened cement paste and concrete," *Transp. Res. Rec.*, no. 2113, pp. 83–91, 2009, doi: 10.3141/2113-10.

[29] S. L. Meyers, "Thermal Coefficient of Expansion of Portland Cement: Long-time tests," *Ind. Eng. Chem.*, vol. 32, no. 8, pp. 1107–1112, 1940, doi: 10.1021/ie50368a018.

[30] D. Cusson and T. J. Hoogeveen, "Measuring early-age coefficient of thermal expansion in high-performance concrete," *NRC Publ. Arch.*, pp. 1–10, Dec. 2005, [Online]. Available: https://www.researchgate.net/publication/44091439_Measuring_early-age_coefficient_of_thermal_expansion_in_high-performance_concrete.

[31] B. Zahabizadeh, A. Edalat-Behbahani, J. Granja, J. G. Gomes, R. Faria, and M. Azenha, "A new test setup for measuring early age coefficient of thermal expansion of concrete," *Cem. Concr. Compos.*, vol. 98, pp. 14–28, Apr. 2019, doi: 10.1016/j.cemconcomp.2019.01.014.

[32] S. Türkel and V. Alabas, "The effect of excessive steam curing on Portland composite cement concrete," *Cem. Concr. Res.*, vol. 35, no. 2, pp. 405–411, Feb. 2005, doi: 10.1016/j.cemconres.2004.07.038.

[33] V. K. R. Kodur, P. P. Bhatt, P. Soroushian, and A. Arablouei, "Temperature and stress development in ultra-high performance concrete during curing," *Constr. Build. Mater.*, vol. 122, pp. 63–71, Sep. 2016, doi: 10.1016/j.conbuildmat.2016.06.052.

[34] T. Lee, J. Lee, and Y. Kim, "Effects of admixtures and accelerators on the development of concrete strength for horizontal form removal upon curing at 10 °C," *Constr. Build. Mater.*, vol. 237, Mar. 2020, doi: 10.1016/j.conbuildmat.2019.117652.

[35] D. Kocáb, R. Halamová, B. Kucharczyková, and P. Daněk, "Development of the modulus of elasticity of cement materials in the early stage of ageing," in *AIP Conference Proceedings 2210*, Feb. 2020, vol. 2210, pp. 20012–20015, doi: 10.1063/5.0000398.

[36] M. E. Robbins, "Predicting the early age temperature response of concrete using isothermal calorimetry," University of Toronto, Toronto, 2007.

[37] A. K. Schindler and K. J. Folliard, "Heat of hydration models for cementitious materials," *ACI Mater. J.*, vol. 102, no. 1, pp. 24–33, Jan. 2005, doi: 10.14359/14246.

[38] ACI Committee 207, "Effect of Restraint, Volume Change, and Reinforcement on Cracking of Mass Concrete," 2002. [Online]. Available:

http://cdnassets.hw.net/a6/60/161538cd484ba9334725b78b1bef/aci-2072r-95-tcm77-2204805.pdf.

[39]   Z. Lu and X. Wang, "Modeling the Heat of Hydration of Concrete Incorporating Fly Ash," *Key Eng. Mater.*, vol. 705, pp. 332–337, Apr. 2016, doi: 10.4028/www.scientific.net/KEM.705.332.

[40]   ACI Committee 318, *Building Code Requirements for Structural Concrete (ACI 318-08) and Commentary*. American Concrete Institute, 2008.

[41]   F. A. Oluokun, "Investigation of physical properties of concrete at early ages - ProQuest," University of Tennessee, Knoxville, 1989.

[42]   A. A. Khan, "Concrete Properties and Thermal Stress Analysis of Members at Early Ages," McGill University, Montreal, 1995.

[43]   J. Zhao, "Mechanical Properties of Concrete at Early Ages," University of Ottawa, Ottawa, 1990.

[44]   W. Piasta, J. Góra, and W. Budzyński, "Stress-strain relationships and modulus of elasticity of rocks and of ordinary and high performance concretes," *Constr. Build. Mater.*, vol. 153, pp. 728–739, Oct. 2017, doi: 10.1016/j.conbuildmat.2017.07.167.

[45]   S. H. Ahmad and S. P. Shah, "Structural Properties of High Strength Concrete and its Implications for Precast Prestressed Concrete," *PCI J.*, vol. 30, no. 6, pp. 92–116, 1985, [Online]. Available: https://www.pci.org/PCI/Publications/PCI_Journal/Issues/1985/November-December/Structural_Properties_of_High_Strength_Concrete_and_its_Implications_for_Precast_Prestressed_Concret.aspx?WebsiteKey=5a7b2064-98c2-4c8e-9b4b-18c80973da1e.

[46]   S. Harsh, Z. Shen, and D. Darwin, "Strain-rate sensitive behavior of cement paste and mortar in compression," *ACI Mater. J.*, vol. 87, no. 5, pp. 508–516, Sep. 1990, doi: 10.14359/1931.

[47]   A. Alsalman, C. N. Dang, G. S. Prinz, and W. M. Hale, "Evaluation of modulus of elasticity of ultra-high performance concrete," *Constr. Build. Mater.*, vol. 153, pp. 918–928, Oct. 2017, doi: 10.1016/j.conbuildmat.2017.07.158.

[48]   K. Yıldız and L. O. Ugur, "The effect of mineral admixture type on the modulus of elasticity of high strength concrete," *Sci. Res. Essay*, vol. 4, no. 8, pp. 791–798, Jul. 2009, [Online]. Available: http://www.academicjournals.org/SRE.

[49]   K.-M. Lee, D.-S. Kim, and J.-S. Kim, "Determination of dynamic Young's modulus of concrete at early ages by impact resonance test," *KSCE J. Civ. Eng.*, vol. 1, no. 1, pp. 11–18, Dec. 1997, doi: 10.1007/bf02830459.

[50]   F. A. Oluokun, E. G. Burdette, and J. H. Deatherage, "Rates of Development of Physical Properties of Concrete at Early Ages," *Transp. Res. Rec.*, no. 1284, pp. 16–21, 1990, [Online]. Available: https://pdfs.semanticscholar.org/a40e/3f742685d90cb98577e84299b078d8e45c83.pdf.

[51]   N. S. Klein, L. A. Lenz, and W. Mazer, "Influence of the granular skeleton packing density

on the static elastic modulus of conventional concretes," *Constr. Build. Mater.*, vol. 242, p. 118086, May 2020, doi: 10.1016/j.conbuildmat.2020.118086.

[52] D. Kocáb, B. Kucharczykova, P. Misak, P. Zitt, and M. Kralikova, "Development of the Elastic Modulus of Concrete under Different Curing Conditions," in *Procedia Engineering*, Jan. 2017, vol. 195, pp. 96–101, doi: 10.1016/j.proeng.2017.04.529.

[53] H. G. Russel and B. A. Graybeal, "Ultra-High Performance Concrete: A State-of-the-Art Report for the Bridge Community," McLean, Jun. 2013. [Online]. Available: https://www.fhwa.dot.gov/publications/research/infrastructure/structures/hpc/13060/1306 0.pdf.

[54] A. A. Khan, "Concrete properties and thermal stress analysis of members at early ages," McGill University, Montreal, 1995.

[55] J. Bensted, "Low Heat Portland Cements," *World Cem.*, vol. 24, no. 11, pp. 42–44, 1993, [Online]. Available: https://search.proquest.com/docview/26064720/7853F489E2D44AC8PQ/12?accountid=1 0920.

[56] K. A. Riding, J. L. Poole, K. J. Folliard, M. C. G. Juenger, and A. K. Schindler, "Modeling hydration of cementitious systems," *ACI Mater. J.*, vol. 109, no. 2, pp. 225–234, Mar. 2012, doi: 10.14359/51683709.

[57] Y. Huaquan, Y. Wang, and Z. Shihua, "Anti-Crack Performance of Low-Heat Portland Cement Concrete," *J. Wuhan Univ. Technol. Sci. Ed*, pp. 555–559, Sep. 2007, doi: 10.1007/s11595-006-3555-7.

[58] K. A. Riding, "Early Age Concrete Thermal Stress Measurement and Modeling," University of Texas at Austin, 2007.

[59] D. Ravina and P. K. Mehta, "Compressive strength of low cement/high fly ash concrete," *Cem. Concr. Res.*, vol. 18, no. 4, pp. 571–583, Jul. 1988, doi: 10.1016/0008-8846(88)90050-6.

[60] R. Bird, W. Stewart, and E. Lightfoot, *Transport Phenomena*. New York: John Wiley and Sons, Inc., 1960.

[61] H. Tokuda and M. Shoya, "Thermal Diffusivity of Concrete as a Composite Material," 1972, [Online]. Available: https://search.proquest.com/docview/87471961/2C2EB73B5FA8420BPQ/1?accountid=10 920.

[62] Z. Bažant and M. Kaplan, *Concrete at high temperatures : material properties and mathematical models* . Harlow: Longman Group Ltd, 1996.

[63] M. Fintel, Ed., *Handbook of Concrete Engineering*, 2nd ed. New York: Van Nostrand Reinhold Company, 1985.

[64] J.-H. Lee, "Experimental and Analytical Investigations of the thermal Behavior of Prestressed Concrete Bridge Girders Including Imperfections," Georgia Institute of Technology, Atlanta, 2010.

[65]   D. Whiting, A. Litvin, and S. E. Goodwin, "Specific Heat of Selected Concretes," *J. Proc.*, vol. 75, no. 7, pp. 299–305, Jul. 1978, doi: 10.14359/10943.

[66]   G. De Schutter and L. Taerwe, "Specific-Heat and Thermal-Diffusivity of Hardening Concrete," *Mag. Concr. Res.*, vol. 47, no. 172, pp. 203–208, Jan. 1995, doi: 10.1680/macr.1995.47.172.203.

[67]   Y. Sun, P. Gao, F. Geng, H. Li, L. Zhang, and H. Liu, "Thermal conductivity and mechanical properties of porous concrete materials," *Mater. Lett.*, vol. 209, pp. 349–352, Dec. 2017, doi: 10.1016/j.matlet.2017.08.046.

[68]   E. Ganjian, "The relationship between porosity and thermal conductivity of concrete," University of Leeds, Leeds, 1990.

[69]   J. A. Gilliland, "Thermal and shrinkage effects in high performance concrete structures during construction," University of Calgary (Canada), Calgary, 2000.

[70]   Figg and Muller Engineers, "Prestressed Concrete Segmental Bridge Construction Manual," 1981.

[71]   G. A. Rombach, "Fugen in Segmentfertigteilbrücken," *Massivbau in ganzer Breite*, no. January 2005, pp. 75–81, 2005, doi: 10.1007/3-540-26827-8_10.

[72]   Deutscher Beton Vereins, "Empfehlungen für Segmentfertigteilbrücken [In German]," 1999.

[73]   G. A. Rombach, "Dry Joint Behavior of Hollow Box Girder Segmental Bridges Design of Unreinforced joints," in *fib Symposium: Segmental Construction in Concrete*, 2004, no. 1998, pp. 26–29.

[74]   T. Shinohe, K. Tashiro, O. Numata, and T. Murakami, "Studies on Strength Development and Durability of High Temperature Steam Cured Concrete," *Tohoku Kogyo Daigaku kiyo*, vol. 1, pp. 139–157, Mar. 1988, [Online]. Available: https://www.engineeringvillage.com/search/doc/abstract.url?&pageType=quickSearch&usageZone=resultslist&usageOrigin=searchresults&searchtype=Quick&SEARCHID=3c1be1441843421b945f13e27aa03870&DOCINDEX=1&ignore_docid=cpx_2263747&database=3&format=quickSearchAb.

[75]   G. A. Rombach and R. Abendeh, "Temperature Induced Deformations in Match-Cast Segments," *IABSE Symp. Rep.*, vol. 88, no. 6, pp. 403–408, Jan. 2004, doi: 10.2749/222137804796291557.

[76]   M. Cervera and J. Oliver, "Thermo-Chemo-Mechanical Model for Concrete," *J. Eng. Mech.*, vol. 9399, no. April, 1999, doi: 10.1061/(ASCE)0733-9399(1999)125.

[77]   F. P. Incropera and D. Dewitt, *Fundamentals of heat and mass transfer*, 3rd ed. New York : John Wiley & Sons, 1990.

[78]   A. K. Schindler, "Effect of temperature on hydration of cementitious materials," *ACI Mater. J.*, vol. 101, no. 1, pp. 72–81, 2004, doi: 10.14359/12990.

[79]   L. D'Aloia and G. Chanvillard, "Determining the 'apparent' activation energy of concrete,"

Cem. Concr. Res., vol. 32, no. 8, pp. 1277–1289, 2002, doi: 10.1016/s0008-8846(02)00791-3.

[80] J. L. Poole, "Modeling Temperature Sensitivity and Heat Evolution of Concrete," 2007.

[81] K. A. Riding, J. L. Poole, A. K. Schindler, M. C. G. Juenger, and K. J. Folliard, "Temperature boundary condition models for concrete bridge members," *ACI Mater. J.*, vol. 104, no. 4, pp. 379–387, 2007, doi: 10.14359/18827.

[82] G. S. Wojcik and D. R. Fitzjarrald, "Energy balances of curing concrete bridge decks," *J. Appl. Meteorol.*, vol. 40, no. 11, pp. 2003–2025, 2001, doi: 10.1175/1520-0450(2001)040<2003:EBOCCB>2.0.CO;2.

[83] ASTM, "ASTM C1074-19 Standard Practice for Estimating Concrete Strength by the Maturity Method," 2019. Accessed: Sep. 07, 2020. [Online]. Available: https://compass.astm.org/EDIT/html_annot.cgi?C1074+19.

[84] M. Viviani, "Monitoring and modelling of construction materials during hardening," EPFL, 2005.

[85] International Federation for Structural Concrete (FIB), "Model Code for Concrete Structures 2010," Laussane, Switzerland, 2010.

[86] M. Larson, "Thermal crack estimation in early age concrete : models and methods for practical application," Doctoral Thesis, Luleå University, Luleå, Sweden, 2003.

[87] M. Aussweger *et al.*, "Early-age evolution of strength, stiffness, and non-aging creep of concretes: Experimental characterization and correlation analysis," *Materials (Basel).*, vol. 12, no. 2, Jan. 2019, doi: 10.3390/ma12020207.

[88] H. Hashida and N. Yamazaki, "Deformation Composed of Autogenous Shrinkage and Thermal Expansion Due to Hydration of High Strength Concrete and Stress in Reinforced Structures," in *Proceedings of the Third International Research Seminar on Self-Desiccation and its Importance in Concrete Technology*, 2002, pp. 77–92.

[89] F. Grondin, M. Bouasker, P. Mounanga, A. Khelidj, and A. Perronnet, "Physico-chemical deformations of solidifying cementitious systems: Multiscale modelling," *Mater. Struct. Constr.*, vol. 43, no. 1–2, pp. 151–165, 2010, doi: 10.1617/s11527-009-9477-z.

[90] European Committee for Standardization (CEN), "Eurocode 2: Design of Concrete Structures EN 1992-1-1," 2004.

[91] ACI Committee 209, "ACI 209.2R-08 Guide for Modeling and Calculating Shrinkage and Creep in Hardened Concrete," 2008.

[92] Y. Liu, "Finite-Element Modeling of Early- Age Concrete Behavior," Auburn University, 2018.

[93] Z. Bažant and F. H. Whitman, "Creep and shrinkage in concrete structures," *Earthq. Eng. Struct. Dyn.*, vol. 11, no. 4, pp. 591–592, Jul. 1983, doi: 10.1002/eqe.4290110413.

[94] Z. Bažant, "Numerical Determination of Long Range Stress History from Strain History in Concrete," *Mater. Struct.*, vol. 5, no. 27, pp. 135–141, 1972.

[95] ASTM, "ASTM C512 / C512M-15 Standard Test Method for Creep of Concrete in Compression," 2015. Accessed: Oct. 23, 2020. [Online]. Available: https://www.astm.org/Standards/C512.

[96] B. E. Byard, A. K. Schindler, K. A. Riding, and K. J. Folliard, "Validation of modified B3 model to predict early-age stress development of concrete," *ACI Mater. J.*, vol. 113, no. 5, pp. 691–700, 2016, doi: 10.14359/51689113.

[97] Z. Bažant and S. Prasannan, "Solidification Theory for Concrete Creep I: Formulation," *Eng. Mech.*, vol. 115, no. 8, pp. 1691–1703, 1990.

[98] B. Z. P. Bazant and S. Prasannan, "Solification Theory for Concrete Creep II: Verification and Application," *Eng. Mech.*, vol. 115, no. 8, pp. 1704–1725, 1990.

[99] G. De Schutter, "Degree of hydration based Kelvin model for the basic creep of early age concrete," *Mater. Struct. Constr.*, vol. 32, no. 218, pp. 260–265, 1999, doi: 10.1007/bf02479595.

[100] b4Cast, "b4Cast User Manual: Mechanical Properties." http://www.b4cast.com/b4cast/help/editmechprop.htm (accessed Oct. 24, 2020).

[101] Diana FEA, "Young Hardening Concrete -Brochure-." 2020, [Online]. Available: https://dianafea.com/.

[102] R. Witasse and M. Hendriks, "Finite Element Modeling of Early Age Concrete Behavior using DIANA," in *Finite Elements in Civil Engineering Applications: Proceedings of the Third DIANA World Conference*, 2002, pp. 129–134, Accessed: Nov. 04, 2020. [Online]. Available: https://books.google.com/books?hl=es&lr=&id=t47ANKyOEf8C&oi=fnd&pg=PR9&dq=witasse+and+hendriks+finite&ots=COQ9Rqja--&sig=Ljp73nrqmYyNUfyFd7o6uMqYdgA#v=onepage&q=witasse and hendriks finite&f=false.

[103] D. Logan, *A First Course in the Finite Element Method*. Boston: PWS Publishers, 1986.

[104] W. Podolny and J. Muller, *Construction and Design of Prestressed Concrete Segmental Bridges*. New York: John Wiley and Sons, Inc., 1982.

[105] Contech Analysis, "b4cast - Simulation of Hardening Concrete," 2021. http://www.b4cast.com/b4cast/b4cast.html.

[106] AASHTO, PCI, and ASBI, "Segmental Box Girder Standards for Span-by-Span and Balanced Cantilever Construction," 2000.

[107] Florida Department of Transportation (FDOT), *Structures Design Guidelines - Structural Manual Volume I*, vol. 1. Tallahassee, 2021.

[108] ASTM, "ASTM C150/C150M-20 Standard Specification for Portland Cement," 2020. doi: 10.1520/C0150.

[109] AASHTO, "AASHTO M 85: Standard Specification for Portland Cement.pdf," 2020.

[110] ASTM, "ASTM C595/C595M-20: Standard Specification for Blended Hydraulic

Cements," 2020. doi: 10.1520/C0595.

[111] AASHTO, "AASHTO M 240M/M 240: Standard Specification for Blended Hydraulic Cement," 2020.

[112] ASTM, "ASTM 1240: Standard Specification for Silica Fume Used in Cementitious Mixtures," 2020. doi: 10.1520/C1240-20.2.

[113] ASTM, "ASTM C494/C494M-19 Standard Specification for Chemical Admixtures for Concrete," no. February, pp. 1–10, 2019, doi: 10.1520/C0494.

[114] N. Yazdani, B. McKinnie, and S. Haroon, "Aggregate-Based Modulus of Elasticity for Florida Concrete," *Transp. Res. Rec.*, no. 1914, pp. 15–23, 2005, doi: 10.3141/1914-03.

[115] A. Tankasala and A. K. Schindler, "Early-Age Cracking of Lightweight Mass Concrete," *ACI Mater. J.*, vol. 117, no. 1, pp. 223–232, 2020, doi: 10.14359/51719082.

[116] Time and Date AS, "Weather in Miami / Weather in Tallahassee," 2022. https://www.timeanddate.com/.

[117] ASTM, "ASTM C171 - 20: Standard Specification for Sheet Materials for Curing Concrete," 2020. doi: 10.1520/C0171-20.

[118] S. Mindess, J. F. Young, and D. Darwin, *Concrete*. Upper Saddle River: Prentice Hall, 2003.

[119] A. Tankasala, A. K. Schindler, and K. A. Riding, "Risk of thermal cracking from use of lightweight aggregate in mass concrete," *Transp. Res. Rec.*, vol. 2629, no. 1, pp. 42–50, 2017, doi: 10.3141/2629-07.

[120] ACI Committee 213, "Guide for Structural Lightweight-Aggregate Concrete," Farmington Hills, MI, 2014.

[121] ACI Committee 211, "Standard Practice for Selecting Proportions for Normal, Heavyweight, and Mass Concrete," 2009.

[122] C. L. Roberts, J. E. Breen, and M. E. Kreger, "Temperature Induced Deformations in Match-cast segments," *PCI J.*, p. 10, 1995.

[123] ConTech Analysis ApS, "b4cast - Manual in Software." 2022.

[124] K. Mehta and P. Monteiro, *Concrete: Microstructure, Properties and Materials*, First Edit. McGraw Hill Professional, 2001.

[125] K. J. Folliard, M. C. G. Juenger, J. L. Poole, K. A. Riding, A. K. Schindler, and S. Slatnick, "Prediction Model for Concrete Behavior," *Univ. Texas Austin. Cent. Transp. Res.*, 2007, [Online]. Available: https://library.ctr.utexas.edu/Presto/content/Detail.aspx?ctID=UHVibGljYXRpb25fMTE2MTA%3D&rID=MTE2MDk%3D&ssid=c2NyZWVuSURfMTQ2MDk%3D&bmdc=MQ==.

[126] Time and Date AS, "Weather in San Antonio - July." https://www.timeanddate.com/weather/usa/san-antonio/historic?month=7&year=2011.

[127] The Weather Company and Weather Underground, "Weather in San Antonio July 1990,"

2022. https://www.wunderground.com/history/daily/us/tx/san-antonio/KSAT/date/1990-7-10.

[128] C-Therm, "The Thermal Conductivity of Unfilled Plastics," 2022. https://ctherm.com/resources/newsroom/blog/the-thermal-conductivity-of-unfilled-plastics/.

[129] F. Beer, *Mecanica de materiales*, 5th ed. McGraw-Hill / Interamericana, 2009.

[130] Incropera, F.P., Dewitt, D.P., Bergman, T.L., Lavine, A.S., Fundamentals of Heat and Mass Transfer, 6th Edition, John Wiley & Sons, Hoboken, N.J., 2007.

Appendix A. Locations of temperature and distortion values examined
Bridge A – Results points of extraction
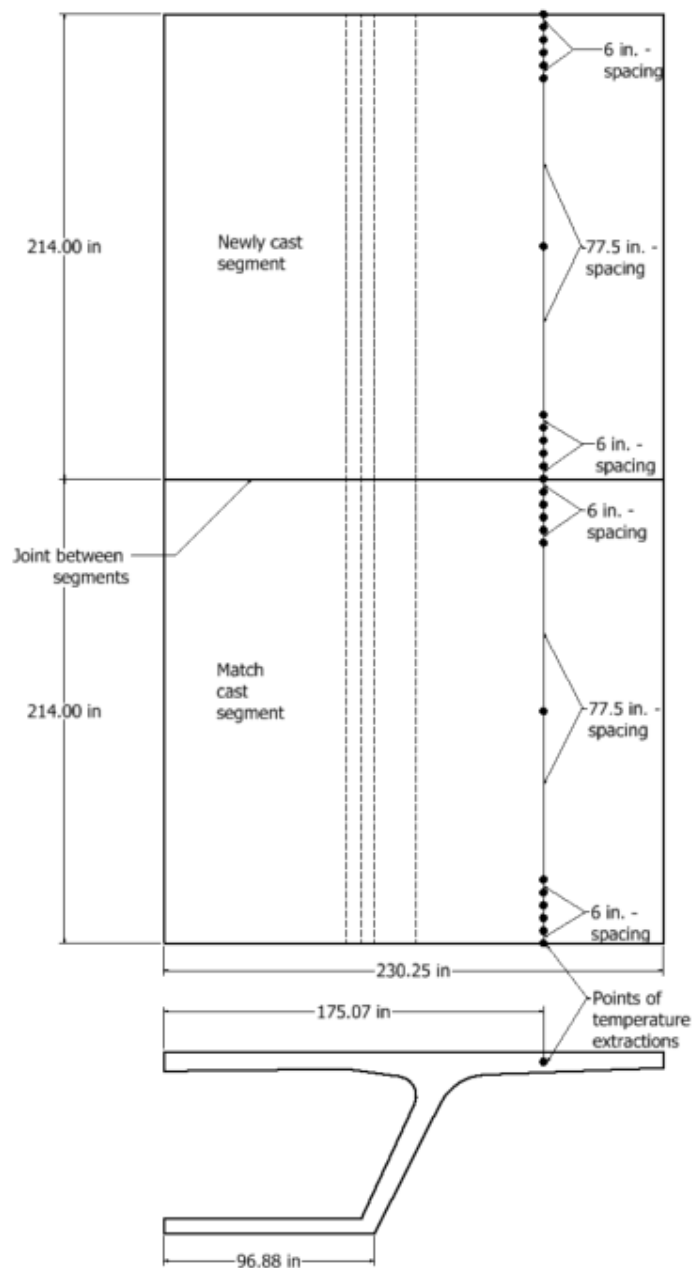
Figure A-1: Locations where temperatures were examined for Bridge A
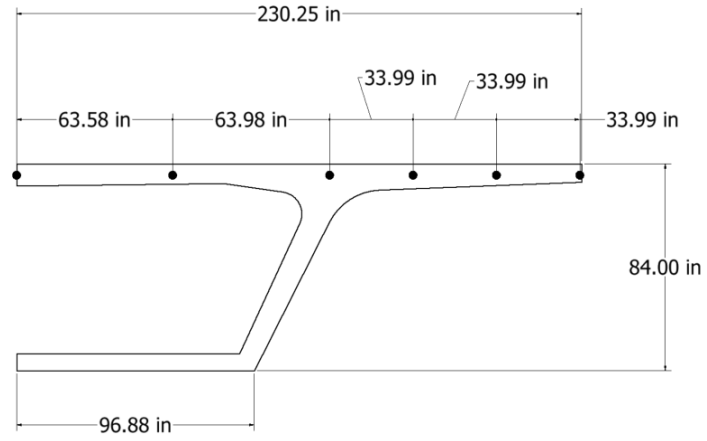
Figure A-2: Locations where deformations were examined for Bridge A

Bridge B – Results points of extraction
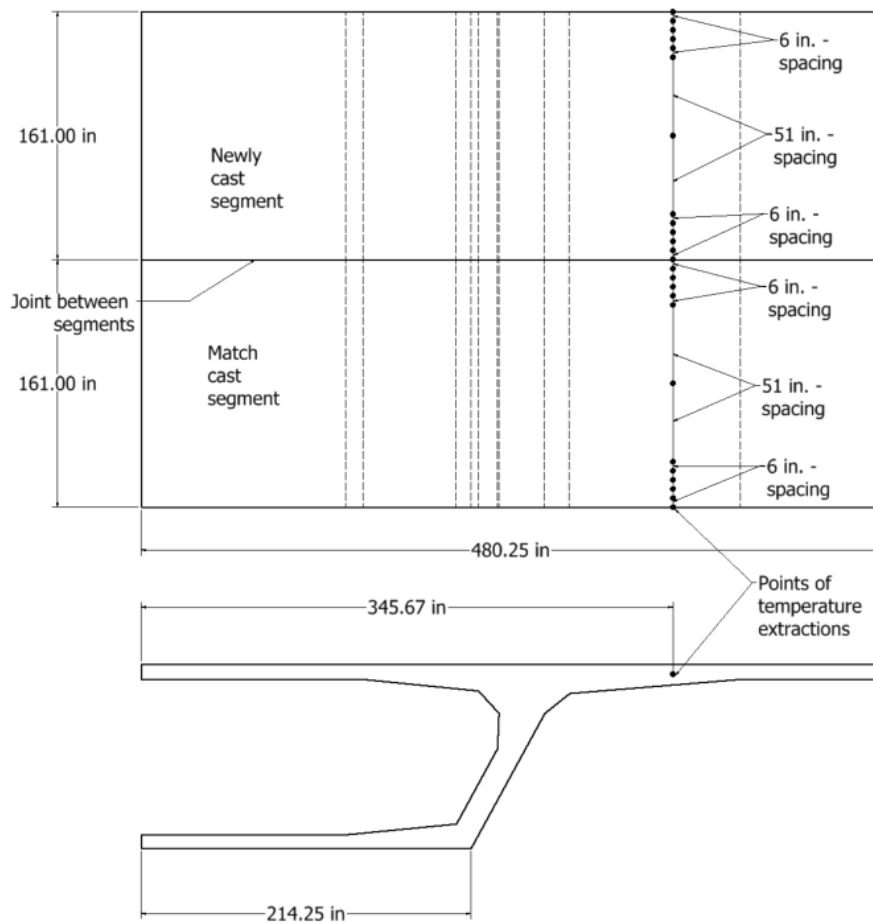
Figure A-3: Locations where temperatures were examined for Bridge B
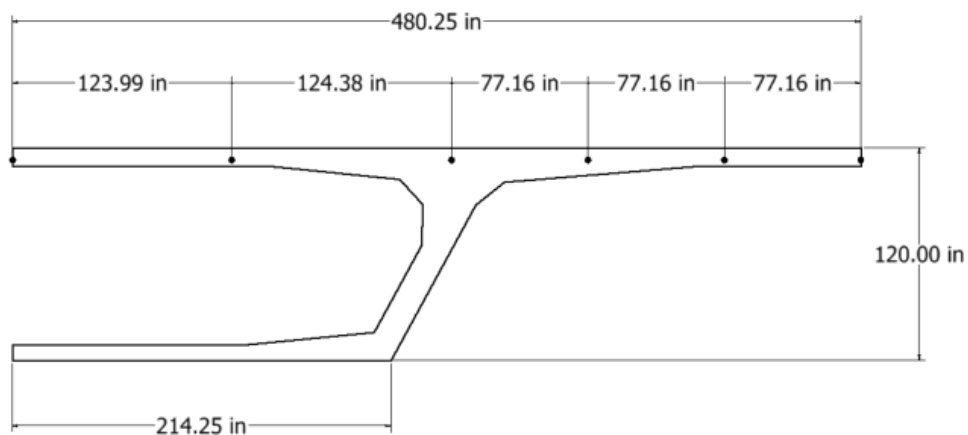
Figure A-4: Locations where deformations were examined for Bridge B

Bridge C – Results points of extraction
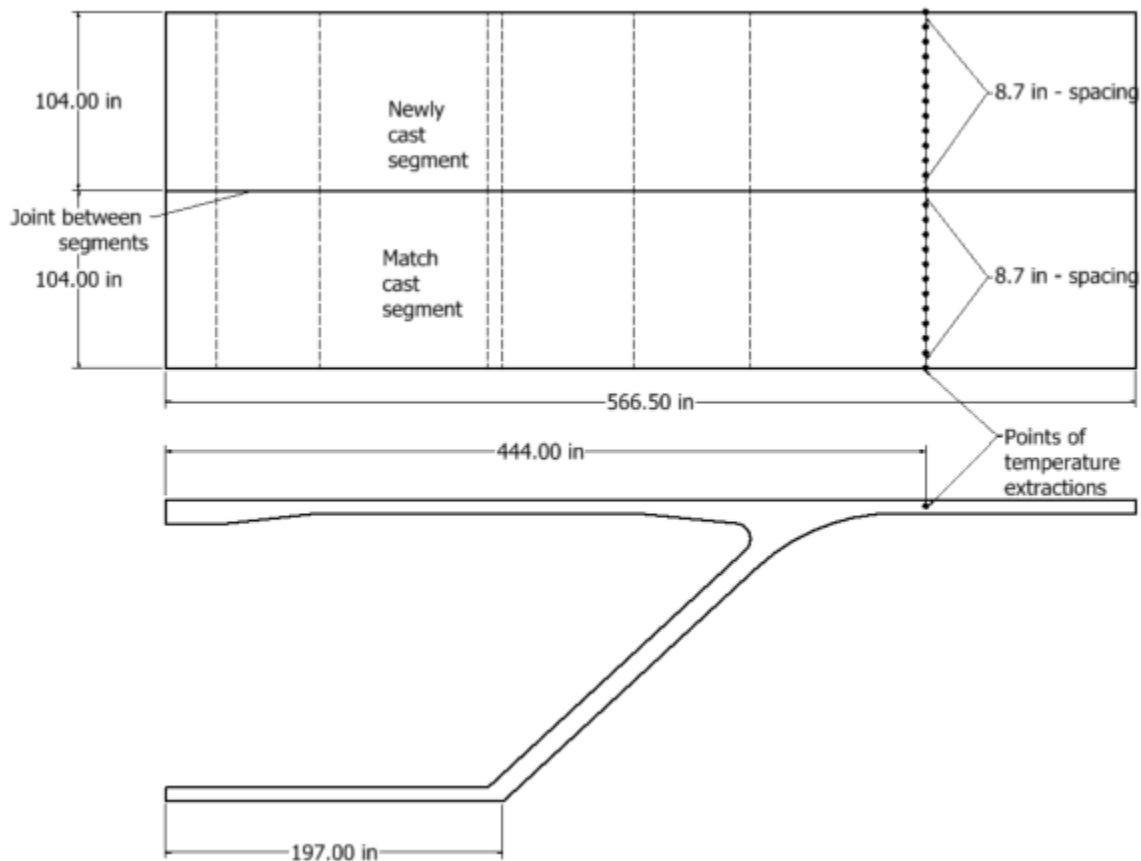
Figure A-5: Locations where temperatures were examined for Bridge C
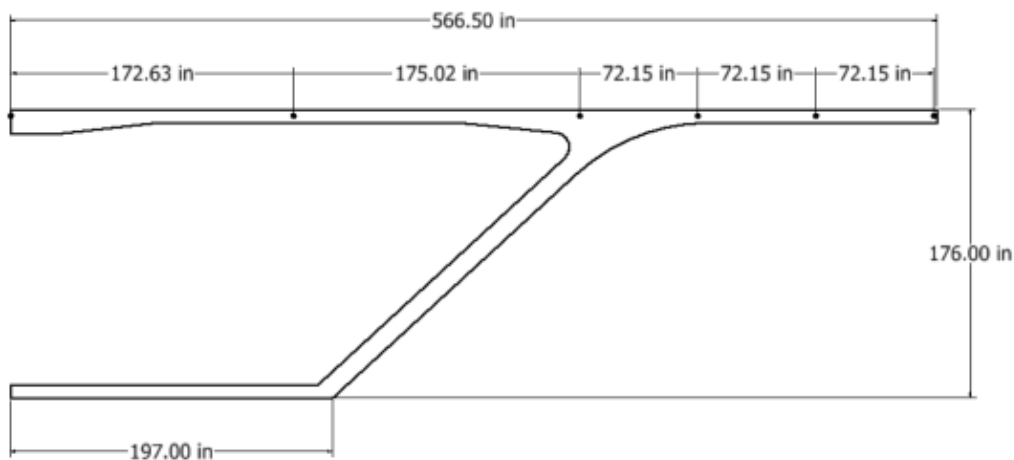
Figure A-6: Locations where deformations were examined for Bridge C

Bridge D – Results points of extraction
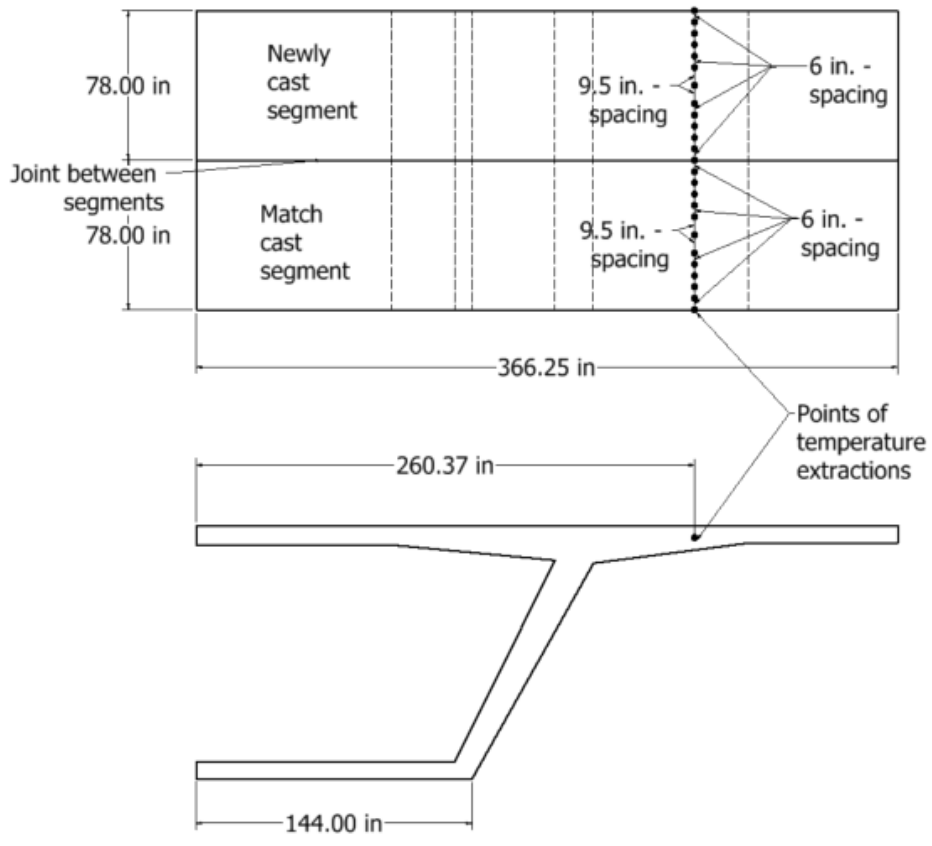
Figure A-7: Locations where temperatures were examined for Bridge D
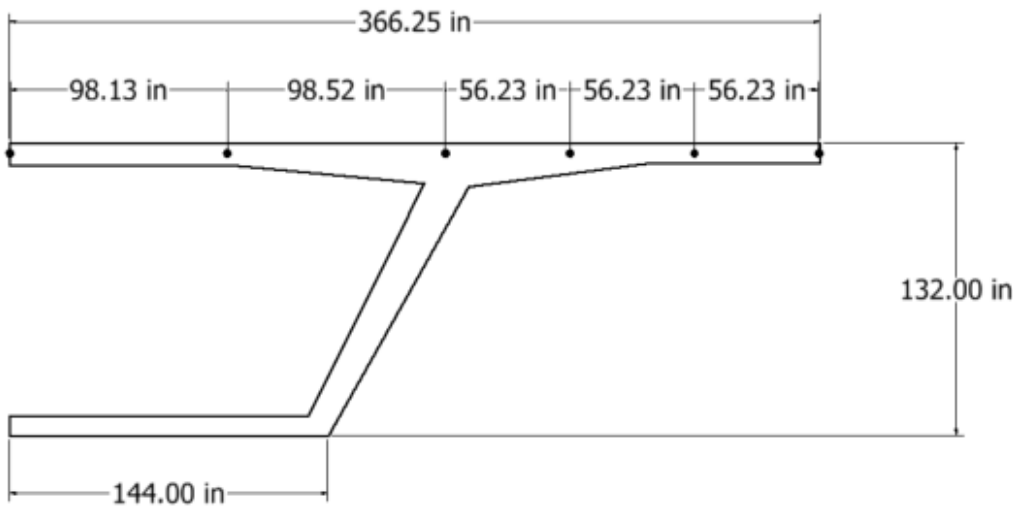
Figure A-8: Locations where deformations were examined for Bridge D

Bridge E – Results points of extraction
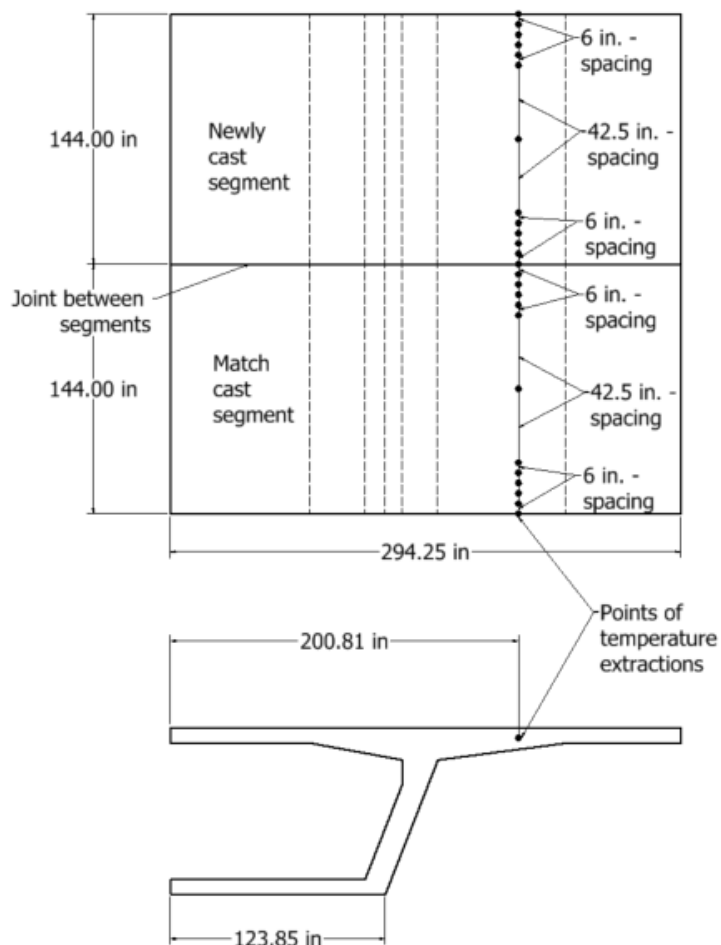
Figure A-9: Locations where temperatures were examined for Bridge E
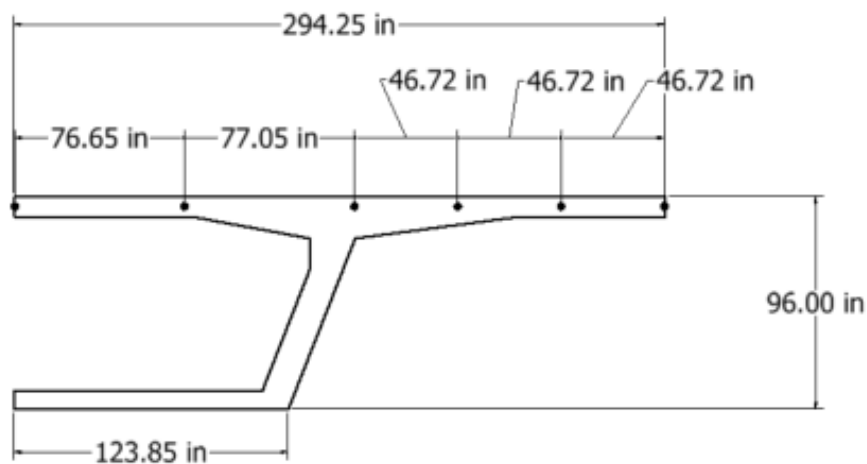
Figure A-10: Locations where deformations were examined for Bridge E

Bridge F – Results points of extraction
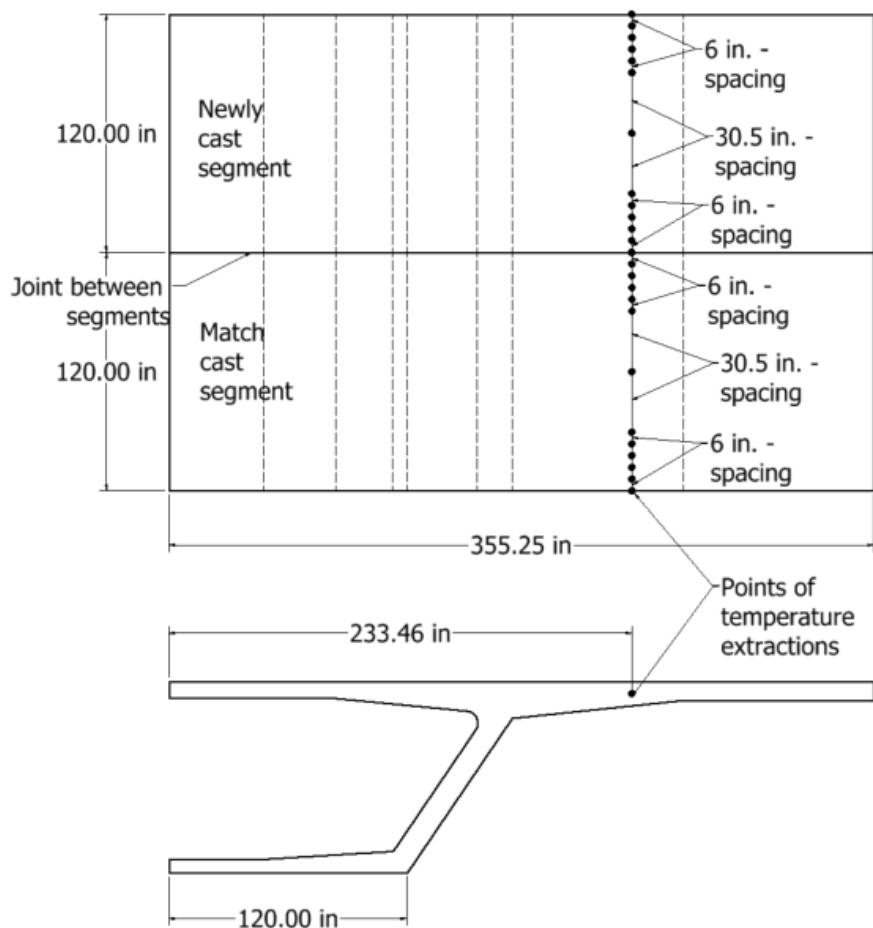
Figure A-11: Locations where temperatures were examined for Bridge F
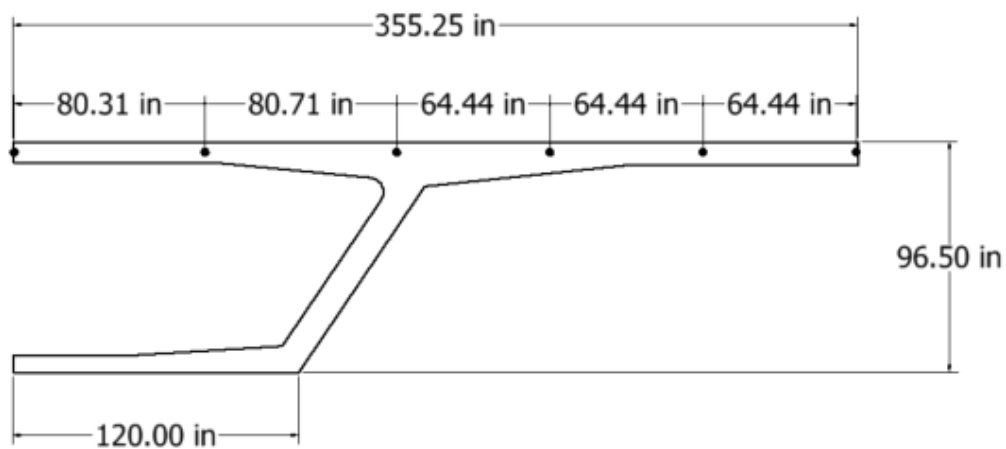
Figure A-12: Locations where deformations were examined for Bridge F

Bang Na – Results points of extraction
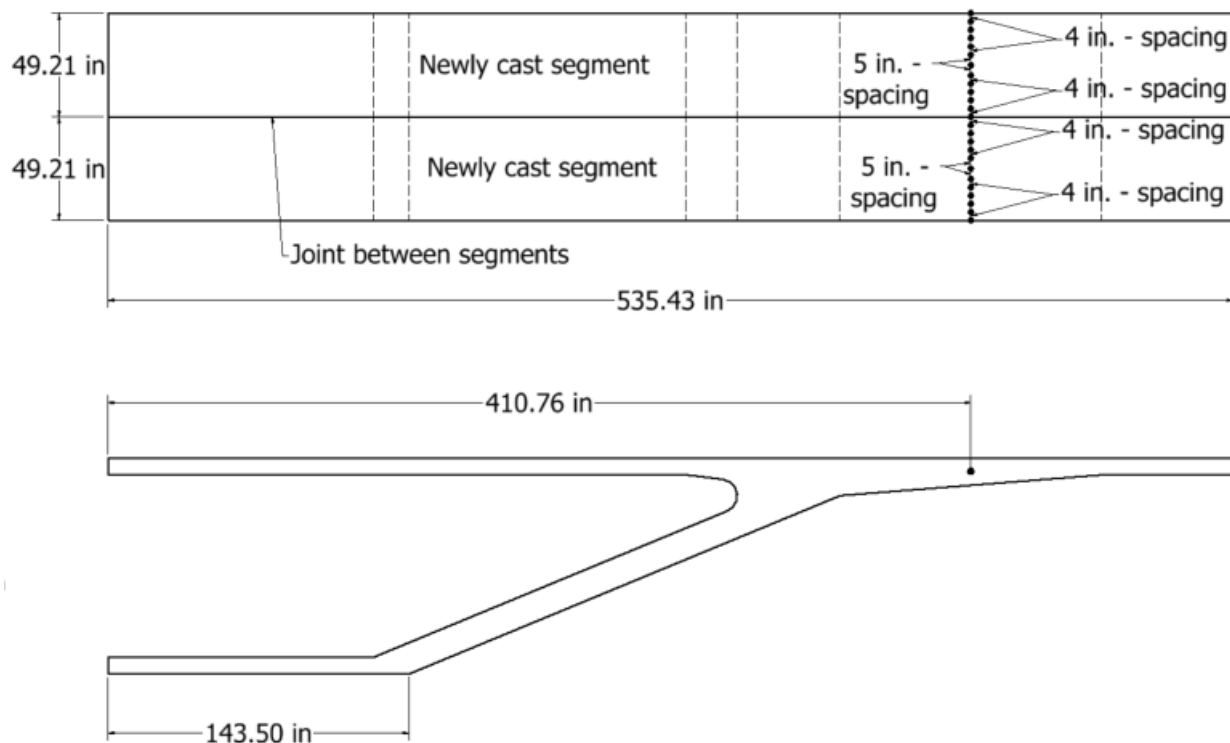
Figure A-13: Locations where temperatures were examined for Bang Na
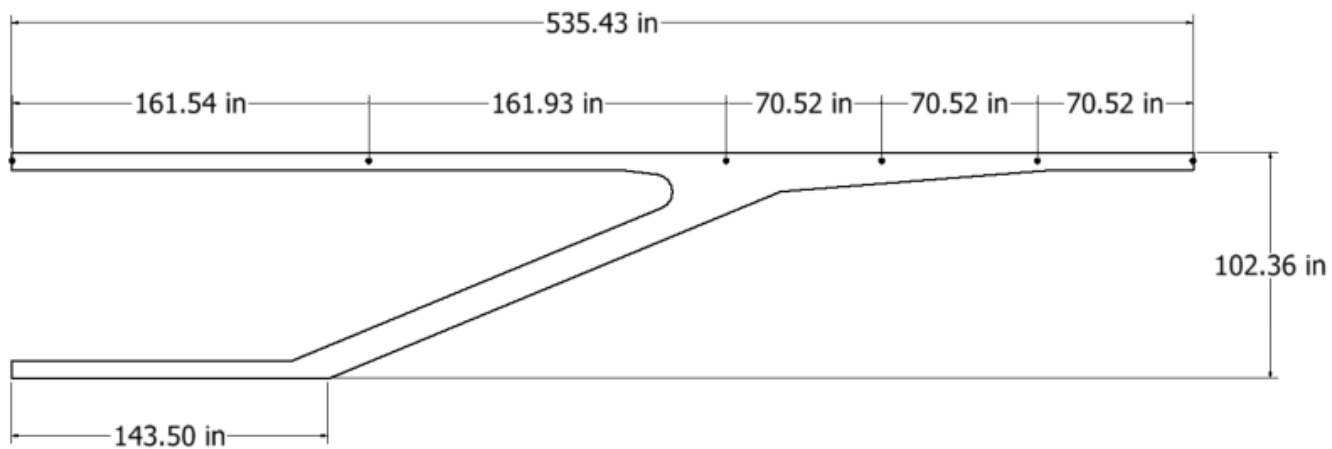
Figure A-14: Locations where deformations were examined for Bang Na

Appendix B. Results summary

Simulation 1 -Results Summary

Table B-1: Model input parameters simulation 1

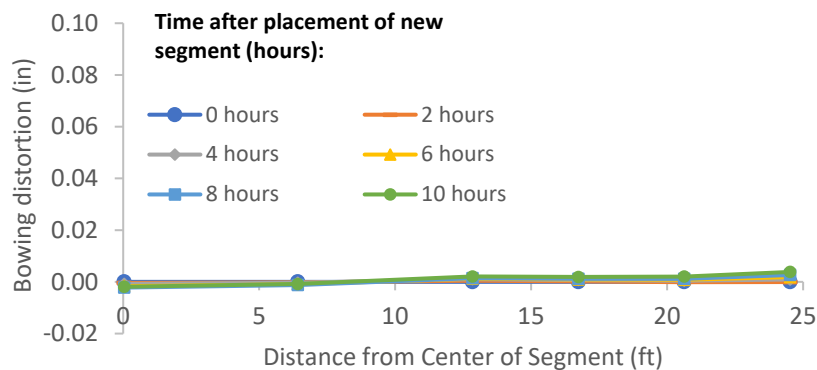| Model details		
Permutation number	1	
Geometry	Florida Bridge E - w/l=4.09	
Max. Mesh Size	2.95	in
Time Step	1	hrs
Placement Temperature	95	°F
Match-cast segment Time of Simulation at Casting	0	hrs
New Segment Time of Simulation at Casting	24	hrs
Concrete Properties		
Cement Content	650.08	lb/yd^3
Activation Energy	36.46	BTU/mol
Heat of Hydration Parameters		
Total Heat Development, $Q_{ult} = \alpha_u \cdot H_u$	103.17	BTU/lb
Time Parameter, τ	12.97	hrs
Curvature Parameter, β	1.14	
Density	3834.891	lb/yd^3
Specific Heat	0.24	BTU/(lb·°F)
Thermal Conductivity	1.608	BTU/(ft·h·°F)
Match-cast segment Elastic Modulus Dev. Parameters		
Final Value	4503.55	ksi
Time Parameter	12.420	hrs
Curvature Parameter	1.068	
New Segment Elastic Modulus Dev. Parameters		
Final Value	14.50	ksi
Time Parameter	n/a	hrs
Curvature Parameter	n/a	
Poisson Ratio	0.17	
Coefficient of Thermal Expansion	4.55	με/°F
Thermal Boundary Conditions (Applied to Appropriate Faces)		
Ambient Temp	Miami - Summer - Morning - Placement		
Wind	Medium-Wind	7.50	mph
Formwork	Steel Formwork	34.60	BTU/(ft·h·°F)
	Thickness	0.118	in
Curing	Burlap	0.18	BTU/(ft·h·°F)
	Thickness	0.39	in

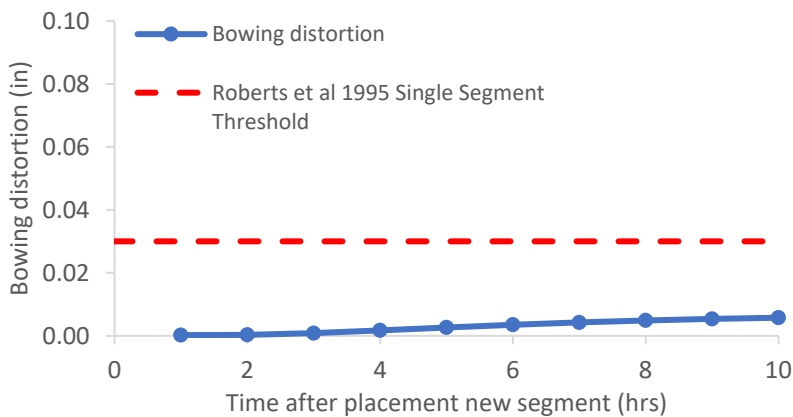Figure B-1: Simulation 1 - Bowing distortion of match-cast segment after placement of the new segment
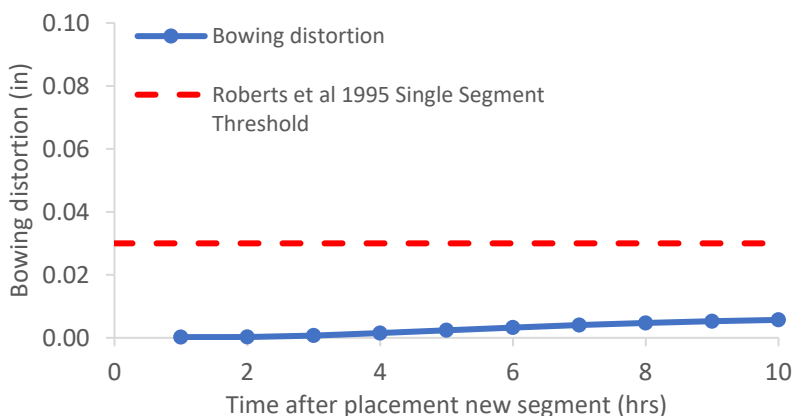
Figure B-2: Simulation 1 - Bowing distortion progression of match-cast segment from time of placement of new segment to 10 hours
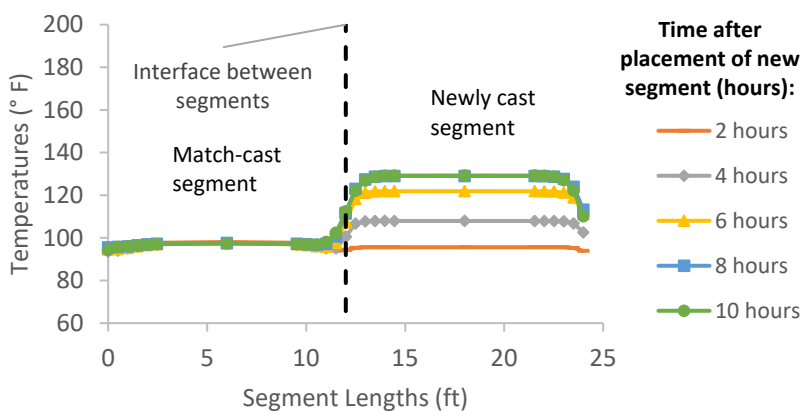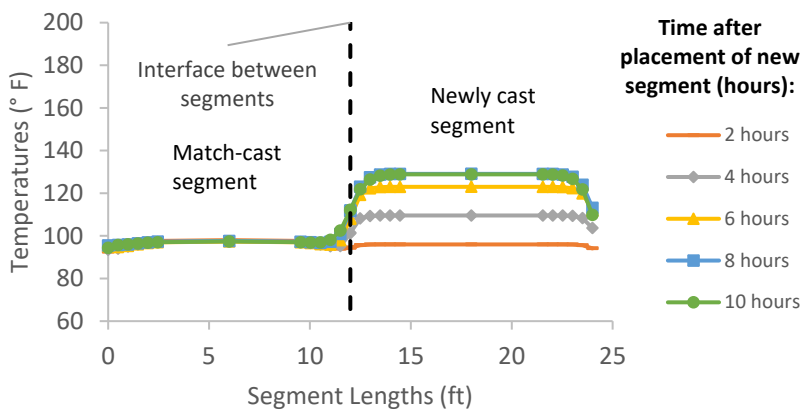

Figure B-3: Simulation 1 - Internal temperatures along the wing of segments

Simulation 2-Results Summary

Table B-2: Model input parameters simulation 2

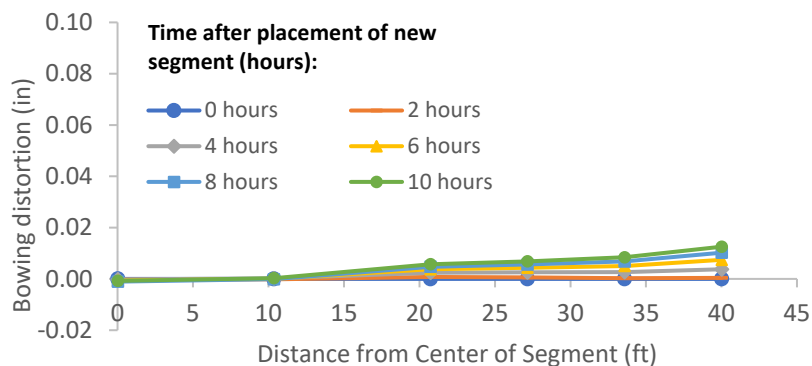| Model details		
Permutation number	2	
Geometry	Florida Bridge B - w/l=5.97	
Max. Mesh Size	3.94	in
Time Step	1	hrs
Placement Temperature	95	°F
Match-cast segment Time of Simulation at Casting	0	hrs
New Segment Time of Simulation at Casting	24	hrs
Concrete Properties		
Cement Content	650.08	lb/yd^3
Activation Energy	36.46	BTU/mol
Heat of Hydration Parameters		
Total Heat Development, $Q_{ult} = \alpha_u \cdot H_u$	103.17	BTU/lb
Time Parameter, τ	12.97	hrs
Curvature Parameter, β	1.14	
Density	3834.891	lb/yd^3
Specific Heat	0.24	BTU/(lb·°F)
Thermal Conductivity	1.608	BTU/(ft·h·°F)
Match-cast segment Elastic Modulus Dev. Parameters		
Final Value	4503.55	ksi
Time Parameter	12.420	hrs
Curvature Parameter	1.068	
New Segment Elastic Modulus Dev. Parameters		
Final Value	14.50	ksi
Time Parameter	n/a	hrs
Curvature Parameter	n/a	
Poisson Ratio	0.17	
Coefficient of Thermal Expansion	4.55	$\mu\varepsilon$/°F
Thermal Boundary Conditions (Applied to Appropriate Faces)			
Ambient Temp	Miami - Summer - Morning - Placement		
Wind	Medium-Wind	7.50	mph
Formwork	Steel Formwork	34.60	BTU/(ft·h·°F)
	Thickness	0.118	in
Curing	Burlap	0.18	BTU/(ft·h·°F)
	Thickness	0.39	in

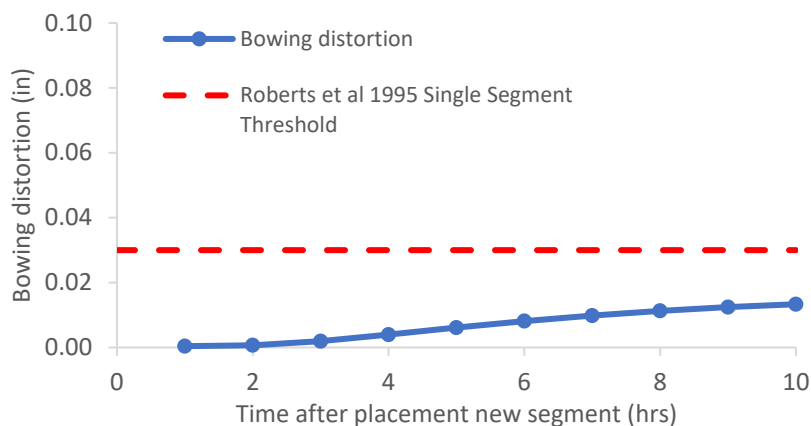Figure B-4: Simulation 2 - Bowing distortion of match-cast segment after placement of the new segment
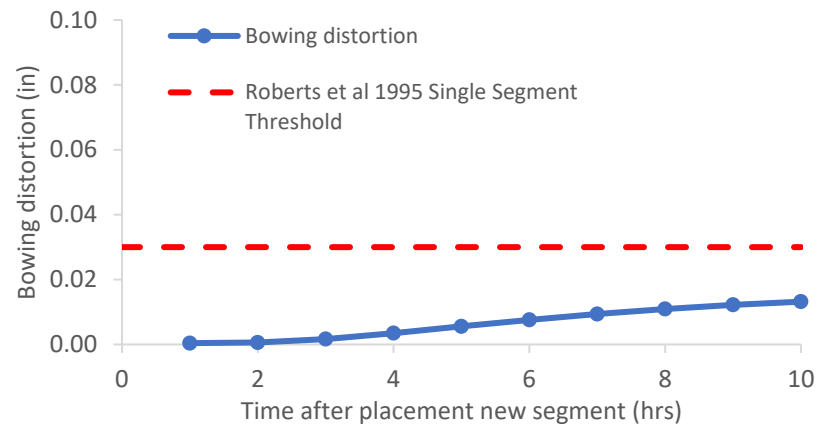
Figure B-5: Simulation 2 - Bowing distortion progression of match-cast segment from time of placement of new segment to 10 hours
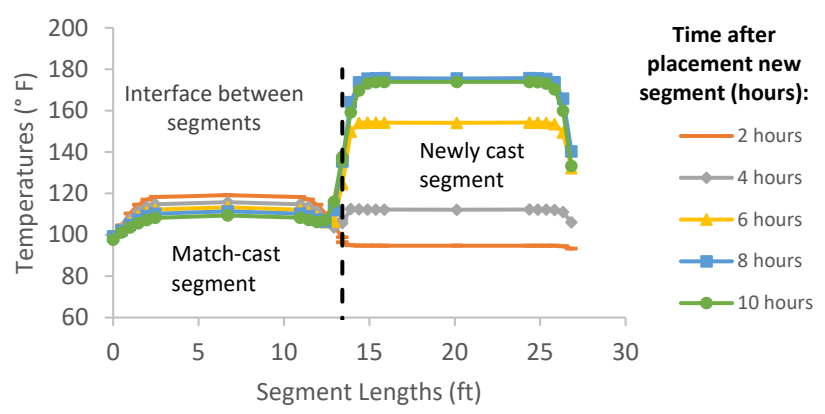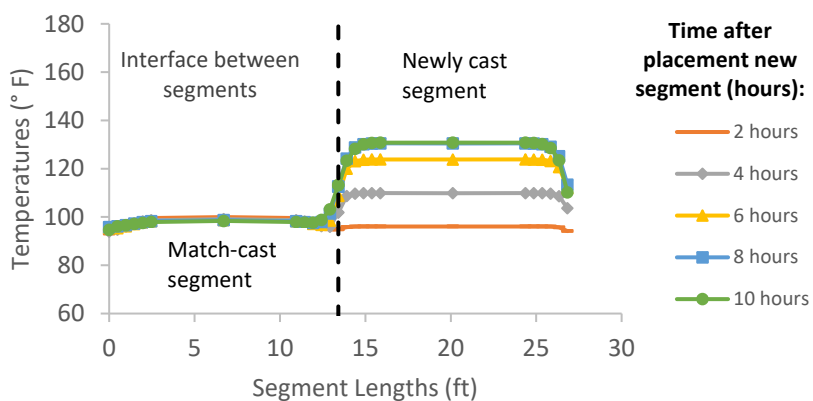

Figure B-6: Simulation 2 - Internal temperatures along the wing of segments

Simulation 3-Results Summary

Table B-3: Model input parameters simulation 3

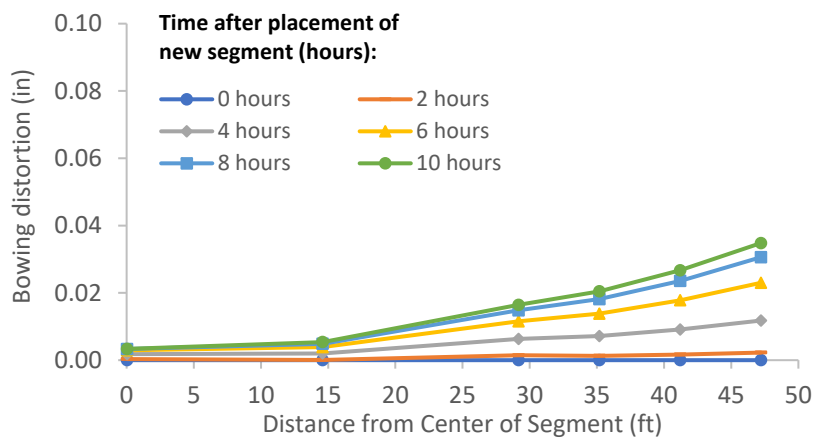| Model details		
Permutation number	3	
Geometry	Florida Bridge C - w/l=10.89	
Max. Mesh Size	3.54	in
Time Step	1	hrs
Placement Temperature	95	°F
Match-cast segment Time of Simulation at Casting	0	hrs
New Segment Time of Simulation at Casting	24	hrs
Concrete Properties		
Cement Content	650.08	lb/yd^3
Activation Energy	36.46	BTU/mol
Heat of Hydration Parameters		
Total Heat Development, $Q_{ult} = \alpha_u \cdot H_u$	103.17	BTU/lb
Time Parameter, τ	12.97	hrs
Curvature Parameter, β	1.14	
Density	3834.891	lb/yd^3
Specific Heat	0.24	BTU/(lb·°F)
Thermal Conductivity	1.608	BTU/(ft·h·°F)
Match-cast segment Elastic Modulus Dev. Parameters		
Final Value	4503.55	ksi
Time Parameter	12.420	hrs
Curvature Parameter	1.068	
New Segment Elastic Modulus Dev. Parameters		
Final Value	14.50	ksi
Time Parameter	n/a	hrs
Curvature Parameter	n/a	
Poisson Ratio	0.17	
Coefficient of Thermal Expansion	4.55	$\mu\varepsilon$/°F
Thermal Boundary Conditions (Applied to Appropriate Faces)		
Ambient Temp	Miami - Summer - Morning - Placement	
Wind	Medium-Wind	7.50	mph
Formwork	Steel Formwork	34.60	BTU/(ft·h·°F)
	Thickness	0.118	in
Curing	Burlap	0.18	BTU/(ft·h·°F)
	Thickness	0.39	in

Figure B-7: Simulation 3 - Bowing distortion of match-cast segment after placement of the new segment
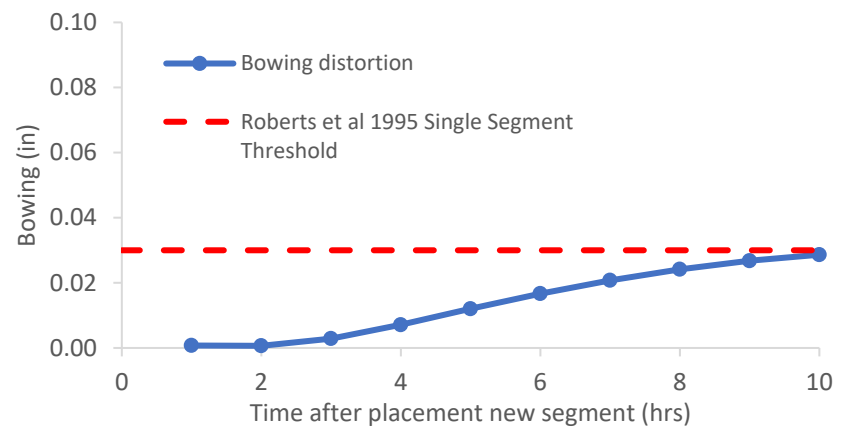
Figure B-8: Simulation 3 - Bowing distortion progression of match-cast segment from time of placement of new segment to 10 hours
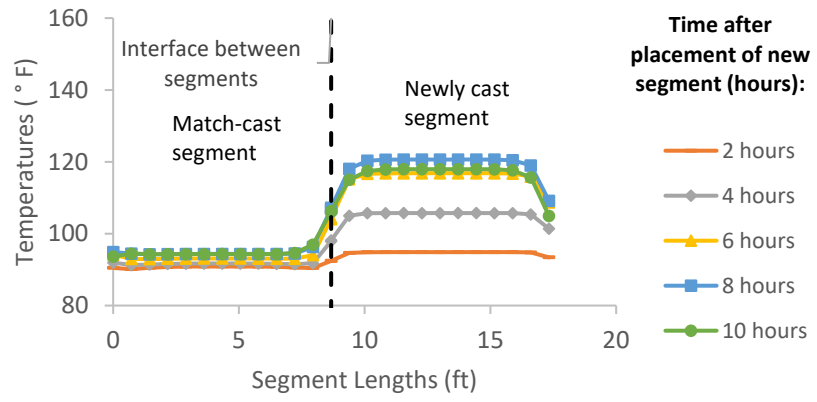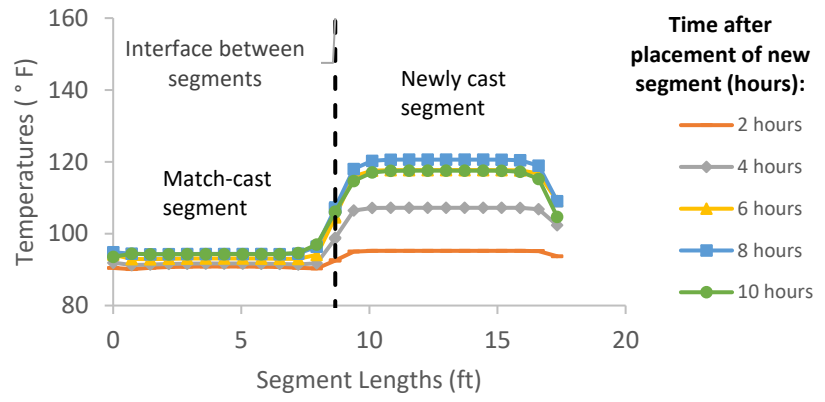

Figure B-9: Simulation 3 - Internal temperatures along the wing of segments

Simulation 4-Results Summary

Table B-4: Model input parameters simulation 4

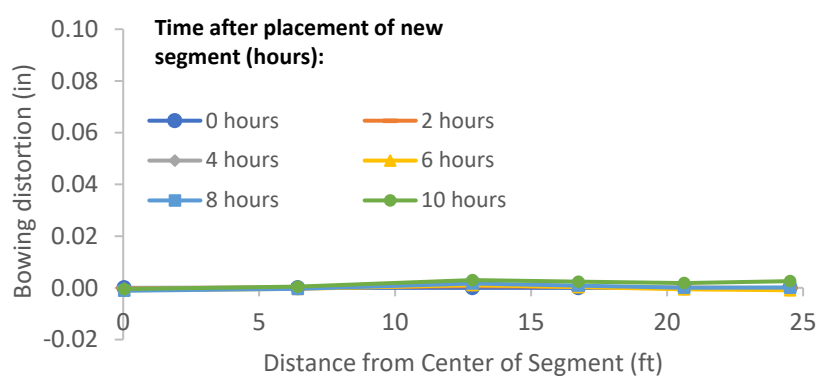| Model details		
Permutation number	4	
Geometry	Florida Bridge E - w/l=4.09	
Max. Mesh Size	2.95	in
Time Step	1	hrs
Placement Temperature	95	°F
Match-cast segment Time of Simulation at Casting	0	hrs
New Segment Time of Simulation at Casting	24	hrs
Concrete Properties		
Cement Content	650.08	lb/yd^3
Activation Energy	32.21	BTU/mol
Heat of Hydration Parameters		
Total Heat Development, $Q_{ult} = \alpha_u \cdot H_u$	103.17	BTU/lb
Time Parameter, τ	11.18	hrs
Curvature Parameter, β	1.14	
Density	3834.891	lb/yd^3
Specific Heat	0.24	BTU/(lb·°F)
Thermal Conductivity	1.608	BTU/(ft·h·°F)
Match-cast segment Elastic Modulus Dev. Parameters		
Final Value	4503.55	ksi
Time Parameter	12.420	hrs
Curvature Parameter	1.068	
New Segment Elastic Modulus Dev. Parameters		
Final Value	14.50	ksi
Time Parameter	n/a	hrs
Curvature Parameter	n/a	
Poisson Ratio	0.17	
Coefficient of Thermal Expansion	4.55	με/°F
Thermal Boundary Conditions (Applied to Appropriate Faces)			
Ambient Temp	Miami - Summer - Morning - Placement		
Wind	Medium-Wind	7.50	mph
Formwork	Steel Formwork	34.60	BTU/(ft·h·°F)
	Thickness	0.118	in
Curing	Burlap	0.18	BTU/(ft·h·°F)
	Thickness	0.39	in

Figure B-10: Simulation 4 - Bowing distortion of match-cast segment after placement of the new segment
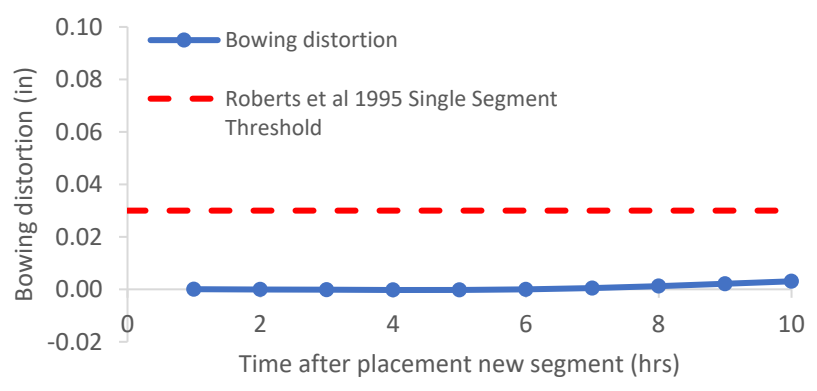

Figure B-10: Simulation 4 - Bowing distortion progression of match-cast segment from time of placement of new segment to 10 hours
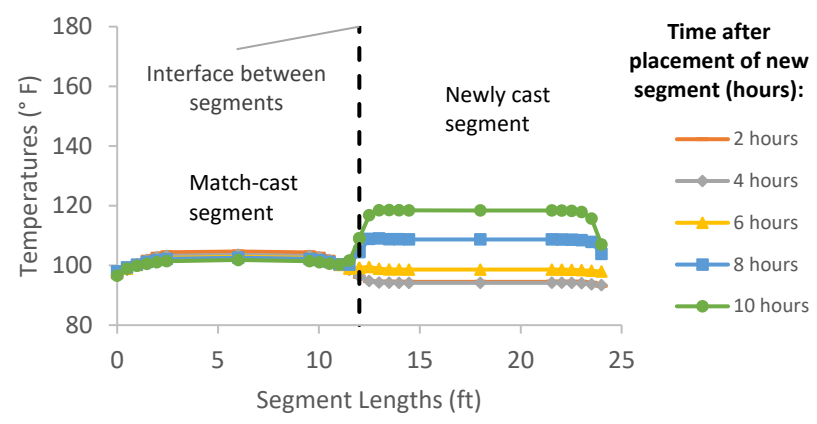

Figure B-12: Simulation 4 - Internal temperatures along the wing of segments

Simulation 5-Results Summary

Table B-5: Model input parameters simulation 5

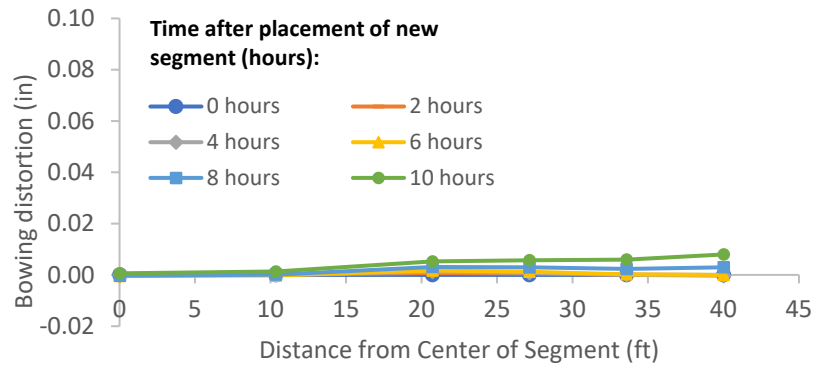| Model details		
Permutation number	5	
Geometry	Florida Bridge B - w/l=5.97	
Max. Mesh Size	3.94	in
Time Step	1	hrs
Placement Temperature	95	°F
Match-cast segment Time of Simulation at Casting	0	hrs
New Segment Time of Simulation at Casting	24	hrs
Concrete Properties		
Cement Content	650.08	lb/yd³
Activation Energy	32.21	BTU/mol
Heat of Hydration Parameters		
Total Heat Development, $Q_{ult} = \alpha_u \cdot H_u$	103.17	BTU/lb
Time Parameter, τ	11.18	hrs
Curvature Parameter, β	1.14	
Density	3834.891	lb/yd³
Specific Heat	0.24	BTU/(lb·°F)
Thermal Conductivity	1.608	BTU/(ft·h·°F)
Match-cast segment Elastic Modulus Dev. Parameters		
Final Value	4503.55	ksi
Time Parameter	12.420	hrs
Curvature Parameter	1.068	
New Segment Elastic Modulus Dev. Parameters		
Final Value	14.50	ksi
Time Parameter	n/a	hrs
Curvature Parameter	n/a	
Poisson Ratio	0.17	
Coefficient of Thermal Expansion	4.55	με/°F
Thermal Boundary Conditions (Applied to Appropriate Faces)		
Ambient Temp	Miami - Summer - Morning - Placement	
Wind	Medium-Wind	7.50	mph
Formwork	Steel Formwork	34.60	BTU/(ft·h·°F)
	Thickness	0.118	in
Curing	Burlap	0.18	BTU/(ft·h·°F)
	Thickness	0.39	in

Figure B-13: Simulation 5 - Bowing distortion of match-cast segment after placement of the new segment
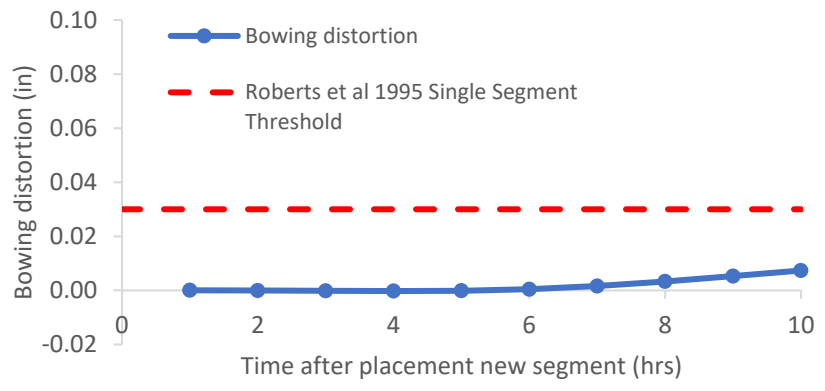

Figure B-14: Simulation 5 - Bowing distortion progression of match-cast segment from time of placement of new segment to 10 hours
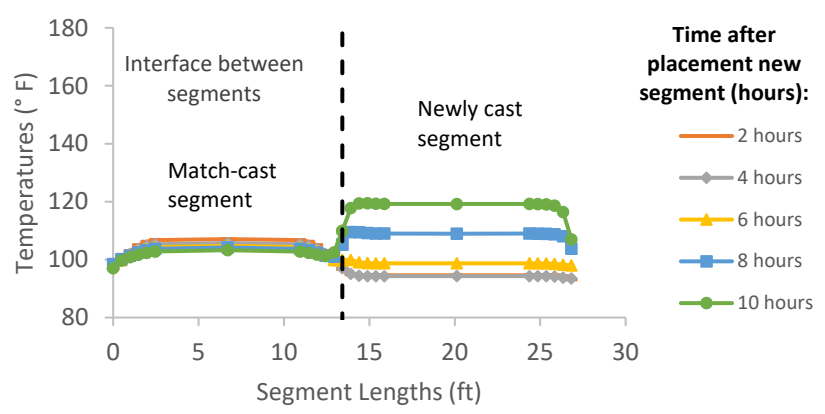

Figure B-15: Simulation 5 - Internal temperatures along the wing of segments

Simulation 6-Results Summary

Table B-6: Model input parameters simulation 6

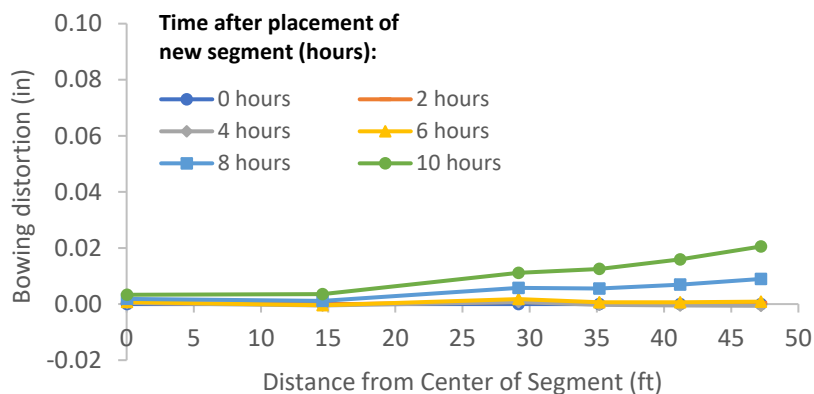| Model details		
Permutation number	6	
Geometry	Florida Bridge C - w/l=10.89	
Max. Mesh Size	3.54	in
Time Step	1	hrs
Placement Temperature	95	°F
Match-cast segment Time of Simulation at Casting	0	hrs
New Segment Time of Simulation at Casting	24	hrs
Concrete Properties		
Cement Content	650.08	lb/yd^3
Activation Energy	32.21	BTU/mol
Heat of Hydration Parameters		
Total Heat Development, $Q_{ult} = \alpha_u \cdot H_u$	103.17	BTU/lb
Time Parameter, τ	11.18	hrs
Curvature Parameter, β	1.14	
Density	3834.891	lb/yd^3
Specific Heat	0.24	BTU/(lb·°F)
Thermal Conductivity	1.608	BTU/(ft·h·°F)
Match-cast segment Elastic Modulus Dev. Parameters		
Final Value	4503.55	ksi
Time Parameter	12.420	hrs
Curvature Parameter	1.068	
New Segment Elastic Modulus Dev. Parameters		
Final Value	14.50	ksi
Time Parameter	n/a	hrs
Curvature Parameter	n/a	
Poisson Ratio	0.17	
Coefficient of Thermal Expansion	4.55	με/°F
Thermal Boundary Conditions (Applied to Appropriate Faces)		
Ambient Temp	Miami - Summer - Morning - Placement	
Wind	Medium-Wind	7.50	mph
Formwork	Steel Formwork	34.60	BTU/(ft·h·°F)
	Thickness	0.118	in
Curing	Burlap	0.18	BTU/(ft·h·°F)
	Thickness	0.39	in

Figure B-16: Simulation 6 - Bowing distortion of match-cast segment after placement of the new segment
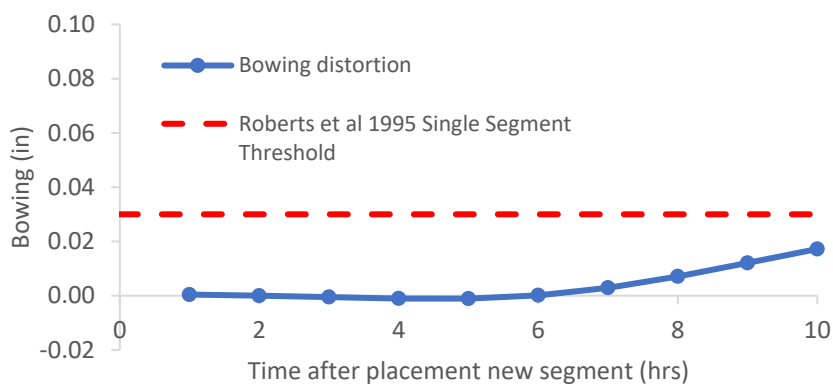

Figure B-17: Simulation 6 - Bowing distortion progression of match-cast segment from time of placement of new segment to 10 hours
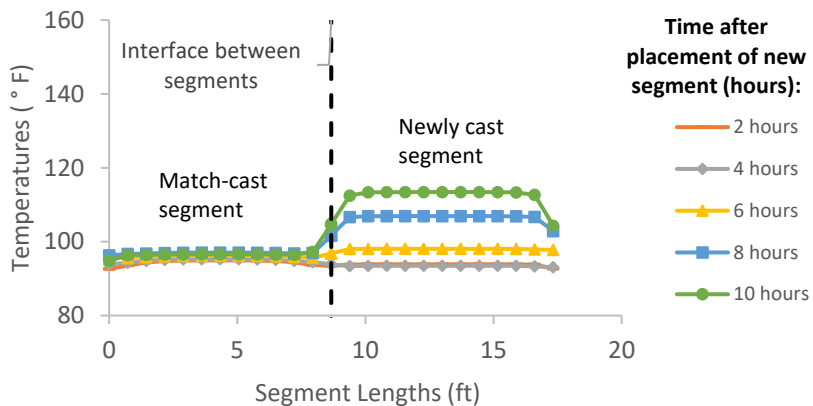

Figure B-18: Simulation 6 - Internal temperatures along the wing of segments

Simulation 7-Results Summary

Table B-7: Model input parameters simulation 7

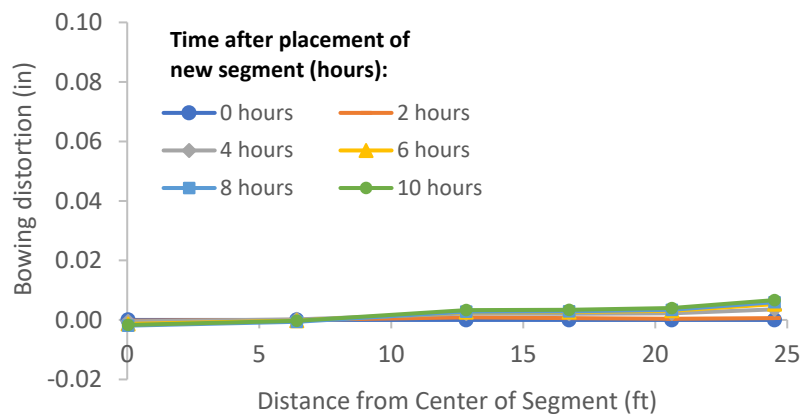| Model details		
Permutation number	7	
Geometry	Florida Bridge E - w/l=4.09	
Max. Mesh Size	2.95	in
Time Step	1	hrs
Placement Temperature	95	°F
Match-cast segment Time of Simulation at Casting	0	hrs
New Segment Time of Simulation at Casting	24	hrs
Concrete Properties		
Cement Content	650.08	lb/yd^3
Activation Energy	26.21	BTU/mol
Heat of Hydration Parameters		
Total Heat Development, $Q_{ult} = \alpha_u \cdot H_u$	107.65	BTU/lb
Time Parameter, τ	18.28	hrs
Curvature Parameter, β	1.65	
Density	3834.891	lb/yd^3
Specific Heat	0.24	BTU/(lb·°F)
Thermal Conductivity	1.608	BTU/(ft·h·°F)
Match-cast segment Elastic Modulus Dev. Parameters		
Final Value	4503.55	ksi
Time Parameter	12.420	hrs
Curvature Parameter	1.068	
New Segment Elastic Modulus Dev. Parameters		
Final Value	14.50	ksi
Time Parameter	n/a	hrs
Curvature Parameter	n/a	
Poisson Ratio	0.17	
Coefficient of Thermal Expansion	4.55	$\mu\varepsilon$/°F
Thermal Boundary Conditions (Applied to Appropriate Faces)			
Ambient Temp	Miami - Summer - Morning - Placement		
Wind	Medium-Wind	7.50	mph
Formwork	Steel Formwork	34.60	BTU/(ft·h·°F)
	Thickness	0.118	in
Curing	Burlap	0.18	BTU/(ft·h·°F)
	Thickness	0.39	in

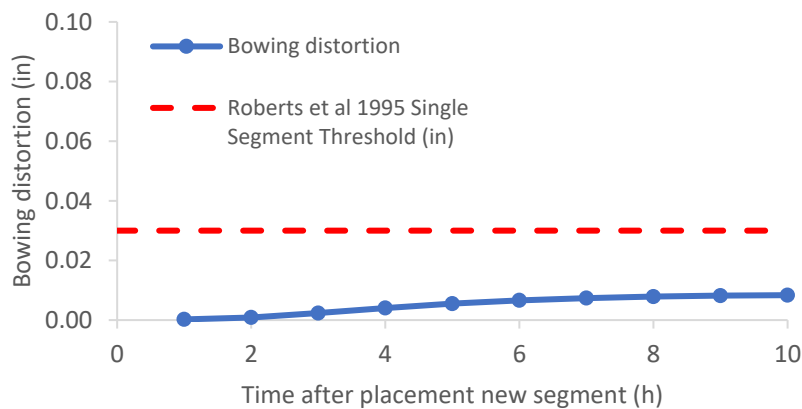Figure B-19: Simulation 7 - Bowing distortion of match-cast segment after placement of the new segment

Figure B-20: Simulation 7 - Bowing distortion progression of match-cast segment from time of placement of new segment to 10 hours
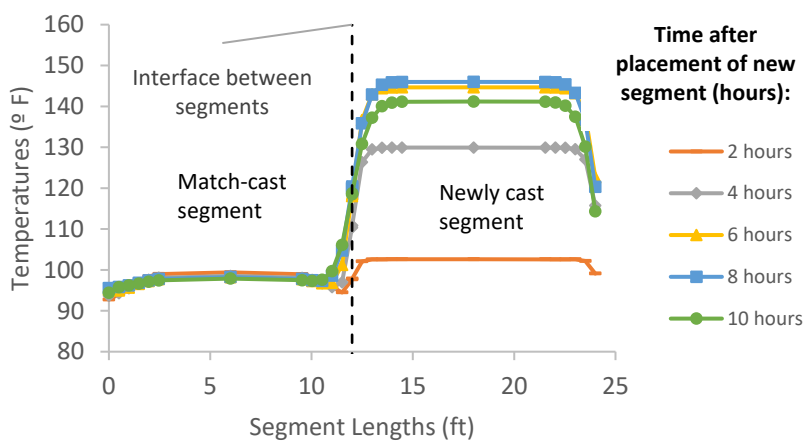

Figure B-21: Simulation 7 - Internal temperatures along the wing of segments

Simulation 8-Results Summary

Table B-8: Model input parameters simulation 8

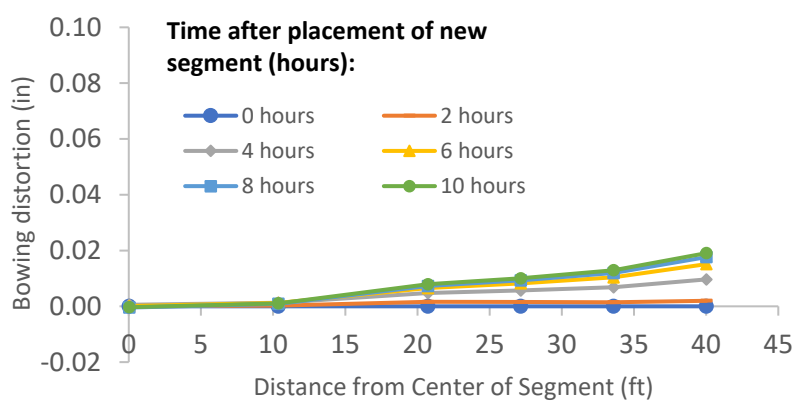| Model details		
Permutation number	8	
Geometry	Florida Bridge B - w/l=5.97	
Max. Mesh Size	3.94	in
Time Step	1	hrs
Placement Temperature	95	°F
Match-cast segment Time of Simulation at Casting	0	hrs
New Segment Time of Simulation at Casting	24	hrs
Concrete Properties		
Cement Content	650.08	lb/yd^3
Activation Energy	26.21	BTU/mol
Heat of Hydration Parameters		
Total Heat Development, $Q_{ult} = \alpha_u \cdot H_u$	107.65	BTU/lb
Time Parameter, τ	18.28	hrs
Curvature Parameter, β	1.65	
Density	3834.891	lb/yd^3
Specific Heat	0.24	BTU/(lb·°F)
Thermal Conductivity	1.608	BTU/(ft·h·°F)
Match-cast segment Elastic Modulus Dev. Parameters		
Final Value	4503.55	ksi
Time Parameter	12.420	hrs
Curvature Parameter	1.068	
New Segment Elastic Modulus Dev. Parameters		
Final Value	14.50	ksi
Time Parameter	n/a	hrs
Curvature Parameter	n/a	
Poisson Ratio	0.17	
Coefficient of Thermal Expansion	4.55	με/°F
Thermal Boundary Conditions (Applied to Appropriate Faces)		
Ambient Temp	Miami - Summer - Morning - Placement		
Wind	Medium-Wind	7.50	mph
Formwork	Steel Formwork	34.60	BTU/(ft·h·°F)
	Thickness	0.118	in
Curing	Burlap	0.18	BTU/(ft·h·°F)
	Thickness	0.39	in

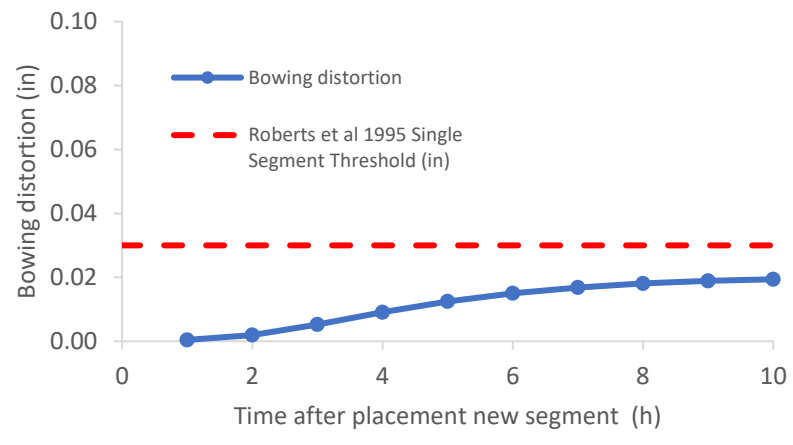Figure B-22: Simulation 8 - Bowing distortion of match-cast segment after placement of the new segment

Figure B-23: Simulation 8 - Bowing distortion progression of match-cast segment from time of placement of new segment to 10 hours
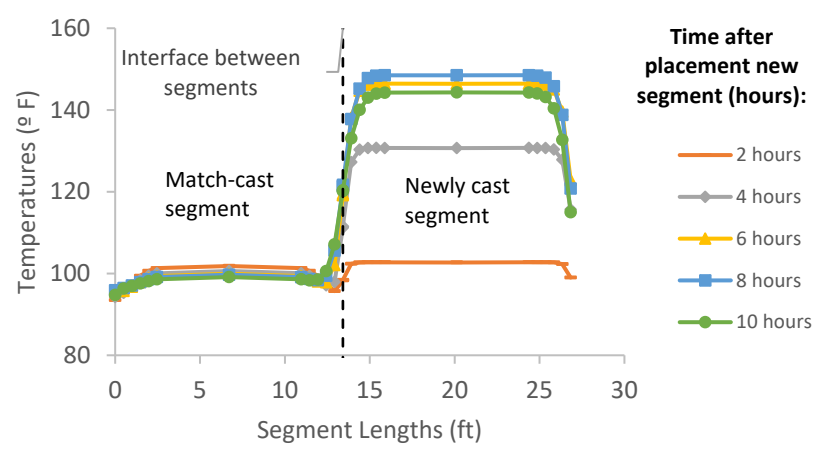

Figure B-24: Simulation 8 - Internal temperatures along the wing of segments

Simulation 9-Results Summary

Table B-9: Model input parameters simulation 9

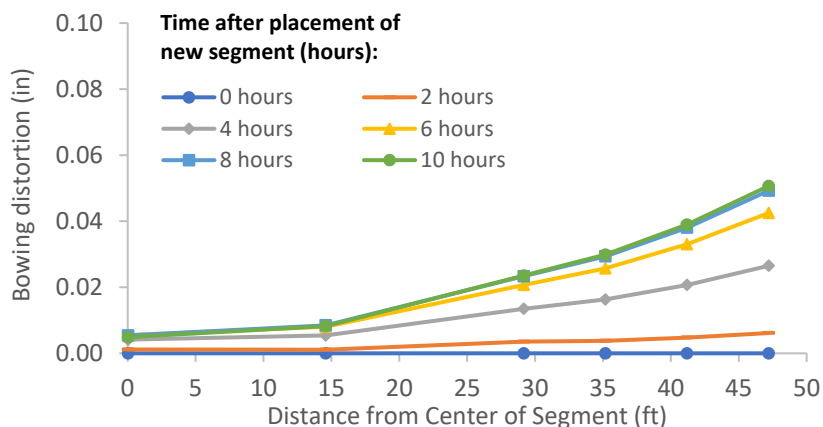| Model details		
Permutation number	9	
Geometry	Florida Bridge C - w/l=10.89	
Max. Mesh Size	3.54	in
Time Step	1	hrs
Placement Temperature	95	°F
Match-cast segment Time of Simulation at Casting	0	hrs
New Segment Time of Simulation at Casting	24	hrs
Concrete Properties		
Cement Content	650.08	lb/yd³
Activation Energy	26.21	BTU/mol
Heat of Hydration Parameters		
Total Heat Development, $Q_{ult} = \alpha_u \cdot H_u$	107.65	BTU/lb
Time Parameter, τ	18.28	hrs
Curvature Parameter, β	1.65	
Density	3834.891	lb/yd³
Specific Heat	0.24	BTU/(lb·°F)
Thermal Conductivity	1.608	BTU/(ft·h·°F)
Match-cast segment Elastic Modulus Dev. Parameters		
Final Value	4503.55	ksi
Time Parameter	12.420	hrs
Curvature Parameter	1.068	
New Segment Elastic Modulus Dev. Parameters		
Final Value	14.50	ksi
Time Parameter	n/a	hrs
Curvature Parameter	n/a	
Poisson Ratio	0.17	
Coefficient of Thermal Expansion	4.55	με/°F
Thermal Boundary Conditions (Applied to Appropriate Faces)		
Ambient Temp	Miami - Summer - Morning - Placement	
Wind	Medium-Wind	7.50	mph
Formwork	Steel Formwork	34.60	BTU/(ft·h·°F)
	Thickness	0.118	in
Curing	Burlap	0.18	BTU/(ft·h·°F)
	Thickness	0.39	in

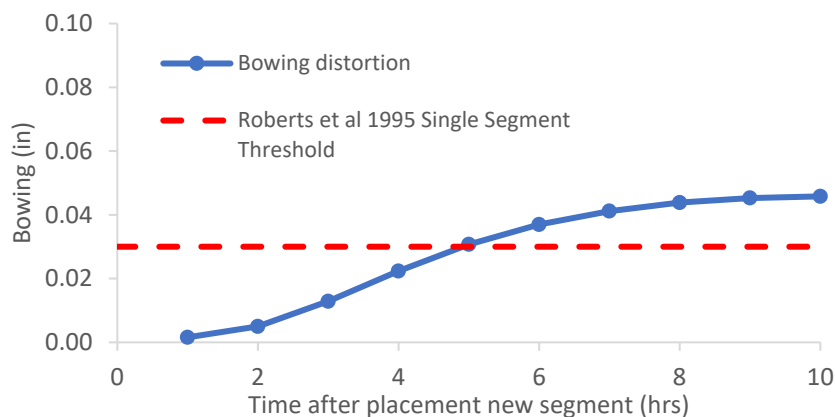Figure B-25: Simulation 9 - Bowing distortion of match-cast segment after placement of the new segment

Figure B-26: Simulation 9 - Bowing distortion progression of match-cast segment from time of placement of new segment to 10 hours
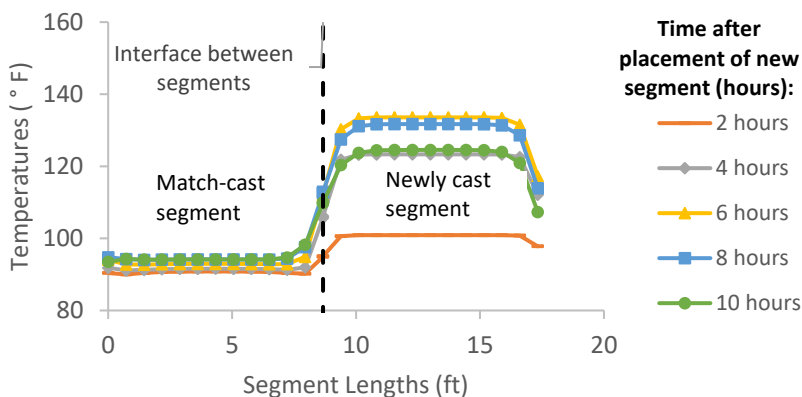

Figure B-27: Simulation 9 - Internal temperatures along the wing of segments

Simulation 10-Results Summary

Table B-10: Model input parameters simulation 10

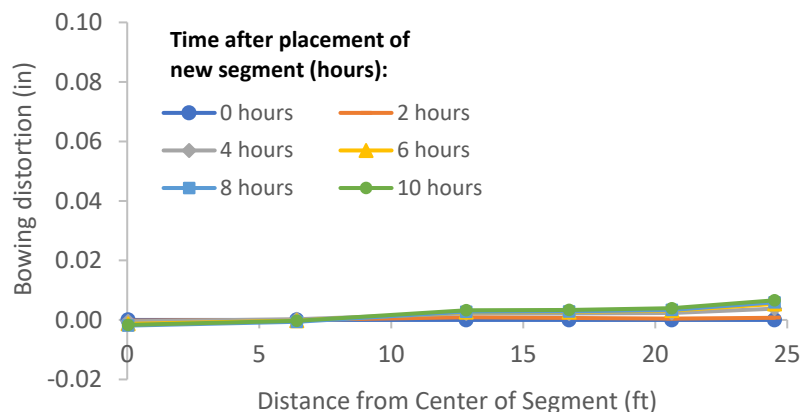| Model details		
Permutation number	10	
Geometry	Florida Bridge E - w/l=4.09	
Max. Mesh Size	2.95	in
Time Step	1	hrs
Placement Temperature	95	°F
Match-cast segment Time of Simulation at Casting	0	hrs
New Segment Time of Simulation at Casting	24	hrs
Concrete Properties		
Cement Content	750.09	lb/yd^3
Activation Energy	34.38	BTU/mol
Heat of Hydration Parameters		
Total Heat Development, $Q_{ult} = \alpha_u \cdot H_u$	117.90	BTU/lb
Time Parameter, τ	9.47	hrs
Curvature Parameter, β	1.03	
Density	3816.577	lb/yd^3
Specific Heat	0.25	BTU/(lb·°F)
Thermal Conductivity	1.557	BTU/(ft·h·°F)
Match-cast segment Elastic Modulus Dev. Parameters		
Final Value	4471.32	ksi
Time Parameter	12.420	hrs
Curvature Parameter	1.068	
New Segment Elastic Modulus Dev. Parameters		
Final Value	14.50	ksi
Time Parameter	n/a	hrs
Curvature Parameter	n/a	
Poisson Ratio	0.17	
Coefficient of Thermal Expansion	4.54	$\mu\varepsilon$/°F
Thermal Boundary Conditions (Applied to Appropriate Faces)		
Ambient Temp	Miami - Summer - Morning - Placement		
Wind	Medium-Wind	7.50	mph
Formwork	Steel Formwork	34.60	BTU/(ft·h·°F)
	Thickness	0.118	in
Curing	Burlap	0.18	BTU/(ft·h·°F)
	Thickness	0.39	in

Figure B-28: Simulation 10 - Bowing distortion of match-cast segment after placement of the new segment
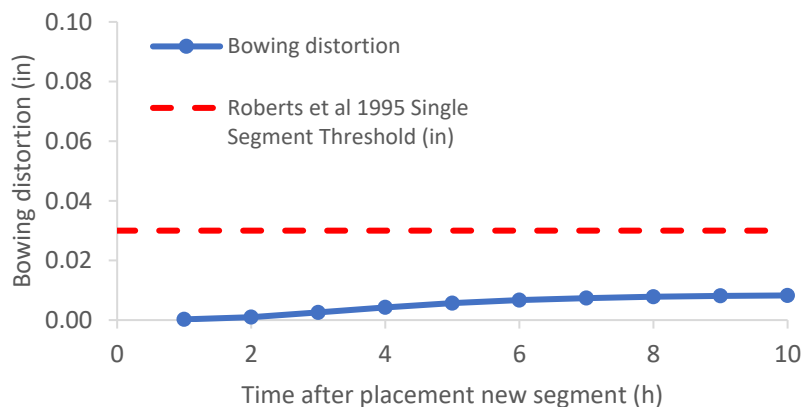

Figure B-29: Simulation 10 - Bowing distortion progression of match-cast segment from time of placement of new segment to 10 hours
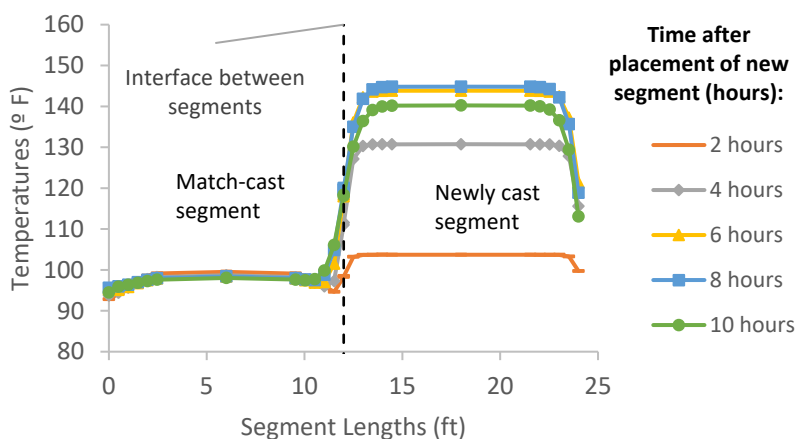

Figure B-30: Simulation 10 - Internal temperatures along the wing of segments

Simulation 11-Results Summary

Table B-11: Model input parameters simulation 11

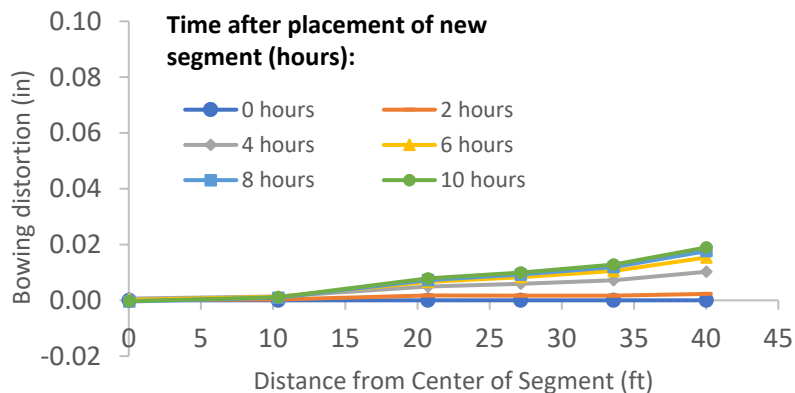| Model details		
Permutation number	11	
Geometry	Florida Bridge B - w/l=5.97	
Max. Mesh Size	3.94	in
Time Step	1	hrs
Placement Temperature	95	°F
Match-cast segment Time of Simulation at Casting	0	hrs
New Segment Time of Simulation at Casting	24	hrs
Concrete Properties		
Cement Content	750.09	lb/yd³
Activation Energy	34.38	BTU/mol
Heat of Hydration Parameters		
Total Heat Development, $Q_{ult} = \alpha_u \cdot H_u$	117.90	BTU/lb
Time Parameter, τ	9.47	hrs
Curvature Parameter, β	1.03	
Density	3816.577	lb/yd³
Specific Heat	0.25	BTU/(lb·°F)
Thermal Conductivity	1.557	BTU/(ft·h·°F)
Match-cast segment Elastic Modulus Dev. Parameters		
Final Value	4471.32	ksi
Time Parameter	12.420	hrs
Curvature Parameter	1.068	
New Segment Elastic Modulus Dev. Parameters		
Final Value	14.50	ksi
Time Parameter	n/a	hrs
Curvature Parameter	n/a	
Poisson Ratio	0.17	
Coefficient of Thermal Expansion	4.54	με/°F
Thermal Boundary Conditions (Applied to Appropriate Faces)		
Ambient Temp	Miami - Summer - Morning - Placement		
Wind	Medium-Wind	7.50	mph
Formwork	Steel Formwork	34.60	BTU/(ft·h·°F)
	Thickness	0.118	in
Curing	Burlap	0.18	BTU/(ft·h·°F)
	Thickness	0.39	in

Figure B-31: Simulation 11 - Bowing distortion of match-cast segment after placement of the new segment
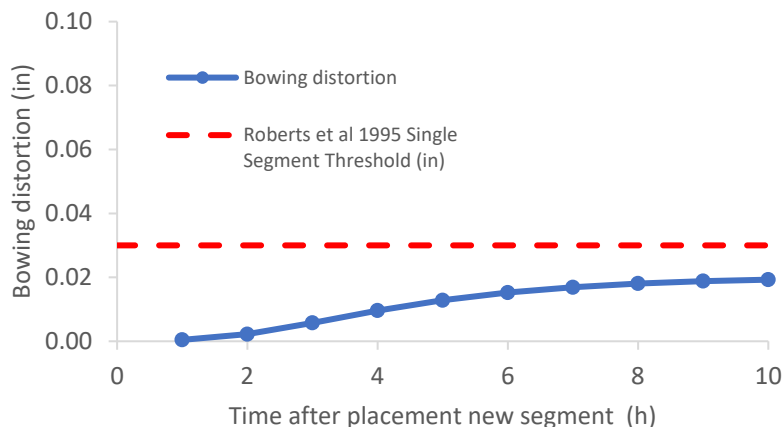

Figure B-32: Simulation 11 - Bowing distortion progression of match-cast segment from time of placement of new segment to 10 hours
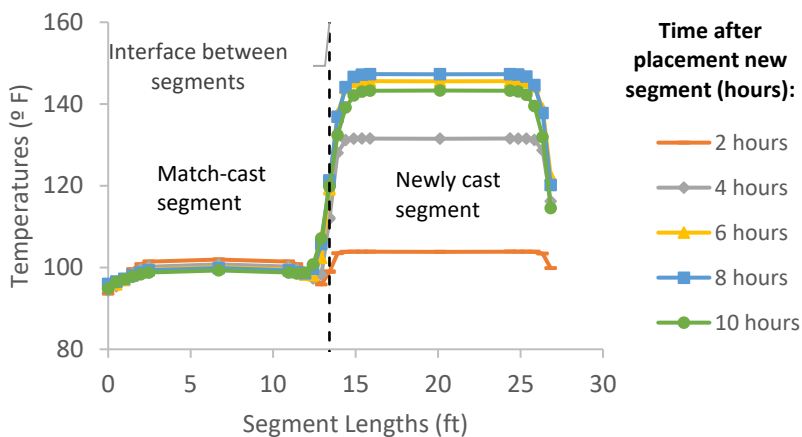

Figure B-33: Simulation 11 - Internal temperatures along the wing of segments

Simulation 12-Results Summary

Table B-12: Model input parameters simulation 12

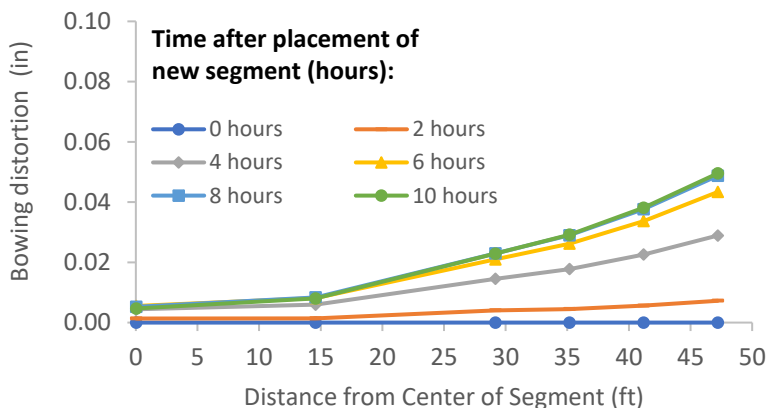| Model details		
Permutation number	12	
Geometry	Florida Bridge C - w/l=10.89	
Max. Mesh Size	3.54	in
Time Step	1	hrs
Placement Temperature	95	°F
Match-cast segment Time of Simulation at Casting	0	hrs
New Segment Time of Simulation at Casting	24	hrs
Concrete Properties		
Cement Content	750.09	lb/yd^3
Activation Energy	34.38	BTU/mol
Heat of Hydration Parameters		
Total Heat Development, $Q_{ult} = \alpha_u \cdot H_u$	117.90	BTU/lb
Time Parameter, τ	9.47	hrs
Curvature Parameter, β	1.03	
Density	3816.577	lb/yd^3
Specific Heat	0.25	BTU/(lb·°F)
Thermal Conductivity	1.557	BTU/(ft·h·°F)
Match-cast segment Elastic Modulus Dev. Parameters		
Final Value	4471.32	ksi
Time Parameter	12.420	hrs
Curvature Parameter	1.068	
New Segment Elastic Modulus Dev. Parameters		
Final Value	14.50	ksi
Time Parameter	n/a	hrs
Curvature Parameter	n/a	
Poisson Ratio	0.17	
Coefficient of Thermal Expansion	4.54	με/°F
Thermal Boundary Conditions (Applied to Appropriate Faces)		
Ambient Temp	Miami - Summer - Morning - Placement		
Wind	Medium-Wind	7.50	mph
Formwork	Steel Formwork	34.60	BTU/(ft·h·°F)
	Thickness	0.118	in
Curing	Burlap	0.18	BTU/(ft·h·°F)
	Thickness	0.39	in

Figure B-34: Simulation 12 - Bowing distortion of match-cast segment after placement of the new segment
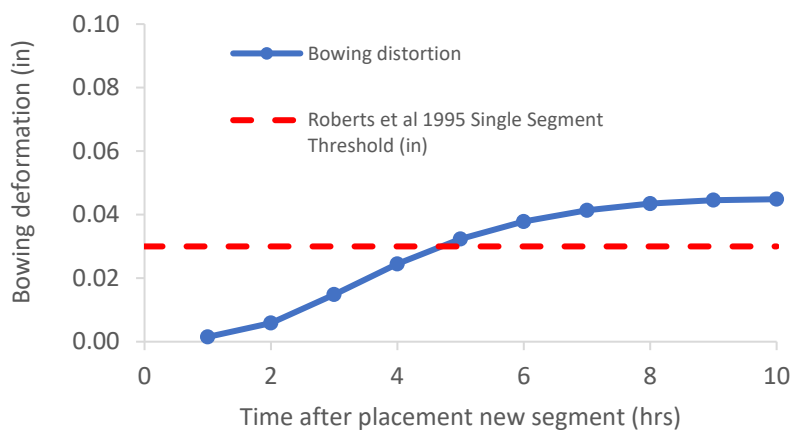

Figure B-35: Simulation 12 - Bowing distortion progression of match-cast segment from time of placement of new segment to 10 hours
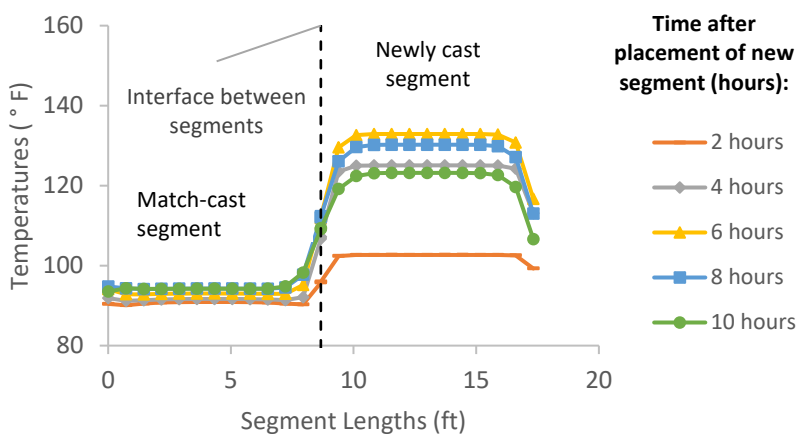

Figure B-36: Simulation 12 - Internal temperatures along the wing of segments

Simulation 13-Results Summary

Table B-13: Model input parameters simulation 13

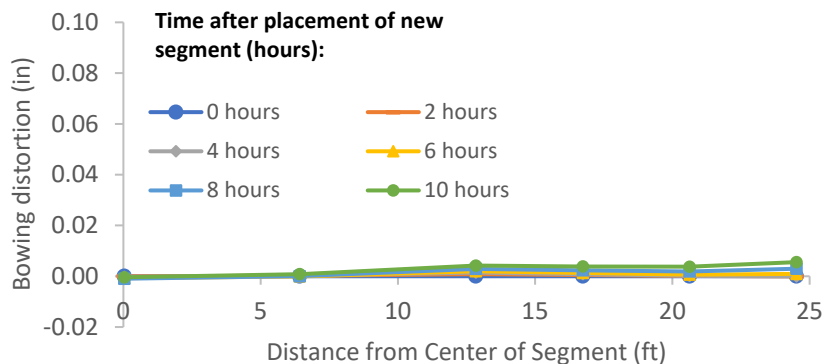| Model details		
Permutation number	13	
Geometry	Florida Bridge E - w/l=4.09	
Max. Mesh Size	2.95	in
Time Step	1	hrs
Placement Temperature	95	°F
Match-cast segment Time of Simulation at Casting	0	hrs
New Segment Time of Simulation at Casting	24	hrs
Concrete Properties		
Cement Content	750.09	lb/yd^3
Activation Energy	30.13	BTU/mol
Heat of Hydration Parameters		
Total Heat Development, $Q_{ult} = \alpha_u \cdot H_u$	117.85	BTU/lb
Time Parameter, τ	8.24	hrs
Curvature Parameter, β	1.03	
Density	3816.577	lb/yd^3
Specific Heat	0.25	BTU/(lb·°F)
Thermal Conductivity	1.557	BTU/(ft·h·°F)
Match-cast segment Elastic Modulus Dev. Parameters		
Final Value	4471.32	ksi
Time Parameter	12.420	hrs
Curvature Parameter	1.068	
New Segment Elastic Modulus Dev. Parameters		
Final Value	14.50	ksi
Time Parameter	n/a	hrs
Curvature Parameter	n/a	
Poisson Ratio	0.17	
Coefficient of Thermal Expansion	4.54	µε/°F
Thermal Boundary Conditions (Applied to Appropriate Faces)		
Ambient Temp	Miami - Summer - Morning - Placement	
Wind	Medium-Wind	7.50	mph
Formwork	Steel Formwork	34.60	BTU/(ft·h·°F)
	Thickness	0.118	in
Curing	Burlap	0.18	BTU/(ft·h·°F)
	Thickness	0.39	in

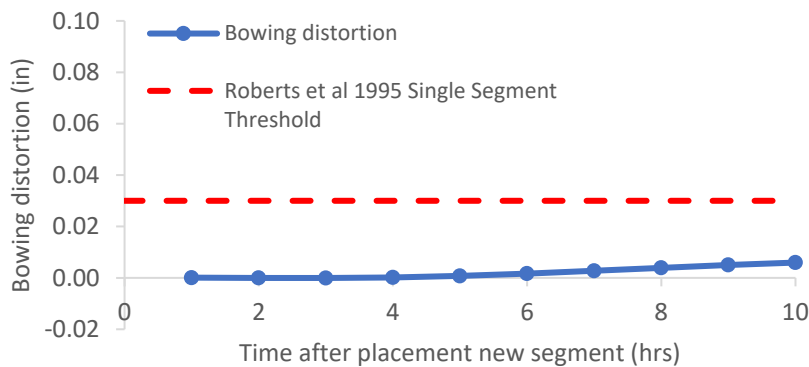Figure B-37: Simulation 13 - Bowing distortion of match-cast segment after placement of the new segment

Figure B-38: Simulation 13 - Bowing distortion progression of match-cast segment from time of placement of new segment to 10 hours
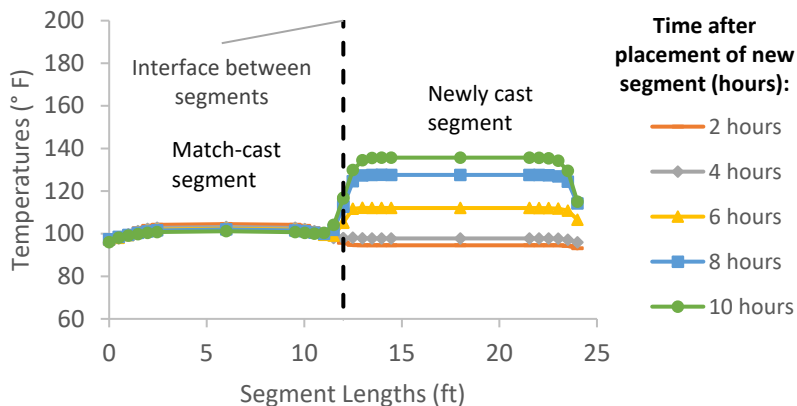

Figure B-39: Simulation 13 - Internal temperatures along the wing of segments

Simulation 14-Results Summary

Table B-14: Model input parameters simulation 14

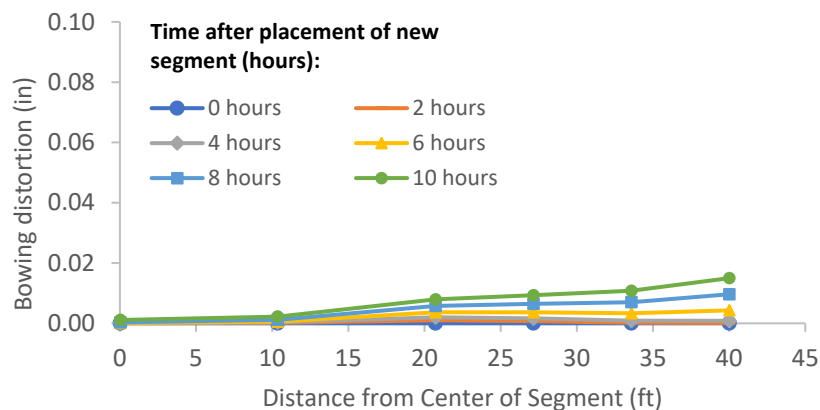| Model details		
Permutation number	14	
Geometry	Florida Bridge B - w/l=5.97	
Max. Mesh Size	3.94	in
Time Step	1	hrs
Placement Temperature	95	°F
Match-cast segment Time of Simulation at Casting	0	hrs
New Segment Time of Simulation at Casting	24	hrs
Concrete Properties		
Cement Content	750.09	lb/yd^3
Activation Energy	30.13	BTU/mol
Heat of Hydration Parameters		
Total Heat Development, $Q_{ult} = \alpha_u \cdot H_u$	117.85	BTU/lb
Time Parameter, τ	8.24	hrs
Curvature Parameter, β	1.03	
Density	3816.577	lb/yd^3
Specific Heat	0.25	BTU/(lb·°F)
Thermal Conductivity	1.557	BTU/(ft·h·°F)
Match-cast segment Elastic Modulus Dev. Parameters		
Final Value	4471.32	ksi
Time Parameter	12.420	hrs
Curvature Parameter	1.068	
New Segment Elastic Modulus Dev. Parameters		
Final Value	14.50	ksi
Time Parameter	n/a	hrs
Curvature Parameter	n/a	
Poisson Ratio	0.17	
Coefficient of Thermal Expansion	4.54	με/°F
Thermal Boundary Conditions (Applied to Appropriate Faces)			
Ambient Temp	Miami - Summer - Morning - Placement		
Wind	Medium-Wind	7.50	mph
Formwork	Steel Formwork	34.60	BTU/(ft·h·°F)
	Thickness	0.118	in
Curing	Burlap	0.18	BTU/(ft·h·°F)
	Thickness	0.39	in

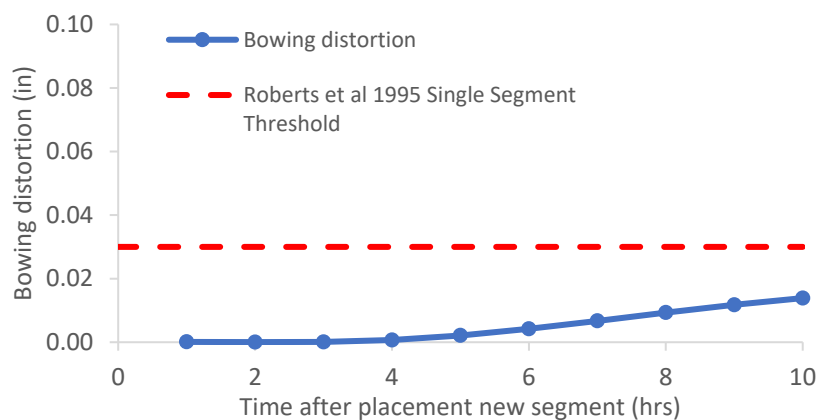Figure B-40: Simulation 14 - Bowing distortion of match-cast segment after placement of the new segment

Figure B-41: Simulation 14 - Bowing distortion progression of match-cast segment from time of placement of new segment to 10 hours
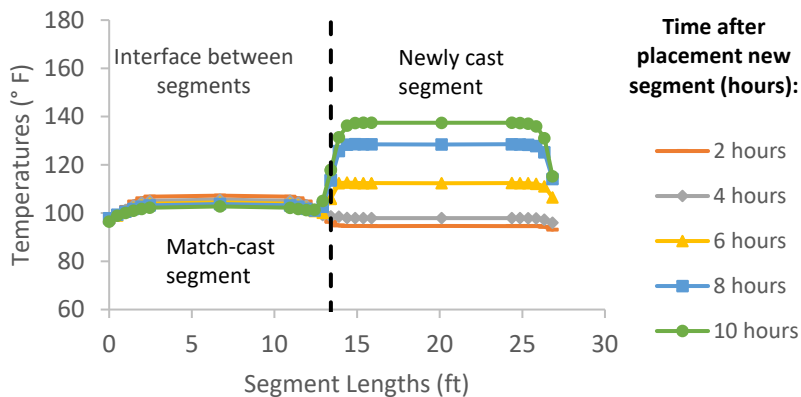

Figure B-42: Simulation 14 - Internal temperatures along the wing of segments

Simulation 15-Results Summary

Table B-15: Model input parameters simulation 15

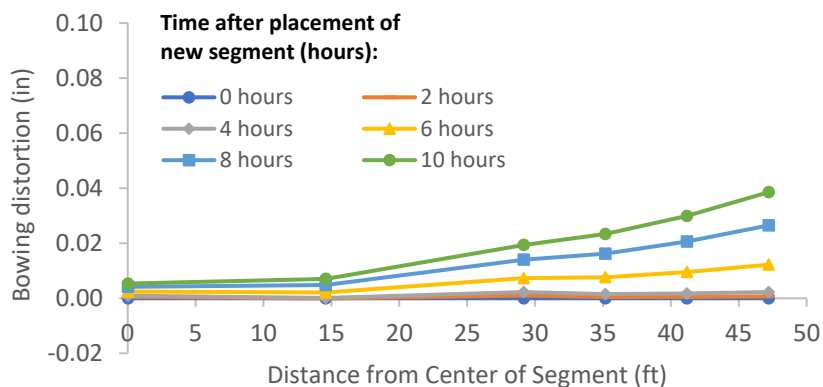| Model details		
Permutation number	15	
Geometry	Florida Bridge C - w/l=10.89	
Max. Mesh Size	3.54	in
Time Step	1	hrs
Placement Temperature	95	°F
Match-cast segment Time of Simulation at Casting	0	hrs
New Segment Time of Simulation at Casting	24	hrs
Concrete Properties		
Cement Content	750.09	lb/yd^3
Activation Energy	30.13	BTU/mol
Heat of Hydration Parameters		
Total Heat Development, $Q_{ult} = \alpha_u \cdot H_u$	117.85	BTU/lb
Time Parameter, τ	8.24	hrs
Curvature Parameter, β	1.03	
Density	3816.577	lb/yd^3
Specific Heat	0.25	BTU/(lb·°F)
Thermal Conductivity	1.557	BTU/(ft·h·°F)
Match-cast segment Elastic Modulus Dev. Parameters		
Final Value	4471.32	ksi
Time Parameter	12.420	hrs
Curvature Parameter	1.068	
New Segment Elastic Modulus Dev. Parameters		
Final Value	14.50	ksi
Time Parameter	n/a	hrs
Curvature Parameter	n/a	
Poisson Ratio	0.17	
Coefficient of Thermal Expansion	4.54	με/°F
Thermal Boundary Conditions (Applied to Appropriate Faces)		
Ambient Temp	Miami - Summer - Morning - Placement	
Wind	Medium-Wind	7.50	mph
Formwork	Steel Formwork	34.60	BTU/(ft·h·°F)
	Thickness	0.118	in
Curing	Burlap	0.18	BTU/(ft·h·°F)
	Thickness	0.39	in

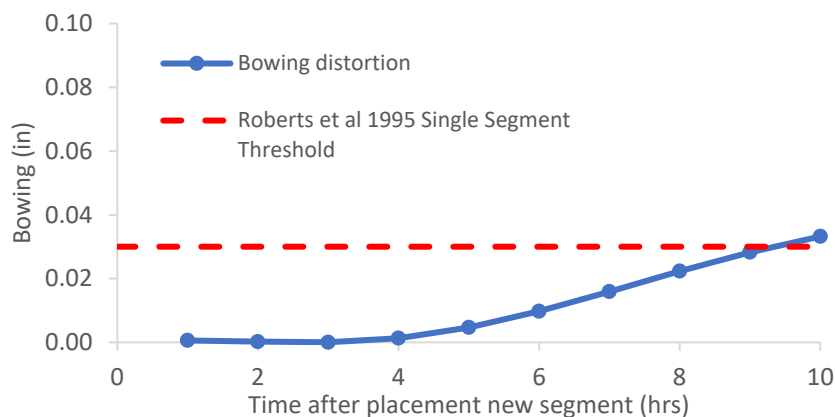Figure B-43: Simulation 15 - Bowing distortion of match-cast segment after placement of the new segment

Figure B-44: Simulation 15 - Bowing distortion progression of match-cast segment from time of placement of new segment to 10 hours
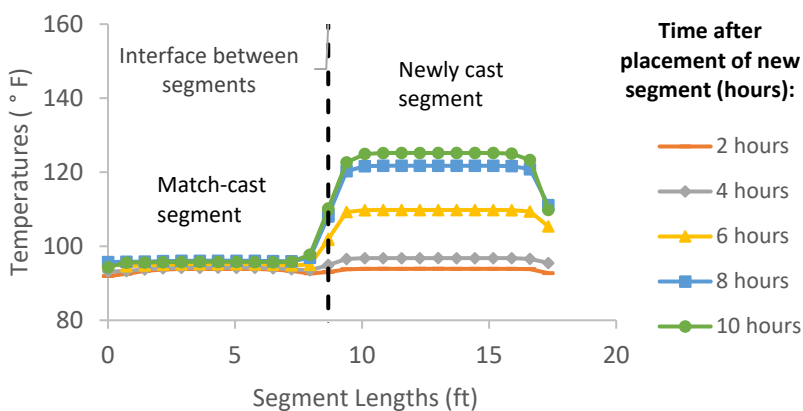

Figure B-45: Simulation 15 - Internal temperatures along the wing of segments

Simulation 16-Results Summary

Table B-16: Model input parameters simulation 16

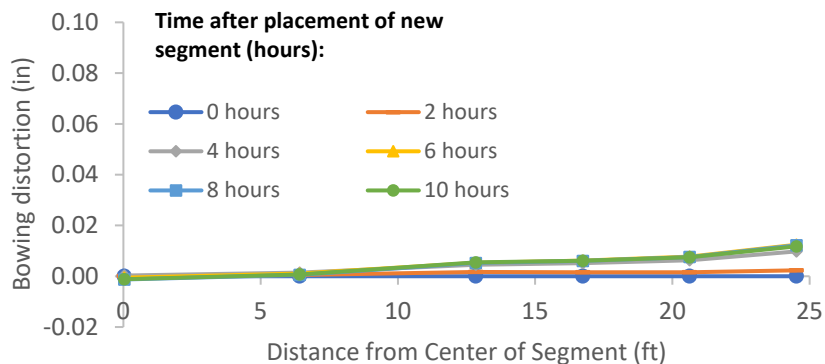| Model details		
Permutation number	16	
Geometry	Florida Bridge E - w/l=4.09	
Max. Mesh Size	2.95	in
Time Step	1	hrs
Placement Temperature	95	°F
Match-cast segment Time of Simulation at Casting	0	hrs
New Segment Time of Simulation at Casting	24	hrs
Concrete Properties		
Cement Content	750.09	lb/yd^3
Activation Energy	24.13	BTU/mol
Heat of Hydration Parameters		
Total Heat Development, $Q_{ult} = \alpha_u \cdot H_u$	111.33	BTU/lb
Time Parameter, τ	13.36	hrs
Curvature Parameter, β	1.49	
Density	3816.577	lb/yd^3
Specific Heat	0.25	BTU/(lb·°F)
Thermal Conductivity	1.557	BTU/(ft·h·°F)
Match-cast segment Elastic Modulus Dev. Parameters		
Final Value	4471.32	ksi
Time Parameter	12.420	hrs
Curvature Parameter	1.068	
New Segment Elastic Modulus Dev. Parameters		
Final Value	14.50	ksi
Time Parameter	n/a	hrs
Curvature Parameter	n/a	
Poisson Ratio	0.17	
Coefficient of Thermal Expansion	4.54	με/°F
Thermal Boundary Conditions (Applied to Appropriate Faces)		
Ambient Temp	Miami - Summer - Morning - Placement	
Wind	Medium-Wind	7.50	mph
Formwork	Steel Formwork	34.60	BTU/(ft·h·°F)
	Thickness	0.118	in
Curing	Burlap	0.18	BTU/(ft·h·°F)
	Thickness	0.39	in

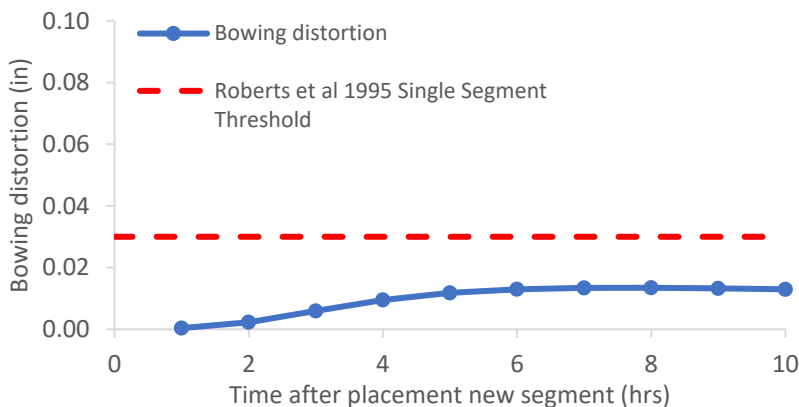Figure B-46: Simulation 16 - Bowing distortion of match-cast segment after placement of the new segment

Figure B-47: Simulation 16 - Bowing distortion progression of match-cast segment from time of placement of new segment to 10 hours
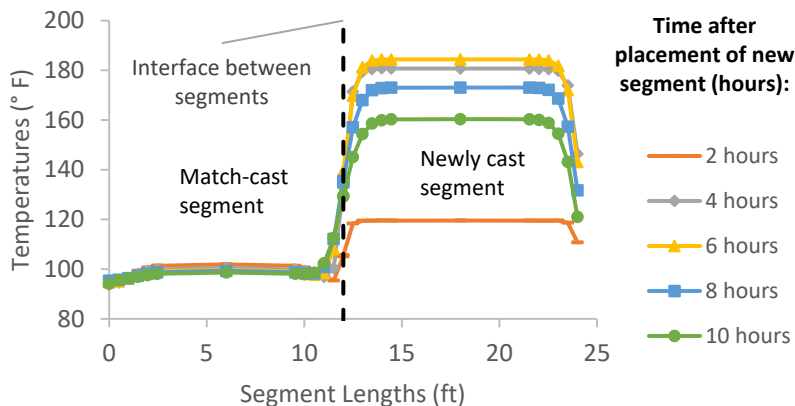

Figure B-48: Simulation 16 - Internal temperatures along the wing of segments

Simulation 17-Results Summary

Table B-17: Model input parameters simulation 17

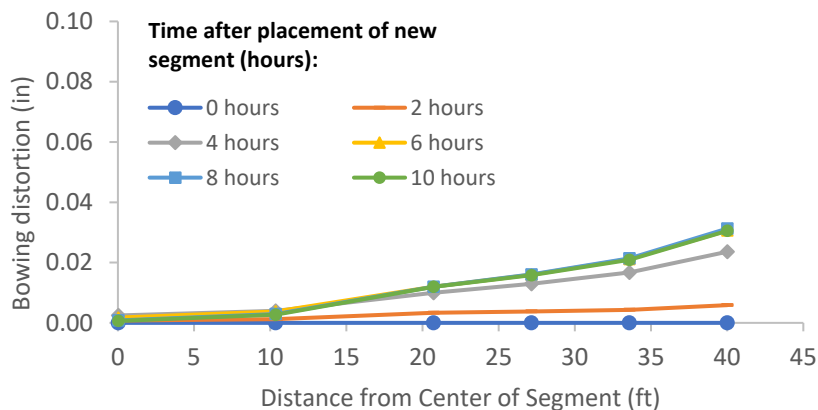| Model details		
Permutation number	17	
Geometry	Florida Bridge B - w/l=5.97	
Max. Mesh Size	3.94	in
Time Step	1	hrs
Placement Temperature	95	°F
Match-cast segment Time of Simulation at Casting	0	hrs
New Segment Time of Simulation at Casting	24	hrs
Concrete Properties		
Cement Content	750.09	lb/yd^3
Activation Energy	24.13	BTU/mol
Heat of Hydration Parameters		
Total Heat Development, $Q_{ult} = \alpha_u \cdot H_u$	111.33	BTU/lb
Time Parameter, τ	13.36	hrs
Curvature Parameter, β	1.49	
Density	3816.577	lb/yd^3
Specific Heat	0.25	BTU/(lb·°F)
Thermal Conductivity	1.557	BTU/(ft·h·°F)
Match-cast segment Elastic Modulus Dev. Parameters		
Final Value	4471.32	ksi
Time Parameter	12.420	hrs
Curvature Parameter	1.068	
New Segment Elastic Modulus Dev. Parameters		
Final Value	14.50	ksi
Time Parameter	n/a	hrs
Curvature Parameter	n/a	
Poisson Ratio	0.17	
Coefficient of Thermal Expansion	4.54	µε/°F
Thermal Boundary Conditions (Applied to Appropriate Faces)		
Ambient Temp	Miami - Summer - Morning - Placement	
Wind	Medium-Wind	7.50	mph
Formwork	Steel Formwork	34.60	BTU/(ft·h·°F)
	Thickness	0.118	in
Curing	Burlap	0.18	BTU/(ft·h·°F)
	Thickness	0.39	in

Figure B-49: Simulation 17 - Bowing distortion of match-cast segment after placement of the new segment
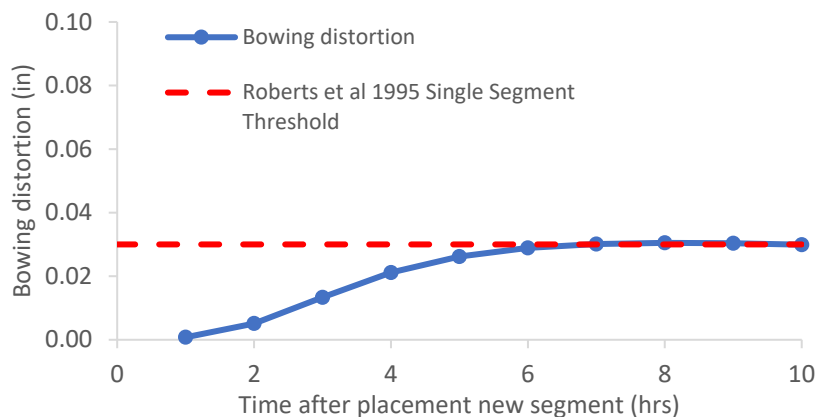

Figure B-50: Simulation 17 - Bowing distortion progression of match-cast segment from time of placement of new segment to 10 hours
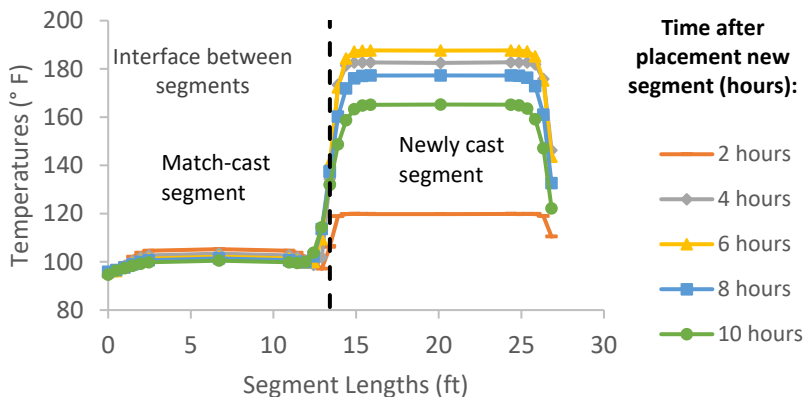

Figure B-51: Simulation 17 - Internal temperatures along the wing of segments

Simulation 18-Results Summary

Table B-18: Model input parameters simulation 18

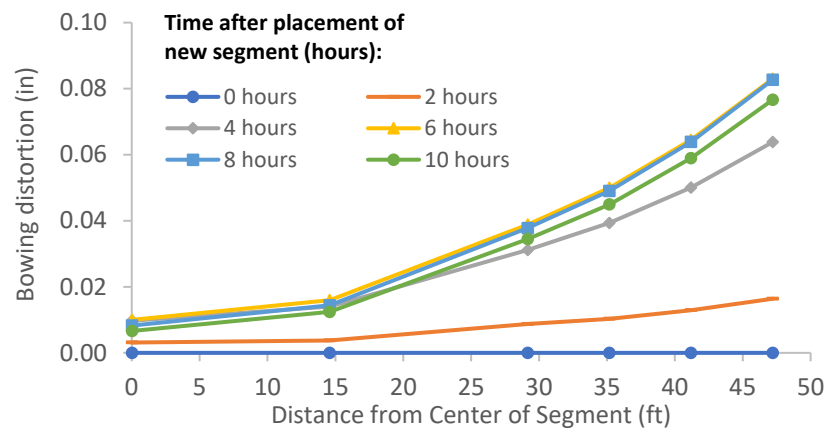| Model details		
Permutation number	18	
Geometry	Florida Bridge C - w/l=10.89	
Max. Mesh Size	3.54	in
Time Step	1	hrs
Placement Temperature	95	°F
Match-cast segment Time of Simulation at Casting	0	hrs
New Segment Time of Simulation at Casting	24	hrs
Concrete Properties		
Cement Content	750.09	lb/yd^3
Activation Energy	24.13	BTU/mol
Heat of Hydration Parameters		
Total Heat Development, $Q_{ult} = \alpha_u \cdot H_u$	111.33	BTU/lb
Time Parameter, τ	13.36	hrs
Curvature Parameter, β	1.49	
Density	3816.577	lb/yd^3
Specific Heat	0.25	BTU/(lb·°F)
Thermal Conductivity	1.557	BTU/(ft·h·°F)
Match-cast segment Elastic Modulus Dev. Parameters		
Final Value	4471.32	ksi
Time Parameter	12.420	hrs
Curvature Parameter	1.068	
New Segment Elastic Modulus Dev. Parameters		
Final Value	14.50	ksi
Time Parameter	n/a	hrs
Curvature Parameter	n/a	
Poisson Ratio	0.17	
Coefficient of Thermal Expansion	4.54	$\mu\varepsilon$/°F
Thermal Boundary Conditions (Applied to Appropriate Faces)		
Ambient Temp	Miami - Summer - Morning - Placement	
Wind	Medium-Wind	7.50	mph
Formwork	Steel Formwork	34.60	BTU/(ft·h·°F)
	Thickness	0.118	in
Curing	Burlap	0.18	BTU/(ft·h·°F)
	Thickness	0.39	in

Figure B-52: Simulation 18 - Bowing distortion of match-cast segment after placement of the new segment
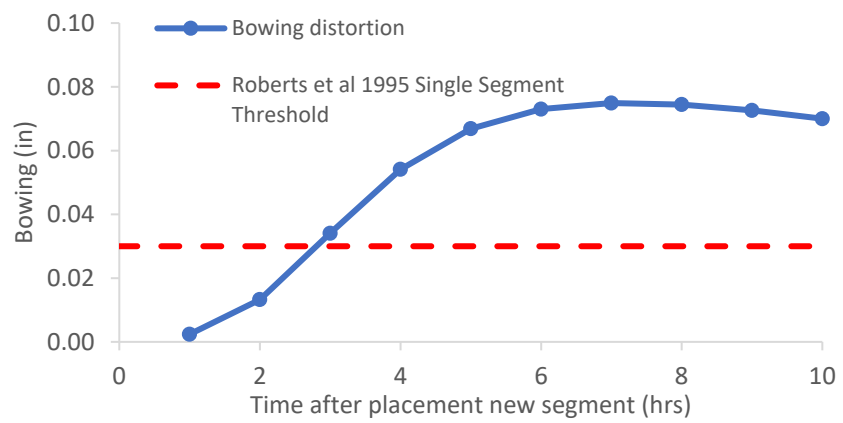

Figure B-53: Simulation 18 - Bowing distortion progression of match-cast segment from time of placement of new segment to 10 hours
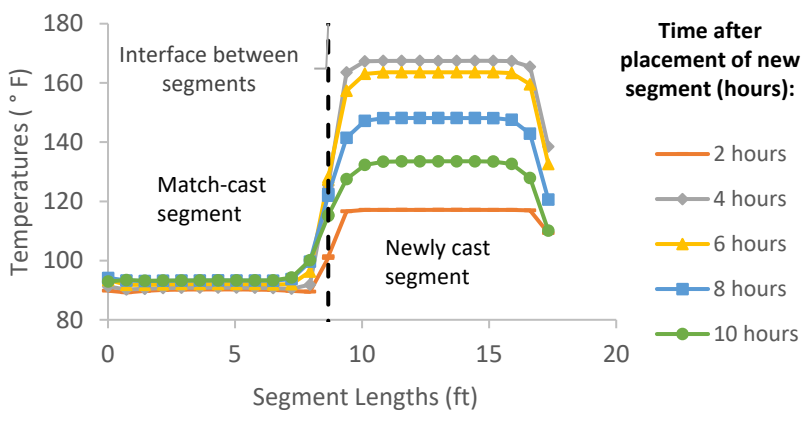

Figure B-54: Simulation 18 - Internal temperatures along the wing of segments

Simulation 19-Results Summary

Table B-19: Model input parameters simulation 19

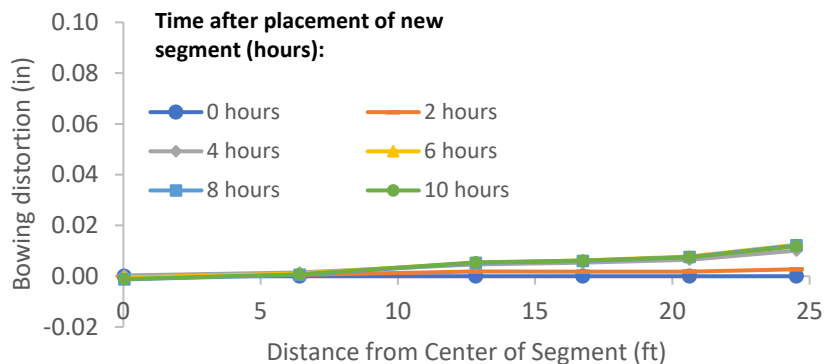| Model details		
Permutation number	19	
Geometry	Florida Bridge E - w/l=4.09	
Max. Mesh Size	2.95	in
Time Step	1	hrs
Placement Temperature	95	°F
Match-cast segment Time of Simulation at Casting	0	hrs
New Segment Time of Simulation at Casting	24	hrs
Concrete Properties		
Cement Content	950.11	lb/yd^3
Activation Energy	38.69	BTU/mol
Heat of Hydration Parameters		
Total Heat Development, $Q_{ult} = \alpha_u \cdot H_u$	129.52	BTU/lb
Time Parameter, τ	7.45	hrs
Curvature Parameter, β	1.10	
Density	3880.948	lb/yd^3
Specific Heat	0.26	BTU/(lb·°F)
Thermal Conductivity	1.502	BTU/(ft·h·°F)
Match-cast segment Elastic Modulus Dev. Parameters		
Final Value	4584.92	ksi
Time Parameter	12.420	hrs
Curvature Parameter	1.068	
New Segment Elastic Modulus Dev. Parameters		
Final Value	14.50	ksi
Time Parameter	n/a	hrs
Curvature Parameter	n/a	
Poisson Ratio	0.17	
Coefficient of Thermal Expansion	4.54	με/°F
Thermal Boundary Conditions (Applied to Appropriate Faces)		
Ambient Temp	Miami - Summer - Morning - Placement		
Wind	Medium-Wind	7.50	mph
Formwork	Steel Formwork	34.60	BTU/(ft·h·°F)
	Thickness	0.118	in
Curing	Burlap	0.18	BTU/(ft·h·°F)
	Thickness	0.39	in

Figure B-55: Simulation 19 - Bowing distortion of match-cast segment after placement of the new segment
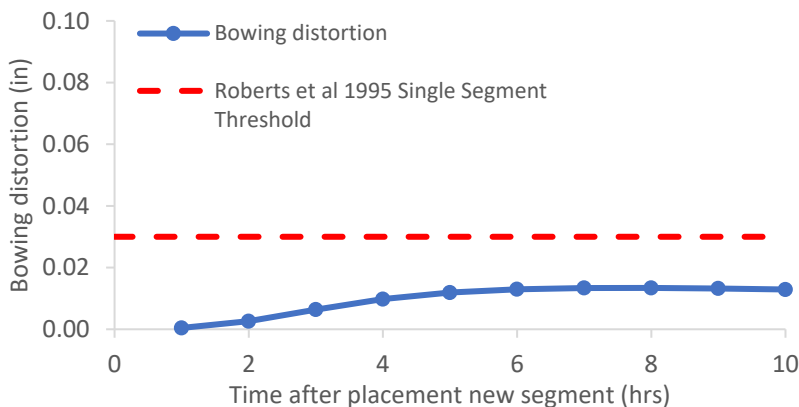

Figure B-56: Simulation 19 - Bowing distortion progression of match-cast segment from time of placement of new segment to 10 hours
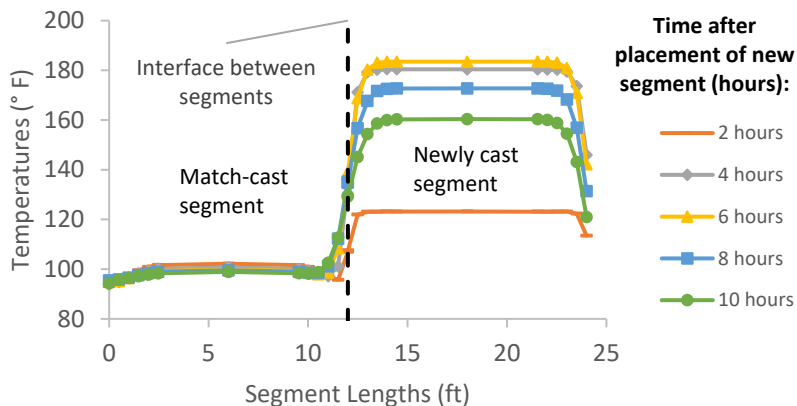

Figure B-57: Simulation 19 - Internal temperatures along the wing of segments

Simulation 20 -Results Summary

Table B-20: Model input parameters simulation 20

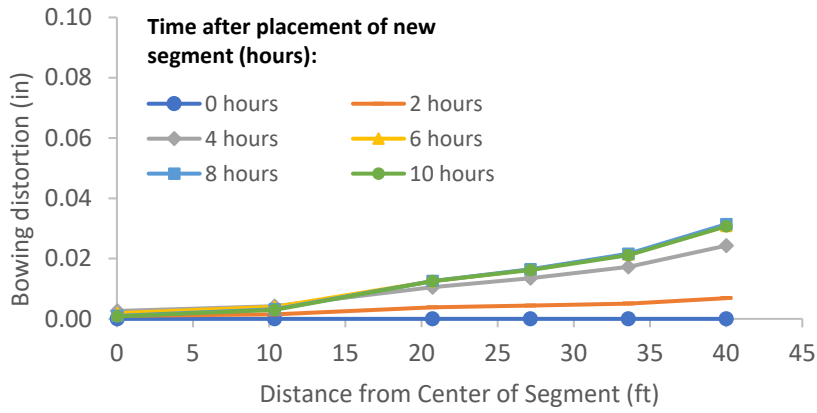| Model details		
Permutation number	20	
Geometry	Florida Bridge B - w/l=5.97	
Max. Mesh Size	3.94	in
Time Step	1	hrs
Placement Temperature	95	°F
Match-cast segment Time of Simulation at Casting	0	hrs
New Segment Time of Simulation at Casting	24	hrs
Concrete Properties		
Cement Content	950.11	lb/yd^3
Activation Energy	38.69	BTU/mol
Heat of Hydration Parameters		
Total Heat Development, $Q_{ult} = \alpha_u \cdot H_u$	129.52	BTU/lb
Time Parameter, τ	7.45	hrs
Curvature Parameter, β	1.10	
Density	3880.948	lb/yd^3
Specific Heat	0.26	BTU/(lb·°F)
Thermal Conductivity	1.502	BTU/(ft·h·°F)
Match-cast segment Elastic Modulus Dev. Parameters		
Final Value	4584.92	ksi
Time Parameter	12.420	hrs
Curvature Parameter	1.068	
New Segment Elastic Modulus Dev. Parameters		
Final Value	14.50	ksi
Time Parameter	n/a	hrs
Curvature Parameter	n/a	
Poisson Ratio	0.17	
Coefficient of Thermal Expansion	4.54	με/°F
Thermal Boundary Conditions (Applied to Appropriate Faces)		
Ambient Temp	Miami - Summer - Morning - Placement	
Wind	Medium-Wind	7.50	mph
Formwork	Steel Formwork	34.60	BTU/(ft·h·°F)
	Thickness	0.118	in
Curing	Burlap	0.18	BTU/(ft·h·°F)
	Thickness	0.39	in

Figure B-58: Simulation 20 - Bowing distortion of match-cast segment after placement of the new segment
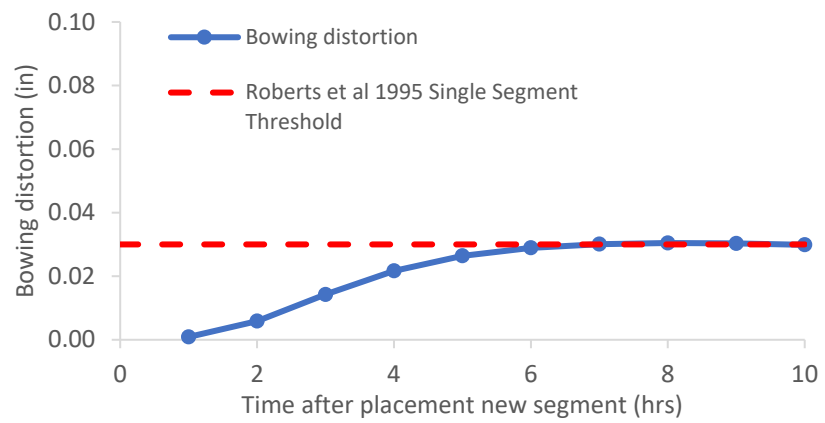

Figure B-59: Simulation 20 - Bowing distortion progression of match-cast segment from time of placement of new segment to 10 hours
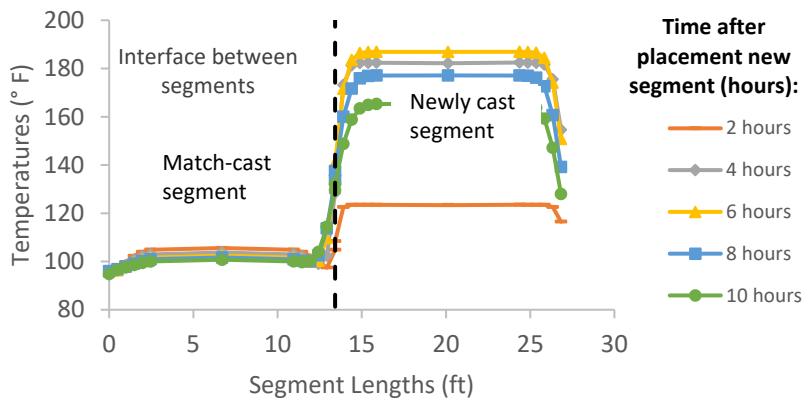

Figure B-60: Simulation 20 - Internal temperatures along the wing of segments

Simulation 21 -Results Summary

Table B-21: Model input parameters simulation 21

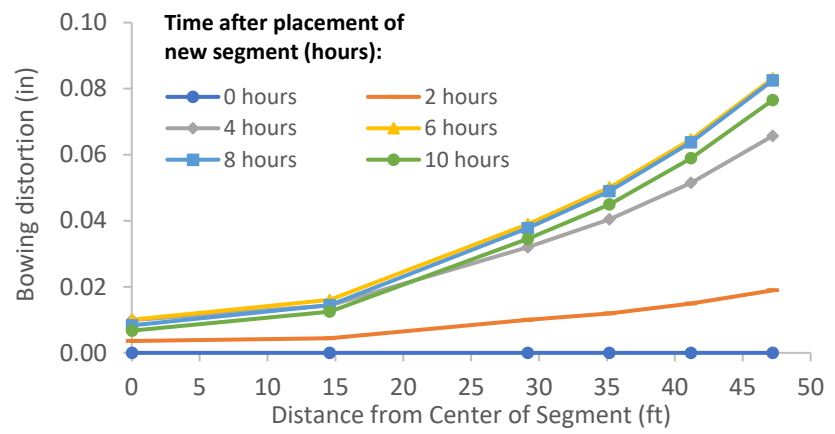| Model details		
Permutation number	21	
Geometry	Florida Bridge C - w/l=10.89	
Max. Mesh Size	3.54	in
Time Step	1	hrs
Placement Temperature	95	°F
Match-cast segment Time of Simulation at Casting	0	hrs
New Segment Time of Simulation at Casting	24	hrs
Concrete Properties		
Cement Content	950.11	lb/yd^3
Activation Energy	38.69	BTU/mol
Heat of Hydration Parameters		
Total Heat Development, $Q_{ult} = \alpha_u \cdot H_u$	129.52	BTU/lb
Time Parameter, τ	7.45	hrs
Curvature Parameter, β	1.10	
Density	3880.948	lb/yd^3
Specific Heat	0.26	BTU/(lb·°F)
Thermal Conductivity	1.502	BTU/(ft·h·°F)
Match-cast segment Elastic Modulus Dev. Parameters		
Final Value	4584.92	ksi
Time Parameter	12.420	hrs
Curvature Parameter	1.068	
New Segment Elastic Modulus Dev. Parameters		
Final Value	14.50	ksi
Time Parameter	n/a	hrs
Curvature Parameter	n/a	
Poisson Ratio	0.17	
Coefficient of Thermal Expansion	4.54	µε/°F
Thermal Boundary Conditions (Applied to Appropriate Faces)		
Ambient Temp	Miami - Summer - Morning - Placement	
Wind	Medium-Wind	7.50	mph
Formwork	Steel Formwork	34.60	BTU/(ft·h·°F)
	Thickness	0.118	in
Curing	Burlap	0.18	BTU/(ft·h·°F)
	Thickness	0.39	in

Figure B-61: Simulation 21 - Bowing distortion of match-cast segment after placement of the new segment
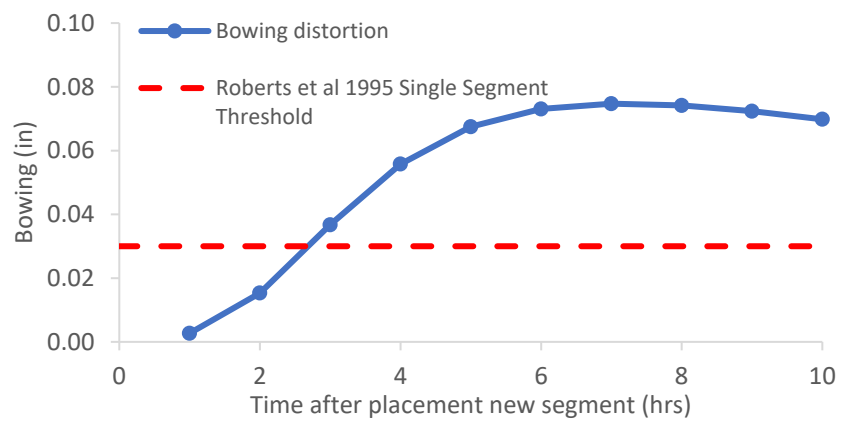

Figure B-62: Simulation 21 - Bowing distortion progression of match-cast segment from time of placement of new segment to 10 hours
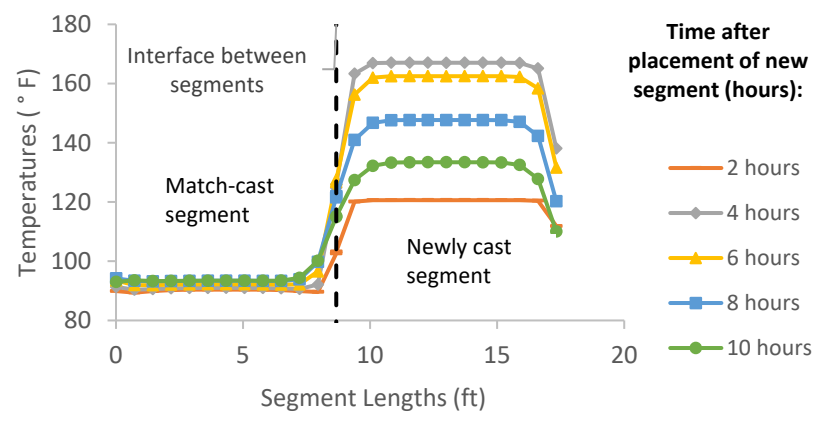

Figure B-63: Simulation 21 - Internal temperatures along the wing of segments

Simulation 22 -Results Summary

Table B-22: Model input parameters simulation 22

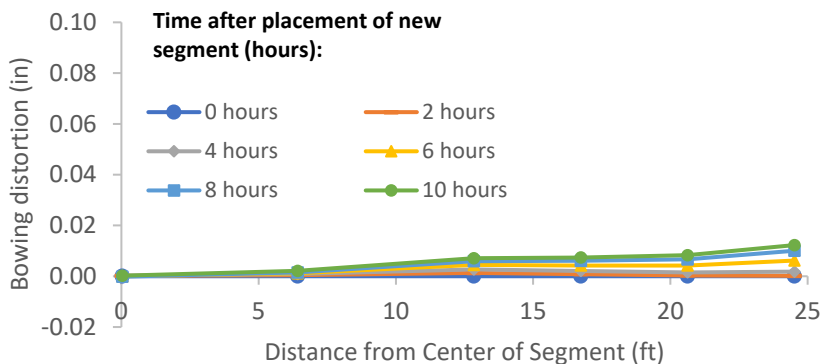| Model details		
Permutation number	22	
Geometry	Florida Bridge E - w/l=4.09	
Max. Mesh Size	2.95	in
Time Step	1	hrs
Placement Temperature	95	°F
Match-cast segment Time of Simulation at Casting	0	hrs
New Segment Time of Simulation at Casting	24	hrs
Concrete Properties		
Cement Content	950.11	lb/yd^3
Activation Energy	34.43	BTU/mol
Heat of Hydration Parameters		
Total Heat Development, $Q_{ult} = \alpha_u \cdot H_u$	129.52	BTU/lb
Time Parameter, τ	6.42	hrs
Curvature Parameter, β	1.10	
Density	3880.948	lb/yd^3
Specific Heat	0.26	BTU/(lb·°F)
Thermal Conductivity	1.502	BTU/(ft·h·°F)
Match-cast segment Elastic Modulus Dev. Parameters		
Final Value	4584.92	ksi
Time Parameter	12.420	hrs
Curvature Parameter	1.068	
New Segment Elastic Modulus Dev. Parameters		
Final Value	14.50	ksi
Time Parameter	n/a	hrs
Curvature Parameter	n/a	
Poisson Ratio	0.17	
Coefficient of Thermal Expansion	4.54	µε/°F
Thermal Boundary Conditions (Applied to Appropriate Faces)		
Ambient Temp	Miami - Summer - Morning - Placement	
Wind	Medium-Wind	7.50	mph
Formwork	Steel Formwork	34.60	BTU/(ft·h·°F)
	Thickness	0.118	in
Curing	Burlap	0.18	BTU/(ft·h·°F)
	Thickness	0.39	in

Figure B-64: Simulation 22 - Bowing distortion of match-cast segment after placement of the new segment
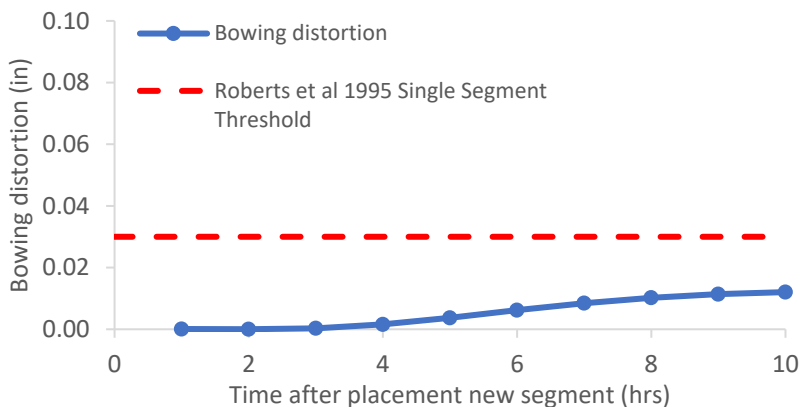

Figure B-65: Simulation 22 - Bowing distortion progression of match-cast segment from time of placement of new segment to 10 hours

Figure B-66: Simulation 22 - Internal temperatures along the wing of segments

Simulation 23 -Results Summary

Table B-23: Model input parameters simulation 23

Model details		
Permutation number	23	
Geometry	Florida Bridge B - w/l=5.97	
Max. Mesh Size	3.94	in
Time Step	1	hrs
Placement Temperature	95	°F
Match-cast segment Time of Simulation at Casting	0	hrs
New Segment Time of Simulation at Casting	24	hrs
Concrete Properties		
Cement Content	950.11	lb/yd^3
Activation Energy	34.43	BTU/mol
Heat of Hydration Parameters		
Total Heat Development, $Q_{ult} = \alpha_u \cdot H_u$	129.52	BTU/lb
Time Parameter, τ	6.42	hrs
Curvature Parameter, β	1.10	
Density	3880.948	lb/yd^3
Specific Heat	0.26	BTU/(lb·°F)
Thermal Conductivity	1.502	BTU/(ft·h·°F)
Match-cast segment Elastic Modulus Dev. Parameters		
Final Value	4584.92	ksi
Time Parameter	12.420	hrs
Curvature Parameter	1.068	
New Segment Elastic Modulus Dev. Parameters		
Final Value	14.50	ksi
Time Parameter	n/a	hrs
Curvature Parameter	n/a	
Poisson Ratio	0.17	
Coefficient of Thermal Expansion	4.54	µε/°F
Thermal Boundary Conditions (Applied to Appropriate Faces)		
Ambient Temp	Miami - Summer - Morning - Placement	
Wind	Medium-Wind	7.50	mph
Formwork	Steel Formwork	34.60	BTU/(ft·h·°F)
	Thickness	0.118	in
Curing	Burlap	0.18	BTU/(ft·h·°F)
	Thickness	0.39	in

Figure B-67: Simulation 23 - Bowing distortion of match-cast segment after placement of the new segment

Figure B-68: Simulation 23 - Bowing distortion progression of match-cast segment from time of placement of new segment to 10 hours
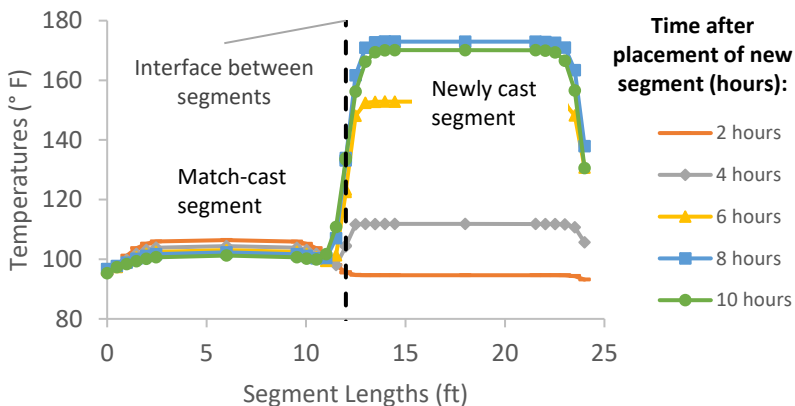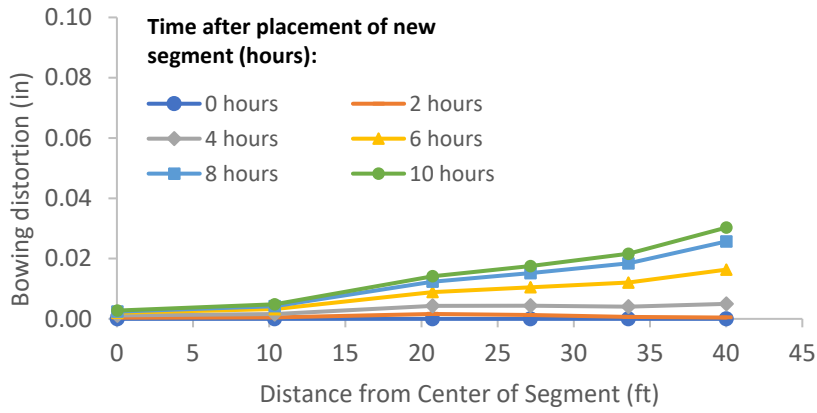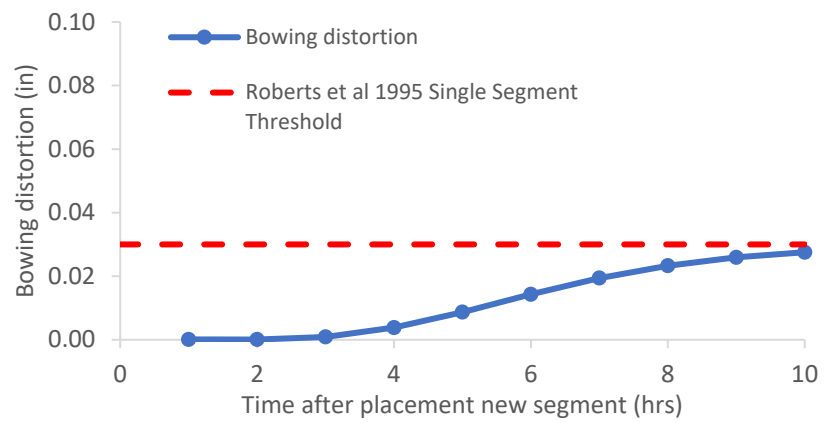

Figure B-69: Simulation 23 - Internal temperatures along the wing of segments

Simulation 24 -Results Summary

Table B-24: Model input parameters simulation 24

Model details		
Permutation number	24	
Geometry	Florida Bridge C - w/l=10.89	
Max. Mesh Size	3.54	in
Time Step	1	hrs
Placement Temperature	95	°F
Match-cast segment Time of Simulation at Casting	0	hrs
New Segment Time of Simulation at Casting	24	hrs
Concrete Properties		
Cement Content	950.11	lb/yd³
Activation Energy	34.43	BTU/mol
Heat of Hydration Parameters		
Total Heat Development, $Q_{ult} = \alpha_u \cdot H_u$	129.52	BTU/lb
Time Parameter, τ	6.42	hrs
Curvature Parameter, β	1.10	
Density	3880.948	lb/yd³
Specific Heat	0.26	BTU/(lb·°F)
Thermal Conductivity	1.502	BTU/(ft·h·°F)
Match-cast segment Elastic Modulus Dev. Parameters		
Final Value	4584.92	ksi
Time Parameter	12.420	hrs
Curvature Parameter	1.068	
New Segment Elastic Modulus Dev. Parameters		
Final Value	14.50	ksi
Time Parameter	n/a	hrs
Curvature Parameter	n/a	
Poisson Ratio	0.17	
Coefficient of Thermal Expansion	4.54	με/°F
Thermal Boundary Conditions (Applied to Appropriate Faces)		
Ambient Temp	Miami - Summer - Morning - Placement	
Wind	Medium-Wind	7.50	mph
Formwork	Steel Formwork	34.60	BTU/(ft·h·°F)
	Thickness	0.118	in
Curing	Burlap	0.18	BTU/(ft·h·°F)
	Thickness	0.39	in

Figure B-70: Simulation 24 - Bowing distortion of match-cast segment after placement of the new segment

Figure B-71: Simulation 24 - Bowing distortion progression of match-cast segment from time of placement of new segment to 10 hours
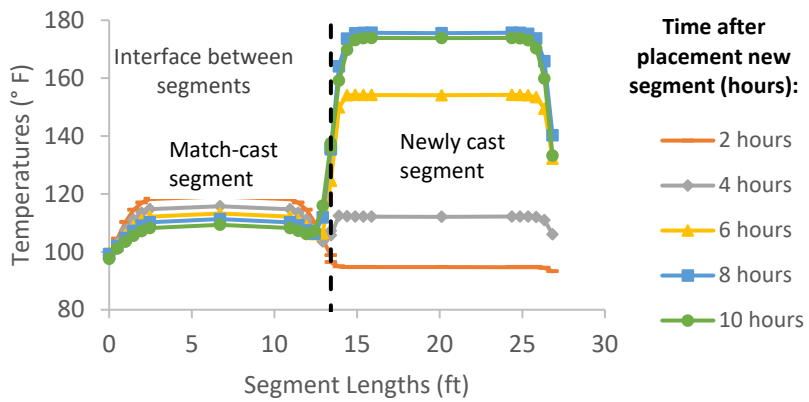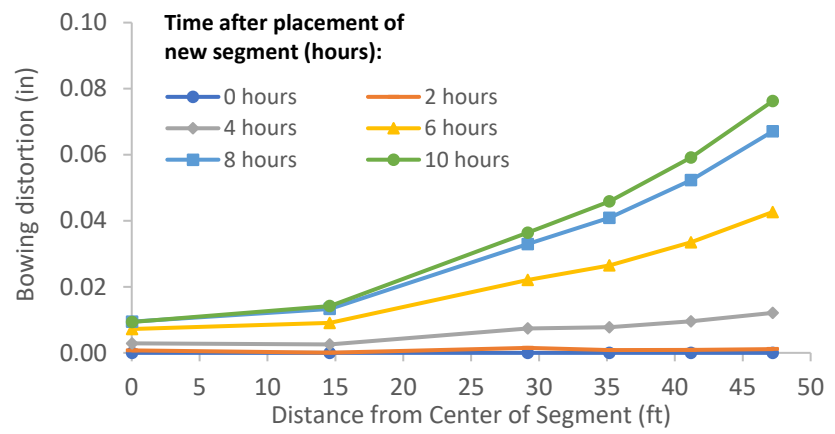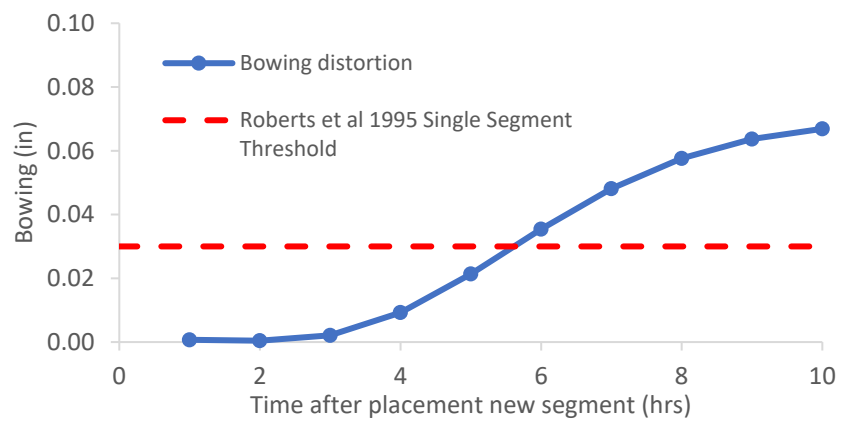

Figure B-72: Simulation 24 - Internal temperatures along the wing of segments

Simulation 25 -Results Summary

Table B-25: Model input parameters simulation 25

Model details		
Permutation number	25	
Geometry	Florida Bridge E - w/l=4.09	
Max. Mesh Size	2.95	in
Time Step	1	hrs
Placement Temperature	95	°F
Match-cast segment Time of Simulation at Casting	0	hrs
New Segment Time of Simulation at Casting	24	hrs
Concrete Properties		
Cement Content	950.11	lb/yd^3
Activation Energy	28.43	BTU/mol
Heat of Hydration Parameters		
Total Heat Development, $Q_{ult} = \alpha_u \cdot H_u$	124.95	BTU/lb
Time Parameter, τ	10.50	hrs
Curvature Parameter, β	1.60	
Density	3880.948	lb/yd^3
Specific Heat	0.26	BTU/(lb·°F)
Thermal Conductivity	1.502	BTU/(ft·h·°F)
Match-cast segment Elastic Modulus Dev. Parameters		
Final Value	4584.92	ksi
Time Parameter	12.420	hrs
Curvature Parameter	1.068	
New Segment Elastic Modulus Dev. Parameters		
Final Value	14.50	ksi
Time Parameter	n/a	hrs
Curvature Parameter	n/a	
Poisson Ratio	0.17	
Coefficient of Thermal Expansion	4.54	με/°F
Thermal Boundary Conditions (Applied to Appropriate Faces)		
Ambient Temp	Miami - Summer - Morning - Placement	
Wind	Medium-Wind	7.50	mph
Formwork	Steel Formwork	34.60	BTU/(ft·h·°F)
	Thickness	0.118	in
Curing	Burlap	0.18	BTU/(ft·h·°F)
	Thickness	0.39	in

Figure B-73: Simulation 25 - Bowing distortion of match-cast segment after placement of the new segment

Figure B-74: Simulation 25 - Bowing distortion progression of match-cast segment from time of placement of new segment to 10 hours
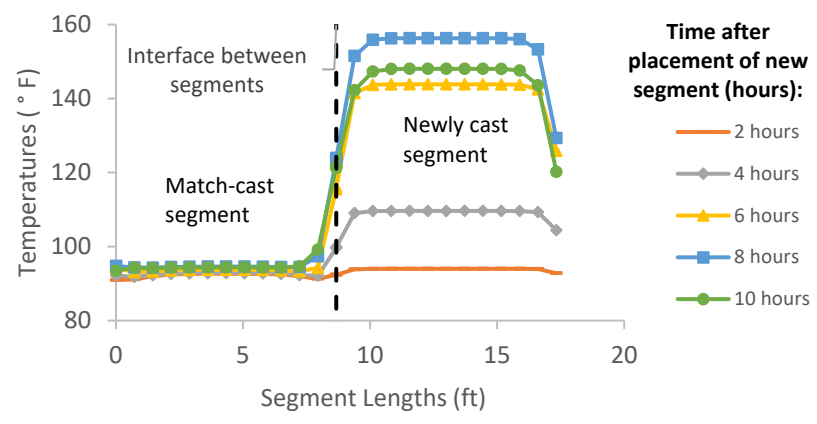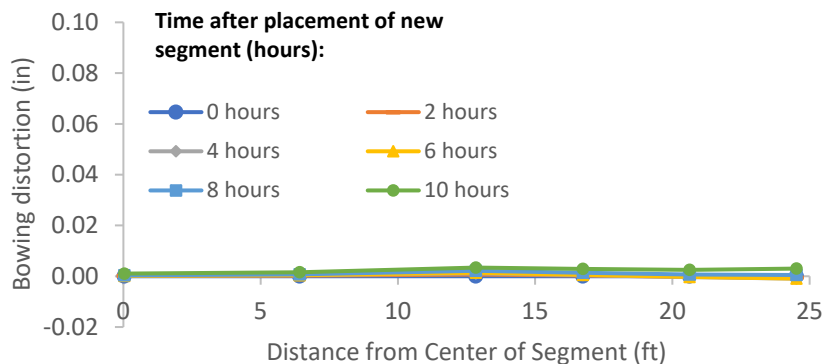

Figure B-75: Simulation 25 - Internal temperatures along the wing of segments

Simulation 26 -Results Summary

Table B-26: Model input parameters simulation 26

Model details		
Permutation number	26	
Geometry	Florida Bridge B - w/l=5.97	
Max. Mesh Size	3.94	in
Time Step	1	hrs
Placement Temperature	95	°F
Match-cast segment Time of Simulation at Casting	0	hrs
New Segment Time of Simulation at Casting	24	hrs
Concrete Properties		
Cement Content	950.11	lb/yd^3
Activation Energy	28.43	BTU/mol
Heat of Hydration Parameters		
Total Heat Development, $Q_{ult} = \alpha_u \cdot H_u$	124.95	BTU/lb
Time Parameter, τ	10.50	hrs
Curvature Parameter, β	1.60	
Density	3880.948	lb/yd^3
Specific Heat	0.26	BTU/(lb·°F)
Thermal Conductivity	1.502	BTU/(ft·h·°F)
Match-cast segment Elastic Modulus Dev. Parameters		
Final Value	4584.92	ksi
Time Parameter	12.420	hrs
Curvature Parameter	1.068	
New Segment Elastic Modulus Dev. Parameters		
Final Value	14.50	ksi
Time Parameter	n/a	hrs
Curvature Parameter	n/a	
Poisson Ratio	0.17	
Coefficient of Thermal Expansion	4.54	με/°F
Thermal Boundary Conditions (Applied to Appropriate Faces)		
Ambient Temp	Miami - Summer - Morning - Placement		
Wind	Medium-Wind	7.50	mph
Formwork	Steel Formwork	34.60	BTU/(ft·h·°F)
	Thickness	0.118	in
Curing	Burlap	0.18	BTU/(ft·h·°F)
	Thickness	0.39	in

Figure B-76: Simulation 26 - Bowing distortion of match-cast segment after placement of the new segment

Figure B-77: Simulation 26 - Bowing distortion progression of match-cast segment from time of placement of new segment to 10 hours
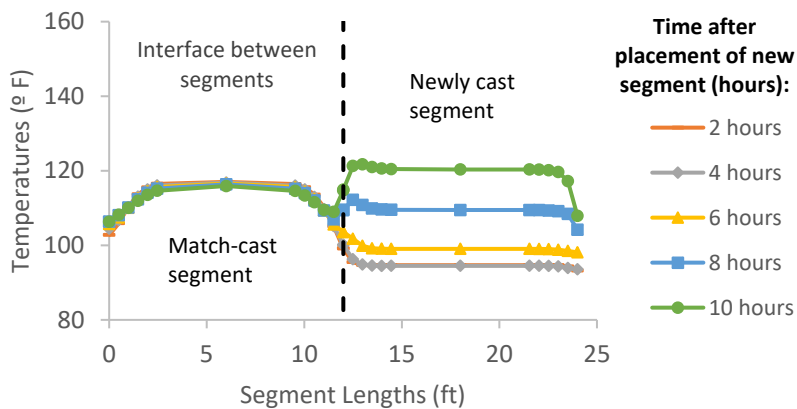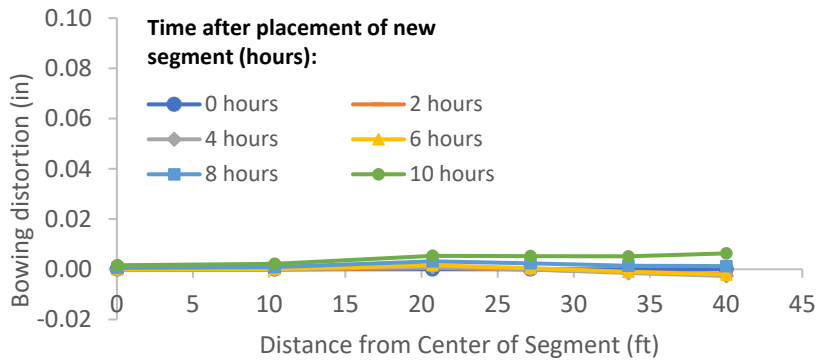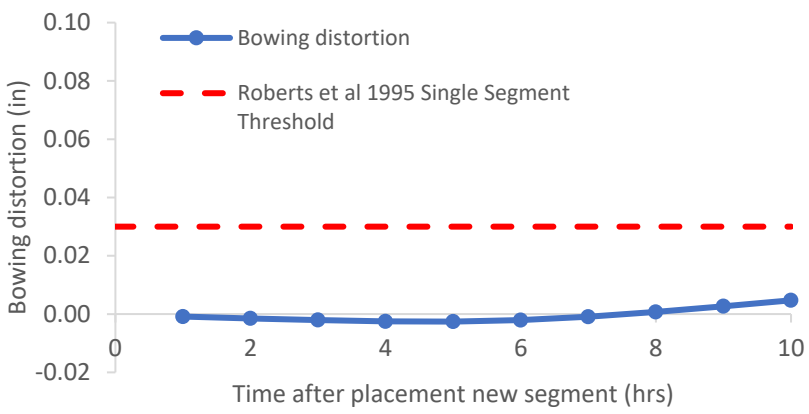

Figure B-78: Simulation 26 - Internal temperatures along the wing of segments

Simulation 27 -Results Summary

Table B-27: Model input parameters simulation 27

Model details		
Permutation number	27	
Geometry	Florida Bridge C - w/l=10.89	
Max. Mesh Size	3.54	in
Time Step	1	hrs
Placement Temperature	95	°F
Match-cast segment Time of Simulation at Casting	0	hrs
New Segment Time of Simulation at Casting	24	hrs
Concrete Properties		
Cement Content	950.11	lb/yd^3
Activation Energy	28.43	BTU/mol
Heat of Hydration Parameters		
Total Heat Development, $Q_{ult} = \alpha_u \cdot H_u$	124.95	BTU/lb
Time Parameter, τ	10.50	hrs
Curvature Parameter, β	1.60	
Density	3880.948	lb/yd^3
Specific Heat	0.26	BTU/(lb·°F)
Thermal Conductivity	1.502	BTU/(ft·h·°F)
Match-cast segment Elastic Modulus Dev. Parameters		
Final Value	4584.92	ksi
Time Parameter	12.420	hrs
Curvature Parameter	1.068	
New Segment Elastic Modulus Dev. Parameters		
Final Value	14.50	ksi
Time Parameter	n/a	hrs
Curvature Parameter	n/a	
Poisson Ratio	0.17	
Coefficient of Thermal Expansion	4.54	με/°F
Thermal Boundary Conditions (Applied to Appropriate Faces)		
Ambient Temp	Miami - Summer - Morning - Placement	
Wind	Medium-Wind	7.50	mph
Formwork	Steel Formwork	34.60	BTU/(ft·h·°F)
	Thickness	0.118	in
Curing	Burlap	0.18	BTU/(ft·h·°F)
	Thickness	0.39	in

Figure B-79: Simulation 27 - Bowing distortion of match-cast segment after placement of the new segment

Figure B-80: Simulation 27 - Bowing distortion progression of match-cast segment from time of placement of new segment to 10 hours
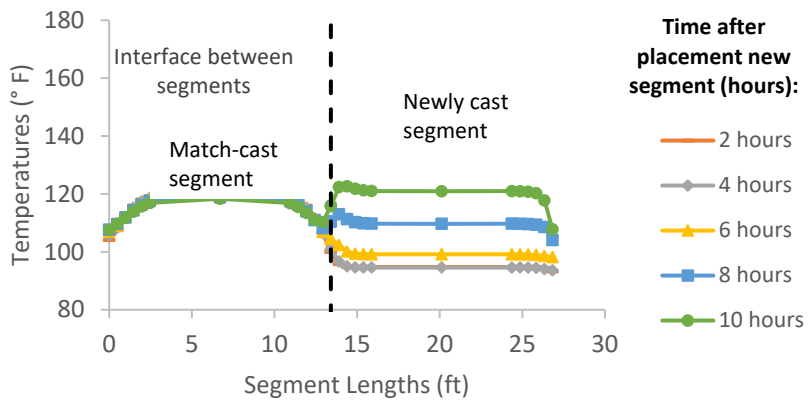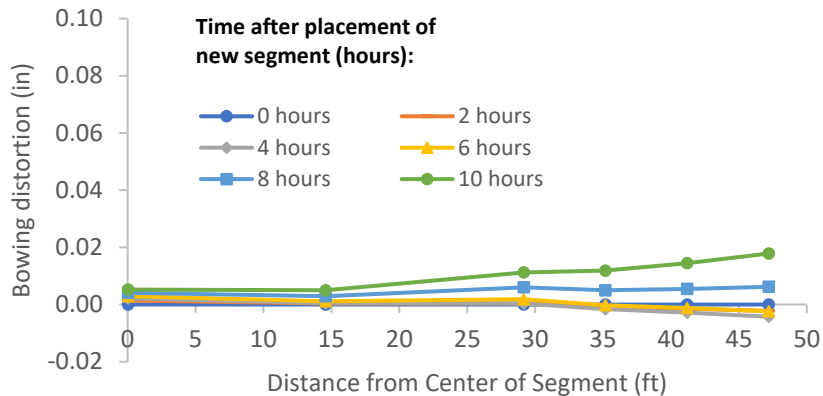

Figure B-81: Simulation 27 - Internal temperatures along the wing of segments

Simulation 28 -Results Summary

Table B-28: Model input parameters simulation 28

Model details		
Permutation number	28	
Geometry	Florida Bridge E - w/l=4.09	
Max. Mesh Size	2.95	in
Time Step	1	hrs
Placement Temperature	95	°F
Match-cast segment Time of Simulation at Casting	0	hrs
New Segment Time of Simulation at Casting	24	hrs
Concrete Properties		
Cement Content	650.08	lb/yd^3
Activation Energy	26.21	BTU/mol
Heat of Hydration Parameters		
Total Heat Development, $Q_{ult} = \alpha_u \cdot H_u$	107.65	BTU/lb
Time Parameter, τ	18.28	hrs
Curvature Parameter, β	1.65	
Density	3834.891	lb/yd^3
Specific Heat	0.24	BTU/(lb·°F)
Thermal Conductivity	1.608	BTU/(ft·h·°F)
Match-cast segment Elastic Modulus Dev. Parameters		
Final Value	4503.55	ksi
Time Parameter	12.420	hrs
Curvature Parameter	1.068	
New Segment Elastic Modulus Dev. Parameters		
Final Value	14.50	ksi
Time Parameter	n/a	hrs
Curvature Parameter	n/a	
Poisson Ratio	0.17	
Coefficient of Thermal Expansion	4.55	µε/°F
Thermal Boundary Conditions (Applied to Appropriate Faces)		
Ambient Temp	Miami - Summer - Morning - Placement	
Wind	Medium-Wind	7.50	mph
Formwork	Steel Formwork	34.60	BTU/(ft·h·°F)
	Thickness	0.118	in
Curing	White Burlap Polyethylene	0.02	BTU/(ft·h·°F)
	Thickness	0.39	in

Figure B-82: Simulation 28 - Bowing distortion of match-cast segment after placement of the new segment
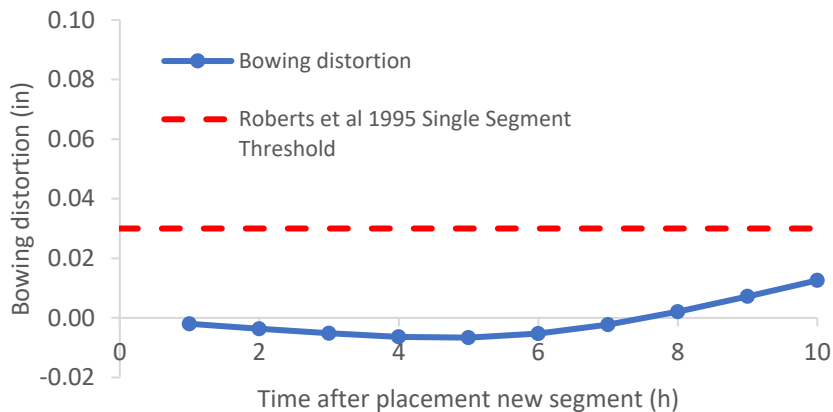

Figure B-83: Simulation 28 - Bowing distortion progression of match-cast segment from time of placement of new segment to 10 hours
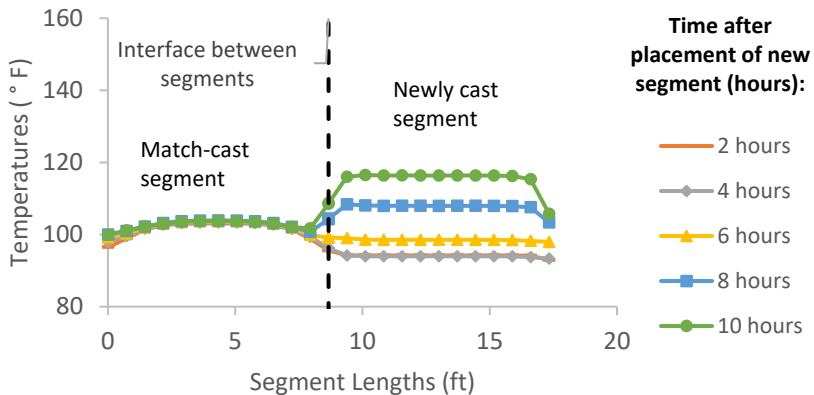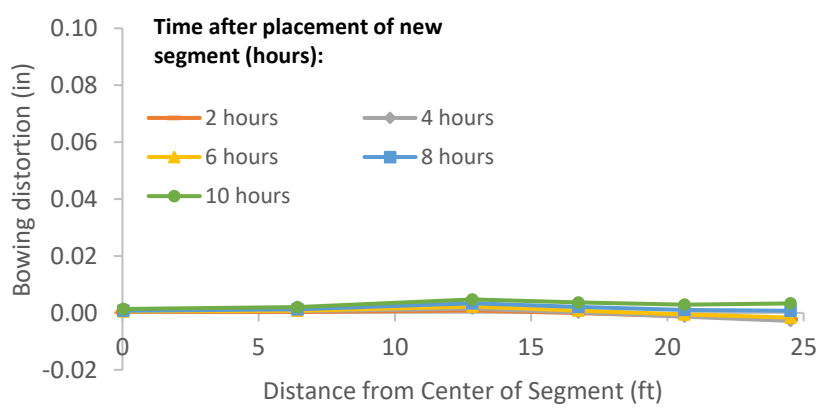

Figure B-84: Simulation 28 - Internal temperatures along the wing of segments

Simulation 29 -Results Summary

Table B-29: Model input parameters simulation 29

Model details		
Permutation number	29	
Geometry	Florida Bridge B - w/l=5.97	
Max. Mesh Size	3.94	in
Time Step	1	hrs
Placement Temperature	95	°F
Match-cast segment Time of Simulation at Casting	0	hrs
New Segment Time of Simulation at Casting	24	hrs
Concrete Properties		
Cement Content	650.08	lb/yd^3
Activation Energy	26.21	BTU/mol
Heat of Hydration Parameters		
Total Heat Development, $Q_{ult} = \alpha_u \cdot H_u$	107.65	BTU/lb
Time Parameter, τ	18.28	hrs
Curvature Parameter, β	1.65	
Density	3834.891	lb/yd^3
Specific Heat	0.24	BTU/(lb·°F)
Thermal Conductivity	1.608	BTU/(ft·h·°F)
Match-cast segment Elastic Modulus Dev. Parameters		
Final Value	4503.55	ksi
Time Parameter	12.420	hrs
Curvature Parameter	1.068	
New Segment Elastic Modulus Dev. Parameters		
Final Value	14.50	ksi
Time Parameter	n/a	hrs
Curvature Parameter	n/a	
Poisson Ratio	0.17	
Coefficient of Thermal Expansion	4.55	με/°F
Thermal Boundary Conditions (Applied to Appropriate Faces)		
Ambient Temp	Miami - Summer - Morning - Placement		
Wind	Medium-Wind	7.50	mph
Formwork	Steel Formwork	34.60	BTU/(ft·h·°F)
	Thickness	0.118	in
Curing	White Burlap Polyethylene	0.02	BTU/(ft·h·°F)
	Thickness	0.39	in

Figure B-85: Simulation 29 - Bowing distortion of match-cast segment after placement of the new segment
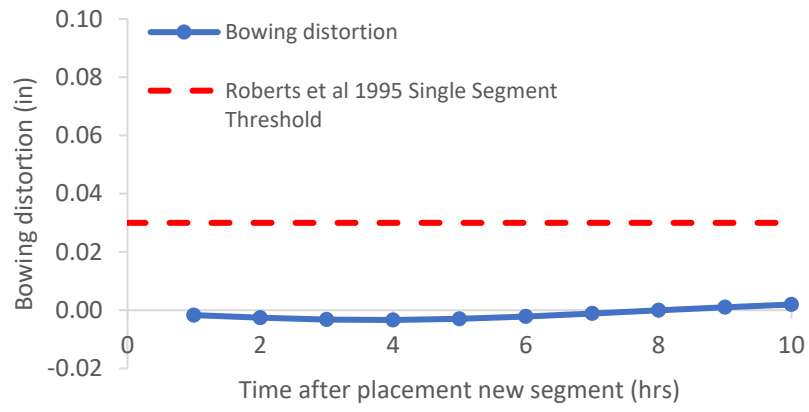

Figure B-86: Simulation 29 - Bowing distortion progression of match-cast segment from time of placement of new segment to 10 hours
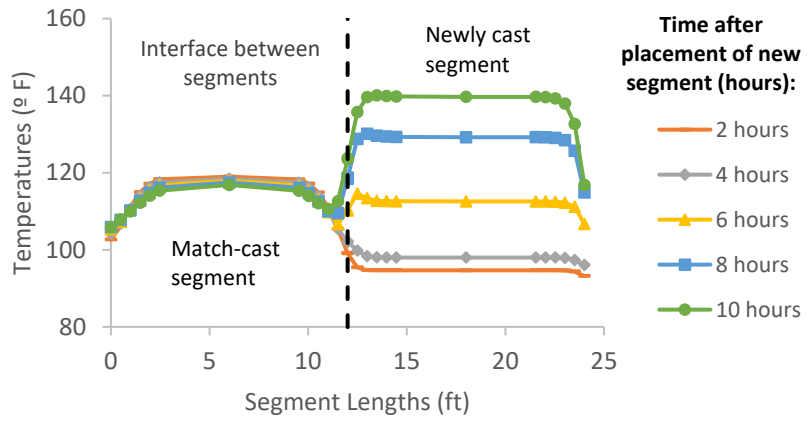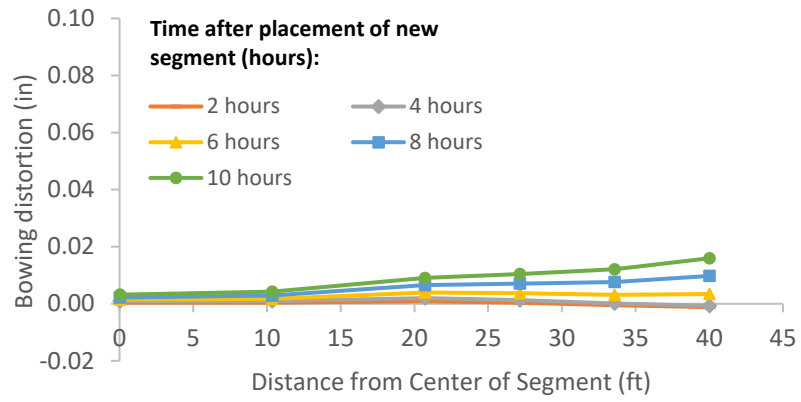

Figure B-87: Simulation 29 - Internal temperatures along the wing of segments

Simulation 30 -Results Summary

Table B-30: Model input parameters simulation 30

Model details		
Permutation number	30	
Geometry	Florida Bridge C - w/l=10.89	
Max. Mesh Size	3.54	in
Time Step	1	hrs
Placement Temperature	95	°F
Match-cast segment Time of Simulation at Casting	0	hrs
New Segment Time of Simulation at Casting	24	hrs
Concrete Properties		
Cement Content	650.08	lb/yd^3
Activation Energy	26.21	BTU/mol
Heat of Hydration Parameters		
Total Heat Development, $Q_{ult} = \alpha_u \cdot H_u$	107.65	BTU/lb
Time Parameter, τ	18.28	hrs
Curvature Parameter, β	1.65	
Density	3834.891	lb/yd^3
Specific Heat	0.24	BTU/(lb·°F)
Thermal Conductivity	1.608	BTU/(ft·h·°F)
Match-cast segment Elastic Modulus Dev. Parameters		
Final Value	4503.55	ksi
Time Parameter	12.420	hrs
Curvature Parameter	1.068	
New Segment Elastic Modulus Dev. Parameters		
Final Value	14.50	ksi
Time Parameter	n/a	hrs
Curvature Parameter	n/a	
Poisson Ratio	0.17	
Coefficient of Thermal Expansion	4.55	$\mu\varepsilon$/°F
Thermal Boundary Conditions (Applied to Appropriate Faces)		
Ambient Temp	Miami - Summer - Morning - Placement	
Wind	Medium-Wind	7.50	mph
Formwork	Steel Formwork	34.60	BTU/(ft·h·°F)
	Thickness	0.118	in
Curing	White Burlap Polyethylene	0.02	BTU/(ft·h·°F)
	Thickness	0.39	in

Figure B-88: Simulation 30 - Bowing distortion of match-cast segment after placement of the new segment
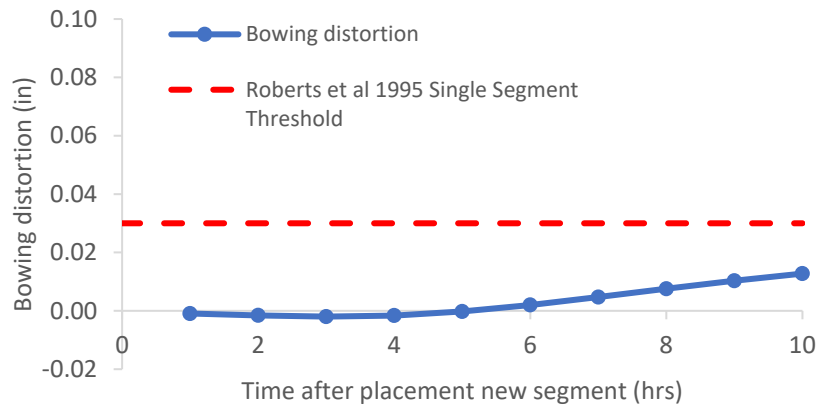

Figure B-89: Simulation 30 - Bowing distortion progression of match-cast segment from time of placement of new segment to 10 hours
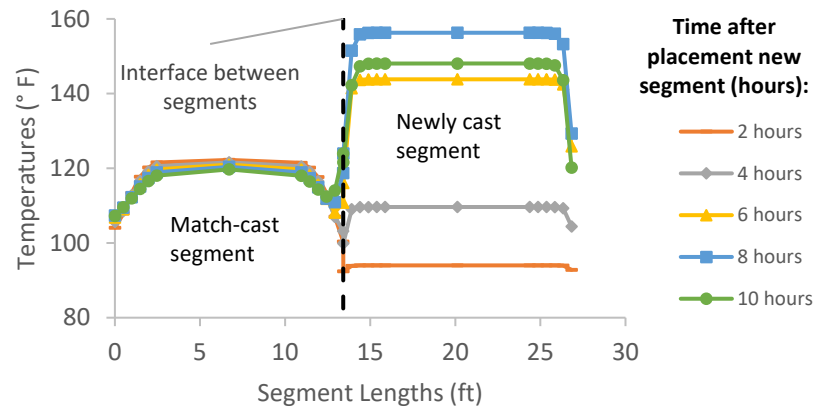

Figure B-90: Simulation 30 - Internal temperatures along the wing of segments

Simulation 31 -Results Summary

Table B-31: Model input parameters simulation 31

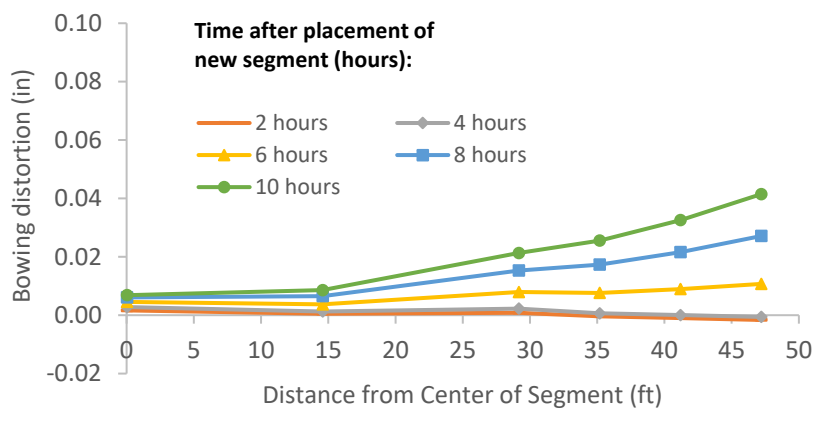| Model details		
Permutation number	31	
Geometry	Florida Bridge E - w/l=4.09	
Max. Mesh Size	2.95	in
Time Step	1	hrs
Placement Temperature	95	°F
Match-cast segment Time of Simulation at Casting	0	hrs
New Segment Time of Simulation at Casting	24	hrs
Concrete Properties		
Cement Content	750.09	lb/yd^3
Activation Energy	24.13	BTU/mol
Heat of Hydration Parameters		
Total Heat Development, $Q_{ult} = \alpha_u \cdot H_u$	111.33	BTU/lb
Time Parameter, τ	13.36	hrs
Curvature Parameter, β	1.49	
Density	3816.577	lb/yd^3
Specific Heat	0.25	BTU/(lb·°F)
Thermal Conductivity	1.557	BTU/(ft·h·°F)
Match-cast segment Elastic Modulus Dev. Parameters		
Final Value	4471.32	ksi
Time Parameter	12.420	hrs
Curvature Parameter	1.068	
New Segment Elastic Modulus Dev. Parameters		
Final Value	14.50	ksi
Time Parameter	n/a	hrs
Curvature Parameter	n/a	
Poisson Ratio	0.17	
Coefficient of Thermal Expansion	4.54	µε/°F
Thermal Boundary Conditions (Applied to Appropriate Faces)		
Ambient Temp	Miami - Summer - Morning - Placement	
Wind	Medium-Wind	7.50	mph
Formwork	Steel Formwork	34.60	BTU/(ft·h·°F)
	Thickness	0.118	in
Curing	White Burlap Polyethylene	0.02	BTU/(ft·h·°F)
	Thickness	0.39	in

Figure B-91: Simulation 31 - Bowing distortion of match-cast segment after placement of the new segment
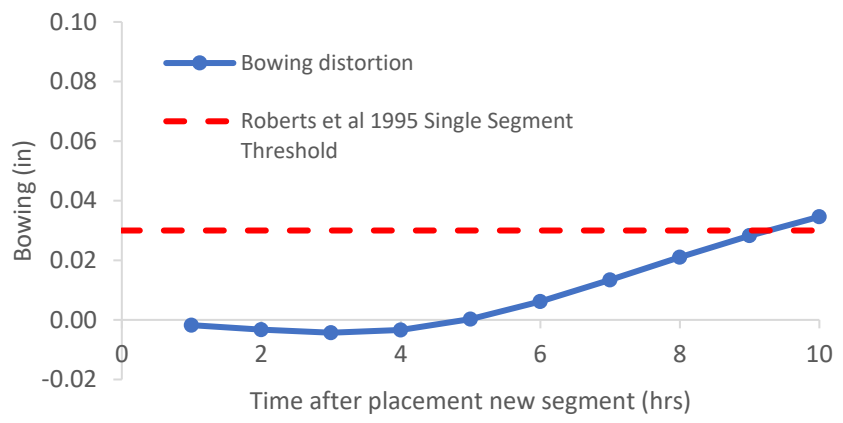

Figure B-92: Simulation 31 - Bowing distortion progression of match-cast segment from time of placement of new segment to 10 hours
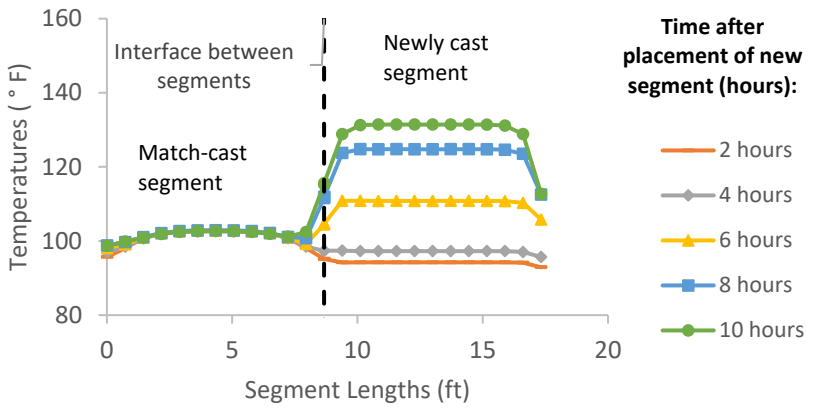

Figure B-93: Simulation 31 - Internal temperatures along the wing of segments

Simulation 32 -Results Summary

Table B-32: Model input parameters simulation 32

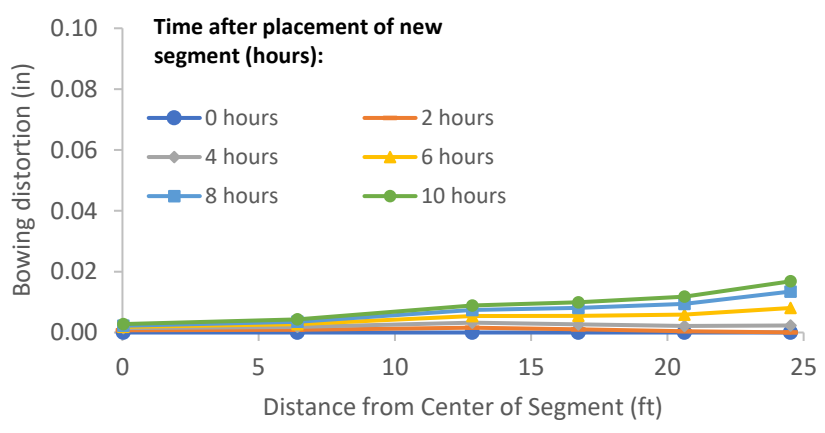| Model details		
Permutation number	32	
Geometry	Florida Bridge B - w/l=5.97	
Max. Mesh Size	3.94	in
Time Step	1	hrs
Placement Temperature	95	°F
Match-cast segment Time of Simulation at Casting	0	hrs
New Segment Time of Simulation at Casting	24	hrs
Concrete Properties		
Cement Content	750.09	lb/yd^3
Activation Energy	24.13	BTU/mol
Heat of Hydration Parameters		
Total Heat Development, $Q_{ult} = \alpha_u \cdot H_u$	111.33	BTU/lb
Time Parameter, τ	13.36	hrs
Curvature Parameter, β	1.49	
Density	3816.577	lb/yd^3
Specific Heat	0.25	BTU/(lb·°F)
Thermal Conductivity	1.557	BTU/(ft·h·°F)
Match-cast segment Elastic Modulus Dev. Parameters		
Final Value	4471.32	ksi
Time Parameter	12.420	hrs
Curvature Parameter	1.068	
New Segment Elastic Modulus Dev. Parameters		
Final Value	14.50	ksi
Time Parameter	n/a	hrs
Curvature Parameter	n/a	
Poisson Ratio	0.17	
Coefficient of Thermal Expansion	4.54	µε/°F
Thermal Boundary Conditions (Applied to Appropriate Faces)		
Ambient Temp	Miami - Summer - Morning - Placement	
Wind	Medium-Wind	7.50	mph
Formwork	Steel Formwork	34.60	BTU/(ft·h·°F)
	Thickness	0.118	in
Curing	White Burlap Polyethylene	0.02	BTU/(ft·h·°F)
	Thickness	0.39	in

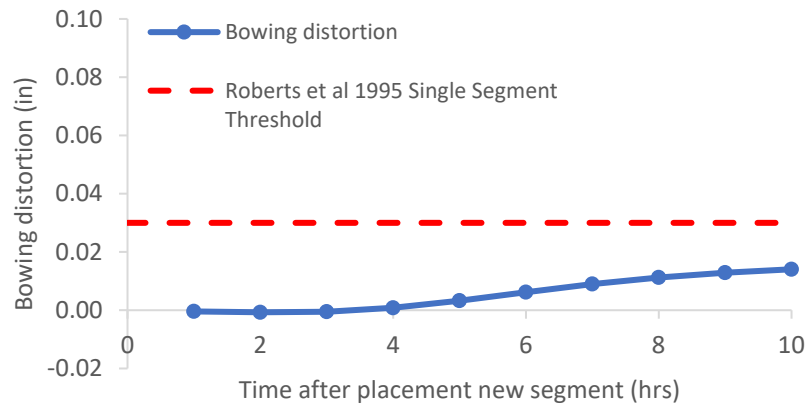Figure B-94: Simulation 32 - Bowing distortion of match-cast segment after placement of the new segment

Figure B-95: Simulation 32 - Bowing distortion progression of match-cast segment from time of placement of new segment to 10 hours
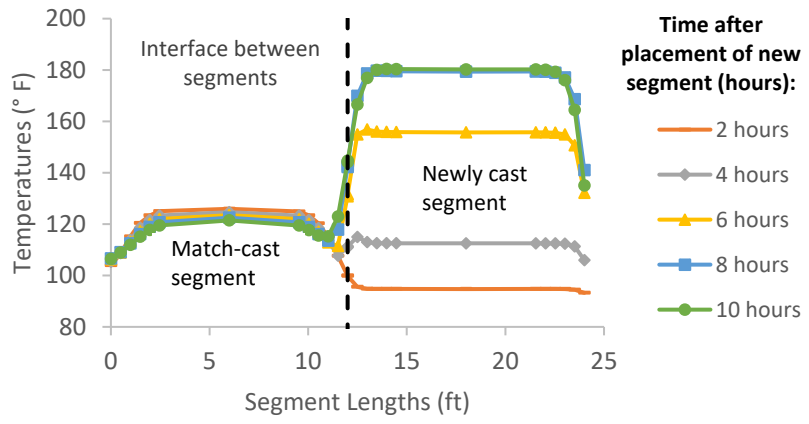

Figure B-96: Simulation 32 - Internal temperatures along the wing of segments

Simulation 33 -Results Summary

Table B-33: Model input parameters simulation 33

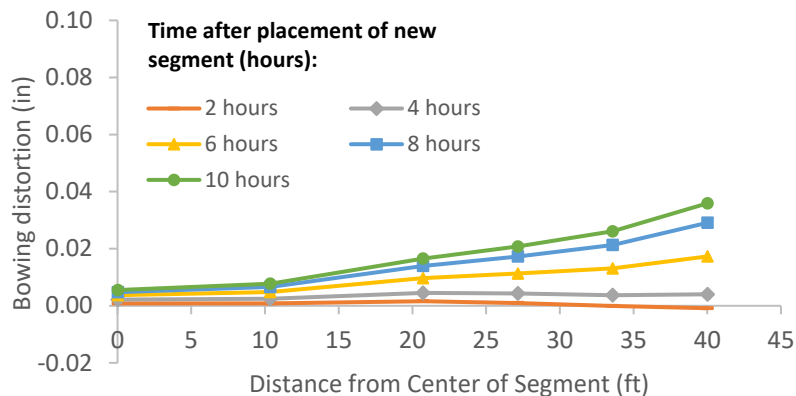| Model details		
Permutation number	33	
Geometry	Florida Bridge C - w/l=10.89	
Max. Mesh Size	3.54	in
Time Step	1	hrs
Placement Temperature	95	°F
Match-cast segment Time of Simulation at Casting	0	hrs
New Segment Time of Simulation at Casting	24	hrs
Concrete Properties		
Cement Content	750.09	lb/yd^3
Activation Energy	24.13	BTU/mol
Heat of Hydration Parameters		
Total Heat Development, $Q_{ult} = \alpha_u \cdot H_u$	111.33	BTU/lb
Time Parameter, τ	13.36	hrs
Curvature Parameter, β	1.49	
Density	3816.577	lb/yd^3
Specific Heat	0.25	BTU/(lb·°F)
Thermal Conductivity	1.557	BTU/(ft·h·°F)
Match-cast segment Elastic Modulus Dev. Parameters		
Final Value	4471.32	ksi
Time Parameter	12.420	hrs
Curvature Parameter	1.068	
New Segment Elastic Modulus Dev. Parameters		
Final Value	14.50	ksi
Time Parameter	n/a	hrs
Curvature Parameter	n/a	
Poisson Ratio	0.17	
Coefficient of Thermal Expansion	4.54	με/°F
Thermal Boundary Conditions (Applied to Appropriate Faces)		
Ambient Temp	Miami - Summer - Morning - Placement	
Wind	Medium-Wind	7.50	mph
Formwork	Steel Formwork	34.60	BTU/(ft·h·°F)
	Thickness	0.118	in
Curing	White Burlap Polyethylene	0.02	BTU/(ft·h·°F)
	Thickness	0.39	in

Figure B-97: Simulation 33 - Bowing distortion of match-cast segment after placement of the new segment

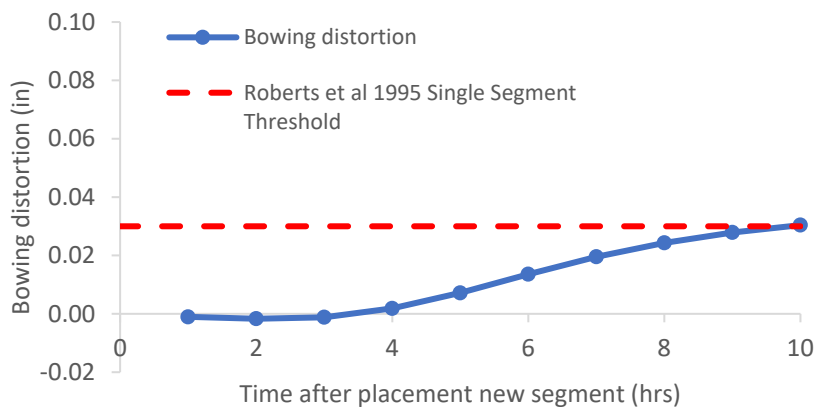Figure B-98: Simulation 33 - Bowing distortion progression of match-cast segment from time of placement of new segment to 10 hours
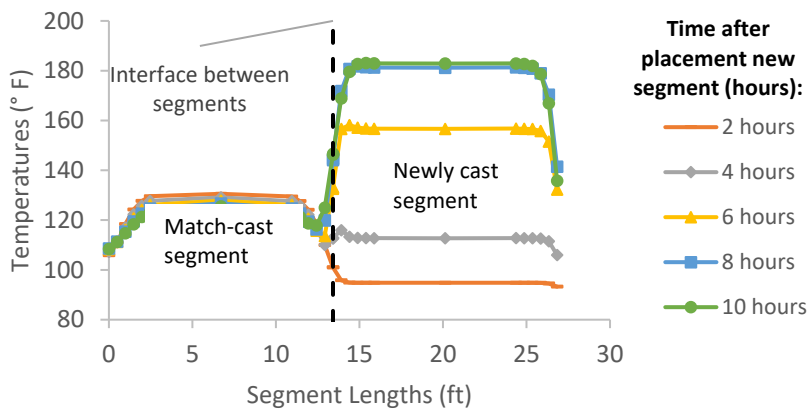

Figure B-99: Simulation 33 - Internal temperatures along the wing of segments

Simulation 34 -Results Summary

Table B-34: Model input parameters simulation 34

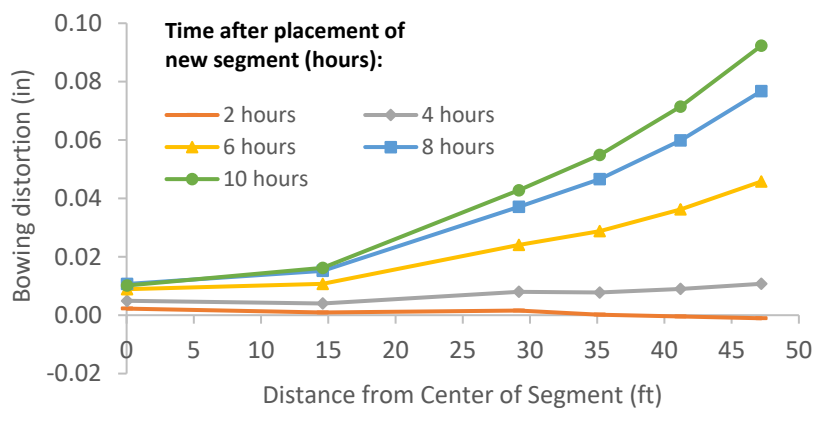| Model details		
Permutation number	34	
Geometry	Florida Bridge E - w/l=4.09	
Max. Mesh Size	2.95	in
Time Step	1	hrs
Placement Temperature	95	°F
Match-cast segment Time of Simulation at Casting	0	hrs
New Segment Time of Simulation at Casting	24	hrs
Concrete Properties		
Cement Content	950.11	lb/yd^3
Activation Energy	28.43	BTU/mol
Heat of Hydration Parameters		
Total Heat Development, $Q_{ult} = \alpha_u \cdot H_u$	124.95	BTU/lb
Time Parameter, τ	10.50	hrs
Curvature Parameter, β	1.60	
Density	3880.948	lb/yd^3
Specific Heat	0.26	BTU/(lb·°F)
Thermal Conductivity	1.502	BTU/(ft·h·°F)
Match-cast segment Elastic Modulus Dev. Parameters		
Final Value	4584.92	ksi
Time Parameter	12.420	hrs
Curvature Parameter	1.068	
New Segment Elastic Modulus Dev. Parameters		
Final Value	14.50	ksi
Time Parameter	n/a	hrs
Curvature Parameter	n/a	
Poisson Ratio	0.17	
Coefficient of Thermal Expansion	4.54	με/°F
Thermal Boundary Conditions (Applied to Appropriate Faces)		
Ambient Temp	Miami - Summer - Morning - Placement	
Wind	Medium-Wind	7.50	mph
Formwork	Steel Formwork	34.60	BTU/(ft·h·°F)
	Thickness	0.118	in
Curing	White Burlap Polyethylene	0.02	BTU/(ft·h·°F)
	Thickness	0.39	in

Figure B-100: Simulation 34 - Bowing distortion of match-cast segment after placement of the new segment

Figure B-101: Simulation 34 - Bowing distortion progression of match-cast segment from time of placement of new segment to 10 hours
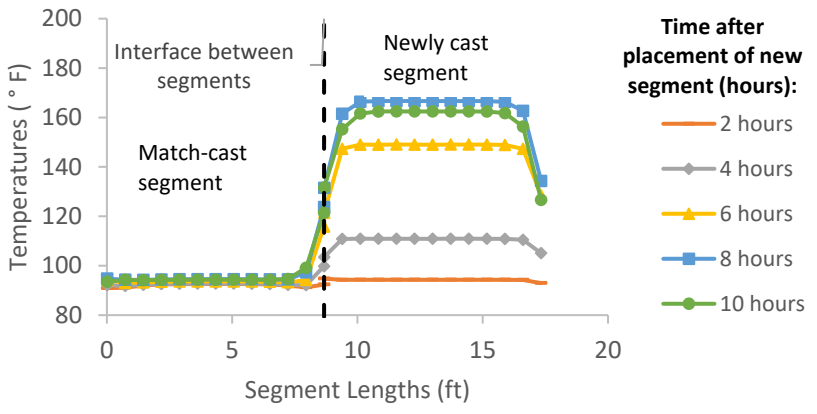

Figure B-102: Simulation 34 - Internal temperatures along the wing of segments

Simulation 35 -Results Summary

Table B-35: Model input parameters simulation 35

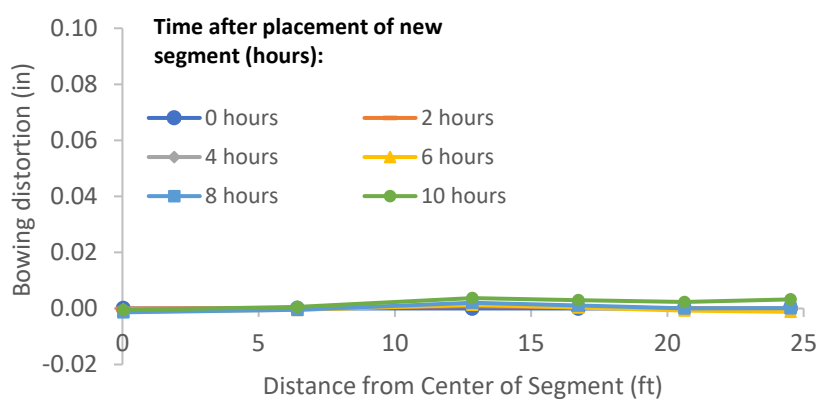| Model details		
Permutation number	35	
Geometry	Florida Bridge B - w/l=5.97	
Max. Mesh Size	3.94	in
Time Step	1	hrs
Placement Temperature	95	°F
Match-cast segment Time of Simulation at Casting	0	hrs
New Segment Time of Simulation at Casting	24	hrs
Concrete Properties		
Cement Content	950.11	lb/yd^3
Activation Energy	28.43	BTU/mol
Heat of Hydration Parameters		
Total Heat Development, $Q_{ult} = \alpha_u \cdot H_u$	124.95	BTU/lb
Time Parameter, τ	10.50	hrs
Curvature Parameter, β	1.60	
Density	3880.948	lb/yd^3
Specific Heat	0.26	BTU/(lb·°F)
Thermal Conductivity	1.502	BTU/(ft·h·°F)
Match-cast segment Elastic Modulus Dev. Parameters		
Final Value	4584.92	ksi
Time Parameter	12.420	hrs
Curvature Parameter	1.068	
New Segment Elastic Modulus Dev. Parameters		
Final Value	14.50	ksi
Time Parameter	n/a	hrs
Curvature Parameter	n/a	
Poisson Ratio	0.17	
Coefficient of Thermal Expansion	4.54	με/°F
Thermal Boundary Conditions (Applied to Appropriate Faces)		
Ambient Temp	Miami - Summer - Morning - Placement	
Wind	Medium-Wind	7.50	mph
Formwork	Steel Formwork	34.60	BTU/(ft·h·°F)
	Thickness	0.118	in
Curing	White Burlap Polyethylene	0.02	BTU/(ft·h·°F)
	Thickness	0.39	in

Figure B-103: Simulation 35 - Bowing distortion of match-cast segment after placement of the new segment

Figure B-104: Simulation 35 - Bowing distortion progression of match-cast segment from time of placement of new segment to 10 hours
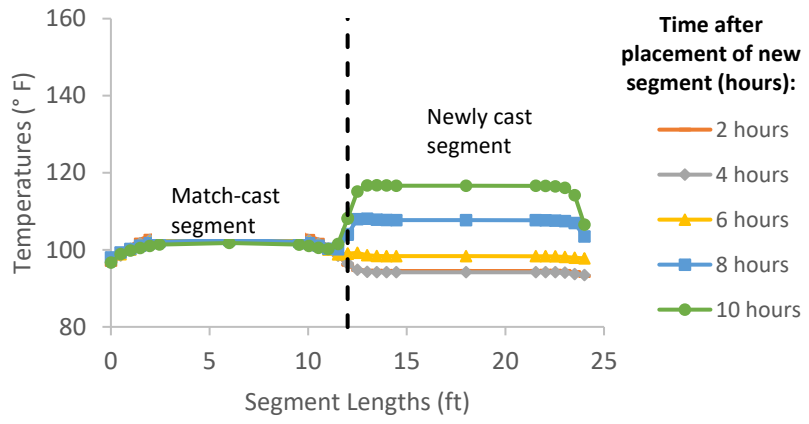

Figure B-105: Simulation 35 - Internal temperatures along the wing of segments

Simulation 36 -Results Summary

Table B-36: Model input parameters simulation 36

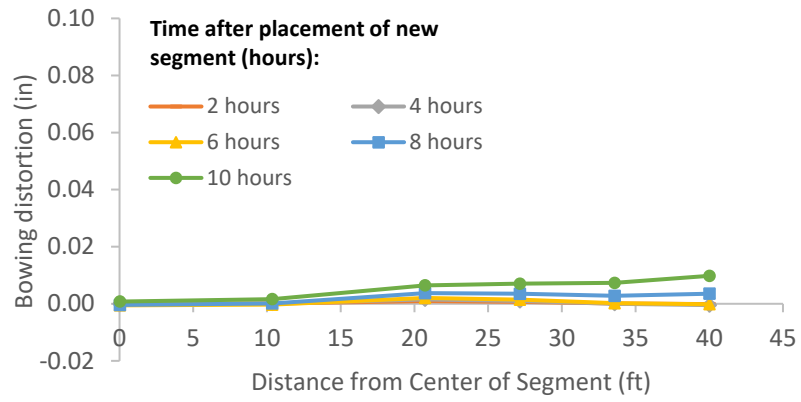| Model details		
Permutation number	36	
Geometry	Florida Bridge C - w/l=10.89	
Max. Mesh Size	3.54	in
Time Step	1	hrs
Placement Temperature	95	°F
Match-cast segment Time of Simulation at Casting	0	hrs
New Segment Time of Simulation at Casting	24	hrs
Concrete Properties		
Cement Content	950.11	lb/yd^3
Activation Energy	28.43	BTU/mol
Heat of Hydration Parameters		
Total Heat Development, $Q_{ult} = \alpha_u \cdot H_u$	124.95	BTU/lb
Time Parameter, τ	10.50	hrs
Curvature Parameter, β	1.60	
Density	3880.948	lb/yd^3
Specific Heat	0.26	BTU/(lb·°F)
Thermal Conductivity	1.502	BTU/(ft·h·°F)
Match-cast segment Elastic Modulus Dev. Parameters		
Final Value	4584.92	ksi
Time Parameter	12.420	hrs
Curvature Parameter	1.068	
New Segment Elastic Modulus Dev. Parameters		
Final Value	14.50	ksi
Time Parameter	n/a	hrs
Curvature Parameter	n/a	
Poisson Ratio	0.17	
Coefficient of Thermal Expansion	4.54	$\mu\varepsilon$/°F
Thermal Boundary Conditions (Applied to Appropriate Faces)		
Ambient Temp	Miami - Summer - Morning - Placement	
Wind	Medium-Wind	7.50	mph
Formwork	Steel Formwork	34.60	BTU/(ft·h·°F)
	Thickness	0.118	in
Curing	White Burlap Polyethylene	0.02	BTU/(ft·h·°F)
	Thickness	0.39	in

Figure B-106: Simulation 36 - Bowing distortion of match-cast segment after placement of the new segment
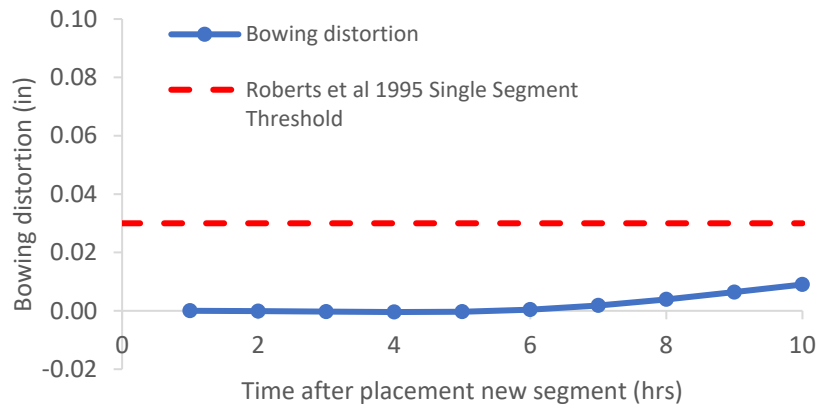

Figure B-107: Simulation 36 - Bowing distortion progression of match-cast segment from time of placement of new segment to 10 hours
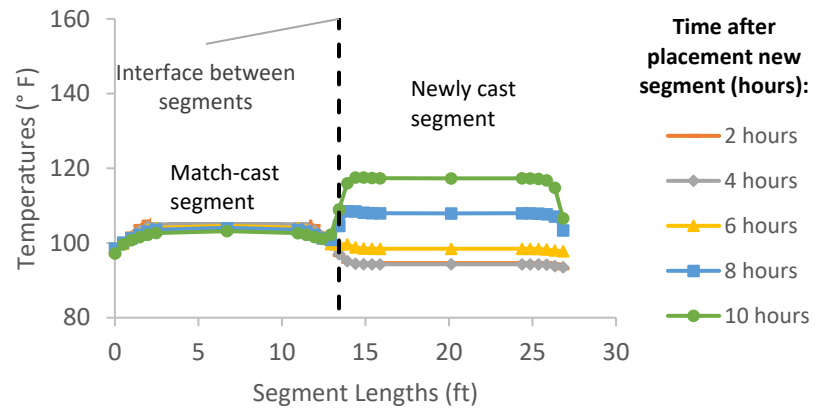

Figure B-108: Simulation 36 - Internal temperatures along the wing of segments

Simulation 37 -Results Summary

Table B-37: Model input parameters simulation 37

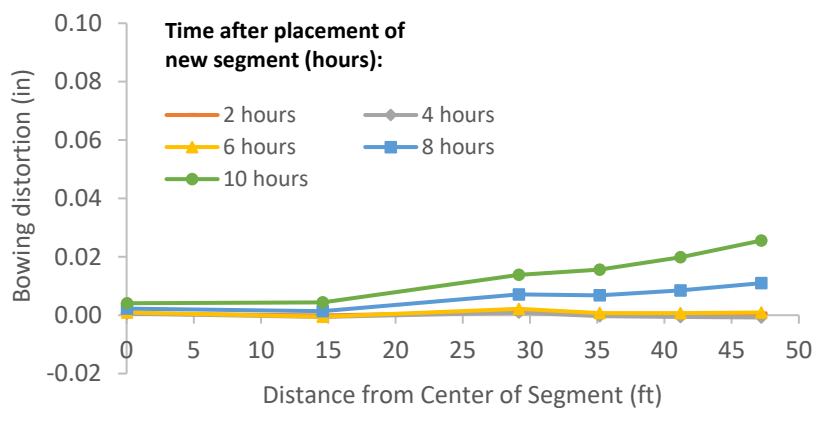| Model details		
Permutation number	37	
Geometry	Florida Bridge E - w/l=4.09	
Max. Mesh Size	2.95	in
Time Step	1	hrs
Placement Temperature	95	°F
Match-cast segment Time of Simulation at Casting	0	hrs
New Segment Time of Simulation at Casting	24	hrs
Concrete Properties		
Cement Content	650.08	lb/yd^3
Activation Energy	26.21	BTU/mol
Heat of Hydration Parameters		
Total Heat Development, $Q_{ult} = \alpha_u \cdot H_u$	107.65	BTU/lb
Time Parameter, τ	18.28	hrs
Curvature Parameter, β	1.65	
Density	3953.252	lb/yd^3
Specific Heat	0.25	BTU/(lb·°F)
Thermal Conductivity	1.810	BTU/(ft·h·°F)
Match-cast segment Elastic Modulus Dev. Parameters		
Final Value	4713.64	ksi
Time Parameter	12.420	hrs
Curvature Parameter	1.068	
New Segment Elastic Modulus Dev. Parameters		
Final Value	14.50	ksi
Time Parameter	n/a	hrs
Curvature Parameter	n/a	
Poisson Ratio	0.17	
Coefficient of Thermal Expansion	6.08	µε/°F
Thermal Boundary Conditions (Applied to Appropriate Faces)		
Ambient Temp	Miami - Summer - Morning - Placement	
Wind	Medium-Wind	7.50	mph
Formwork	Steel Formwork	34.60	BTU/(ft·h·°F)
	Thickness	0.118	in
Curing	Burlap	0.18	BTU/(ft·h·°F)
	Thickness	0.39	in

Figure B-109: Simulation 37 - Bowing distortion of match-cast segment after placement of the new segment
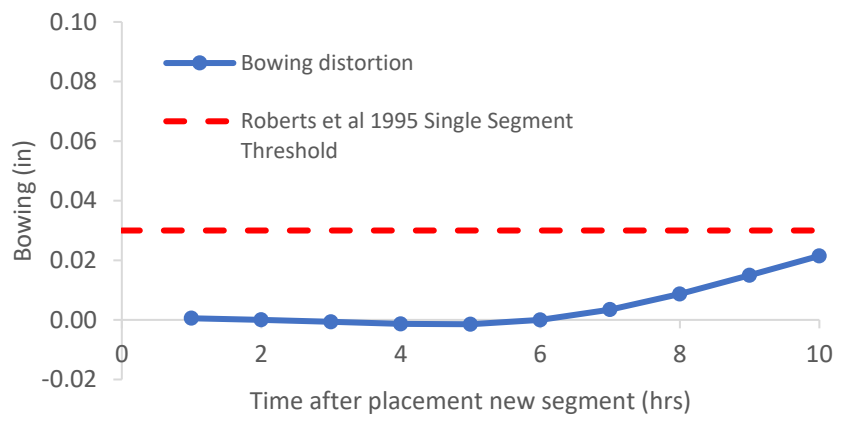

Figure B-110: Simulation 37 - Bowing distortion progression of match-cast segment from time of placement of new segment to 10 hours
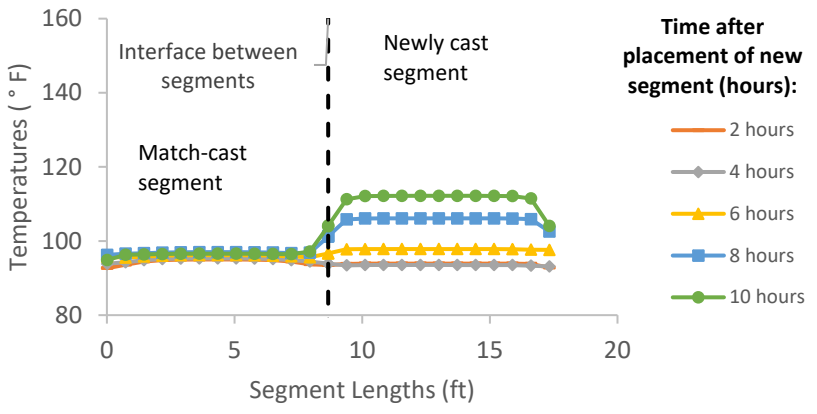

Figure B-111: Simulation 37 - Internal temperatures along the wing of segments

Simulation 38 -Results Summary

Table B-38: Model input parameters simulation 38

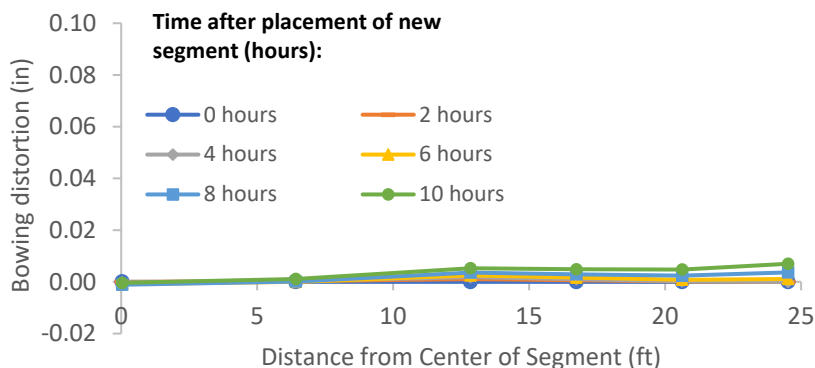| Model details		
Permutation number	38	
Geometry	Florida Bridge B - w/l=5.97	
Max. Mesh Size	3.94	in
Time Step	1	hrs
Placement Temperature	95	°F
Match-cast segment Time of Simulation at Casting	0	hrs
New Segment Time of Simulation at Casting	24	hrs
Concrete Properties		
Cement Content	650.08	lb/yd^3
Activation Energy	26.21	BTU/mol
Heat of Hydration Parameters		
Total Heat Development, $Q_{ult} = \alpha_u \cdot H_u$	107.65	BTU/lb
Time Parameter, τ	18.28	hrs
Curvature Parameter, β	1.65	
Density	3953.252	lb/yd^3
Specific Heat	0.25	BTU/(lb·°F)
Thermal Conductivity	1.810	BTU/(ft·h·°F)
Match-cast segment Elastic Modulus Dev. Parameters		
Final Value	4713.64	ksi
Time Parameter	12.420	hrs
Curvature Parameter	1.068	
New Segment Elastic Modulus Dev. Parameters		
Final Value	14.50	ksi
Time Parameter	n/a	hrs
Curvature Parameter	n/a	
Poisson Ratio	0.17	
Coefficient of Thermal Expansion	6.08	µε/°F
Thermal Boundary Conditions (Applied to Appropriate Faces)		
Ambient Temp	Miami - Summer - Morning - Placement	
Wind	Medium-Wind	7.50	mph
Formwork	Steel Formwork	34.60	BTU/(ft·h·°F)
	Thickness	0.118	in
Curing	Burlap	0.18	BTU/(ft·h·°F)
	Thickness	0.39	in

Figure B-112: Simulation 38 - Bowing distortion of match-cast segment after placement of the new segment

Figure B-113: Simulation 38 - Bowing distortion progression of match-cast segment from time of placement of new segment to 10 hours
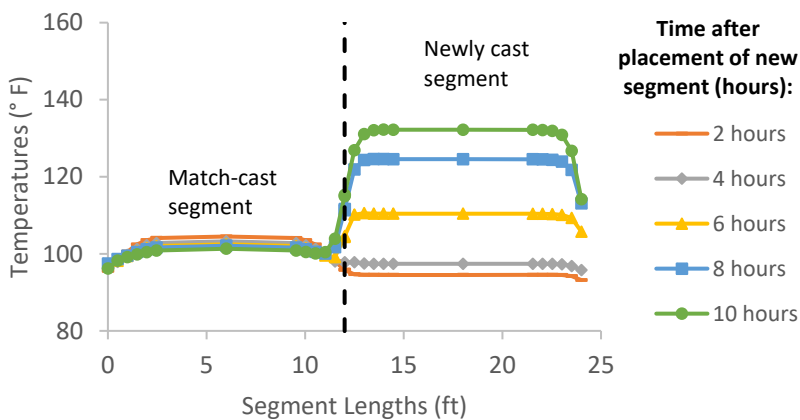

Figure B-114: Simulation 38 - Internal temperatures along the wing of segments

Simulation 39 -Results Summary

Table B-39: Model input parameters simulation 39

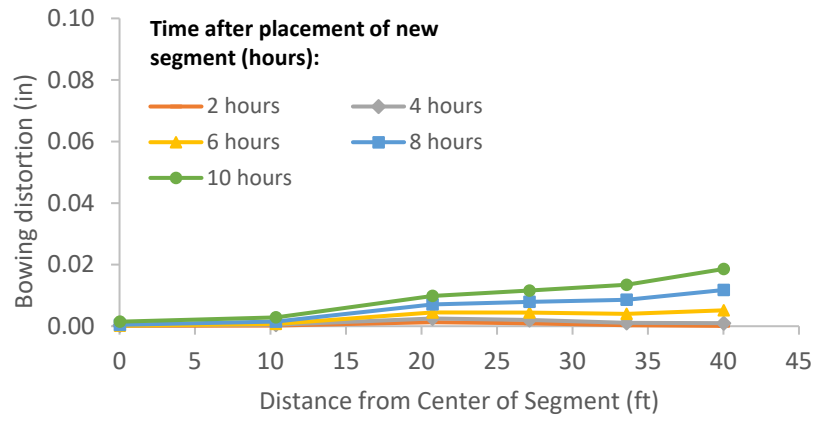| Model details		
Permutation number	39	
Geometry	Florida Bridge C - w/l=10.89	
Max. Mesh Size	3.54	in
Time Step	1	hrs
Placement Temperature	95	°F
Match-cast segment Time of Simulation at Casting	0	hrs
New Segment Time of Simulation at Casting	24	hrs
Concrete Properties		
Cement Content	650.08	lb/yd^3
Activation Energy	26.21	BTU/mol
Heat of Hydration Parameters		
Total Heat Development, $Q_{ult} = \alpha_u \cdot H_u$	107.65	BTU/lb
Time Parameter, τ	18.28	hrs
Curvature Parameter, β	1.65	
Density	3953.252	lb/yd^3
Specific Heat	0.25	BTU/(lb·°F)
Thermal Conductivity	1.810	BTU/(ft·h·°F)
Match-cast segment Elastic Modulus Dev. Parameters		
Final Value	4713.64	ksi
Time Parameter	12.420	hrs
Curvature Parameter	1.068	
New Segment Elastic Modulus Dev. Parameters		
Final Value	14.50	ksi
Time Parameter	n/a	hrs
Curvature Parameter	n/a	
Poisson Ratio	0.17	
Coefficient of Thermal Expansion	6.08	με/°F
Thermal Boundary Conditions (Applied to Appropriate Faces)		
Ambient Temp	Miami - Summer - Morning - Placement	
Wind	Medium-Wind	7.50	mph
Formwork	Steel Formwork	34.60	BTU/(ft·h·°F)
	Thickness	0.118	in
Curing	Burlap	0.18	BTU/(ft·h·°F)
	Thickness	0.39	in

Figure B-115: Simulation 39 - Bowing distortion of match-cast segment after placement of the new segment
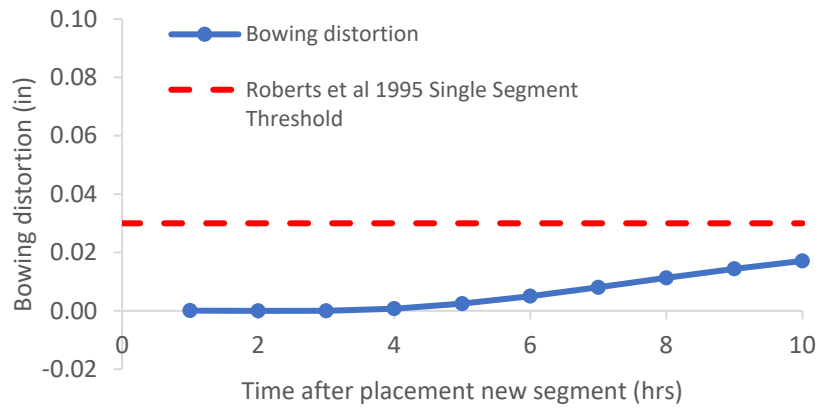

Figure B-116: Simulation 39 - Bowing distortion progression of match-cast segment from time of placement of new segment to 10 hours
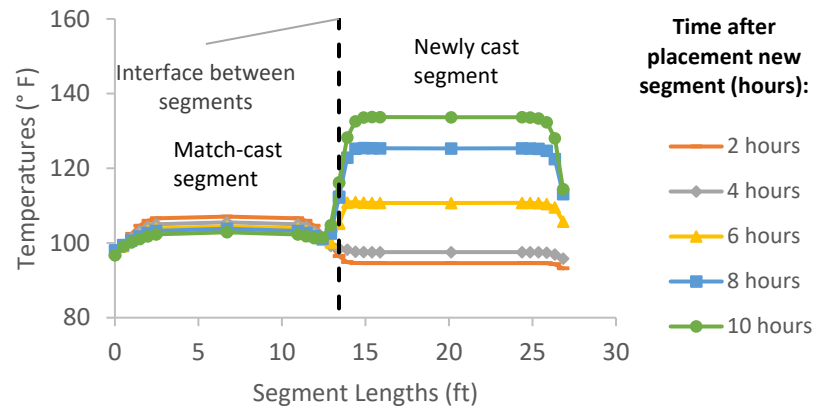

Figure B-117: Simulation 39 - Internal temperatures along the wing of segments

Simulation 40 -Results Summary

Table B-40: Model input parameters simulation 40

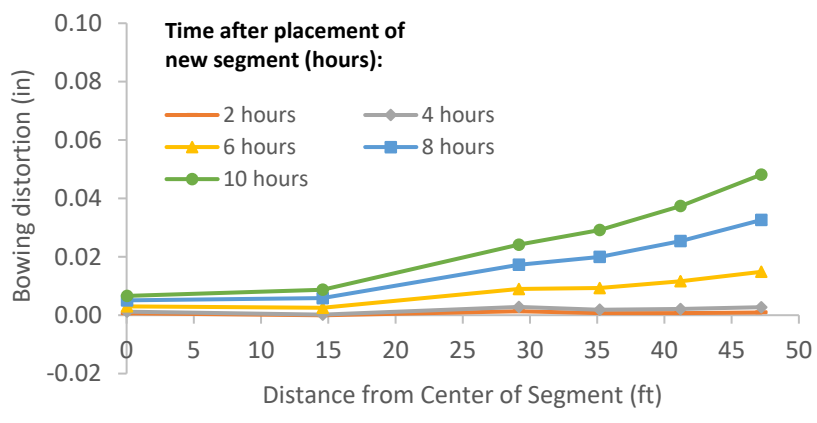| Model details		
Permutation number	40	
Geometry	Florida Bridge E - w/l=4.09	
Max. Mesh Size	2.95	in
Time Step	1	hrs
Placement Temperature	95	°F
Match-cast segment Time of Simulation at Casting	0	hrs
New Segment Time of Simulation at Casting	24	hrs
Concrete Properties		
Cement Content	750.09	lb/yd³
Activation Energy	24.13	BTU/mol
Heat of Hydration Parameters		
Total Heat Development, $Q_{ult} = \alpha_u \cdot H_u$	111.33	BTU/lb
Time Parameter, τ	13.36	hrs
Curvature Parameter, β	1.49	
Density	3934.937	lb/yd³
Specific Heat	0.26	BTU/(lb·°F)
Thermal Conductivity	1.759	BTU/(ft·h·°F)
Match-cast segment Elastic Modulus Dev. Parameters		
Final Value	4680.92	ksi
Time Parameter	12.420	hrs
Curvature Parameter	1.068	
New Segment Elastic Modulus Dev. Parameters		
Final Value	14.50	ksi
Time Parameter	n/a	hrs
Curvature Parameter	n/a	
Poisson Ratio	0.17	
Coefficient of Thermal Expansion	6.08	με/°F
Thermal Boundary Conditions (Applied to Appropriate Faces)		
Ambient Temp	Miami - Summer - Morning - Placement	
Wind	Medium-Wind	7.50	mph
Formwork	Steel Formwork	34.60	BTU/(ft·h·°F)
	Thickness	0.118	in
Curing	Burlap	0.18	BTU/(ft·h·°F)
	Thickness	0.39	in

Figure B-118: Simulation 40 - Bowing distortion of match-cast segment after placement of the new segment
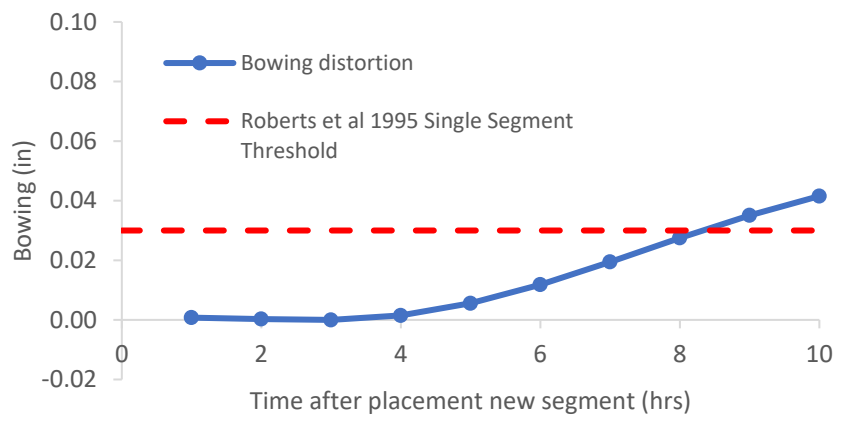

Figure B-119: Simulation 40 - Bowing distortion progression of match-cast segment from time of placement of new segment to 10 hours
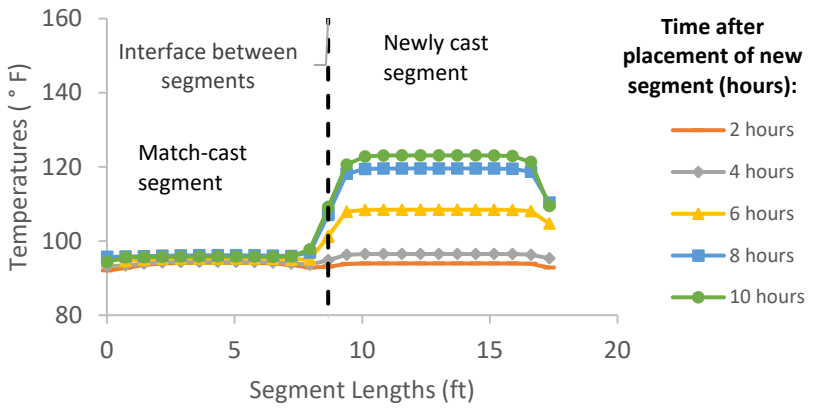

Figure B-120: Simulation 40 - Internal temperatures along the wing of segments

Simulation 41 -Results Summary

Table B-41: Model input parameters simulation 41

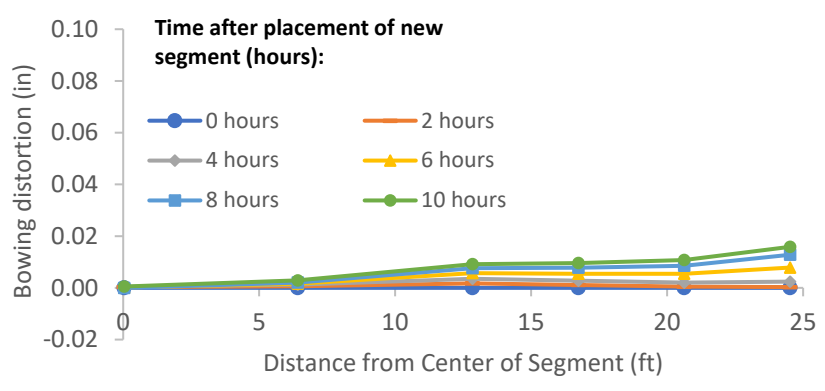| Model details		
Permutation number	41	
Geometry	Florida Bridge B - w/l=5.97	
Max. Mesh Size	3.94	in
Time Step	1	hrs
Placement Temperature	95	°F
Match-cast segment Time of Simulation at Casting	0	hrs
New Segment Time of Simulation at Casting	24	hrs
Concrete Properties		
Cement Content	750.09	lb/yd³
Activation Energy	24.13	BTU/mol
Heat of Hydration Parameters		
Total Heat Development, $Q_{ult} = \alpha_u \cdot H_u$	111.33	BTU/lb
Time Parameter, τ	13.36	hrs
Curvature Parameter, β	1.49	
Density	3934.937	lb/yd³
Specific Heat	0.26	BTU/(lb·°F)
Thermal Conductivity	1.759	BTU/(ft·h·°F)
Match-cast segment Elastic Modulus Dev. Parameters		
Final Value	4680.92	ksi
Time Parameter	12.420	hrs
Curvature Parameter	1.068	
New Segment Elastic Modulus Dev. Parameters		
Final Value	14.50	ksi
Time Parameter	n/a	hrs
Curvature Parameter	n/a	
Poisson Ratio	0.17	
Coefficient of Thermal Expansion	6.08	µε/°F
Thermal Boundary Conditions (Applied to Appropriate Faces)		
Ambient Temp	Miami - Summer - Morning - Placement	
Wind	Medium-Wind	7.50	mph
Formwork	Steel Formwork	34.60	BTU/(ft·h·°F)
	Thickness	0.118	in
Curing	Burlap	0.18	BTU/(ft·h·°F)
	Thickness	0.39	in

Figure B-121: Simulation 41 - Bowing distortion of match-cast segment after placement of the new segment
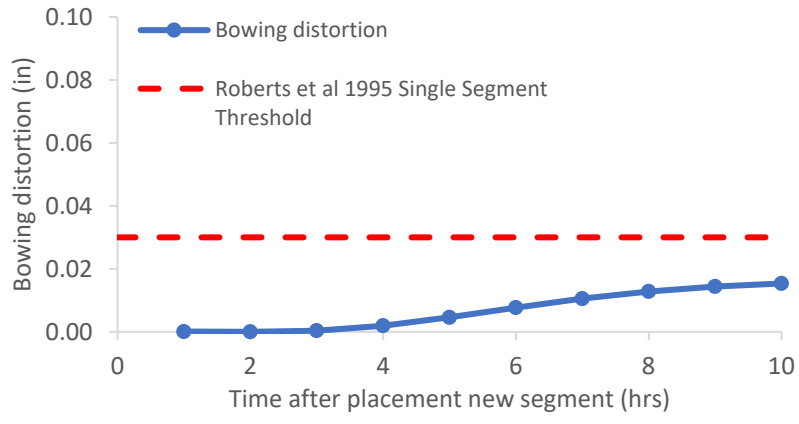

Figure B-122: Simulation 41 - Bowing distortion progression of match-cast segment from time of placement of new segment to 10 hours
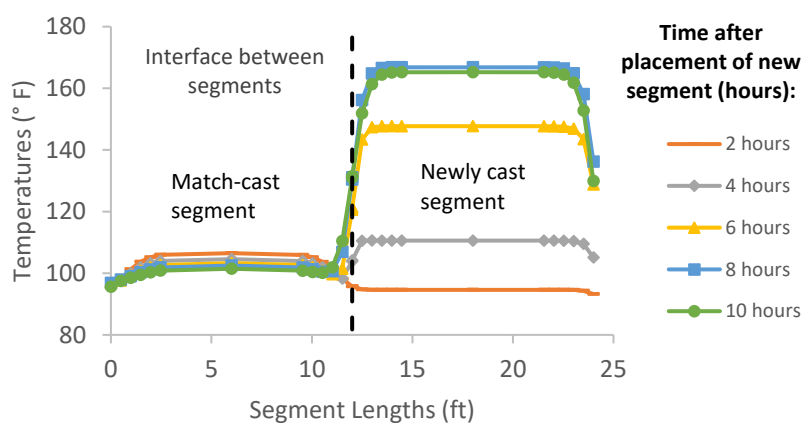

Figure B-123: Simulation 41 - Internal temperatures along the wing of segments

Simulation 42 -Results Summary

Table B-42: Model input parameters simulation 42

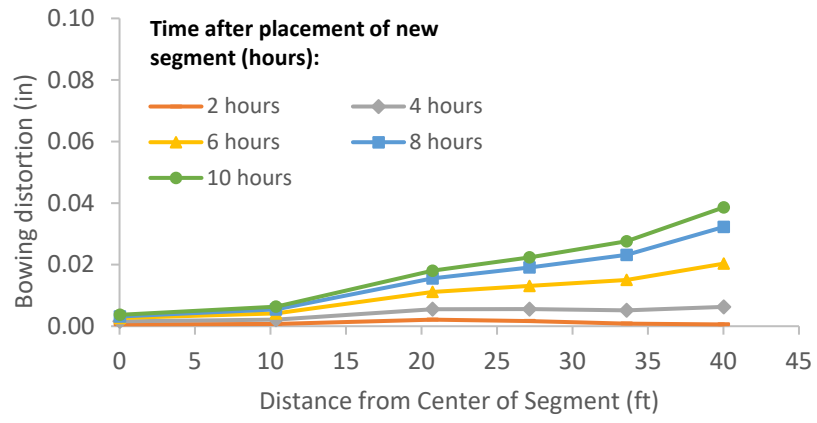| Model details		
Permutation number	42	
Geometry	Florida Bridge C - w/l=10.89	
Max. Mesh Size	3.54	in
Time Step	1	hrs
Placement Temperature	95	°F
Match-cast segment Time of Simulation at Casting	0	hrs
New Segment Time of Simulation at Casting	24	hrs
Concrete Properties		
Cement Content	750.09	lb/yd^3
Activation Energy	24.13	BTU/mol
Heat of Hydration Parameters		
Total Heat Development, $Q_{ult} = \alpha_u \cdot H_u$	111.33	BTU/lb
Time Parameter, τ	13.36	hrs
Curvature Parameter, β	1.49	
Density	3934.937	lb/yd^3
Specific Heat	0.26	BTU/(lb·°F)
Thermal Conductivity	1.759	BTU/(ft·h·°F)
Match-cast segment Elastic Modulus Dev. Parameters		
Final Value	4680.92	ksi
Time Parameter	12.420	hrs
Curvature Parameter	1.068	
New Segment Elastic Modulus Dev. Parameters		
Final Value	14.50	ksi
Time Parameter	n/a	hrs
Curvature Parameter	n/a	
Poisson Ratio	0.17	
Coefficient of Thermal Expansion	6.08	µε/°F
Thermal Boundary Conditions (Applied to Appropriate Faces)		
Ambient Temp	Miami - Summer - Morning - Placement	
Wind	Medium-Wind	7.50	mph
Formwork	Steel Formwork	34.60	BTU/(ft·h·°F)
	Thickness	0.118	in
Curing	Burlap	0.18	BTU/(ft·h·°F)
	Thickness	0.39	in

Figure B-124: Simulation 42 - Bowing distortion of match-cast segment after placement of the new segment
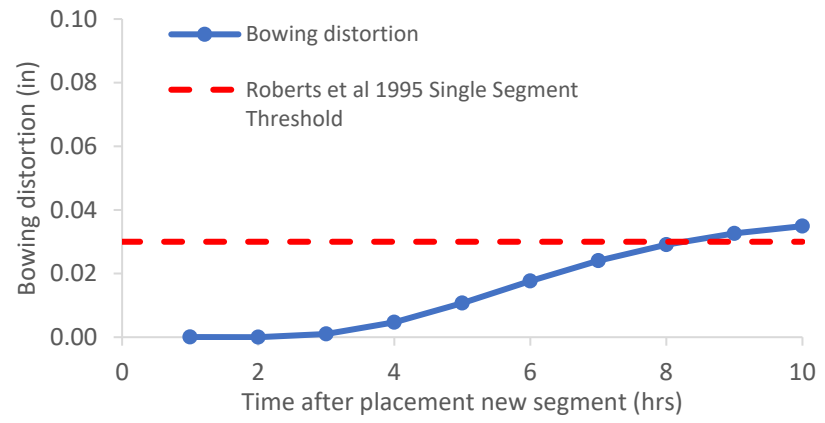

Figure B-125: Simulation 42 - Bowing distortion progression of match-cast segment from time of placement of new segment to 10 hours
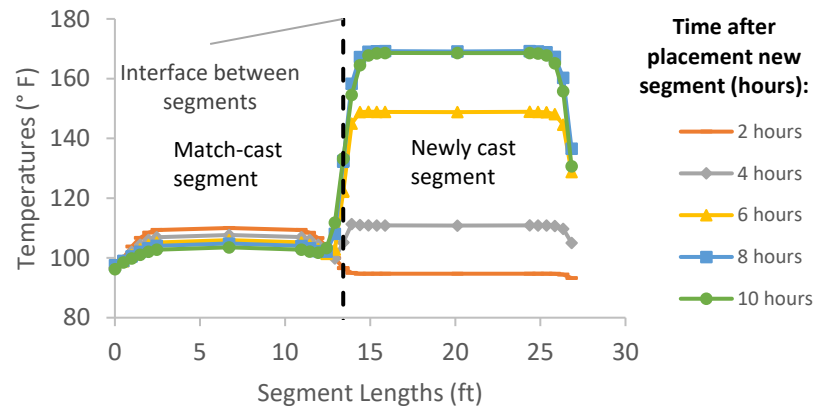

Figure B-126: Simulation 42 - Internal temperatures along the wing of segments

Simulation 43 -Results Summary

Table B-43: Model input parameters simulation 43

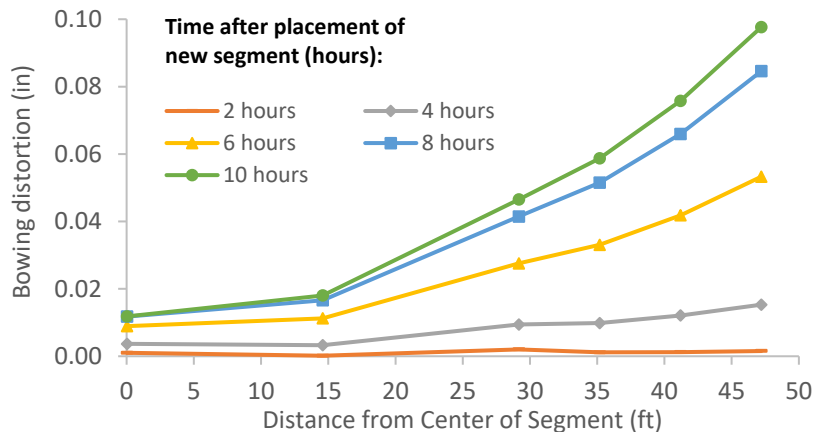| Model details		
Permutation number	43	
Geometry	Florida Bridge E - w/l=4.09	
Max. Mesh Size	2.95	in
Time Step	1	hrs
Placement Temperature	95	°F
Match-cast segment Time of Simulation at Casting	0	hrs
New Segment Time of Simulation at Casting	24	hrs
Concrete Properties		
Cement Content	950.11	lb/yd³
Activation Energy	28.43	BTU/mol
Heat of Hydration Parameters		
Total Heat Development, $Q_{ult} = \alpha_u \cdot H_u$	124.95	BTU/lb
Time Parameter, τ	10.50	hrs
Curvature Parameter, β	1.60	
Density	3999.308	lb/yd³
Specific Heat	0.27	BTU/(lb·°F)
Thermal Conductivity	1.705	BTU/(ft·h·°F)
Match-cast segment Elastic Modulus Dev. Parameters		
Final Value	4796.26	ksi
Time Parameter	12.420	hrs
Curvature Parameter	1.068	
New Segment Elastic Modulus Dev. Parameters		
Final Value	14.50	ksi
Time Parameter	n/a	hrs
Curvature Parameter	n/a	
Poisson Ratio	0.17	
Coefficient of Thermal Expansion	6.07	με/°F
Thermal Boundary Conditions (Applied to Appropriate Faces)		
Ambient Temp	Miami - Summer - Morning - Placement	
Wind	Medium-Wind	7.50	mph
Formwork	Steel Formwork	34.60	BTU/(ft·h·°F)
	Thickness	0.118	in
Curing	Burlap	0.18	BTU/(ft·h·°F)
	Thickness	0.39	in

Figure B-127: Simulation 43 - Bowing distortion of match-cast segment after placement of the new segment
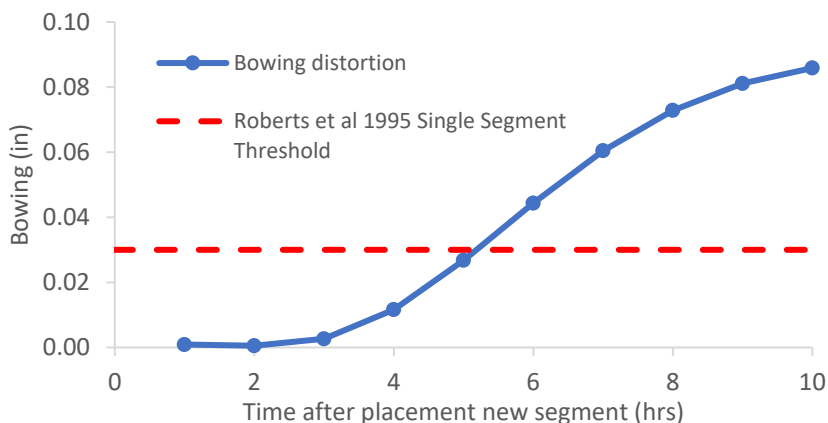

Figure B-128: Simulation 43 - Bowing distortion progression of match-cast segment from time of placement of new segment to 10 hours
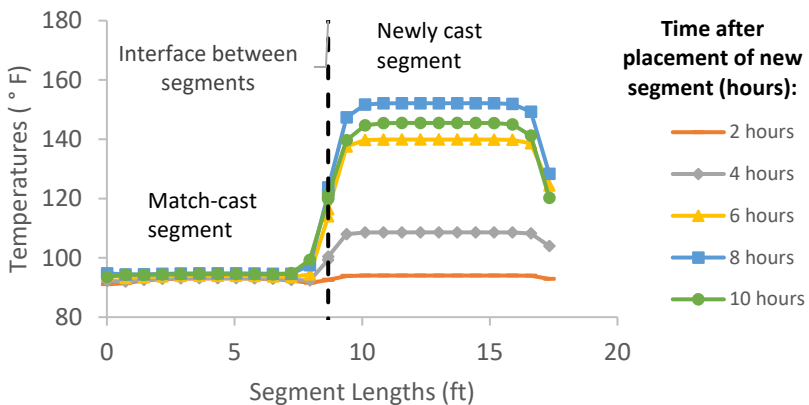

Figure B-129: Simulation 43 - Internal temperatures along the wing of segments

Simulation 44 -Results Summary

Table B-44: Model input parameters simulation 44

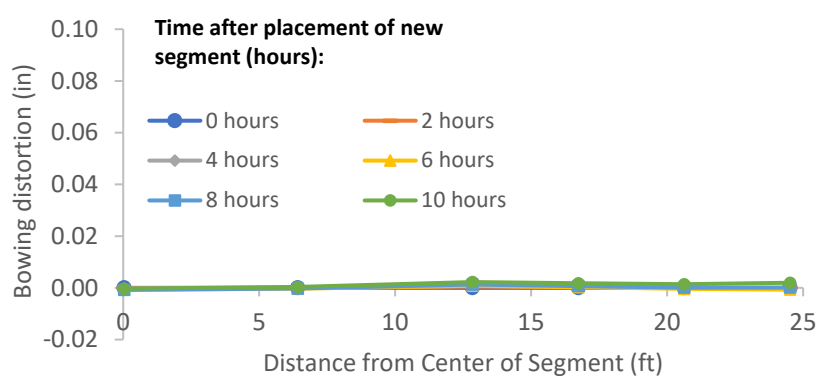| Model details		
Permutation number	44	
Geometry	Florida Bridge B - w/l=5.97	
Max. Mesh Size	3.94	in
Time Step	1	hrs
Placement Temperature	95	°F
Match-cast segment Time of Simulation at Casting	0	hrs
New Segment Time of Simulation at Casting	24	hrs
Concrete Properties		
Cement Content	950.11	lb/yd^3
Activation Energy	28.43	BTU/mol
Heat of Hydration Parameters		
Total Heat Development, $Q_{ult} = \alpha_u \cdot H_u$	124.95	BTU/lb
Time Parameter, τ	10.50	hrs
Curvature Parameter, β	1.60	
Density	3999.308	lb/yd^3
Specific Heat	0.27	BTU/(lb·°F)
Thermal Conductivity	1.705	BTU/(ft·h·°F)
Match-cast segment Elastic Modulus Dev. Parameters		
Final Value	4796.26	ksi
Time Parameter	12.420	hrs
Curvature Parameter	1.068	
New Segment Elastic Modulus Dev. Parameters		
Final Value	14.50	ksi
Time Parameter	n/a	hrs
Curvature Parameter	n/a	
Poisson Ratio	0.17	
Coefficient of Thermal Expansion	6.07	με/°F
Thermal Boundary Conditions (Applied to Appropriate Faces)		
Ambient Temp	Miami - Summer - Morning - Placement	
Wind	Medium-Wind	7.50	mph
Formwork	Steel Formwork	34.60	BTU/(ft·h·°F)
	Thickness	0.118	in
Curing	Burlap	0.18	BTU/(ft·h·°F)
	Thickness	0.39	in

Figure B-130: Simulation 44 - Bowing distortion of match-cast segment after placement of the new segment
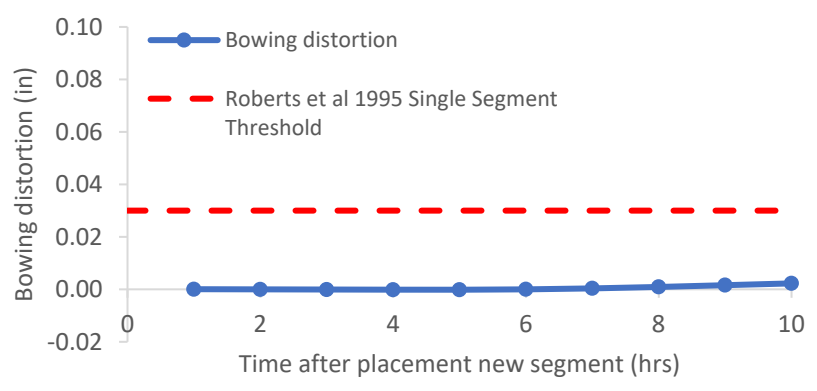

Figure B-131: Simulation 44 - Bowing distortion progression of match-cast segment from time of placement of new segment to 10 hours
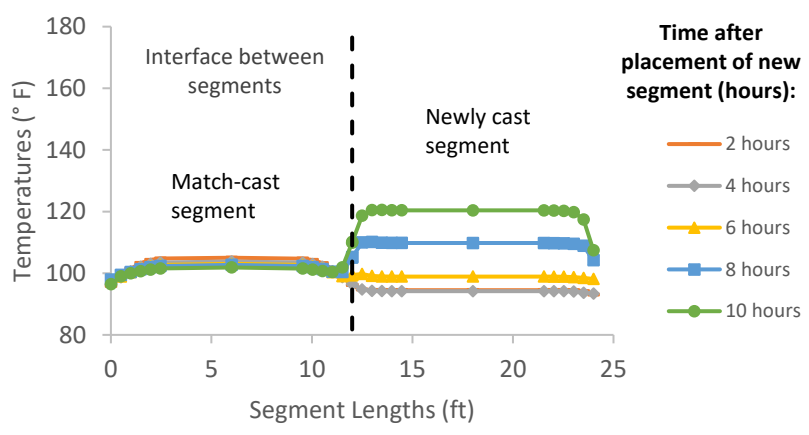

Figure B-132: Simulation 44 - Internal temperatures along the wing of segments

Simulation 45 -Results Summary

Table B-45: Model input parameters simulation 45

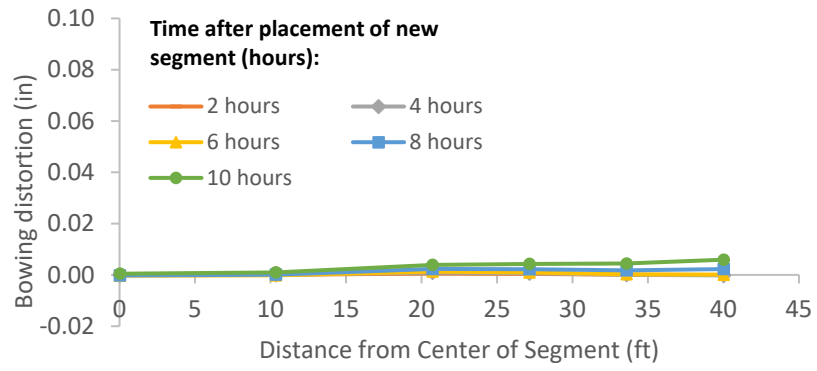| Model details		
Permutation number	45	
Geometry	Florida Bridge C - w/l=10.89	
Max. Mesh Size	3.54	in
Time Step	1	hrs
Placement Temperature	95	°F
Match-cast segment Time of Simulation at Casting	0	hrs
New Segment Time of Simulation at Casting	24	hrs
Concrete Properties		
Cement Content	950.11	lb/yd^3
Activation Energy	28.43	BTU/mol
Heat of Hydration Parameters		
Total Heat Development, $Q_{ult} = \alpha_u \cdot H_u$	124.95	BTU/lb
Time Parameter, τ	10.50	hrs
Curvature Parameter, β	1.60	
Density	3999.308	lb/yd^3
Specific Heat	0.27	BTU/(lb·°F)
Thermal Conductivity	1.705	BTU/(ft·h·°F)
Match-cast segment Elastic Modulus Dev. Parameters		
Final Value	4796.26	ksi
Time Parameter	12.420	hrs
Curvature Parameter	1.068	
New Segment Elastic Modulus Dev. Parameters		
Final Value	14.50	ksi
Time Parameter	n/a	hrs
Curvature Parameter	n/a	
Poisson Ratio	0.17	
Coefficient of Thermal Expansion	6.07	με/°F
Thermal Boundary Conditions (Applied to Appropriate Faces)		
Ambient Temp	Miami - Summer - Morning - Placement	
Wind	Medium-Wind	7.50	mph
Formwork	Steel Formwork	34.60	BTU/(ft·h·°F)
	Thickness	0.118	in
Curing	Burlap	0.18	BTU/(ft·h·°F)
	Thickness	0.39	in

Figure B-133: Simulation 45 - Bowing distortion of match-cast segment after placement of the new segment
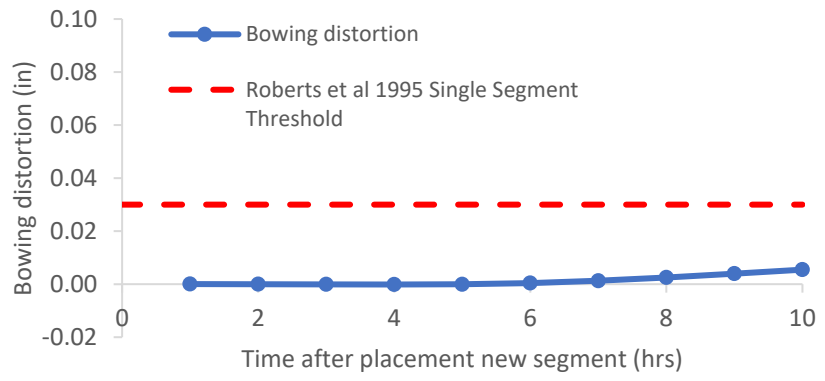

Figure B-134: Simulation 45 - Bowing distortion progression of match-cast segment from time of placement of new segment to 10 hours
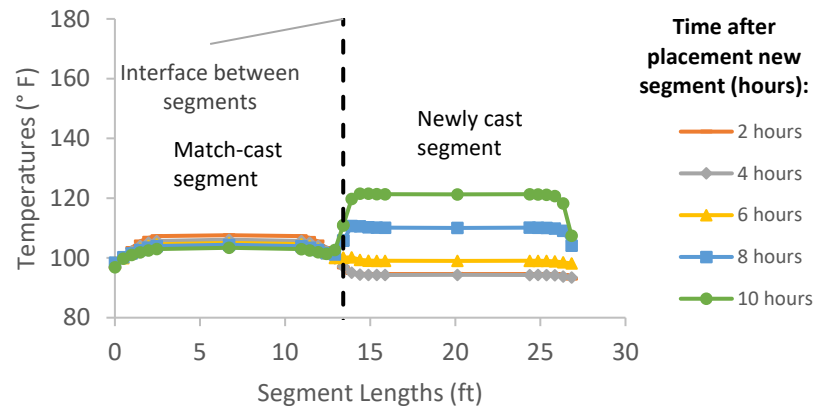

Figure B-135: Simulation 45 - Internal temperatures along the wing of segments

Simulation 46 -Results Summary

Table B-46: Model input parameters simulation 46

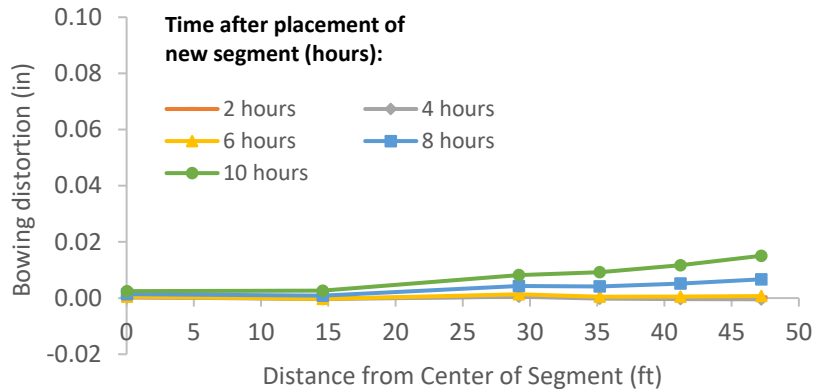| Model details		
Permutation number	46	
Geometry	Florida Bridge E - w/l=4.09	
Max. Mesh Size	2.95	in
Time Step	1	hrs
Placement Temperature	95	°F
Match-cast segment Time of Simulation at Casting	0	hrs
New Segment Time of Simulation at Casting	24	hrs
Concrete Properties		
Cement Content	650.08	lb/yd^3
Activation Energy	26.21	BTU/mol
Heat of Hydration Parameters		
Total Heat Development, $Q_{ult} = \alpha_u \cdot H_u$	107.65	BTU/lb
Time Parameter, τ	18.28	hrs
Curvature Parameter, β	1.65	
Density	3724.899	lb/yd^3
Specific Heat	0.23	BTU/(lb·°F)
Thermal Conductivity	1.419	BTU/(ft·h·°F)
Match-cast segment Elastic Modulus Dev. Parameters		
Final Value	4311.19	ksi
Time Parameter	12.420	hrs
Curvature Parameter	1.068	
New Segment Elastic Modulus Dev. Parameters		
Final Value	14.50	ksi
Time Parameter	n/a	hrs
Curvature Parameter	n/a	
Poisson Ratio	0.17	
Coefficient of Thermal Expansion	3.12	με/°F
Thermal Boundary Conditions (Applied to Appropriate Faces)		
Ambient Temp	Miami - Summer - Morning - Placement		
Wind	Medium-Wind	7.50	mph
Formwork	Steel Formwork	34.60	BTU/(ft·h·°F)
	Thickness	0.118	in
Curing	Burlap	0.18	BTU/(ft·h·°F)
	Thickness	0.39	in

Figure B-136: Simulation 46 - Bowing distortion of match-cast segment after placement of the new segment
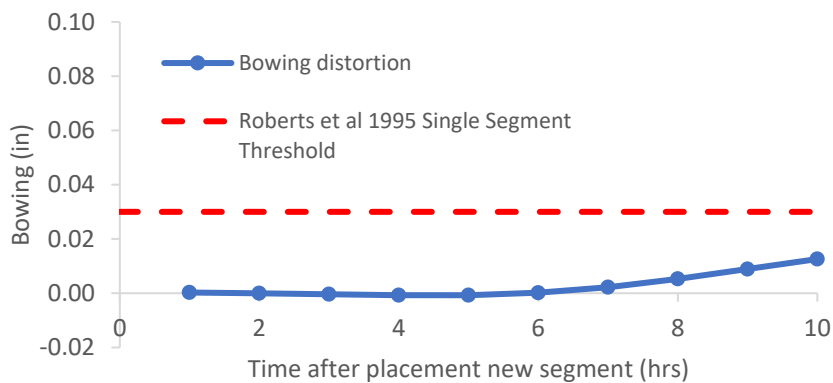

Figure B-137: Simulation 46 - Bowing distortion progression of match-cast segment from time of placement of new segment to 10 hours
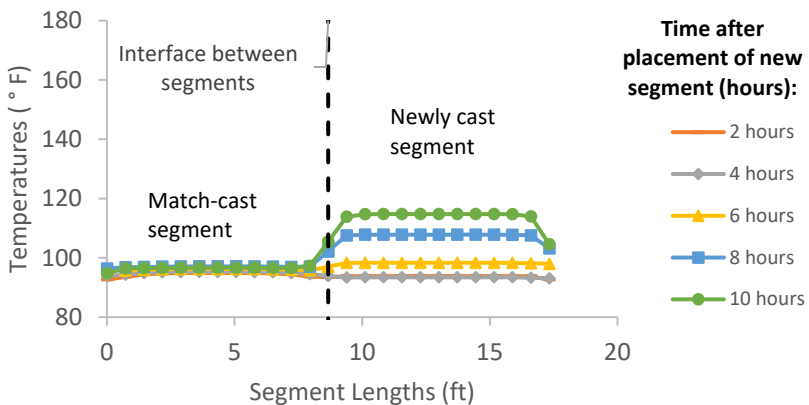

Figure B-138: Simulation 46 - Internal temperatures along the wing of segments

Simulation 47 -Results Summary

Table B-47: Model input parameters simulation 47

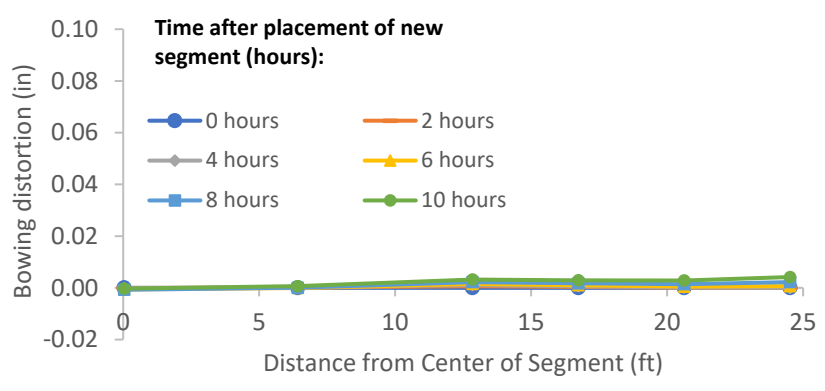| Model details		
Permutation number	47	
Geometry	Florida Bridge B - w/l=5.97	
Max. Mesh Size	3.94	in
Time Step	1	hrs
Placement Temperature	95	°F
Match-cast segment Time of Simulation at Casting	0	hrs
New Segment Time of Simulation at Casting	24	hrs
Concrete Properties		
Cement Content	650.08	lb/yd³
Activation Energy	26.21	BTU/mol
Heat of Hydration Parameters		
Total Heat Development, $Q_{ult} = \alpha_u \cdot H_u$	107.65	BTU/lb
Time Parameter, τ	18.28	hrs
Curvature Parameter, β	1.65	
Density	3724.899	lb/yd³
Specific Heat	0.23	BTU/(lb·°F)
Thermal Conductivity	1.419	BTU/(ft·h·°F)
Match-cast segment Elastic Modulus Dev. Parameters		
Final Value	4311.19	ksi
Time Parameter	12.420	hrs
Curvature Parameter	1.068	
New Segment Elastic Modulus Dev. Parameters		
Final Value	14.50	ksi
Time Parameter	n/a	hrs
Curvature Parameter	n/a	
Poisson Ratio	0.17	
Coefficient of Thermal Expansion	3.12	µε/°F
Thermal Boundary Conditions (Applied to Appropriate Faces)		
Ambient Temp	Miami - Summer - Morning - Placement	
Wind	Medium-Wind	7.50	mph
Formwork	Steel Formwork	34.60	BTU/(ft·h·°F)
	Thickness	0.118	in
Curing	Burlap	0.18	BTU/(ft·h·°F)
	Thickness	0.39	in

Figure B-139: Simulation 47 - Bowing distortion of match-cast segment after placement of the new segment
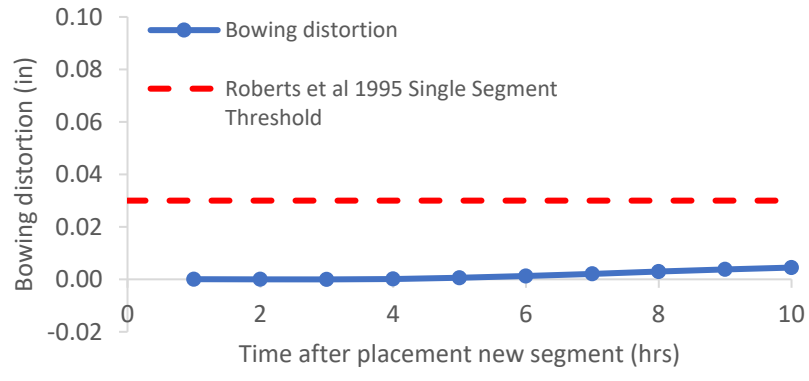

Figure B-140: Simulation 47 - Bowing distortion progression of match-cast segment from time of placement of new segment to 10 hours
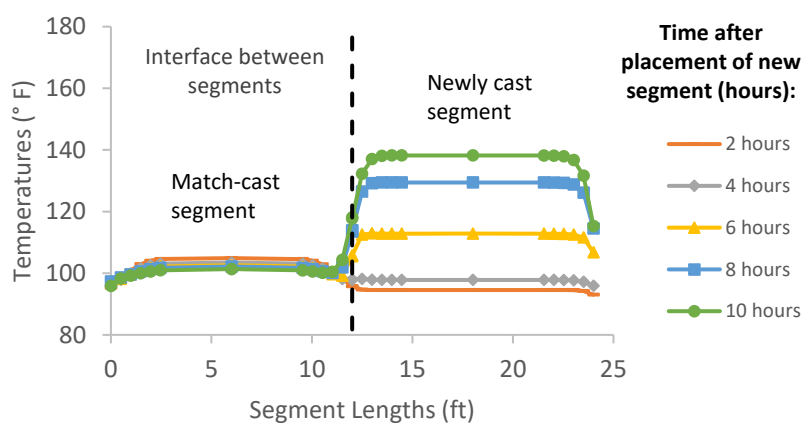

Figure B-141: Simulation 47 - Internal temperatures along the wing of segments

Simulation 48 -Results Summary

Table B-48: Model input parameters simulation 48

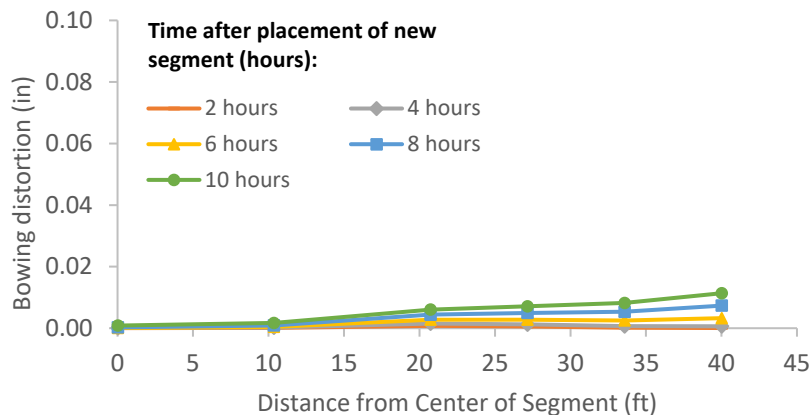| Model details		
Permutation number	48	
Geometry	Florida Bridge C - w/l=10.89	
Max. Mesh Size	3.54	in
Time Step	1	hrs
Placement Temperature	95	°F
Match-cast segment Time of Simulation at Casting	0	hrs
New Segment Time of Simulation at Casting	24	hrs
Concrete Properties		
Cement Content	650.08	lb/yd³
Activation Energy	26.21	BTU/mol
Heat of Hydration Parameters		
Total Heat Development, $Q_{ult} = \alpha_u \cdot H_u$	107.65	BTU/lb
Time Parameter, τ	18.28	hrs
Curvature Parameter, β	1.65	
Density	3724.899	lb/yd³
Specific Heat	0.23	BTU/(lb·°F)
Thermal Conductivity	1.419	BTU/(ft·h·°F)
Match-cast segment Elastic Modulus Dev. Parameters		
Final Value	4311.19	ksi
Time Parameter	12.420	hrs
Curvature Parameter	1.068	
New Segment Elastic Modulus Dev. Parameters		
Final Value	14.50	ksi
Time Parameter	n/a	hrs
Curvature Parameter	n/a	
Poisson Ratio	0.17	
Coefficient of Thermal Expansion	3.12	με/°F
Thermal Boundary Conditions (Applied to Appropriate Faces)		
Ambient Temp	Miami - Summer - Morning - Placement	
Wind	Medium-Wind	7.50	mph
Formwork	Steel Formwork	34.60	BTU/(ft·h·°F)
	Thickness	0.118	in
Curing	Burlap	0.18	BTU/(ft·h·°F)
	Thickness	0.39	in

Figure B-142: Simulation 48 - Bowing distortion of match-cast segment after placement of the new segment
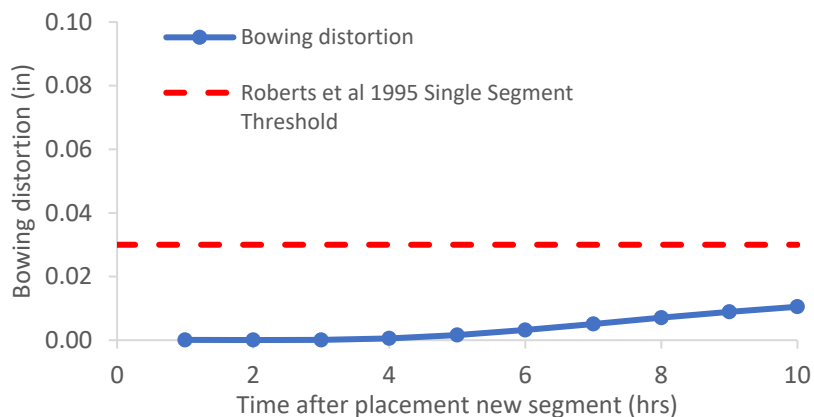

Figure B-143: Simulation 48 - Bowing distortion progression of match-cast segment from time of placement of new segment to 10 hours
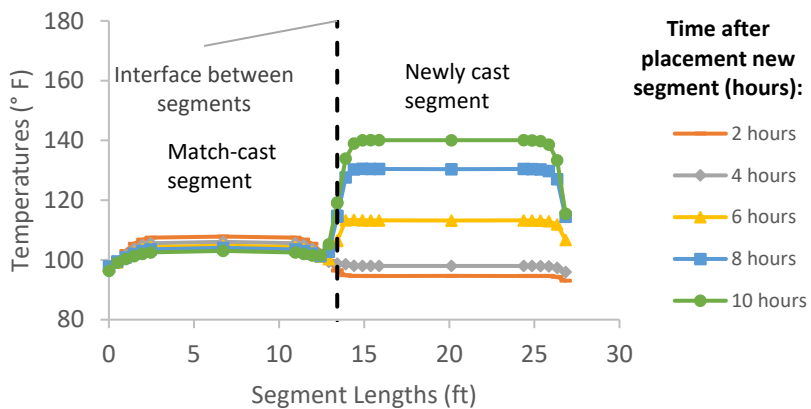

Figure B-144: Simulation 48 - Internal temperatures along the wing of segments

Simulation 49 -Results Summary

Table B-49: Model input parameters simulation 49

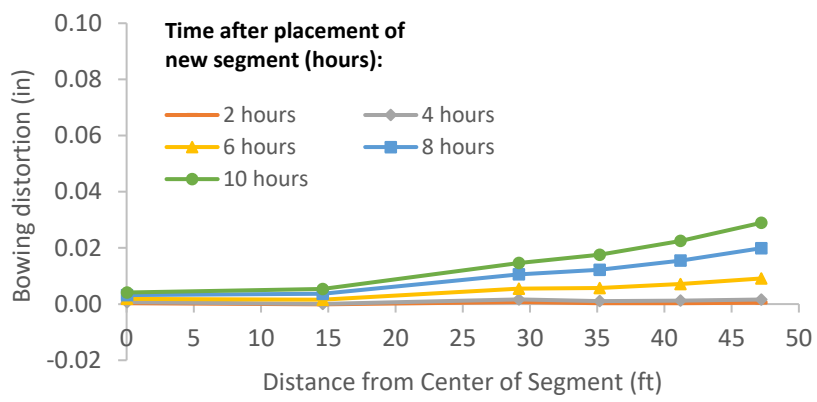| Model details		
Permutation number	49	
Geometry	Florida Bridge E - w/l=4.09	
Max. Mesh Size	2.95	in
Time Step	1	hrs
Placement Temperature	95	°F
Match-cast segment Time of Simulation at Casting	0	hrs
New Segment Time of Simulation at Casting	24	hrs
Concrete Properties		
Cement Content	750.09	lb/yd^3
Activation Energy	24.13	BTU/mol
Heat of Hydration Parameters		
Total Heat Development, $Q_{ult} = \alpha_u \cdot H_u$	111.33	BTU/lb
Time Parameter, τ	13.36	hrs
Curvature Parameter, β	1.49	
Density	3730.970	lb/yd^3
Specific Heat	0.24	BTU/(lb·°F)
Thermal Conductivity	1.375	BTU/(ft·h·°F)
Match-cast segment Elastic Modulus Dev. Parameters		
Final Value	4321.73	ksi
Time Parameter	12.420	hrs
Curvature Parameter	1.068	
New Segment Elastic Modulus Dev. Parameters		
Final Value	14.50	ksi
Time Parameter	n/a	hrs
Curvature Parameter	n/a	
Poisson Ratio	0.17	
Coefficient of Thermal Expansion	3.30	µε/°F
Thermal Boundary Conditions (Applied to Appropriate Faces)		
Ambient Temp	Miami - Summer - Morning - Placement	
Wind	Medium-Wind	7.50	mph
Formwork	Steel Formwork	34.60	BTU/(ft·h·°F)
	Thickness	0.118	in
Curing	Burlap	0.18	BTU/(ft·h·°F)
	Thickness	0.39	in

Figure B-145: Simulation 49 - Bowing distortion of match-cast segment after placement of the new segment
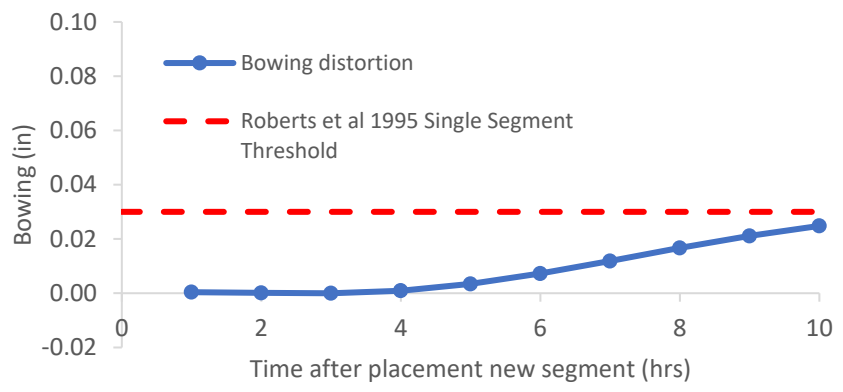

Figure B-146: Simulation 49 - Bowing distortion progression of match-cast segment from time of placement of new segment to 10 hours
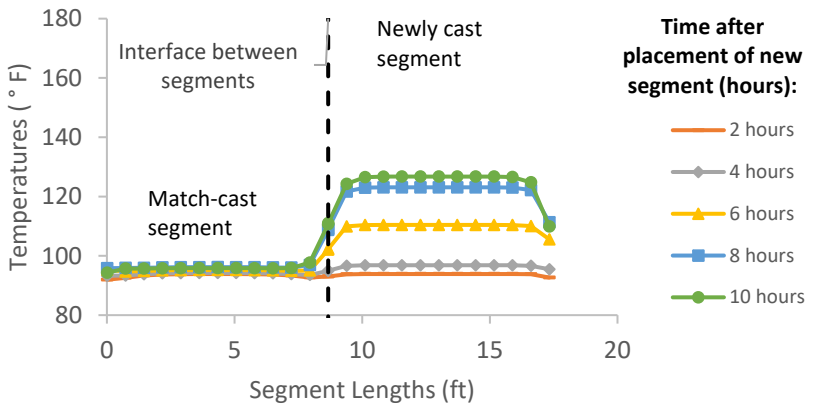

Figure B-147: Simulation 49 - Internal temperatures along the wing of segments

Simulation 50 -Results Summary

Table B-50: Model input parameters simulation 50

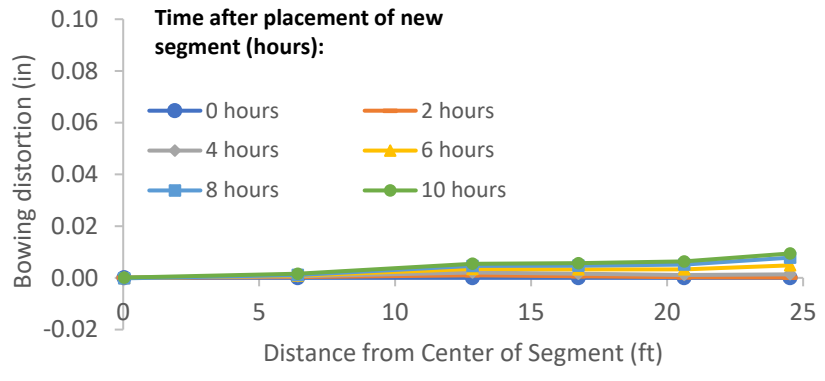| Model details		
Permutation number	50	
Geometry	Florida Bridge B - w/l=5.97	
Max. Mesh Size	3.94	in
Time Step	1	hrs
Placement Temperature	95	°F
Match-cast segment Time of Simulation at Casting	0	hrs
New Segment Time of Simulation at Casting	24	hrs
Concrete Properties		
Cement Content	750.09	lb/yd^3
Activation Energy	24.13	BTU/mol
Heat of Hydration Parameters		
Total Heat Development, $Q_{ult} = \alpha_u \cdot H_u$	111.33	BTU/lb
Time Parameter, τ	13.36	hrs
Curvature Parameter, β	1.49	
Density	3730.970	lb/yd^3
Specific Heat	0.24	BTU/(lb·°F)
Thermal Conductivity	1.375	BTU/(ft·h·°F)
Match-cast segment Elastic Modulus Dev. Parameters		
Final Value	4321.73	ksi
Time Parameter	12.420	hrs
Curvature Parameter	1.068	
New Segment Elastic Modulus Dev. Parameters		
Final Value	14.50	ksi
Time Parameter	n/a	hrs
Curvature Parameter	n/a	
Poisson Ratio	0.17	
Coefficient of Thermal Expansion	3.30	µε/°F
Thermal Boundary Conditions (Applied to Appropriate Faces)		
Ambient Temp	Miami - Summer - Morning - Placement	
Wind	Medium-Wind	7.50	mph
Formwork	Steel Formwork	34.60	BTU/(ft·h·°F)
	Thickness	0.118	in
Curing	Burlap	0.18	BTU/(ft·h·°F)
	Thickness	0.39	in

Figure B-148: Simulation 50 - Bowing distortion of match-cast segment after placement of the new segment
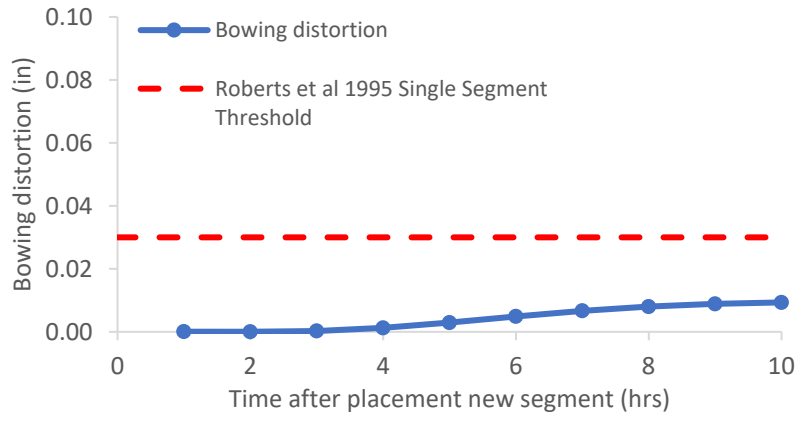

Figure B-149: Simulation 50 - Bowing distortion progression of match-cast segment from time of placement of new segment to 10 hours
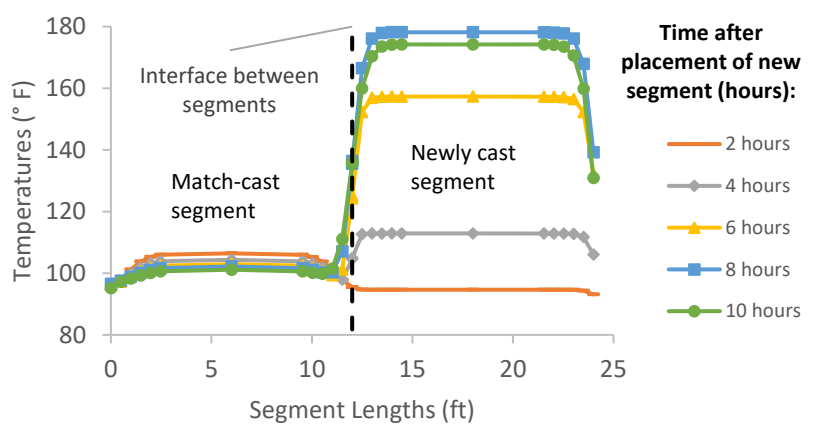

Figure B-150: Simulation 50 - Internal temperatures along the wing of segments

Simulation 51 -Results Summary

Table B-51: Model input parameters simulation 51

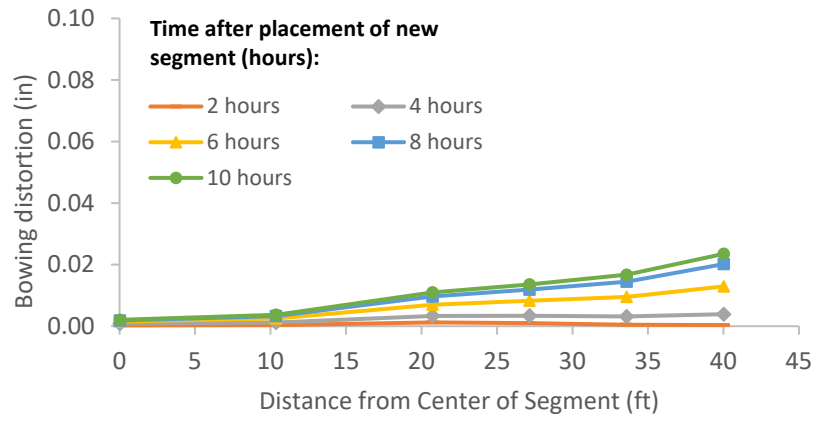| Model details		
Permutation number	51	
Geometry	Florida Bridge C - w/l=10.89	
Max. Mesh Size	3.54	in
Time Step	1	hrs
Placement Temperature	95	°F
Match-cast segment Time of Simulation at Casting	0	hrs
New Segment Time of Simulation at Casting	24	hrs
Concrete Properties		
Cement Content	750.09	lb/yd^3
Activation Energy	24.13	BTU/mol
Heat of Hydration Parameters		
Total Heat Development, $Q_{ult} = \alpha_u \cdot H_u$	111.33	BTU/lb
Time Parameter, τ	13.36	hrs
Curvature Parameter, β	1.49	
Density	3730.970	lb/yd^3
Specific Heat	0.24	BTU/(lb·°F)
Thermal Conductivity	1.375	BTU/(ft·h·°F)
Match-cast segment Elastic Modulus Dev. Parameters		
Final Value	4321.73	ksi
Time Parameter	12.420	hrs
Curvature Parameter	1.068	
New Segment Elastic Modulus Dev. Parameters		
Final Value	14.50	ksi
Time Parameter	n/a	hrs
Curvature Parameter	n/a	
Poisson Ratio	0.17	
Coefficient of Thermal Expansion	3.30	µε/°F
Thermal Boundary Conditions (Applied to Appropriate Faces)		
Ambient Temp	Miami - Summer - Morning - Placement		
Wind	Medium-Wind	7.50	mph
Formwork	Steel Formwork	34.60	BTU/(ft·h·°F)
	Thickness	0.118	in
Curing	Burlap	0.18	BTU/(ft·h·°F)
	Thickness	0.39	in

Figure B-151: Simulation 51 - Bowing distortion of match-cast segment after placement of the new segment
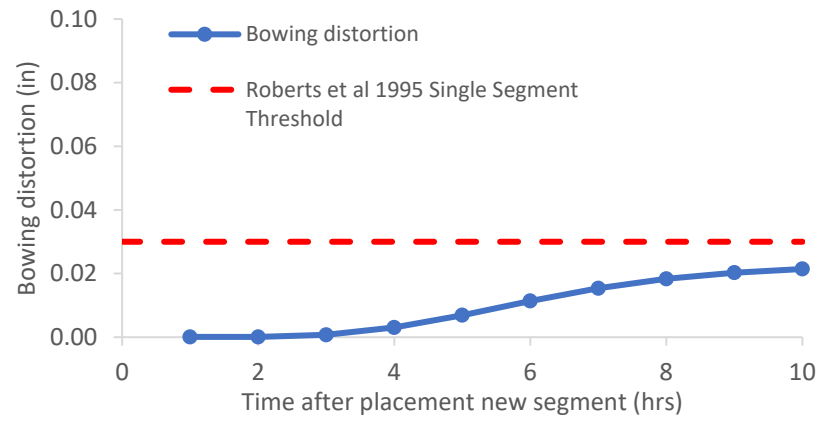

Figure B-152: Simulation 51 - Bowing distortion progression of match-cast segment from time of placement of new segment to 10 hours
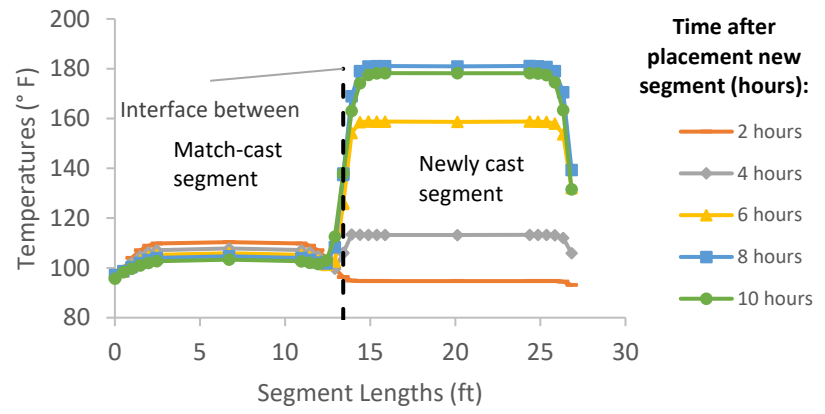

Figure B-153: Simulation 51 - Internal temperatures along the wing of segments

Simulation 52 -Results Summary

Table B-52: Model input parameters simulation 52

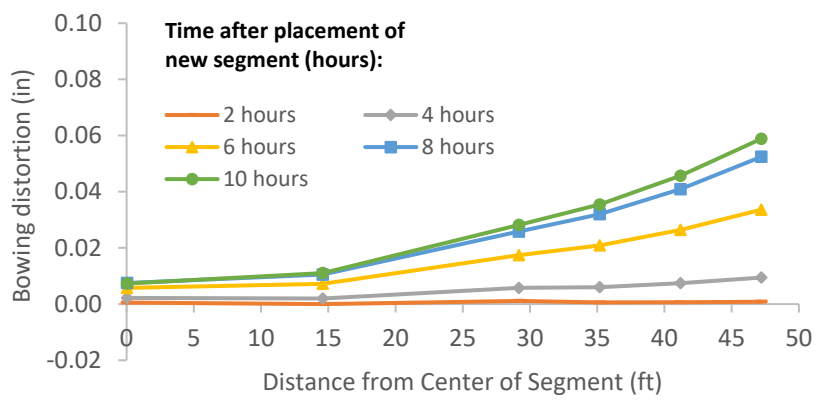| Model details		
Permutation number	52	
Geometry	Florida Bridge E - w/l=4.09	
Max. Mesh Size	2.95	in
Time Step	1	hrs
Placement Temperature	95	°F
Match-cast segment Time of Simulation at Casting	0	hrs
New Segment Time of Simulation at Casting	24	hrs
Concrete Properties		
Cement Content	950.11	lb/yd^3
Activation Energy	28.43	BTU/mol
Heat of Hydration Parameters		
Total Heat Development, $Q_{ult} = \alpha_u \cdot H_u$	124.95	BTU/lb
Time Parameter, τ	10.50	hrs
Curvature Parameter, β	1.60	
Density	3792.929	lb/yd^3
Specific Heat	0.25	BTU/(lb·°F)
Thermal Conductivity	1.352	BTU/(ft·h·°F)
Match-cast segment Elastic Modulus Dev. Parameters		
Final Value	4429.83	ksi
Time Parameter	12.420	hrs
Curvature Parameter	1.068	
New Segment Elastic Modulus Dev. Parameters		
Final Value	14.50	ksi
Time Parameter	n/a	hrs
Curvature Parameter	n/a	
Poisson Ratio	0.17	
Coefficient of Thermal Expansion	3.40	με/°F
Thermal Boundary Conditions (Applied to Appropriate Faces)		
Ambient Temp	Miami - Summer - Morning - Placement	
Wind	Medium-Wind	7.50	mph
Formwork	Steel Formwork	34.60	BTU/(ft·h·°F)
	Thickness	0.118	in
Curing	Burlap	0.18	BTU/(ft·h·°F)
	Thickness	0.39	in

Figure B-154: Simulation 52 - Bowing distortion of match-cast segment after placement of the new segment
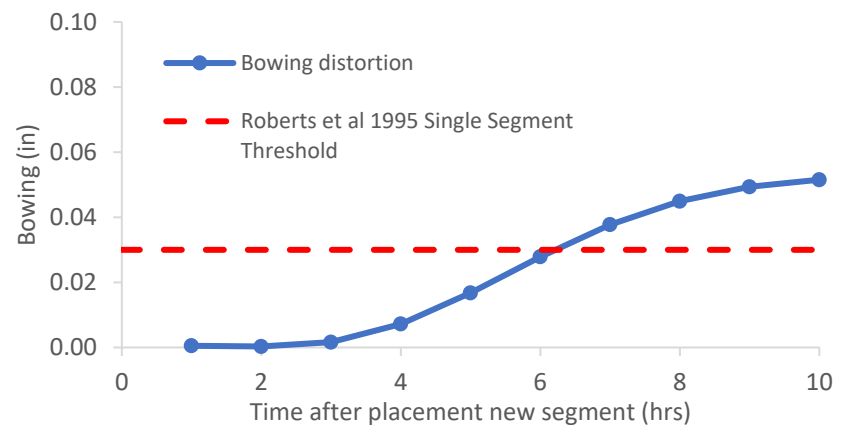

Figure B-155: Simulation 52 - Bowing distortion progression of match-cast segment from time of placement of new segment to 10 hours
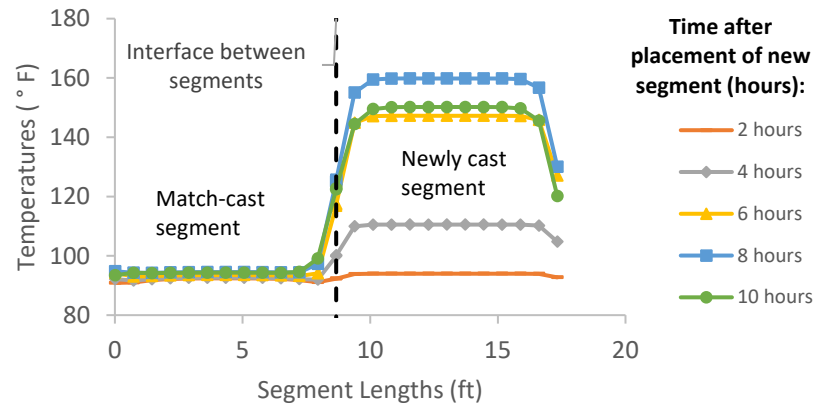

Figure B-156: Simulation 52 - Internal temperatures along the wing of segments

Simulation 53 -Results Summary

Table B-53: Model input parameters simulation 53

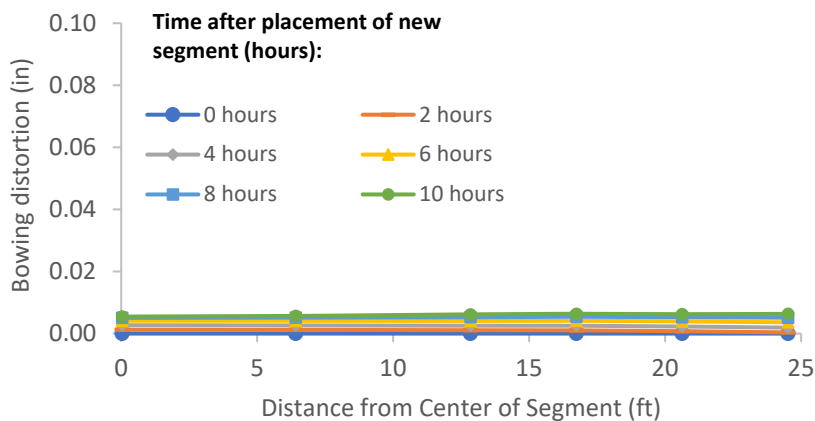| Model details		
Permutation number	53	
Geometry	Florida Bridge B - w/l=5.97	
Max. Mesh Size	3.94	in
Time Step	1	hrs
Placement Temperature	95	°F
Match-cast segment Time of Simulation at Casting	0	hrs
New Segment Time of Simulation at Casting	24	hrs
Concrete Properties		
Cement Content	950.11	lb/yd^3
Activation Energy	28.43	BTU/mol
Heat of Hydration Parameters		
Total Heat Development, $Q_{ult} = \alpha_u \cdot H_u$	124.95	BTU/lb
Time Parameter, τ	10.50	hrs
Curvature Parameter, β	1.60	
Density	3792.929	lb/yd^3
Specific Heat	0.25	BTU/(lb·°F)
Thermal Conductivity	1.352	BTU/(ft·h·°F)
Match-cast segment Elastic Modulus Dev. Parameters		
Final Value	4429.83	ksi
Time Parameter	12.420	hrs
Curvature Parameter	1.068	
New Segment Elastic Modulus Dev. Parameters		
Final Value	14.50	ksi
Time Parameter	n/a	hrs
Curvature Parameter	n/a	
Poisson Ratio	0.17	
Coefficient of Thermal Expansion	3.40	με/°F
Thermal Boundary Conditions (Applied to Appropriate Faces)		
Ambient Temp	Miami - Summer - Morning - Placement	
Wind	Medium-Wind	7.50	mph
Formwork	Steel Formwork	34.60	BTU/(ft·h·°F)
	Thickness	0.118	in
Curing	Burlap	0.18	BTU/(ft·h·°F)
	Thickness	0.39	in

Figure B-157: Simulation 53 - Bowing distortion of match-cast segment after placement of the new segment
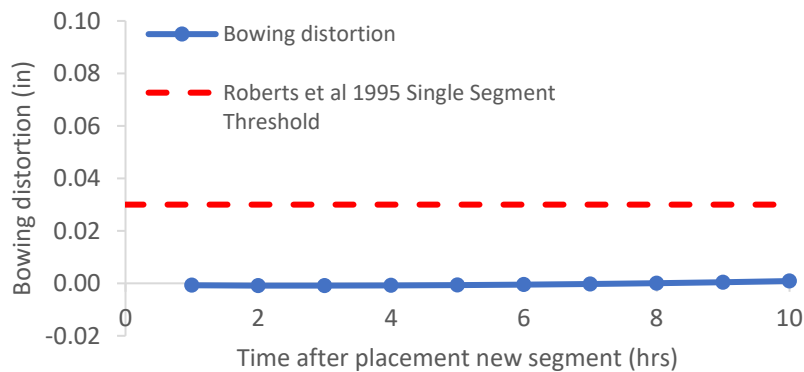

Figure B-158: Simulation 53 - Bowing distortion progression of match-cast segment from time of placement of new segment to 10 hours
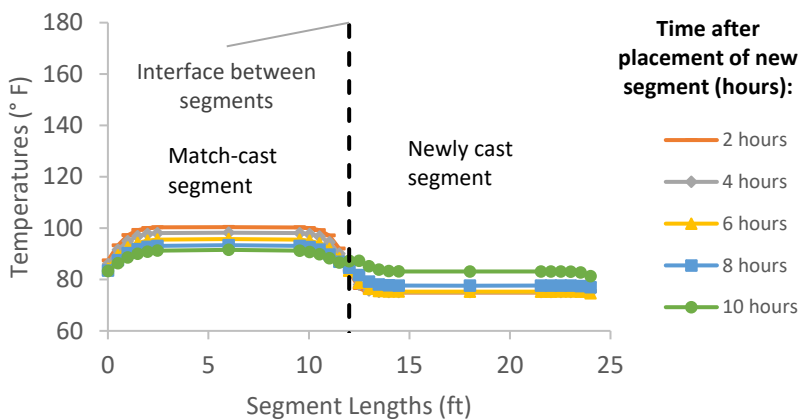

Figure B-159: Simulation 53 - Internal temperatures along the wing of segments

Simulation 54 -Results Summary

Table B-54: Model input parameters simulation 54

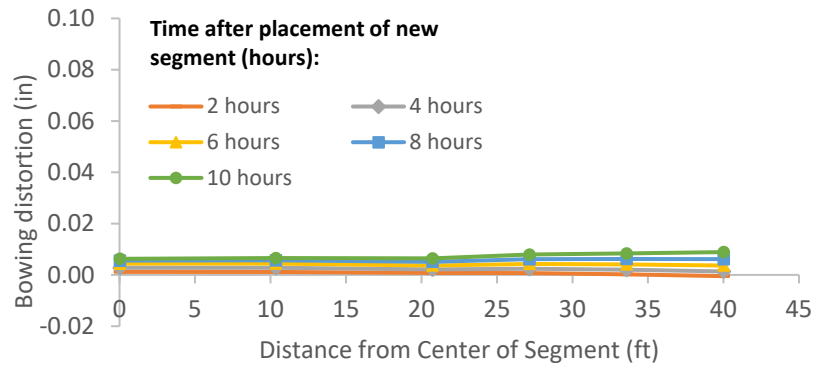| Model details		
Permutation number	54	
Geometry	Florida Bridge C - w/l=10.89	
Max. Mesh Size	3.54	in
Time Step	1	hrs
Placement Temperature	95	°F
Match-cast segment Time of Simulation at Casting	0	hrs
New Segment Time of Simulation at Casting	24	hrs
Concrete Properties		
Cement Content	950.11	lb/yd^3
Activation Energy	28.43	BTU/mol
Heat of Hydration Parameters		
Total Heat Development, $Q_{ult} = \alpha_u \cdot H_u$	124.95	BTU/lb
Time Parameter, τ	10.50	hrs
Curvature Parameter, β	1.60	
Density	3792.929	lb/yd^3
Specific Heat	0.25	BTU/(lb·°F)
Thermal Conductivity	1.352	BTU/(ft·h·°F)
Match-cast segment Elastic Modulus Dev. Parameters		
Final Value	4429.83	ksi
Time Parameter	12.420	hrs
Curvature Parameter	1.068	
New Segment Elastic Modulus Dev. Parameters		
Final Value	14.50	ksi
Time Parameter	n/a	hrs
Curvature Parameter	n/a	
Poisson Ratio	0.17	
Coefficient of Thermal Expansion	3.40	με/°F
Thermal Boundary Conditions (Applied to Appropriate Faces)		
Ambient Temp	Miami - Summer - Morning - Placement	
Wind	Medium-Wind	7.50	mph
Formwork	Steel Formwork	34.60	BTU/(ft·h·°F)
	Thickness	0.118	in
Curing	Burlap	0.18	BTU/(ft·h·°F)
	Thickness	0.39	in

Figure B-160: Simulation 54 - Bowing distortion of match-cast segment after placement of the new segment
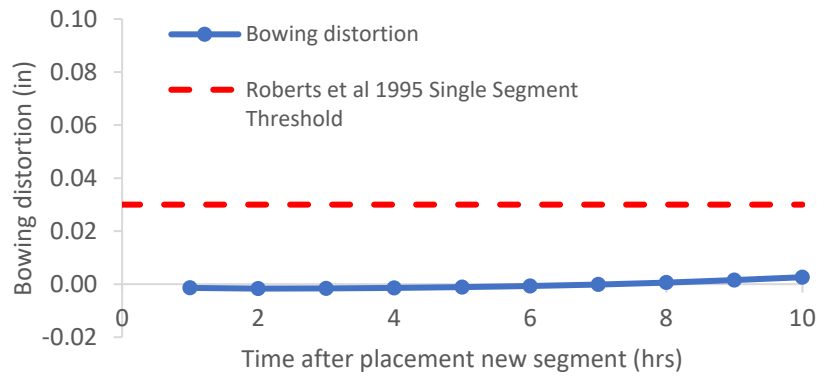

Figure B-161: Simulation 54 - Bowing distortion progression of match-cast segment from time of placement of new segment to 10 hours

Figure B-162: Simulation 54 - Internal temperatures along the wing of segments

Simulation 55 -Results Summary

Table B-55: Model input parameters simulation 55

Model details		
Permutation number	55	
Geometry	Florida Bridge E - w/l=4.09	
Max. Mesh Size	2.95	in
Time Step	1	hrs
Placement Temperature	75	°F
Match-cast segment Time of Simulation at Casting	0	hrs
New Segment Time of Simulation at Casting	24	hrs
Concrete Properties		
Cement Content	650.08	lb/yd^3
Activation Energy	26.21	BTU/mol
Heat of Hydration Parameters		
Total Heat Development, $Q_{ult} = \alpha_u \cdot H_u$	107.65	BTU/lb
Time Parameter, τ	18.28	hrs
Curvature Parameter, β	1.65	
Density	3834.891	lb/yd^3
Specific Heat	0.24	BTU/(lb·°F)
Thermal Conductivity	1.608	BTU/(ft·h·°F)
Match-cast segment Elastic Modulus Dev. Parameters		
Final Value	4503.55	ksi
Time Parameter	12.420	hrs
Curvature Parameter	1.068	
New Segment Elastic Modulus Dev. Parameters		
Final Value	14.50	ksi
Time Parameter	n/a	hrs
Curvature Parameter	n/a	
Poisson Ratio	0.17	
Coefficient of Thermal Expansion	4.55	με/°F
Thermal Boundary Conditions (Applied to Appropriate Faces)		
Ambient Temp	Miami - Summer - Night - Placement	
Wind	Medium-Wind	7.50	mph
Formwork	Steel Formwork	34.60	BTU/(ft·h·°F)
	Thickness	0.118	in
Curing	Burlap	0.18	BTU/(ft·h·°F)
	Thickness	0.39	in

Figure B-163: Simulation 55 - Bowing distortion of match-cast segment after placement of the new segment

Figure B-164: Simulation 55 - Bowing distortion progression of match-cast segment from time of placement of new segment to 10 hours
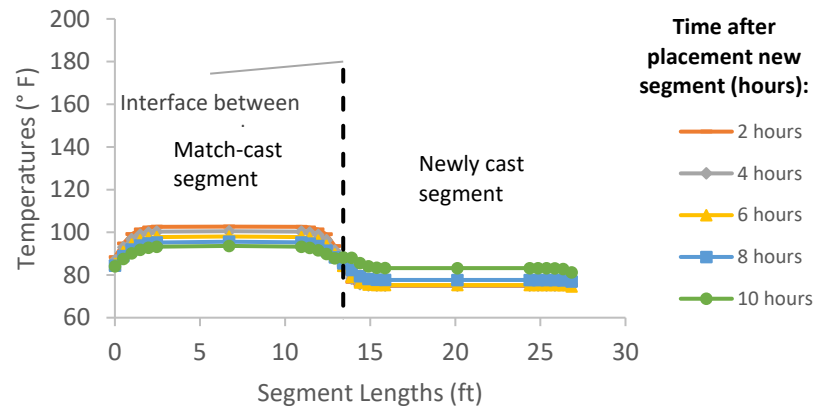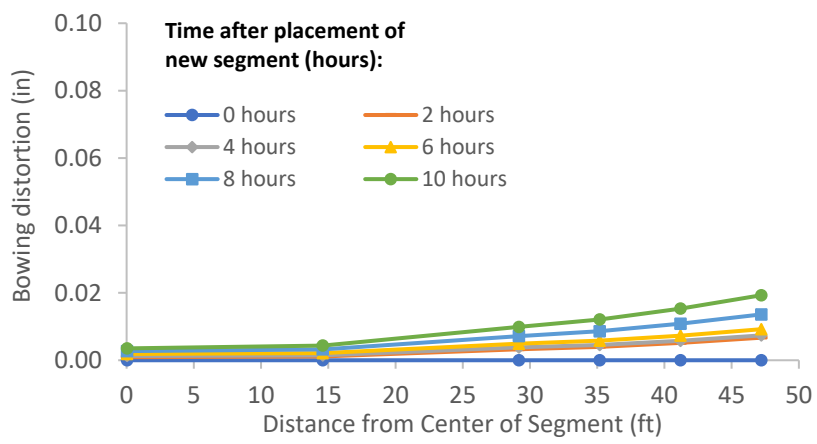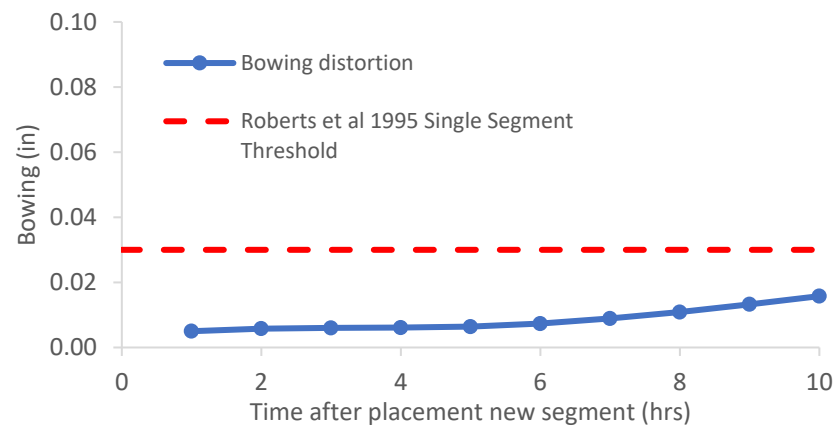

Figure B-165: Simulation 55 - Internal temperatures along the wing of segments

Simulation 56 -Results Summary

Table B-56: Model input parameters simulation 56

Model details		
Permutation number	56	
Geometry	Florida Bridge B - w/l=5.97	
Max. Mesh Size	3.94	in
Time Step	1	hrs
Placement Temperature	75	°F
Match-cast segment Time of Simulation at Casting	0	hrs
New Segment Time of Simulation at Casting	24	hrs
Concrete Properties		
Cement Content	650.08	lb/yd^3
Activation Energy	26.21	BTU/mol
Heat of Hydration Parameters		
Total Heat Development, $Q_{ult} = \alpha_u \cdot H_u$	107.65	BTU/lb
Time Parameter, τ	18.28	hrs
Curvature Parameter, β	1.65	
Density	3834.891	lb/yd^3
Specific Heat	0.24	BTU/(lb·°F)
Thermal Conductivity	1.608	BTU/(ft·h·°F)
Match-cast segment Elastic Modulus Dev. Parameters		
Final Value	4503.55	ksi
Time Parameter	12.420	hrs
Curvature Parameter	1.068	
New Segment Elastic Modulus Dev. Parameters		
Final Value	14.50	ksi
Time Parameter	n/a	hrs
Curvature Parameter	n/a	
Poisson Ratio	0.17	
Coefficient of Thermal Expansion	4.55	με/°F
Thermal Boundary Conditions (Applied to Appropriate Faces)		
Ambient Temp	Miami - Summer - Night - Placement	
Wind	Medium-Wind	7.50	mph
Formwork	Steel Formwork	34.60	BTU/(ft·h·°F)
	Thickness	0.118	in
Curing	Burlap	0.18	BTU/(ft·h·°F)
	Thickness	0.39	in

Figure B-166: Simulation 56 - Bowing distortion of match-cast segment after placement of the new segment

Figure B-167: Simulation 56 - Bowing distortion progression of match-cast segment from time of placement of new segment to 10 hours
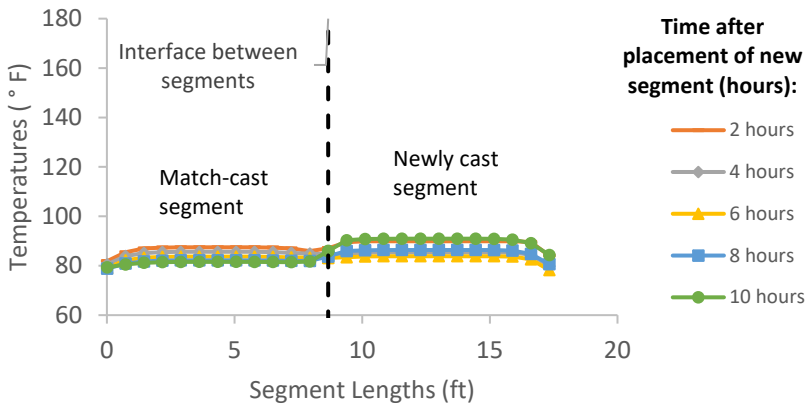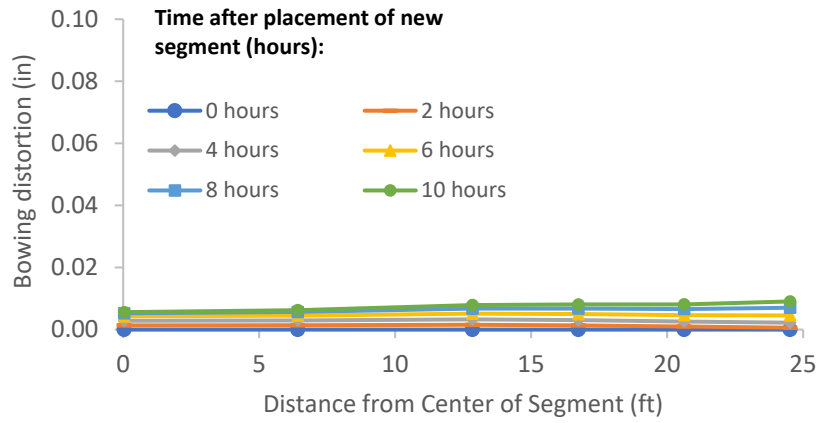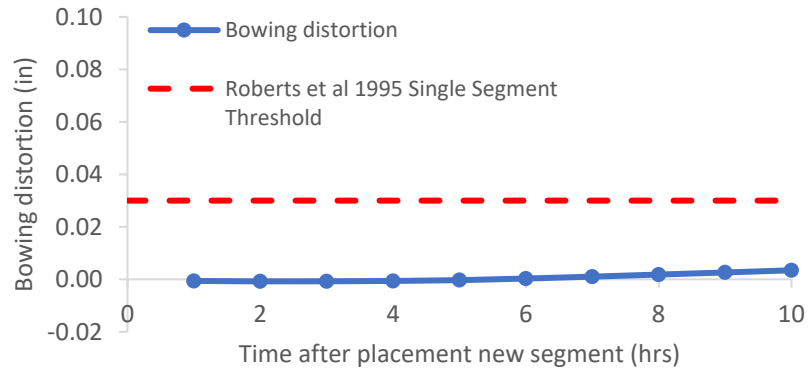

Figure B-168: Simulation 56 - Internal temperatures along the wing of segments

Simulation 57 -Results Summary

Table B-57: Model input parameters simulation 57

Model details		
Permutation number	57	
Geometry	Florida Bridge C - w/l=10.89	
Max. Mesh Size	3.54	in
Time Step	1	hrs
Placement Temperature	75	°F
Match-cast segment Time of Simulation at Casting	0	hrs
New Segment Time of Simulation at Casting	24	hrs
Concrete Properties		
Cement Content	650.08	lb/yd^3
Activation Energy	26.21	BTU/mol
Heat of Hydration Parameters		
Total Heat Development, $Q_{ult} = \alpha_u \cdot H_u$	107.65	BTU/lb
Time Parameter, τ	18.28	hrs
Curvature Parameter, β	1.65	
Density	3834.891	lb/yd^3
Specific Heat	0.24	BTU/(lb·°F)
Thermal Conductivity	1.608	BTU/(ft·h·°F)
Match-cast segment Elastic Modulus Dev. Parameters		
Final Value	4503.55	ksi
Time Parameter	12.420	hrs
Curvature Parameter	1.068	
New Segment Elastic Modulus Dev. Parameters		
Final Value	14.50	ksi
Time Parameter	n/a	hrs
Curvature Parameter	n/a	
Poisson Ratio	0.17	
Coefficient of Thermal Expansion	4.55	με/°F
Thermal Boundary Conditions (Applied to Appropriate Faces)		
Ambient Temp	Miami - Summer - Night - Placement	
Wind	Medium-Wind	7.50	mph
Formwork	Steel Formwork	34.60	BTU/(ft·h·°F)
	Thickness	0.118	in
Curing	Burlap	0.18	BTU/(ft·h·°F)
	Thickness	0.39	in

Figure B-169: Simulation 57 - Bowing distortion of match-cast segment after placement of the new segment

Figure B-170: Simulation 57 - Bowing distortion progression of match-cast segment from time of placement of new segment to 10 hours
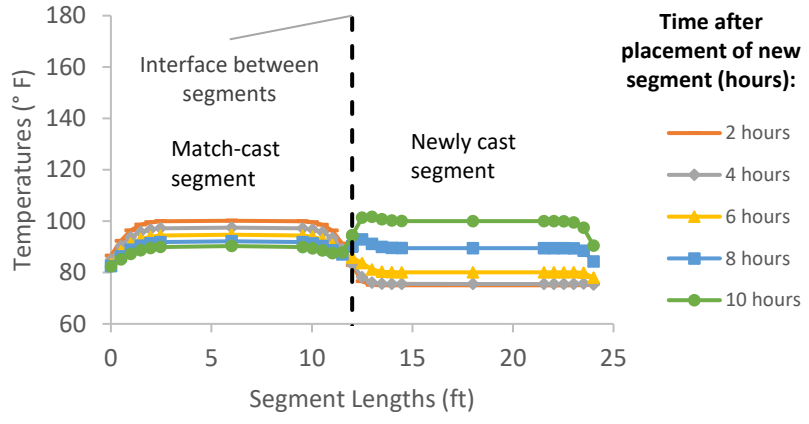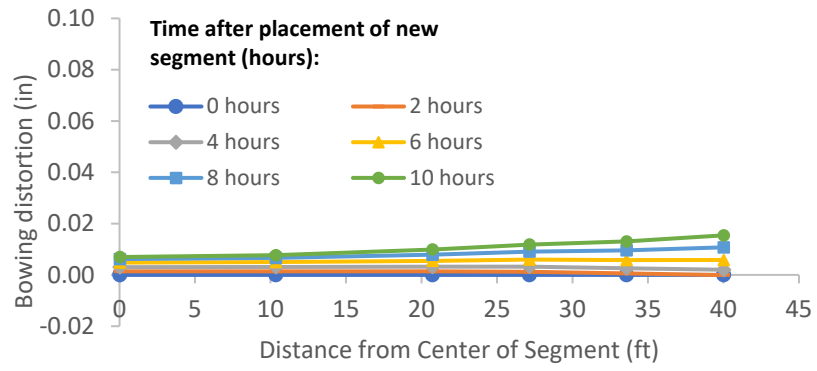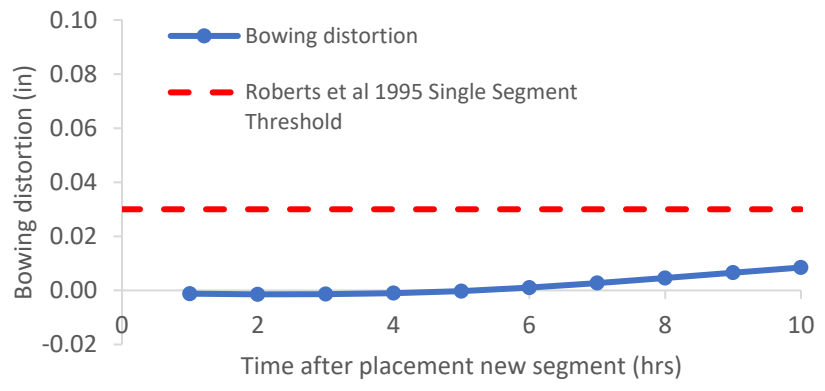

Figure B-171: Simulation 57 - Internal temperatures along the wing of segments

Simulation 58 -Results Summary

Table B-58: Model input parameters simulation 58

Model details		
Permutation number	58	
Geometry	Florida Bridge E - w/l=4.09	
Max. Mesh Size	2.95	in
Time Step	1	hrs
Placement Temperature	75	°F
Match-cast segment Time of Simulation at Casting	0	hrs
New Segment Time of Simulation at Casting	24	hrs
Concrete Properties		
Cement Content	750.09	lb/yd^3
Activation Energy	24.13	BTU/mol
Heat of Hydration Parameters		
Total Heat Development, $Q_{ult} = \alpha_u \cdot H_u$	111.33	BTU/lb
Time Parameter, τ	13.36	hrs
Curvature Parameter, β	1.49	
Density	3816.577	lb/yd^3
Specific Heat	0.25	BTU/(lb·°F)
Thermal Conductivity	1.557	BTU/(ft·h·°F)
Match-cast segment Elastic Modulus Dev. Parameters		
Final Value	4471.32	ksi
Time Parameter	12.420	hrs
Curvature Parameter	1.068	
New Segment Elastic Modulus Dev. Parameters		
Final Value	14.50	ksi
Time Parameter	n/a	hrs
Curvature Parameter	n/a	
Poisson Ratio	0.17	
Coefficient of Thermal Expansion	4.54	$\mu\varepsilon$/°F
Thermal Boundary Conditions (Applied to Appropriate Faces)		
Ambient Temp	Miami - Summer - Night - Placement	
Wind	Medium-Wind	7.50	mph
Formwork	Steel Formwork	34.60	BTU/(ft·h·°F)
	Thickness	0.118	in
Curing	Burlap	0.18	BTU/(ft·h·°F)
	Thickness	0.39	in

Figure B-172: Simulation 58 - Bowing distortion of match-cast segment after placement of the new segment

Figure B-173: Simulation 58 - Bowing distortion progression of match-cast segment from time of placement of new segment to 10 hours
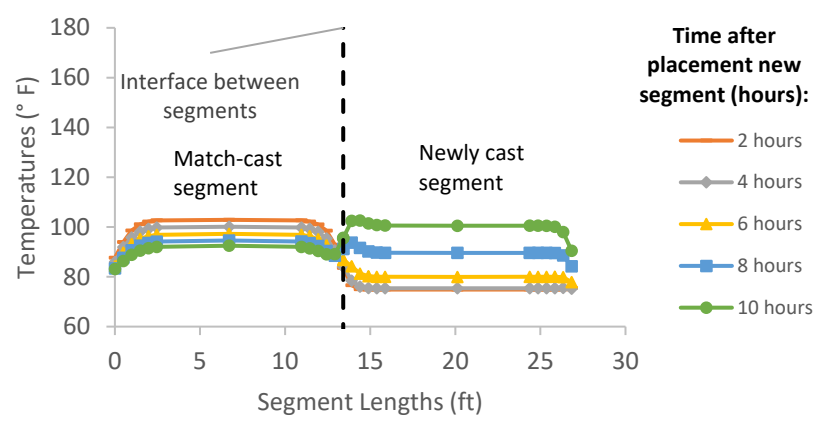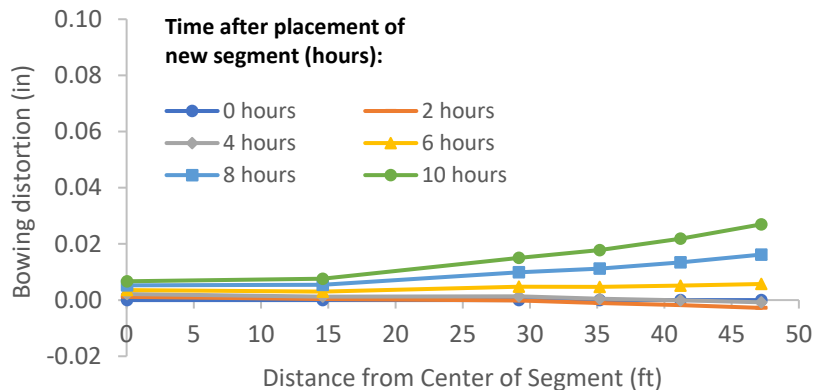

Figure B-174: Simulation 58 - Internal temperatures along the wing of segments

Simulation 59 -Results Summary

Table B-59: Model input parameters simulation 59

Model details		
Permutation number	59	
Geometry	Florida Bridge B - w/l=5.97	
Max. Mesh Size	3.94	in
Time Step	1	hrs
Placement Temperature	75	°F
Match-cast segment Time of Simulation at Casting	0	hrs
New Segment Time of Simulation at Casting	24	hrs
Concrete Properties		
Cement Content	750.09	lb/yd^3
Activation Energy	24.13	BTU/mol
Heat of Hydration Parameters		
Total Heat Development, $Q_{ult} = \alpha_u \cdot H_u$	111.33	BTU/lb
Time Parameter, τ	13.36	hrs
Curvature Parameter, β	1.49	
Density	3816.577	lb/yd^3
Specific Heat	0.25	BTU/(lb·°F)
Thermal Conductivity	1.557	BTU/(ft·h·°F)
Match-cast segment Elastic Modulus Dev. Parameters		
Final Value	4471.32	ksi
Time Parameter	12.420	hrs
Curvature Parameter	1.068	
New Segment Elastic Modulus Dev. Parameters		
Final Value	14.50	ksi
Time Parameter	n/a	hrs
Curvature Parameter	n/a	
Poisson Ratio	0.17	
Coefficient of Thermal Expansion	4.54	µε/°F
Thermal Boundary Conditions (Applied to Appropriate Faces)		
Ambient Temp	Miami - Summer - Night - Placement	
Wind	Medium-Wind	7.50	mph
Formwork	Steel Formwork	34.60	BTU/(ft·h·°F)
	Thickness	0.118	in
Curing	Burlap	0.18	BTU/(ft·h·°F)
	Thickness	0.39	in

Figure B-175: Simulation 59 - Bowing distortion of match-cast segment after placement of the new segment
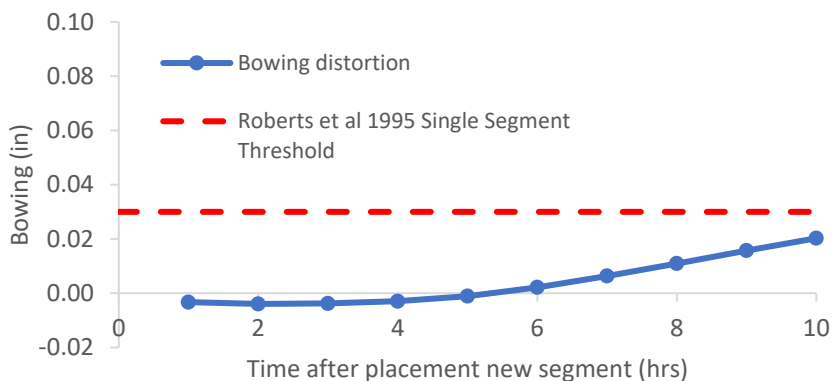

Figure B-:176 Simulation 59 - Bowing distortion progression of match-cast segment from time of placement of new segment to 10 hours
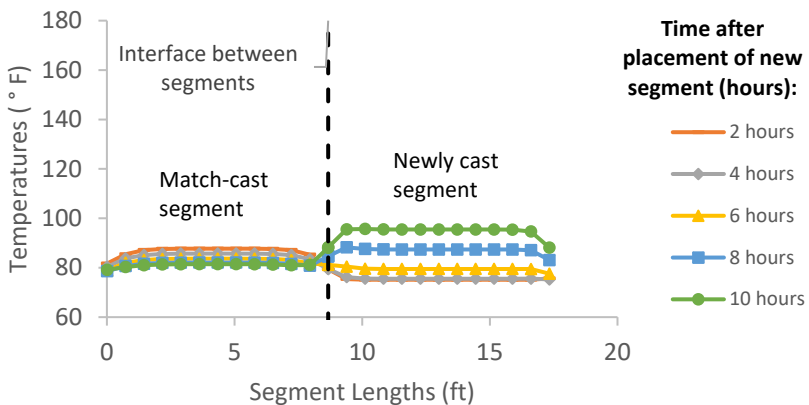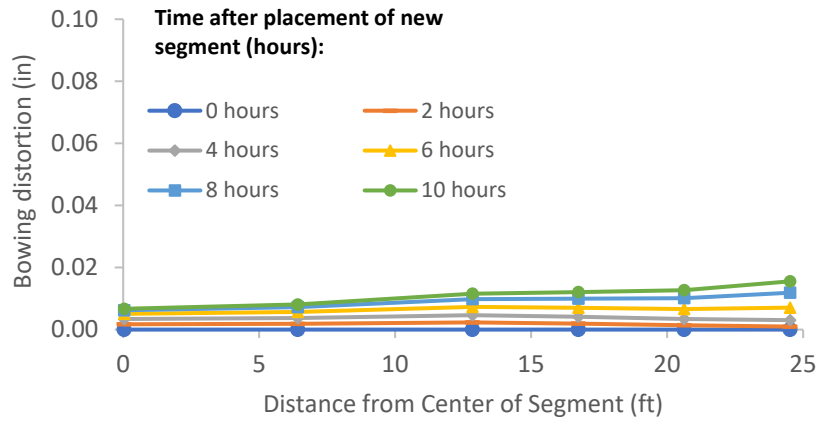

Figure B-177: Simulation 59 - Internal temperatures along the wing of segments

Simulation 60 -Results Summary

Table B-60: Model input parameters simulation 60

Model details		
Permutation number	60	
Geometry	Florida Bridge C - w/l=10.89	
Max. Mesh Size	3.54	in
Time Step	1	hrs
Placement Temperature	75	°F
Match-cast segment Time of Simulation at Casting	0	hrs
New Segment Time of Simulation at Casting	24	hrs
Concrete Properties		
Cement Content	750.09	lb/yd^3
Activation Energy	24.13	BTU/mol
Heat of Hydration Parameters		
Total Heat Development, $Q_{ult} = \alpha_u \cdot H_u$	111.33	BTU/lb
Time Parameter, τ	13.36	hrs
Curvature Parameter, β	1.49	
Density	3816.577	lb/yd^3
Specific Heat	0.25	BTU/(lb·°F)
Thermal Conductivity	1.557	BTU/(ft·h·°F)
Match-cast segment Elastic Modulus Dev. Parameters		
Final Value	4471.32	ksi
Time Parameter	12.420	hrs
Curvature Parameter	1.068	
New Segment Elastic Modulus Dev. Parameters		
Final Value	14.50	ksi
Time Parameter	n/a	hrs
Curvature Parameter	n/a	
Poisson Ratio	0.17	
Coefficient of Thermal Expansion	4.54	$\mu\varepsilon$/°F
Thermal Boundary Conditions (Applied to Appropriate Faces)		
Ambient Temp	Miami - Summer - Night - Placement	
Wind	Medium-Wind	7.50	mph
Formwork	Steel Formwork	34.60	BTU/(ft·h·°F)
	Thickness	0.118	in
Curing	Burlap	0.18	BTU/(ft·h·°F)
	Thickness	0.39	in

Figure B-178: Simulation 60 - Bowing distortion of match-cast segment after placement of the new segment
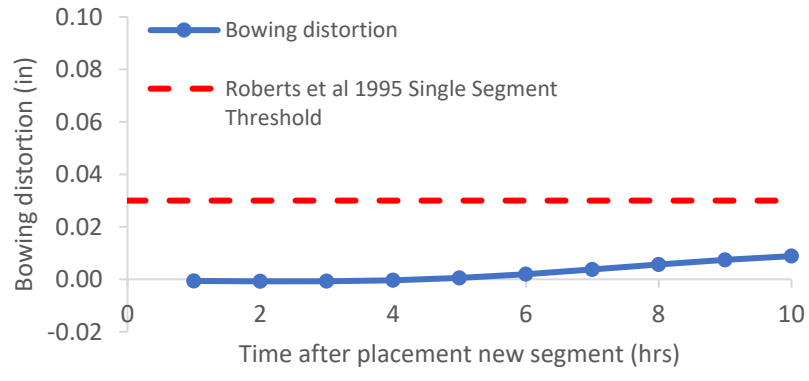

Figure B-179: Simulation 60 - Bowing distortion progression of match-cast segment from time of placement of new segment to 10 hours
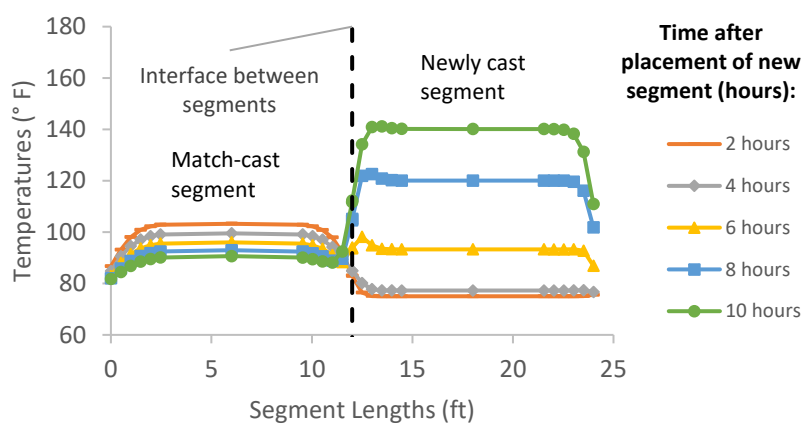

Figure B-180: Simulation 60 - Internal temperatures along the wing of segments

Simulation 61 -Results Summary

Table B-61: Model input parameters simulation 61

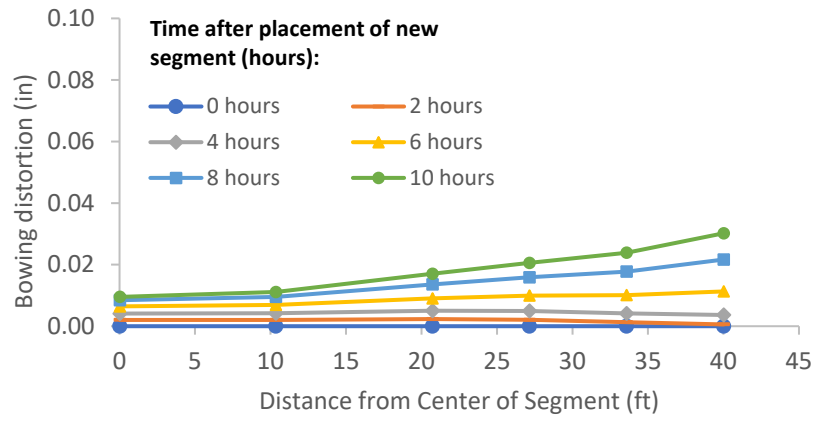| Model details		
Permutation number	61	
Geometry	Florida Bridge E - w/l=4.09	
Max. Mesh Size	2.95	in
Time Step	1	hrs
Placement Temperature	75	°F
Match-cast segment Time of Simulation at Casting	0	hrs
New Segment Time of Simulation at Casting	24	hrs
Concrete Properties		
Cement Content	950.11	lb/yd^3
Activation Energy	28.43	BTU/mol
Heat of Hydration Parameters		
Total Heat Development, $Q_{ult} = \alpha_u \cdot H_u$	124.95	BTU/lb
Time Parameter, τ	10.50	hrs
Curvature Parameter, β	1.60	
Density	3880.948	lb/yd^3
Specific Heat	0.26	BTU/(lb·°F)
Thermal Conductivity	1.502	BTU/(ft·h·°F)
Match-cast segment Elastic Modulus Dev. Parameters		
Final Value	4584.92	ksi
Time Parameter	12.420	hrs
Curvature Parameter	1.068	
New Segment Elastic Modulus Dev. Parameters		
Final Value	14.50	ksi
Time Parameter	n/a	hrs
Curvature Parameter	n/a	
Poisson Ratio	0.17	
Coefficient of Thermal Expansion	4.54	µε/°F
Thermal Boundary Conditions (Applied to Appropriate Faces)		
Ambient Temp	Miami - Summer - Night - Placement	
Wind	Medium-Wind	7.50	mph
Formwork	Steel Formwork	34.60	BTU/(ft·h·°F)
	Thickness	0.118	in
Curing	Burlap	0.18	BTU/(ft·h·°F)
	Thickness	0.39	in

Figure B-181: Simulation 61 - Bowing distortion of match-cast segment after placement of the new segment
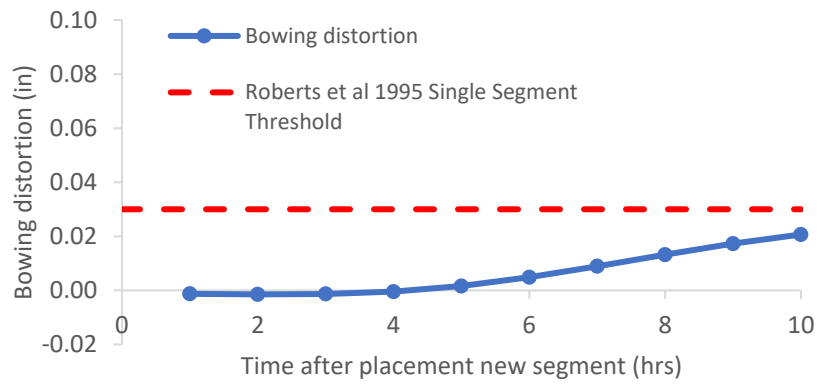

Figure B-182: Simulation 61 - Bowing distortion progression of match-cast segment from time of placement of new segment to 10 hours
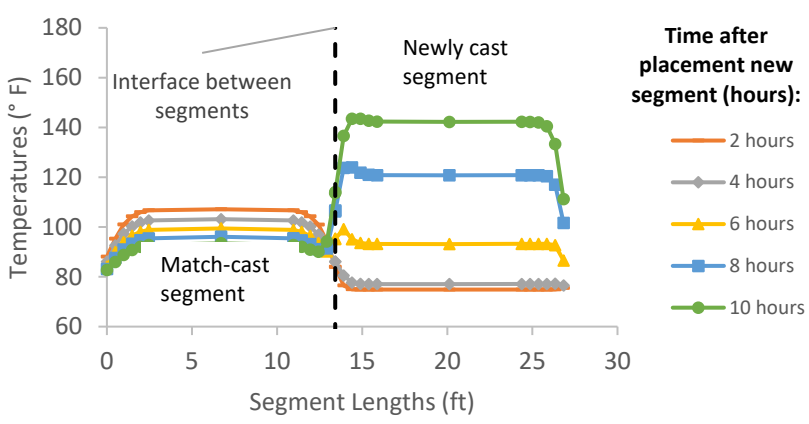

Figure B-183: Simulation 61 - Internal temperatures along the wing of segments

Simulation 62 -Results Summary

Table B-62: Model input parameters simulation 62

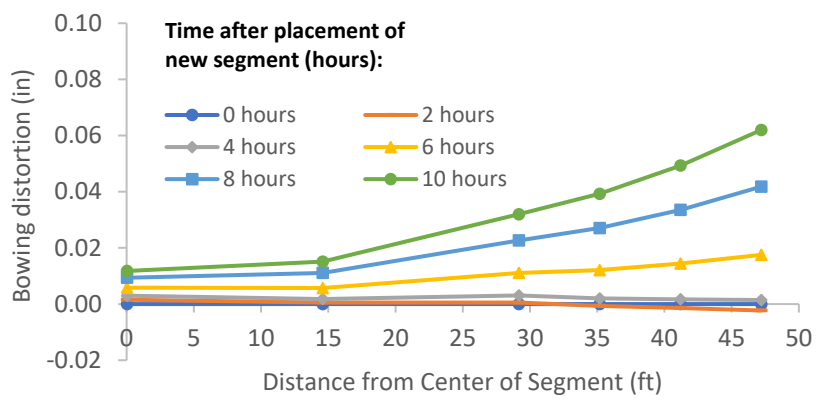| Model details		
Permutation number	62	
Geometry	Florida Bridge B - w/l=5.97	
Max. Mesh Size	3.94	in
Time Step	1	hrs
Placement Temperature	75	°F
Match-cast segment Time of Simulation at Casting	0	hrs
New Segment Time of Simulation at Casting	24	hrs
Concrete Properties		
Cement Content	950.11	lb/yd^3
Activation Energy	28.43	BTU/mol
Heat of Hydration Parameters		
Total Heat Development, $Q_{ult} = \alpha_u \cdot H_u$	124.95	BTU/lb
Time Parameter, τ	10.50	hrs
Curvature Parameter, β	1.60	
Density	3880.948	lb/yd^3
Specific Heat	0.26	BTU/(lb·°F)
Thermal Conductivity	1.502	BTU/(ft·h·°F)
Match-cast segment Elastic Modulus Dev. Parameters		
Final Value	4584.92	ksi
Time Parameter	12.420	hrs
Curvature Parameter	1.068	
New Segment Elastic Modulus Dev. Parameters		
Final Value	14.50	ksi
Time Parameter	n/a	hrs
Curvature Parameter	n/a	
Poisson Ratio	0.17	
Coefficient of Thermal Expansion	4.54	με/°F
Thermal Boundary Conditions (Applied to Appropriate Faces)		
Ambient Temp	Miami - Summer - Night - Placement	
Wind	Medium-Wind	7.50	mph
Formwork	Steel Formwork	34.60	BTU/(ft·h·°F)
	Thickness	0.118	in
Curing	Burlap	0.18	BTU/(ft·h·°F)
	Thickness	0.39	in

Figure B-184: Simulation 62 - Bowing distortion of match-cast segment after placement of the new segment
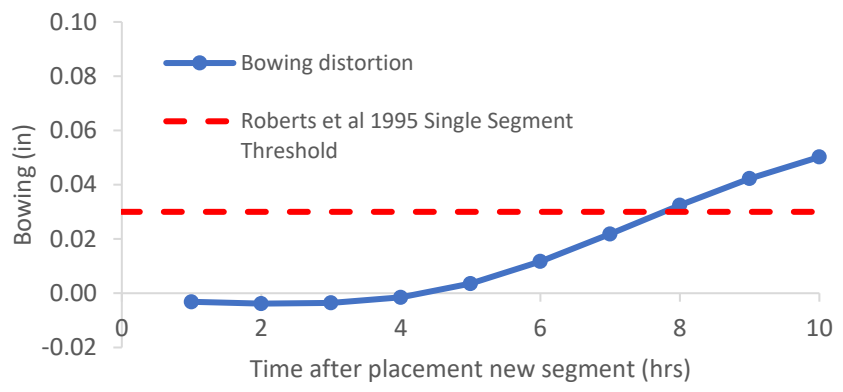

Figure B-185: Simulation 62 - Bowing distortion progression of match-cast segment from time of placement of new segment to 10 hours
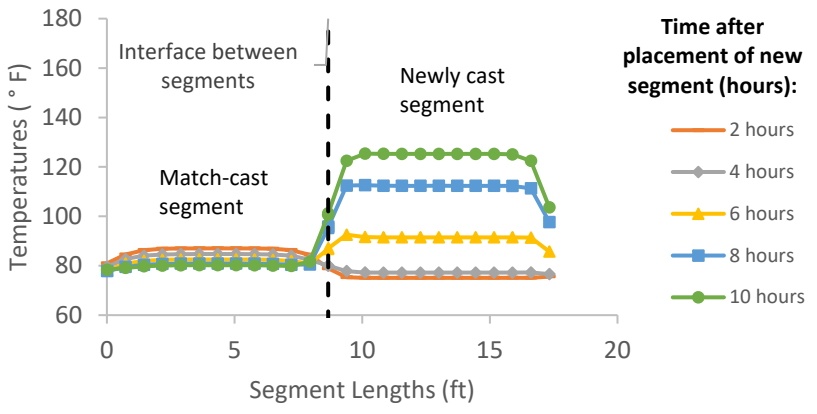

Figure B-186: Simulation 62 - Internal temperatures along the wing of segments

Simulation 63 -Results Summary

Table B-63: Model input parameters simulation 63

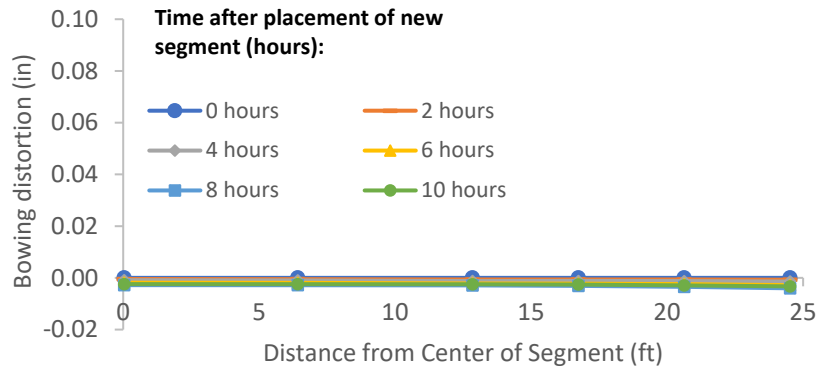| Model details		
Permutation number	63	
Geometry	Florida Bridge C - w/l=10.89	
Max. Mesh Size	3.54	in
Time Step	1	hrs
Placement Temperature	75	°F
Match-cast segment Time of Simulation at Casting	0	hrs
New Segment Time of Simulation at Casting	24	hrs
Concrete Properties		
Cement Content	950.11	lb/yd^3
Activation Energy	28.43	BTU/mol
Heat of Hydration Parameters		
Total Heat Development, $Q_{ult} = \alpha_u \cdot H_u$	124.95	BTU/lb
Time Parameter, τ	10.50	hrs
Curvature Parameter, β	1.60	
Density	3880.948	lb/yd^3
Specific Heat	0.26	BTU/(lb·°F)
Thermal Conductivity	1.502	BTU/(ft·h·°F)
Match-cast segment Elastic Modulus Dev. Parameters		
Final Value	4584.92	ksi
Time Parameter	12.420	hrs
Curvature Parameter	1.068	
New Segment Elastic Modulus Dev. Parameters		
Final Value	14.50	ksi
Time Parameter	n/a	hrs
Curvature Parameter	n/a	
Poisson Ratio	0.17	
Coefficient of Thermal Expansion	4.54	με/°F
Thermal Boundary Conditions (Applied to Appropriate Faces)		
Ambient Temp	Miami - Summer - Night - Placement	
Wind	Medium-Wind	7.50	mph
Formwork	Steel Formwork	34.60	BTU/(ft·h·°F)
	Thickness	0.118	in
Curing	Burlap	0.18	BTU/(ft·h·°F)
	Thickness	0.39	in

Figure B-187: Simulation 63 - Bowing distortion of match-cast segment after placement of the new segment
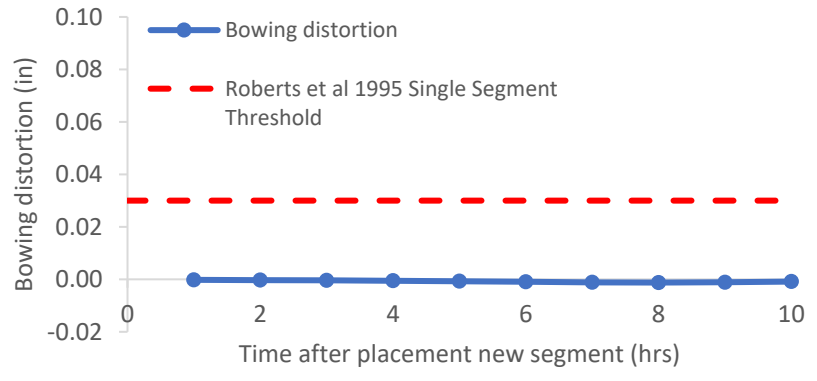

Figure B-188: Simulation 63 - Bowing distortion progression of match-cast segment from time of placement of new segment to 10 hours
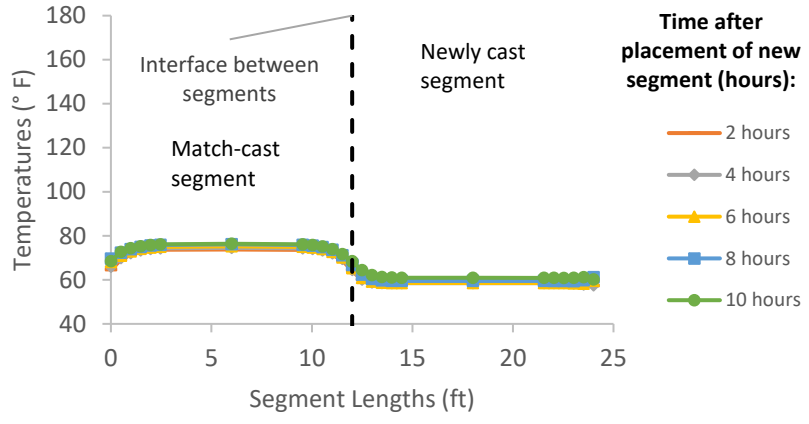

Figure B-189: Simulation 63 - Internal temperatures along the wing of segments

Simulation 64 -Results Summary

Table B-64: Model input parameters simulation 64

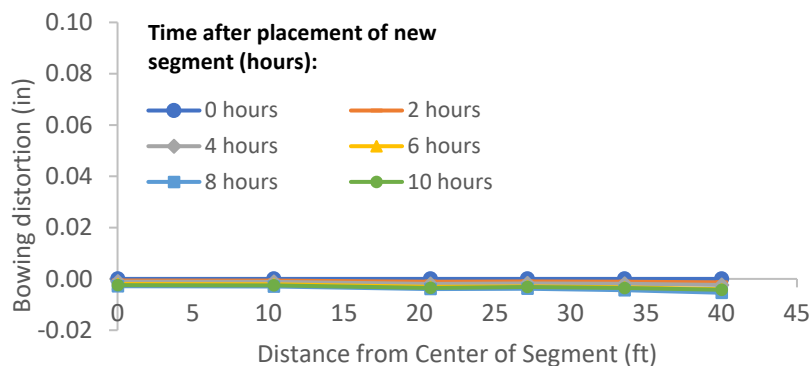| Model details		
Permutation number	64	
Geometry	Florida Bridge E - w/l=4.09	
Max. Mesh Size	2.95	in
Time Step	1	hrs
Placement Temperature	60	°F
Match-cast segment Time of Simulation at Casting	0	hrs
New Segment Time of Simulation at Casting	24	hrs
Concrete Properties		
Cement Content	650.08	lb/yd³
Activation Energy	26.21	BTU/mol
Heat of Hydration Parameters		
Total Heat Development, $Q_{ult} = \alpha_u \cdot H_u$	107.65	BTU/lb
Time Parameter, τ	18.28	hrs
Curvature Parameter, β	1.65	
Density	3834.891	lb/yd³
Specific Heat	0.24	BTU/(lb·°F)
Thermal Conductivity	1.608	BTU/(ft·h·°F)
Match-cast segment Elastic Modulus Dev. Parameters		
Final Value	4503.55	ksi
Time Parameter	12.420	hrs
Curvature Parameter	1.068	
New Segment Elastic Modulus Dev. Parameters		
Final Value	14.50	ksi
Time Parameter	n/a	hrs
Curvature Parameter	n/a	
Poisson Ratio	0.17	
Coefficient of Thermal Expansion	4.55	με/°F
Thermal Boundary Conditions (Applied to Appropriate Faces)		
Ambient Temp	Tallahassee - Winter - Morning - Placement	
Wind	Medium-Wind	7.50	mph
Formwork	Steel Formwork	34.60	BTU/(ft·h·°F)
	Thickness	0.118	in
Curing	Burlap	0.18	BTU/(ft·h·°F)
	Thickness	0.39	in

Figure B-190: Simulation 64 - Bowing distortion of match-cast segment after placement of the new segment
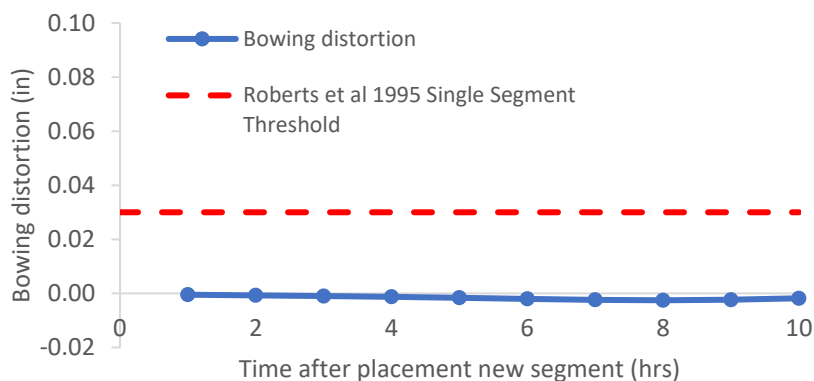

Figure B-191: Simulation 64 - Bowing distortion progression of match-cast segment from time of placement of new segment to 10 hours
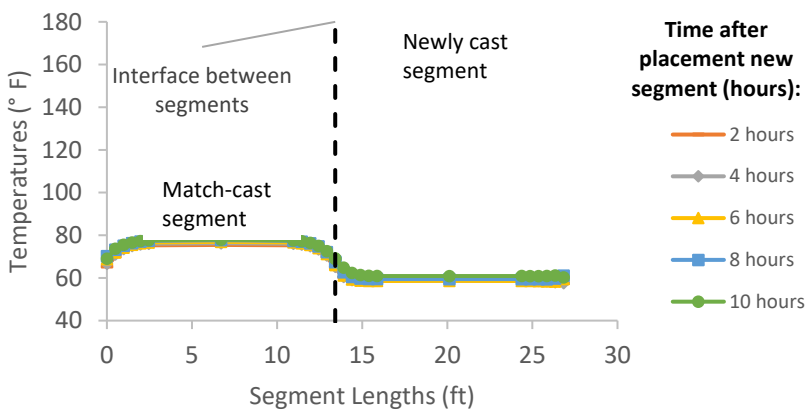

Figure B-192: Simulation 64 - Internal temperatures along the wing of segments

Simulation 65 -Results Summary

Table B-65: Model input parameters simulation 65

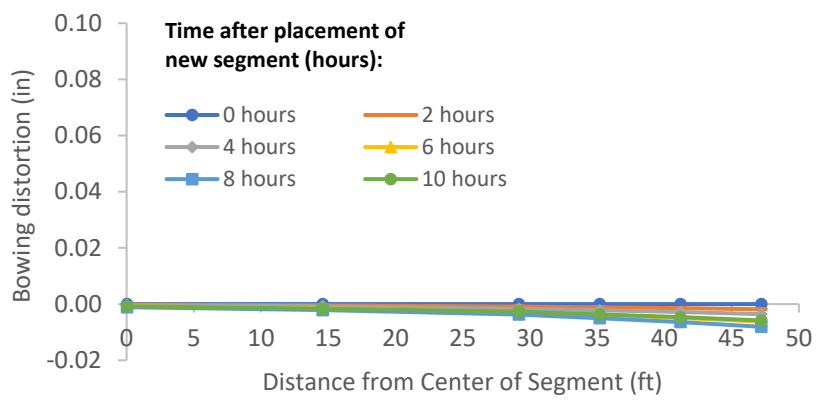| Model details		
Permutation number	65	
Geometry	Florida Bridge B - w/l=5.97	
Max. Mesh Size	3.94	in
Time Step	1	hrs
Placement Temperature	60	°F
Match-cast segment Time of Simulation at Casting	0	hrs
New Segment Time of Simulation at Casting	24	hrs
Concrete Properties		
Cement Content	650.08	lb/yd^3
Activation Energy	26.21	BTU/mol
Heat of Hydration Parameters		
Total Heat Development, $Q_{ult} = \alpha_u \cdot H_u$	107.65	BTU/lb
Time Parameter, τ	18.28	hrs
Curvature Parameter, β	1.65	
Density	3834.891	lb/yd^3
Specific Heat	0.24	BTU/(lb·°F)
Thermal Conductivity	1.608	BTU/(ft·h·°F)
Match-cast segment Elastic Modulus Dev. Parameters		
Final Value	4503.55	ksi
Time Parameter	12.420	hrs
Curvature Parameter	1.068	
New Segment Elastic Modulus Dev. Parameters		
Final Value	14.50	ksi
Time Parameter	n/a	hrs
Curvature Parameter	n/a	
Poisson Ratio	0.17	
Coefficient of Thermal Expansion	4.55	µε/°F
Thermal Boundary Conditions (Applied to Appropriate Faces)			
Ambient Temp	Tallahassee - Winter - Morning - Placement		
Wind	Medium-Wind	7.50	mph
Formwork	Steel Formwork	34.60	BTU/(ft·h·°F)
	Thickness	0.118	in
Curing	Burlap	0.18	BTU/(ft·h·°F)
	Thickness	0.39	in

Figure B-193: Simulation 65 - Bowing distortion of match-cast segment after placement of the new segment
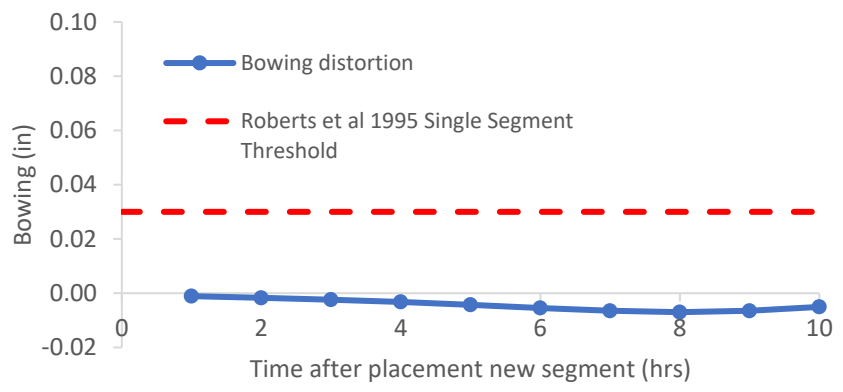

Figure B-194: Simulation 65 - Bowing distortion progression of match-cast segment from time of placement of new segment to 10 hours
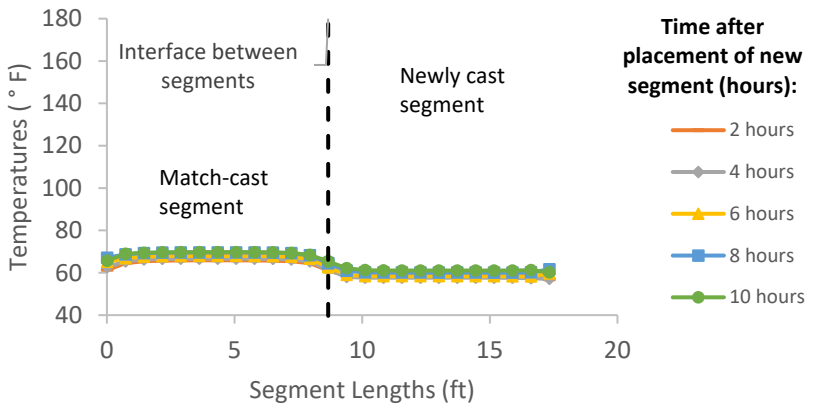

Figure B-195: Simulation 65 - Internal temperatures along the wing of segments

Simulation 66 -Results Summary

Table B-66: Model input parameters simulation 66

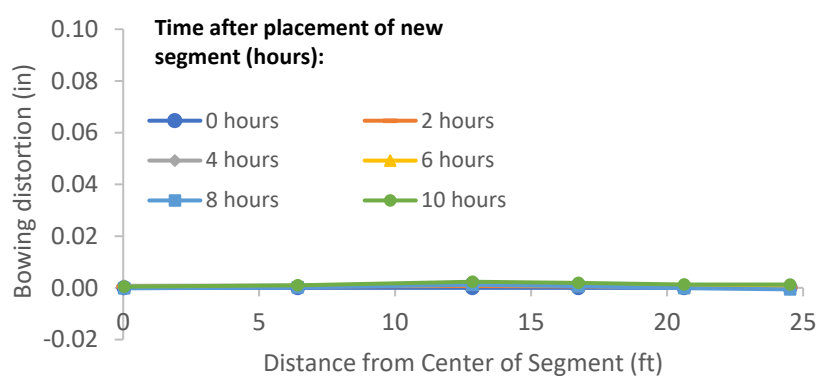| Model details		
Permutation number	66	
Geometry	Florida Bridge C - w/l=10.89	
Max. Mesh Size	3.54	in
Time Step	1	hrs
Placement Temperature	60	°F
Match-cast segment Time of Simulation at Casting	0	hrs
New Segment Time of Simulation at Casting	24	hrs
Concrete Properties		
Cement Content	650.08	lb/yd^3
Activation Energy	26.21	BTU/mol
Heat of Hydration Parameters		
Total Heat Development, $Q_{ult} = \alpha_u \cdot H_u$	107.65	BTU/lb
Time Parameter, τ	18.28	hrs
Curvature Parameter, β	1.65	
Density	3834.891	lb/yd^3
Specific Heat	0.24	BTU/(lb·°F)
Thermal Conductivity	1.608	BTU/(ft·h·°F)
Match-cast segment Elastic Modulus Dev. Parameters		
Final Value	4503.55	ksi
Time Parameter	12.420	hrs
Curvature Parameter	1.068	
New Segment Elastic Modulus Dev. Parameters		
Final Value	14.50	ksi
Time Parameter	n/a	hrs
Curvature Parameter	n/a	
Poisson Ratio	0.17	
Coefficient of Thermal Expansion	4.55	με/°F
Thermal Boundary Conditions (Applied to Appropriate Faces)		
Ambient Temp	Tallahassee - Winter - Morning - Placement	
Wind	Medium-Wind	7.50	mph
Formwork	Steel Formwork	34.60	BTU/(ft·h·°F)
	Thickness	0.118	in
Curing	Burlap	0.18	BTU/(ft·h·°F)
	Thickness	0.39	in

Figure B-196: Simulation 66 - Bowing distortion of match-cast segment after placement of the new segment
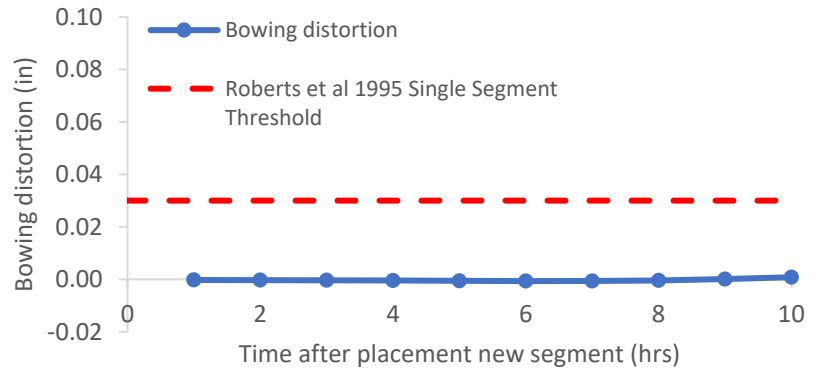

Figure B-197: Simulation 66 - Bowing distortion progression of match-cast segment from time of placement of new segment to 10 hours
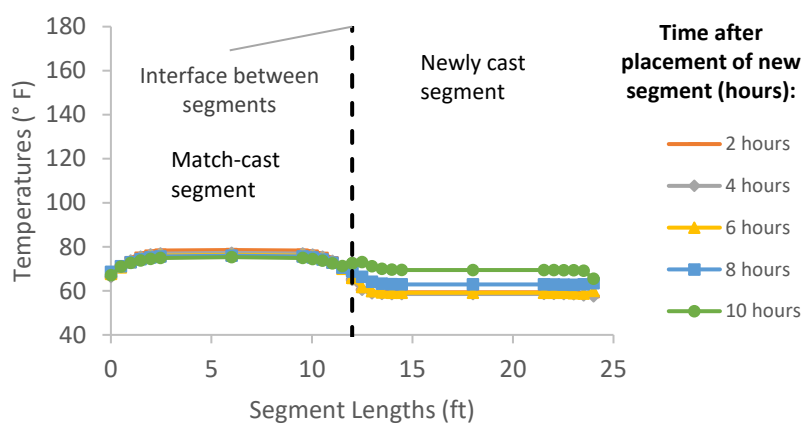

Figure B-198: Simulation 66 - Internal temperatures along the wing of segments

Simulation 67 -Results Summary

Table B-67: Model input parameters simulation 67

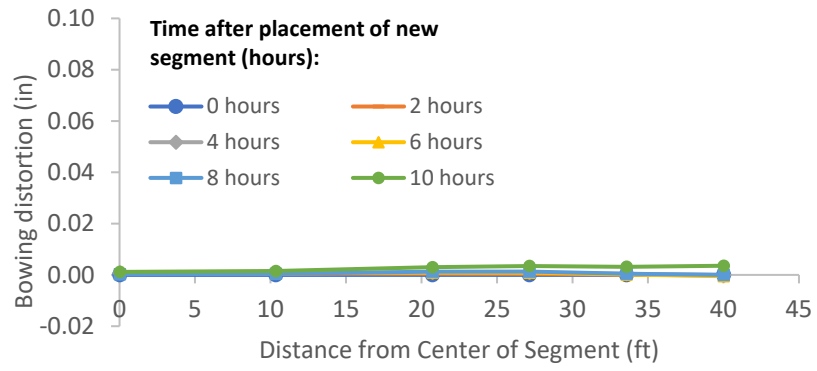| Model details		
Permutation number	67	
Geometry	Florida Bridge E - w/l=4.09	
Max. Mesh Size	2.95	in
Time Step	1	hrs
Placement Temperature	60	°F
Match-cast segment Time of Simulation at Casting	0	hrs
New Segment Time of Simulation at Casting	24	hrs
Concrete Properties		
Cement Content	750.09	lb/yd^3
Activation Energy	24.13	BTU/mol
Heat of Hydration Parameters		
Total Heat Development, $Q_{ult} = \alpha_u \cdot H_u$	111.33	BTU/lb
Time Parameter, τ	13.36	hrs
Curvature Parameter, β	1.49	
Density	3816.577	lb/yd^3
Specific Heat	0.25	BTU/(lb·°F)
Thermal Conductivity	1.557	BTU/(ft·h·°F)
Match-cast segment Elastic Modulus Dev. Parameters		
Final Value	4471.32	ksi
Time Parameter	12.420	hrs
Curvature Parameter	1.068	
New Segment Elastic Modulus Dev. Parameters		
Final Value	14.50	ksi
Time Parameter	n/a	hrs
Curvature Parameter	n/a	
Poisson Ratio	0.17	
Coefficient of Thermal Expansion	4.54	µε/°F
Thermal Boundary Conditions (Applied to Appropriate Faces)		
Ambient Temp	Tallahassee - Winter - Morning - Placement	
Wind	Medium-Wind	7.50	mph
Formwork	Steel Formwork	34.60	BTU/(ft·h·°F)
	Thickness	0.118	in
Curing	Burlap	0.18	BTU/(ft·h·°F)
	Thickness	0.39	in

Figure B-199: Simulation 67 - Bowing distortion of match-cast segment after placement of the new segment
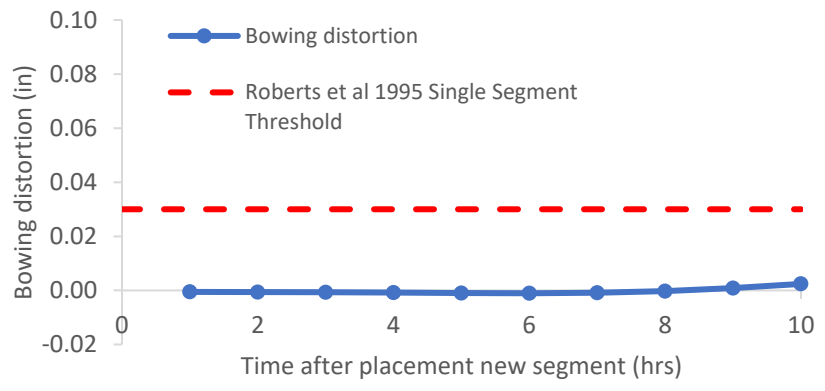

Figure B-200: Simulation 67 - Bowing distortion progression of match-cast segment from time of placement of new segment to 10 hours
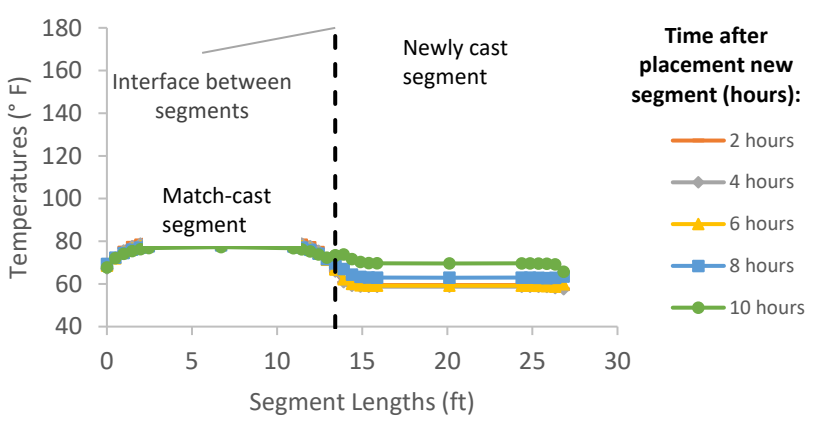

Figure B-201: Simulation 67 - Internal temperatures along the wing of segments

Simulation 68 -Results Summary

Table B-68: Model input parameters simulation 68

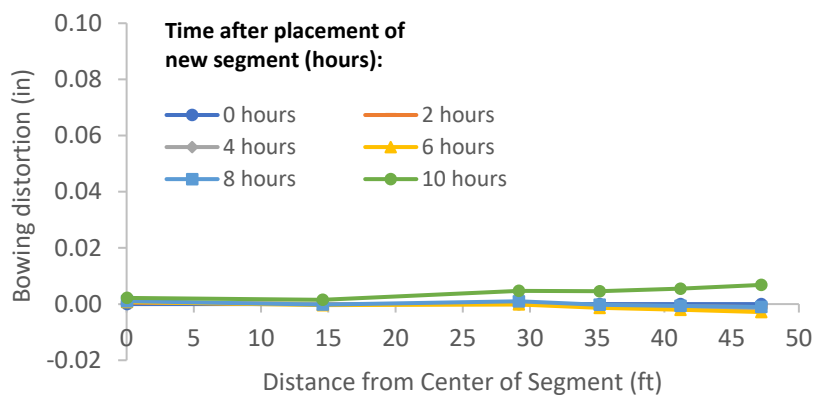| Model details		
Permutation number	68	
Geometry	Florida Bridge B - w/l=5.97	
Max. Mesh Size	3.94	in
Time Step	1	hrs
Placement Temperature	60	°F
Match-cast segment Time of Simulation at Casting	0	hrs
New Segment Time of Simulation at Casting	24	hrs
Concrete Properties		
Cement Content	750.09	lb/yd^3
Activation Energy	24.13	BTU/mol
Heat of Hydration Parameters		
Total Heat Development, $Q_{ult} = \alpha_u \cdot H_u$	111.33	BTU/lb
Time Parameter, τ	13.36	hrs
Curvature Parameter, β	1.49	
Density	3816.577	lb/yd^3
Specific Heat	0.25	BTU/(lb·°F)
Thermal Conductivity	1.557	BTU/(ft·h·°F)
Match-cast segment Elastic Modulus Dev. Parameters		
Final Value	4471.32	ksi
Time Parameter	12.420	hrs
Curvature Parameter	1.068	
New Segment Elastic Modulus Dev. Parameters		
Final Value	14.50	ksi
Time Parameter	n/a	hrs
Curvature Parameter	n/a	
Poisson Ratio	0.17	
Coefficient of Thermal Expansion	4.54	$\mu\varepsilon$/°F
Thermal Boundary Conditions (Applied to Appropriate Faces)		
Ambient Temp	Tallahassee - Winter - Morning - Placement	
Wind	Medium-Wind	7.50	mph
Formwork	Steel Formwork	34.60	BTU/(ft·h·°F)
	Thickness	0.118	in
Curing	Burlap	0.18	BTU/(ft·h·°F)
	Thickness	0.39	in

Figure B-202: Simulation 68 - Bowing distortion of match-cast segment after placement of the new segment
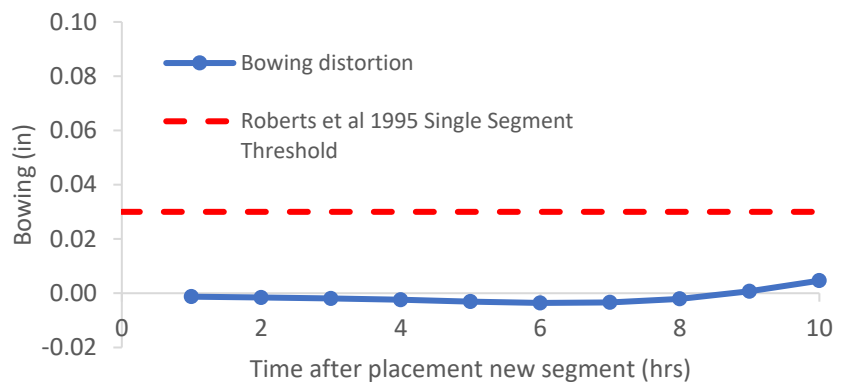

Figure B-203: Simulation 68 - Bowing distortion progression of match-cast segment from time of placement of new segment to 10 hours
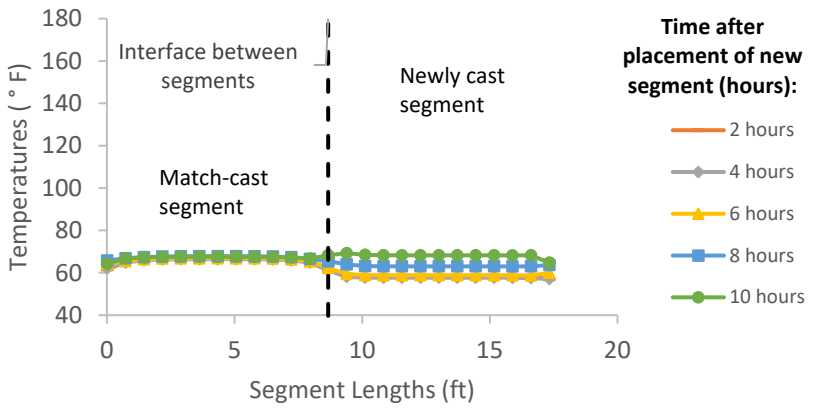

Figure B-204: Simulation 68 - Internal temperatures along the wing of segments

Simulation 69 -Results Summary

Table B-69: Model input parameters simulation 69

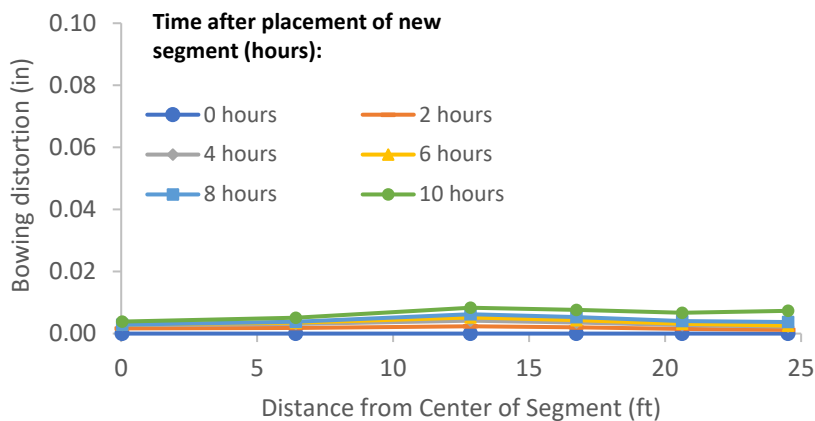| Model details		
Permutation number	69	
Geometry	Florida Bridge C - w/l=10.89	
Max. Mesh Size	3.54	in
Time Step	1	hrs
Placement Temperature	60	°F
Match-cast segment Time of Simulation at Casting	0	hrs
New Segment Time of Simulation at Casting	24	hrs
Concrete Properties		
Cement Content	750.09	lb/yd^3
Activation Energy	24.13	BTU/mol
Heat of Hydration Parameters		
Total Heat Development, $Q_{ult} = \alpha_u \cdot H_u$	111.33	BTU/lb
Time Parameter, τ	13.36	hrs
Curvature Parameter, β	1.49	
Density	3816.577	lb/yd^3
Specific Heat	0.25	BTU/(lb·°F)
Thermal Conductivity	1.557	BTU/(ft·h·°F)
Match-cast segment Elastic Modulus Dev. Parameters		
Final Value	4471.32	ksi
Time Parameter	12.420	hrs
Curvature Parameter	1.068	
New Segment Elastic Modulus Dev. Parameters		
Final Value	14.50	ksi
Time Parameter	n/a	hrs
Curvature Parameter	n/a	
Poisson Ratio	0.17	
Coefficient of Thermal Expansion	4.54	µε/°F
Thermal Boundary Conditions (Applied to Appropriate Faces)		
Ambient Temp	Tallahassee - Winter - Morning - Placement	
Wind	Medium-Wind	7.50	mph
Formwork	Steel Formwork	34.60	BTU/(ft·h·°F)
	Thickness	0.118	in
Curing	Burlap	0.18	BTU/(ft·h·°F)
	Thickness	0.39	in

Figure B-205: Simulation 69 - Bowing distortion of match-cast segment after placement of the new segment
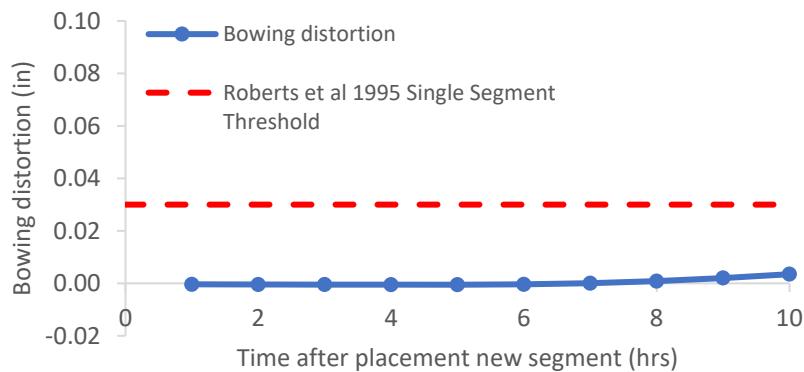

Figure B-206: Simulation 69 - Bowing distortion progression of match-cast segment from time of placement of new segment to 10 hours
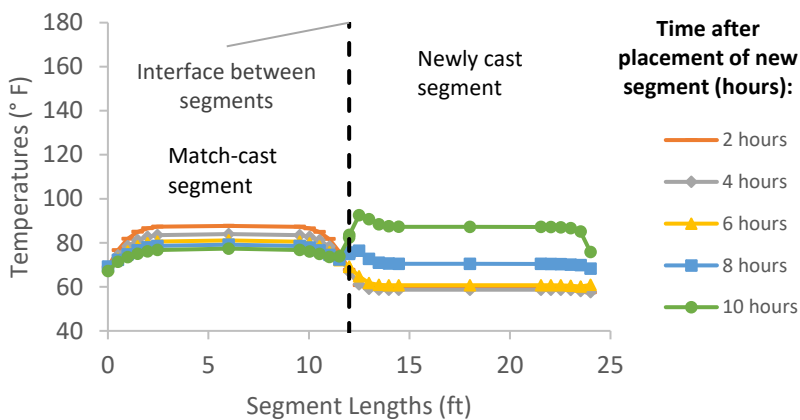

Figure B-207: Simulation 69 - Internal temperatures along the wing of segments

Simulation 70 -Results Summary

Table B-70: Model input parameters simulation 70

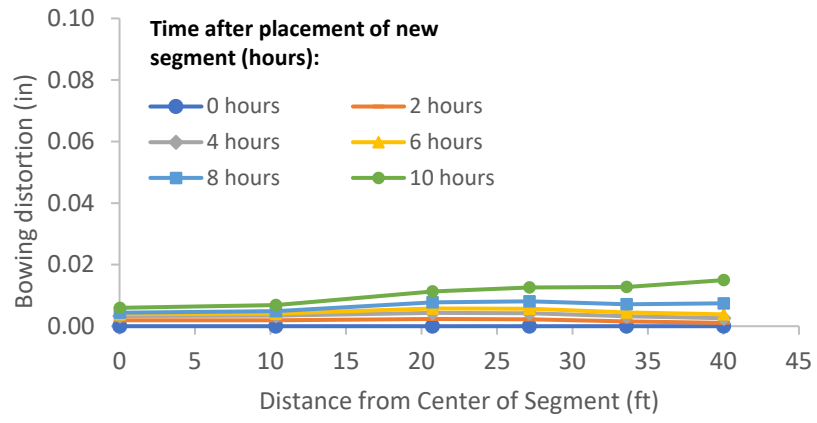| Model details		
Permutation number	70	
Geometry	Florida Bridge E - w/l=4.09	
Max. Mesh Size	2.95	in
Time Step	1	hrs
Placement Temperature	60	°F
Match-cast segment Time of Simulation at Casting	0	hrs
New Segment Time of Simulation at Casting	24	hrs
Concrete Properties		
Cement Content	950.11	lb/yd³
Activation Energy	28.43	BTU/mol
Heat of Hydration Parameters		
Total Heat Development, $Q_{ult} = \alpha_u \cdot H_u$	124.95	BTU/lb
Time Parameter, τ	10.50	hrs
Curvature Parameter, β	1.60	
Density	3880.948	lb/yd³
Specific Heat	0.26	BTU/(lb·°F)
Thermal Conductivity	1.502	BTU/(ft·h·°F)
Match-cast segment Elastic Modulus Dev. Parameters		
Final Value	4584.92	ksi
Time Parameter	12.420	hrs
Curvature Parameter	1.068	
New Segment Elastic Modulus Dev. Parameters		
Final Value	14.50	ksi
Time Parameter	n/a	hrs
Curvature Parameter	n/a	
Poisson Ratio	0.17	
Coefficient of Thermal Expansion	4.54	με/°F
Thermal Boundary Conditions (Applied to Appropriate Faces)		
Ambient Temp	Tallahassee - Winter - Morning - Placement	
Wind	Medium-Wind	7.50	mph
Formwork	Steel Formwork	34.60	BTU/(ft·h·°F)
	Thickness	0.118	in
Curing	Burlap	0.18	BTU/(ft·h·°F)
	Thickness	0.39	in

Figure B-208: Simulation 70 - Bowing distortion of match-cast segment after placement of the new segment
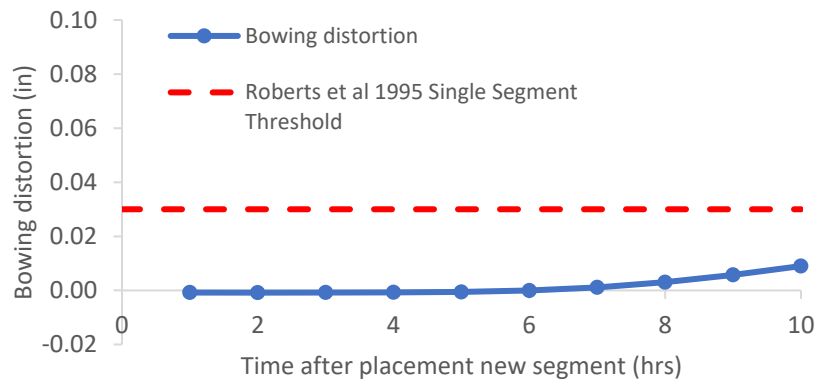

Figure B-209: Simulation 70 - Bowing distortion progression of match-cast segment from time of placement of new segment to 10 hours
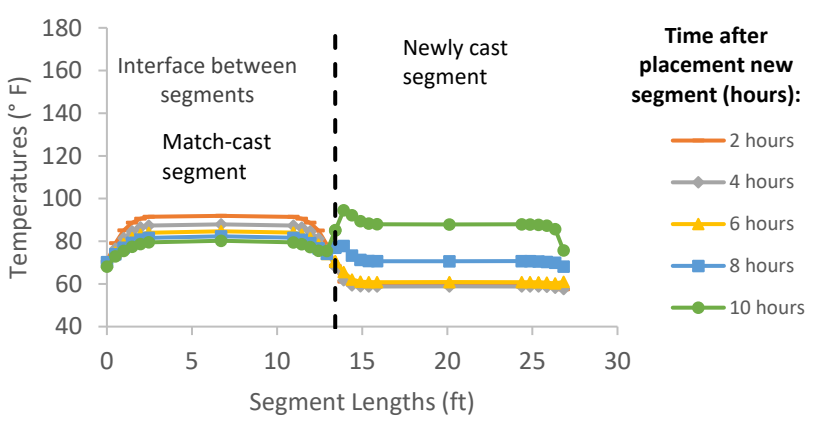

Figure B-210: Simulation 70 - Internal temperatures along the wing of segments

Simulation 71 -Results Summary

Table B-71: Model input parameters simulation 71

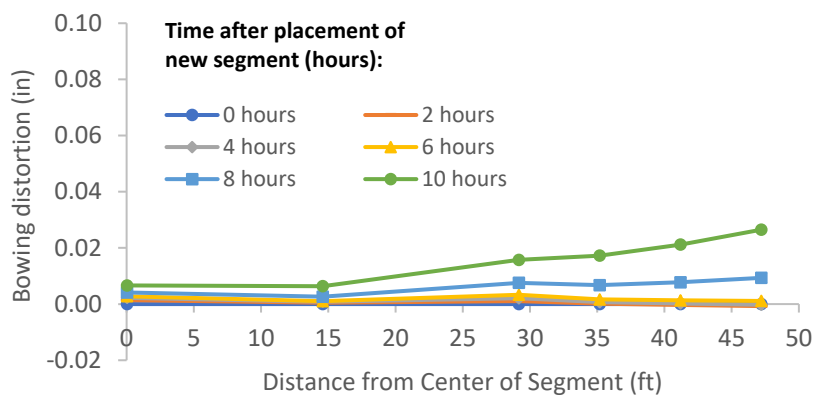| Model details		
Permutation number	71	
Geometry	Florida Bridge B - w/l=5.97	
Max. Mesh Size	3.94	in
Time Step	1	hrs
Placement Temperature	60	°F
Match-cast segment Time of Simulation at Casting	0	hrs
New Segment Time of Simulation at Casting	24	hrs
Concrete Properties		
Cement Content	950.11	lb/yd³
Activation Energy	28.43	BTU/mol
Heat of Hydration Parameters		
Total Heat Development, $Q_{ult} = \alpha_u \cdot H_u$	124.95	BTU/lb
Time Parameter, τ	10.50	hrs
Curvature Parameter, β	1.60	
Density	3880.948	lb/yd³
Specific Heat	0.26	BTU/(lb·°F)
Thermal Conductivity	1.502	BTU/(ft·h·°F)
Match-cast segment Elastic Modulus Dev. Parameters		
Final Value	4584.92	ksi
Time Parameter	12.420	hrs
Curvature Parameter	1.068	
New Segment Elastic Modulus Dev. Parameters		
Final Value	14.50	ksi
Time Parameter	n/a	hrs
Curvature Parameter	n/a	
Poisson Ratio	0.17	
Coefficient of Thermal Expansion	4.54	με/°F
Thermal Boundary Conditions (Applied to Appropriate Faces)		
Ambient Temp	Tallahassee - Winter - Morning - Placement	
Wind	Medium-Wind	7.50	mph
Formwork	Steel Formwork	34.60	BTU/(ft·h·°F)
	Thickness	0.118	in
Curing	Burlap	0.18	BTU/(ft·h·°F)
	Thickness	0.39	in

Figure B-211: Simulation 71 - Bowing distortion of match-cast segment after placement of the new segment
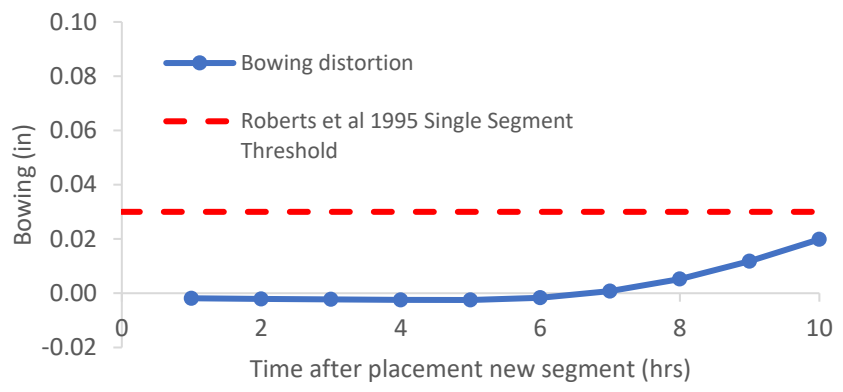

Figure B-212: Simulation 71 - Bowing distortion progression of match-cast segment from time of placement of new segment to 10 hours
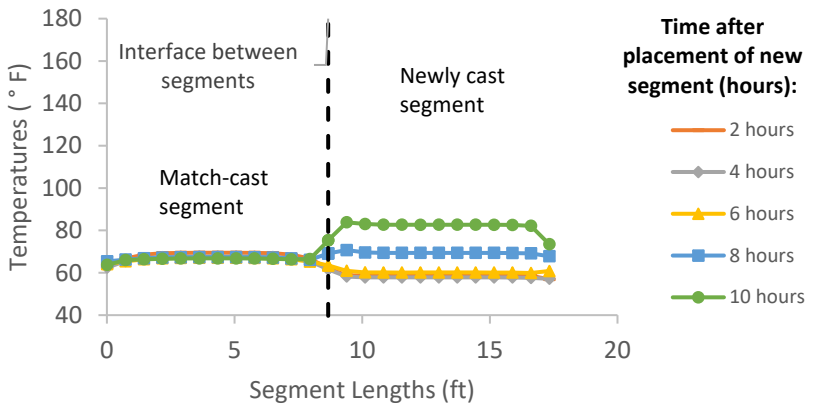

Figure B-213: Simulation 71 - Internal temperatures along the wing of segments

Simulation 72 -Results Summary

Table B-72: Model input parameters simulation 72

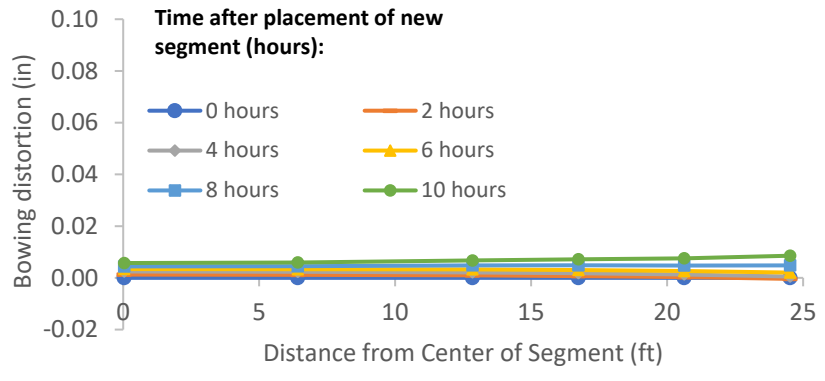| Model details		
Permutation number	72	
Geometry	Florida Bridge C - w/l=10.89	
Max. Mesh Size	3.54	in
Time Step	1	hrs
Placement Temperature	60	°F
Match-cast segment Time of Simulation at Casting	0	hrs
New Segment Time of Simulation at Casting	24	hrs
Concrete Properties		
Cement Content	950.11	lb/yd^3
Activation Energy	28.43	BTU/mol
Heat of Hydration Parameters		
Total Heat Development, $Q_{ult} = \alpha_u \cdot H_u$	124.95	BTU/lb
Time Parameter, τ	10.50	hrs
Curvature Parameter, β	1.60	
Density	3880.948	lb/yd^3
Specific Heat	0.26	BTU/(lb·°F)
Thermal Conductivity	1.502	BTU/(ft·h·°F)
Match-cast segment Elastic Modulus Dev. Parameters		
Final Value	4584.92	ksi
Time Parameter	12.420	hrs
Curvature Parameter	1.068	
New Segment Elastic Modulus Dev. Parameters		
Final Value	14.50	ksi
Time Parameter	n/a	hrs
Curvature Parameter	n/a	
Poisson Ratio	0.17	
Coefficient of Thermal Expansion	4.54	με/°F
Thermal Boundary Conditions (Applied to Appropriate Faces)		
Ambient Temp	Tallahassee - Winter - Morning - Placement	
Wind	Medium-Wind	7.50	mph
Formwork	Steel Formwork	34.60	BTU/(ft·h·°F)
	Thickness	0.118	in
Curing	Burlap	0.18	BTU/(ft·h·°F)
	Thickness	0.39	in

Figure B-214: Simulation 72 - Bowing distortion of match-cast segment after placement of the new segment
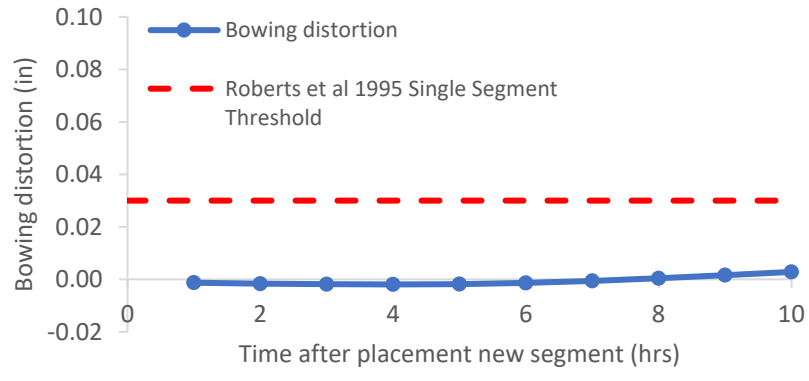

Figure B-215: Simulation 72 - Bowing distortion progression of match-cast segment from time of placement of new segment to 10 hours
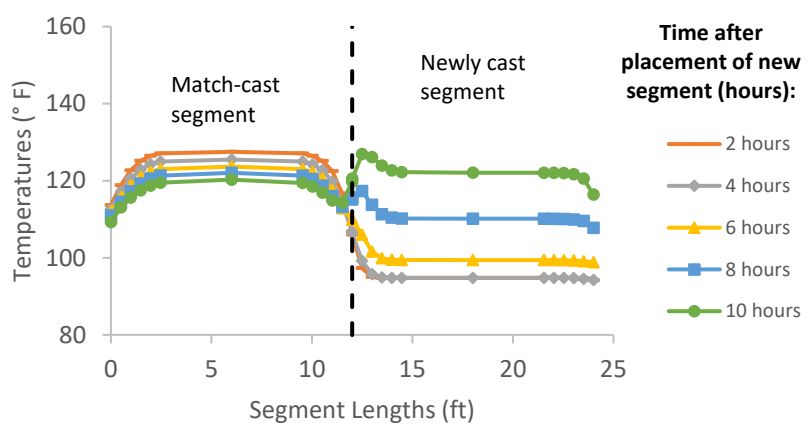

Figure B-216: Simulation 72 - Internal temperatures along the wing of segments

Simulation 73 -Results Summary

Table B-73: Model input parameters simulation 73

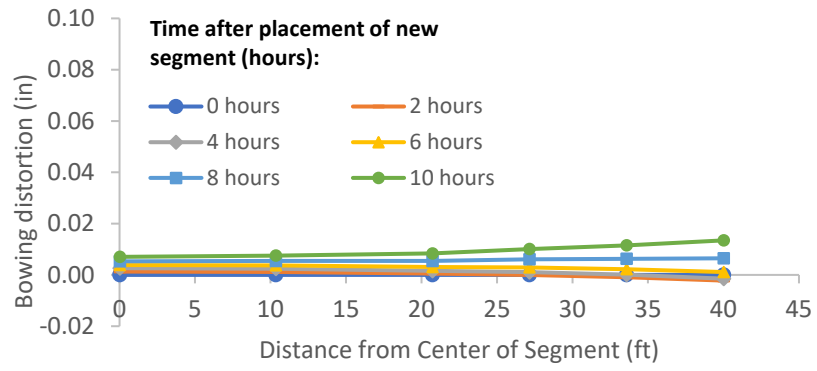| Model details		
Permutation number	73	
Geometry	Florida Bridge E - w/l=4.09	
Max. Mesh Size	2.95	in
Time Step	1	hrs
Placement Temperature	95	°F
Match-cast segment Time of Simulation at Casting	0	hrs
New Segment Time of Simulation at Casting	24	hrs
Concrete Properties		
Cement Content	650.08	lb/yd^3
Activation Energy	26.21	BTU/mol
Heat of Hydration Parameters		
Total Heat Development, $Q_{ult} = \alpha_u \cdot H_u$	107.65	BTU/lb
Time Parameter, τ	18.28	hrs
Curvature Parameter, β	1.65	
Density	3834.891	lb/yd^3
Specific Heat	0.24	BTU/(lb·°F)
Thermal Conductivity	1.608	BTU/(ft·h·°F)
Match-cast segment Elastic Modulus Dev. Parameters		
Final Value	4503.55	ksi
Time Parameter	12.420	hrs
Curvature Parameter	1.068	
New Segment Elastic Modulus Dev. Parameters		
Final Value	14.50	ksi
Time Parameter	n/a	hrs
Curvature Parameter	n/a	
Poisson Ratio	0.17	
Coefficient of Thermal Expansion	4.55	µε/°F
Thermal Boundary Conditions (Applied to Appropriate Faces)		
Ambient Temp	Miami - Summer - Morning - Placement	
Wind	Low-Wind	0.00	mph
Formwork	Steel Formwork	34.60	BTU/(ft·h·°F)
	Thickness	0.118	in
Curing	Burlap	0.18	BTU/(ft·h·°F)
	Thickness	0.39	in

Figure B-217: Simulation 73 - Bowing distortion of match-cast segment after placement of the new segment
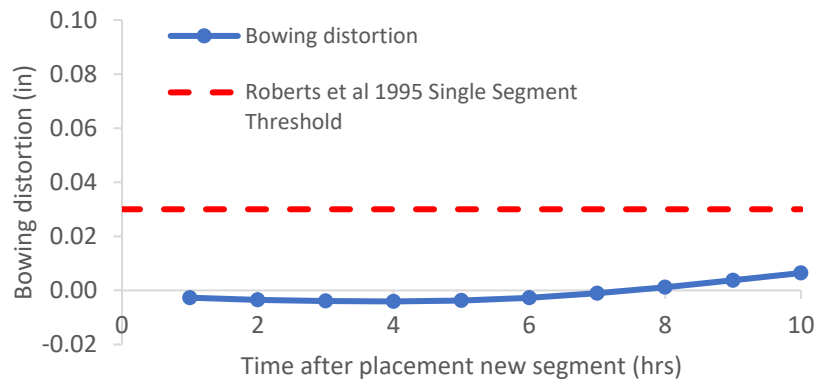

Figure B-218: Simulation 73 - Bowing distortion progression of match-cast segment from time of placement of new segment to 10 hours
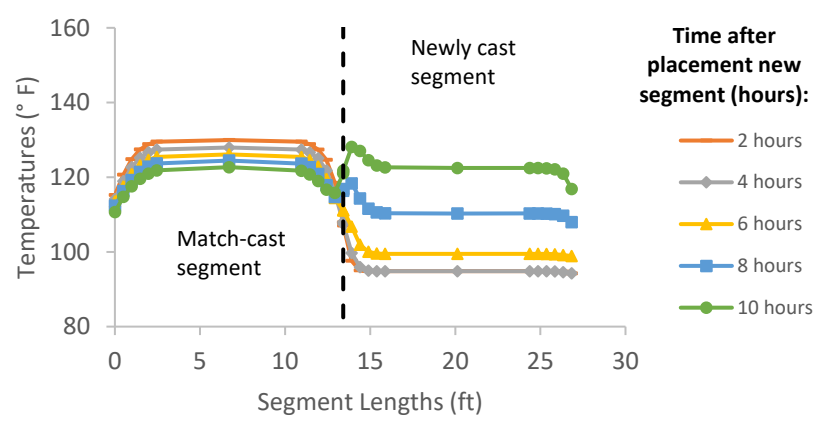

Figure B-219: Simulation 73 - Internal temperatures along the wing of segments

Simulation 74 -Results Summary

Table B-74: Model input parameters simulation 74

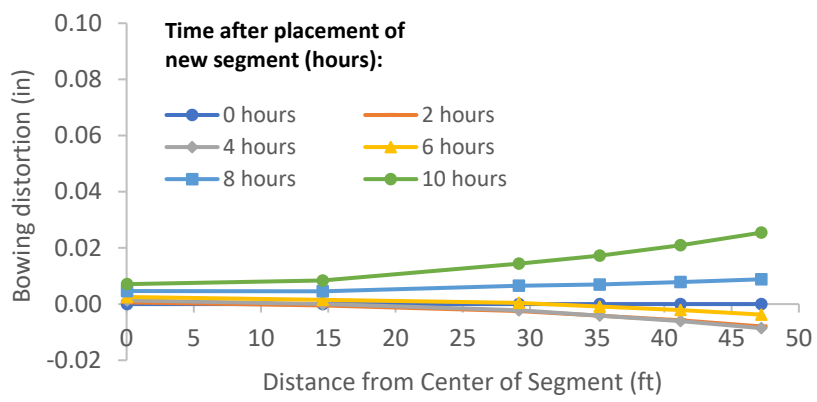| Model details		
Permutation number	74	
Geometry	Florida Bridge B - w/l=5.97	
Max. Mesh Size	3.94	in
Time Step	1	hrs
Placement Temperature	95	°F
Match-cast segment Time of Simulation at Casting	0	hrs
New Segment Time of Simulation at Casting	24	hrs
Concrete Properties		
Cement Content	650.08	lb/yd^3
Activation Energy	26.21	BTU/mol
Heat of Hydration Parameters		
Total Heat Development, $Q_{ult} = \alpha_u \cdot H_u$	107.65	BTU/lb
Time Parameter, τ	18.28	hrs
Curvature Parameter, β	1.65	
Density	3834.891	lb/yd^3
Specific Heat	0.24	BTU/(lb·°F)
Thermal Conductivity	1.608	BTU/(ft·h·°F)
Match-cast segment Elastic Modulus Dev. Parameters		
Final Value	4503.55	ksi
Time Parameter	12.420	hrs
Curvature Parameter	1.068	
New Segment Elastic Modulus Dev. Parameters		
Final Value	14.50	ksi
Time Parameter	n/a	hrs
Curvature Parameter	n/a	
Poisson Ratio	0.17	
Coefficient of Thermal Expansion	4.55	με/°F
Thermal Boundary Conditions (Applied to Appropriate Faces)		
Ambient Temp	Miami - Summer - Morning - Placement	
Wind	Low-Wind	0.00	mph
Formwork	Steel Formwork	34.60	BTU/(ft·h·°F)
	Thickness	0.118	in
Curing	Burlap	0.18	BTU/(ft·h·°F)
	Thickness	0.39	in

Figure B-220: Simulation 74 - Bowing distortion of match-cast segment after placement of the new segment
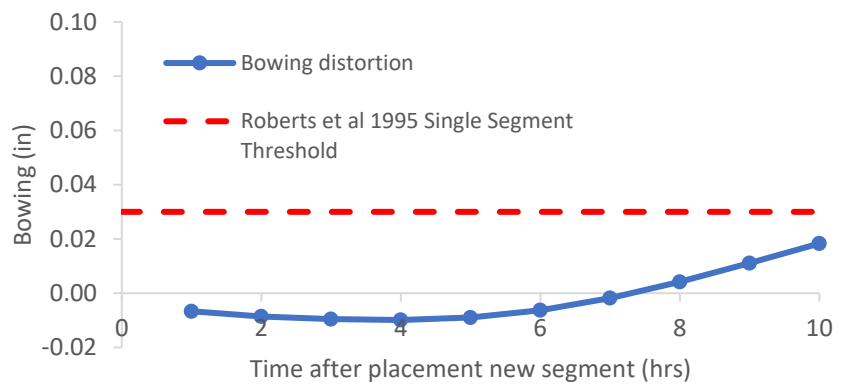

Figure B-221: Simulation 74 - Bowing distortion progression of match-cast segment from time of placement of new segment to 10 hours
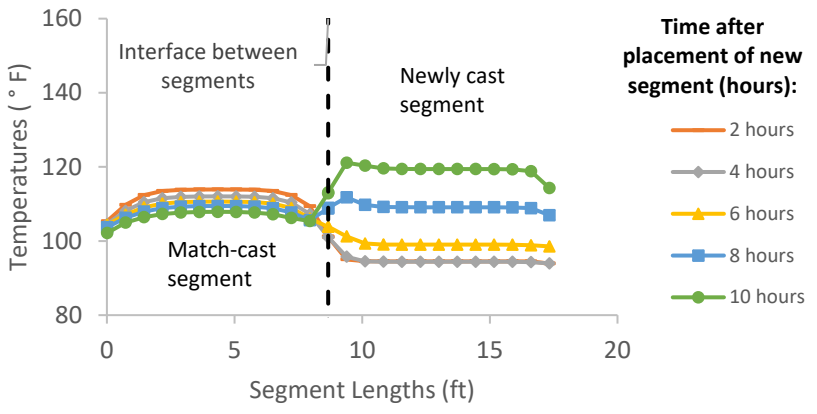

Figure B-222: Simulation 74 - Internal temperatures along the wing of segments

Simulation 75 -Results Summary

Table B-75: Model input parameters simulation 75

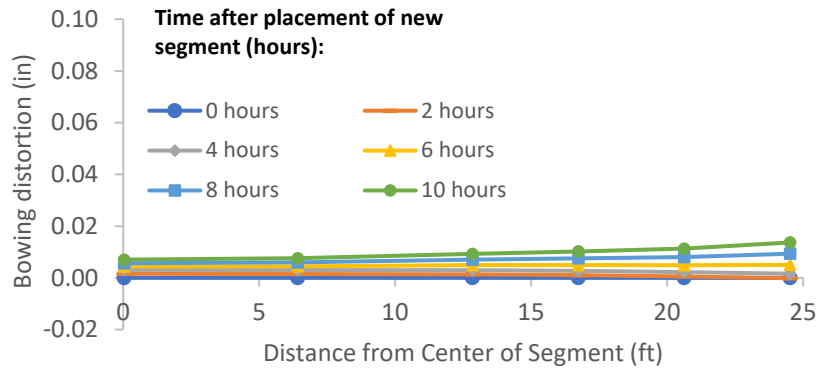| Model details		
Permutation number	75	
Geometry	Florida Bridge C - w/l=10.89	
Max. Mesh Size	3.54	in
Time Step	1	hrs
Placement Temperature	95	°F
Match-cast segment Time of Simulation at Casting	0	hrs
New Segment Time of Simulation at Casting	24	hrs
Concrete Properties		
Cement Content	650.08	lb/yd^3
Activation Energy	26.21	BTU/mol
Heat of Hydration Parameters		
Total Heat Development, $Q_{ult} = \alpha_u \cdot H_u$	107.65	BTU/lb
Time Parameter, τ	18.28	hrs
Curvature Parameter, β	1.65	
Density	3834.891	lb/yd^3
Specific Heat	0.24	BTU/(lb·°F)
Thermal Conductivity	1.608	BTU/(ft·h·°F)
Match-cast segment Elastic Modulus Dev. Parameters		
Final Value	4503.55	ksi
Time Parameter	12.420	hrs
Curvature Parameter	1.068	
New Segment Elastic Modulus Dev. Parameters		
Final Value	14.50	ksi
Time Parameter	n/a	hrs
Curvature Parameter	n/a	
Poisson Ratio	0.17	
Coefficient of Thermal Expansion	4.55	µε/°F
Thermal Boundary Conditions (Applied to Appropriate Faces)		
Ambient Temp	Miami - Summer - Morning - Placement	
Wind	Low-Wind	0.00	mph
Formwork	Steel Formwork	34.60	BTU/(ft·h·°F)
	Thickness	0.118	in
Curing	Burlap	0.18	BTU/(ft·h·°F)
	Thickness	0.39	in

Figure B-223: Simulation 75 - Bowing distortion of match-cast segment after placement of the new segment
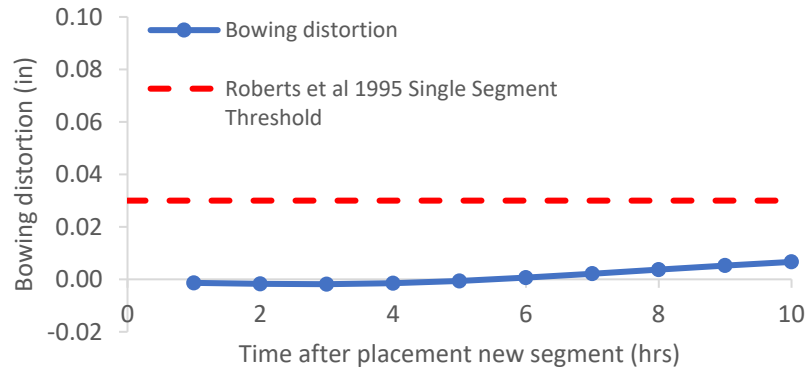

Figure B-224: Simulation 75 - Bowing distortion progression of match-cast segment from time of placement of new segment to 10 hours
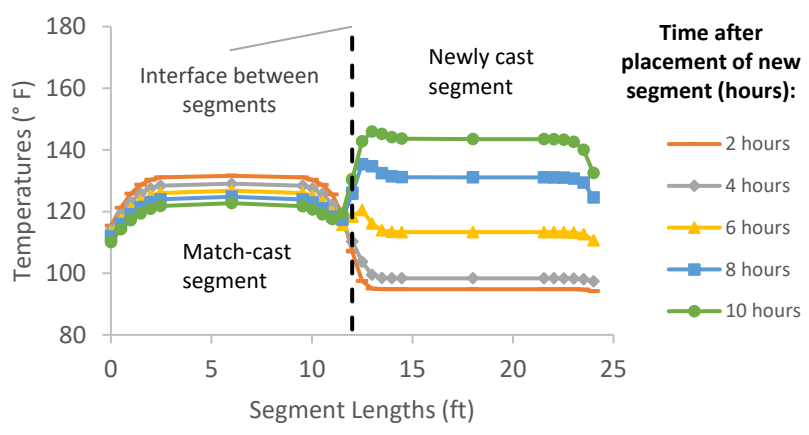

Figure B-225: Simulation 75 - Internal temperatures along the wing of segments

Simulation 76 -Results Summary

Table B-76: Model input parameters simulation 76

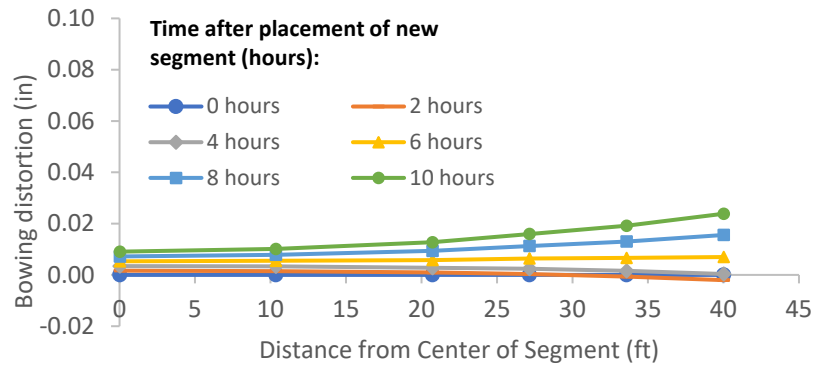| Model details		
Permutation number	76	
Geometry	Florida Bridge E - w/l=4.09	
Max. Mesh Size	2.95	in
Time Step	1	hrs
Placement Temperature	95	°F
Match-cast segment Time of Simulation at Casting	0	hrs
New Segment Time of Simulation at Casting	24	hrs
Concrete Properties		
Cement Content	750.09	lb/yd^3
Activation Energy	24.13	BTU/mol
Heat of Hydration Parameters		
Total Heat Development, $Q_{ult} = \alpha_u \cdot H_u$	111.33	BTU/lb
Time Parameter, τ	13.36	hrs
Curvature Parameter, β	1.49	
Density	3816.577	lb/yd^3
Specific Heat	0.25	BTU/(lb·°F)
Thermal Conductivity	1.557	BTU/(ft·h·°F)
Match-cast segment Elastic Modulus Dev. Parameters		
Final Value	4471.32	ksi
Time Parameter	12.420	hrs
Curvature Parameter	1.068	
New Segment Elastic Modulus Dev. Parameters		
Final Value	14.50	ksi
Time Parameter	n/a	hrs
Curvature Parameter	n/a	
Poisson Ratio	0.17	
Coefficient of Thermal Expansion	4.54	με/°F
Thermal Boundary Conditions (Applied to Appropriate Faces)		
Ambient Temp	Miami - Summer - Morning - Placement	
Wind	Low-Wind	0.00	mph
Formwork	Steel Formwork	34.60	BTU/(ft·h·°F)
	Thickness	0.118	in
Curing	Burlap	0.18	BTU/(ft·h·°F)
	Thickness	0.39	in

Figure B-226: Simulation 76 - Bowing distortion of match-cast segment after placement of the new segment
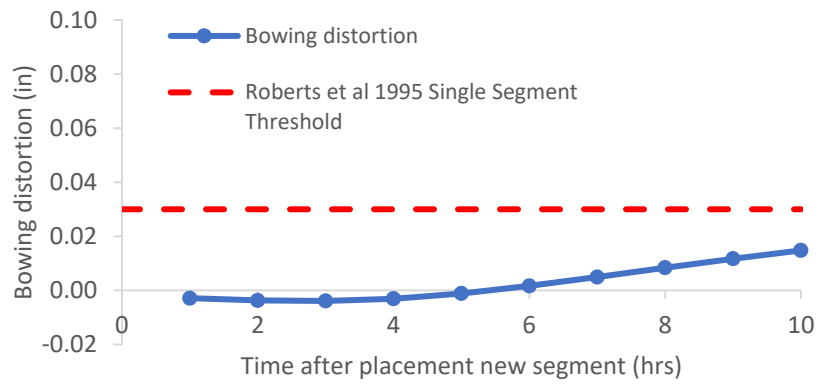

Figure B-227: Simulation 76 - Bowing distortion progression of match-cast segment from time of placement of new segment to 10 hours
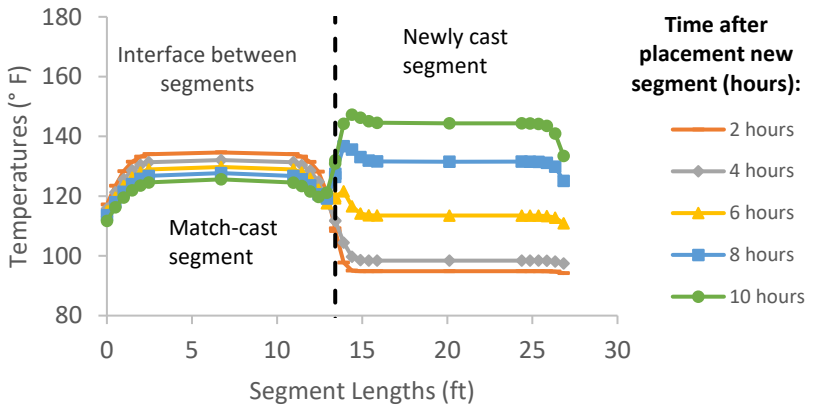

Figure B-228: Simulation 76 - Internal temperatures along the wing of segments

Simulation 77 -Results Summary

Table B-77: Model input parameters simulation 77

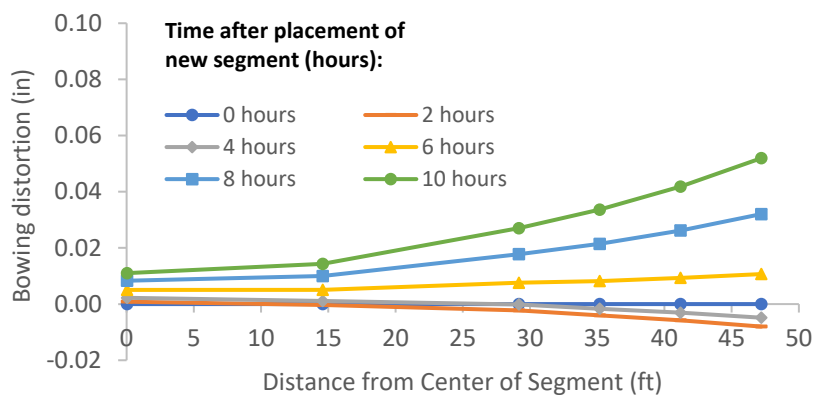| Model details		
Permutation number	77	
Geometry	Florida Bridge B - w/l=5.97	
Max. Mesh Size	3.94	in
Time Step	1	hrs
Placement Temperature	95	°F
Match-cast segment Time of Simulation at Casting	0	hrs
New Segment Time of Simulation at Casting	24	hrs
Concrete Properties		
Cement Content	750.09	lb/yd^3
Activation Energy	24.13	BTU/mol
Heat of Hydration Parameters		
Total Heat Development, $Q_{ult} = \alpha_u \cdot H_u$	111.33	BTU/lb
Time Parameter, τ	13.36	hrs
Curvature Parameter, β	1.49	
Density	3816.577	lb/yd^3
Specific Heat	0.25	BTU/(lb·°F)
Thermal Conductivity	1.557	BTU/(ft·h·°F)
Match-cast segment Elastic Modulus Dev. Parameters		
Final Value	4471.32	ksi
Time Parameter	12.420	hrs
Curvature Parameter	1.068	
New Segment Elastic Modulus Dev. Parameters		
Final Value	14.50	ksi
Time Parameter	n/a	hrs
Curvature Parameter	n/a	
Poisson Ratio	0.17	
Coefficient of Thermal Expansion	4.54	με/°F
Thermal Boundary Conditions (Applied to Appropriate Faces)		
Ambient Temp	Miami - Summer - Morning - Placement	
Wind	Low-Wind	0.00	mph
Formwork	Steel Formwork	34.60	BTU/(ft·h·°F)
	Thickness	0.118	in
Curing	Burlap	0.18	BTU/(ft·h·°F)
	Thickness	0.39	in

Figure B-229: Simulation 77 - Bowing distortion of match-cast segment after placement of the new segment
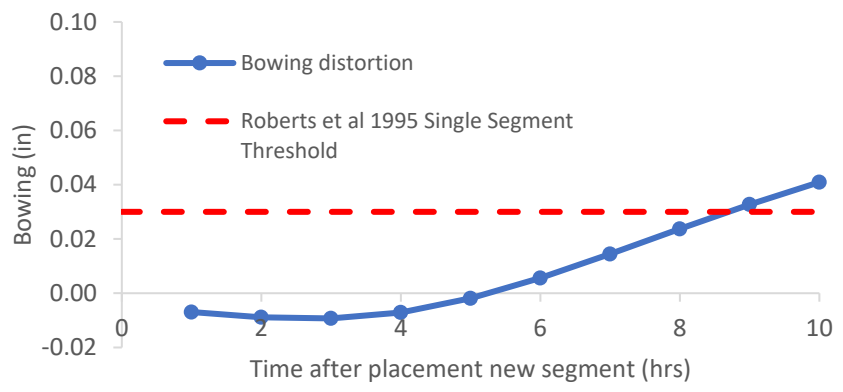

Figure B-230: Simulation 77 - Bowing distortion progression of match-cast segment from time of placement of new segment to 10 hours

Figure B-231: Simulation 77 - Internal temperatures along the wing of segments

Simulation 78 -Results Summary

Table B-78: Model input parameters simulation 78

Model details		
Permutation number	78	
Geometry	Florida Bridge C - w/l=10.89	
Max. Mesh Size	3.54	in
Time Step	1	hrs
Placement Temperature	95	°F
Match-cast segment Time of Simulation at Casting	0	hrs
New Segment Time of Simulation at Casting	24	hrs
Concrete Properties		
Cement Content	750.09	lb/yd^3
Activation Energy	24.13	BTU/mol
Heat of Hydration Parameters		
Total Heat Development, $Q_{ult} = \alpha_u \cdot H_u$	111.33	BTU/lb
Time Parameter, τ	13.36	hrs
Curvature Parameter, β	1.49	
Density	3816.577	lb/yd^3
Specific Heat	0.25	BTU/(lb·°F)
Thermal Conductivity	1.557	BTU/(ft·h·°F)
Match-cast segment Elastic Modulus Dev. Parameters		
Final Value	4471.32	ksi
Time Parameter	12.420	hrs
Curvature Parameter	1.068	
New Segment Elastic Modulus Dev. Parameters		
Final Value	14.50	ksi
Time Parameter	n/a	hrs
Curvature Parameter	n/a	
Poisson Ratio	0.17	
Coefficient of Thermal Expansion	4.54	µε/°F
Thermal Boundary Conditions (Applied to Appropriate Faces)		
Ambient Temp	Miami - Summer - Morning - Placement	
Wind	Low-Wind	0.00	mph
Formwork	Steel Formwork	34.60	BTU/(ft·h·°F)
	Thickness	0.118	in
Curing	Burlap	0.18	BTU/(ft·h·°F)
	Thickness	0.39	in

Figure B-232: Simulation 78 - Bowing distortion of match-cast segment after placement of the new segment

Figure B-233: Simulation 78 - Bowing distortion progression of match-cast segment from time of placement of new segment to 10 hours
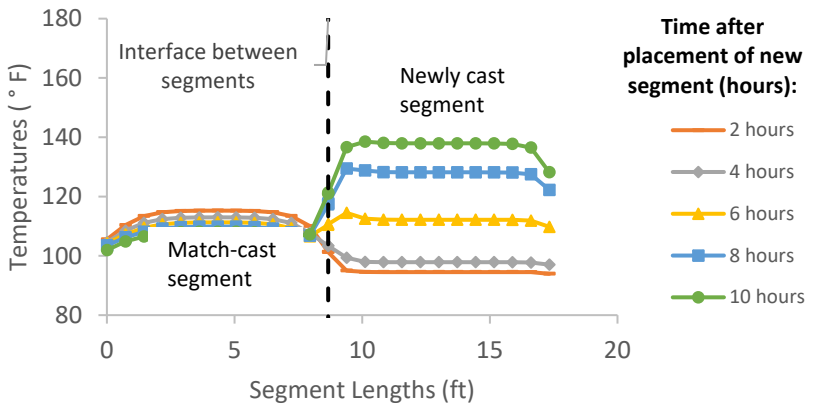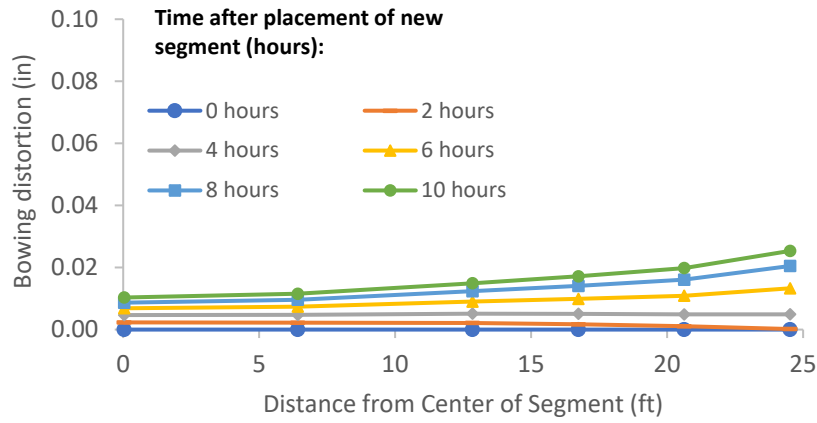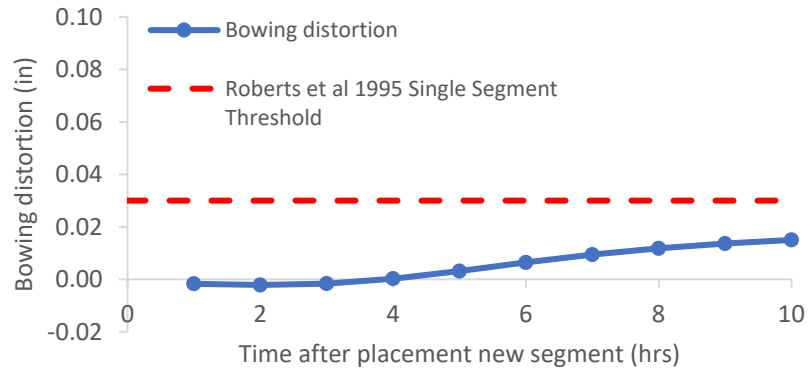

Figure B-234: Simulation 78 - Internal temperatures along the wing of segments

Simulation 79 -Results Summary

Table B-79: Model input parameters simulation 79

Model details		
Permutation number	79	
Geometry	Florida Bridge E - w/l=4.09	
Max. Mesh Size	2.95	in
Time Step	1	hrs
Placement Temperature	95	°F
Match-cast segment Time of Simulation at Casting	0	hrs
New Segment Time of Simulation at Casting	24	hrs
Concrete Properties		
Cement Content	950.11	lb/yd^3
Activation Energy	28.43	BTU/mol
Heat of Hydration Parameters		
Total Heat Development, $Q_{ult} = \alpha_u \cdot H_u$	124.95	BTU/lb
Time Parameter, τ	10.50	hrs
Curvature Parameter, β	1.60	
Density	3880.948	lb/yd^3
Specific Heat	0.26	BTU/(lb·°F)
Thermal Conductivity	1.502	BTU/(ft·h·°F)
Match-cast segment Elastic Modulus Dev. Parameters		
Final Value	4584.92	ksi
Time Parameter	12.420	hrs
Curvature Parameter	1.068	
New Segment Elastic Modulus Dev. Parameters		
Final Value	14.50	ksi
Time Parameter	n/a	hrs
Curvature Parameter	n/a	
Poisson Ratio	0.17	
Coefficient of Thermal Expansion	4.54	με/°F
Thermal Boundary Conditions (Applied to Appropriate Faces)		
Ambient Temp	Miami - Summer - Morning - Placement	
Wind	Low-Wind	0.00	mph
Formwork	Steel Formwork	34.60	BTU/(ft·h·°F)
	Thickness	0.118	in
Curing	Burlap	0.18	BTU/(ft·h·°F)
	Thickness	0.39	in

Figure B-235: Simulation 79 - Bowing distortion of match-cast segment after placement of the new segment

Figure B-236: Simulation 79 - Bowing distortion progression of match-cast segment from time of placement of new segment to 10 hours
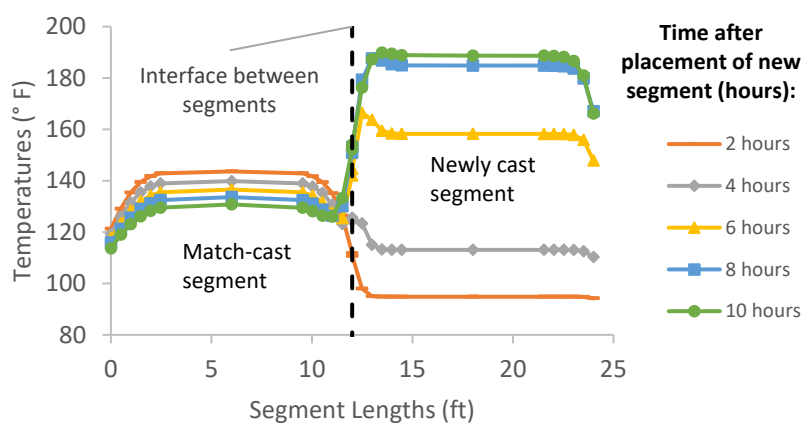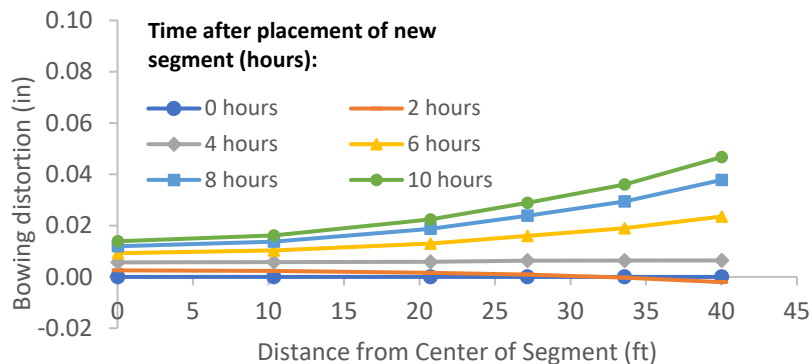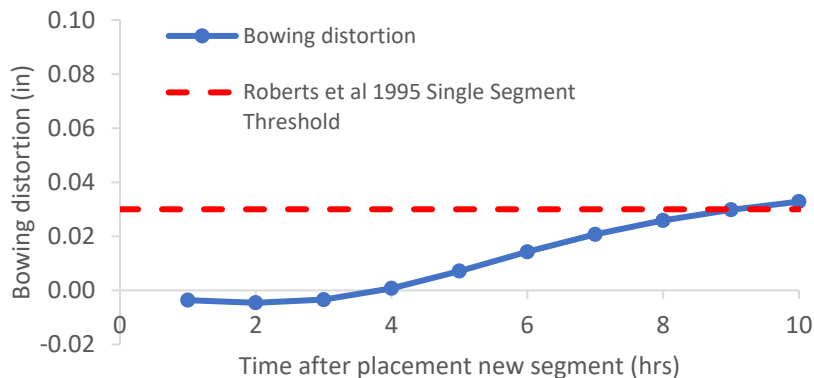

Figure B-237: Simulation 79 - Internal temperatures along the wing of segments

Simulation 80 -Results Summary

Table B-80: Model input parameters simulation 80

Model details		
Permutation number	80	
Geometry	Florida Bridge B - w/l=5.97	
Max. Mesh Size	3.94	in
Time Step	1	hrs
Placement Temperature	95	°F
Match-cast segment Time of Simulation at Casting	0	hrs
New Segment Time of Simulation at Casting	24	hrs
Concrete Properties		
Cement Content	950.11	lb/yd^3
Activation Energy	28.43	BTU/mol
Heat of Hydration Parameters		
Total Heat Development, $Q_{ult} = \alpha_u \cdot H_u$	124.95	BTU/lb
Time Parameter, τ	10.50	hrs
Curvature Parameter, β	1.60	
Density	3880.948	lb/yd^3
Specific Heat	0.26	BTU/(lb·°F)
Thermal Conductivity	1.502	BTU/(ft·h·°F)
Match-cast segment Elastic Modulus Dev. Parameters		
Final Value	4584.92	ksi
Time Parameter	12.420	hrs
Curvature Parameter	1.068	
New Segment Elastic Modulus Dev. Parameters		
Final Value	14.50	ksi
Time Parameter	n/a	hrs
Curvature Parameter	n/a	
Poisson Ratio	0.17	
Coefficient of Thermal Expansion	4.54	με/°F
Thermal Boundary Conditions (Applied to Appropriate Faces)		
Ambient Temp	Miami - Summer - Morning - Placement	
Wind	Low-Wind	0.00	mph
Formwork	Steel Formwork	34.60	BTU/(ft·h·°F)
	Thickness	0.118	in
Curing	Burlap	0.18	BTU/(ft·h·°F)
	Thickness	0.39	in

Figure B-238: Simulation 80 - Bowing distortion of match-cast segment after placement of the new segment

Figure B-239: Simulation 80 - Bowing distortion progression of match-cast segment from time of placement of new segment to 10 hours
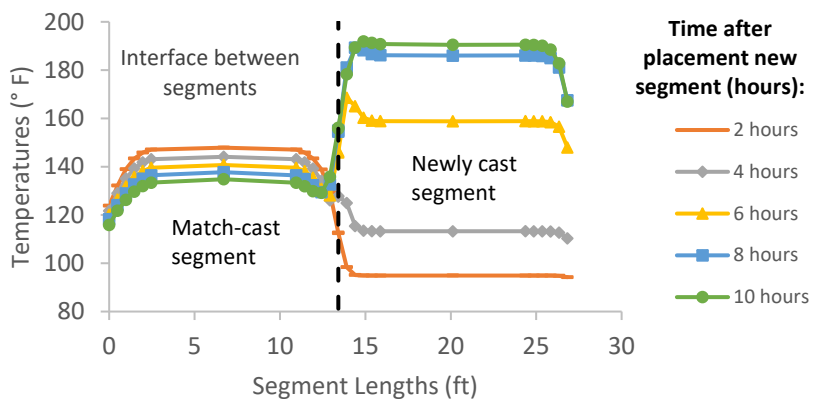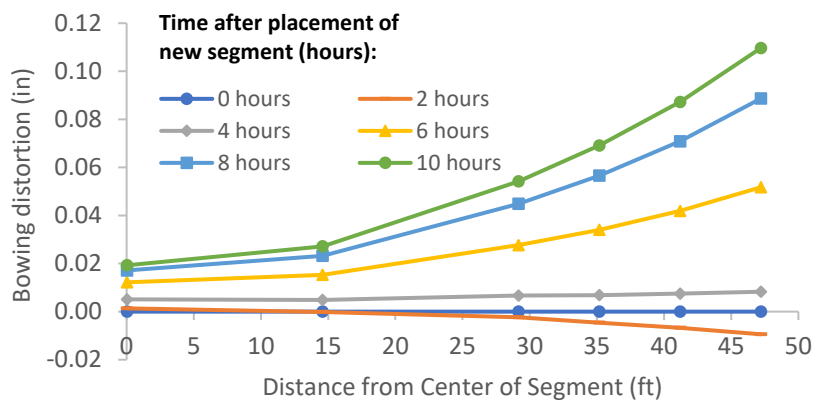

Figure B-240: Simulation 80 - Internal temperatures along the wing of segments

Simulation 81 -Results Summary

Table B-81: Model input parameters simulation 81

Model details		
Permutation number	81	
Geometry	Florida Bridge C - w/l=10.89	
Max. Mesh Size	3.54	in
Time Step	1	hrs
Placement Temperature	95	°F
Match-cast segment Time of Simulation at Casting	0	hrs
New Segment Time of Simulation at Casting	24	hrs
Concrete Properties		
Cement Content	950.11	lb/yd^3
Activation Energy	28.43	BTU/mol
Heat of Hydration Parameters		
Total Heat Development, $Q_{ult} = \alpha_u \cdot H_u$	124.95	BTU/lb
Time Parameter, τ	10.50	hrs
Curvature Parameter, β	1.60	
Density	3880.948	lb/yd^3
Specific Heat	0.26	BTU/(lb·°F)
Thermal Conductivity	1.502	BTU/(ft·h·°F)
Match-cast segment Elastic Modulus Dev. Parameters		
Final Value	4584.92	ksi
Time Parameter	12.420	hrs
Curvature Parameter	1.068	
New Segment Elastic Modulus Dev. Parameters		
Final Value	14.50	ksi
Time Parameter	n/a	hrs
Curvature Parameter	n/a	
Poisson Ratio	0.17	
Coefficient of Thermal Expansion	4.54	µε/°F
Thermal Boundary Conditions (Applied to Appropriate Faces)		
Ambient Temp	Miami - Summer - Morning - Placement	
Wind	Low-Wind	0.00	mph
Formwork	Steel Formwork	34.60	BTU/(ft·h·°F)
	Thickness	0.118	in
Curing	Burlap	0.18	BTU/(ft·h·°F)
	Thickness	0.39	in

Figure B-241: Simulation 81 - Bowing distortion of match-cast segment after placement of the new segment
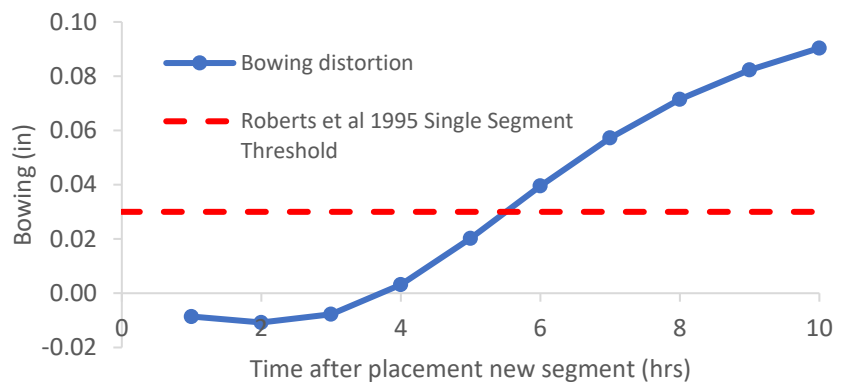

Figure B-242: Simulation 81 - Bowing distortion progression of match-cast segment from time of placement of new segment to 10 hours
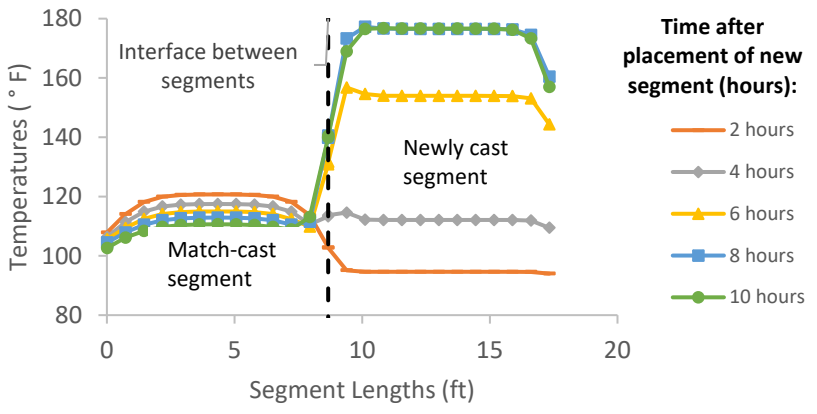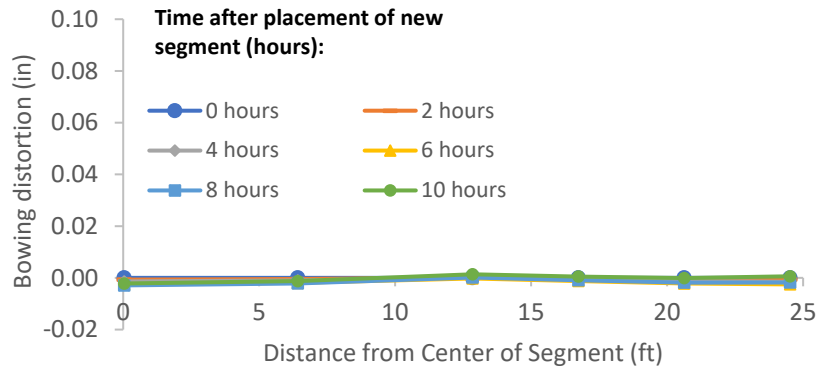

Figure B-243: Simulation 81 - Internal temperatures along the wing of segments

Simulation 82 -Results Summary

Table B-82: Model input parameters simulation 82

Model details		
Permutation number	82	
Geometry	Florida Bridge E - w/l=4.09	
Max. Mesh Size	2.95	in
Time Step	1	hrs
Placement Temperature	95	°F
Match-cast segment Time of Simulation at Casting	0	hrs
New Segment Time of Simulation at Casting	24	hrs
Concrete Properties		
Cement Content	650.08	lb/yd^3
Activation Energy	26.21	BTU/mol
Heat of Hydration Parameters		
Total Heat Development, $Q_{ult} = \alpha_u \cdot H_u$	107.65	BTU/lb
Time Parameter, τ	18.28	hrs
Curvature Parameter, β	1.65	
Density	3834.891	lb/yd^3
Specific Heat	0.24	BTU/(lb·°F)
Thermal Conductivity	1.608	BTU/(ft·h·°F)
Match-cast segment Elastic Modulus Dev. Parameters		
Final Value	4503.55	ksi
Time Parameter	12.420	hrs
Curvature Parameter	1.068	
New Segment Elastic Modulus Dev. Parameters		
Final Value	14.50	ksi
Time Parameter	n/a	hrs
Curvature Parameter	n/a	
Poisson Ratio	0.17	
Coefficient of Thermal Expansion	4.55	με/°F
Thermal Boundary Conditions (Applied to Appropriate Faces)		
Ambient Temp	Miami - Summer - Morning - Placement	
Wind	High-Wind	15.00	mph
Formwork	Steel Formwork	34.60	BTU/(ft·h·°F)
	Thickness	0.118	in
Curing	Burlap	0.18	BTU/(ft·h·°F)
	Thickness	0.39	in

Figure B-244: Simulation 82 - Bowing distortion of match-cast segment after placement of the new segment
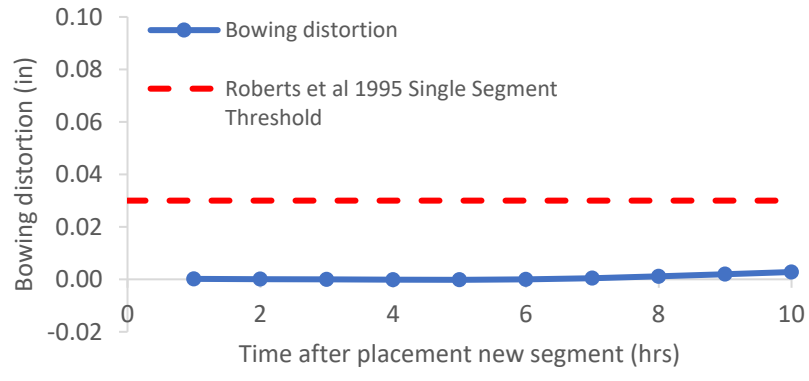

Figure B-245: Simulation 82 - Bowing distortion progression of match-cast segment from time of placement of new segment to 10 hours
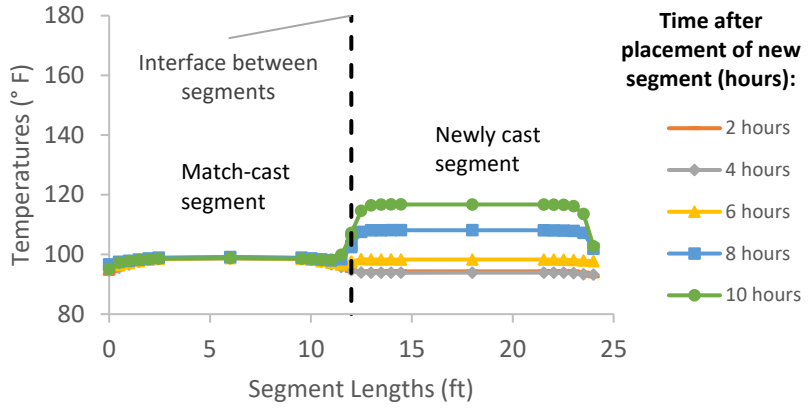

Figure B-246: Simulation 82 - Internal temperatures along the wing of segments

Simulation 83 -Results Summary

Table B-83: Model input parameters simulation 83

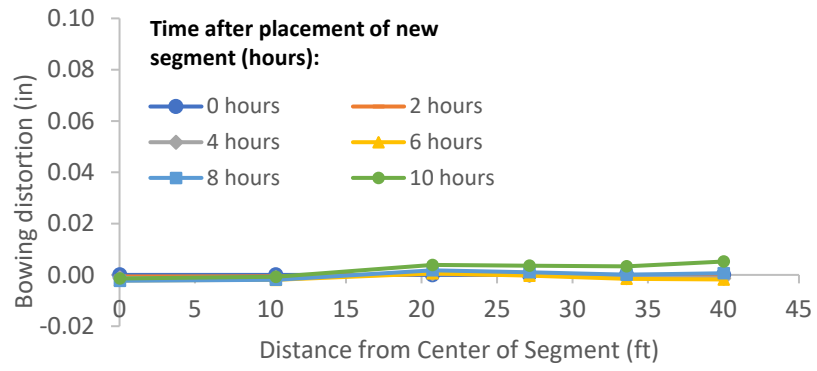| Model details		
Permutation number	83	
Geometry	Florida Bridge B - w/l=5.97	
Max. Mesh Size	3.94	in
Time Step	1	hrs
Placement Temperature	95	°F
Match-cast segment Time of Simulation at Casting	0	hrs
New Segment Time of Simulation at Casting	24	hrs
Concrete Properties		
Cement Content	650.08	lb/yd^3
Activation Energy	26.21	BTU/mol
Heat of Hydration Parameters		
Total Heat Development, $Q_{ult} = \alpha_u \cdot H_u$	107.65	BTU/lb
Time Parameter, τ	18.28	hrs
Curvature Parameter, β	1.65	
Density	3834.891	lb/yd^3
Specific Heat	0.24	BTU/(lb·°F)
Thermal Conductivity	1.608	BTU/(ft·h·°F)
Match-cast segment Elastic Modulus Dev. Parameters		
Final Value	4503.55	ksi
Time Parameter	12.420	hrs
Curvature Parameter	1.068	
New Segment Elastic Modulus Dev. Parameters		
Final Value	14.50	ksi
Time Parameter	n/a	hrs
Curvature Parameter	n/a	
Poisson Ratio	0.17	
Coefficient of Thermal Expansion	4.55	με/°F
Thermal Boundary Conditions (Applied to Appropriate Faces)		
Ambient Temp	Miami - Summer - Morning - Placement	
Wind	High-Wind	15.00	mph
Formwork	Steel Formwork	34.60	BTU/(ft·h·°F)
	Thickness	0.118	in
Curing	Burlap	0.18	BTU/(ft·h·°F)
	Thickness	0.39	in

Figure B-247: Simulation 83 - Bowing distortion of match-cast segment after placement of the new segment
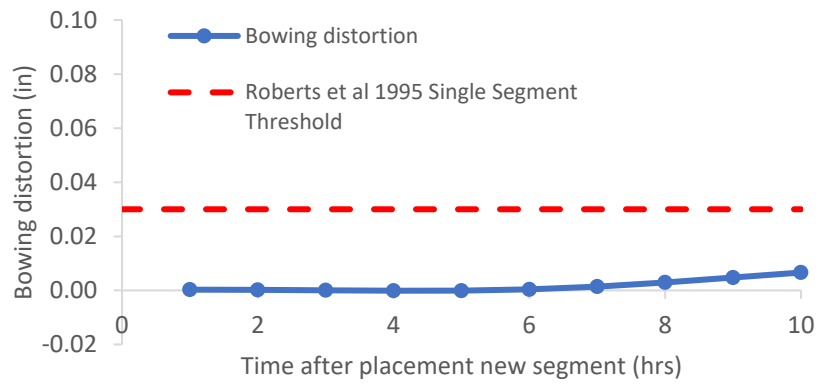

Figure B-248: Simulation 83 - Bowing distortion progression of match-cast segment from time of placement of new segment to 10 hours
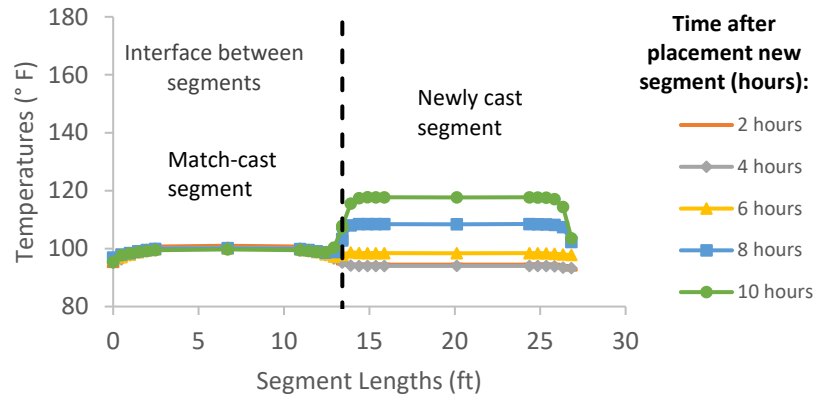

Figure B-249: Simulation 83 - Internal temperatures along the wing of segments

Simulation 84 -Results Summary

Table B-84: Model input parameters simulation 84

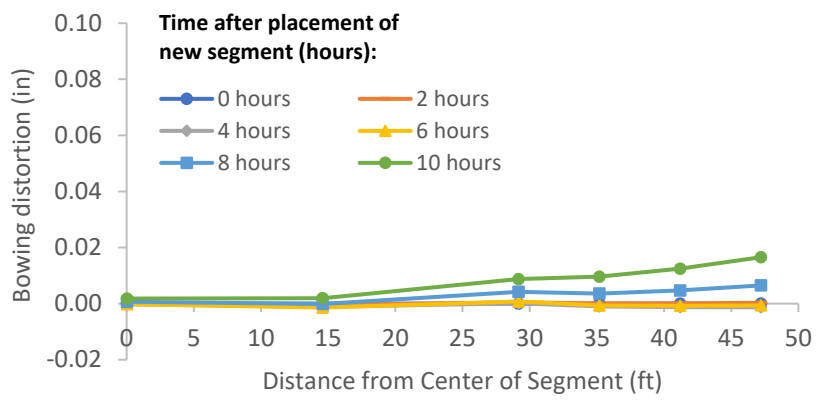| Model details		
Permutation number	84	
Geometry	Florida Bridge C - w/l=10.89	
Max. Mesh Size	3.54	in
Time Step	1	hrs
Placement Temperature	95	°F
Match-cast segment Time of Simulation at Casting	0	hrs
New Segment Time of Simulation at Casting	24	hrs
Concrete Properties		
Cement Content	650.08	lb/yd³
Activation Energy	26.21	BTU/mol
Heat of Hydration Parameters		
Total Heat Development, $Q_{ult} = \alpha_u \cdot H_u$	107.65	BTU/lb
Time Parameter, τ	18.28	hrs
Curvature Parameter, β	1.65	
Density	3834.891	lb/yd³
Specific Heat	0.24	BTU/(lb·°F)
Thermal Conductivity	1.608	BTU/(ft·h·°F)
Match-cast segment Elastic Modulus Dev. Parameters		
Final Value	4503.55	ksi
Time Parameter	12.420	hrs
Curvature Parameter	1.068	
New Segment Elastic Modulus Dev. Parameters		
Final Value	14.50	ksi
Time Parameter	n/a	hrs
Curvature Parameter	n/a	
Poisson Ratio	0.17	
Coefficient of Thermal Expansion	4.55	με/°F
Thermal Boundary Conditions (Applied to Appropriate Faces)		
Ambient Temp	Miami - Summer - Morning - Placement	
Wind	High-Wind	15.00	mph
Formwork	Steel Formwork	34.60	BTU/(ft·h·°F)
	Thickness	0.118	in
Curing	Burlap	0.18	BTU/(ft·h·°F)
	Thickness	0.39	in

Figure B-250: Simulation 84 - Bowing distortion of match-cast segment after placement of the new segment
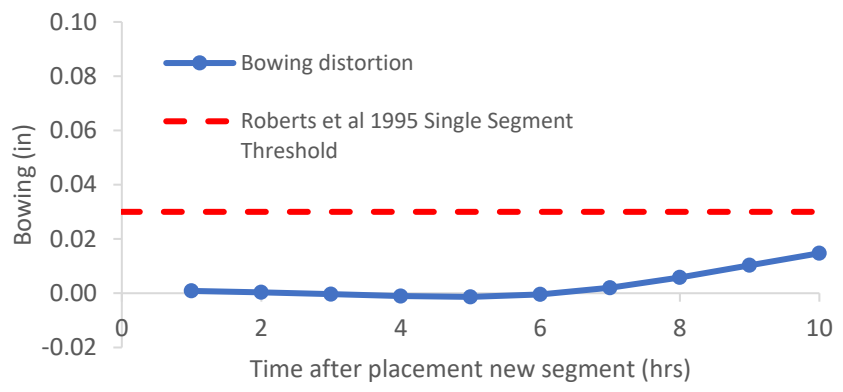

Figure B-251: Simulation 84 - Bowing distortion progression of match-cast segment from time of placement of new segment to 10 hours
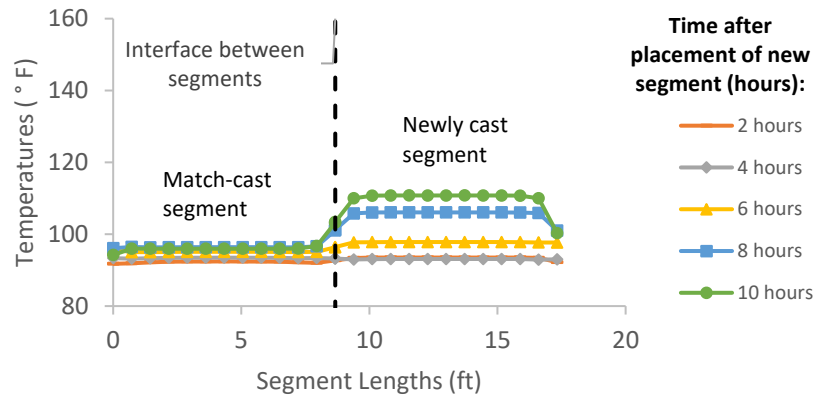

Figure B-252: Simulation 84 - Internal temperatures along the wing of segments

Simulation 85 -Results Summary

Table B-85: Model input parameters simulation 85

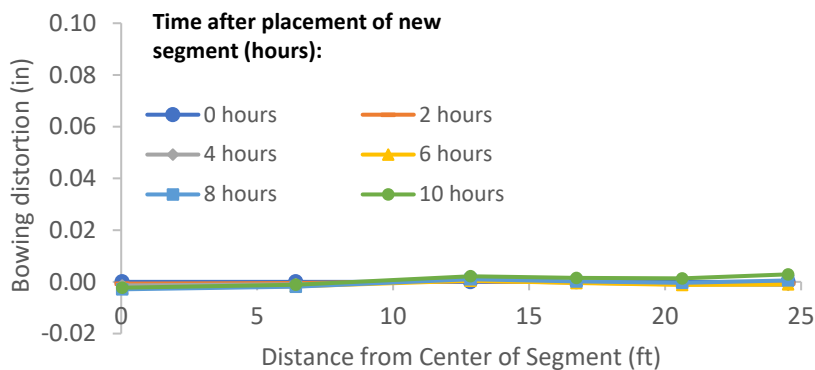| Model details		
Permutation number	85	
Geometry	Florida Bridge E - w/l=4.09	
Max. Mesh Size	2.95	in
Time Step	1	hrs
Placement Temperature	95	°F
Match-cast segment Time of Simulation at Casting	0	hrs
New Segment Time of Simulation at Casting	24	hrs
Concrete Properties		
Cement Content	750.09	lb/yd^3
Activation Energy	24.13	BTU/mol
Heat of Hydration Parameters		
Total Heat Development, $Q_{ult} = \alpha_u \cdot H_u$	111.33	BTU/lb
Time Parameter, τ	13.36	hrs
Curvature Parameter, β	1.49	
Density	3816.577	lb/yd^3
Specific Heat	0.25	BTU/(lb·°F)
Thermal Conductivity	1.557	BTU/(ft·h·°F)
Match-cast segment Elastic Modulus Dev. Parameters		
Final Value	4471.32	ksi
Time Parameter	12.420	hrs
Curvature Parameter	1.068	
New Segment Elastic Modulus Dev. Parameters		
Final Value	14.50	ksi
Time Parameter	n/a	hrs
Curvature Parameter	n/a	
Poisson Ratio	0.17	
Coefficient of Thermal Expansion	4.54	με/°F
Thermal Boundary Conditions (Applied to Appropriate Faces)		
Ambient Temp	Miami - Summer - Morning - Placement		
Wind	High-Wind	15.00	mph
Formwork	Steel Formwork	34.60	BTU/(ft·h·°F)
	Thickness	0.118	in
Curing	Burlap	0.18	BTU/(ft·h·°F)
	Thickness	0.39	in

Figure B-253: Simulation 85 - Bowing distortion of match-cast segment after placement of the new segment
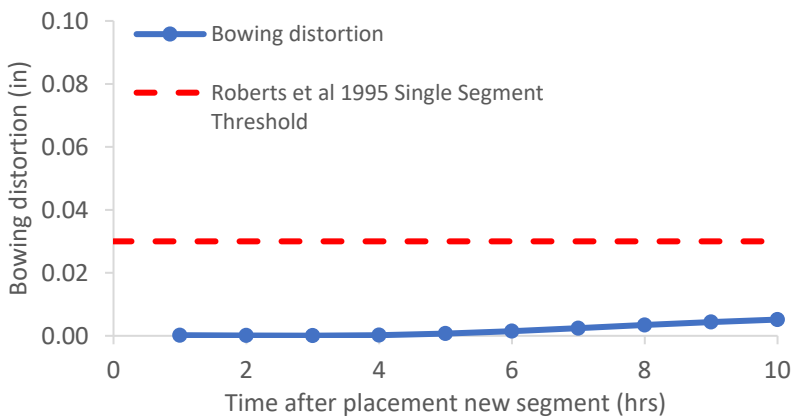

Figure B-254: Simulation 85 - Bowing distortion progression of match-cast segment from time of placement of new segment to 10 hours
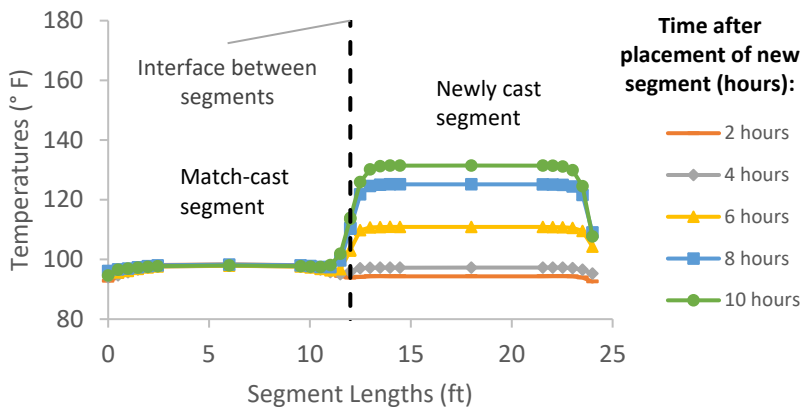

Figure B-255: Simulation 85 - Internal temperatures along the wing of segments

Simulation 86 -Results Summary

Table B-86: Model input parameters simulation 86

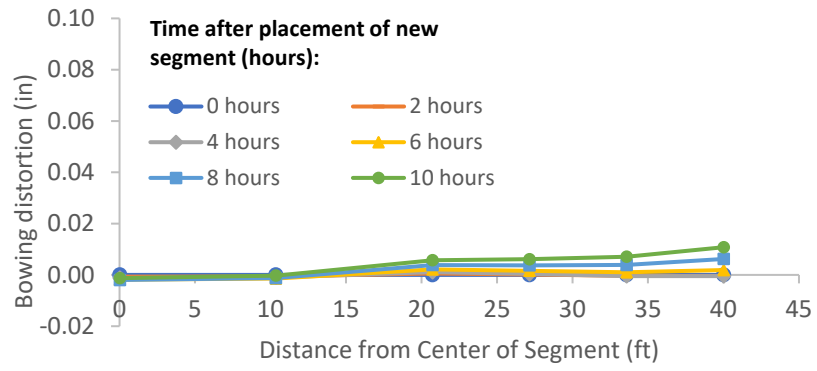| Model details		
Permutation number	86	
Geometry	Florida Bridge B - w/l=5.97	
Max. Mesh Size	3.94	in
Time Step	1	hrs
Placement Temperature	95	°F
Match-cast segment Time of Simulation at Casting	0	hrs
New Segment Time of Simulation at Casting	24	hrs
Concrete Properties		
Cement Content	750.09	lb/yd³
Activation Energy	24.13	BTU/mol
Heat of Hydration Parameters		
Total Heat Development, $Q_{ult} = \alpha_u \cdot H_u$	111.33	BTU/lb
Time Parameter, τ	13.36	hrs
Curvature Parameter, β	1.49	
Density	3816.577	lb/yd³
Specific Heat	0.25	BTU/(lb·°F)
Thermal Conductivity	1.557	BTU/(ft·h·°F)
Match-cast segment Elastic Modulus Dev. Parameters		
Final Value	4471.32	ksi
Time Parameter	12.420	hrs
Curvature Parameter	1.068	
New Segment Elastic Modulus Dev. Parameters		
Final Value	14.50	ksi
Time Parameter	n/a	hrs
Curvature Parameter	n/a	
Poisson Ratio	0.17	
Coefficient of Thermal Expansion	4.54	με/°F
Thermal Boundary Conditions (Applied to Appropriate Faces)		
Ambient Temp	Miami - Summer - Morning - Placement		
Wind	High-Wind	15.00	mph
Formwork	Steel Formwork	34.60	BTU/(ft·h·°F)
	Thickness	0.118	in
Curing	Burlap	0.18	BTU/(ft·h·°F)
	Thickness	0.39	in

Figure B-256: Simulation 86 - Bowing distortion of match-cast segment after placement of the new segment
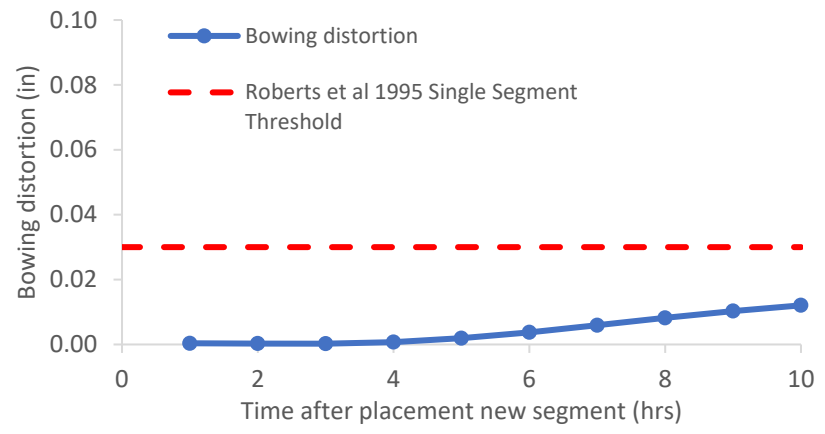

Figure B-257: Simulation 86 - Bowing distortion progression of match-cast segment from time of placement of new segment to 10 hours
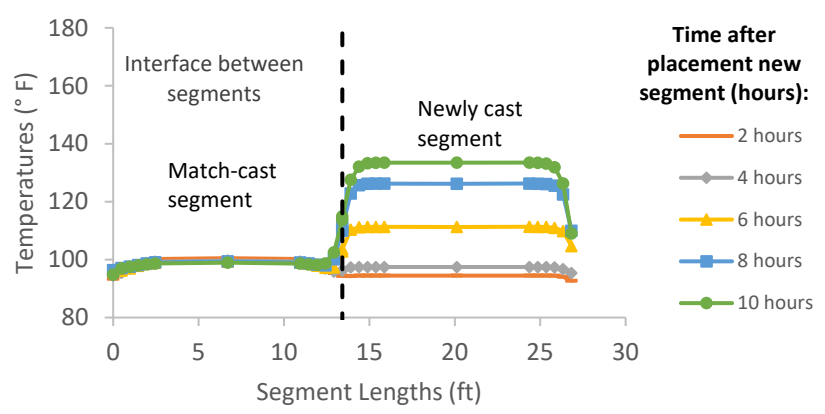

Figure B-258: Simulation 86 - Internal temperatures along the wing of segments

Simulation 87 -Results Summary

Table B-87: Model input parameters simulation 87

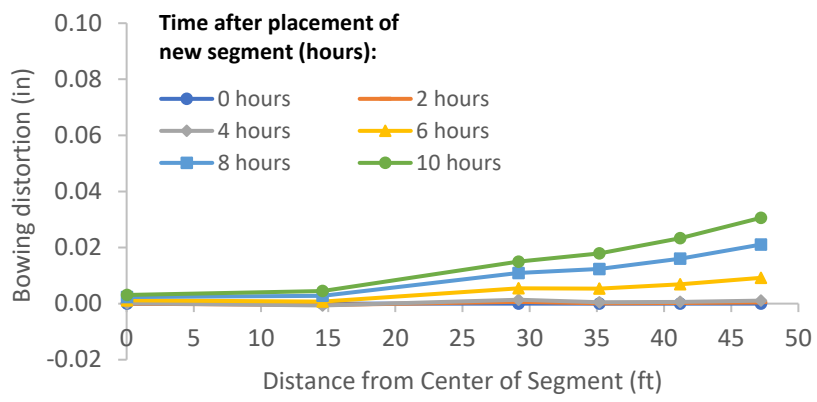| Model details		
Permutation number	87	
Geometry	Florida Bridge C - w/l=10.89	
Max. Mesh Size	3.54	in
Time Step	1	hrs
Placement Temperature	95	°F
Match-cast segment Time of Simulation at Casting	0	hrs
New Segment Time of Simulation at Casting	24	hrs
Concrete Properties		
Cement Content	750.09	lb/yd^3
Activation Energy	24.13	BTU/mol
Heat of Hydration Parameters		
Total Heat Development, $Q_{ult} = \alpha_u \cdot H_u$	111.33	BTU/lb
Time Parameter, τ	13.36	hrs
Curvature Parameter, β	1.49	
Density	3816.577	lb/yd^3
Specific Heat	0.25	BTU/(lb·°F)
Thermal Conductivity	1.557	BTU/(ft·h·°F)
Match-cast segment Elastic Modulus Dev. Parameters		
Final Value	4471.32	ksi
Time Parameter	12.420	hrs
Curvature Parameter	1.068	
New Segment Elastic Modulus Dev. Parameters		
Final Value	14.50	ksi
Time Parameter	n/a	hrs
Curvature Parameter	n/a	
Poisson Ratio	0.17	
Coefficient of Thermal Expansion	4.54	με/°F
Thermal Boundary Conditions (Applied to Appropriate Faces)		
Ambient Temp	Miami - Summer - Morning - Placement	
Wind	High-Wind	15.00	mph
Formwork	Steel Formwork	34.60	BTU/(ft·h·°F)
	Thickness	0.118	in
Curing	Burlap	0.18	BTU/(ft·h·°F)
	Thickness	0.39	in

Figure B-259: Simulation 87 - Bowing distortion of match-cast segment after placement of the new segment
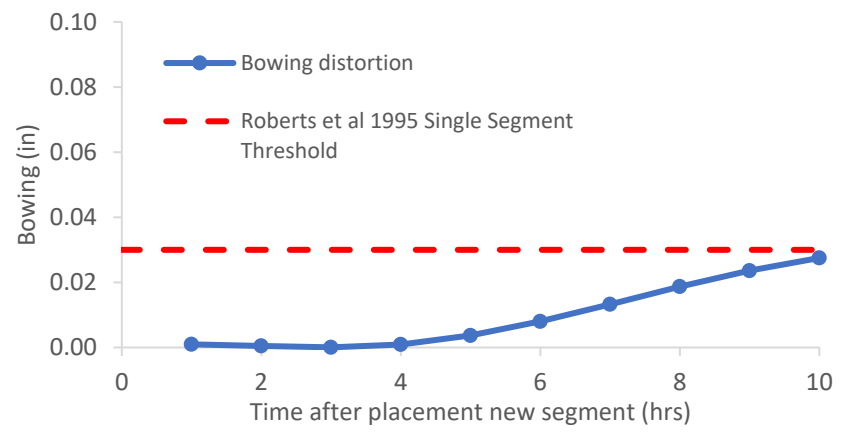

Figure B-260: Simulation 87 - Bowing distortion progression of match-cast segment from time of placement of new segment to 10 hours
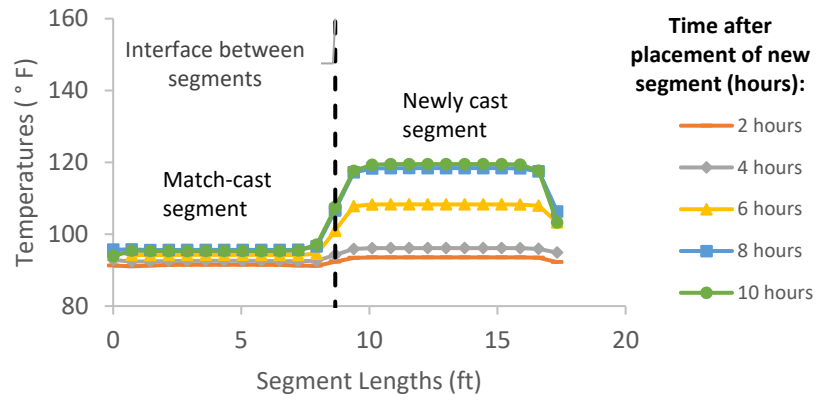

Figure B-261: Simulation 87 - Internal temperatures along the wing of segments

Simulation 88 -Results Summary

Table B-88: Model input parameters simulation 88

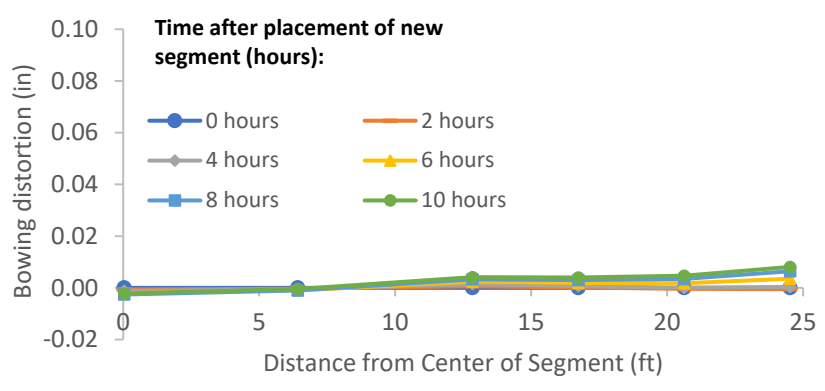| Model details		
Permutation number	88	
Geometry	Florida Bridge E - w/l=4.09	
Max. Mesh Size	2.95	in
Time Step	1	hrs
Placement Temperature	95	°F
Match-cast segment Time of Simulation at Casting	0	hrs
New Segment Time of Simulation at Casting	24	hrs
Concrete Properties		
Cement Content	950.11	lb/yd³
Activation Energy	28.43	BTU/mol
Heat of Hydration Parameters		
Total Heat Development, $Q_{ult} = \alpha_u \cdot H_u$	124.95	BTU/lb
Time Parameter, τ	10.50	hrs
Curvature Parameter, β	1.60	
Density	3880.948	lb/yd³
Specific Heat	0.26	BTU/(lb·°F)
Thermal Conductivity	1.502	BTU/(ft·h·°F)
Match-cast segment Elastic Modulus Dev. Parameters		
Final Value	4584.92	ksi
Time Parameter	12.420	hrs
Curvature Parameter	1.068	
New Segment Elastic Modulus Dev. Parameters		
Final Value	14.50	ksi
Time Parameter	n/a	hrs
Curvature Parameter	n/a	
Poisson Ratio	0.17	
Coefficient of Thermal Expansion	4.54	με/°F
Thermal Boundary Conditions (Applied to Appropriate Faces)		
Ambient Temp	Miami - Summer - Morning - Placement		
Wind	High-Wind	15.00	mph
Formwork	Steel Formwork	34.60	BTU/(ft·h·°F)
	Thickness	0.118	in
Curing	Burlap	0.18	BTU/(ft·h·°F)
	Thickness	0.39	in

Figure B-262: Simulation 88 - Bowing distortion of match-cast segment after placement of the new segment
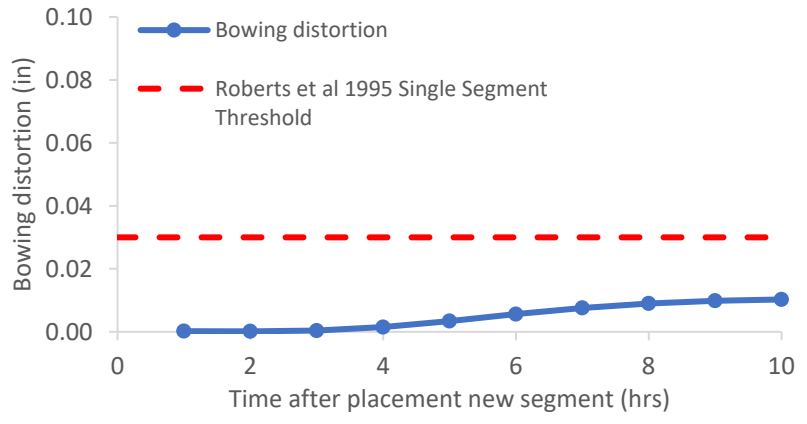

Figure B-263: Simulation 88 - Bowing distortion progression of match-cast segment from time of placement of new segment to 10 hours
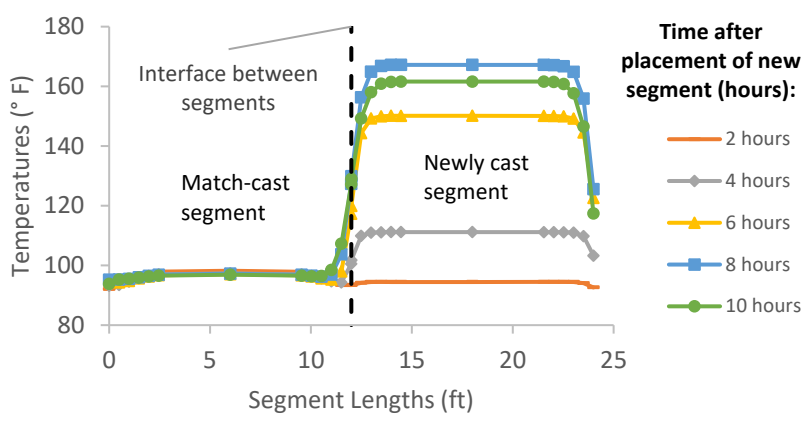

Figure B-264: Simulation 88 - Internal temperatures along the wing of segments

Simulation 89 -Results Summary

Table B-89: Model input parameters simulation 89

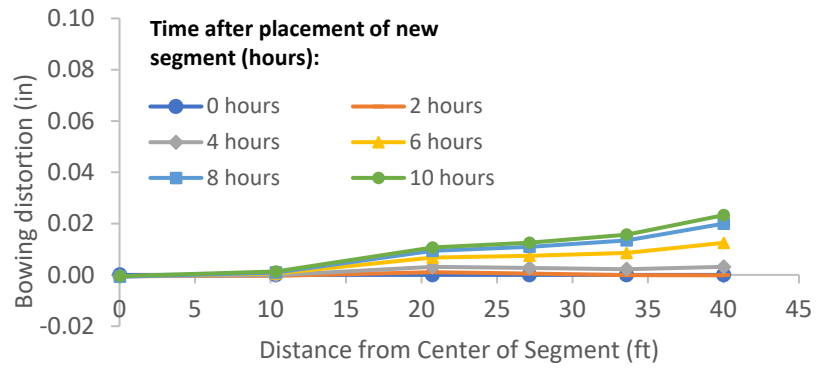| Model details		
Permutation number	89	
Geometry	Florida Bridge B - w/l=5.97	
Max. Mesh Size	3.94	in
Time Step	1	hrs
Placement Temperature	95	°F
Match-cast segment Time of Simulation at Casting	0	hrs
New Segment Time of Simulation at Casting	24	hrs
Concrete Properties		
Cement Content	950.11	lb/yd^3
Activation Energy	28.43	BTU/mol
Heat of Hydration Parameters		
Total Heat Development, $Q_{ult} = \alpha_u \cdot H_u$	124.95	BTU/lb
Time Parameter, τ	10.50	hrs
Curvature Parameter, β	1.60	
Density	3880.948	lb/yd^3
Specific Heat	0.26	BTU/(lb·°F)
Thermal Conductivity	1.502	BTU/(ft·h·°F)
Match-cast segment Elastic Modulus Dev. Parameters		
Final Value	4584.92	ksi
Time Parameter	12.420	hrs
Curvature Parameter	1.068	
New Segment Elastic Modulus Dev. Parameters		
Final Value	14.50	ksi
Time Parameter	n/a	hrs
Curvature Parameter	n/a	
Poisson Ratio	0.17	
Coefficient of Thermal Expansion	4.54	με/°F
Thermal Boundary Conditions (Applied to Appropriate Faces)		
Ambient Temp	Miami - Summer - Morning - Placement	
Wind	High-Wind	15.00	mph
Formwork	Steel Formwork	34.60	BTU/(ft·h·°F)
	Thickness	0.118	in
Curing	Burlap	0.18	BTU/(ft·h·°F)
	Thickness	0.39	in

Figure B-265: Simulation 89 - Bowing distortion of match-cast segment after placement of the new segment
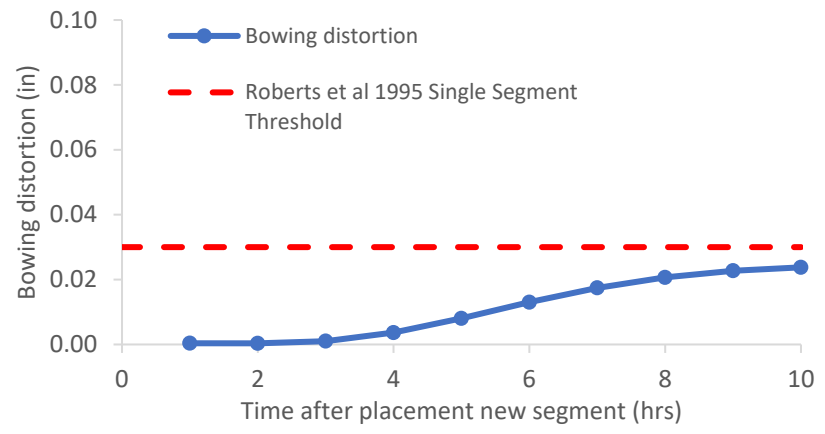

Figure B-266: Simulation 89 - Bowing distortion progression of match-cast segment from time of placement of new segment to 10 hours
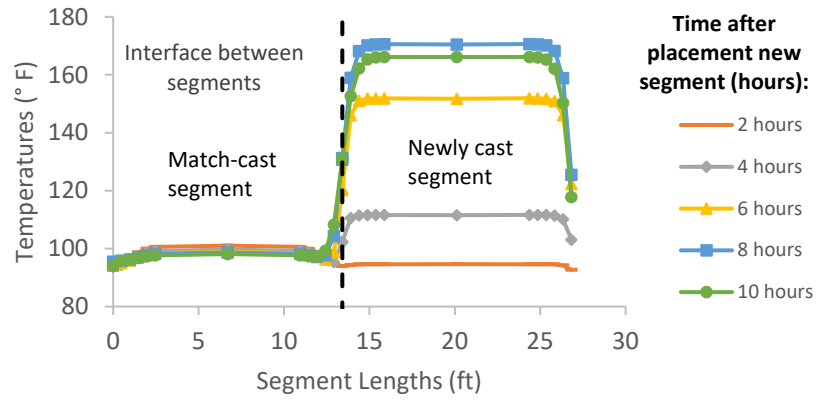

Figure B-267: Simulation 89 - Internal temperatures along the wing of segments

Simulation 90 -Results Summary

Table B-90: Model input parameters simulation 90

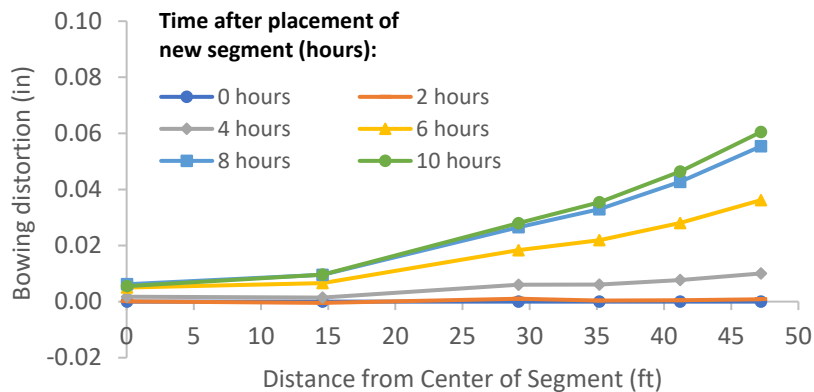| Model details		
Permutation number	90	
Geometry	Florida Bridge C - w/l=10.89	
Max. Mesh Size	3.54	in
Time Step	1	hrs
Placement Temperature	95	°F
Match-cast segment Time of Simulation at Casting	0	hrs
New Segment Time of Simulation at Casting	24	hrs
Concrete Properties		
Cement Content	950.11	lb/yd^3
Activation Energy	28.43	BTU/mol
Heat of Hydration Parameters		
Total Heat Development, $Q_{ult} = \alpha_u \cdot H_u$	124.95	BTU/lb
Time Parameter, τ	10.50	hrs
Curvature Parameter, β	1.60	
Density	3880.948	lb/yd^3
Specific Heat	0.26	BTU/(lb·°F)
Thermal Conductivity	1.502	BTU/(ft·h·°F)
Match-cast segment Elastic Modulus Dev. Parameters		
Final Value	4584.92	ksi
Time Parameter	12.420	hrs
Curvature Parameter	1.068	
New Segment Elastic Modulus Dev. Parameters		
Final Value	14.50	ksi
Time Parameter	n/a	hrs
Curvature Parameter	n/a	
Poisson Ratio	0.17	
Coefficient of Thermal Expansion	4.54	$\mu\varepsilon$/°F
Thermal Boundary Conditions (Applied to Appropriate Faces)		
Ambient Temp	Miami - Summer - Morning - Placement	
Wind	High-Wind	15.00	mph
Formwork	Steel Formwork	34.60	BTU/(ft·h·°F)
	Thickness	0.118	in
Curing	Burlap	0.18	BTU/(ft·h·°F)
	Thickness	0.39	in

Figure B-268: Simulation 90 - Bowing distortion of match-cast segment after placement of the new segment
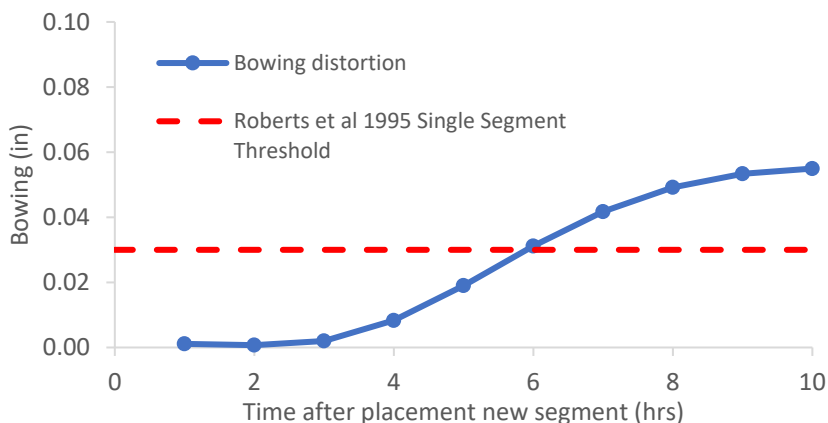

Figure B-269: Simulation 90 - Bowing distortion progression of match-cast segment from time of placement of new segment to 10 hours
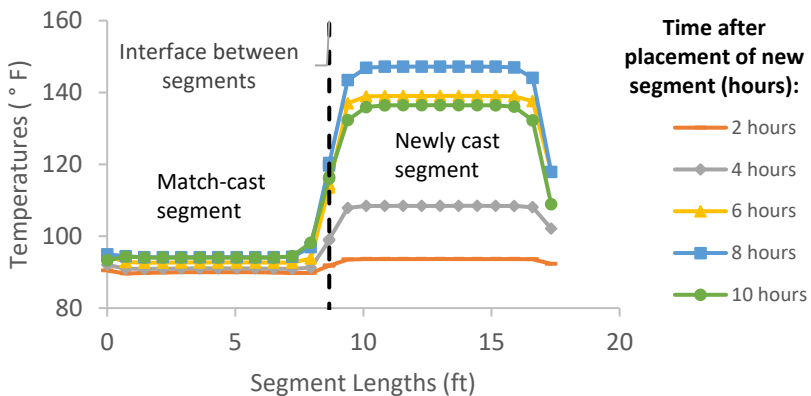

Figure B-270: Simulation 90 - Internal temperatures along the wing of segments

Simulation 91 -Results Summary

Table B-91: Model input parameters simulation 91

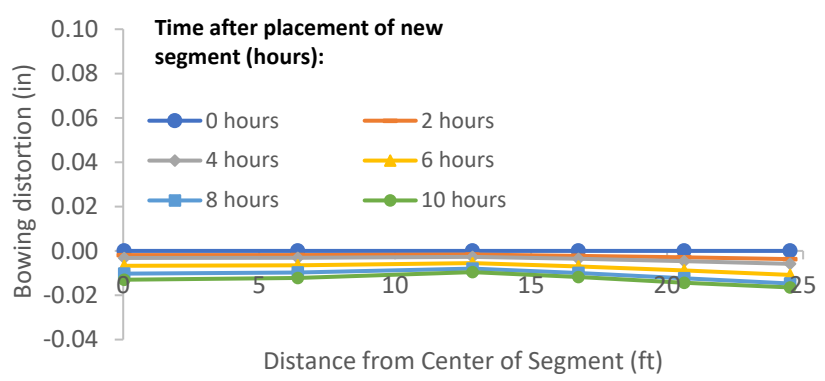| Model details		
Permutation number	91	
Geometry	Florida Bridge E - w/l=4.09	
Max. Mesh Size	2.95	in
Time Step	1	hrs
Placement Temperature	80	°F
Match-cast segment Time of Simulation at Casting	0	hrs
New Segment Time of Simulation at Casting	24	hrs
Concrete Properties		
Cement Content	650.08	lb/yd³
Activation Energy	26.21	BTU/mol
Heat of Hydration Parameters		
Total Heat Development, $Q_{ult} = \alpha_u \cdot H_u$	107.65	BTU/lb
Time Parameter, τ	18.28	hrs
Curvature Parameter, β	1.65	
Density	3834.891	lb/yd³
Specific Heat	0.24	BTU/(lb·°F)
Thermal Conductivity	1.608	BTU/(ft·h·°F)
Match-cast segment Elastic Modulus Dev. Parameters		
Final Value	4503.55	ksi
Time Parameter	12.420	hrs
Curvature Parameter	1.068	
New Segment Elastic Modulus Dev. Parameters		
Final Value	14.50	ksi
Time Parameter	n/a	hrs
Curvature Parameter	n/a	
Poisson Ratio	0.17	
Coefficient of Thermal Expansion	4.55	με/°F
Thermal Boundary Conditions (Applied to Appropriate Faces)		
Ambient Temp	Steam-curing-130°F-cycle	
Wind	Low-Wind	0.00	mph
Formwork	Steel Formwork	34.60	BTU/(ft·h·°F)
	Thickness	0.118	in
Curing	Burlap	0.18	BTU/(ft·h·°F)
	Thickness	0.39	in

Figure B-271: Simulation 91 - Bowing distortion of match-cast segment after placement of the new segment
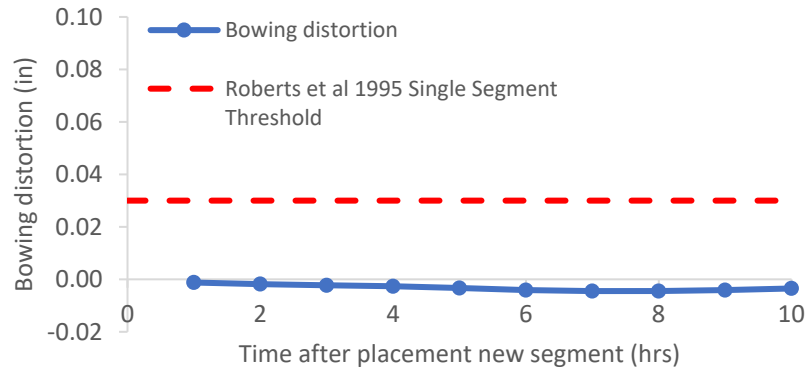

Figure B-272: Simulation 91 - Bowing distortion progression of match-cast segment from time of placement of new segment to 10 hours
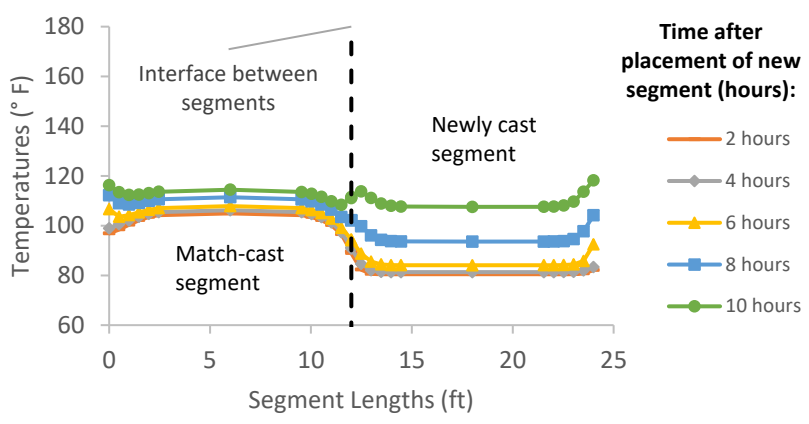

Figure B-273: Simulation 91 - Internal temperatures along the wing of segments

Simulation 92 -Results Summary

Table B-92: Model input parameters simulation 92

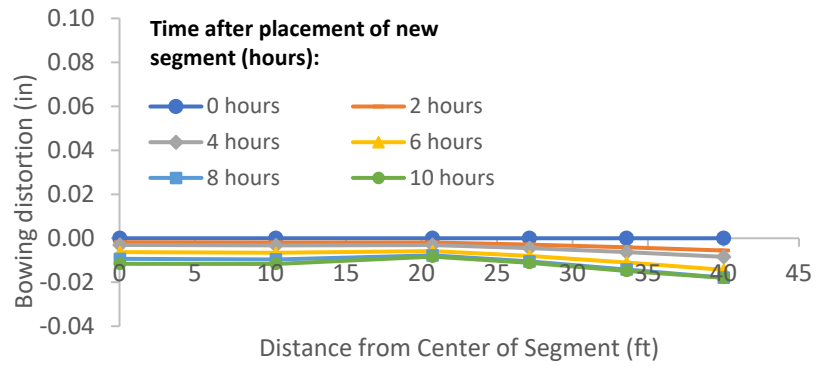| Model details		
Permutation number	92	
Geometry	Florida Bridge B - w/l=5.97	
Max. Mesh Size	3.94	in
Time Step	1	hrs
Placement Temperature	80	°F
Match-cast segment Time of Simulation at Casting	0	hrs
New Segment Time of Simulation at Casting	24	hrs
Concrete Properties		
Cement Content	650.08	lb/yd³
Activation Energy	26.21	BTU/mol
Heat of Hydration Parameters		
Total Heat Development, $Q_{ult} = \alpha_u \cdot H_u$	107.65	BTU/lb
Time Parameter, τ	18.28	hrs
Curvature Parameter, β	1.65	
Density	3834.891	lb/yd³
Specific Heat	0.24	BTU/(lb·°F)
Thermal Conductivity	1.608	BTU/(ft·h·°F)
Match-cast segment Elastic Modulus Dev. Parameters		
Final Value	4503.55	ksi
Time Parameter	12.420	hrs
Curvature Parameter	1.068	
New Segment Elastic Modulus Dev. Parameters		
Final Value	14.50	ksi
Time Parameter	n/a	hrs
Curvature Parameter	n/a	
Poisson Ratio	0.17	
Coefficient of Thermal Expansion	4.55	με/°F
Thermal Boundary Conditions (Applied to Appropriate Faces)		
Ambient Temp	Steam-curing-130°F-cycle	
Wind	Low-Wind	0.00	mph
Formwork	Steel Formwork	34.60	BTU/(ft·h·°F)
	Thickness	0.118	in
Curing	Burlap	0.18	BTU/(ft·h·°F)
	Thickness	0.39	in

Figure B-274: Simulation 92 - Bowing distortion of match-cast segment after placement of the new segment
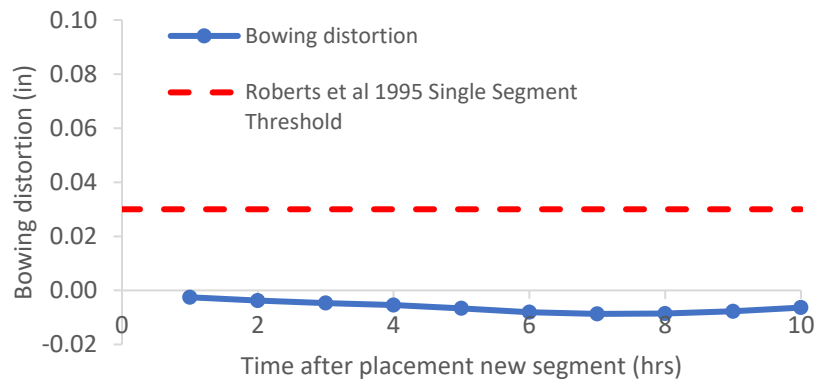

Figure B-275: Simulation 92 - Bowing distortion progression of match-cast segment from time of placement of new segment to 10 hours
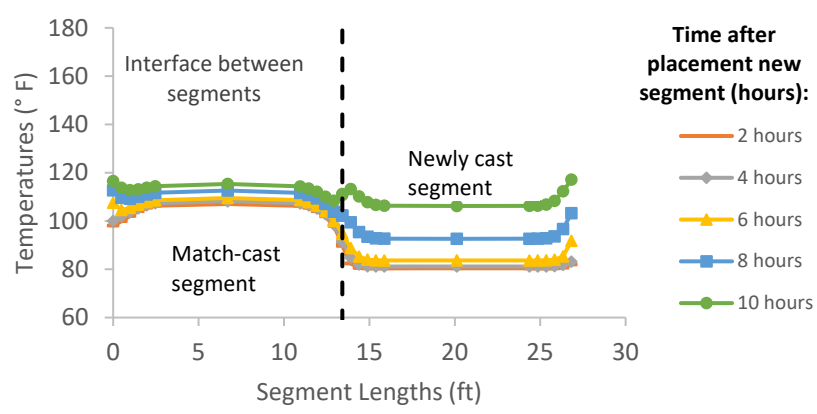

Figure B-276: Simulation 92 - Internal temperatures along the wing of segments

Simulation 93 -Results Summary

Table B-93: Model input parameters simulation 93

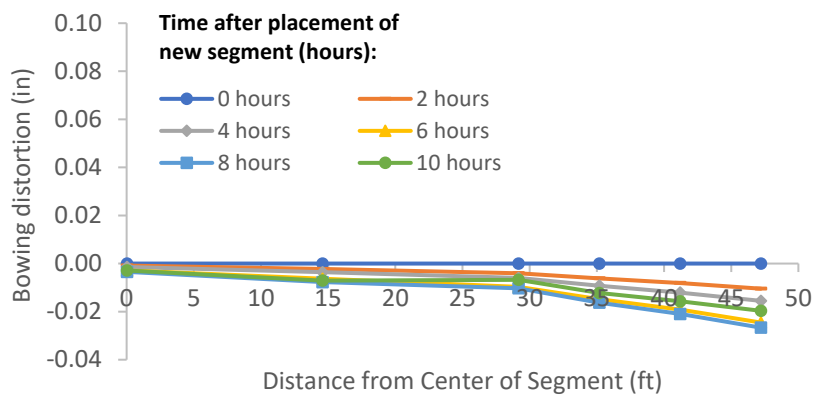| Model details		
Permutation number	93	
Geometry	Florida Bridge C - w/l=10.89	
Max. Mesh Size	3.54	in
Time Step	1	hrs
Placement Temperature	80	°F
Match-cast segment Time of Simulation at Casting	0	hrs
New Segment Time of Simulation at Casting	24	hrs
Concrete Properties		
Cement Content	650.08	lb/yd^3
Activation Energy	26.21	BTU/mol
Heat of Hydration Parameters		
Total Heat Development, $Q_{ult} = \alpha_u \cdot H_u$	107.65	BTU/lb
Time Parameter, τ	18.28	hrs
Curvature Parameter, β	1.65	
Density	3834.891	lb/yd^3
Specific Heat	0.24	BTU/(lb·°F)
Thermal Conductivity	1.608	BTU/(ft·h·°F)
Match-cast segment Elastic Modulus Dev. Parameters		
Final Value	4503.55	ksi
Time Parameter	12.420	hrs
Curvature Parameter	1.068	
New Segment Elastic Modulus Dev. Parameters		
Final Value	14.50	ksi
Time Parameter	n/a	hrs
Curvature Parameter	n/a	
Poisson Ratio	0.17	
Coefficient of Thermal Expansion	4.55	µε/°F
Thermal Boundary Conditions (Applied to Appropriate Faces)		
Ambient Temp	Steam-curing-130°F-cycle	
Wind	Low-Wind	0.00	mph
Formwork	Steel Formwork	34.60	BTU/(ft·h·°F)
	Thickness	0.118	in
Curing	Burlap	0.18	BTU/(ft·h·°F)
	Thickness	0.39	in

Figure B-277: Simulation 93 - Bowing distortion of match-cast segment after placement of the new segment
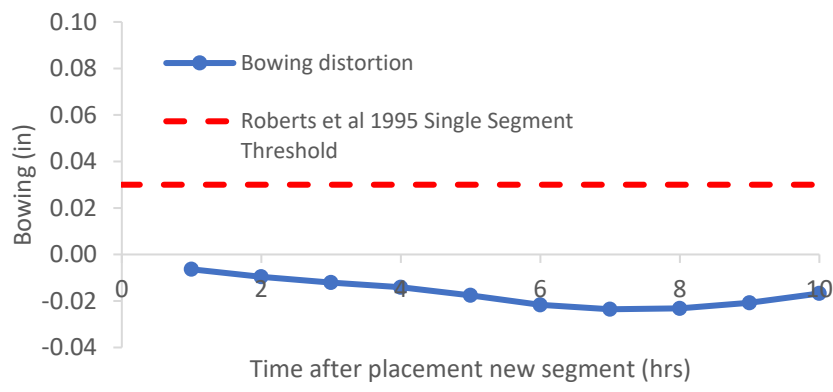

Figure B-278: Simulation 93 - Bowing distortion progression of match-cast segment from time of placement of new segment to 10 hours
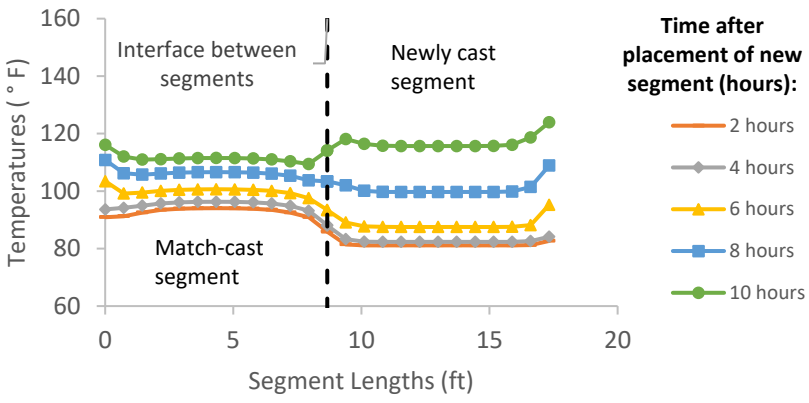

Figure B-279: Simulation 93 - Internal temperatures along the wing of segments

Simulation 94 -Results Summary

Table B-94: Model input parameters simulation 94

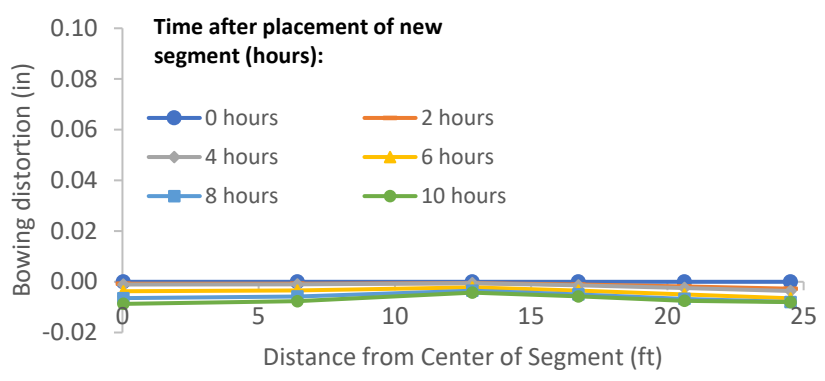| Model details		
Permutation number	94	
Geometry	Florida Bridge E - w/l=4.09	
Max. Mesh Size	2.95	in
Time Step	1	hrs
Placement Temperature	80	°F
Match-cast segment Time of Simulation at Casting	0	hrs
New Segment Time of Simulation at Casting	24	hrs
Concrete Properties		
Cement Content	750.09	lb/yd³
Activation Energy	24.13	BTU/mol
Heat of Hydration Parameters		
Total Heat Development, $Q_{ult} = \alpha_u \cdot H_u$	111.33	BTU/lb
Time Parameter, τ	13.36	hrs
Curvature Parameter, β	1.49	
Density	3816.577	lb/yd³
Specific Heat	0.25	BTU/(lb·°F)
Thermal Conductivity	1.557	BTU/(ft·h·°F)
Match-cast segment Elastic Modulus Dev. Parameters		
Final Value	4471.32	ksi
Time Parameter	12.420	hrs
Curvature Parameter	1.068	
New Segment Elastic Modulus Dev. Parameters		
Final Value	14.50	ksi
Time Parameter	n/a	hrs
Curvature Parameter	n/a	
Poisson Ratio	0.17	
Coefficient of Thermal Expansion	4.54	µε/°F
Thermal Boundary Conditions (Applied to Appropriate Faces)		
Ambient Temp	Steam-curing-130°F-cycle	
Wind	Low-Wind	0.00	mph
Formwork	Steel Formwork	34.60	BTU/(ft·h·°F)
	Thickness	0.118	in
Curing	Burlap	0.18	BTU/(ft·h·°F)
	Thickness	0.39	in

Figure B-280: Simulation 94 - Bowing distortion of match-cast segment after placement of the new segment
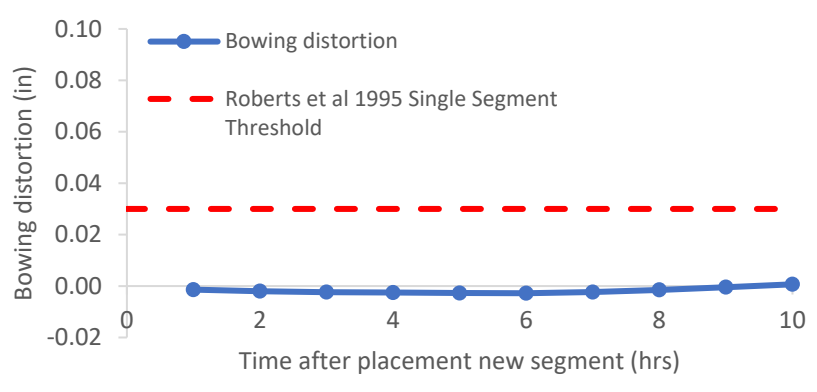

Figure B-281: Simulation 94 - Bowing distortion progression of match-cast segment from time of placement of new segment to 10 hours
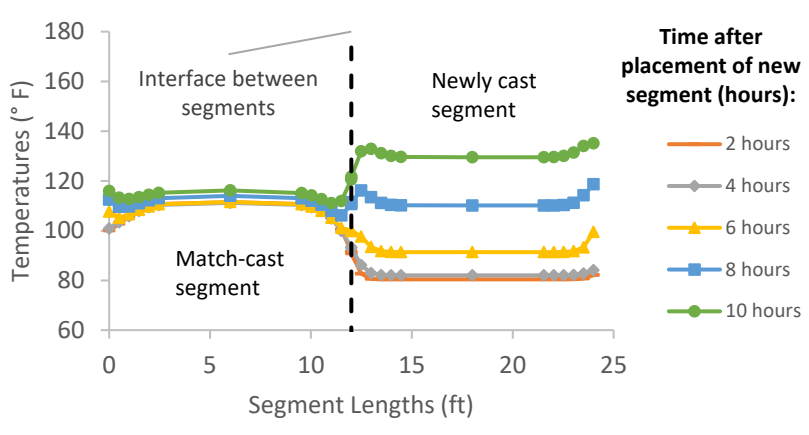

Figure B-282: Simulation 94 - Internal temperatures along the wing of segments

Simulation 95 -Results Summary

Table B-95: Model input parameters simulation 95

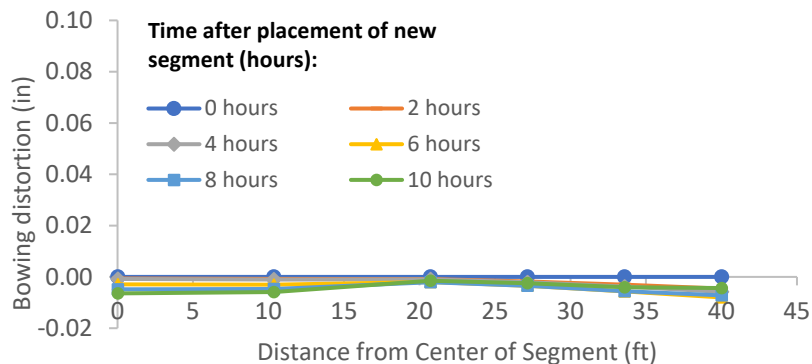| Model details		
Permutation number	95	
Geometry	Florida Bridge B - w/l=5.97	
Max. Mesh Size	3.94	in
Time Step	1	hrs
Placement Temperature	80	°F
Match-cast segment Time of Simulation at Casting	0	hrs
New Segment Time of Simulation at Casting	24	hrs
Concrete Properties		
Cement Content	750.09	lb/yd^3
Activation Energy	24.13	BTU/mol
Heat of Hydration Parameters		
Total Heat Development, $Q_{ult} = \alpha_u \cdot H_u$	111.33	BTU/lb
Time Parameter, τ	13.36	hrs
Curvature Parameter, β	1.49	
Density	3816.577	lb/yd^3
Specific Heat	0.25	BTU/(lb·°F)
Thermal Conductivity	1.557	BTU/(ft·h·°F)
Match-cast segment Elastic Modulus Dev. Parameters		
Final Value	4471.32	ksi
Time Parameter	12.420	hrs
Curvature Parameter	1.068	
New Segment Elastic Modulus Dev. Parameters		
Final Value	14.50	ksi
Time Parameter	n/a	hrs
Curvature Parameter	n/a	
Poisson Ratio	0.17	
Coefficient of Thermal Expansion	4.54	µε/°F
Thermal Boundary Conditions (Applied to Appropriate Faces)		
Ambient Temp	Steam-curing-130°F-cycle	
Wind	Low-Wind	0.00	mph
Formwork	Steel Formwork	34.60	BTU/(ft·h·°F)
	Thickness	0.118	in
Curing	Burlap	0.18	BTU/(ft·h·°F)
	Thickness	0.39	in

Figure B-283: Simulation 95 - Bowing distortion of match-cast segment after placement of the new segment
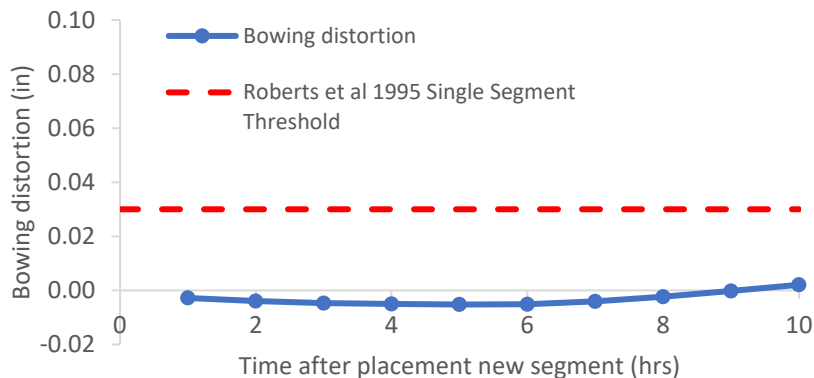

Figure B-284: Simulation 95 - Bowing distortion progression of match-cast segment from time of placement of new segment to 10 hours
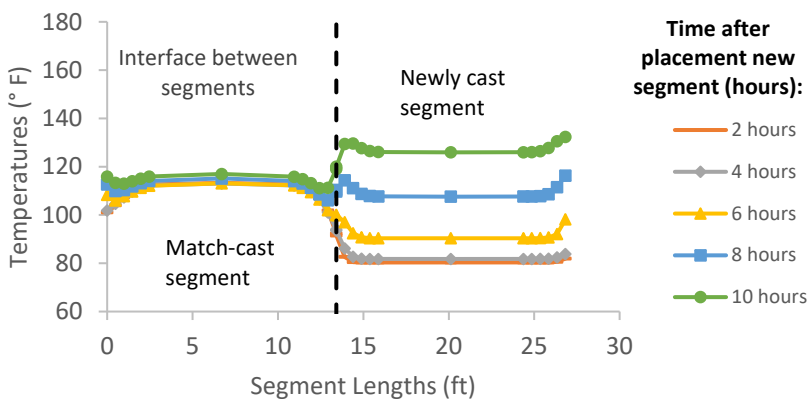

Figure B-285: Simulation 95 - Internal temperatures along the wing of segments

Simulation 96 -Results Summary

Table B-96: Model input parameters simulation 96

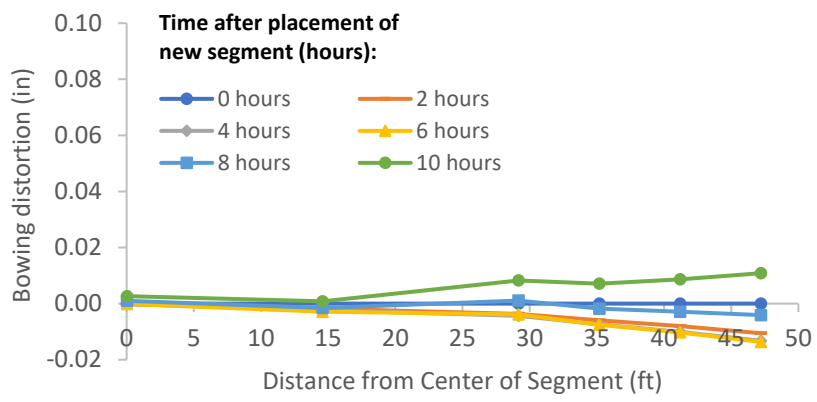| Model details		
Permutation number	96	
Geometry	Florida Bridge C - w/l=10.89	
Max. Mesh Size	3.54	in
Time Step	1	hrs
Placement Temperature	80	°F
Match-cast segment Time of Simulation at Casting	0	hrs
New Segment Time of Simulation at Casting	24	hrs
Concrete Properties		
Cement Content	750.09	lb/yd^3
Activation Energy	24.13	BTU/mol
Heat of Hydration Parameters		
Total Heat Development, $Q_{ult} = \alpha_u \cdot H_u$	111.33	BTU/lb
Time Parameter, τ	13.36	hrs
Curvature Parameter, β	1.49	
Density	3816.577	lb/yd^3
Specific Heat	0.25	BTU/(lb·°F)
Thermal Conductivity	1.557	BTU/(ft·h·°F)
Match-cast segment Elastic Modulus Dev. Parameters		
Final Value	4471.32	ksi
Time Parameter	12.420	hrs
Curvature Parameter	1.068	
New Segment Elastic Modulus Dev. Parameters		
Final Value	14.50	ksi
Time Parameter	n/a	hrs
Curvature Parameter	n/a	
Poisson Ratio	0.17	
Coefficient of Thermal Expansion	4.54	µε/°F
Thermal Boundary Conditions (Applied to Appropriate Faces)		
Ambient Temp	Steam-curing-130°F-cycle	
Wind	Low-Wind	0.00	mph
Formwork	Steel Formwork	34.60	BTU/(ft·h·°F)
	Thickness	0.118	in
Curing	Burlap	0.18	BTU/(ft·h·°F)
	Thickness	0.39	in

Figure B-286: Simulation 96 - Bowing distortion of match-cast segment after placement of the new segment
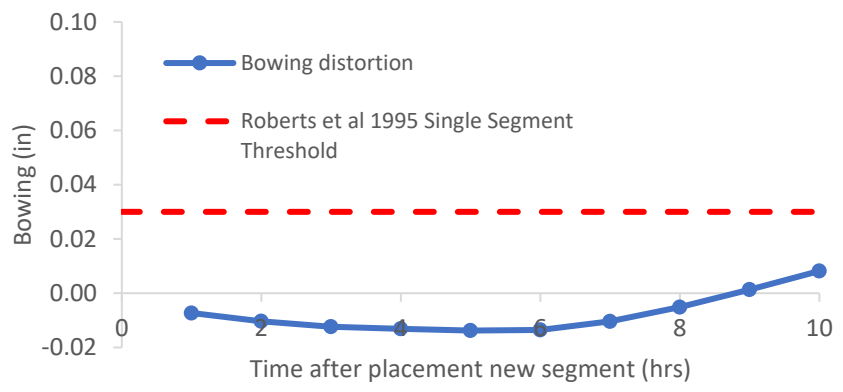

Figure B-287: Simulation 96 - Bowing distortion progression of match-cast segment from time of placement of new segment to 10 hours
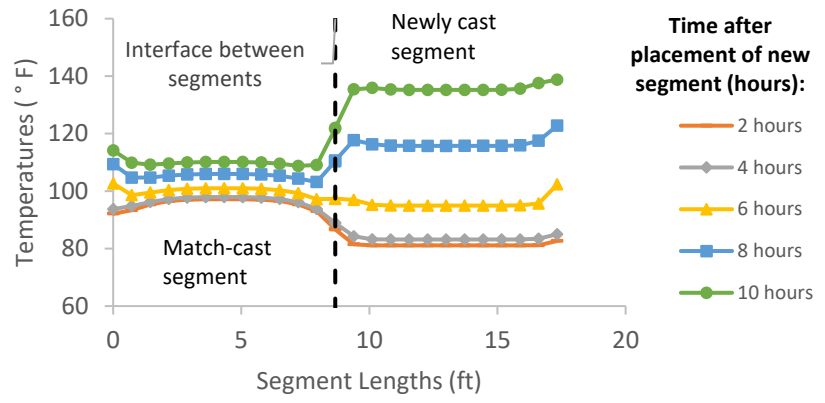

Figure B-288: Simulation 96 - Internal temperatures along the wing of segments

Simulation 97 -Results Summary

Table B-97: Model input parameters simulation 97

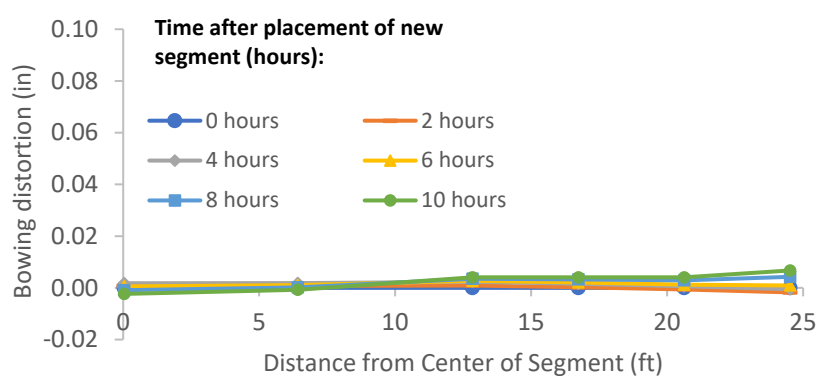| Model details		
Permutation number	97	
Geometry	Florida Bridge E - w/l=4.09	
Max. Mesh Size	2.95	in
Time Step	1	hrs
Placement Temperature	80	°F
Match-cast segment Time of Simulation at Casting	0	hrs
New Segment Time of Simulation at Casting	24	hrs
Concrete Properties		
Cement Content	950.11	lb/yd^3
Activation Energy	28.43	BTU/mol
Heat of Hydration Parameters		
Total Heat Development, $Q_{ult} = \alpha_u \cdot H_u$	124.95	BTU/lb
Time Parameter, τ	10.50	hrs
Curvature Parameter, β	1.60	
Density	3880.948	lb/yd^3
Specific Heat	0.26	BTU/(lb·°F)
Thermal Conductivity	1.502	BTU/(ft·h·°F)
Match-cast segment Elastic Modulus Dev. Parameters		
Final Value	4584.92	ksi
Time Parameter	12.420	hrs
Curvature Parameter	1.068	
New Segment Elastic Modulus Dev. Parameters		
Final Value	14.50	ksi
Time Parameter	n/a	hrs
Curvature Parameter	n/a	
Poisson Ratio	0.17	
Coefficient of Thermal Expansion	4.54	με/°F
Thermal Boundary Conditions (Applied to Appropriate Faces)		
Ambient Temp	Steam-curing-130°F-cycle	
Wind	Low-Wind	0.00	mph
Formwork	Steel Formwork	34.60	BTU/(ft·h·°F)
	Thickness	0.118	in
Curing	Burlap	0.18	BTU/(ft·h·°F)
	Thickness	0.39	in

Figure B-289: Simulation 97 - Bowing distortion of match-cast segment after placement of the new segment
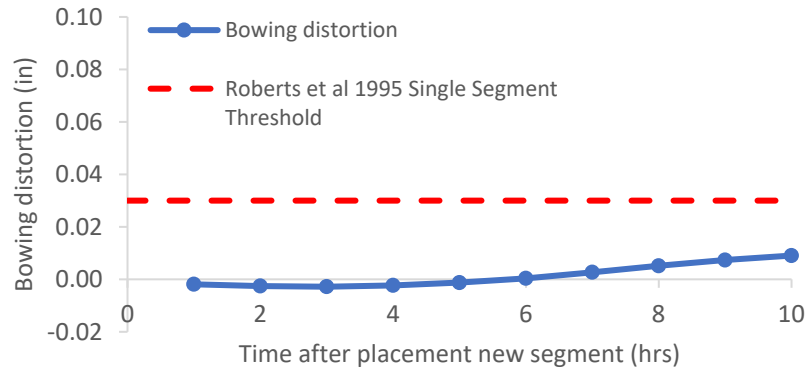

Figure B-290: Simulation 97 - Bowing distortion progression of match-cast segment from time of placement of new segment to 10 hours
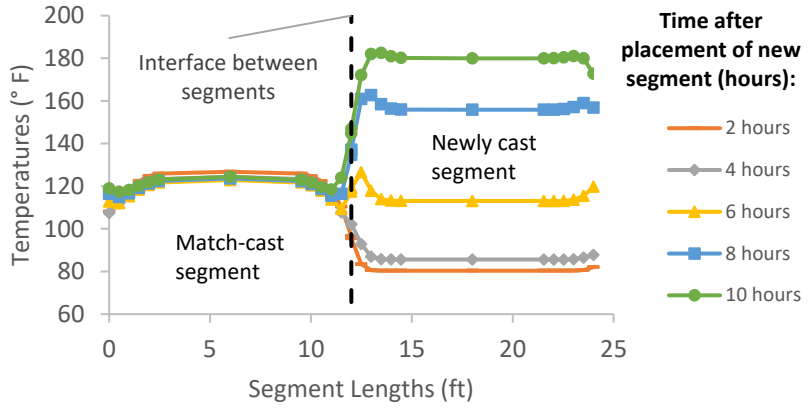

Figure B-291: Simulation 97 - Internal temperatures along the wing of segments

Simulation 98 -Results Summary

Table B-98: Model input parameters simulation 98

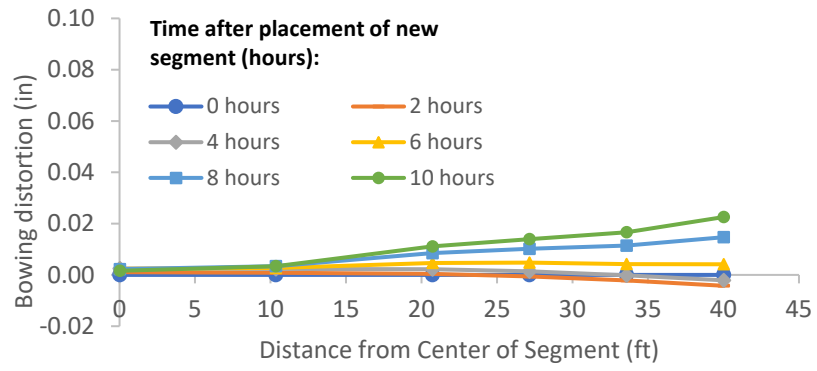| Model details		
Permutation number	98	
Geometry	Florida Bridge B - w/l=5.97	
Max. Mesh Size	3.94	in
Time Step	1	hrs
Placement Temperature	80	°F
Match-cast segment Time of Simulation at Casting	0	hrs
New Segment Time of Simulation at Casting	24	hrs
Concrete Properties		
Cement Content	950.11	lb/yd³
Activation Energy	28.43	BTU/mol
Heat of Hydration Parameters		
Total Heat Development, $Q_{ult} = \alpha_u \cdot H_u$	124.95	BTU/lb
Time Parameter, τ	10.50	hrs
Curvature Parameter, β	1.60	
Density	3880.948	lb/yd³
Specific Heat	0.26	BTU/(lb·°F)
Thermal Conductivity	1.502	BTU/(ft·h·°F)
Match-cast segment Elastic Modulus Dev. Parameters		
Final Value	4584.92	ksi
Time Parameter	12.420	hrs
Curvature Parameter	1.068	
New Segment Elastic Modulus Dev. Parameters		
Final Value	14.50	ksi
Time Parameter	n/a	hrs
Curvature Parameter	n/a	
Poisson Ratio	0.17	
Coefficient of Thermal Expansion	4.54	με/°F
Thermal Boundary Conditions (Applied to Appropriate Faces)		
Ambient Temp	Steam-curing-130°F-cycle	
Wind	Low-Wind	0.00	mph
Formwork	Steel Formwork	34.60	BTU/(ft·h·°F)
	Thickness	0.118	in
Curing	Burlap	0.18	BTU/(ft·h·°F)
	Thickness	0.39	in

Figure B-292: Simulation 98 - Bowing distortion of match-cast segment after placement of the new segment
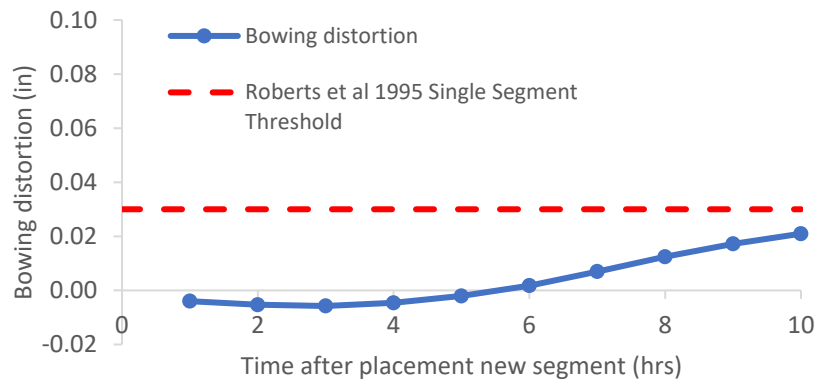

Figure B-293: Simulation 98 - Bowing distortion progression of match-cast segment from time of placement of new segment to 10 hours
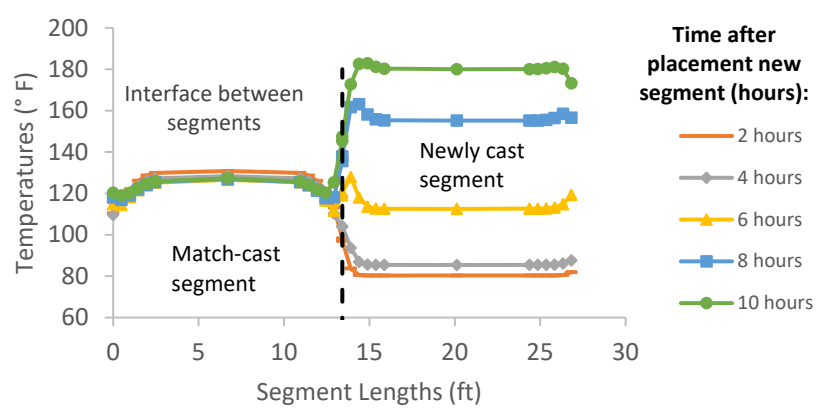

Figure B-294: Simulation 98 - Internal temperatures along the wing of segments

Simulation 99 -Results Summary

Table B-99: Model input parameters simulation 99

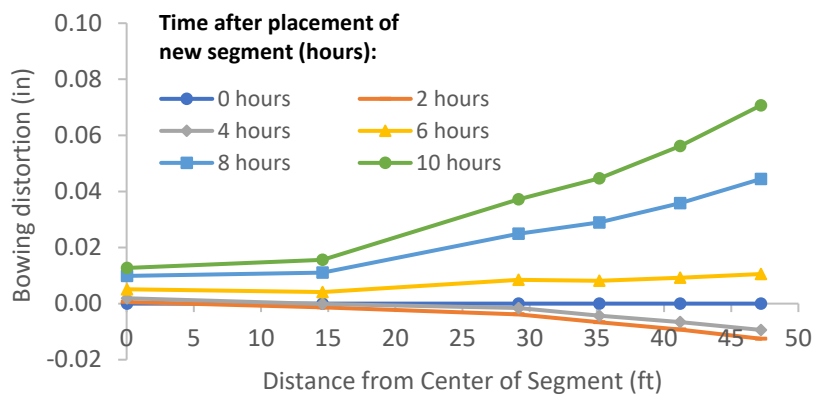| Model details		
Permutation number	99	
Geometry	Florida Bridge C - w/l=10.89	
Max. Mesh Size	3.54	in
Time Step	1	hrs
Placement Temperature	80	°F
Match-cast segment Time of Simulation at Casting	0	hrs
New Segment Time of Simulation at Casting	24	hrs
Concrete Properties		
Cement Content	950.11	lb/yd^3
Activation Energy	28.43	BTU/mol
Heat of Hydration Parameters		
Total Heat Development, $Q_{ult} = \alpha_u \cdot H_u$	124.95	BTU/lb
Time Parameter, τ	10.50	hrs
Curvature Parameter, β	1.60	
Density	3880.948	lb/yd^3
Specific Heat	0.26	BTU/(lb·°F)
Thermal Conductivity	1.502	BTU/(ft·h·°F)
Match-cast segment Elastic Modulus Dev. Parameters		
Final Value	4584.92	ksi
Time Parameter	12.420	hrs
Curvature Parameter	1.068	
New Segment Elastic Modulus Dev. Parameters		
Final Value	14.50	ksi
Time Parameter	n/a	hrs
Curvature Parameter	n/a	
Poisson Ratio	0.17	
Coefficient of Thermal Expansion	4.54	με/°F
Thermal Boundary Conditions (Applied to Appropriate Faces)		
Ambient Temp	Steam-curing-130°F-cycle	
Wind	Low-Wind	0.00	mph
Formwork	Steel Formwork	34.60	BTU/(ft·h·°F)
	Thickness	0.118	in
Curing	Burlap	0.18	BTU/(ft·h·°F)
	Thickness	0.39	in

Figure B-295: Simulation 99 - Bowing distortion of match-cast segment after placement of the new segment
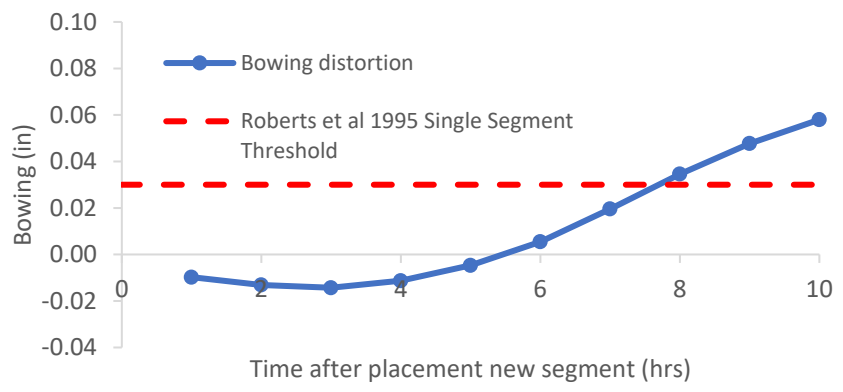

Figure B-296: Simulation 99 - Bowing distortion progression of match-cast segment from time of placement of new segment to 10 hours
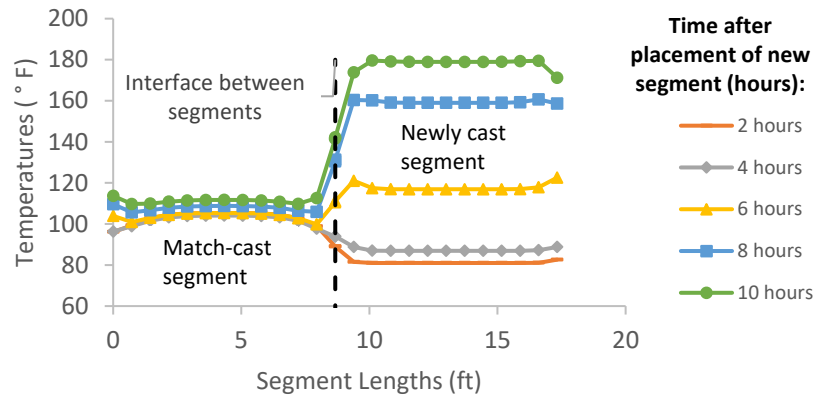

Figure B-297: Simulation 99 - Internal temperatures along the wing of segments

Simulation 100 -Results Summary

Table B-100: Model input parameters simulation 100

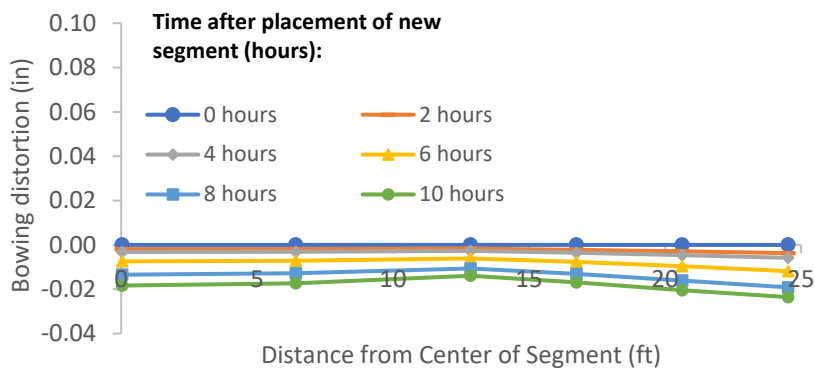| Model details		
Permutation number	100	
Geometry	Florida Bridge E - w/l=4.09	
Max. Mesh Size	2.95	in
Time Step	1	hrs
Placement Temperature	80	°F
Match-cast segment Time of Simulation at Casting	0	hrs
New Segment Time of Simulation at Casting	24	hrs
Concrete Properties		
Cement Content	650.08	lb/yd^3
Activation Energy	26.21	BTU/mol
Heat of Hydration Parameters		
Total Heat Development, $Q_{ult} = \alpha_u \cdot H_u$	107.65	BTU/lb
Time Parameter, τ	18.28	hrs
Curvature Parameter, β	1.65	
Density	3834.891	lb/yd^3
Specific Heat	0.24	BTU/(lb·°F)
Thermal Conductivity	1.608	BTU/(ft·h·°F)
Match-cast segment Elastic Modulus Dev. Parameters		
Final Value	4503.55	ksi
Time Parameter	12.420	hrs
Curvature Parameter	1.068	
New Segment Elastic Modulus Dev. Parameters		
Final Value	14.50	ksi
Time Parameter	n/a	hrs
Curvature Parameter	n/a	
Poisson Ratio	0.17	
Coefficient of Thermal Expansion	4.55	µε/°F
Thermal Boundary Conditions (Applied to Appropriate Faces)		
Ambient Temp	Steam-curing-160°F-cycle	
Wind	Low-Wind	0.00	mph
Formwork	Steel Formwork	34.60	BTU/(ft·h·°F)
	Thickness	0.118	in
Curing	Burlap	0.18	BTU/(ft·h·°F)
	Thickness	0.39	in

Figure B-298: Simulation 100 - Bowing distortion of match-cast segment after placement of the new segment
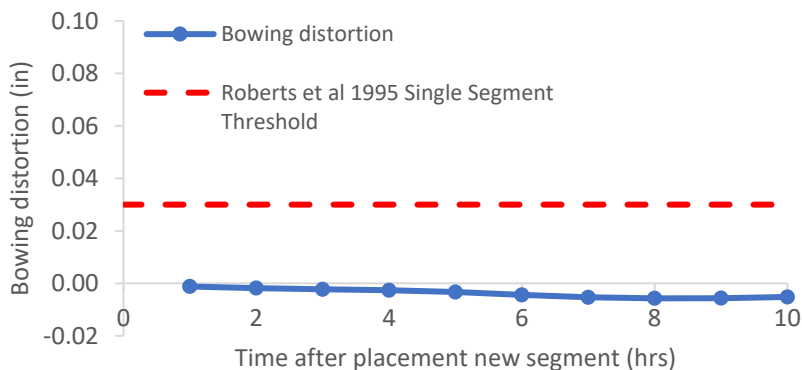

Figure B-299: Simulation 100 - Bowing distortion progression of match-cast segment from time of placement of new segment to 10 hours

Figure B-300: Simulation 100 - Internal temperatures along the wing of segments

Simulation 101 -Results Summary

Table B-101: Model input parameters simulation 101

Model details		
Permutation number	101	
Geometry	Florida Bridge B - w/l=5.97	
Max. Mesh Size	3.94	in
Time Step	1	hrs
Placement Temperature	80	°F
Match-cast segment Time of Simulation at Casting	0	hrs
New Segment Time of Simulation at Casting	24	hrs
Concrete Properties		
Cement Content	650.08	lb/yd³
Activation Energy	26.21	BTU/mol
Heat of Hydration Parameters		
Total Heat Development, $Q_{ult} = \alpha_u \cdot H_u$	107.65	BTU/lb
Time Parameter, τ	18.28	hrs
Curvature Parameter, β	1.65	
Density	3834.891	lb/yd³
Specific Heat	0.24	BTU/(lb·°F)
Thermal Conductivity	1.608	BTU/(ft·h·°F)
Match-cast segment Elastic Modulus Dev. Parameters		
Final Value	4503.55	ksi
Time Parameter	12.420	hrs
Curvature Parameter	1.068	
New Segment Elastic Modulus Dev. Parameters		
Final Value	14.50	ksi
Time Parameter	n/a	hrs
Curvature Parameter	n/a	
Poisson Ratio	0.17	
Coefficient of Thermal Expansion	4.55	με/°F
Thermal Boundary Conditions (Applied to Appropriate Faces)		
Ambient Temp	Steam-curing-160°F-cycle	
Wind	Low-Wind	0.00	mph
Formwork	Steel Formwork	34.60	BTU/(ft·h·°F)
	Thickness	0.118	in
Curing	Burlap	0.18	BTU/(ft·h·°F)
	Thickness	0.39	in

Figure B-301: Simulation 101 - Bowing distortion of match-cast segment after placement of the new segment

Figure B-302: Simulation 101 - Bowing distortion progression of match-cast segment from time of placement of new segment to 10 hours
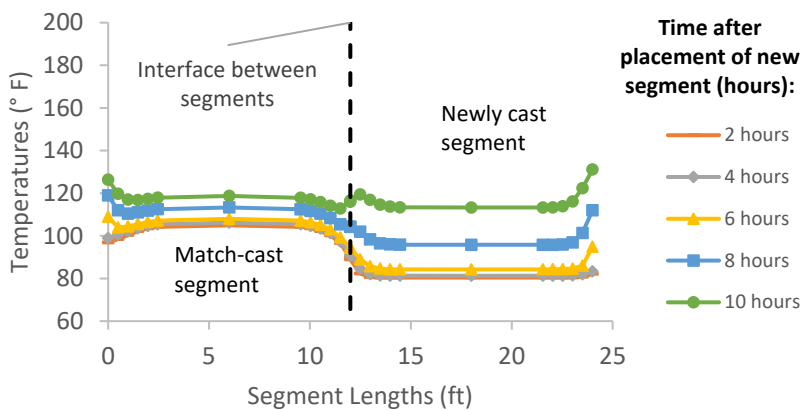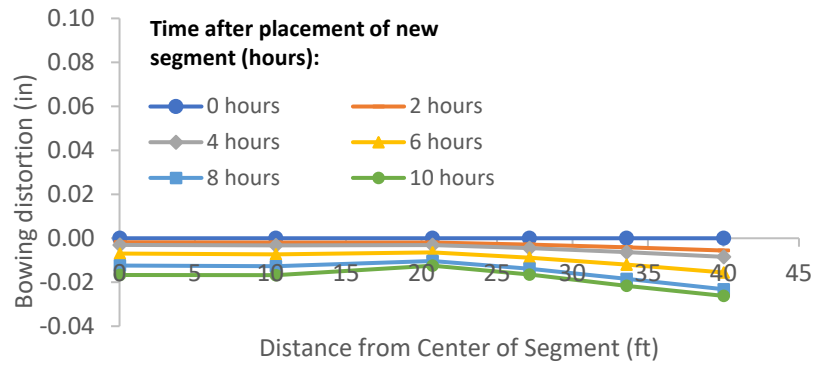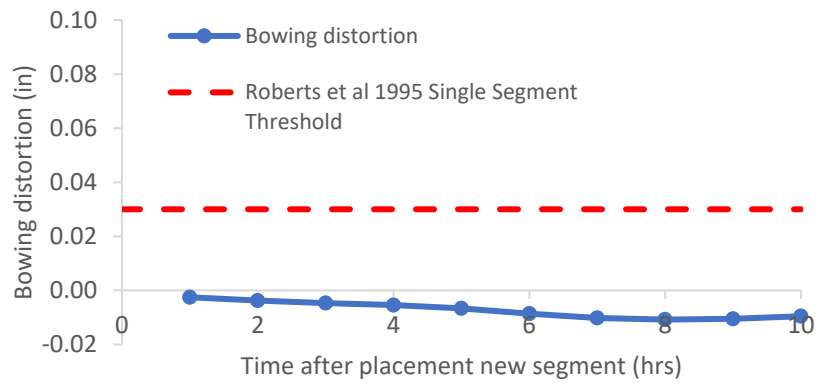

Figure B-303: Simulation 101 - Internal temperatures along the wing of segments

Simulation 102 -Results Summary

Table B-102: Model input parameters simulation 102

Model details		
Permutation number	102	
Geometry	Florida Bridge C - w/l=10.89	
Max. Mesh Size	3.54	in
Time Step	1	hrs
Placement Temperature	80	°F
Match-cast segment Time of Simulation at Casting	0	hrs
New Segment Time of Simulation at Casting	24	hrs
Concrete Properties		
Cement Content	650.08	lb/yd^3
Activation Energy	26.21	BTU/mol
Heat of Hydration Parameters		
Total Heat Development, $Q_{ult} = \alpha_u \cdot H_u$	107.65	BTU/lb
Time Parameter, τ	18.28	hrs
Curvature Parameter, β	1.65	
Density	3834.891	lb/yd^3
Specific Heat	0.24	BTU/(lb·°F)
Thermal Conductivity	1.608	BTU/(ft·h·°F)
Match-cast segment Elastic Modulus Dev. Parameters		
Final Value	4503.55	ksi
Time Parameter	12.420	hrs
Curvature Parameter	1.068	
New Segment Elastic Modulus Dev. Parameters		
Final Value	14.50	ksi
Time Parameter	n/a	hrs
Curvature Parameter	n/a	
Poisson Ratio	0.17	
Coefficient of Thermal Expansion	4.55	με/°F
Thermal Boundary Conditions (Applied to Appropriate Faces)		
Ambient Temp	Steam-curing-160°F-cycle	
Wind	Low-Wind	0.00	mph
Formwork	Steel Formwork	34.60	BTU/(ft·h·°F)
	Thickness	0.118	in
Curing	Burlap	0.18	BTU/(ft·h·°F)
	Thickness	0.39	in

Figure B-304: Simulation 102 - Bowing distortion of match-cast segment after placement of the new segment

Figure B-305: Simulation 102 - Bowing distortion progression of match-cast segment from time of placement of new segment to 10 hours
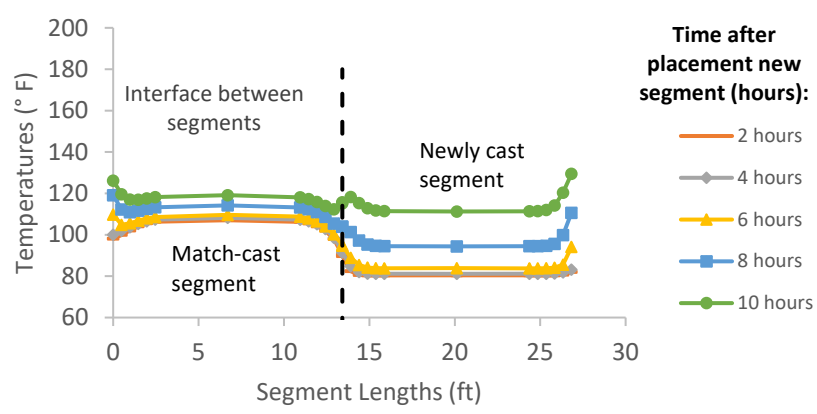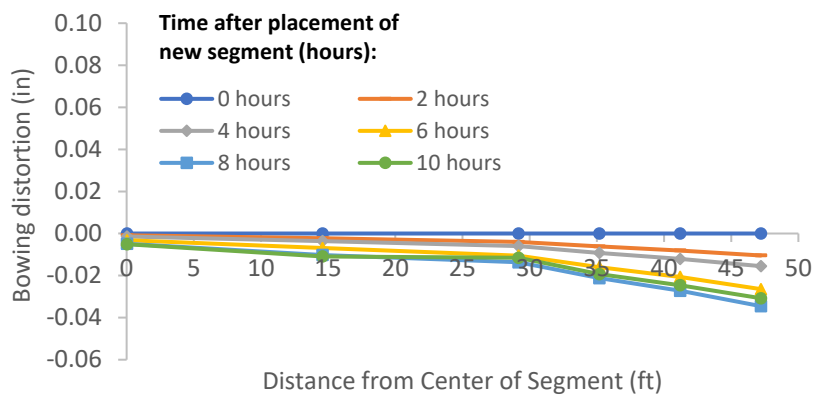

Figure B-306: Simulation 102 - Internal temperatures along the wing of segments

Simulation 103 -Results Summary

Table B-103: Model input parameters simulation 103

Model details		
Permutation number	103	
Geometry	Florida Bridge E - w/l=4.09	
Max. Mesh Size	2.95	in
Time Step	1	hrs
Placement Temperature	80	°F
Match-cast segment Time of Simulation at Casting	0	hrs
New Segment Time of Simulation at Casting	24	hrs
Concrete Properties		
Cement Content	750.09	lb/yd^3
Activation Energy	24.13	BTU/mol
Heat of Hydration Parameters		
Total Heat Development, $Q_{ult} = \alpha_u \cdot H_u$	111.33	BTU/lb
Time Parameter, τ	13.36	hrs
Curvature Parameter, β	1.49	
Density	3816.577	lb/yd^3
Specific Heat	0.25	BTU/(lb·°F)
Thermal Conductivity	1.557	BTU/(ft·h·°F)
Match-cast segment Elastic Modulus Dev. Parameters		
Final Value	4471.32	ksi
Time Parameter	12.420	hrs
Curvature Parameter	1.068	
New Segment Elastic Modulus Dev. Parameters		
Final Value	14.50	ksi
Time Parameter	n/a	hrs
Curvature Parameter	n/a	
Poisson Ratio	0.17	
Coefficient of Thermal Expansion	4.54	µε/°F
Thermal Boundary Conditions (Applied to Appropriate Faces)		
Ambient Temp	Steam-curing-160°F-cycle	
Wind	Low-Wind	0.00	mph
Formwork	Steel Formwork	34.60	BTU/(ft·h·°F)
	Thickness	0.118	in
Curing	Burlap	0.18	BTU/(ft·h·°F)
	Thickness	0.39	in

Figure B-307: Simulation 103 - Bowing distortion of match-cast segment after placement of the new segment
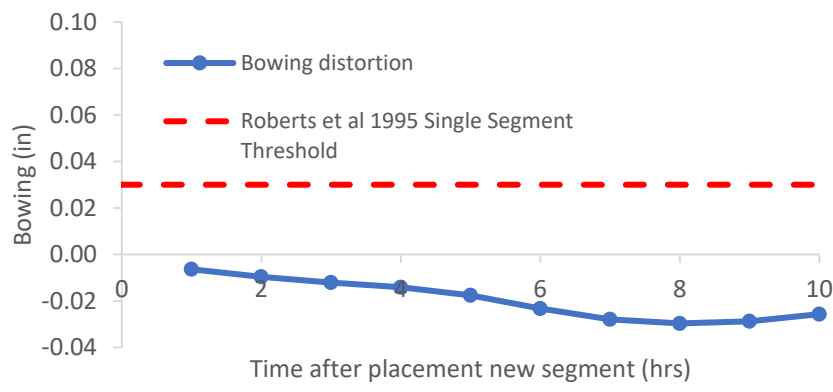

Figure B-308: Simulation 103 - Bowing distortion progression of match-cast segment from time of placement of new segment to 10 hours
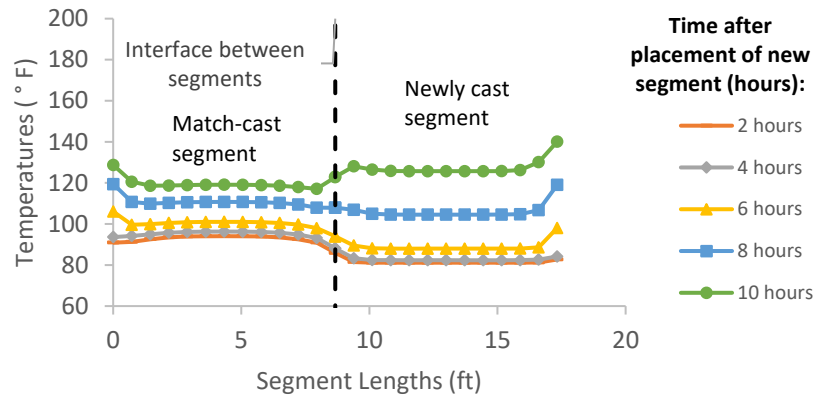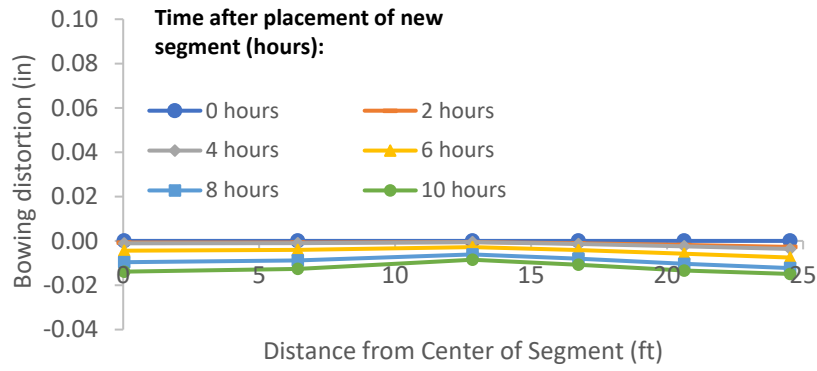

Figure B-309: Simulation 103 - Internal temperatures along the wing of segments

Simulation 104 -Results Summary

Table B-104: Model input parameters simulation 104

Model details		
Permutation number	104	
Geometry	Florida Bridge B - w/l=5.97	
Max. Mesh Size	3.94	in
Time Step	1	hrs
Placement Temperature	80	°F
Match-cast segment Time of Simulation at Casting	0	hrs
New Segment Time of Simulation at Casting	24	hrs
Concrete Properties		
Cement Content	750.09	lb/yd^3
Activation Energy	24.13	BTU/mol
Heat of Hydration Parameters		
Total Heat Development, $Q_{ult} = \alpha_u \cdot H_u$	111.33	BTU/lb
Time Parameter, τ	13.36	hrs
Curvature Parameter, β	1.49	
Density	3816.577	lb/yd^3
Specific Heat	0.25	BTU/(lb·°F)
Thermal Conductivity	1.557	BTU/(ft·h·°F)
Match-cast segment Elastic Modulus Dev. Parameters		
Final Value	4471.32	ksi
Time Parameter	12.420	hrs
Curvature Parameter	1.068	
New Segment Elastic Modulus Dev. Parameters		
Final Value	14.50	ksi
Time Parameter	n/a	hrs
Curvature Parameter	n/a	
Poisson Ratio	0.17	
Coefficient of Thermal Expansion	4.54	με/°F
Thermal Boundary Conditions (Applied to Appropriate Faces)		
Ambient Temp	Steam-curing-160°F-cycle	
Wind	Low-Wind	0.00	mph
Formwork	Steel Formwork	34.60	BTU/(ft·h·°F)
	Thickness	0.118	in
Curing	Burlap	0.18	BTU/(ft·h·°F)
	Thickness	0.39	in

Figure B-310: Simulation 104 - Bowing distortion of match-cast segment after placement of the new segment
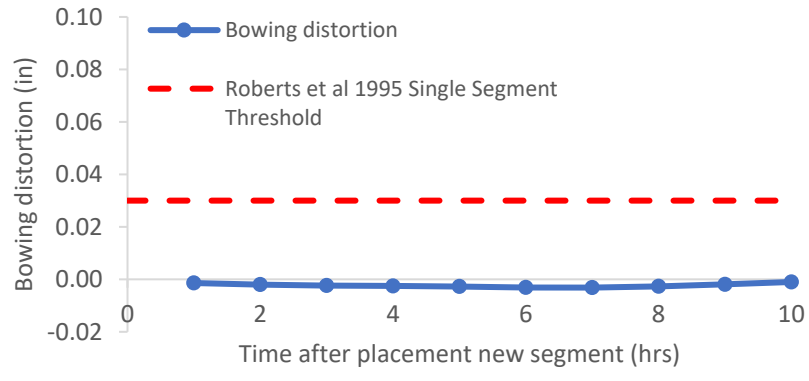

Figure B-311: Simulation 104 - Bowing distortion progression of match-cast segment from time of placement of new segment to 10 hours
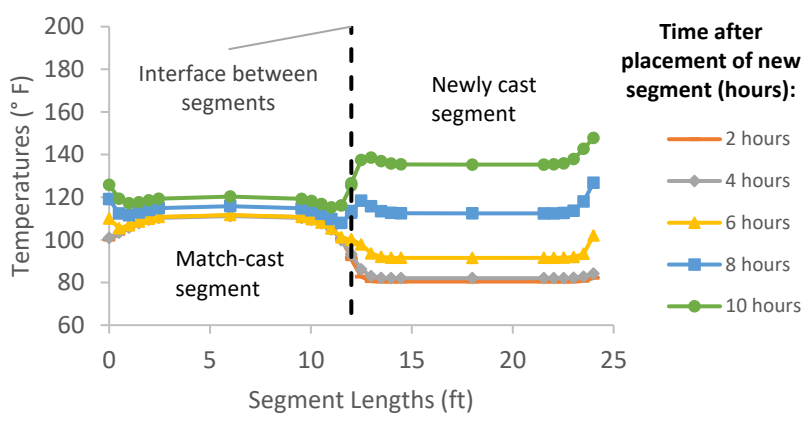

Figure B-312: Simulation 104 - Internal temperatures along the wing of segments

Simulation 105 -Results Summary

Table B-105: Model input parameters simulation 105

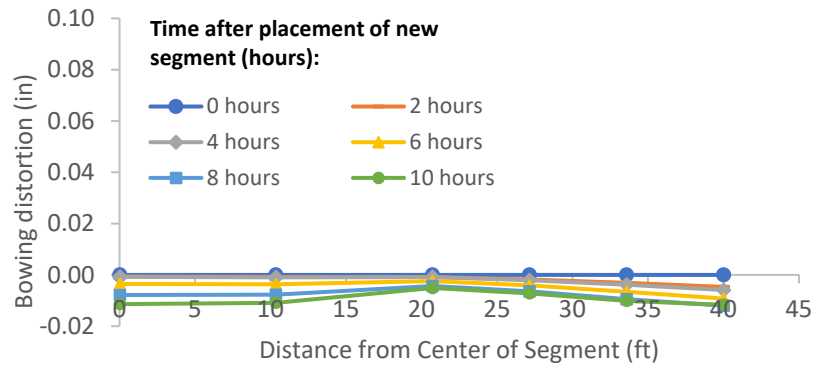| Model details		
Permutation number	105	
Geometry	Florida Bridge C - w/l=10.89	
Max. Mesh Size	3.54	in
Time Step	1	hrs
Placement Temperature	80	°F
Match-cast segment Time of Simulation at Casting	0	hrs
New Segment Time of Simulation at Casting	24	hrs
Concrete Properties		
Cement Content	750.09	lb/yd³
Activation Energy	24.13	BTU/mol
Heat of Hydration Parameters		
Total Heat Development, $Q_{ult} = \alpha_u \cdot H_u$	111.33	BTU/lb
Time Parameter, τ	13.36	hrs
Curvature Parameter, β	1.49	
Density	3816.577	lb/yd³
Specific Heat	0.25	BTU/(lb·°F)
Thermal Conductivity	1.557	BTU/(ft·h·°F)
Match-cast segment Elastic Modulus Dev. Parameters		
Final Value	4471.32	ksi
Time Parameter	12.420	hrs
Curvature Parameter	1.068	
New Segment Elastic Modulus Dev. Parameters		
Final Value	14.50	ksi
Time Parameter	n/a	hrs
Curvature Parameter	n/a	
Poisson Ratio	0.17	
Coefficient of Thermal Expansion	4.54	µε/°F
Thermal Boundary Conditions (Applied to Appropriate Faces)		
Ambient Temp	Steam-curing-160°F-cycle	
Wind	Low-Wind	0.00	mph
Formwork	Steel Formwork	34.60	BTU/(ft·h·°F)
	Thickness	0.118	in
Curing	Burlap	0.18	BTU/(ft·h·°F)
	Thickness	0.39	in

Figure B-313: Simulation 105 - Bowing distortion of match-cast segment after placement of the new segment
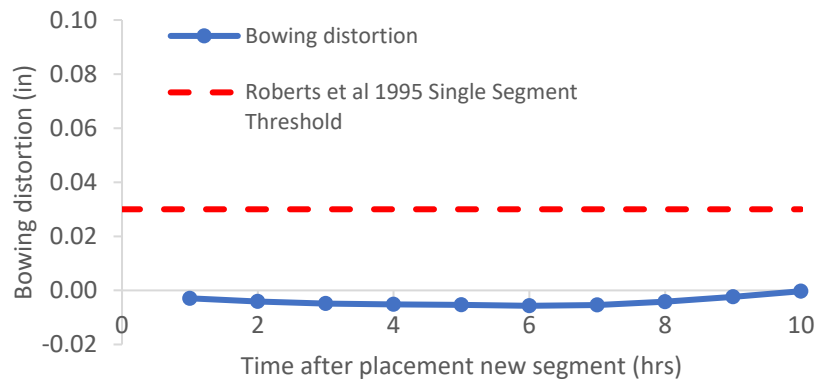

Figure B-314: Simulation 105 - Bowing distortion progression of match-cast segment from time of placement of new segment to 10 hours
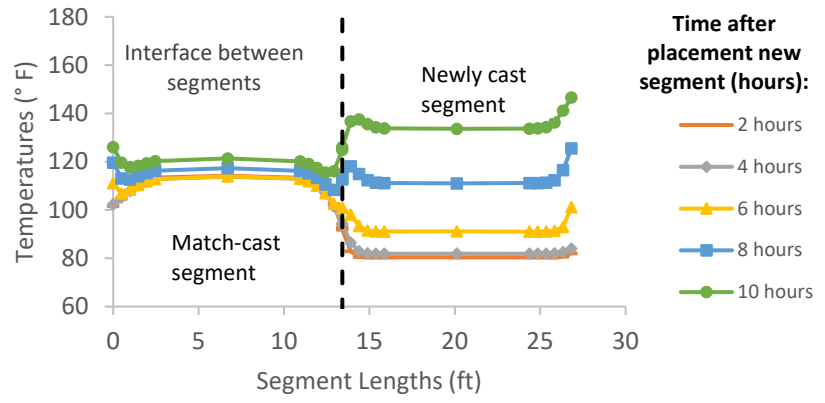

Figure B-315: Simulation 105 - Internal temperatures along the wing of segments

Simulation 106 -Results Summary

Table B-106: Model input parameters simulation 106

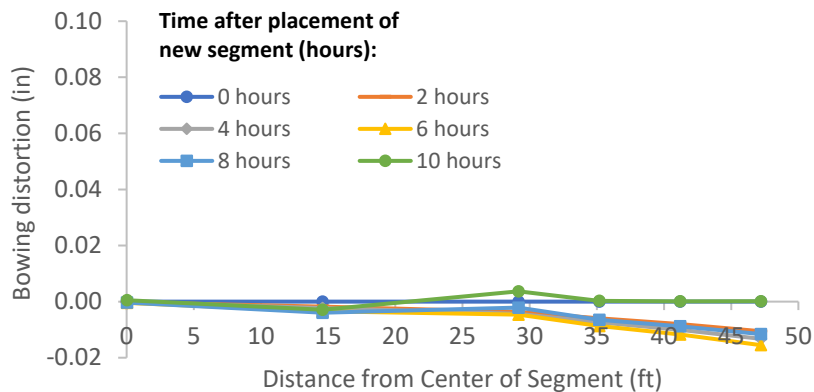| Model details		
Permutation number	106	
Geometry	Florida Bridge E - w/l=4.09	
Max. Mesh Size	2.95	in
Time Step	1	hrs
Placement Temperature	80	°F
Match-cast segment Time of Simulation at Casting	0	hrs
New Segment Time of Simulation at Casting	24	hrs
Concrete Properties		
Cement Content	950.11	lb/yd³
Activation Energy	28.43	BTU/mol
Heat of Hydration Parameters		
Total Heat Development, $Q_{ult} = \alpha_u \cdot H_u$	124.95	BTU/lb
Time Parameter, τ	10.50	hrs
Curvature Parameter, β	1.60	
Density	3880.948	lb/yd³
Specific Heat	0.26	BTU/(lb·°F)
Thermal Conductivity	1.502	BTU/(ft·h·°F)
Match-cast segment Elastic Modulus Dev. Parameters		
Final Value	4584.92	ksi
Time Parameter	12.420	hrs
Curvature Parameter	1.068	
New Segment Elastic Modulus Dev. Parameters		
Final Value	14.50	ksi
Time Parameter	n/a	hrs
Curvature Parameter	n/a	
Poisson Ratio	0.17	
Coefficient of Thermal Expansion	4.54	με/°F
Thermal Boundary Conditions (Applied to Appropriate Faces)		
Ambient Temp	Steam-curing-160°F-cycle	
Wind	Low-Wind	0.00	mph
Formwork	Steel Formwork	34.60	BTU/(ft·h·°F)
	Thickness	0.118	in
Curing	Burlap	0.18	BTU/(ft·h·°F)
	Thickness	0.39	in

Figure B-316: Simulation 106 - Bowing distortion of match-cast segment after placement of the new segment
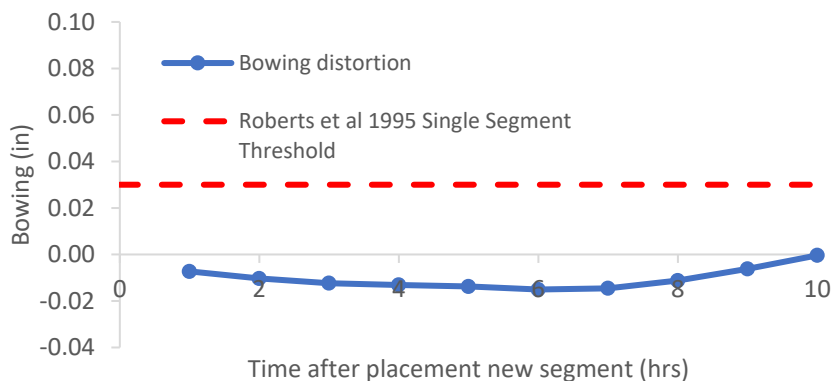

Figure B-317: Simulation 106 - Bowing distortion progression of match-cast segment from time of placement of new segment to 10 hours
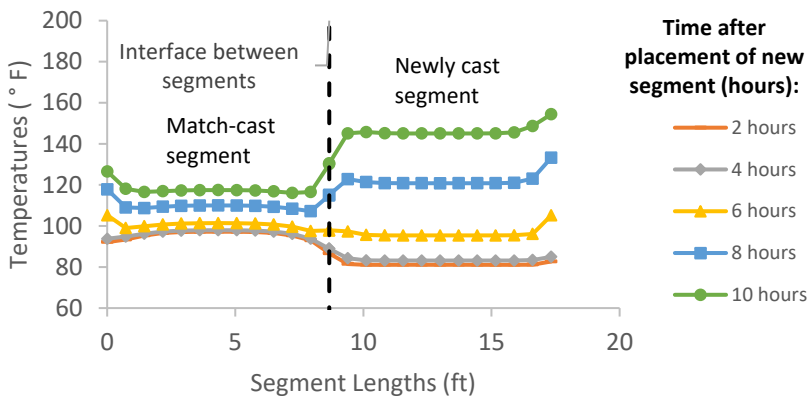

Figure B-318: Simulation 106 - Internal temperatures along the wing of segments

Simulation 107 -Results Summary

Table B-107: Model input parameters simulation 107

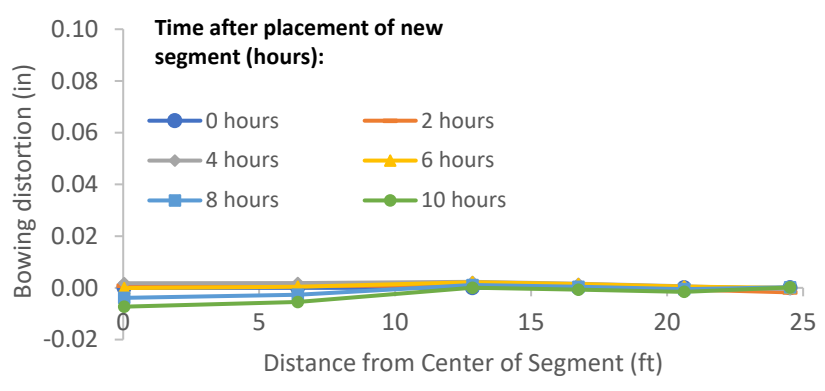| Model details		
Permutation number	107	
Geometry	Florida Bridge B - w/l=5.97	
Max. Mesh Size	3.94	in
Time Step	1	hrs
Placement Temperature	80	°F
Match-cast segment Time of Simulation at Casting	0	hrs
New Segment Time of Simulation at Casting	24	hrs
Concrete Properties		
Cement Content	950.11	lb/yd³
Activation Energy	28.43	BTU/mol
Heat of Hydration Parameters		
Total Heat Development, $Q_{ult} = \alpha_u \cdot H_u$	124.95	BTU/lb
Time Parameter, τ	10.50	hrs
Curvature Parameter, β	1.60	
Density	3880.948	lb/yd³
Specific Heat	0.26	BTU/(lb·°F)
Thermal Conductivity	1.502	BTU/(ft·h·°F)
Match-cast segment Elastic Modulus Dev. Parameters		
Final Value	4584.92	ksi
Time Parameter	12.420	hrs
Curvature Parameter	1.068	
New Segment Elastic Modulus Dev. Parameters		
Final Value	14.50	ksi
Time Parameter	n/a	hrs
Curvature Parameter	n/a	
Poisson Ratio	0.17	
Coefficient of Thermal Expansion	4.54	$\mu\varepsilon$/°F
Thermal Boundary Conditions (Applied to Appropriate Faces)		
Ambient Temp	Steam-curing-160°F-cycle	
Wind	Low-Wind	0.00	mph
Formwork	Steel Formwork	34.60	BTU/(ft·h·°F)
	Thickness	0.118	in
Curing	Burlap	0.18	BTU/(ft·h·°F)
	Thickness	0.39	in

Figure B-319: Simulation 107 - Bowing distortion of match-cast segment after placement of the new segment
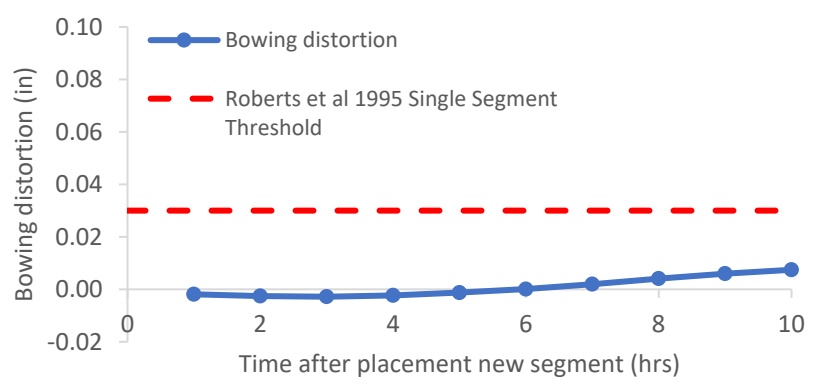

Figure B-320: Simulation 107 - Bowing distortion progression of match-cast segment from time of placement of new segment to 10 hours
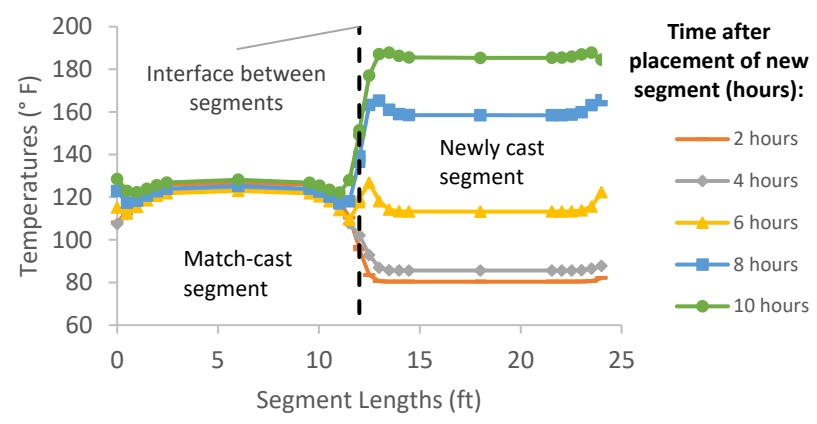

Figure B-321: Simulation 107 - Internal temperatures along the wing of segments

Simulation 108 -Results Summary

Table B-108: Model input parameters simulation 108

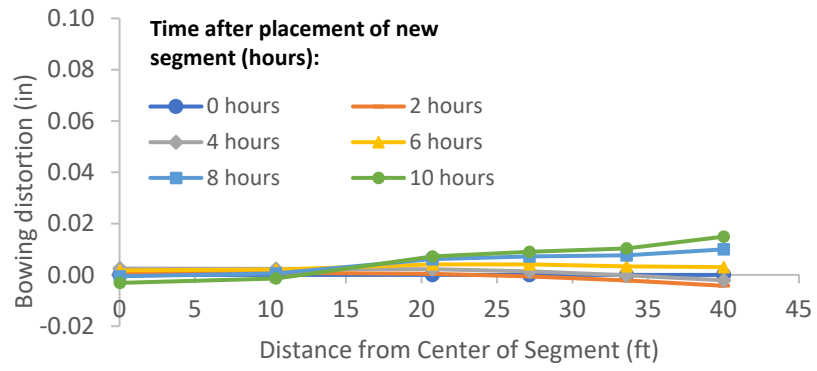| Model details		
Permutation number	108	
Geometry	Florida Bridge C - w/l=10.89	
Max. Mesh Size	3.54	in
Time Step	1	hrs
Placement Temperature	80	°F
Match-cast segment Time of Simulation at Casting	0	hrs
New Segment Time of Simulation at Casting	24	hrs
Concrete Properties		
Cement Content	950.11	lb/yd^3
Activation Energy	28.43	BTU/mol
Heat of Hydration Parameters		
Total Heat Development, $Q_{ult} = \alpha_u \cdot H_u$	124.95	BTU/lb
Time Parameter, τ	10.50	hrs
Curvature Parameter, β	1.60	
Density	3880.948	lb/yd^3
Specific Heat	0.26	BTU/(lb·°F)
Thermal Conductivity	1.502	BTU/(ft·h·°F)
Match-cast segment Elastic Modulus Dev. Parameters		
Final Value	4584.92	ksi
Time Parameter	12.420	hrs
Curvature Parameter	1.068	
New Segment Elastic Modulus Dev. Parameters		
Final Value	14.50	ksi
Time Parameter	n/a	hrs
Curvature Parameter	n/a	
Poisson Ratio	0.17	
Coefficient of Thermal Expansion	4.54	µε/°F
Thermal Boundary Conditions (Applied to Appropriate Faces)		
Ambient Temp	Steam-curing-160°F-cycle	
Wind	Low-Wind	0.00	mph
Formwork	Steel Formwork	34.60	BTU/(ft·h·°F)
	Thickness	0.118	in
Curing	Burlap	0.18	BTU/(ft·h·°F)
	Thickness	0.39	in

Figure B-322: Simulation 108 - Bowing distortion of match-cast segment after placement of the new segment
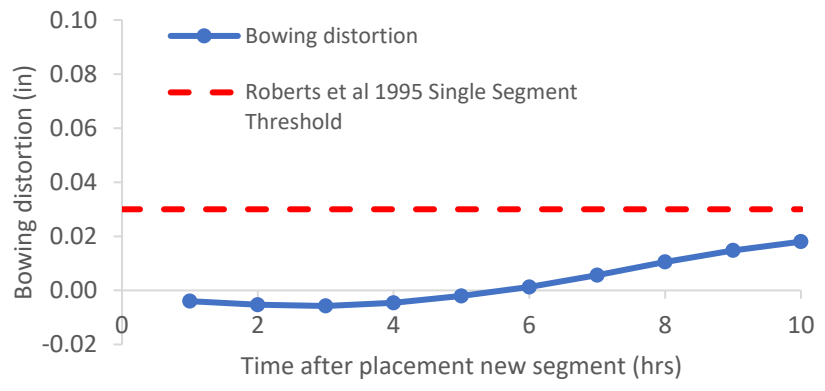

Figure B-323: Simulation 108 - Bowing distortion progression of match-cast segment from time of placement of new segment to 10 hours
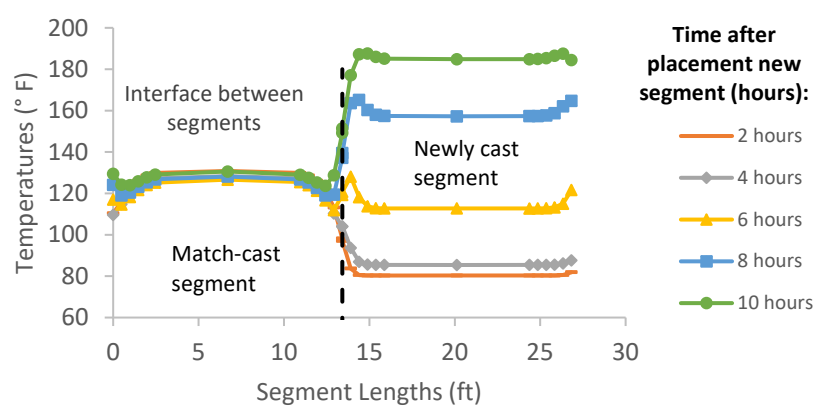

Figure B-324: Simulation 108 - Internal temperatures along the wing of segments

Simulation 109 -Results Summary

Table B-109: Model input parameters simulation 109

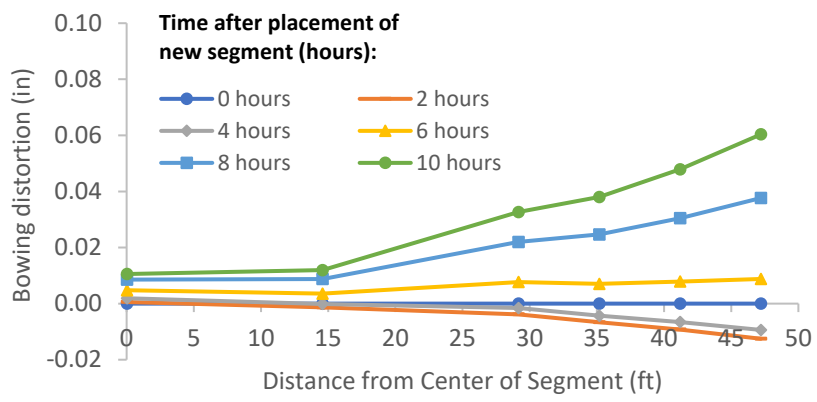| Model details		
Permutation number	109	
Geometry	Florida Bridge A - w/l=2.15	
Max. Mesh Size	2.76	in
Time Step	1	hrs
Placement Temperature	95	°F
Match-cast segment Time of Simulation at Casting	0	hrs
New Segment Time of Simulation at Casting	24	hrs
Concrete Properties		
Cement Content	950.11	lb/yd^3
Activation Energy	28.43	BTU/mol
Heat of Hydration Parameters		
Total Heat Development, $Q_{ult} = \alpha_u \cdot H_u$	124.95	BTU/lb
Time Parameter, τ	10.50	hrs
Curvature Parameter, β	1.60	
Density	3880.948	lb/yd^3
Specific Heat	0.26	BTU/(lb·°F)
Thermal Conductivity	1.502	BTU/(ft·h·°F)
Match-cast segment Elastic Modulus Dev. Parameters		
Final Value	4584.92	ksi
Time Parameter	12.420	hrs
Curvature Parameter	1.068	
New Segment Elastic Modulus Dev. Parameters		
Final Value	14.50	ksi
Time Parameter	n/a	hrs
Curvature Parameter	n/a	
Poisson Ratio	0.17	
Coefficient of Thermal Expansion	4.54	µε/°F
Thermal Boundary Conditions (Applied to Appropriate Faces)		
Ambient Temp	Miami - Summer - Morning - Placement	
Wind	Medium-Wind	7.50	mph
Formwork	Steel Formwork	34.60	BTU/(ft·h·°F)
	Thickness	0.118	in
Curing	Burlap	0.18	BTU/(ft·h·°F)
	Thickness	0.39	in

Figure B-325: Simulation 109 - Bowing distortion of match-cast segment after placement of the new segment
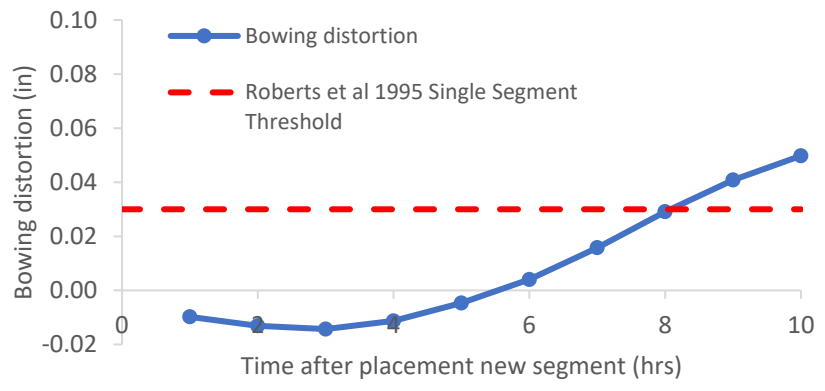

Figure B-326: Simulation 109 - Bowing distortion progression of match-cast segment from time of placement of new segment to 10 hours
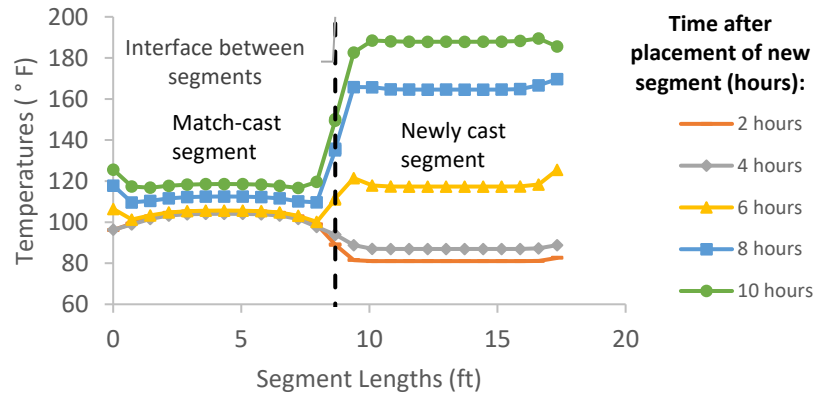

Figure B-327: Simulation 109 - Internal temperatures along the wing of segments

Simulation 110 -Results Summary

Table B-110: Model input parameters simulation 110

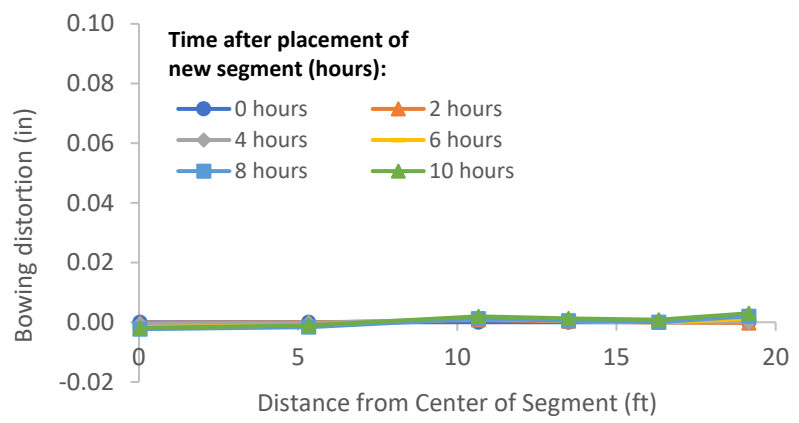| Model details		
Permutation number	110	
Geometry	Florida Bridge F - w/l=5.92	
Max. Mesh Size	3.15	in
Time Step	1	hrs
Placement Temperature	95	°F
Match-cast segment Time of Simulation at Casting	0	hrs
New Segment Time of Simulation at Casting	24	hrs
Concrete Properties		
Cement Content	950.11	lb/yd³
Activation Energy	28.43	BTU/mol
Heat of Hydration Parameters		
Total Heat Development, $Q_{ult} = \alpha_u \cdot H_u$	124.95	BTU/lb
Time Parameter, τ	10.50	hrs
Curvature Parameter, β	1.60	
Density	3880.948	lb/yd³
Specific Heat	0.26	BTU/(lb·°F)
Thermal Conductivity	1.502	BTU/(ft·h·°F)
Match-cast segment Elastic Modulus Dev. Parameters		
Final Value	4584.92	ksi
Time Parameter	12.420	hrs
Curvature Parameter	1.068	
New Segment Elastic Modulus Dev. Parameters		
Final Value	14.50	ksi
Time Parameter	n/a	hrs
Curvature Parameter	n/a	
Poisson Ratio	0.17	
Coefficient of Thermal Expansion	4.54	µε/°F
Thermal Boundary Conditions (Applied to Appropriate Faces)		
Ambient Temp	Miami - Summer - Morning - Placement	
Wind	Medium-Wind	7.50	mph
Formwork	Steel Formwork	34.60	BTU/(ft·h·°F)
	Thickness	0.118	in
Curing	Burlap	0.18	BTU/(ft·h·°F)
	Thickness	0.39	in

Figure B-328: Simulation 110 - Bowing distortion of match-cast segment after placement of the new segment

Figure B-329: Simulation 110 - Bowing distortion progression of match-cast segment from time of placement of new segment to 10 hours
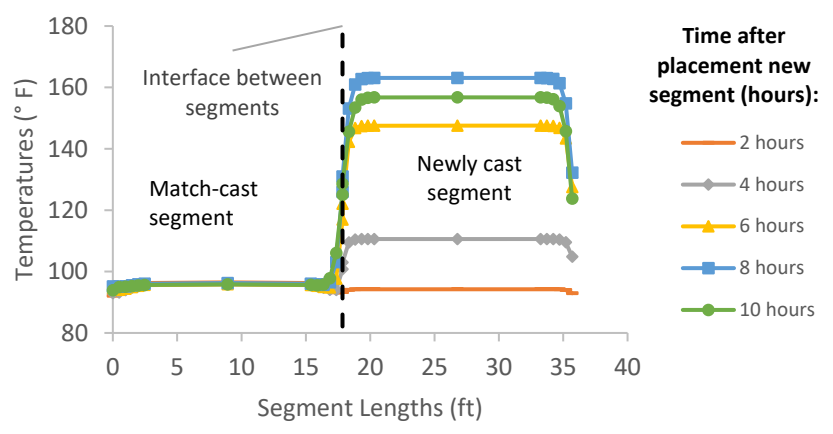

Figure B-330: Simulation 110 - Internal temperatures along the wing of segments

Simulation 111 -Results Summary

Table B-111: Model input parameters simulation 111

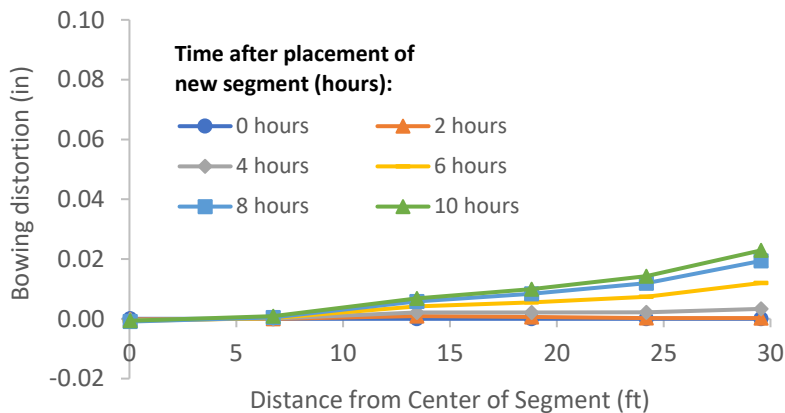| Model details		
Permutation number	111	
Geometry	Florida Bridge D - w/l=9.39	
Max. Mesh Size	3.15	in
Time Step	1	hrs
Placement Temperature	95	°F
Match-cast segment Time of Simulation at Casting	0	hrs
New Segment Time of Simulation at Casting	24	hrs
Concrete Properties		
Cement Content	950.11	lb/yd^3
Activation Energy	28.43	BTU/mol
Heat of Hydration Parameters		
Total Heat Development, $Q_{ult} = \alpha_u \cdot H_u$	124.95	BTU/lb
Time Parameter, τ	10.50	hrs
Curvature Parameter, β	1.60	
Density	3880.948	lb/yd^3
Specific Heat	0.26	BTU/(lb·°F)
Thermal Conductivity	1.502	BTU/(ft·h·°F)
Match-cast segment Elastic Modulus Dev. Parameters		
Final Value	4584.92	ksi
Time Parameter	12.420	hrs
Curvature Parameter	1.068	
New Segment Elastic Modulus Dev. Parameters		
Final Value	14.50	ksi
Time Parameter	n/a	hrs
Curvature Parameter	n/a	
Poisson Ratio	0.17	
Coefficient of Thermal Expansion	4.54	με/°F
Thermal Boundary Conditions (Applied to Appropriate Faces)		
Ambient Temp	Miami - Summer - Morning - Placement	
Wind	Medium-Wind	7.50	mph
Formwork	Steel Formwork	34.60	BTU/(ft·h·°F)
	Thickness	0.118	in
Curing	Burlap	0.18	BTU/(ft·h·°F)
	Thickness	0.39	in

Figure B-331: Simulation 111 - Bowing distortion of match-cast segment after placement of the new segment
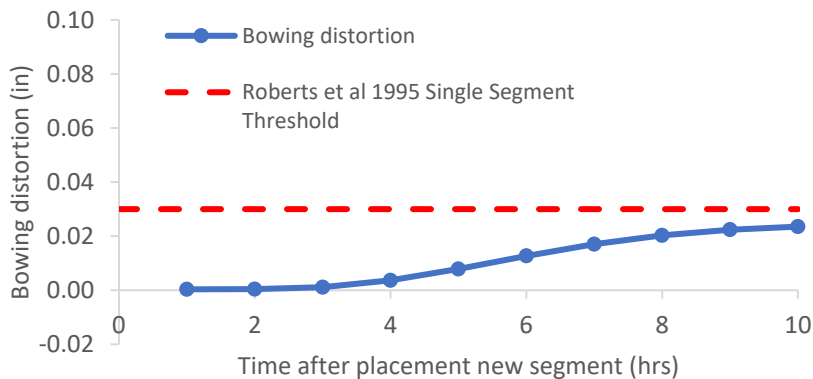

Figure B-332: Simulation 111 - Bowing distortion progression of match-cast segment from time of placement of new segment to 10 hours
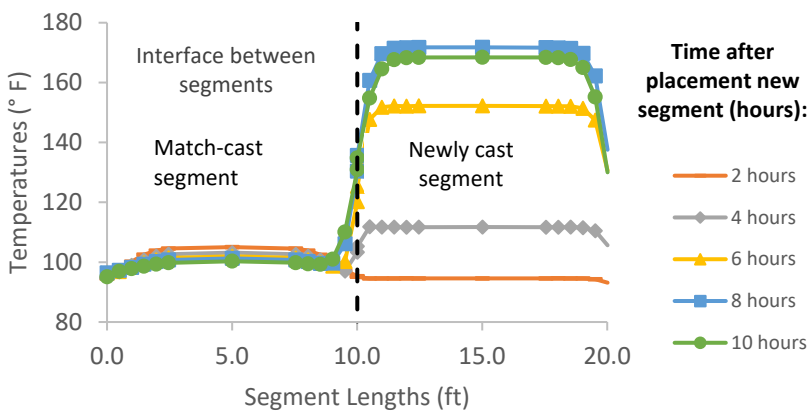

Figure B-333: Simulation 111 - Internal temperatures along the wing of segments

Simulation 112 -Results Summary

Table B-112: Model input parameters simulation 112

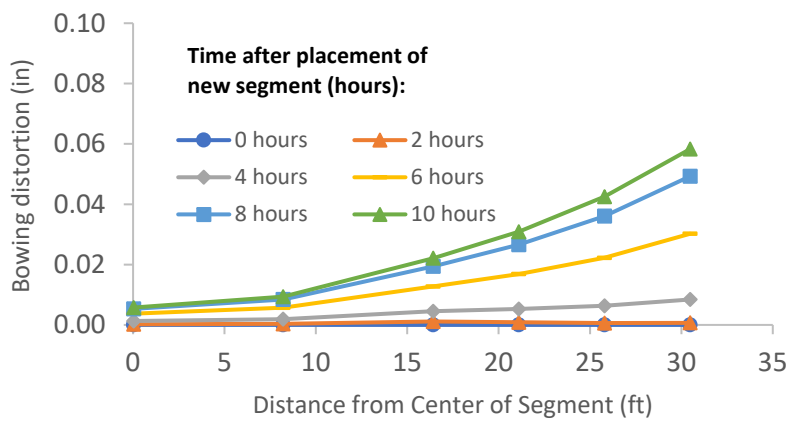| Model details		
Permutation number	112	
Geometry	Bridge Bang Na Pier - w/l=21.80	
Max. Mesh Size	2.76	in
Time Step	1	hrs
Placement Temperature	95	°F
Match-cast segment Time of Simulation at Casting	0	hrs
New Segment Time of Simulation at Casting	24	hrs
Concrete Properties		
Cement Content	950.11	lb/yd^3
Activation Energy	28.43	BTU/mol
Heat of Hydration Parameters		
Total Heat Development, $Q_{ult} = \alpha_u \cdot H_u$	124.95	BTU/lb
Time Parameter, τ	10.50	hrs
Curvature Parameter, β	1.60	
Density	3880.948	lb/yd^3
Specific Heat	0.26	BTU/(lb·°F)
Thermal Conductivity	1.502	BTU/(ft·h·°F)
Match-cast segment Elastic Modulus Dev. Parameters		
Final Value	4584.92	ksi
Time Parameter	12.420	hrs
Curvature Parameter	1.068	
New Segment Elastic Modulus Dev. Parameters		
Final Value	14.50	ksi
Time Parameter	n/a	hrs
Curvature Parameter	n/a	
Poisson Ratio	0.17	
Coefficient of Thermal Expansion	4.54	με/°F
Thermal Boundary Conditions (Applied to Appropriate Faces)		
Ambient Temp	Miami - Summer - Morning - Placement		
Wind	Medium-Wind	7.50	mph
Formwork	Steel Formwork	34.60	BTU/(ft·h·°F)
	Thickness	0.118	in
Curing	Burlap	0.18	BTU/(ft·h·°F)
	Thickness	0.39	in

Figure B-334: Simulation 112 - Bowing distortion of match-cast segment after placement of the new segment
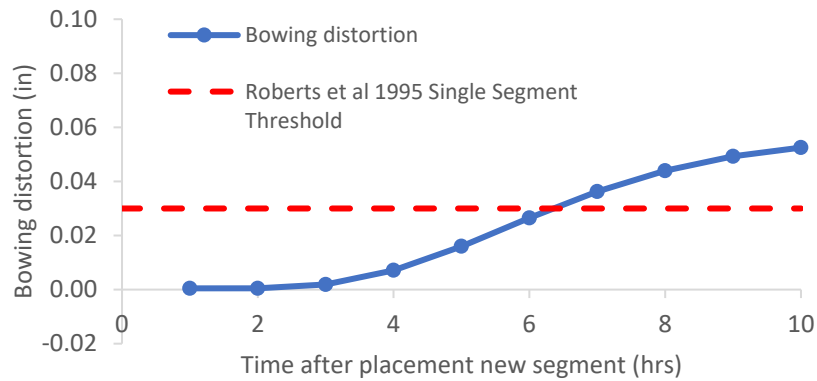

Figure B-335: Simulation 112 - Bowing distortion progression of match-cast segment from time of placement of new segment to 10 hours
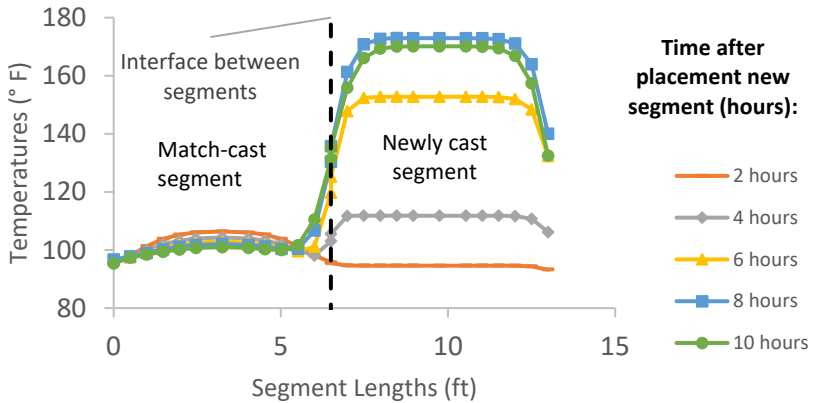

Figure B-336: Simulation 112 - Internal temperatures along the wing of segments

Simulation 113 -Results Summary

Table B-113: Model input parameters simulation 113

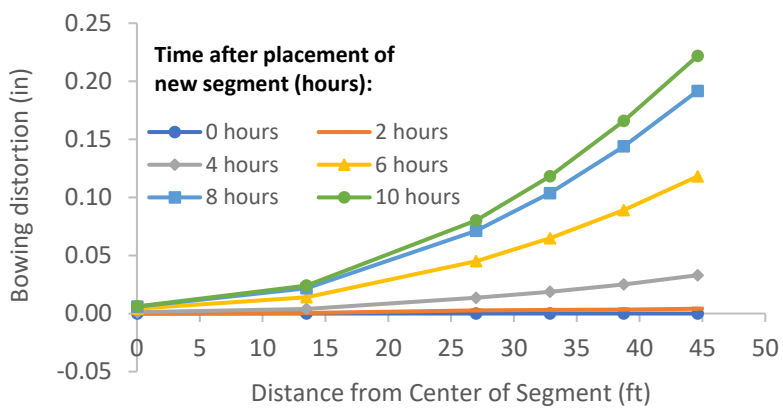| Model details		
Permutation number	113	
Geometry	Florida Bridge A - w/l=2.15	
Max. Mesh Size	2.76	in
Time Step	1	hrs
Placement Temperature	95	°F
Match-cast segment Time of Simulation at Casting	0	hrs
New Segment Time of Simulation at Casting	24	hrs
Concrete Properties		
Cement Content	950.11	lb/yd³
Activation Energy	28.43	BTU/mol
Heat of Hydration Parameters		
Total Heat Development, $Q_{ult} = \alpha_u \cdot H_u$	124.95	BTU/lb
Time Parameter, τ	10.50	hrs
Curvature Parameter, β	1.60	
Density	3880.948	lb/yd³
Specific Heat	0.26	BTU/(lb·°F)
Thermal Conductivity	1.502	BTU/(ft·h·°F)
Match-cast segment Elastic Modulus Dev. Parameters		
Final Value	4584.92	ksi
Time Parameter	12.420	hrs
Curvature Parameter	1.068	
New Segment Elastic Modulus Dev. Parameters		
Final Value	14.50	ksi
Time Parameter	n/a	hrs
Curvature Parameter	n/a	
Poisson Ratio	0.17	
Coefficient of Thermal Expansion	4.54	με/°F
Thermal Boundary Conditions (Applied to Appropriate Faces)		
Ambient Temp	Miami - Summer - Morning - Placement	
Wind	Medium-Wind	7.50	mph
Formwork	Steel Formwork	34.60	BTU/(ft·h·°F)
	Thickness	0.118	in
Curing	White Burlap Polyethylene	0.02	BTU/(ft·h·°F)
	Thickness	0.39	in

Figure B-337: Simulation 113 - Bowing distortion of match-cast segment after placement of the new segment
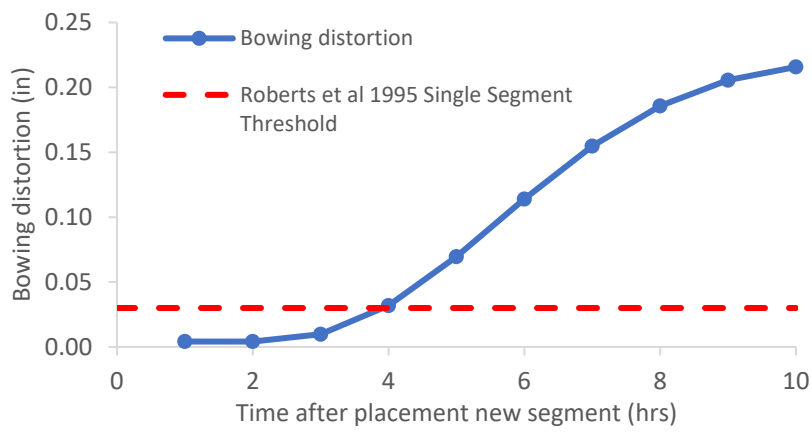

Figure B-338: Simulation 113 - Bowing distortion progression of match-cast segment from time of placement of new segment to 10 hours
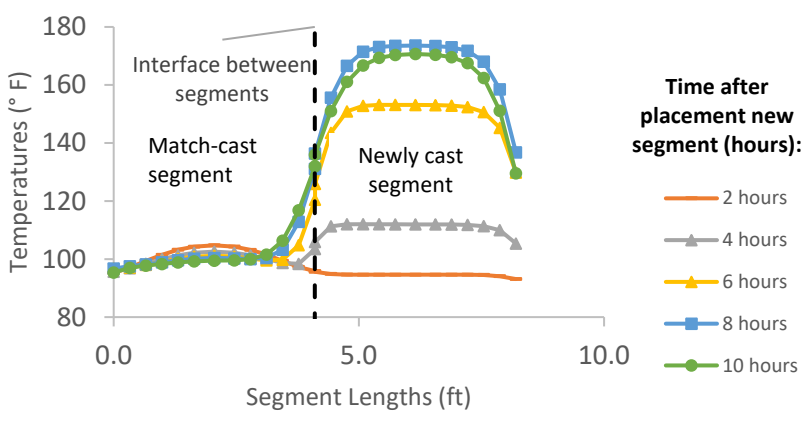

Figure B-339: Simulation 113 - Internal temperatures along the wing of segments

Simulation 114 -Results Summary

Table B-114: Model input parameters simulation 114

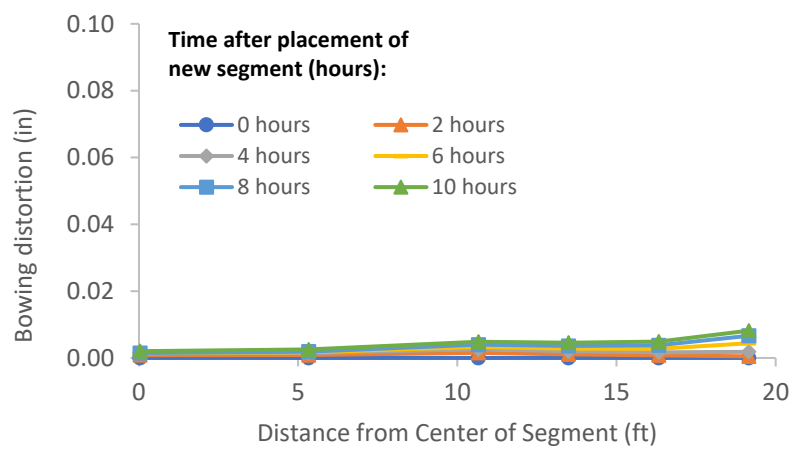| Model details		
Permutation number	114	
Geometry	Florida Bridge F - w/l=5.92	
Max. Mesh Size	3.15	in
Time Step	1	hrs
Placement Temperature	95	°F
Match-cast segment Time of Simulation at Casting	0	hrs
New Segment Time of Simulation at Casting	24	hrs
Concrete Properties		
Cement Content	950.11	lb/yd^3
Activation Energy	28.43	BTU/mol
Heat of Hydration Parameters		
Total Heat Development, $Q_{ult} = \alpha_u \cdot H_u$	124.95	BTU/lb
Time Parameter, τ	10.50	hrs
Curvature Parameter, β	1.60	
Density	3880.948	lb/yd^3
Specific Heat	0.26	BTU/(lb·°F)
Thermal Conductivity	1.502	BTU/(ft·h·°F)
Match-cast segment Elastic Modulus Dev. Parameters		
Final Value	4584.92	ksi
Time Parameter	12.420	hrs
Curvature Parameter	1.068	
New Segment Elastic Modulus Dev. Parameters		
Final Value	14.50	ksi
Time Parameter	n/a	hrs
Curvature Parameter	n/a	
Poisson Ratio	0.17	
Coefficient of Thermal Expansion	4.54	με/°F
Thermal Boundary Conditions (Applied to Appropriate Faces)		
Ambient Temp	Miami - Summer - Morning - Placement	
Wind	Medium-Wind	7.50	mph
Formwork	Steel Formwork	34.60	BTU/(ft·h·°F)
	Thickness	0.118	in
Curing	White Burlap Polyethylene	0.02	BTU/(ft·h·°F)
	Thickness	0.39	in

Figure B-340: Simulation 114 - Bowing distortion of match-cast segment after placement of the new segment

Figure B-341: Simulation 114 - Bowing distortion progression of match-cast segment from time of placement of new segment to 10 hours
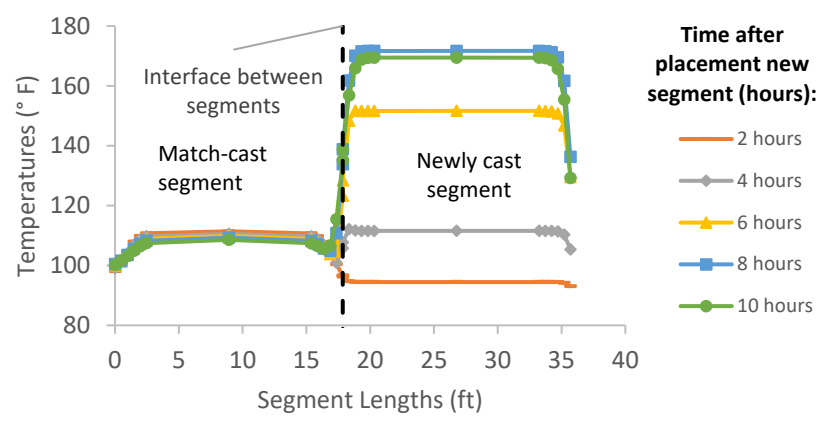

Figure B-342: Simulation 114 - Internal temperatures along the wing of segments

Simulation 115 -Results Summary

Table B-115: Model input parameters simulation 115

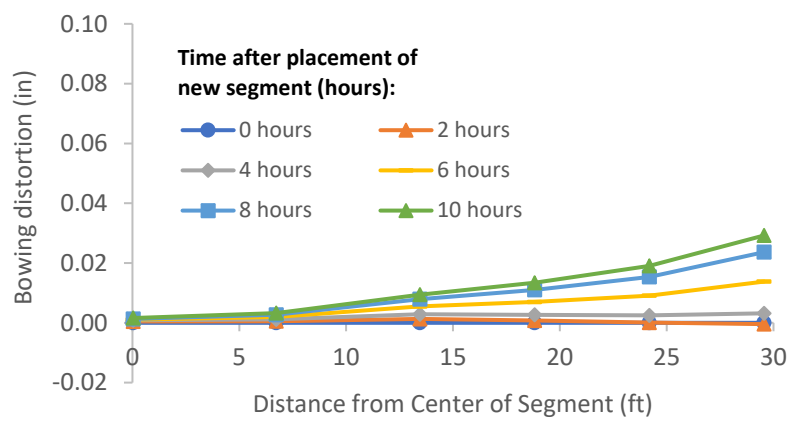| Model details		
Permutation number	115	
Geometry	Florida Bridge D - w/l=9.39	
Max. Mesh Size	3.15	in
Time Step	1	hrs
Placement Temperature	95	°F
Match-cast segment Time of Simulation at Casting	0	hrs
New Segment Time of Simulation at Casting	24	hrs
Concrete Properties		
Cement Content	950.11	lb/yd^3
Activation Energy	28.43	BTU/mol
Heat of Hydration Parameters		
Total Heat Development, $Q_{ult} = \alpha_u \cdot H_u$	124.95	BTU/lb
Time Parameter, τ	10.50	hrs
Curvature Parameter, β	1.60	
Density	3880.948	lb/yd^3
Specific Heat	0.26	BTU/(lb·°F)
Thermal Conductivity	1.502	BTU/(ft·h·°F)
Match-cast segment Elastic Modulus Dev. Parameters		
Final Value	4584.92	ksi
Time Parameter	12.420	hrs
Curvature Parameter	1.068	
New Segment Elastic Modulus Dev. Parameters		
Final Value	14.50	ksi
Time Parameter	n/a	hrs
Curvature Parameter	n/a	
Poisson Ratio	0.17	
Coefficient of Thermal Expansion	4.54	µε/°F
Thermal Boundary Conditions (Applied to Appropriate Faces)		
Ambient Temp	Miami - Summer - Morning - Placement		
Wind	Medium-Wind	7.50	mph
Formwork	Steel Formwork	34.60	BTU/(ft·h·°F)
	Thickness	0.118	in
Curing	White Burlap Polyethylene	0.02	BTU/(ft·h·°F)
	Thickness	0.39	in

Figure B-343: Simulation 115 - Bowing distortion of match-cast segment after placement of the new segment
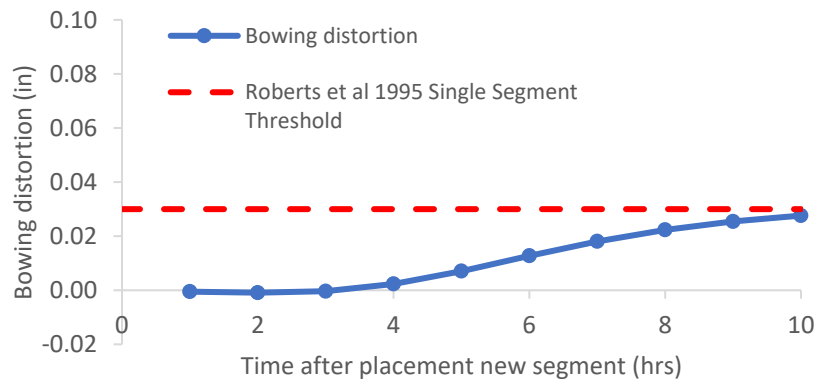

Figure B-344: Simulation 115 - Bowing distortion progression of match-cast segment from time of placement of new segment to 10 hours
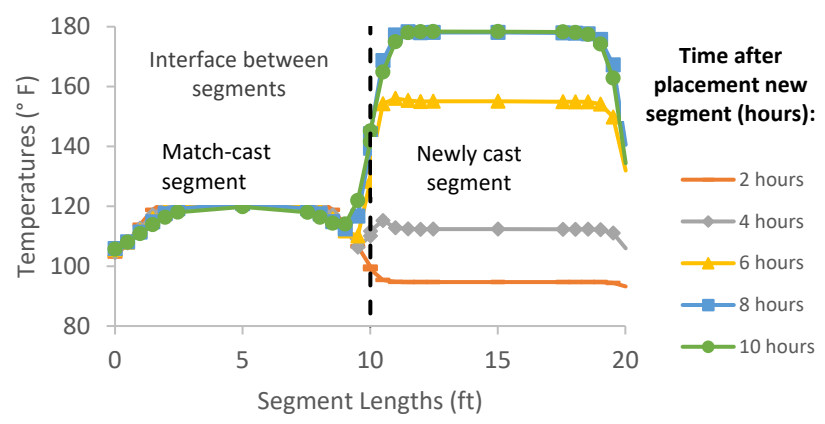

Figure B-345: Simulation 115 - Internal temperatures along the wing of segments

Simulation 116 -Results Summary

Table B-116: Model input parameters simulation 116

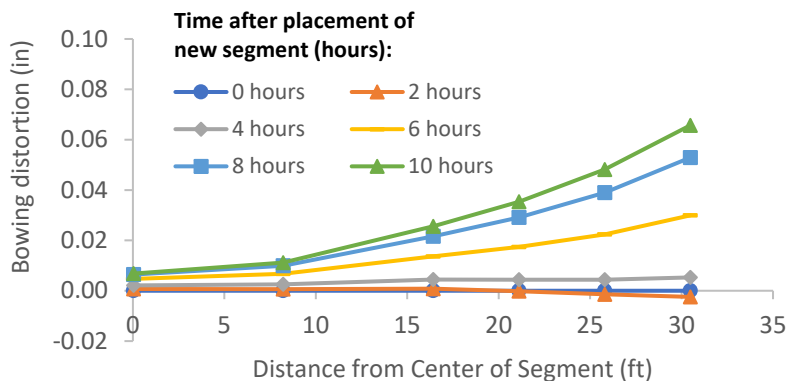| Model details		
Permutation number	116	
Geometry	Bridge Bang Na Pier - w/l=21.80	
Max. Mesh Size	2.76	in
Time Step	1	hrs
Placement Temperature	95	°F
Match-cast segment Time of Simulation at Casting	0	hrs
New Segment Time of Simulation at Casting	24	hrs
Concrete Properties		
Cement Content	950.11	lb/yd^3
Activation Energy	28.43	BTU/mol
Heat of Hydration Parameters		
Total Heat Development, $Q_{ult} = \alpha_u \cdot H_u$	124.95	BTU/lb
Time Parameter, τ	10.50	hrs
Curvature Parameter, β	1.60	
Density	3880.948	lb/yd^3
Specific Heat	0.26	BTU/(lb·°F)
Thermal Conductivity	1.502	BTU/(ft·h·°F)
Match-cast segment Elastic Modulus Dev. Parameters		
Final Value	4584.92	ksi
Time Parameter	12.420	hrs
Curvature Parameter	1.068	
New Segment Elastic Modulus Dev. Parameters		
Final Value	14.50	ksi
Time Parameter	n/a	hrs
Curvature Parameter	n/a	
Poisson Ratio	0.17	
Coefficient of Thermal Expansion	4.54	με/°F
Thermal Boundary Conditions (Applied to Appropriate Faces)		
Ambient Temp	Miami - Summer - Morning - Placement	
Wind	Medium-Wind	7.50	mph
Formwork	Steel Formwork	34.60	BTU/(ft·h·°F)
	Thickness	0.118	in
Curing	White Burlap Polyethylene	0.02	BTU/(ft·h·°F)
	Thickness	0.39	in

Figure B-346: Simulation 116 - Bowing distortion of match-cast segment after placement of the new segment
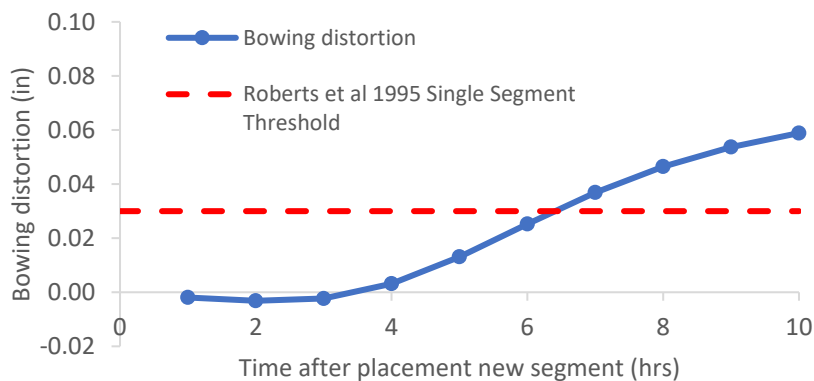

Figure B-347: Simulation 116 - Bowing distortion progression of match-cast segment from time of placement of new segment to 10 hours
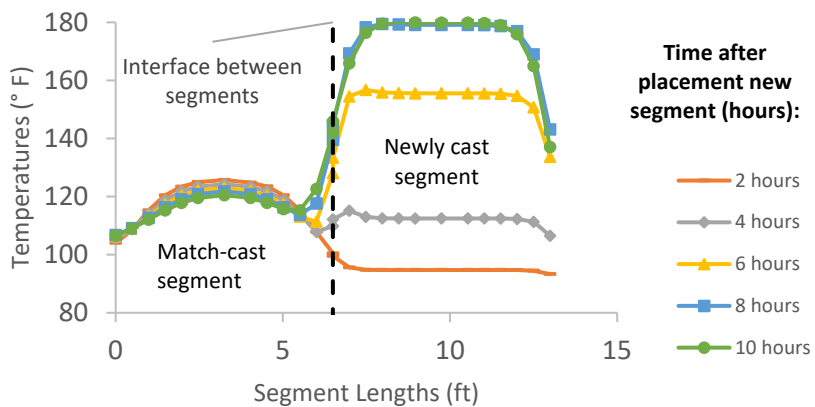

Figure B-348: Simulation 116 - Internal temperatures along the wing of segments

Simulation 117 -Results Summary

Table B-117: Model input parameters simulation 117

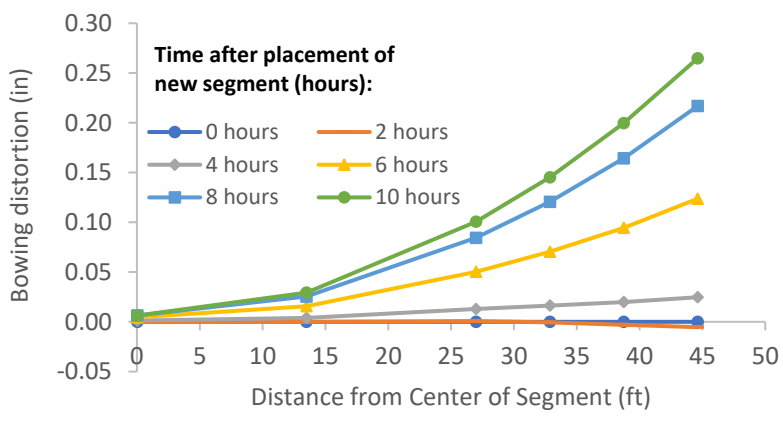| Model details		
Permutation number	117	
Geometry	Florida Bridge A - w/l=2.15	
Max. Mesh Size	2.76	in
Time Step	1	hrs
Placement Temperature	95	°F
Match-cast segment Time of Simulation at Casting	0	hrs
New Segment Time of Simulation at Casting	24	hrs
Concrete Properties		
Cement Content	950.11	lb/yd^3
Activation Energy	28.43	BTU/mol
Heat of Hydration Parameters		
Total Heat Development, $Q_{ult} = \alpha_u \cdot H_u$	124.95	BTU/lb
Time Parameter, τ	10.50	hrs
Curvature Parameter, β	1.60	
Density	3999.308	lb/yd^3
Specific Heat	0.27	BTU/(lb·°F)
Thermal Conductivity	1.705	BTU/(ft·h·°F)
Match-cast segment Elastic Modulus Dev. Parameters		
Final Value	4796.26	ksi
Time Parameter	12.420	hrs
Curvature Parameter	1.068	
New Segment Elastic Modulus Dev. Parameters		
Final Value	14.50	ksi
Time Parameter	n/a	hrs
Curvature Parameter	n/a	
Poisson Ratio	0.17	
Coefficient of Thermal Expansion	6.07	µε/°F
Thermal Boundary Conditions (Applied to Appropriate Faces)		
Ambient Temp	Miami - Summer - Morning - Placement	
Wind	Medium-Wind	7.50	mph
Formwork	Steel Formwork	34.60	BTU/(ft·h·°F)
	Thickness	0.118	in
Curing	Burlap	0.18	BTU/(ft·h·°F)
	Thickness	0.39	in

Figure B-349: Simulation 117 - Bowing distortion of match-cast segment after placement of the new segment
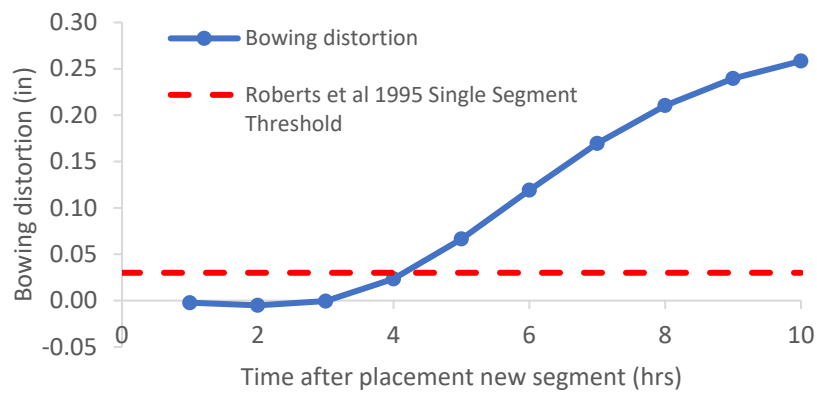

Figure B-350: Simulation 117 - Bowing distortion progression of match-cast segment from time of placement of new segment to 10 hours
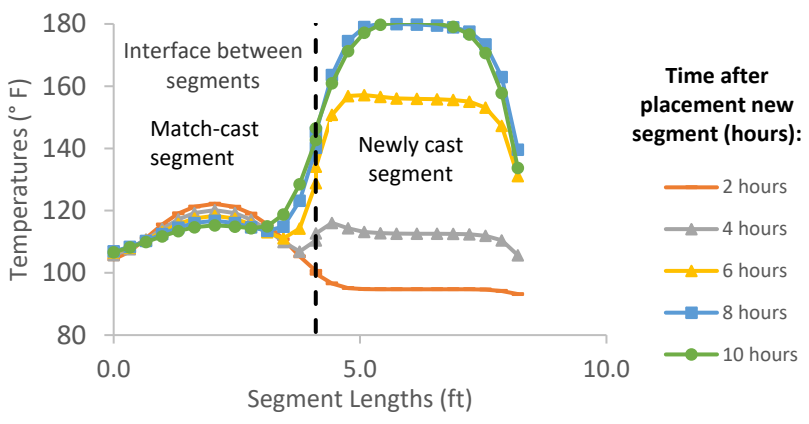

Figure B-351: Simulation 117 - Internal temperatures along the wing of segments

Simulation 118 -Results Summary

Table B-118: Model input parameters simulation 118

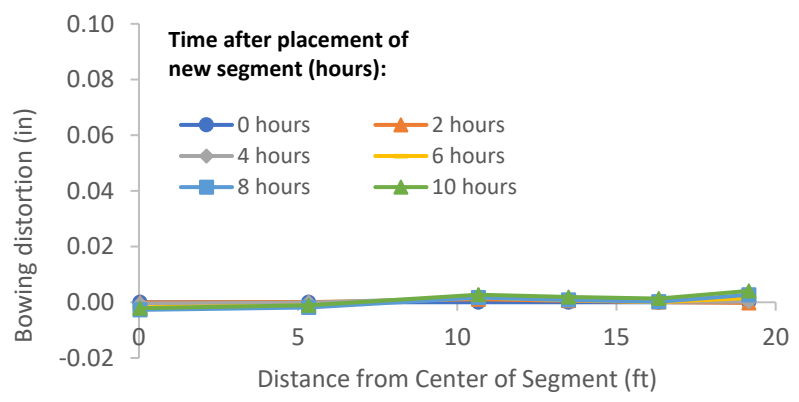| Model details		
Permutation number	118	
Geometry	Florida Bridge F - w/l=5.92	
Max. Mesh Size	3.15	in
Time Step	1	hrs
Placement Temperature	95	°F
Match-cast segment Time of Simulation at Casting	0	hrs
New Segment Time of Simulation at Casting	24	hrs
Concrete Properties		
Cement Content	950.11	lb/yd^3
Activation Energy	28.43	BTU/mol
Heat of Hydration Parameters		
Total Heat Development, $Q_{ult} = \alpha_u \cdot H_u$	124.95	BTU/lb
Time Parameter, τ	10.50	hrs
Curvature Parameter, β	1.60	
Density	3999.308	lb/yd^3
Specific Heat	0.27	BTU/(lb·°F)
Thermal Conductivity	1.705	BTU/(ft·h·°F)
Match-cast segment Elastic Modulus Dev. Parameters		
Final Value	4796.26	ksi
Time Parameter	12.420	hrs
Curvature Parameter	1.068	
New Segment Elastic Modulus Dev. Parameters		
Final Value	14.50	ksi
Time Parameter	n/a	hrs
Curvature Parameter	n/a	
Poisson Ratio	0.17	
Coefficient of Thermal Expansion	6.07	µε/°F
Thermal Boundary Conditions (Applied to Appropriate Faces)		
Ambient Temp	Miami - Summer - Morning - Placement		
Wind	Medium-Wind	7.50	mph
Formwork	Steel Formwork	34.60	BTU/(ft·h·°F)
	Thickness	0.118	in
Curing	Burlap	0.18	BTU/(ft·h·°F)
	Thickness	0.39	in

Figure B-352: Simulation 118 - Bowing distortion of match-cast segment after placement of the new segment
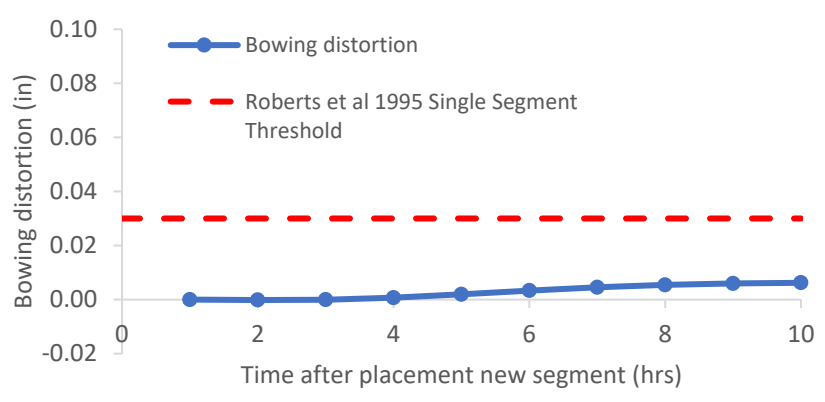

Figure B-353: Simulation 118 - Bowing distortion progression of match-cast segment from time of placement of new segment to 10 hours
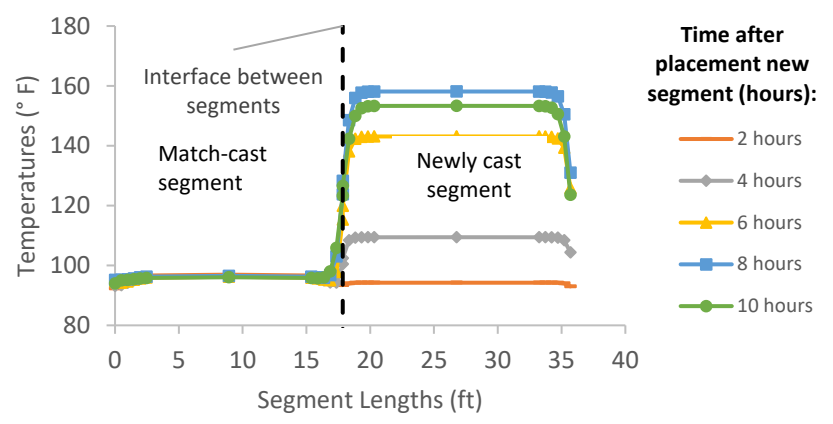

Figure B-354: Simulation 118 - Internal temperatures along the wing of segments

Simulation 119 -Results Summary

Table B-119: Model input parameters simulation 119

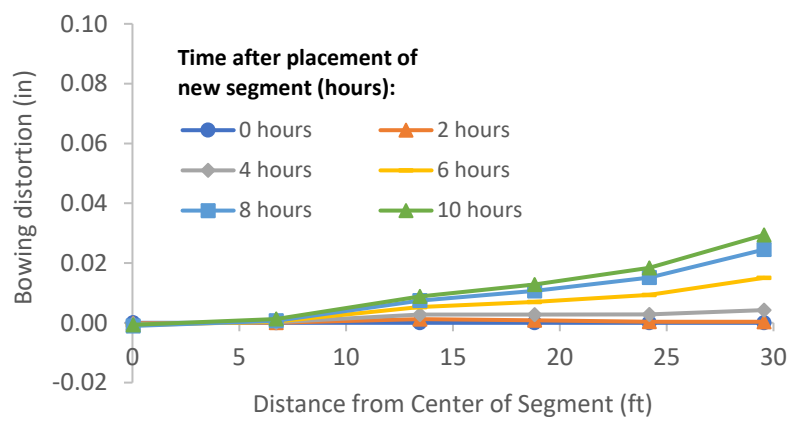| Model details		
Permutation number	119	
Geometry	Florida Bridge D - w/l=9.39	
Max. Mesh Size	3.15	in
Time Step	1	hrs
Placement Temperature	95	°F
Match-cast segment Time of Simulation at Casting	0	hrs
New Segment Time of Simulation at Casting	24	hrs
Concrete Properties		
Cement Content	950.11	lb/yd^3
Activation Energy	28.43	BTU/mol
Heat of Hydration Parameters		
Total Heat Development, $Q_{ult} = \alpha_u \cdot H_u$	124.95	BTU/lb
Time Parameter, τ	10.50	hrs
Curvature Parameter, β	1.60	
Density	3999.308	lb/yd^3
Specific Heat	0.27	BTU/(lb·°F)
Thermal Conductivity	1.705	BTU/(ft·h·°F)
Match-cast segment Elastic Modulus Dev. Parameters		
Final Value	4796.26	ksi
Time Parameter	12.420	hrs
Curvature Parameter	1.068	
New Segment Elastic Modulus Dev. Parameters		
Final Value	14.50	ksi
Time Parameter	n/a	hrs
Curvature Parameter	n/a	
Poisson Ratio	0.17	
Coefficient of Thermal Expansion	6.07	με/°F
Thermal Boundary Conditions (Applied to Appropriate Faces)			
Ambient Temp	Miami - Summer - Morning - Placement		
Wind	Medium-Wind	7.50	mph
Formwork	Steel Formwork	34.60	BTU/(ft·h·°F)
	Thickness	0.118	in
Curing	Burlap	0.18	BTU/(ft·h·°F)
	Thickness	0.39	in

Figure B-355: Simulation 119 - Bowing distortion of match-cast segment after placement of the new segment
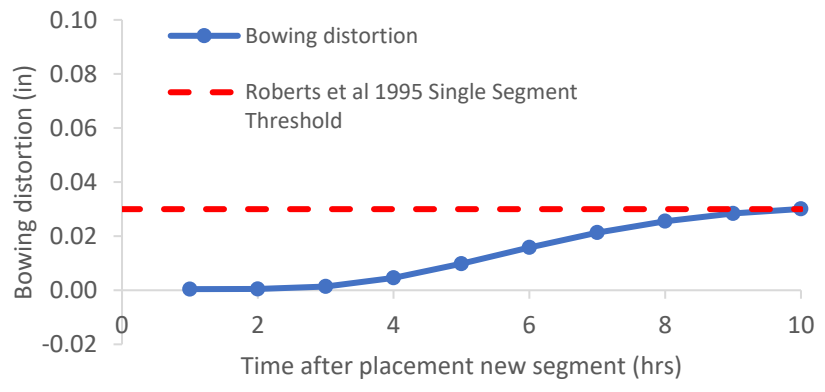

Figure B-356: Simulation 119 - Bowing distortion progression of match-cast segment from time of placement of new segment to 10 hours
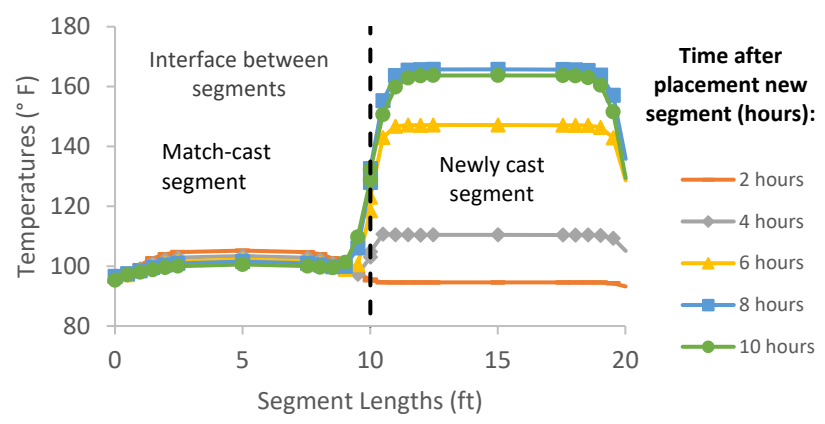

Figure B-357: Simulation 119 - Internal temperatures along the wing of segments

Simulation 120 -Results Summary

Table B-120: Model input parameters simulation 120

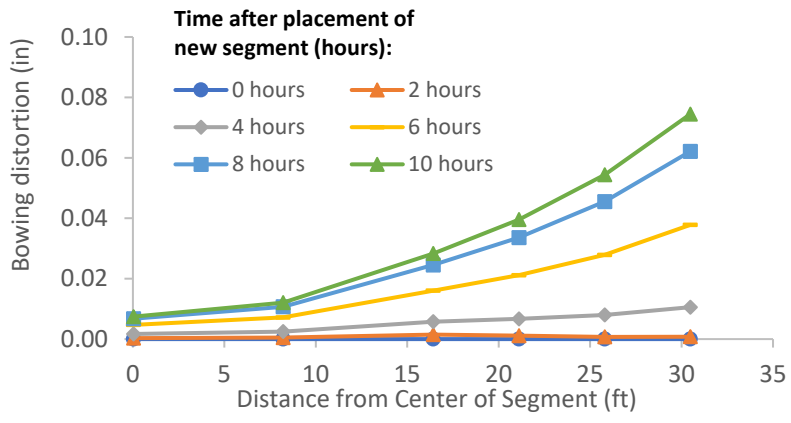| Model details		
Permutation number	120	
Geometry	Bridge Bang Na Pier - w/l=21.80	
Max. Mesh Size	2.76	in
Time Step	1	hrs
Placement Temperature	95	°F
Match-cast segment Time of Simulation at Casting	0	hrs
New Segment Time of Simulation at Casting	24	hrs
Concrete Properties		
Cement Content	950.11	lb/yd^3
Activation Energy	28.43	BTU/mol
Heat of Hydration Parameters		
Total Heat Development, $Q_{ult} = \alpha_u \cdot H_u$	124.95	BTU/lb
Time Parameter, τ	10.50	hrs
Curvature Parameter, β	1.60	
Density	3999.308	lb/yd^3
Specific Heat	0.27	BTU/(lb·°F)
Thermal Conductivity	1.705	BTU/(ft·h·°F)
Match-cast segment Elastic Modulus Dev. Parameters		
Final Value	4796.26	ksi
Time Parameter	12.420	hrs
Curvature Parameter	1.068	
New Segment Elastic Modulus Dev. Parameters		
Final Value	14.50	ksi
Time Parameter	n/a	hrs
Curvature Parameter	n/a	
Poisson Ratio	0.17	
Coefficient of Thermal Expansion	6.07	$\mu\varepsilon$/°F
Thermal Boundary Conditions (Applied to Appropriate Faces)		
Ambient Temp	Miami - Summer - Morning - Placement	
Wind	Medium-Wind	7.50	mph
Formwork	Steel Formwork	34.60	BTU/(ft·h·°F)
	Thickness	0.118	in
Curing	Burlap	0.18	BTU/(ft·h·°F)
	Thickness	0.39	in

Figure B-358: Simulation 120 - Bowing distortion of match-cast segment after placement of the new segment
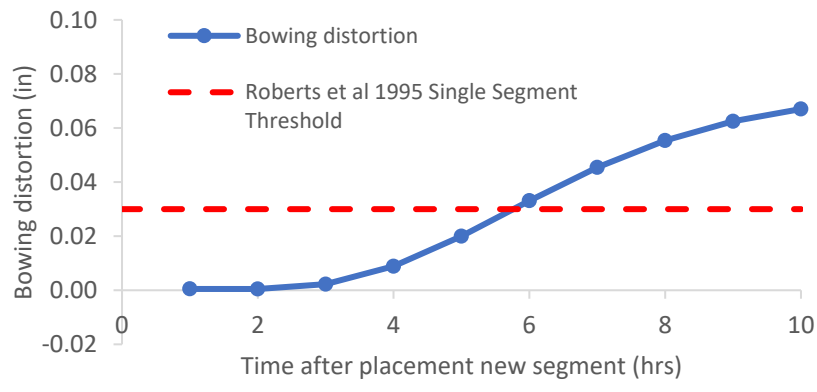

Figure B-359: Simulation 120 - Bowing distortion progression of match-cast segment from time of placement of new segment to 10 hours
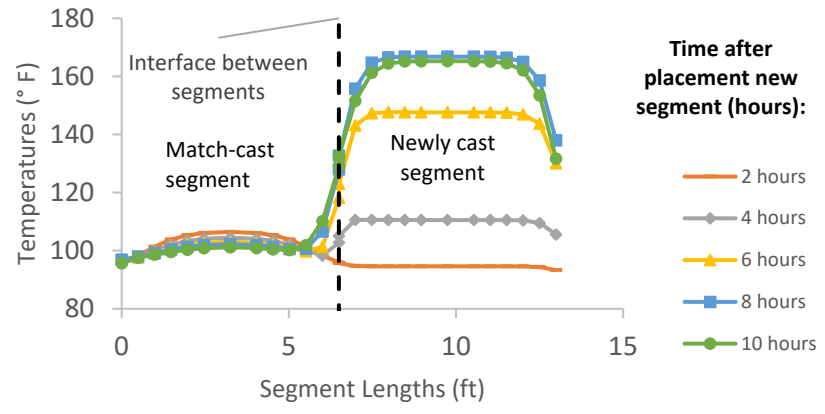

Figure B-360: Simulation 120 - Internal temperatures along the wing of segments

Simulation 121 -Results Summary

Table B-121: Model input parameters simulation 121

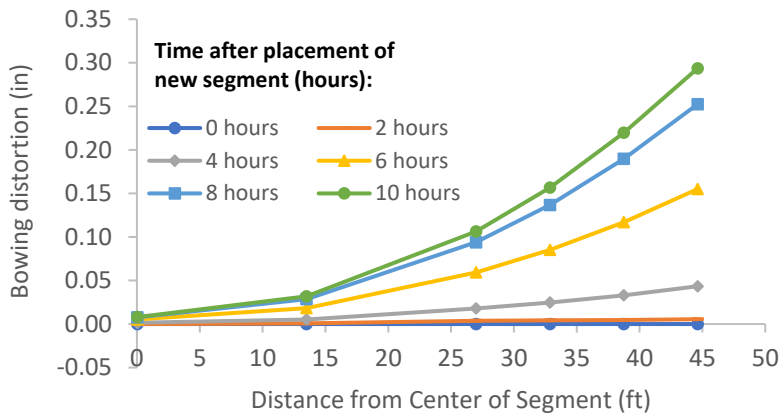| Model details		
Permutation number	121	
Geometry	Florida Bridge A - w/l=2.15	
Max. Mesh Size	2.76	in
Time Step	1	hrs
Placement Temperature	95	°F
Match-cast segment Time of Simulation at Casting	0	hrs
New Segment Time of Simulation at Casting	24	hrs
Concrete Properties		
Cement Content	950.11	lb/yd^3
Activation Energy	28.43	BTU/mol
Heat of Hydration Parameters		
Total Heat Development, $Q_{ult} = \alpha_u \cdot H_u$	124.95	BTU/lb
Time Parameter, τ	10.50	hrs
Curvature Parameter, β	1.60	
Density	3792.929	lb/yd^3
Specific Heat	0.25	BTU/(lb·°F)
Thermal Conductivity	1.352	BTU/(ft·h·°F)
Match-cast segment Elastic Modulus Dev. Parameters		
Final Value	4429.83	ksi
Time Parameter	12.420	hrs
Curvature Parameter	1.068	
New Segment Elastic Modulus Dev. Parameters		
Final Value	14.50	ksi
Time Parameter	n/a	hrs
Curvature Parameter	n/a	
Poisson Ratio	0.17	
Coefficient of Thermal Expansion	3.40	με/°F
Thermal Boundary Conditions (Applied to Appropriate Faces)		
Ambient Temp	Miami - Summer - Morning - Placement	
Wind	Medium-Wind	7.50	mph
Formwork	Steel Formwork	34.60	BTU/(ft·h·°F)
	Thickness	0.118	in
Curing	Burlap	0.18	BTU/(ft·h·°F)
	Thickness	0.39	in

Figure B-361: Simulation 121 - Bowing distortion of match-cast segment after placement of the new segment
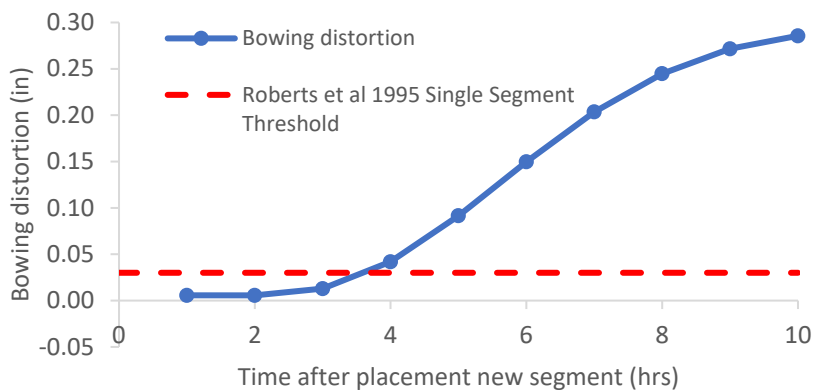

Figure B-362: Simulation 121 - Bowing distortion progression of match-cast segment from time of placement of new segment to 10 hours
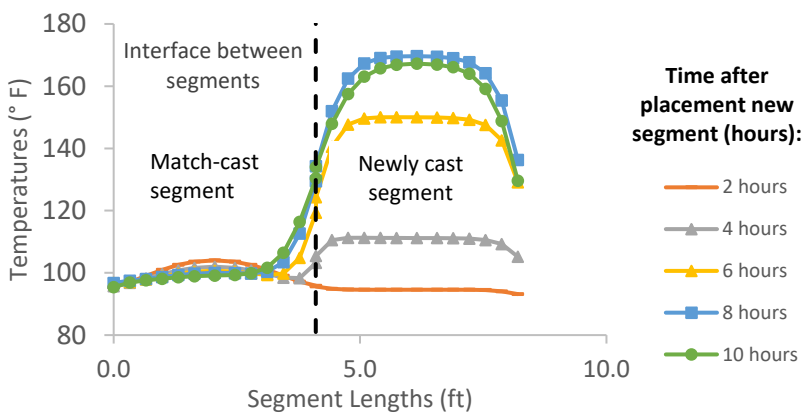

Figure B-363: Simulation 121 - Internal temperatures along the wing of segments

Simulation 122 -Results Summary

Table B-122: Model input parameters simulation 122

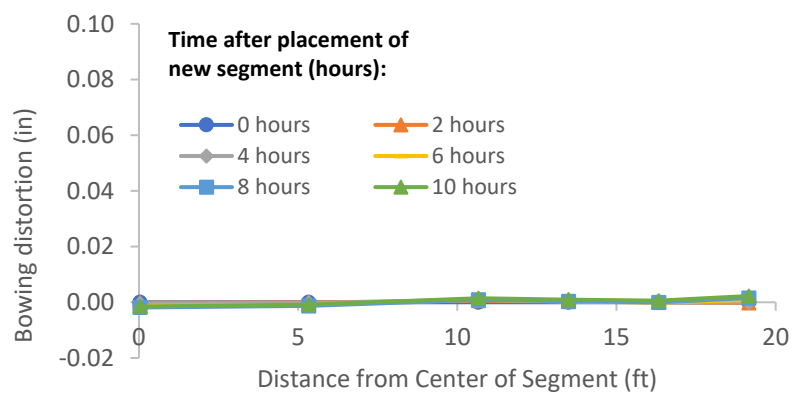| Model details		
Permutation number	122	
Geometry	Florida Bridge F - w/l=5.92	
Max. Mesh Size	3.15	in
Time Step	1	hrs
Placement Temperature	95	°F
Match-cast segment Time of Simulation at Casting	0	hrs
New Segment Time of Simulation at Casting	24	hrs
Concrete Properties		
Cement Content	950.11	lb/yd^3
Activation Energy	28.43	BTU/mol
Heat of Hydration Parameters		
Total Heat Development, $Q_{ult} = \alpha_u \cdot H_u$	124.95	BTU/lb
Time Parameter, τ	10.50	hrs
Curvature Parameter, β	1.60	
Density	3792.929	lb/yd^3
Specific Heat	0.25	BTU/(lb·°F)
Thermal Conductivity	1.352	BTU/(ft·h·°F)
Match-cast segment Elastic Modulus Dev. Parameters		
Final Value	4429.83	ksi
Time Parameter	12.420	hrs
Curvature Parameter	1.068	
New Segment Elastic Modulus Dev. Parameters		
Final Value	14.50	ksi
Time Parameter	n/a	hrs
Curvature Parameter	n/a	
Poisson Ratio	0.17	
Coefficient of Thermal Expansion	3.40	με/°F
Thermal Boundary Conditions (Applied to Appropriate Faces)		
Ambient Temp	Miami - Summer - Morning - Placement	
Wind	Medium-Wind	7.50	mph
Formwork	Steel Formwork	34.60	BTU/(ft·h·°F)
	Thickness	0.118	in
Curing	Burlap	0.18	BTU/(ft·h·°F)
	Thickness	0.39	in

Figure B-364: Simulation 122 - Bowing distortion of match-cast segment after placement of the new segment
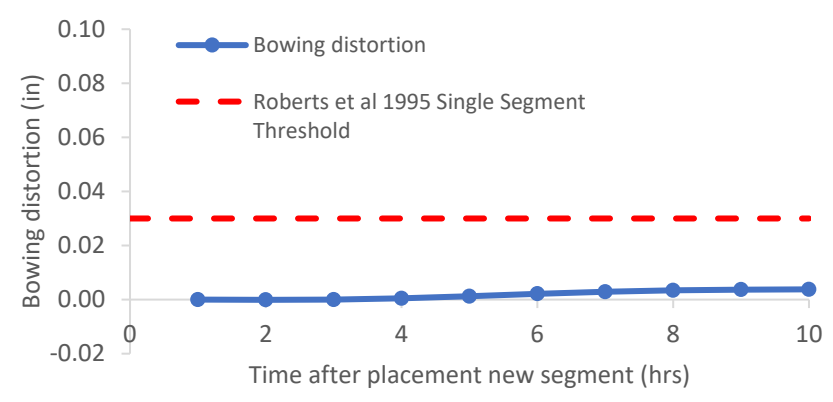

Figure B-365: Simulation 122 - Bowing distortion progression of match-cast segment from time of placement of new segment to 10 hours
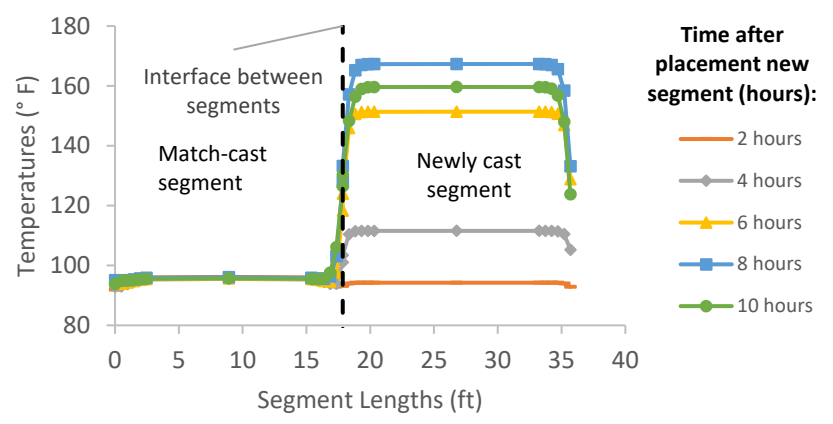

Figure B-366: Simulation 122 - Internal temperatures along the wing of segments

Simulation 123 -Results Summary

Table B-123: Model input parameters simulation 123

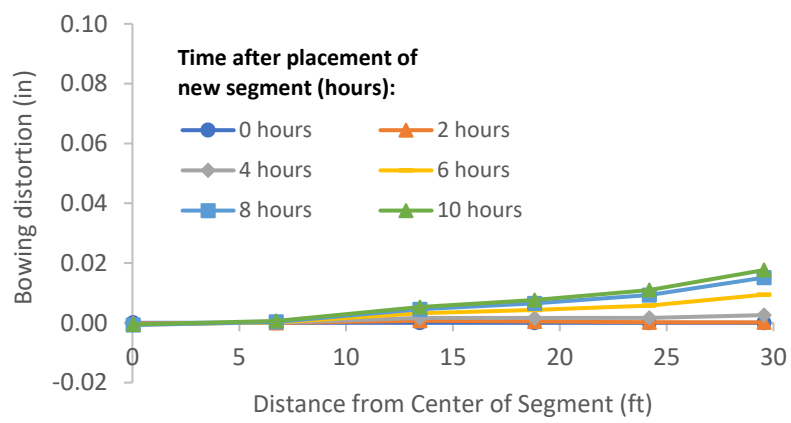| Model details		
Permutation number	123	
Geometry	Florida Bridge D - w/l=9.39	
Max. Mesh Size	3.15	in
Time Step	1	hrs
Placement Temperature	95	°F
Match-cast segment Time of Simulation at Casting	0	hrs
New Segment Time of Simulation at Casting	24	hrs
Concrete Properties		
Cement Content	950.11	lb/yd^3
Activation Energy	28.43	BTU/mol
Heat of Hydration Parameters		
Total Heat Development, $Q_{ult} = \alpha_u \cdot H_u$	124.95	BTU/lb
Time Parameter, τ	10.50	hrs
Curvature Parameter, β	1.60	
Density	3792.929	lb/yd^3
Specific Heat	0.25	BTU/(lb·°F)
Thermal Conductivity	1.352	BTU/(ft·h·°F)
Match-cast segment Elastic Modulus Dev. Parameters		
Final Value	4429.83	ksi
Time Parameter	12.420	hrs
Curvature Parameter	1.068	
New Segment Elastic Modulus Dev. Parameters		
Final Value	14.50	ksi
Time Parameter	n/a	hrs
Curvature Parameter	n/a	
Poisson Ratio	0.17	
Coefficient of Thermal Expansion	3.40	µε/°F
Thermal Boundary Conditions (Applied to Appropriate Faces)		
Ambient Temp	Miami - Summer - Morning - Placement	
Wind	Medium-Wind	7.50	mph
Formwork	Steel Formwork	34.60	BTU/(ft·h·°F)
	Thickness	0.118	in
Curing	Burlap	0.18	BTU/(ft·h·°F)
	Thickness	0.39	in

Figure B-367: Simulation 123 - Bowing distortion of match-cast segment after placement of the new segment
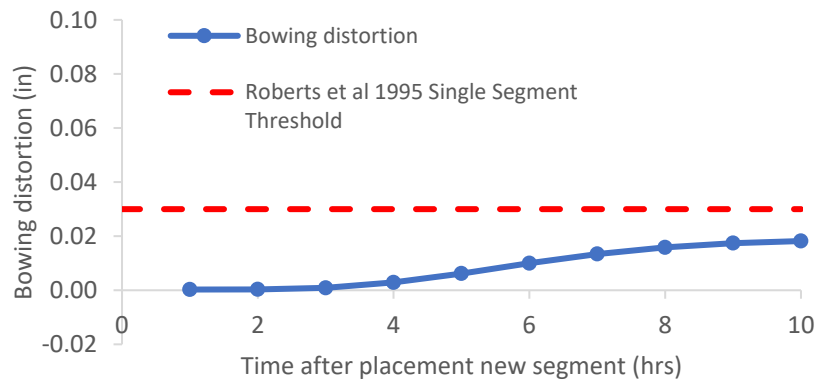

Figure B-368: Simulation 123 - Bowing distortion progression of match-cast segment from time of placement of new segment to 10 hours
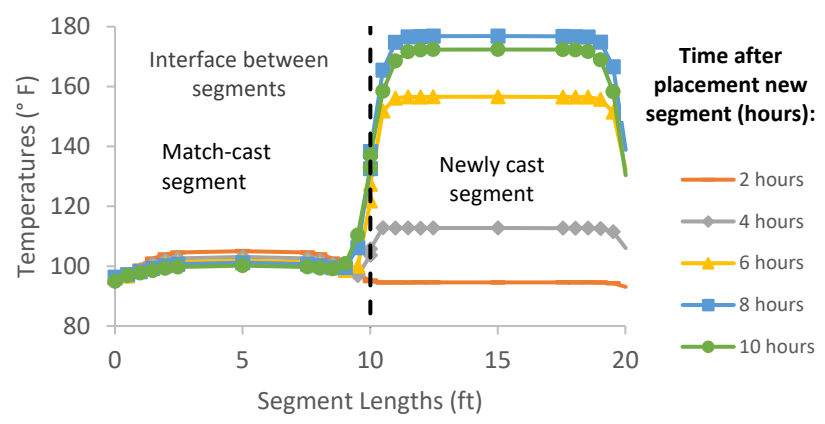

Figure B-369: Simulation 123 - Internal temperatures along the wing of segments

Simulation 124 -Results Summary

Table B-124: Model input parameters simulation 124

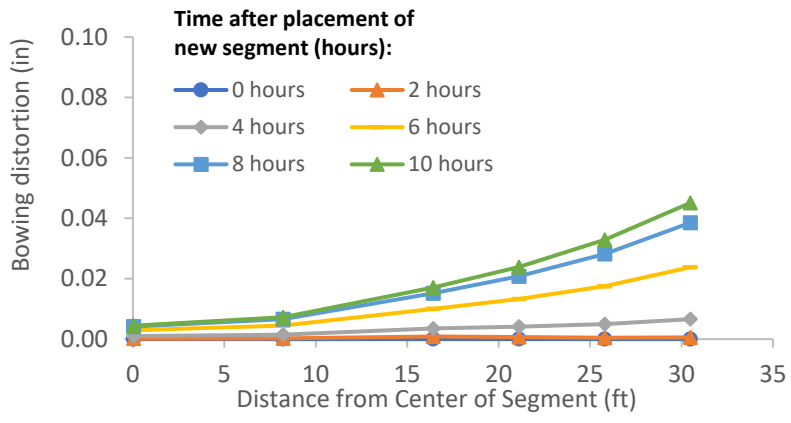| Model details		
Permutation number	124	
Geometry	Bridge Bang Na Pier - w/l=21.80	
Max. Mesh Size	2.76	in
Time Step	1	hrs
Placement Temperature	95	°F
Match-cast segment Time of Simulation at Casting	0	hrs
New Segment Time of Simulation at Casting	24	hrs
Concrete Properties		
Cement Content	950.11	lb/yd^3
Activation Energy	28.43	BTU/mol
Heat of Hydration Parameters		
Total Heat Development, $Q_{ult} = \alpha_u \cdot H_u$	124.95	BTU/lb
Time Parameter, τ	10.50	hrs
Curvature Parameter, β	1.60	
Density	3792.929	lb/yd^3
Specific Heat	0.25	BTU/(lb·°F)
Thermal Conductivity	1.352	BTU/(ft·h·°F)
Match-cast segment Elastic Modulus Dev. Parameters		
Final Value	4429.83	ksi
Time Parameter	12.420	hrs
Curvature Parameter	1.068	
New Segment Elastic Modulus Dev. Parameters		
Final Value	14.50	ksi
Time Parameter	n/a	hrs
Curvature Parameter	n/a	
Poisson Ratio	0.17	
Coefficient of Thermal Expansion	3.40	με/°F
Thermal Boundary Conditions (Applied to Appropriate Faces)		
Ambient Temp	Miami - Summer - Morning - Placement		
Wind	Medium-Wind	7.50	mph
Formwork	Steel Formwork	34.60	BTU/(ft·h·°F)
	Thickness	0.118	in
Curing	Burlap	0.18	BTU/(ft·h·°F)
	Thickness	0.39	in

Figure B-370: Simulation 124 - Bowing distortion of match-cast segment after placement of the new segment
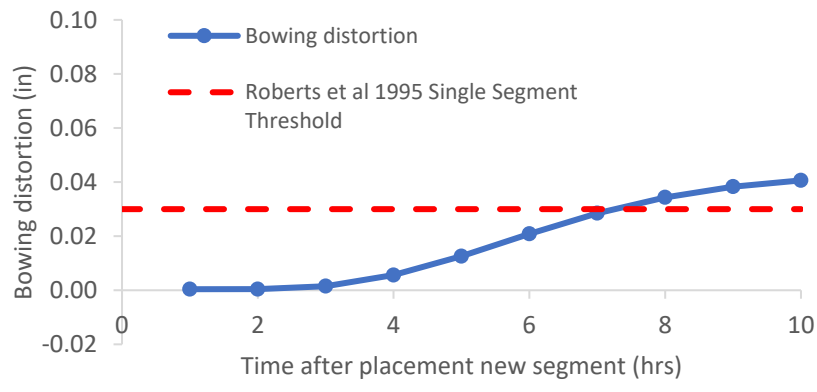

Figure B-371: Simulation 124 - Bowing distortion progression of match-cast segment from time of placement of new segment to 10 hours
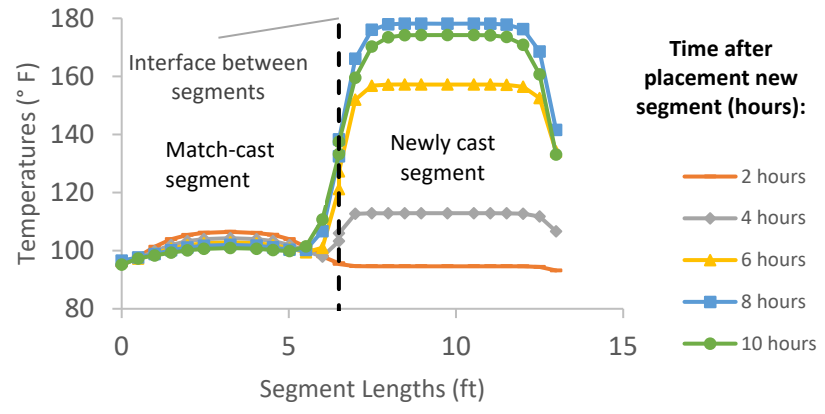

Figure B-372: Simulation 124 - Internal temperatures along the wing of segments

Simulation 125 -Results Summary

Table B-125: Model input parameters simulation 125

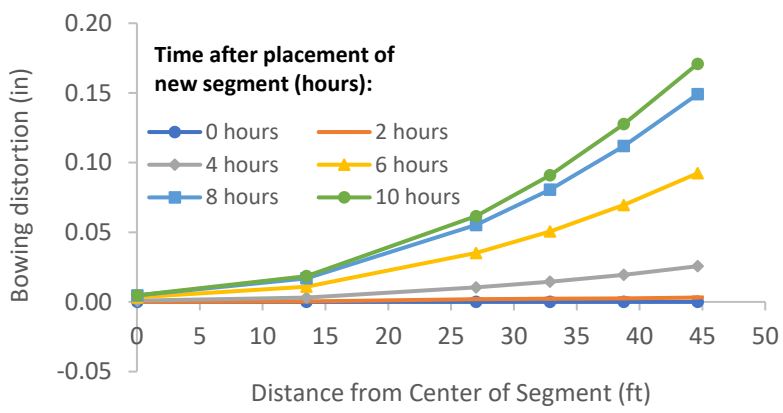| Model details		
Permutation number	125	
Geometry	Florida Bridge A - w/l=2.15	
Max. Mesh Size	2.76	in
Time Step	1	hrs
Placement Temperature	75	°F
Match-cast segment Time of Simulation at Casting	0	hrs
New Segment Time of Simulation at Casting	24	hrs
Concrete Properties		
Cement Content	950.11	lb/yd^3
Activation Energy	28.43	BTU/mol
Heat of Hydration Parameters		
Total Heat Development, $Q_{ult} = \alpha_u \cdot H_u$	124.95	BTU/lb
Time Parameter, τ	10.50	hrs
Curvature Parameter, β	1.60	
Density	3880.948	lb/yd^3
Specific Heat	0.26	BTU/(lb·°F)
Thermal Conductivity	1.502	BTU/(ft·h·°F)
Match-cast segment Elastic Modulus Dev. Parameters		
Final Value	4584.92	ksi
Time Parameter	12.420	hrs
Curvature Parameter	1.068	
New Segment Elastic Modulus Dev. Parameters		
Final Value	14.50	ksi
Time Parameter	n/a	hrs
Curvature Parameter	n/a	
Poisson Ratio	0.17	
Coefficient of Thermal Expansion	4.54	με/°F
Thermal Boundary Conditions (Applied to Appropriate Faces)		
Ambient Temp	Miami - Summer - Night - Placement	
Wind	Medium-Wind	7.50	mph
Formwork	Steel Formwork	34.60	BTU/(ft·h·°F)
	Thickness	0.118	in
Curing	Burlap	0.18	BTU/(ft·h·°F)
	Thickness	0.39	in

Figure B-373: Simulation 125 - Bowing distortion of match-cast segment after placement of the new segment
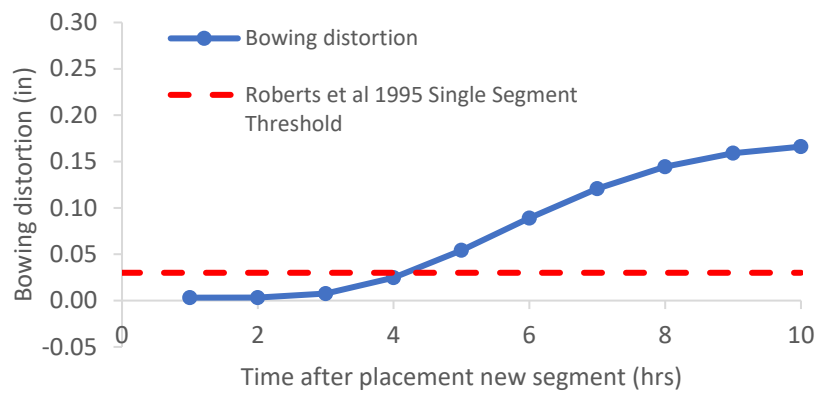

Figure B-374: Simulation 125 - Bowing distortion progression of match-cast segment from time of placement of new segment to 10 hours
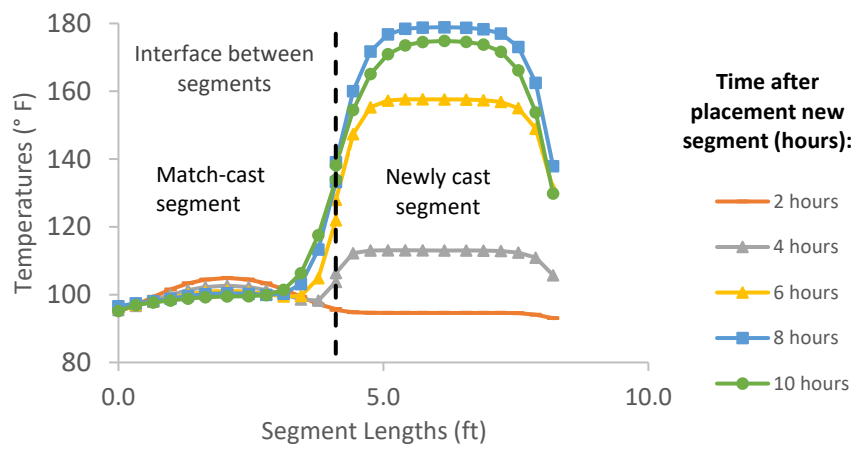

Figure B-375: Simulation 125 - Internal temperatures along the wing of segments

Simulation 126 -Results Summary

Table B-126: Model input parameters simulation 126

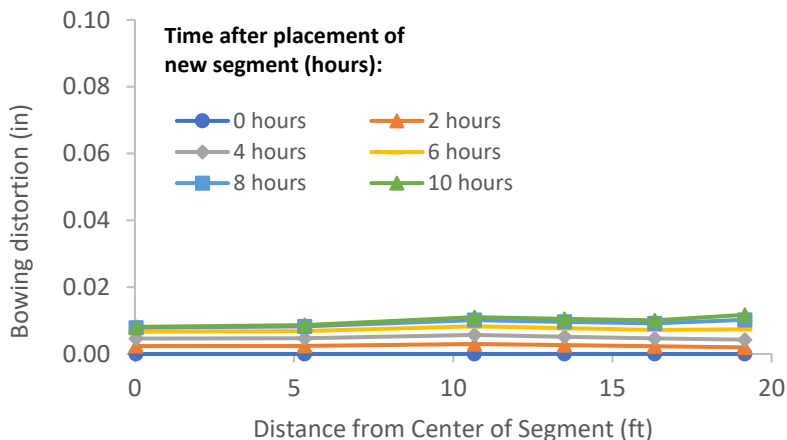| Model details		
Permutation number	126	
Geometry	Florida Bridge F - w/l=5.92	
Max. Mesh Size	3.15	in
Time Step	1	hrs
Placement Temperature	75	°F
Match-cast segment Time of Simulation at Casting	0	hrs
New Segment Time of Simulation at Casting	24	hrs
Concrete Properties		
Cement Content	950.11	lb/yd^3
Activation Energy	28.43	BTU/mol
Heat of Hydration Parameters		
Total Heat Development, $Q_{ult} = \alpha_u \cdot H_u$	124.95	BTU/lb
Time Parameter, τ	10.50	hrs
Curvature Parameter, β	1.60	
Density	3880.948	lb/yd^3
Specific Heat	0.26	BTU/(lb·°F)
Thermal Conductivity	1.502	BTU/(ft·h·°F)
Match-cast segment Elastic Modulus Dev. Parameters		
Final Value	4584.92	ksi
Time Parameter	12.420	hrs
Curvature Parameter	1.068	
New Segment Elastic Modulus Dev. Parameters		
Final Value	14.50	ksi
Time Parameter	n/a	hrs
Curvature Parameter	n/a	
Poisson Ratio	0.17	
Coefficient of Thermal Expansion	4.54	$\mu\varepsilon$/°F
Thermal Boundary Conditions (Applied to Appropriate Faces)		
Ambient Temp	Miami - Summer - Night - Placement	
Wind	Medium-Wind	7.50	mph
Formwork	Steel Formwork	34.60	BTU/(ft·h·°F)
	Thickness	0.118	in
Curing	Burlap	0.18	BTU/(ft·h·°F)
	Thickness	0.39	in

Figure B-376: Simulation 126 - Bowing distortion of match-cast segment after placement of the new segment

Figure B-377: Simulation 126 - Bowing distortion progression of match-cast segment from time of placement of new segment to 10 hours
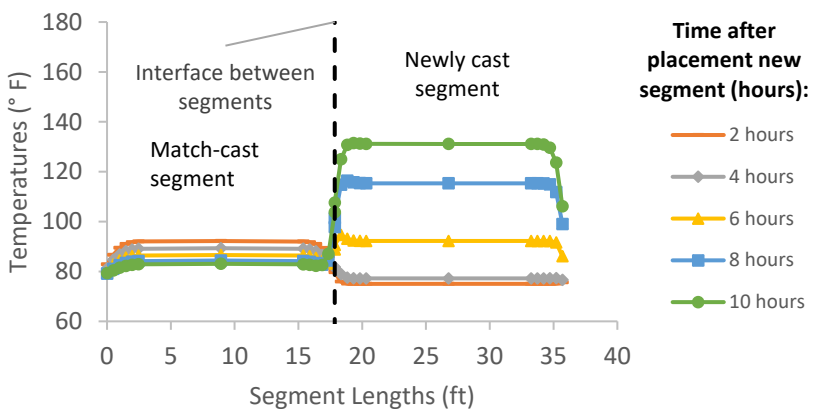

Figure B-378: Simulation 126 - Internal temperatures along the wing of segments

Simulation 127 -Results Summary

Table B-127: Model input parameters simulation 127

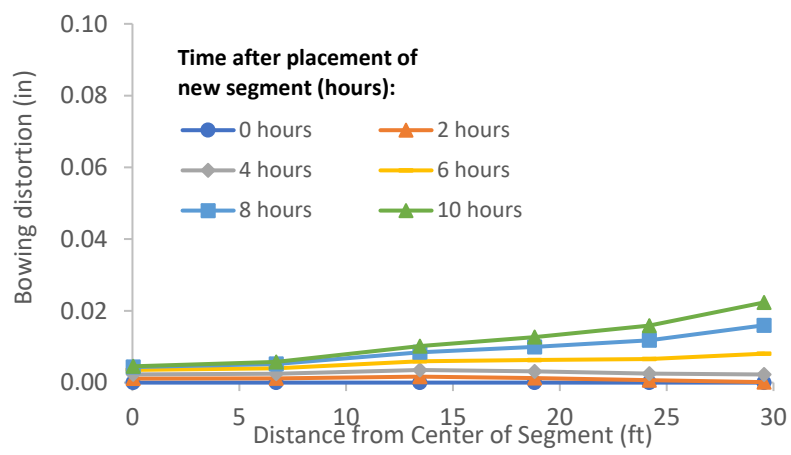| Model details		
Permutation number	127	
Geometry	Florida Bridge D - w/l=9.39	
Max. Mesh Size	3.15	in
Time Step	1	hrs
Placement Temperature	75	°F
Match-cast segment Time of Simulation at Casting	0	hrs
New Segment Time of Simulation at Casting	24	hrs
Concrete Properties		
Cement Content	950.11	lb/yd^3
Activation Energy	28.43	BTU/mol
Heat of Hydration Parameters		
Total Heat Development, $Q_{ult} = \alpha_u \cdot H_u$	124.95	BTU/lb
Time Parameter, τ	10.50	hrs
Curvature Parameter, β	1.60	
Density	3880.948	lb/yd^3
Specific Heat	0.26	BTU/(lb·°F)
Thermal Conductivity	1.502	BTU/(ft·h·°F)
Match-cast segment Elastic Modulus Dev. Parameters		
Final Value	4584.92	ksi
Time Parameter	12.420	hrs
Curvature Parameter	1.068	
New Segment Elastic Modulus Dev. Parameters		
Final Value	14.50	ksi
Time Parameter	n/a	hrs
Curvature Parameter	n/a	
Poisson Ratio	0.17	
Coefficient of Thermal Expansion	4.54	με/°F
Thermal Boundary Conditions (Applied to Appropriate Faces)		
Ambient Temp	Miami - Summer - Night - Placement	
Wind	Medium-Wind	7.50	mph
Formwork	Steel Formwork	34.60	BTU/(ft·h·°F)
	Thickness	0.118	in
Curing	Burlap	0.18	BTU/(ft·h·°F)
	Thickness	0.39	in

Figure B-379: Simulation 127 - Bowing distortion of match-cast segment after placement of the new segment
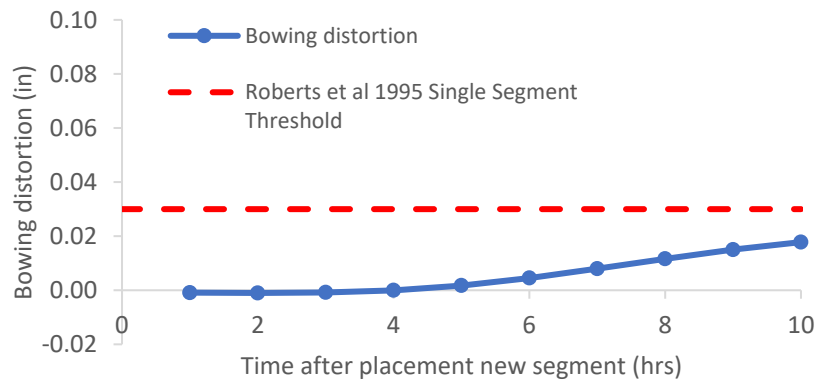

Figure B-380: Simulation 127 - Bowing distortion progression of match-cast segment from time of placement of new segment to 10 hours
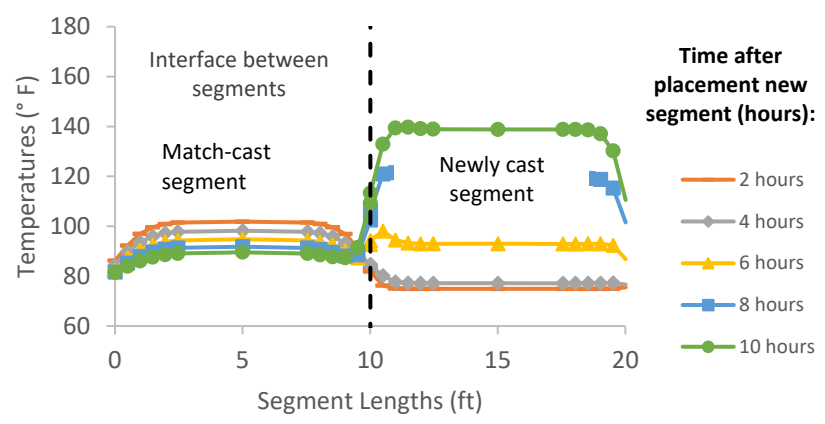

Figure B-381: Simulation 127 - Internal temperatures along the wing of segments

Simulation 128 -Results Summary

Table B-128: Model input parameters simulation 128

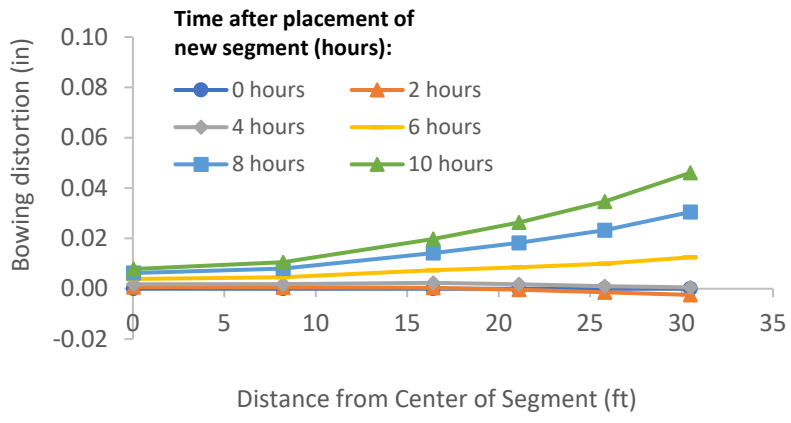| Model details		
Permutation number	128	
Geometry	Bridge Bang Na Pier - w/l=21.80	
Max. Mesh Size	2.76	in
Time Step	1	hrs
Placement Temperature	75	°F
Match-cast segment Time of Simulation at Casting	0	hrs
New Segment Time of Simulation at Casting	24	hrs
Concrete Properties		
Cement Content	950.11	lb/yd^3
Activation Energy	28.43	BTU/mol
Heat of Hydration Parameters		
Total Heat Development, $Q_{ult} = \alpha_u \cdot H_u$	124.95	BTU/lb
Time Parameter, τ	10.50	hrs
Curvature Parameter, β	1.60	
Density	3880.948	lb/yd^3
Specific Heat	0.26	BTU/(lb·°F)
Thermal Conductivity	1.502	BTU/(ft·h·°F)
Match-cast segment Elastic Modulus Dev. Parameters		
Final Value	4584.92	ksi
Time Parameter	12.420	hrs
Curvature Parameter	1.068	
New Segment Elastic Modulus Dev. Parameters		
Final Value	14.50	ksi
Time Parameter	n/a	hrs
Curvature Parameter	n/a	
Poisson Ratio	0.17	
Coefficient of Thermal Expansion	4.54	με/°F
Thermal Boundary Conditions (Applied to Appropriate Faces)		
Ambient Temp	Miami - Summer - Night - Placement	
Wind	Medium-Wind	7.50	mph
Formwork	Steel Formwork	34.60	BTU/(ft·h·°F)
	Thickness	0.118	in
Curing	Burlap	0.18	BTU/(ft·h·°F)
	Thickness	0.39	in

Figure B-382: Simulation 128 - Bowing distortion of match-cast segment after placement of the new segment
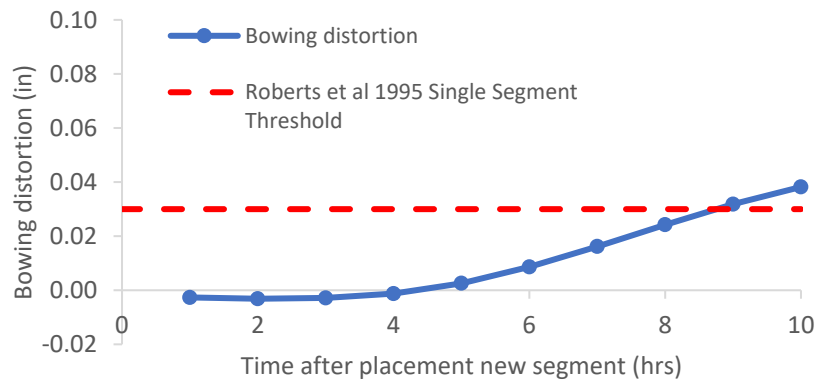

Figure B-383: Simulation 128 - Bowing distortion progression of match-cast segment from time of placement of new segment to 10 hours
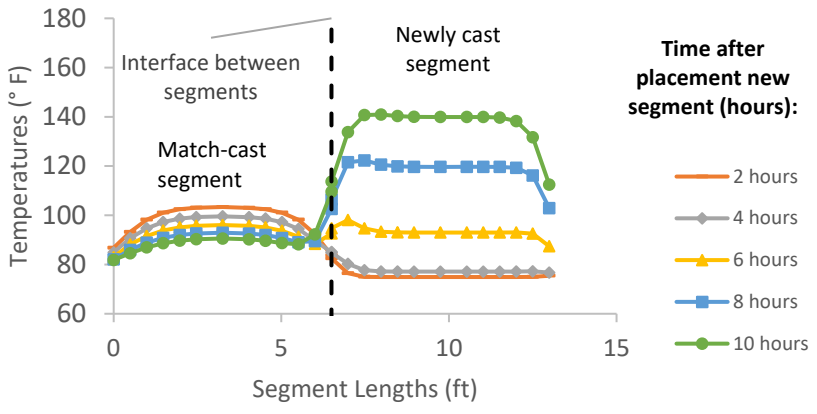

Figure B-384: Simulation 128 - Internal temperatures along the wing of segments

Simulation 129 -Results Summary

Table B-129: Model input parameters simulation 129

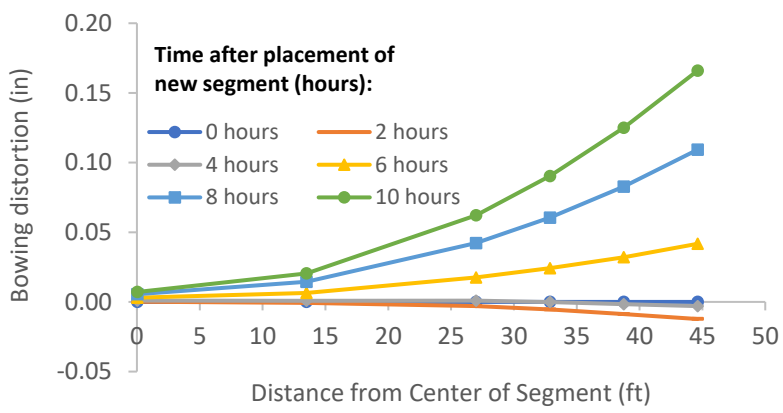| Model details		
Permutation number	129	
Geometry	Florida Bridge A - w/l=2.15	
Max. Mesh Size	2.76	in
Time Step	1	hrs
Placement Temperature	50	°F
Match-cast segment Time of Simulation at Casting	0	hrs
New Segment Time of Simulation at Casting	24	hrs
Concrete Properties		
Cement Content	950.11	lb/yd³
Activation Energy	28.43	BTU/mol
Heat of Hydration Parameters		
Total Heat Development, $Q_{ult} = \alpha_u \cdot H_u$	124.95	BTU/lb
Time Parameter, τ	10.50	hrs
Curvature Parameter, β	1.60	
Density	3880.948	lb/yd³
Specific Heat	0.26	BTU/(lb·°F)
Thermal Conductivity	1.502	BTU/(ft·h·°F)
Match-cast segment Elastic Modulus Dev. Parameters		
Final Value	4584.92	ksi
Time Parameter	12.420	hrs
Curvature Parameter	1.068	
New Segment Elastic Modulus Dev. Parameters		
Final Value	14.50	ksi
Time Parameter	n/a	hrs
Curvature Parameter	n/a	
Poisson Ratio	0.17	
Coefficient of Thermal Expansion	4.54	με/°F
Thermal Boundary Conditions (Applied to Appropriate Faces)		
Ambient Temp	Tallahassee - Winter - Afternoon - Placement	
Wind	Medium-Wind	7.50	mph
Formwork	Steel Formwork	34.60	BTU/(ft·h·°F)
	Thickness	0.118	in
Curing	Burlap	0.18	BTU/(ft·h·°F)
	Thickness	0.39	in

Figure B-385: Simulation 129 - Bowing distortion of match-cast segment after placement of the new segment
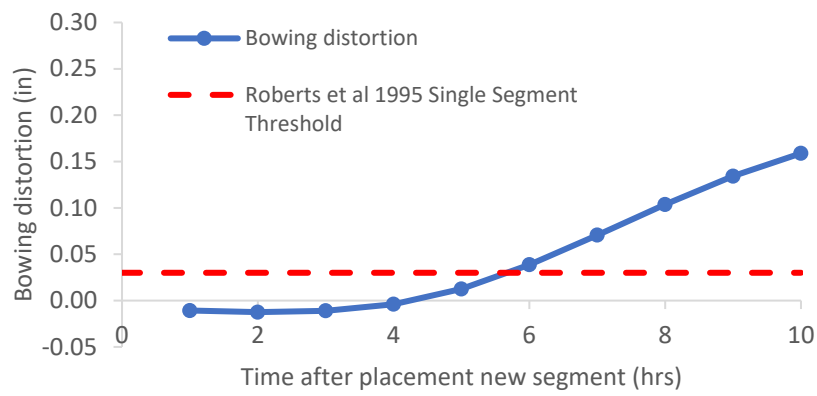

Figure B-386: Simulation 129 - Bowing distortion progression of match-cast segment from time of placement of new segment to 10 hours
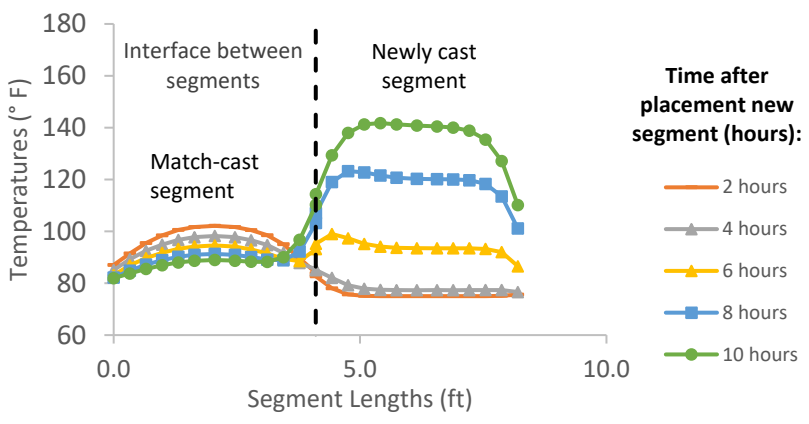

Figure B-387: Simulation 129 - Internal temperatures along the wing of segments

Simulation 130 -Results Summary

Table B-130: Model input parameters simulation 130

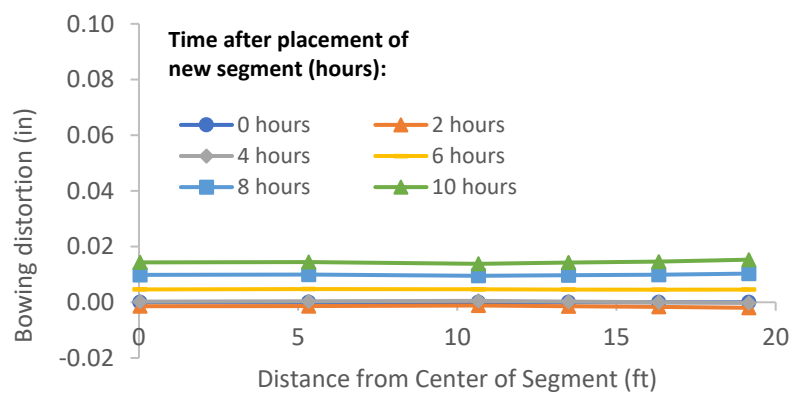| Model details		
Permutation number	130	
Geometry	Florida Bridge F - w/l=5.92	
Max. Mesh Size	3.15	in
Time Step	1	hrs
Placement Temperature	50	°F
Match-cast segment Time of Simulation at Casting	0	hrs
New Segment Time of Simulation at Casting	24	hrs
Concrete Properties		
Cement Content	950.11	lb/yd^3
Activation Energy	28.43	BTU/mol
Heat of Hydration Parameters		
Total Heat Development, $Q_{ult} = \alpha_u \cdot H_u$	124.95	BTU/lb
Time Parameter, τ	10.50	hrs
Curvature Parameter, β	1.60	
Density	3880.948	lb/yd^3
Specific Heat	0.26	BTU/(lb·°F)
Thermal Conductivity	1.502	BTU/(ft·h·°F)
Match-cast segment Elastic Modulus Dev. Parameters		
Final Value	4584.92	ksi
Time Parameter	12.420	hrs
Curvature Parameter	1.068	
New Segment Elastic Modulus Dev. Parameters		
Final Value	14.50	ksi
Time Parameter	n/a	hrs
Curvature Parameter	n/a	
Poisson Ratio	0.17	
Coefficient of Thermal Expansion	4.54	με/°F
Thermal Boundary Conditions (Applied to Appropriate Faces)		
Ambient Temp	Tallahassee - Winter - Afternoon - Placement	
Wind	Medium-Wind	7.50	mph
Formwork	Steel Formwork	34.60	BTU/(ft·h·°F)
	Thickness	0.118	in
Curing	Burlap	0.18	BTU/(ft·h·°F)
	Thickness	0.39	in

Figure B-388: Simulation 130 - Bowing distortion of match-cast segment after placement of the new segment

Figure B-389: Simulation 130 - Bowing distortion progression of match-cast segment from time of placement of new segment to 10 hours
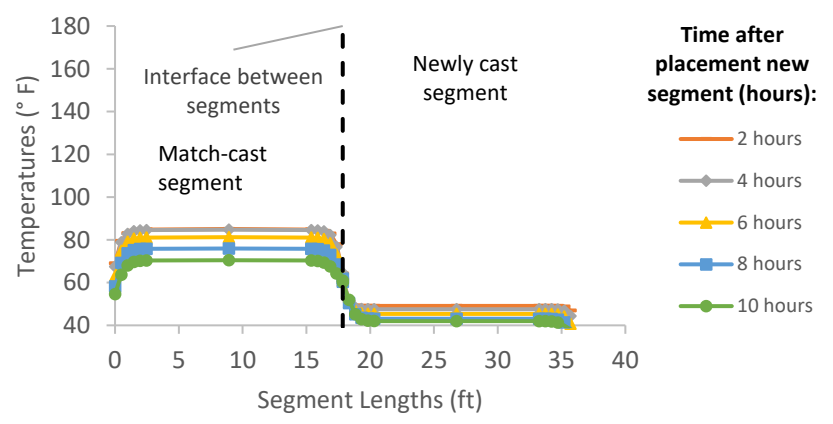

Figure B-390: Simulation 130 - Internal temperatures along the wing of segments

Simulation 131 -Results Summary

Table B-131: Model input parameters simulation 131

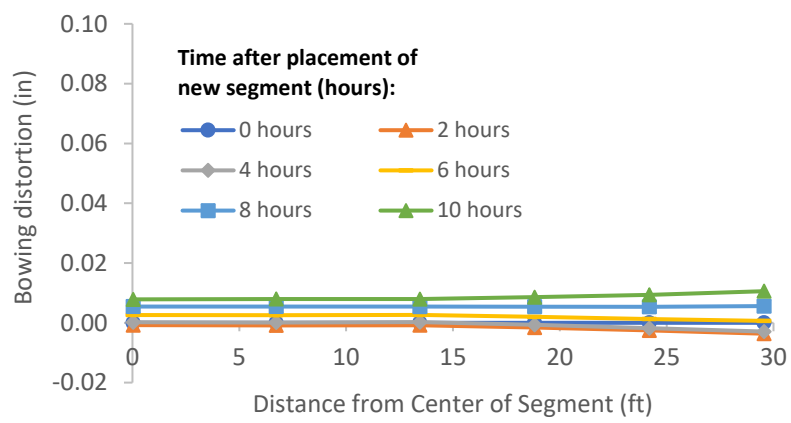| Model details		
Permutation number	131	
Geometry	Florida Bridge D - w/l=9.39	
Max. Mesh Size	3.15	in
Time Step	1	hrs
Placement Temperature	50	°F
Match-cast segment Time of Simulation at Casting	0	hrs
New Segment Time of Simulation at Casting	24	hrs
Concrete Properties		
Cement Content	950.11	lb/yd³
Activation Energy	28.43	BTU/mol
Heat of Hydration Parameters		
Total Heat Development, $Q_{ult} = \alpha_u \cdot H_u$	124.95	BTU/lb
Time Parameter, τ	10.50	hrs
Curvature Parameter, β	1.60	
Density	3880.948	lb/yd³
Specific Heat	0.26	BTU/(lb·°F)
Thermal Conductivity	1.502	BTU/(ft·h·°F)
Match-cast segment Elastic Modulus Dev. Parameters		
Final Value	4584.92	ksi
Time Parameter	12.420	hrs
Curvature Parameter	1.068	
New Segment Elastic Modulus Dev. Parameters		
Final Value	14.50	ksi
Time Parameter	n/a	hrs
Curvature Parameter	n/a	
Poisson Ratio	0.17	
Coefficient of Thermal Expansion	4.54	µε/°F
Thermal Boundary Conditions (Applied to Appropriate Faces)		
Ambient Temp	Tallahassee - Winter - Afternoon - Placement	
Wind	Medium-Wind	7.50	mph
Formwork	Steel Formwork	34.60	BTU/(ft·h·°F)
	Thickness	0.118	in
Curing	Burlap	0.18	BTU/(ft·h·°F)
	Thickness	0.39	in

Figure B-391: Simulation 131 - Bowing distortion of match-cast segment after placement of the new segment

Figure B-392: Simulation 131 - Bowing distortion progression of match-cast segment from time of placement of new segment to 10 hours
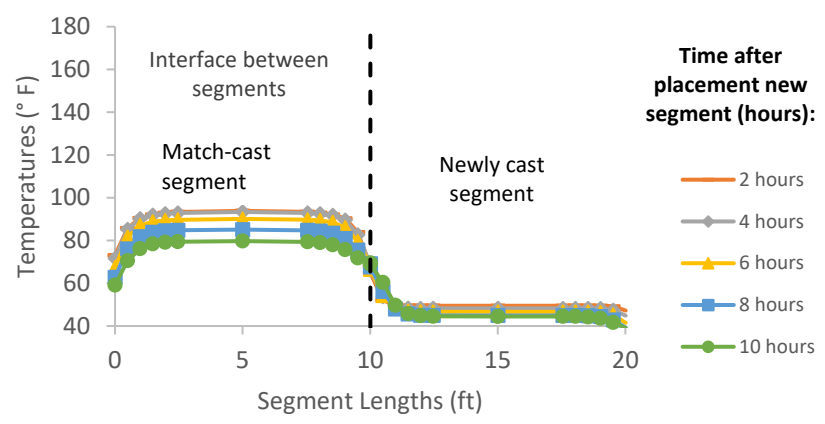

Figure B-393: Simulation 131 - Internal temperatures along the wing of segments

Simulation 132 -Results Summary

Table B-132: Model input parameters simulation 132

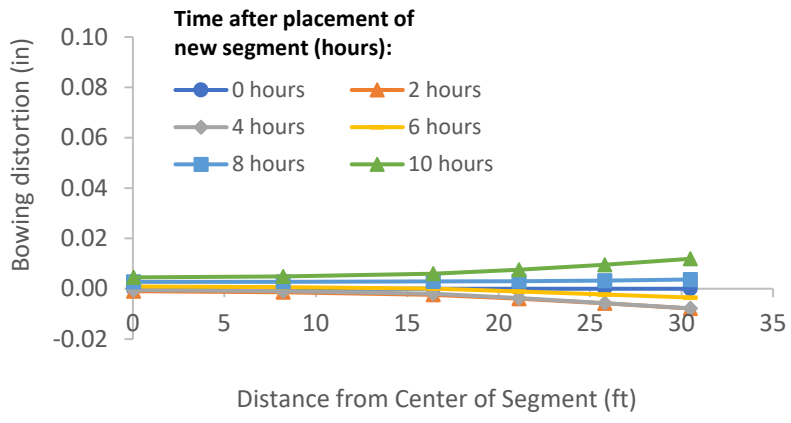| Model details		
Permutation number	132	
Geometry	Bridge Bang Na Pier - w/l=21.80	
Max. Mesh Size	2.76	in
Time Step	1	hrs
Placement Temperature	50	°F
Match-cast segment Time of Simulation at Casting	0	hrs
New Segment Time of Simulation at Casting	24	hrs
Concrete Properties		
Cement Content	950.11	lb/yd^3
Activation Energy	28.43	BTU/mol
Heat of Hydration Parameters		
Total Heat Development, $Q_{ult} = \alpha_u \cdot H_u$	124.95	BTU/lb
Time Parameter, τ	10.50	hrs
Curvature Parameter, β	1.60	
Density	3880.948	lb/yd^3
Specific Heat	0.26	BTU/(lb·°F)
Thermal Conductivity	1.502	BTU/(ft·h·°F)
Match-cast segment Elastic Modulus Dev. Parameters		
Final Value	4584.92	ksi
Time Parameter	12.420	hrs
Curvature Parameter	1.068	
New Segment Elastic Modulus Dev. Parameters		
Final Value	14.50	ksi
Time Parameter	n/a	hrs
Curvature Parameter	n/a	
Poisson Ratio	0.17	
Coefficient of Thermal Expansion	4.54	µε/°F
Thermal Boundary Conditions (Applied to Appropriate Faces)		
Ambient Temp	Tallahassee - Winter - Afternoon - Placement		
Wind	Medium-Wind	7.50	mph
Formwork	Steel Formwork	34.60	BTU/(ft·h·°F)
	Thickness	0.118	in
Curing	Burlap	0.18	BTU/(ft·h·°F)
	Thickness	0.39	in

Figure B-394: Simulation 132 - Bowing distortion of match-cast segment after placement of the new segment
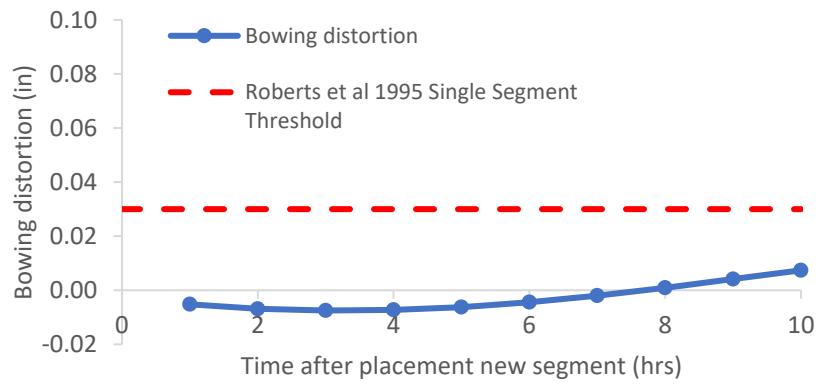

Figure B-395: Simulation 132 - Bowing distortion progression of match-cast segment from time of placement of new segment to 10 hours
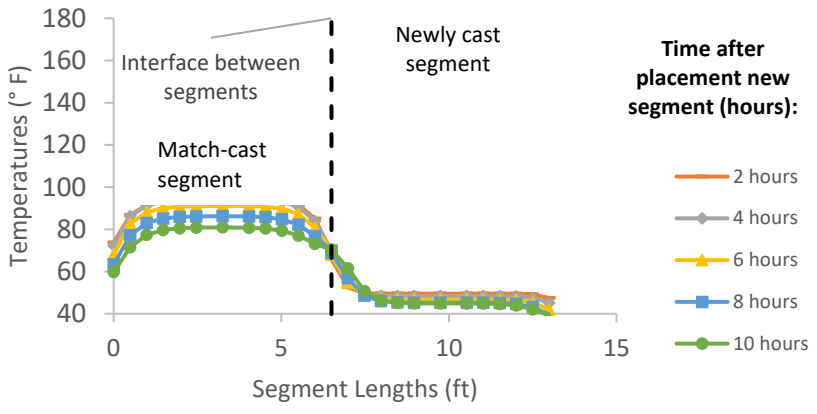

Figure B-396: Simulation 132 - Internal temperatures along the wing of segments

Simulation 133 -Results Summary

Table B-133: Model input parameters simulation 133

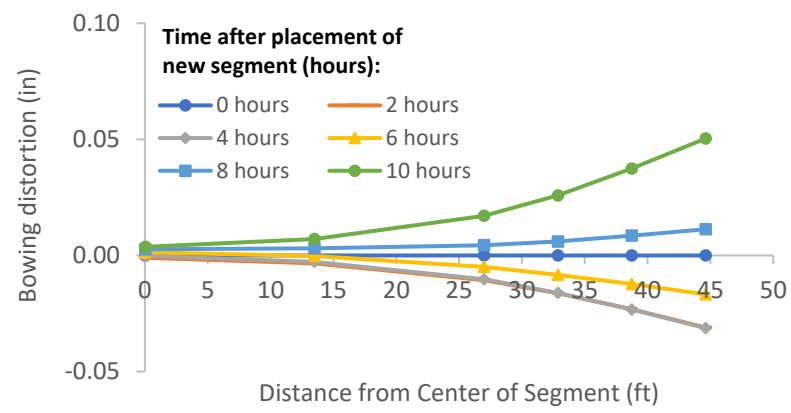| Model details		
Permutation number	133	
Geometry	Florida Bridge A - w/l=2.15	
Max. Mesh Size	2.76	in
Time Step	1	hrs
Placement Temperature	95	°F
Match-cast segment Time of Simulation at Casting	0	hrs
New Segment Time of Simulation at Casting	24	hrs
Concrete Properties		
Cement Content	950.11	lb/yd^3
Activation Energy	28.43	BTU/mol
Heat of Hydration Parameters		
Total Heat Development, $Q_{ult} = \alpha_u \cdot H_u$	124.95	BTU/lb
Time Parameter, τ	10.50	hrs
Curvature Parameter, β	1.60	
Density	3880.948	lb/yd^3
Specific Heat	0.26	BTU/(lb·°F)
Thermal Conductivity	1.502	BTU/(ft·h·°F)
Match-cast segment Elastic Modulus Dev. Parameters		
Final Value	4584.92	ksi
Time Parameter	12.420	hrs
Curvature Parameter	1.068	
New Segment Elastic Modulus Dev. Parameters		
Final Value	14.50	ksi
Time Parameter	n/a	hrs
Curvature Parameter	n/a	
Poisson Ratio	0.17	
Coefficient of Thermal Expansion	4.54	µε/°F
Thermal Boundary Conditions (Applied to Appropriate Faces)		
Ambient Temp	Miami - Summer - Morning - Placement	
Wind	Low-Wind	0.00	mph
Formwork	Steel Formwork	34.60	BTU/(ft·h·°F)
	Thickness	0.118	in
Curing	Burlap	0.18	BTU/(ft·h·°F)
	Thickness	0.39	in

Figure B-397: Simulation 133 - Bowing distortion of match-cast segment after placement of the new segment
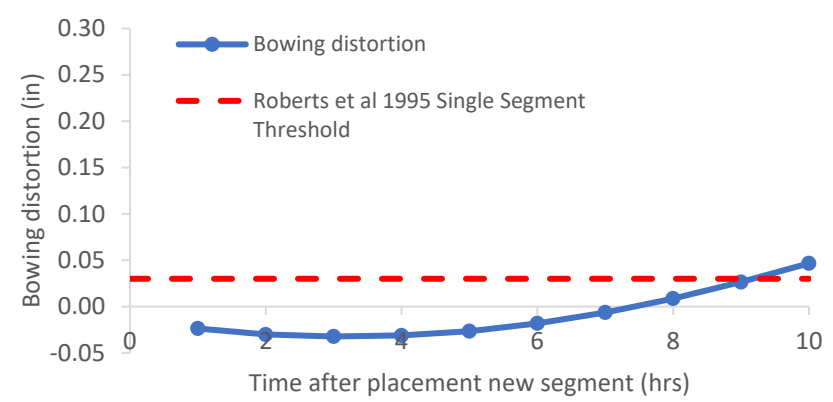

Figure B-398: Simulation 133 - Bowing distortion progression of match-cast segment from time of placement of new segment to 10 hours

Figure B-399: Simulation 133 - Internal temperatures along the wing of segments

Simulation 134 -Results Summary

Table B-134: Model input parameters simulation 134

Model details		
Permutation number	134	
Geometry	Florida Bridge F - w/l=5.92	
Max. Mesh Size	3.15	in
Time Step	1	hrs
Placement Temperature	95	°F
Match-cast segment Time of Simulation at Casting	0	hrs
New Segment Time of Simulation at Casting	24	hrs
Concrete Properties		
Cement Content	950.11	lb/yd^3
Activation Energy	28.43	BTU/mol
Heat of Hydration Parameters		
Total Heat Development, $Q_{ult} = \alpha_u \cdot H_u$	124.95	BTU/lb
Time Parameter, τ	10.50	hrs
Curvature Parameter, β	1.60	
Density	3880.948	lb/yd^3
Specific Heat	0.26	BTU/(lb·°F)
Thermal Conductivity	1.502	BTU/(ft·h·°F)
Match-cast segment Elastic Modulus Dev. Parameters		
Final Value	4584.92	ksi
Time Parameter	12.420	hrs
Curvature Parameter	1.068	
New Segment Elastic Modulus Dev. Parameters		
Final Value	14.50	ksi
Time Parameter	n/a	hrs
Curvature Parameter	n/a	
Poisson Ratio	0.17	
Coefficient of Thermal Expansion	4.54	µε/°F
Thermal Boundary Conditions (Applied to Appropriate Faces)		
Ambient Temp	Miami - Summer - Morning - Placement	
Wind	Low-Wind	0.00	mph
Formwork	Steel Formwork	34.60	BTU/(ft·h·°F)
	Thickness	0.118	in
Curing	Burlap	0.18	BTU/(ft·h·°F)
	Thickness	0.39	in

Figure B-400: Simulation 134 - Bowing distortion of match-cast segment after placement of the new segment

Figure B-401: Simulation 134 - Bowing distortion progression of match-cast segment from time of placement of new segment to 10 hours
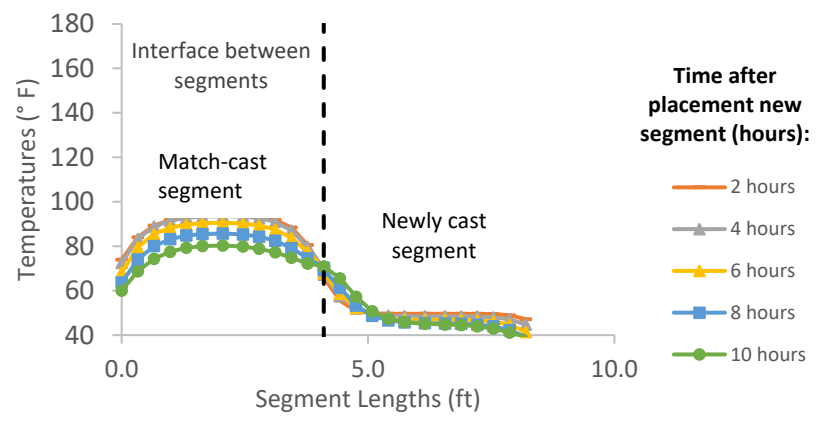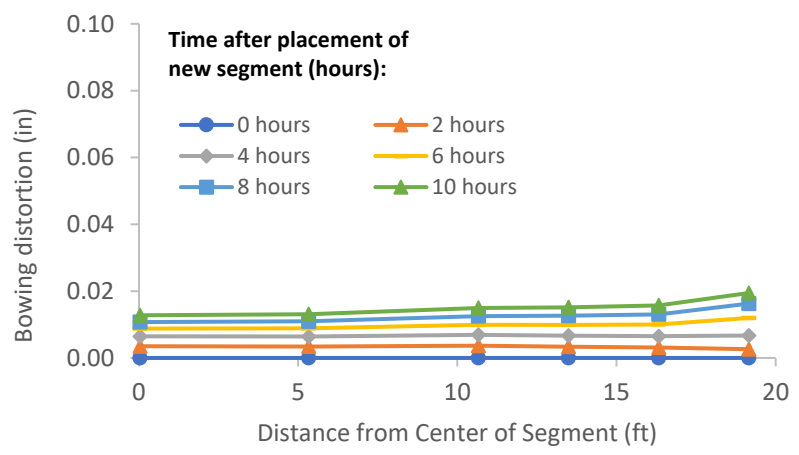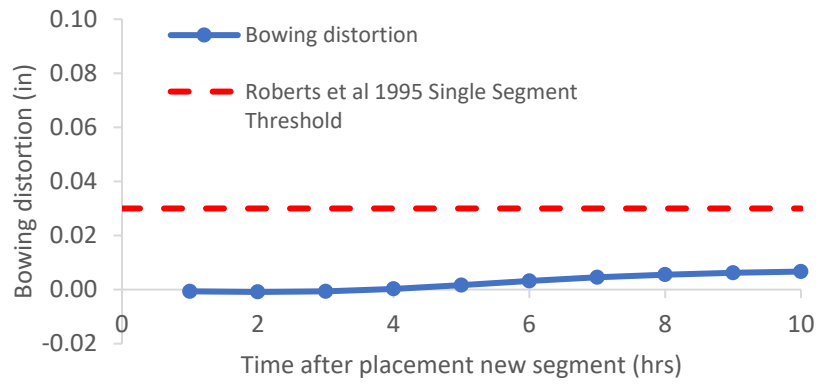

Figure B-402: Simulation 134 - Internal temperatures along the wing of segments

Simulation 135 -Results Summary

Table B-135: Model input parameters simulation 135

Model details		
Permutation number	135	
Geometry	Florida Bridge D - w/l=9.39	
Max. Mesh Size	3.15	in
Time Step	1	hrs
Placement Temperature	95	°F
Match-cast segment Time of Simulation at Casting	0	hrs
New Segment Time of Simulation at Casting	24	hrs
Concrete Properties		
Cement Content	950.11	lb/yd^3
Activation Energy	28.43	BTU/mol
Heat of Hydration Parameters		
Total Heat Development, $Q_{ult} = \alpha_u \cdot H_u$	124.95	BTU/lb
Time Parameter, τ	10.50	hrs
Curvature Parameter, β	1.60	
Density	3880.948	lb/yd^3
Specific Heat	0.26	BTU/(lb·°F)
Thermal Conductivity	1.502	BTU/(ft·h·°F)
Match-cast segment Elastic Modulus Dev. Parameters		
Final Value	4584.92	ksi
Time Parameter	12.420	hrs
Curvature Parameter	1.068	
New Segment Elastic Modulus Dev. Parameters		
Final Value	14.50	ksi
Time Parameter	n/a	hrs
Curvature Parameter	n/a	
Poisson Ratio	0.17	
Coefficient of Thermal Expansion	4.54	με/°F
Thermal Boundary Conditions (Applied to Appropriate Faces)		
Ambient Temp	Miami - Summer - Morning - Placement	
Wind	Low-Wind	0.00	mph
Formwork	Steel Formwork	34.60	BTU/(ft·h·°F)
	Thickness	0.118	in
Curing	Burlap	0.18	BTU/(ft·h·°F)
	Thickness	0.39	in

Figure B-403: Simulation 135 - Bowing distortion of match-cast segment after placement of the new segment

Figure B-404: Simulation 135 - Bowing distortion progression of match-cast segment from time of placement of new segment to 10 hours
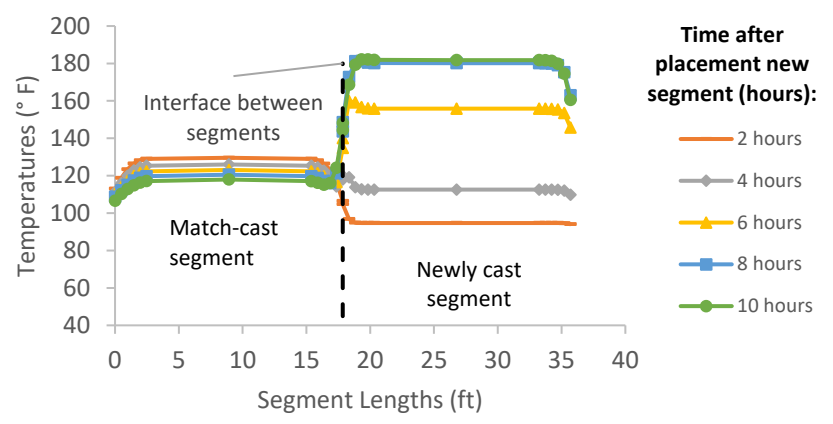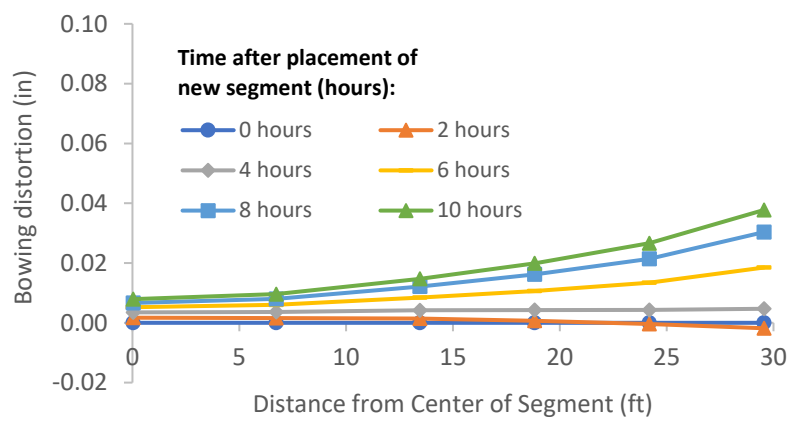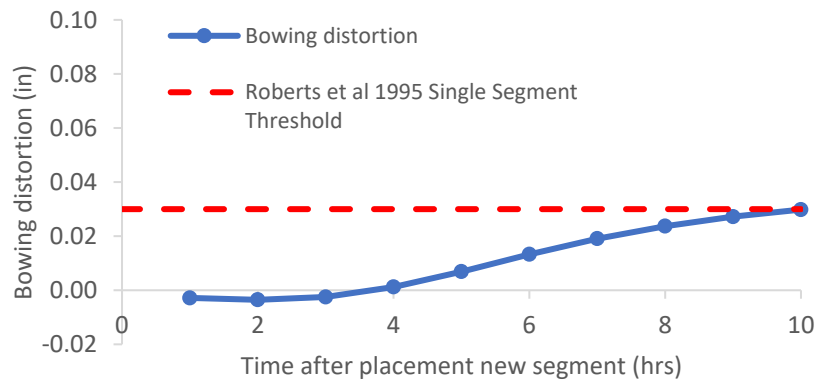

Figure B-405: Simulation 135 - Internal temperatures along the wing of segments

Simulation 136 -Results Summary

Table B-136: Model input parameters simulation 136

Model details		
Permutation number	136	
Geometry	Bridge Bang Na Pier - w/l=21.80	
Max. Mesh Size	2.76	in
Time Step	1	hrs
Placement Temperature	95	°F
Match-cast segment Time of Simulation at Casting	0	hrs
New Segment Time of Simulation at Casting	24	hrs
Concrete Properties		
Cement Content	950.11	lb/yd^3
Activation Energy	28.43	BTU/mol
Heat of Hydration Parameters		
Total Heat Development, $Q_{ult} = \alpha_u \cdot H_u$	124.95	BTU/lb
Time Parameter, τ	10.50	hrs
Curvature Parameter, β	1.60	
Density	3880.948	lb/yd^3
Specific Heat	0.26	BTU/(lb·°F)
Thermal Conductivity	1.502	BTU/(ft·h·°F)
Match-cast segment Elastic Modulus Dev. Parameters		
Final Value	4584.92	ksi
Time Parameter	12.420	hrs
Curvature Parameter	1.068	
New Segment Elastic Modulus Dev. Parameters		
Final Value	14.50	ksi
Time Parameter	n/a	hrs
Curvature Parameter	n/a	
Poisson Ratio	0.17	
Coefficient of Thermal Expansion	4.54	$\mu\varepsilon$/°F
Thermal Boundary Conditions (Applied to Appropriate Faces)		
Ambient Temp	Miami - Summer - Morning - Placement	
Wind	Low-Wind	0.00	mph
Formwork	Steel Formwork	34.60	BTU/(ft·h·°F)
	Thickness	0.118	in
Curing	Burlap	0.18	BTU/(ft·h·°F)
	Thickness	0.39	in

Figure B-406: Simulation 136 - Bowing distortion of match-cast segment after placement of the new segment

Figure B-407: Simulation 136 - Bowing distortion progression of match-cast segment from time of placement of new segment to 10 hours
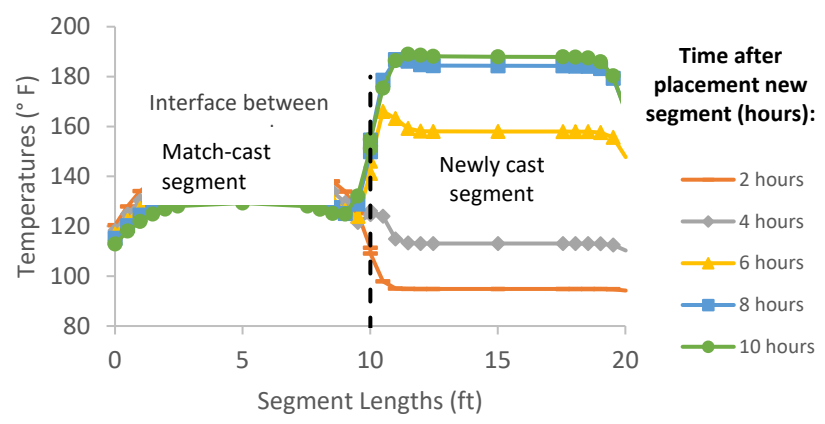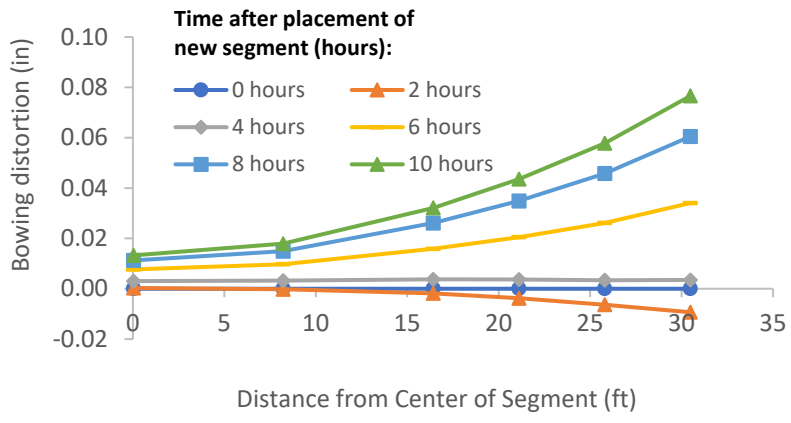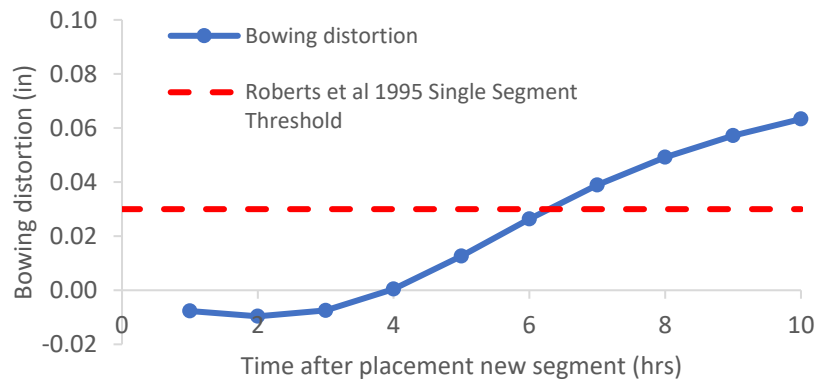

Figure B-408: Simulation 136 - Internal temperatures along the wing of segments

Simulation 137 -Results Summary

Table B-137: Model input parameters simulation 137

Model details		
Permutation number	137	
Geometry	Florida Bridge A - w/l=2.15	
Max. Mesh Size	2.76	in
Time Step	1	hrs
Placement Temperature	95	°F
Match-cast segment Time of Simulation at Casting	0	hrs
New Segment Time of Simulation at Casting	24	hrs
Concrete Properties		
Cement Content	950.11	lb/yd^3
Activation Energy	28.43	BTU/mol
Heat of Hydration Parameters		
Total Heat Development, $Q_{ult} = \alpha_u \cdot H_u$	124.95	BTU/lb
Time Parameter, τ	10.50	hrs
Curvature Parameter, β	1.60	
Density	3880.948	lb/yd^3
Specific Heat	0.26	BTU/(lb·°F)
Thermal Conductivity	1.502	BTU/(ft·h·°F)
Match-cast segment Elastic Modulus Dev. Parameters		
Final Value	4584.92	ksi
Time Parameter	12.420	hrs
Curvature Parameter	1.068	
New Segment Elastic Modulus Dev. Parameters		
Final Value	14.50	ksi
Time Parameter	n/a	hrs
Curvature Parameter	n/a	
Poisson Ratio	0.17	
Coefficient of Thermal Expansion	4.54	µε/°F
Thermal Boundary Conditions (Applied to Appropriate Faces)		
Ambient Temp	Miami - Summer - Morning - Placement	
Wind	High-Wind	15.00	mph
Formwork	Steel Formwork	34.60	BTU/(ft·h·°F)
	Thickness	0.118	in
Curing	Burlap	0.18	BTU/(ft·h·°F)
	Thickness	0.39	in

Figure B-409: Simulation 137 - Bowing distortion of match-cast segment after placement of the new segment

Figure B-410: Simulation 137 - Bowing distortion progression of match-cast segment from time of placement of new segment to 10 hours
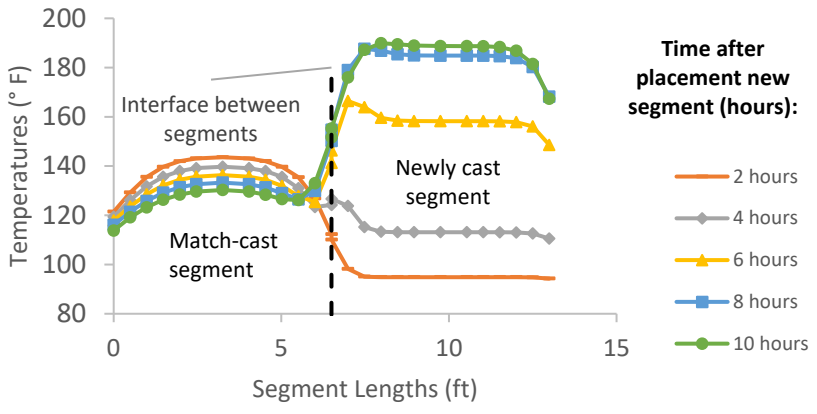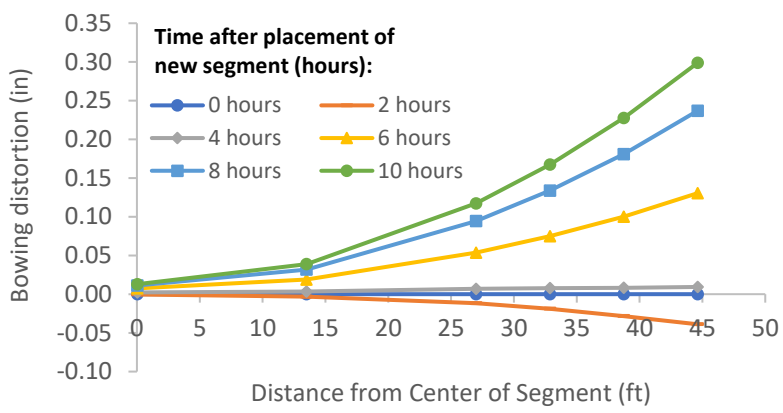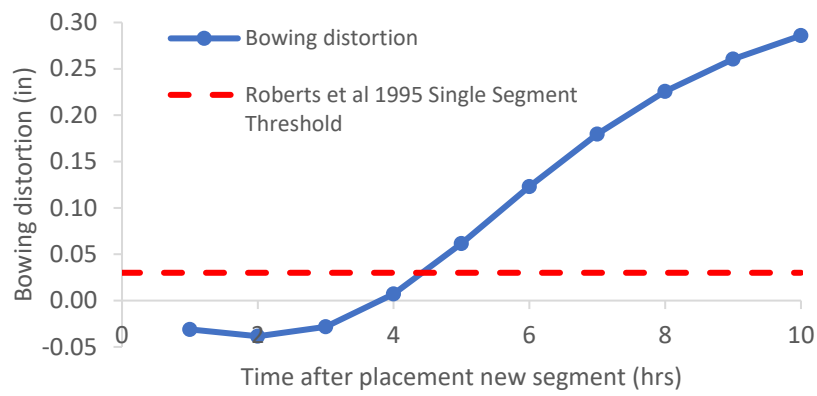

Figure B-411: Simulation 137 - Internal temperatures along the wing of segments

Simulation 138 -Results Summary

Table B-138: Model input parameters simulation 138

Model details		
Permutation number	138	
Geometry	Florida Bridge F - w/l=5.92	
Max. Mesh Size	3.15	in
Time Step	1	hrs
Placement Temperature	95	°F
Match-cast segment Time of Simulation at Casting	0	hrs
New Segment Time of Simulation at Casting	24	hrs
Concrete Properties		
Cement Content	950.11	lb/yd^3
Activation Energy	28.43	BTU/mol
Heat of Hydration Parameters		
Total Heat Development, $Q_{ult} = \alpha_u \cdot H_u$	124.95	BTU/lb
Time Parameter, τ	10.50	hrs
Curvature Parameter, β	1.60	
Density	3880.948	lb/yd^3
Specific Heat	0.26	BTU/(lb·°F)
Thermal Conductivity	1.502	BTU/(ft·h·°F)
Match-cast segment Elastic Modulus Dev. Parameters		
Final Value	4584.92	ksi
Time Parameter	12.420	hrs
Curvature Parameter	1.068	
New Segment Elastic Modulus Dev. Parameters		
Final Value	14.50	ksi
Time Parameter	n/a	hrs
Curvature Parameter	n/a	
Poisson Ratio	0.17	
Coefficient of Thermal Expansion	4.54	µε/°F
Thermal Boundary Conditions (Applied to Appropriate Faces)		
Ambient Temp	Miami - Summer - Morning - Placement	
Wind	High-Wind	15.00	mph
Formwork	Steel Formwork	34.60	BTU/(ft·h·°F)
	Thickness	0.118	in
Curing	Burlap	0.18	BTU/(ft·h·°F)
	Thickness	0.39	in

Figure B-412: Simulation 138 - Bowing distortion of match-cast segment after placement of the new segment

Figure B-413: Simulation 138 - Bowing distortion progression of match-cast segment from time of placement of new segment to 10 hours
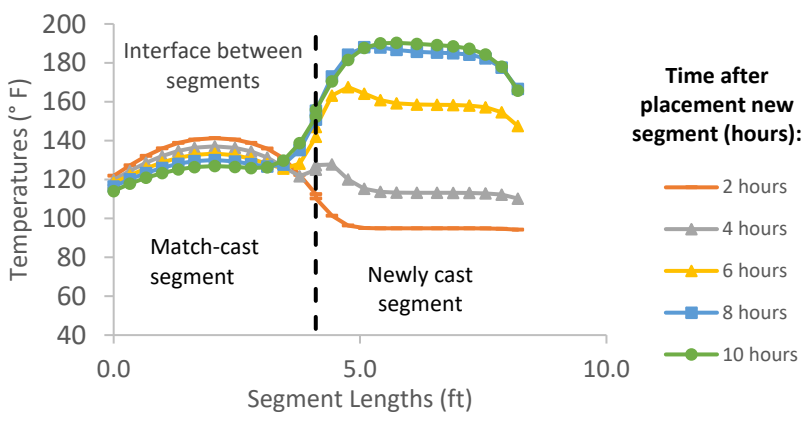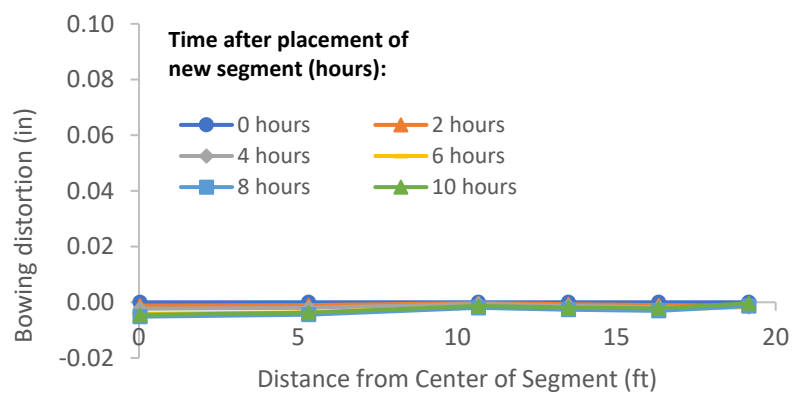

Figure B-414: Simulation 138 - Internal temperatures along the wing of segments

Simulation 139 -Results Summary

Table B-139: Model input parameters simulation 139

Model details		
Permutation number	139	
Geometry	Florida Bridge D - w/l=9.39	
Max. Mesh Size	3.15	in
Time Step	1	hrs
Placement Temperature	95	°F
Match-cast segment Time of Simulation at Casting	0	hrs
New Segment Time of Simulation at Casting	24	hrs
Concrete Properties		
Cement Content	950.11	lb/yd³
Activation Energy	28.43	BTU/mol
Heat of Hydration Parameters		
Total Heat Development, $Q_{ult} = \alpha_u \cdot H_u$	124.95	BTU/lb
Time Parameter, τ	10.50	hrs
Curvature Parameter, β	1.60	
Density	3880.948	lb/yd³
Specific Heat	0.26	BTU/(lb·°F)
Thermal Conductivity	1.502	BTU/(ft·h·°F)
Match-cast segment Elastic Modulus Dev. Parameters		
Final Value	4584.92	ksi
Time Parameter	12.420	hrs
Curvature Parameter	1.068	
New Segment Elastic Modulus Dev. Parameters		
Final Value	14.50	ksi
Time Parameter	n/a	hrs
Curvature Parameter	n/a	
Poisson Ratio	0.17	
Coefficient of Thermal Expansion	4.54	με/°F
Thermal Boundary Conditions (Applied to Appropriate Faces)		
Ambient Temp	Miami - Summer - Morning - Placement	
Wind	High-Wind	15.00	mph
Formwork	Steel Formwork	34.60	BTU/(ft·h·°F)
	Thickness	0.118	in
Curing	Burlap	0.18	BTU/(ft·h·°F)
	Thickness	0.39	in

Figure B-415: Simulation 139 - Bowing distortion of match-cast segment after placement of the new segment
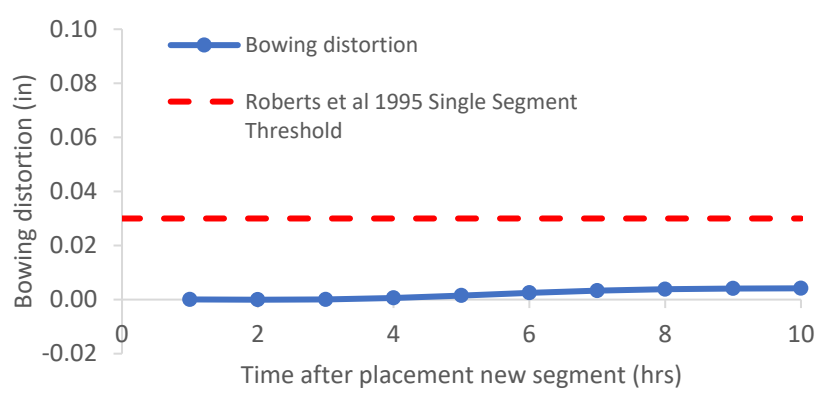

Figure B-416: Simulation 139 - Bowing distortion progression of match-cast segment from time of placement of new segment to 10 hours
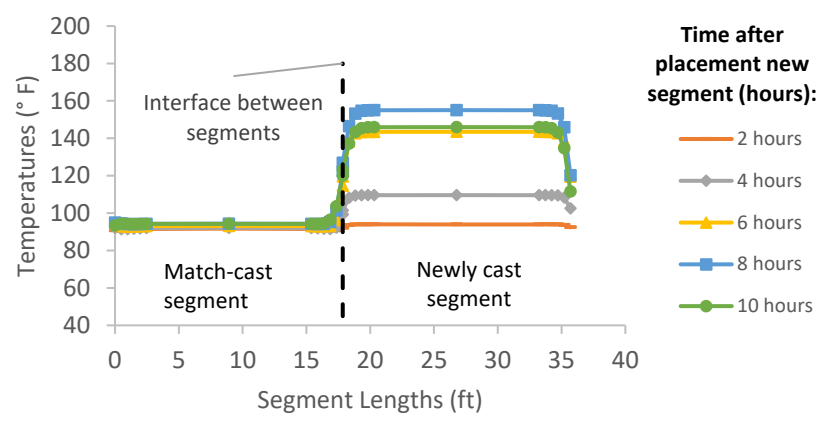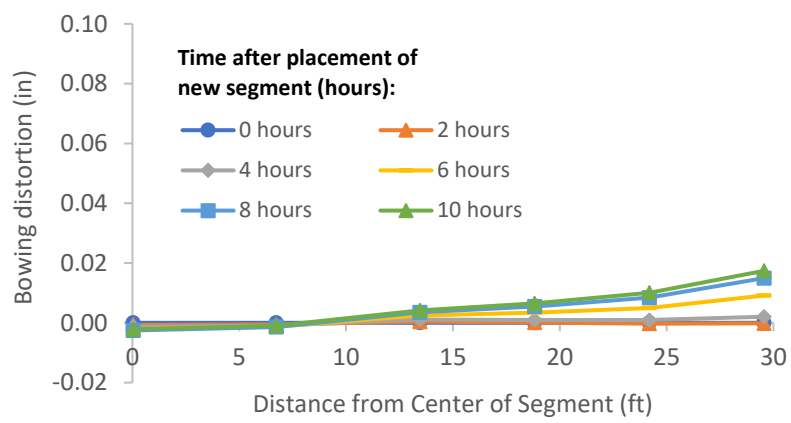

Figure B-417: Simulation 139 - Internal temperatures along the wing of segments

Simulation 140 -Results Summary

Table B-140: Model input parameters simulation 140

Model details		
Permutation number	140	
Geometry	Bridge Bang Na Pier - w/l=21.80	
Max. Mesh Size	2.76	in
Time Step	1	hrs
Placement Temperature	95	°F
Match-cast segment Time of Simulation at Casting	0	hrs
New Segment Time of Simulation at Casting	24	hrs
Concrete Properties		
Cement Content	950.11	lb/yd^3
Activation Energy	28.43	BTU/mol
Heat of Hydration Parameters		
Total Heat Development, $Q_{ult} = \alpha_u \cdot H_u$	124.95	BTU/lb
Time Parameter, τ	10.50	hrs
Curvature Parameter, β	1.60	
Density	3880.948	lb/yd^3
Specific Heat	0.26	BTU/(lb·°F)
Thermal Conductivity	1.502	BTU/(ft·h·°F)
Match-cast segment Elastic Modulus Dev. Parameters		
Final Value	4584.92	ksi
Time Parameter	12.420	hrs
Curvature Parameter	1.068	
New Segment Elastic Modulus Dev. Parameters		
Final Value	14.50	ksi
Time Parameter	n/a	hrs
Curvature Parameter	n/a	
Poisson Ratio	0.17	
Coefficient of Thermal Expansion	4.54	µε/°F
Thermal Boundary Conditions (Applied to Appropriate Faces)		
Ambient Temp	Miami - Summer - Morning - Placement	
Wind	High-Wind	15.00	mph
Formwork	Steel Formwork	34.60	BTU/(ft·h·°F)
	Thickness	0.118	in
Curing	Burlap	0.18	BTU/(ft·h·°F)
	Thickness	0.39	in

Figure B-418: Simulation 140 - Bowing distortion of match-cast segment after placement of the new segment
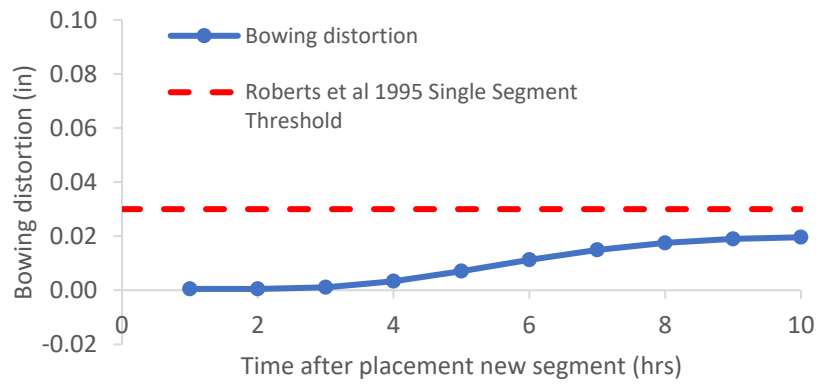

Figure B-419: Simulation 140 - Bowing distortion progression of match-cast segment from time of placement of new segment to 10 hours
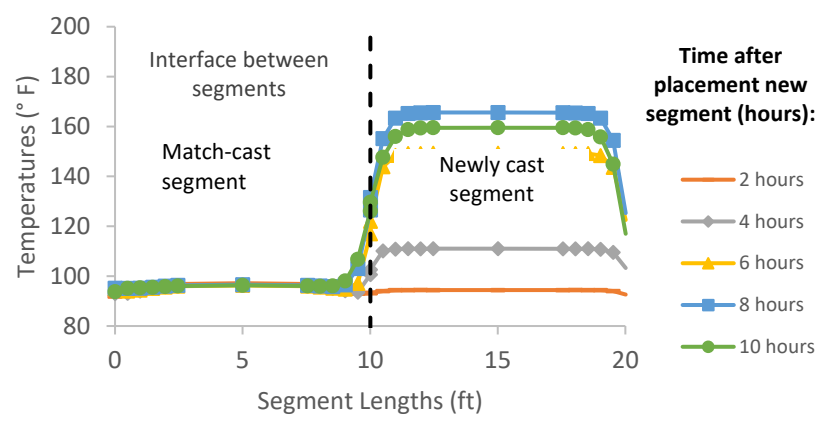

Figure B-420: Simulation 140 - Internal temperatures along the wing of segments

Simulation 141 -Results Summary

Table B-141: Model input parameters simulation 141

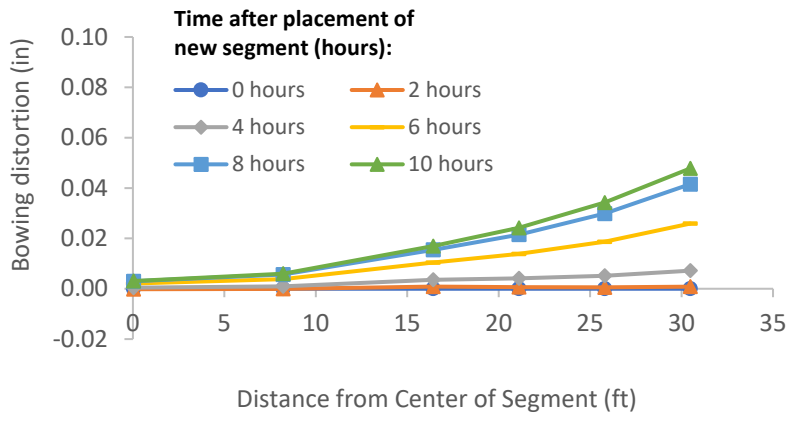| Model details		
Permutation number	141	
Geometry	Florida Bridge A - w/l=2.15	
Max. Mesh Size	2.76	in
Time Step	1	hrs
Placement Temperature	80	°F
Match-cast segment Time of Simulation at Casting	0	hrs
New Segment Time of Simulation at Casting	24	hrs
Concrete Properties		
Cement Content	950.11	lb/yd^3
Activation Energy	28.43	BTU/mol
Heat of Hydration Parameters		
Total Heat Development, $Q_{ult} = \alpha_u \cdot H_u$	124.95	BTU/lb
Time Parameter, τ	10.50	hrs
Curvature Parameter, β	1.60	
Density	3880.948	lb/yd^3
Specific Heat	0.26	BTU/(lb·°F)
Thermal Conductivity	1.502	BTU/(ft·h·°F)
Match-cast segment Elastic Modulus Dev. Parameters		
Final Value	4584.92	ksi
Time Parameter	12.420	hrs
Curvature Parameter	1.068	
New Segment Elastic Modulus Dev. Parameters		
Final Value	14.50	ksi
Time Parameter	n/a	hrs
Curvature Parameter	n/a	
Poisson Ratio	0.17	
Coefficient of Thermal Expansion	4.54	με/°F
Thermal Boundary Conditions (Applied to Appropriate Faces)		
Ambient Temp	Steam-curing-130°F-cycle	
Wind	Low-Wind	0.00	mph
Formwork	Steel Formwork	34.60	BTU/(ft·h·°F)
	Thickness	0.118	in
Curing	Burlap	0.18	BTU/(ft·h·°F)
	Thickness	0.39	in

Figure B-421: Simulation 141 - Bowing distortion of match-cast segment after placement of the new segment
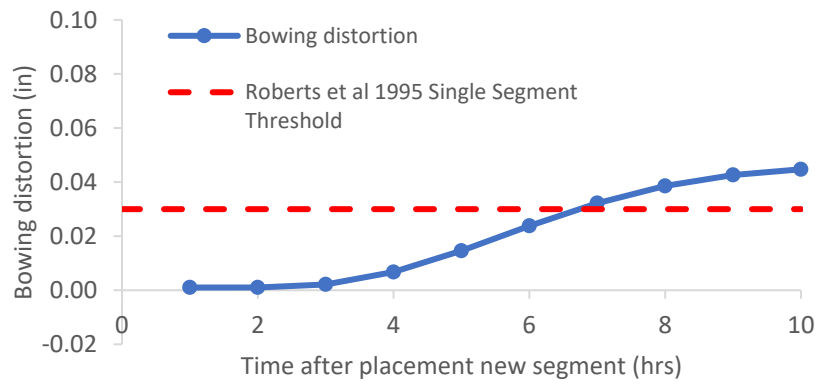

Figure B-422: Simulation 141 - Bowing distortion progression of match-cast segment from time of placement of new segment to 10 hours
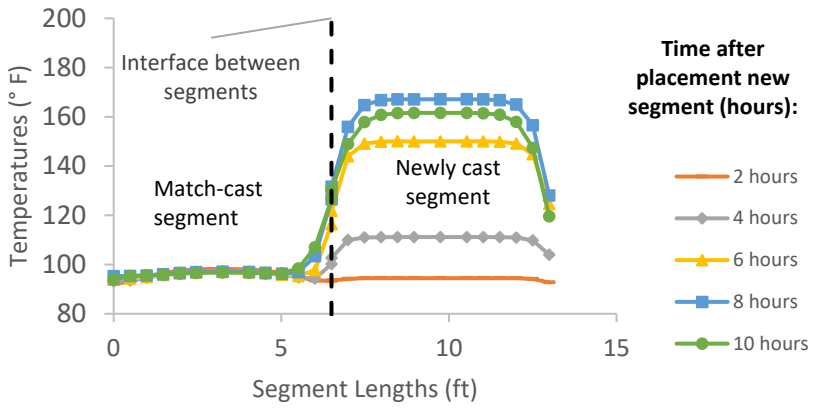

Figure B-423: Simulation 141 - Internal temperatures along the wing of segments

Simulation 142 -Results Summary

Table B-142: Model input parameters simulation 142

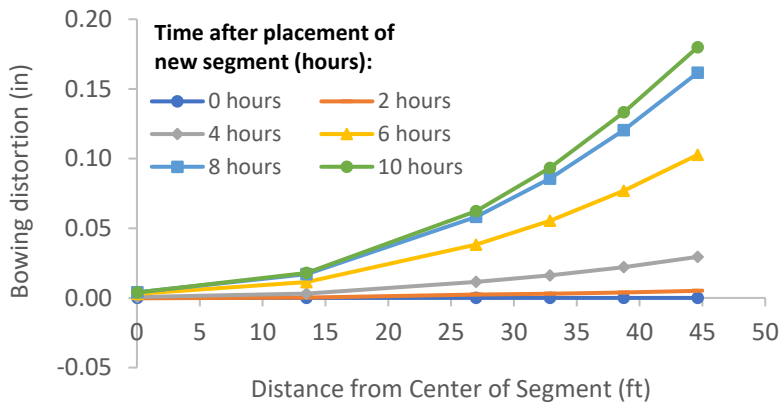| Model details		
Permutation number	142	
Geometry	Florida Bridge F - w/l=5.92	
Max. Mesh Size	3.15	in
Time Step	1	hrs
Placement Temperature	80	°F
Match-cast segment Time of Simulation at Casting	0	hrs
New Segment Time of Simulation at Casting	24	hrs
Concrete Properties		
Cement Content	950.11	lb/yd^3
Activation Energy	28.43	BTU/mol
Heat of Hydration Parameters		
Total Heat Development, $Q_{ult} = \alpha_u \cdot H_u$	124.95	BTU/lb
Time Parameter, τ	10.50	hrs
Curvature Parameter, β	1.60	
Density	3880.948	lb/yd^3
Specific Heat	0.26	BTU/(lb·°F)
Thermal Conductivity	1.502	BTU/(ft·h·°F)
Match-cast segment Elastic Modulus Dev. Parameters		
Final Value	4584.92	ksi
Time Parameter	12.420	hrs
Curvature Parameter	1.068	
New Segment Elastic Modulus Dev. Parameters		
Final Value	14.50	ksi
Time Parameter	n/a	hrs
Curvature Parameter	n/a	
Poisson Ratio	0.17	
Coefficient of Thermal Expansion	4.54	µε/°F
Thermal Boundary Conditions (Applied to Appropriate Faces)		
Ambient Temp	Steam-curing-130°F-cycle	
Wind	Low-Wind	0.00	mph
Formwork	Steel Formwork	34.60	BTU/(ft·h·°F)
	Thickness	0.118	in
Curing	Burlap	0.18	BTU/(ft·h·°F)
	Thickness	0.39	in

Figure B-424: Simulation 142 - Bowing distortion of match-cast segment after placement of the new segment
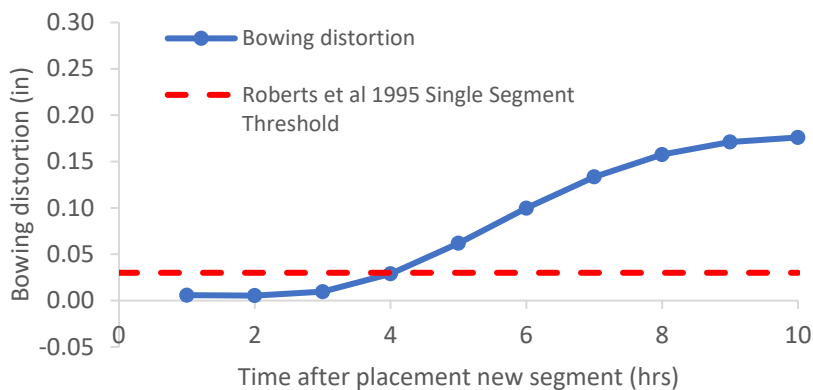

Figure B-425: Simulation 142 - Bowing distortion progression of match-cast segment from time of placement of new segment to 10 hours
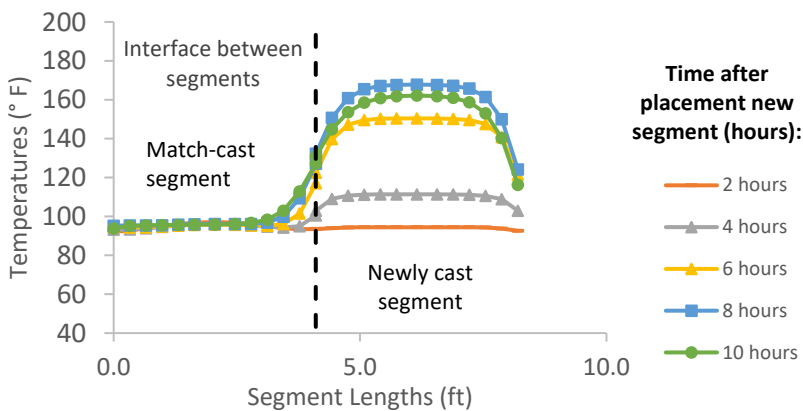

Figure B-426: Simulation 142 - Internal temperatures along the wing of segments

Simulation 143 -Results Summary

Table B-143: Model input parameters simulation 143

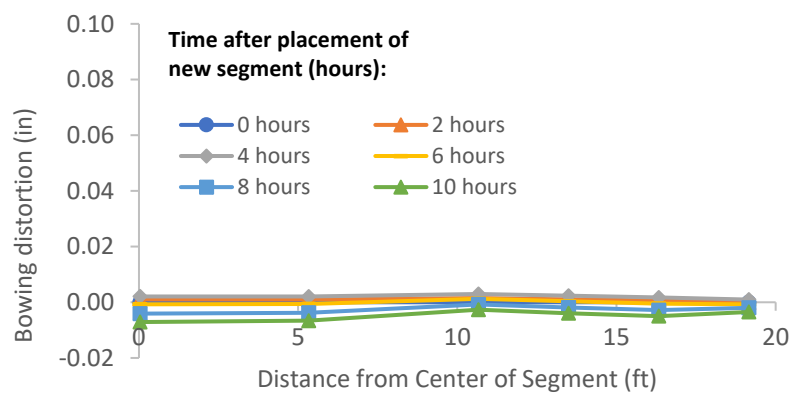| Model details		
Permutation number	143	
Geometry	Florida Bridge D - w/l=9.39	
Max. Mesh Size	3.15	in
Time Step	1	hrs
Placement Temperature	80	°F
Match-cast segment Time of Simulation at Casting	0	hrs
New Segment Time of Simulation at Casting	24	hrs
Concrete Properties		
Cement Content	950.11	lb/yd^3
Activation Energy	28.43	BTU/mol
Heat of Hydration Parameters		
Total Heat Development, $Q_{ult} = \alpha_u \cdot H_u$	124.95	BTU/lb
Time Parameter, τ	10.50	hrs
Curvature Parameter, β	1.60	
Density	3880.948	lb/yd^3
Specific Heat	0.26	BTU/(lb·°F)
Thermal Conductivity	1.502	BTU/(ft·h·°F)
Match-cast segment Elastic Modulus Dev. Parameters		
Final Value	4584.92	ksi
Time Parameter	12.420	hrs
Curvature Parameter	1.068	
New Segment Elastic Modulus Dev. Parameters		
Final Value	14.50	ksi
Time Parameter	n/a	hrs
Curvature Parameter	n/a	
Poisson Ratio	0.17	
Coefficient of Thermal Expansion	4.54	µε/°F
Thermal Boundary Conditions (Applied to Appropriate Faces)		
Ambient Temp	Steam-curing-130°F-cycle	
Wind	Low-Wind	0.00	mph
Formwork	Steel Formwork	34.60	BTU/(ft·h·°F)
	Thickness	0.118	in
Curing	Burlap	0.18	BTU/(ft·h·°F)
	Thickness	0.39	in

Figure B-427: Simulation 143 - Bowing distortion of match-cast segment after placement of the new segment

Figure B-428: Simulation 143 - Bowing distortion progression of match-cast segment from time of placement of new segment to 10 hours
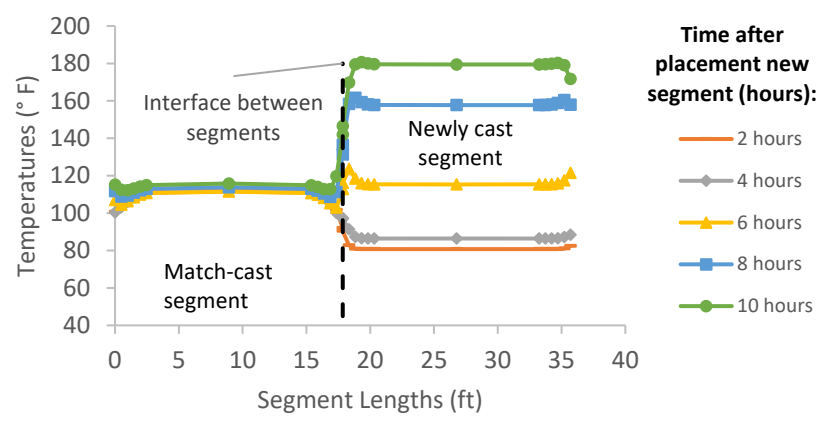

Figure B-429: Simulation 143 - Internal temperatures along the wing of segments

Simulation 144 -Results Summary

Table B-144: Model input parameters simulation 144

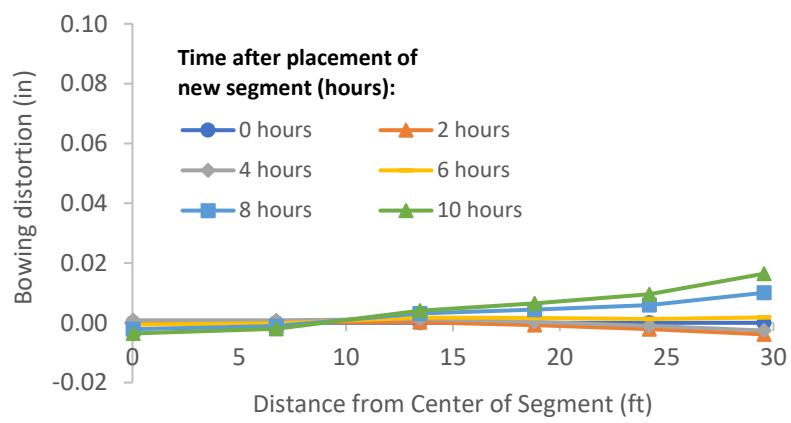| Model details		
Permutation number	144	
Geometry	Bridge Bang Na Pier - w/l=21.80	
Max. Mesh Size	2.76	in
Time Step	1	hrs
Placement Temperature	80	°F
Match-cast segment Time of Simulation at Casting	0	hrs
New Segment Time of Simulation at Casting	24	hrs
Concrete Properties		
Cement Content	950.11	lb/yd^3
Activation Energy	28.43	BTU/mol
Heat of Hydration Parameters		
Total Heat Development, $Q_{ult} = \alpha_u \cdot H_u$	124.95	BTU/lb
Time Parameter, τ	10.50	hrs
Curvature Parameter, β	1.60	
Density	3880.948	lb/yd^3
Specific Heat	0.26	BTU/(lb·°F)
Thermal Conductivity	1.502	BTU/(ft·h·°F)
Match-cast segment Elastic Modulus Dev. Parameters		
Final Value	4584.92	ksi
Time Parameter	12.420	hrs
Curvature Parameter	1.068	
New Segment Elastic Modulus Dev. Parameters		
Final Value	14.50	ksi
Time Parameter	n/a	hrs
Curvature Parameter	n/a	
Poisson Ratio	0.17	
Coefficient of Thermal Expansion	4.54	με/°F
Thermal Boundary Conditions (Applied to Appropriate Faces)		
Ambient Temp	Steam-curing-130°F-cycle	
Wind	Low-Wind	0.00	mph
Formwork	Steel Formwork	34.60	BTU/(ft·h·°F)
	Thickness	0.118	in
Curing	Burlap	0.18	BTU/(ft·h·°F)
	Thickness	0.39	in

Figure B-430: Simulation 144 - Bowing distortion of match-cast segment after placement of the new segment
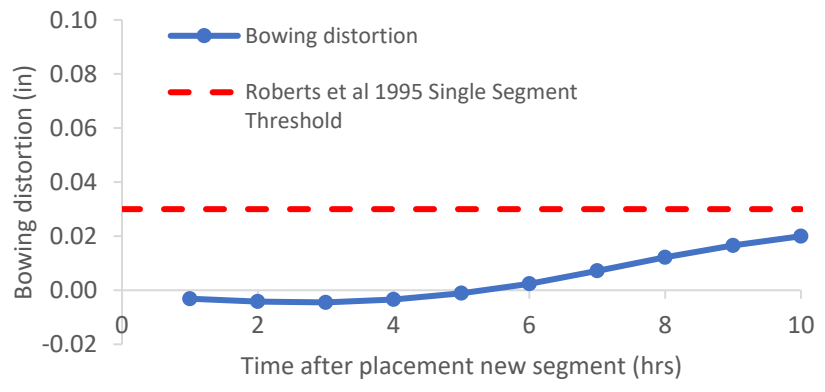

Figure B-431: Simulation 144 - Bowing distortion progression of match-cast segment from time of placement of new segment to 10 hours
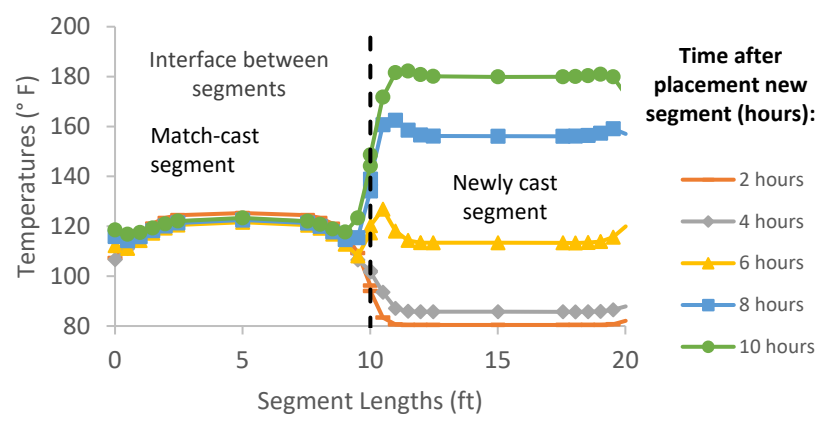

Figure B-432: Simulation 144 - Internal temperatures along the wing of segments

Simulation 145 -Results Summary

Table B-145: Model input parameters simulation 145

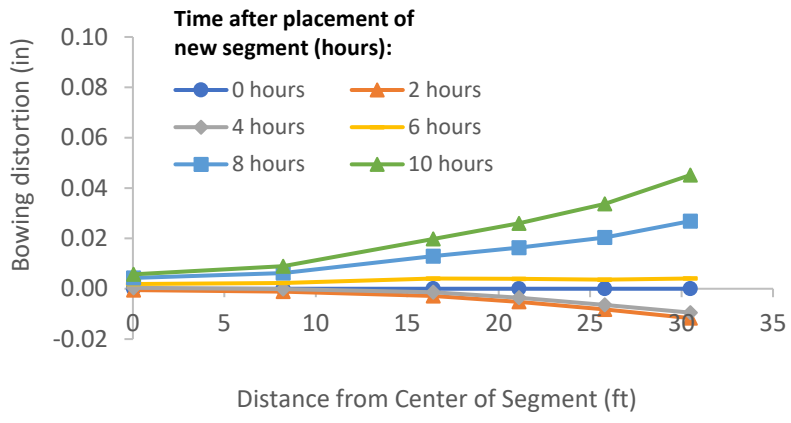| Model details		
Permutation number	145	
Geometry	Florida Bridge A - w/l=2.15	
Max. Mesh Size	2.76	in
Time Step	1	hrs
Placement Temperature	80	°F
Match-cast segment Time of Simulation at Casting	0	hrs
New Segment Time of Simulation at Casting	24	hrs
Concrete Properties		
Cement Content	950.11	lb/yd^3
Activation Energy	28.43	BTU/mol
Heat of Hydration Parameters		
Total Heat Development, $Q_{ult} = \alpha_u \cdot H_u$	124.95	BTU/lb
Time Parameter, τ	10.50	hrs
Curvature Parameter, β	1.60	
Density	3880.948	lb/yd^3
Specific Heat	0.26	BTU/(lb·°F)
Thermal Conductivity	1.502	BTU/(ft·h·°F)
Match-cast segment Elastic Modulus Dev. Parameters		
Final Value	4584.92	ksi
Time Parameter	12.420	hrs
Curvature Parameter	1.068	
New Segment Elastic Modulus Dev. Parameters		
Final Value	14.50	ksi
Time Parameter	n/a	hrs
Curvature Parameter	n/a	
Poisson Ratio	0.17	
Coefficient of Thermal Expansion	4.54	με/°F
Thermal Boundary Conditions (Applied to Appropriate Faces)		
Ambient Temp	Steam-curing-160°F-cycle	
Wind	Low-Wind	0.00	mph
Formwork	Steel Formwork	34.60	BTU/(ft·h·°F)
	Thickness	0.118	in
Curing	Burlap	0.18	BTU/(ft·h·°F)
	Thickness	0.39	in

Figure B-433: Simulation 145 - Bowing distortion of match-cast segment after placement of the new segment
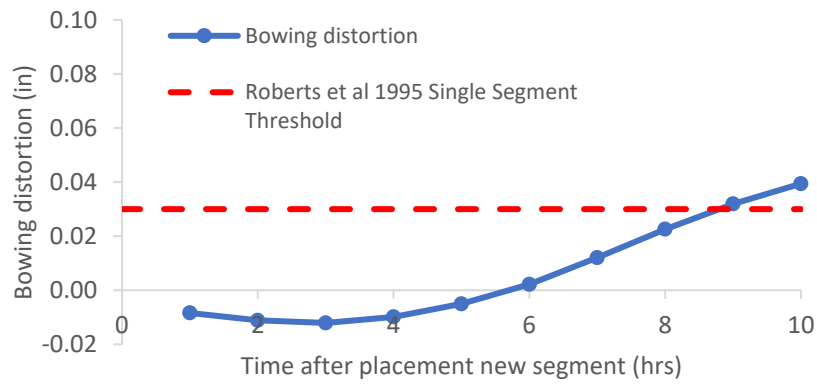

Figure B-434: Simulation 145 - Bowing distortion progression of match-cast segment from time of placement of new segment to 10 hours
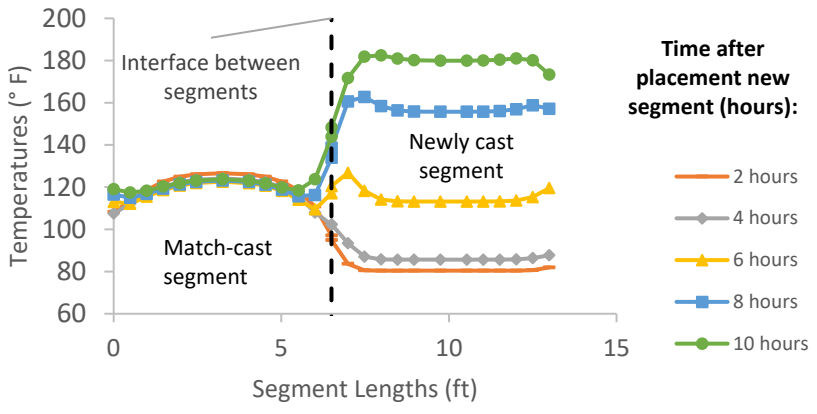

Figure B-435: Simulation 145 - Internal temperatures along the wing of segments

Simulation 146 -Results Summary

Table B-146: Model input parameters simulation 146

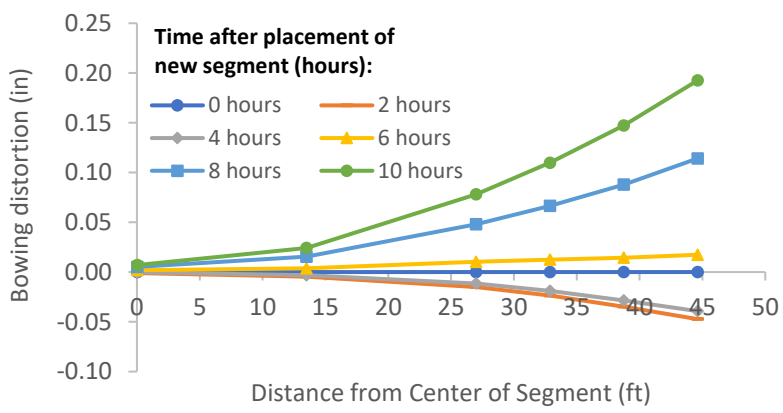| Model details		
Permutation number	146	
Geometry	Florida Bridge F - w/l=5.92	
Max. Mesh Size	3.15	in
Time Step	1	hrs
Placement Temperature	80	°F
Match-cast segment Time of Simulation at Casting	0	hrs
New Segment Time of Simulation at Casting	24	hrs
Concrete Properties		
Cement Content	950.11	lb/yd³
Activation Energy	28.43	BTU/mol
Heat of Hydration Parameters		
Total Heat Development, $Q_{ult} = \alpha_u \cdot H_u$	124.95	BTU/lb
Time Parameter, τ	10.50	hrs
Curvature Parameter, β	1.60	
Density	3880.948	lb/yd³
Specific Heat	0.26	BTU/(lb·°F)
Thermal Conductivity	1.502	BTU/(ft·h·°F)
Match-cast segment Elastic Modulus Dev. Parameters		
Final Value	4584.92	ksi
Time Parameter	12.420	hrs
Curvature Parameter	1.068	
New Segment Elastic Modulus Dev. Parameters		
Final Value	14.50	ksi
Time Parameter	n/a	hrs
Curvature Parameter	n/a	
Poisson Ratio	0.17	
Coefficient of Thermal Expansion	4.54	με/°F
Thermal Boundary Conditions (Applied to Appropriate Faces)		
Ambient Temp	Steam-curing-160°F-cycle	
Wind	Low-Wind	0.00	mph
Formwork	Steel Formwork	34.60	BTU/(ft·h·°F)
	Thickness	0.118	in
Curing	Burlap	0.18	BTU/(ft·h·°F)
	Thickness	0.39	in

Figure B-436: Simulation 146 - Bowing distortion of match-cast segment after placement of the new segment
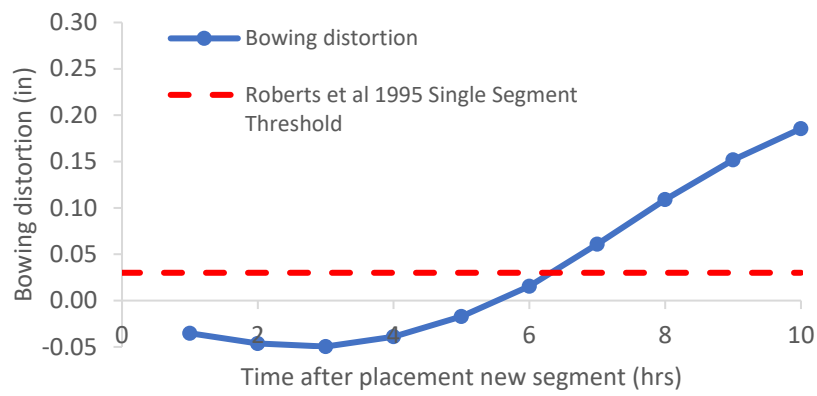

Figure B-437: Simulation 146 - Bowing distortion progression of match-cast segment from time of placement of new segment to 10 hours
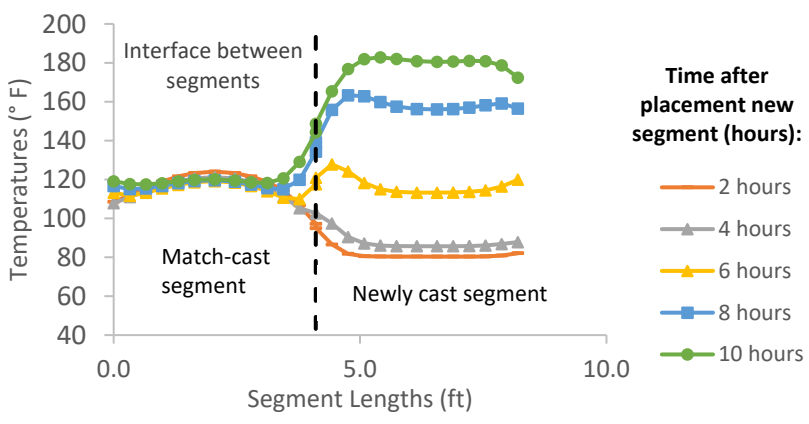

Figure B-438: Simulation 146 - Internal temperatures along the wing of segments

Simulation 147 -Results Summary

Table B-147: Model input parameters simulation 147

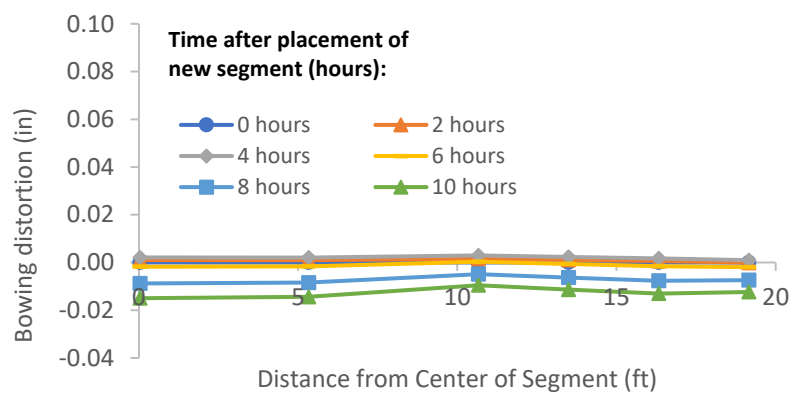| Model details		
Permutation number	147	
Geometry	Florida Bridge D - w/l=9.39	
Max. Mesh Size	3.15	in
Time Step	1	hrs
Placement Temperature	80	°F
Match-cast segment Time of Simulation at Casting	0	hrs
New Segment Time of Simulation at Casting	24	hrs
Concrete Properties		
Cement Content	950.11	lb/yd³
Activation Energy	28.43	BTU/mol
Heat of Hydration Parameters		
Total Heat Development, $Q_{ult} = \alpha_u \cdot H_u$	124.95	BTU/lb
Time Parameter, τ	10.50	hrs
Curvature Parameter, β	1.60	
Density	3880.948	lb/yd³
Specific Heat	0.26	BTU/(lb·°F)
Thermal Conductivity	1.502	BTU/(ft·h·°F)
Match-cast segment Elastic Modulus Dev. Parameters		
Final Value	4584.92	ksi
Time Parameter	12.420	hrs
Curvature Parameter	1.068	
New Segment Elastic Modulus Dev. Parameters		
Final Value	14.50	ksi
Time Parameter	n/a	hrs
Curvature Parameter	n/a	
Poisson Ratio	0.17	
Coefficient of Thermal Expansion	4.54	µε/°F
Thermal Boundary Conditions (Applied to Appropriate Faces)		
Ambient Temp	Steam-curing-160°F-cycle	
Wind	Low-Wind	0.00	mph
Formwork	Steel Formwork	34.60	BTU/(ft·h·°F)
	Thickness	0.118	in
Curing	Burlap	0.18	BTU/(ft·h·°F)
	Thickness	0.39	in

Figure B-439: Simulation 147 - Bowing distortion of match-cast segment after placement of the new segment

Figure B-440: Simulation 147 - Bowing distortion progression of match-cast segment from time of placement of new segment to 10 hours
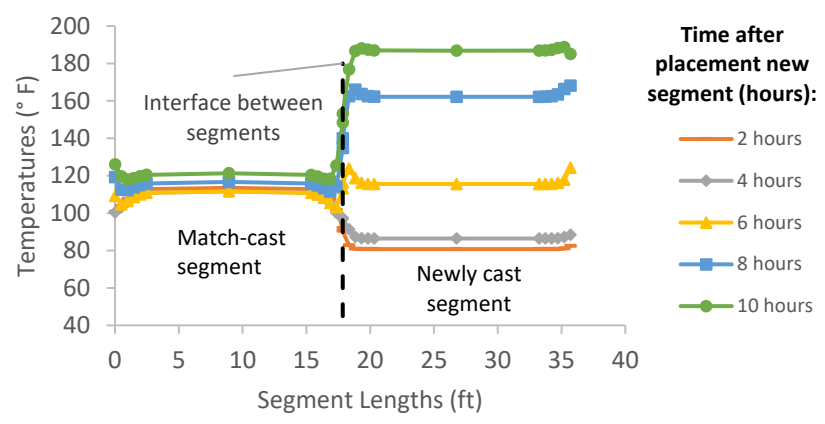

Figure B-441: Simulation 147 - Internal temperatures along the wing of segments

Simulation 148 -Results Summary

Table B-148: Model input parameters simulation 148

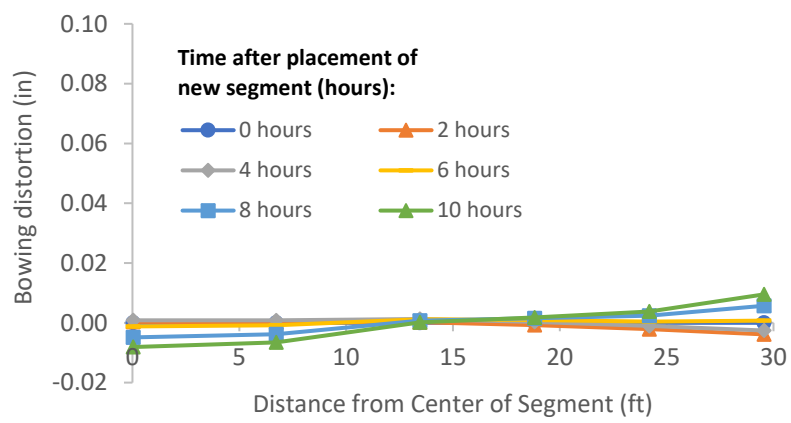| Model details		
Permutation number	148	
Geometry	Bridge Bang Na Pier - w/l=21.80	
Max. Mesh Size	2.76	in
Time Step	1	hrs
Placement Temperature	80	°F
Match-cast segment Time of Simulation at Casting	0	hrs
New Segment Time of Simulation at Casting	24	hrs
Concrete Properties		
Cement Content	950.11	lb/yd^3
Activation Energy	28.43	BTU/mol
Heat of Hydration Parameters		
Total Heat Development, $Q_{ult} = \alpha_u \cdot H_u$	124.95	BTU/lb
Time Parameter, τ	10.50	hrs
Curvature Parameter, β	1.60	
Density	3880.948	lb/yd^3
Specific Heat	0.26	BTU/(lb·°F)
Thermal Conductivity	1.502	BTU/(ft·h·°F)
Match-cast segment Elastic Modulus Dev. Parameters		
Final Value	4584.92	ksi
Time Parameter	12.420	hrs
Curvature Parameter	1.068	
New Segment Elastic Modulus Dev. Parameters		
Final Value	14.50	ksi
Time Parameter	n/a	hrs
Curvature Parameter	n/a	
Poisson Ratio	0.17	
Coefficient of Thermal Expansion	4.54	µε/°F
Thermal Boundary Conditions (Applied to Appropriate Faces)		
Ambient Temp	Steam-curing-160°F-cycle	
Wind	Low-Wind	0.00	mph
Formwork	Steel Formwork	34.60	BTU/(ft·h·°F)
	Thickness	0.118	in
Curing	Burlap	0.18	BTU/(ft·h·°F)
	Thickness	0.39	in

Figure B-442: Simulation 148 - Bowing distortion of match-cast segment after placement of the new segment
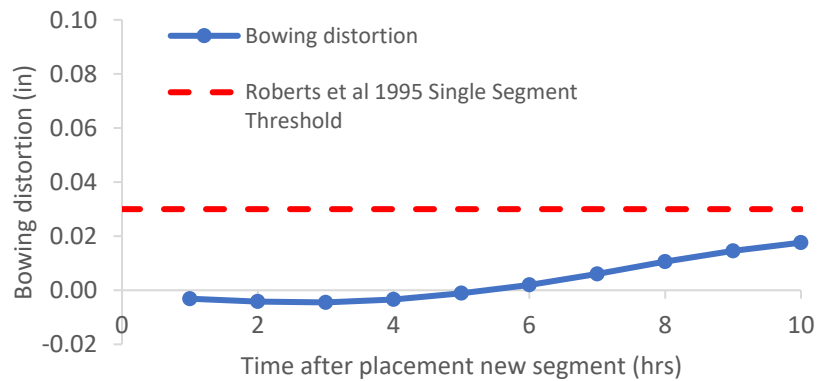

Figure B-443: Simulation 148 - Bowing distortion progression of match-cast segment from time of placement of new segment to 10 hours
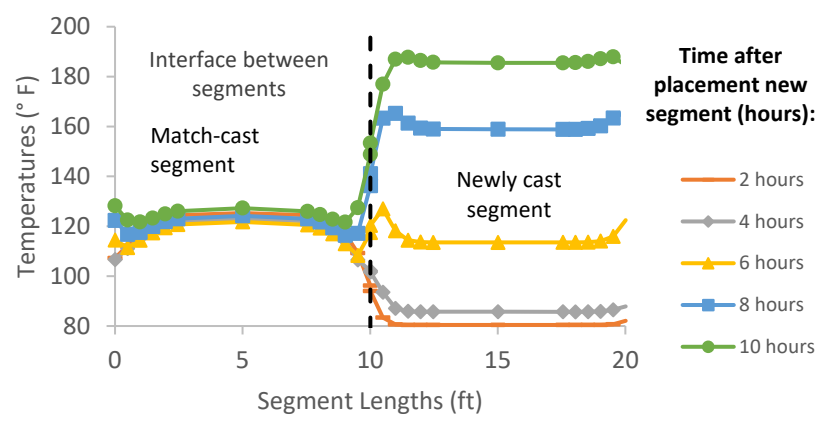

Figure B-444: Simulation 148 - Internal temperatures along the wing of segments

Simulation 149 -Results Summary

Table B-149: Model input parameters simulation 149

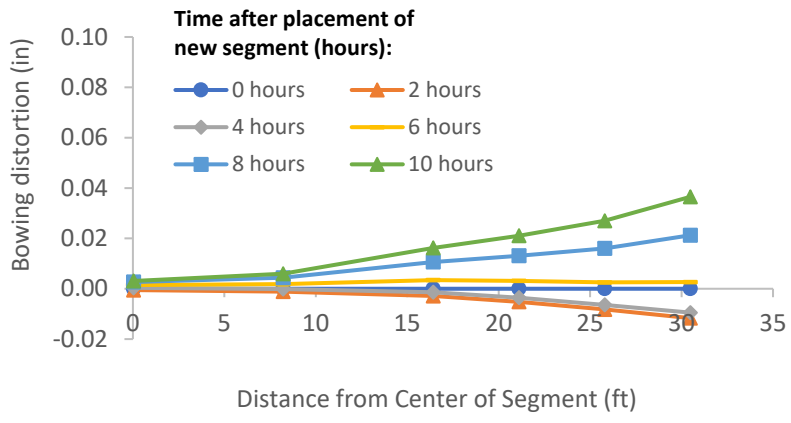| Model details		
Permutation number	149	
Geometry	Florida Bridge E - w/l=4.09	
Max. Mesh Size	2.95	in
Time Step	1	hrs
Placement Temperature	95	°F
Match-cast segment Time of Simulation at Casting	0	hrs
New Segment Time of Simulation at Casting	24	hrs
Concrete Properties		
Cement Content	650.08	lb/yd³
Activation Energy	26.21	BTU/mol
Heat of Hydration Parameters		
Total Heat Development, $Q_{ult} = \alpha_u \cdot H_u$	107.65	BTU/lb
Time Parameter, τ	18.28	hrs
Curvature Parameter, β	1.65	
Density	3034.390	lb/yd³
Specific Heat	0.21	BTU/(lb·°F)
Thermal Conductivity	1.084	BTU/(ft·h·°F)
Match-cast segment Elastic Modulus Dev. Parameters		
Final Value	3100.00	ksi
Time Parameter	12.420	hrs
Curvature Parameter	1.068	
New Segment Elastic Modulus Dev. Parameters		
Final Value	14.50	ksi
Time Parameter	n/a	hrs
Curvature Parameter	n/a	
Poisson Ratio	0.17	
Coefficient of Thermal Expansion	5.10	με/°F
Thermal Boundary Conditions (Applied to Appropriate Faces)		
Ambient Temp	Miami - Summer - Morning - Placement	
Wind	Medium-Wind	7.50	mph
Formwork	Steel Formwork	34.60	BTU/(ft·h·°F)
	Thickness	0.118	in
Curing	Burlap	0.18	BTU/(ft·h·°F)
	Thickness	0.39	in

Figure B-445: Simulation 149 - Bowing distortion of match-cast segment after placement of the new segment
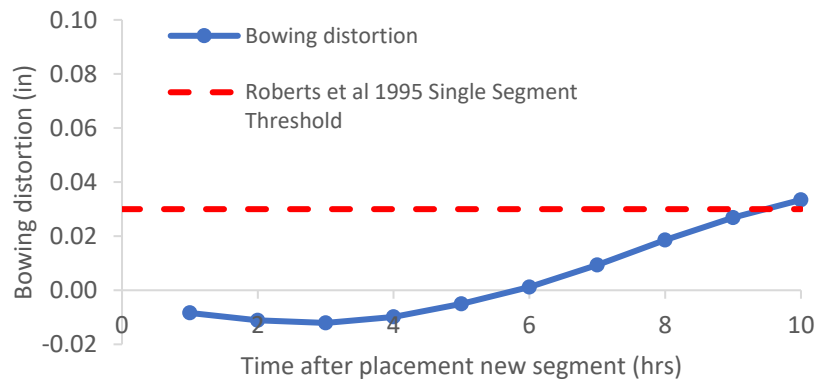

Figure B-446: Simulation 149 - Bowing distortion progression of match-cast segment from time of placement of new segment to 10 hours
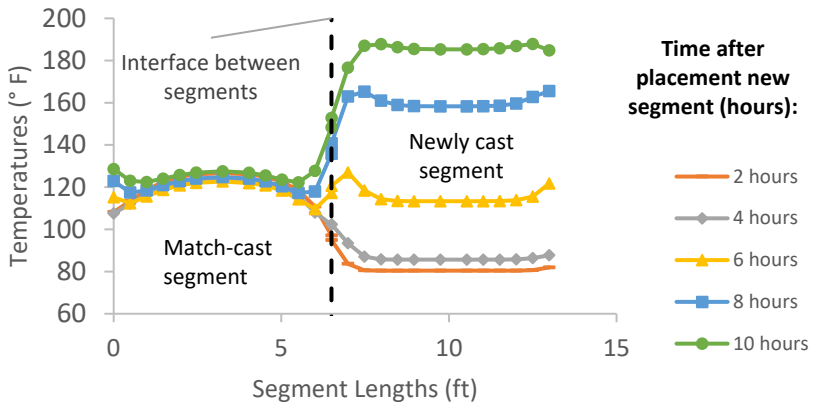

Figure B-447: Simulation 149 - Internal temperatures along the wing of segments

Simulation 150 -Results Summary

Table B-150: Model input parameters simulation 150

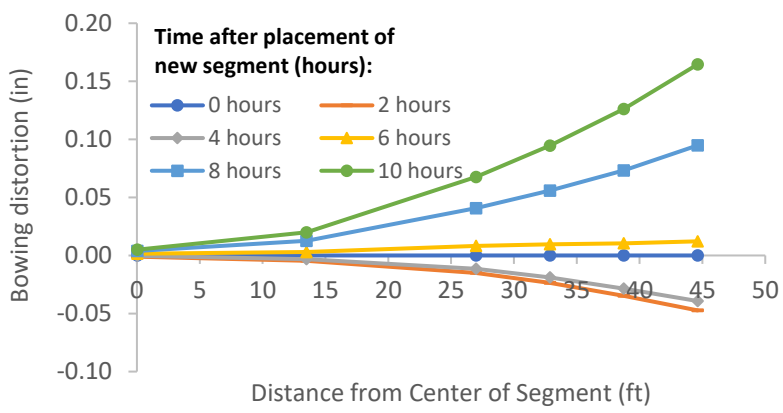| Model details		
Permutation number	150	
Geometry	Florida Bridge B - w/l=5.97	
Max. Mesh Size	3.94	in
Time Step	1	hrs
Placement Temperature	95	°F
Match-cast segment Time of Simulation at Casting	0	hrs
New Segment Time of Simulation at Casting	24	hrs
Concrete Properties		
Cement Content	650.08	lb/yd^3
Activation Energy	26.21	BTU/mol
Heat of Hydration Parameters		
Total Heat Development, $Q_{ult} = \alpha_u \cdot H_u$	107.65	BTU/lb
Time Parameter, τ	18.28	hrs
Curvature Parameter, β	1.65	
Density	3034.390	lb/yd^3
Specific Heat	0.21	BTU/(lb·°F)
Thermal Conductivity	1.084	BTU/(ft·h·°F)
Match-cast segment Elastic Modulus Dev. Parameters		
Final Value	3100.00	ksi
Time Parameter	12.420	hrs
Curvature Parameter	1.068	
New Segment Elastic Modulus Dev. Parameters		
Final Value	14.50	ksi
Time Parameter	n/a	hrs
Curvature Parameter	n/a	
Poisson Ratio	0.17	
Coefficient of Thermal Expansion	5.10	με/°F
Thermal Boundary Conditions (Applied to Appropriate Faces)		
Ambient Temp	Miami - Summer - Morning - Placement	
Wind	Medium-Wind	7.50	mph
Formwork	Steel Formwork	34.60	BTU/(ft·h·°F)
	Thickness	0.118	in
Curing	Burlap	0.18	BTU/(ft·h·°F)
	Thickness	0.39	in

Figure B-448: Simulation 150 - Bowing distortion of match-cast segment after placement of the new segment
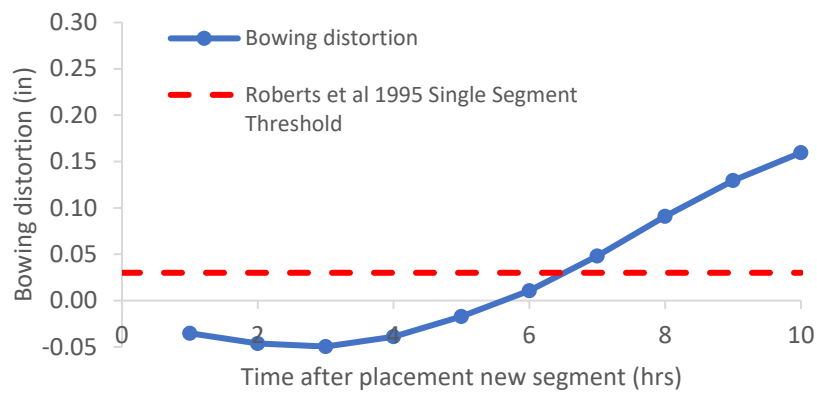

Figure B-449: Simulation 150 - Bowing distortion progression of match-cast segment from time of placement of new segment to 10 hours
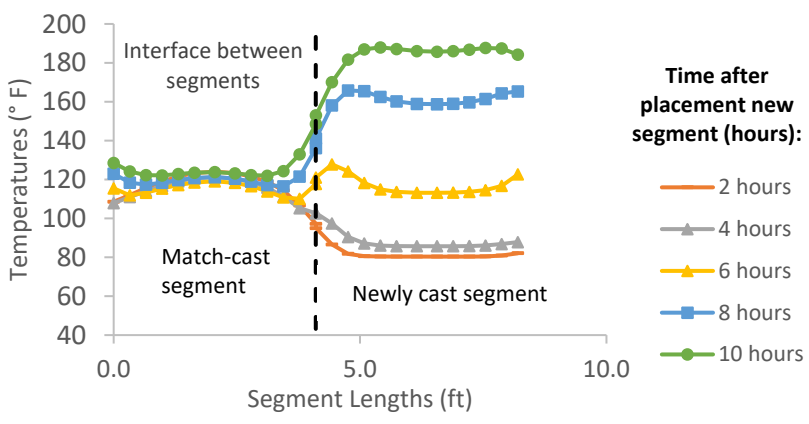

Figure B-450: Simulation 150 - Internal temperatures along the wing of segments

Simulation 151 -Results Summary

Table B-151: Model input parameters simulation 151

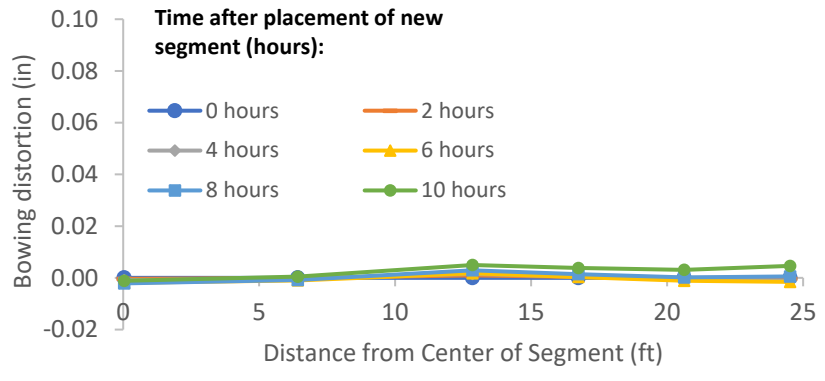| Model details		
Permutation number	151	
Geometry	Florida Bridge C - w/l=10.89	
Max. Mesh Size	3.54	in
Time Step	1	hrs
Placement Temperature	95	°F
Match-cast segment Time of Simulation at Casting	0	hrs
New Segment Time of Simulation at Casting	24	hrs
Concrete Properties		
Cement Content	650.08	lb/yd^3
Activation Energy	26.21	BTU/mol
Heat of Hydration Parameters		
Total Heat Development, $Q_{ult} = \alpha_u \cdot H_u$	107.65	BTU/lb
Time Parameter, τ	18.28	hrs
Curvature Parameter, β	1.65	
Density	3034.390	lb/yd^3
Specific Heat	0.21	BTU/(lb·°F)
Thermal Conductivity	1.084	BTU/(ft·h·°F)
Match-cast segment Elastic Modulus Dev. Parameters		
Final Value	3100.00	ksi
Time Parameter	12.420	hrs
Curvature Parameter	1.068	
New Segment Elastic Modulus Dev. Parameters		
Final Value	14.50	ksi
Time Parameter	n/a	hrs
Curvature Parameter	n/a	
Poisson Ratio	0.17	
Coefficient of Thermal Expansion	5.10	με/°F
Thermal Boundary Conditions (Applied to Appropriate Faces)		
Ambient Temp	Miami - Summer - Morning - Placement	
Wind	Medium-Wind	7.50	mph
Formwork	Steel Formwork	34.60	BTU/(ft·h·°F)
	Thickness	0.118	in
Curing	Burlap	0.18	BTU/(ft·h·°F)
	Thickness	0.39	in

Figure B-451: Simulation 151 - Bowing distortion of match-cast segment after placement of the new segment
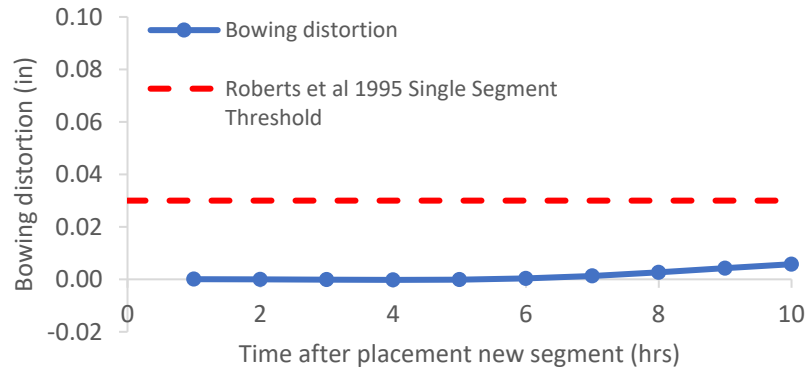

Figure B-452: Simulation 151 - Bowing distortion progression of match-cast segment from time of placement of new segment to 10 hours
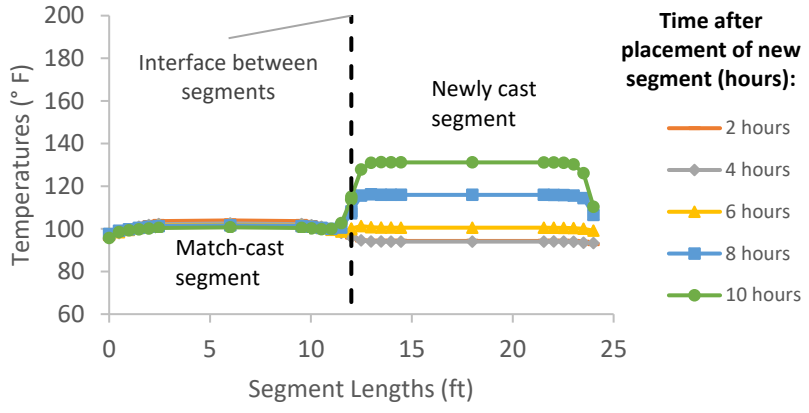

Figure B-453: Simulation 151 - Internal temperatures along the wing of segments

Simulation 152 -Results Summary

Table B-152: Model input parameters simulation 152

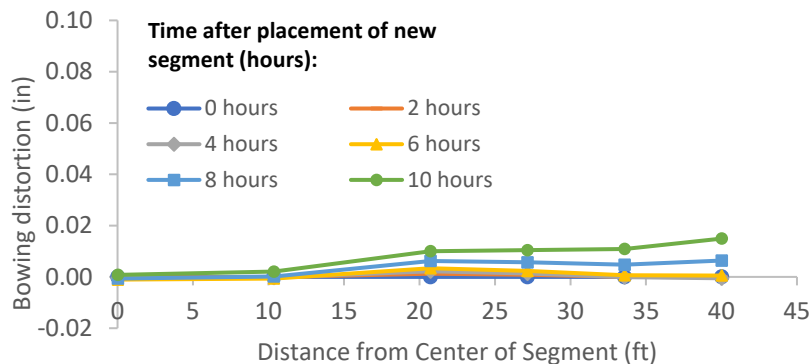| Model details		
Permutation number	152	
Geometry	Florida Bridge E - w/l=4.09	
Max. Mesh Size	2.95	in
Time Step	1	hrs
Placement Temperature	95	°F
Match-cast segment Time of Simulation at Casting	0	hrs
New Segment Time of Simulation at Casting	24	hrs
Concrete Properties		
Cement Content	750.09	lb/yd³
Activation Energy	24.13	BTU/mol
Heat of Hydration Parameters		
Total Heat Development, $Q_{ult} = \alpha_u \cdot H_u$	111.33	BTU/lb
Time Parameter, τ	13.36	hrs
Curvature Parameter, β	1.49	
Density	3034.390	lb/yd³
Specific Heat	0.21	BTU/(lb·°F)
Thermal Conductivity	1.084	BTU/(ft·h·°F)
Match-cast segment Elastic Modulus Dev. Parameters		
Final Value	3100.00	ksi
Time Parameter	12.420	hrs
Curvature Parameter	1.068	
New Segment Elastic Modulus Dev. Parameters		
Final Value	14.50	ksi
Time Parameter	n/a	hrs
Curvature Parameter	n/a	
Poisson Ratio	0.17	
Coefficient of Thermal Expansion	5.10	με/°F
Thermal Boundary Conditions (Applied to Appropriate Faces)		
Ambient Temp	Miami - Summer - Morning - Placement	
Wind	Medium-Wind	7.50	mph
Formwork	Steel Formwork	34.60	BTU/(ft·h·°F)
	Thickness	0.118	in
Curing	Burlap	0.18	BTU/(ft·h·°F)
	Thickness	0.39	in

Figure B-454: Simulation 152 - Bowing distortion of match-cast segment after placement of the new segment

Figure B-455: Simulation 152 - Bowing distortion progression of match-cast segment from time of placement of new segment to 10 hours
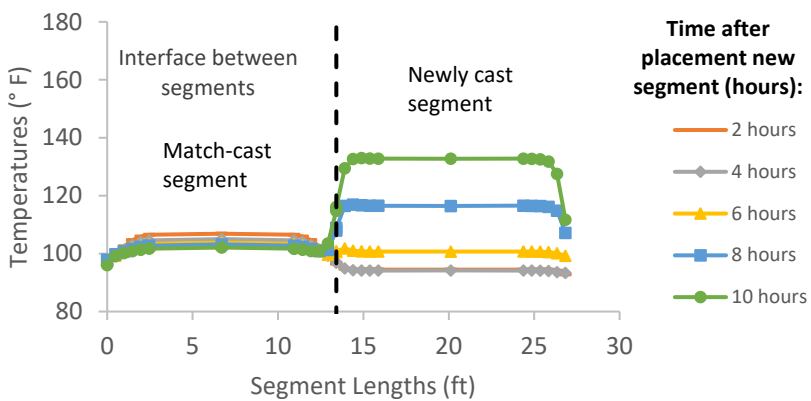

Figure B-456: Simulation 152 - Internal temperatures along the wing of segments

Simulation 153 -Results Summary

Table B-153: Model input parameters simulation 153

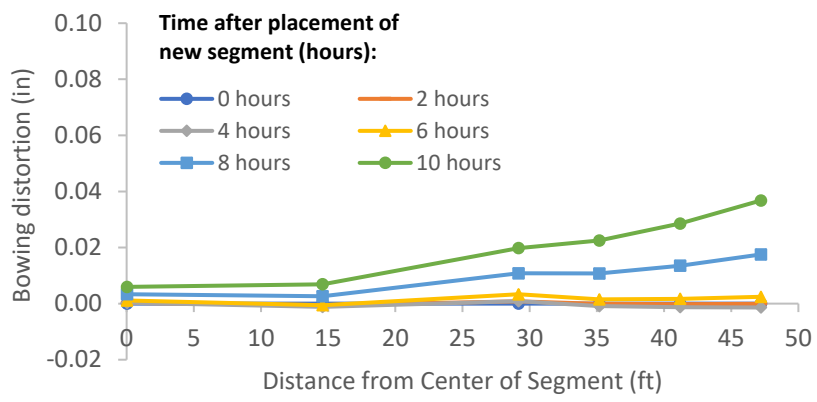| Model details		
Permutation number	153	
Geometry	Florida Bridge B - w/l=5.97	
Max. Mesh Size	3.94	in
Time Step	1	hrs
Placement Temperature	95	°F
Match-cast segment Time of Simulation at Casting	0	hrs
New Segment Time of Simulation at Casting	24	hrs
Concrete Properties		
Cement Content	750.09	lb/yd^3
Activation Energy	24.13	BTU/mol
Heat of Hydration Parameters		
Total Heat Development, $Q_{ult} = \alpha_u \cdot H_u$	111.33	BTU/lb
Time Parameter, τ	13.36	hrs
Curvature Parameter, β	1.49	
Density	3034.390	lb/yd^3
Specific Heat	0.21	BTU/(lb·°F)
Thermal Conductivity	1.084	BTU/(ft·h·°F)
Match-cast segment Elastic Modulus Dev. Parameters		
Final Value	3100.00	ksi
Time Parameter	12.420	hrs
Curvature Parameter	1.068	
New Segment Elastic Modulus Dev. Parameters		
Final Value	14.50	ksi
Time Parameter	n/a	hrs
Curvature Parameter	n/a	
Poisson Ratio	0.17	
Coefficient of Thermal Expansion	5.10	με/°F
Thermal Boundary Conditions (Applied to Appropriate Faces)		
Ambient Temp	Miami - Summer - Morning - Placement	
Wind	Medium-Wind	7.50	mph
Formwork	Steel Formwork	34.60	BTU/(ft·h·°F)
	Thickness	0.118	in
Curing	Burlap	0.18	BTU/(ft·h·°F)
	Thickness	0.39	in

Figure B-457: Simulation 153 - Bowing distortion of match-cast segment after placement of the new segment
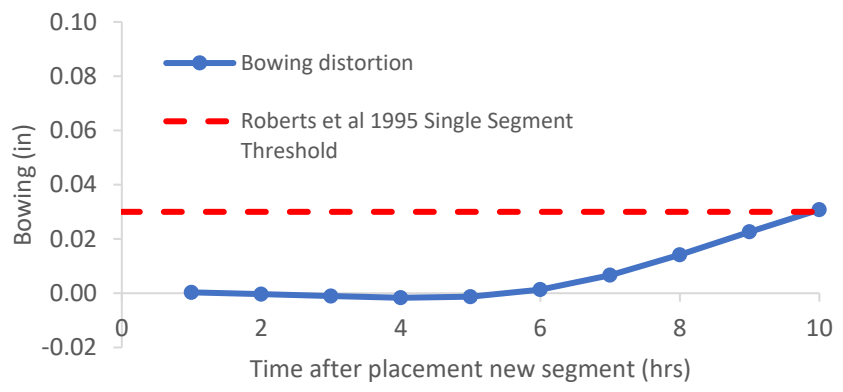

Figure B-458: Simulation 153 - Bowing distortion progression of match-cast segment from time of placement of new segment to 10 hours
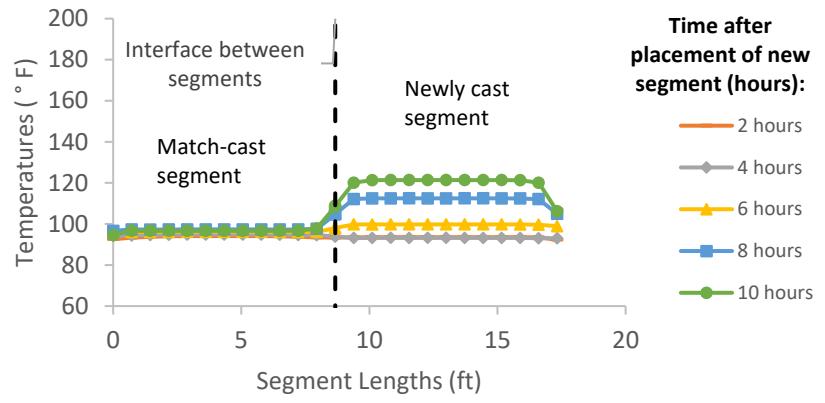

Figure B-459: Simulation 153 - Internal temperatures along the wing of segments

Simulation 154 -Results Summary

Table B-154: Model input parameters simulation 154

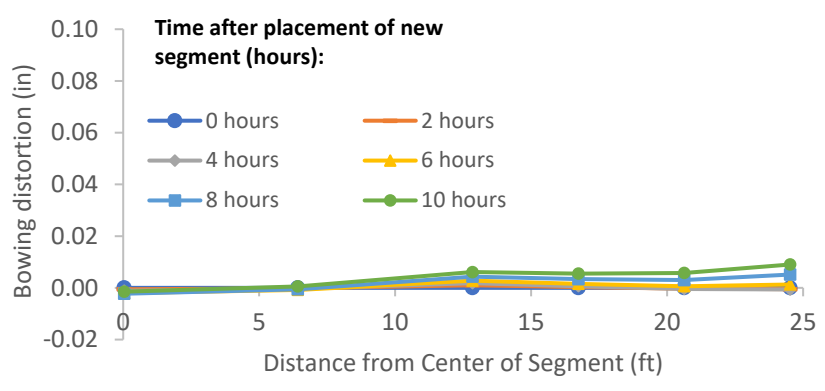| Model details		
Permutation number	154	
Geometry	Florida Bridge C - w/l=10.89	
Max. Mesh Size	3.54	in
Time Step	1	hrs
Placement Temperature	95	°F
Match-cast segment Time of Simulation at Casting	0	hrs
New Segment Time of Simulation at Casting	24	hrs
Concrete Properties		
Cement Content	750.09	lb/yd^3
Activation Energy	24.13	BTU/mol
Heat of Hydration Parameters		
Total Heat Development, $Q_{ult} = \alpha_u \cdot H_u$	111.33	BTU/lb
Time Parameter, τ	13.36	hrs
Curvature Parameter, β	1.49	
Density	3034.390	lb/yd^3
Specific Heat	0.21	BTU/(lb·°F)
Thermal Conductivity	1.084	BTU/(ft·h·°F)
Match-cast segment Elastic Modulus Dev. Parameters		
Final Value	3100.00	ksi
Time Parameter	12.420	hrs
Curvature Parameter	1.068	
New Segment Elastic Modulus Dev. Parameters		
Final Value	14.50	ksi
Time Parameter	n/a	hrs
Curvature Parameter	n/a	
Poisson Ratio	0.17	
Coefficient of Thermal Expansion	5.10	με/°F
Thermal Boundary Conditions (Applied to Appropriate Faces)		
Ambient Temp	Miami - Summer - Morning - Placement	
Wind	Medium-Wind	7.50	mph
Formwork	Steel Formwork	34.60	BTU/(ft·h·°F)
	Thickness	0.118	in
Curing	Burlap	0.18	BTU/(ft·h·°F)
	Thickness	0.39	in

Figure B-460: Simulation 154 - Bowing distortion of match-cast segment after placement of the new segment
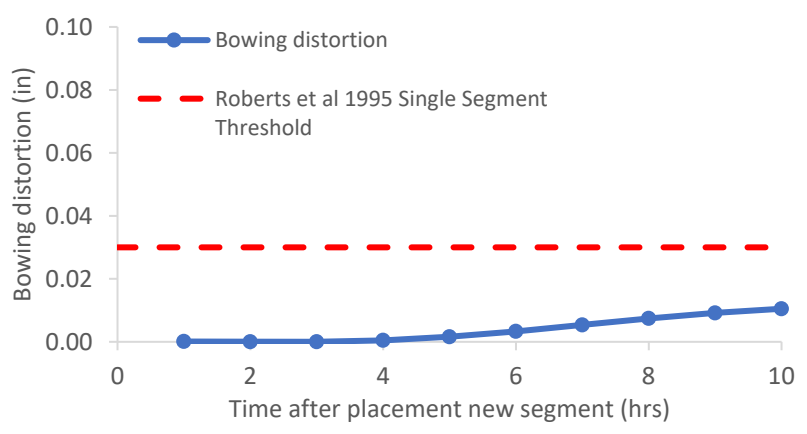

Figure B-461: Simulation 154 - Bowing distortion progression of match-cast segment from time of placement of new segment to 10 hours
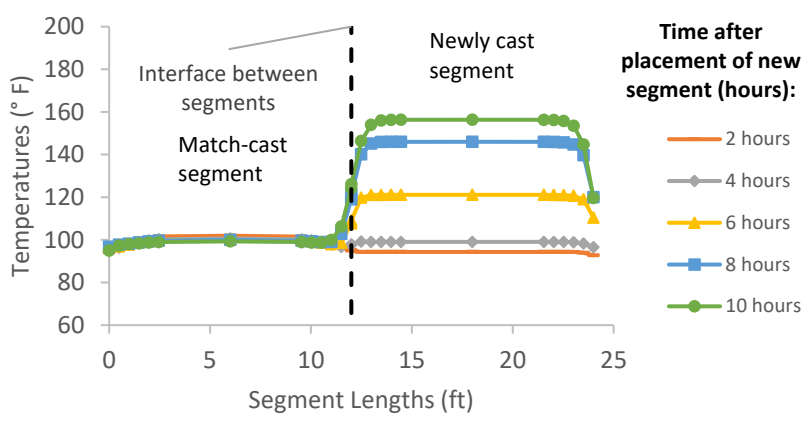

Figure B-462: Simulation 154 - Internal temperatures along the wing of segments

Simulation 155 -Results Summary

Table B-155: Model input parameters simulation 155

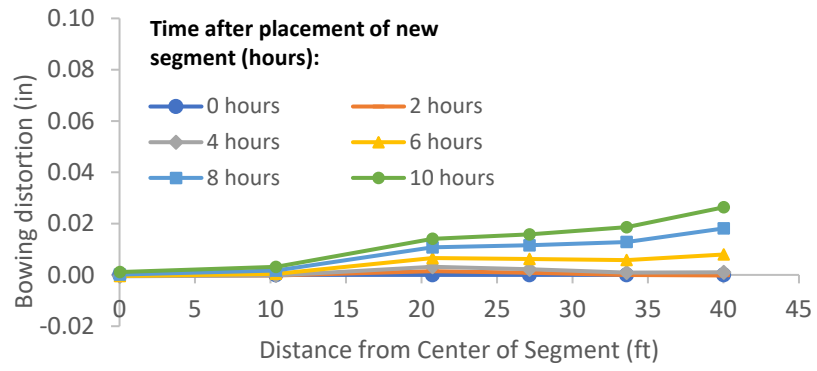| Model details		
Permutation number	155	
Geometry	Florida Bridge E - w/l=4.09	
Max. Mesh Size	2.95	in
Time Step	1	hrs
Placement Temperature	95	°F
Match-cast segment Time of Simulation at Casting	0	hrs
New Segment Time of Simulation at Casting	24	hrs
Concrete Properties		
Cement Content	950.11	lb/yd^3
Activation Energy	28.43	BTU/mol
Heat of Hydration Parameters		
Total Heat Development, $Q_{ult} = \alpha_u \cdot H_u$	124.95	BTU/lb
Time Parameter, τ	10.50	hrs
Curvature Parameter, β	1.60	
Density	3034.390	lb/yd^3
Specific Heat	0.21	BTU/(lb·°F)
Thermal Conductivity	1.084	BTU/(ft·h·°F)
Match-cast segment Elastic Modulus Dev. Parameters		
Final Value	3100.00	ksi
Time Parameter	12.420	hrs
Curvature Parameter	1.068	
New Segment Elastic Modulus Dev. Parameters		
Final Value	14.50	ksi
Time Parameter	n/a	hrs
Curvature Parameter	n/a	
Poisson Ratio	0.17	
Coefficient of Thermal Expansion	5.10	µε/°F
Thermal Boundary Conditions (Applied to Appropriate Faces)		
Ambient Temp	Miami - Summer - Morning - Placement		
Wind	Medium-Wind	7.50	mph
Formwork	Steel Formwork	34.60	BTU/(ft·h·°F)
	Thickness	0.118	in
Curing	Burlap	0.18	BTU/(ft·h·°F)
	Thickness	0.39	in

Figure B-463: Simulation 155 - Bowing distortion of match-cast segment after placement of the new segment
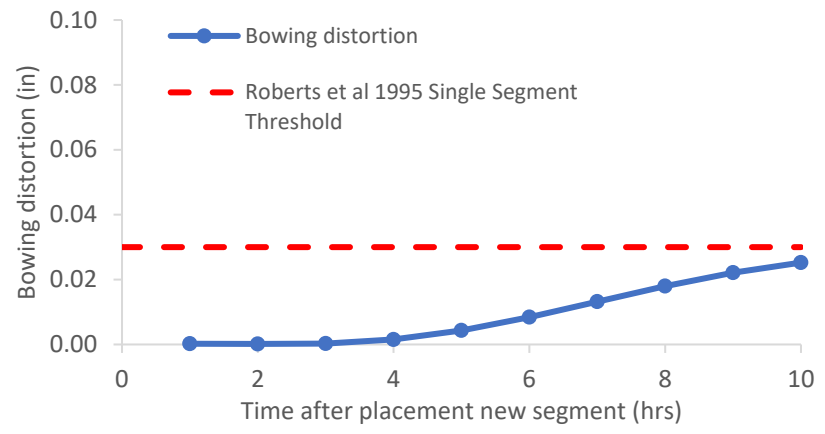

Figure B-464: Simulation 155 - Bowing distortion progression of match-cast segment from time of placement of new segment to 10 hours
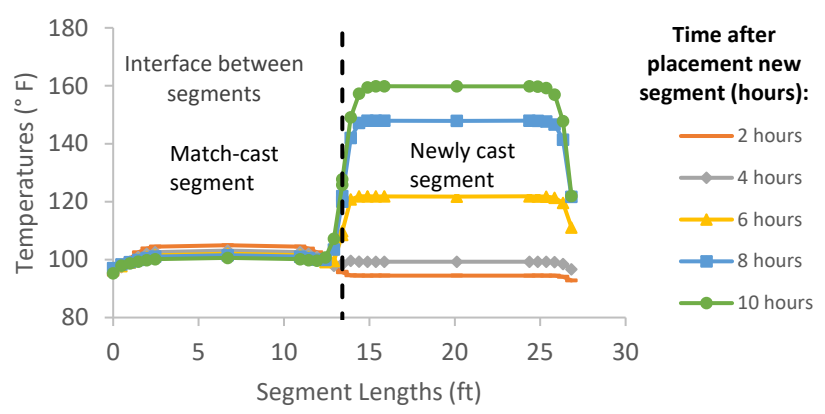

Figure B-465: Simulation 155 - Internal temperatures along the wing of segments

Simulation 156 -Results Summary

Table B-156: Model input parameters simulation 156

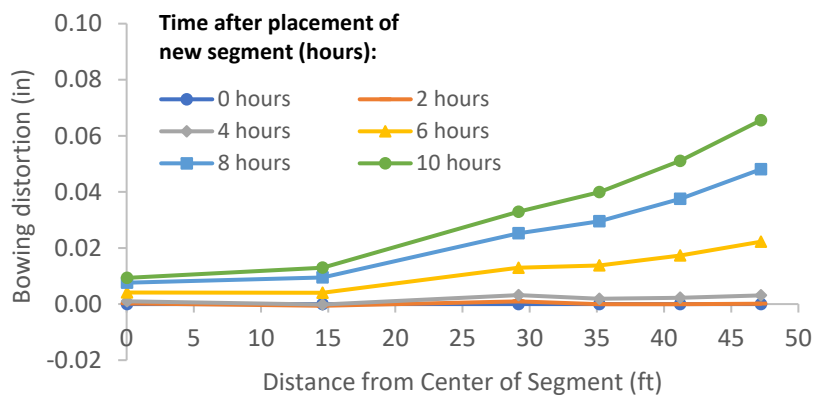| Model details		
Permutation number	156	
Geometry	Florida Bridge B - w/l=5.97	
Max. Mesh Size	3.94	in
Time Step	1	hrs
Placement Temperature	95	°F
Match-cast segment Time of Simulation at Casting	0	hrs
New Segment Time of Simulation at Casting	24	hrs
Concrete Properties		
Cement Content	950.11	lb/yd^3
Activation Energy	28.43	BTU/mol
Heat of Hydration Parameters		
Total Heat Development, $Q_{ult} = \alpha_u \cdot H_u$	124.95	BTU/lb
Time Parameter, τ	10.50	hrs
Curvature Parameter, β	1.60	
Density	3034.390	lb/yd^3
Specific Heat	0.21	BTU/(lb·°F)
Thermal Conductivity	1.084	BTU/(ft·h·°F)
Match-cast segment Elastic Modulus Dev. Parameters		
Final Value	3100.00	ksi
Time Parameter	12.420	hrs
Curvature Parameter	1.068	
New Segment Elastic Modulus Dev. Parameters		
Final Value	14.50	ksi
Time Parameter	n/a	hrs
Curvature Parameter	n/a	
Poisson Ratio	0.17	
Coefficient of Thermal Expansion	5.10	$\mu\varepsilon$/°F
Thermal Boundary Conditions (Applied to Appropriate Faces)		
Ambient Temp	Miami - Summer - Morning - Placement	
Wind	Medium-Wind	7.50	mph
Formwork	Steel Formwork	34.60	BTU/(ft·h·°F)
	Thickness	0.118	in
Curing	Burlap	0.18	BTU/(ft·h·°F)
	Thickness	0.39	in

Figure B-466: Simulation 156 - Bowing distortion of match-cast segment after placement of the new segment
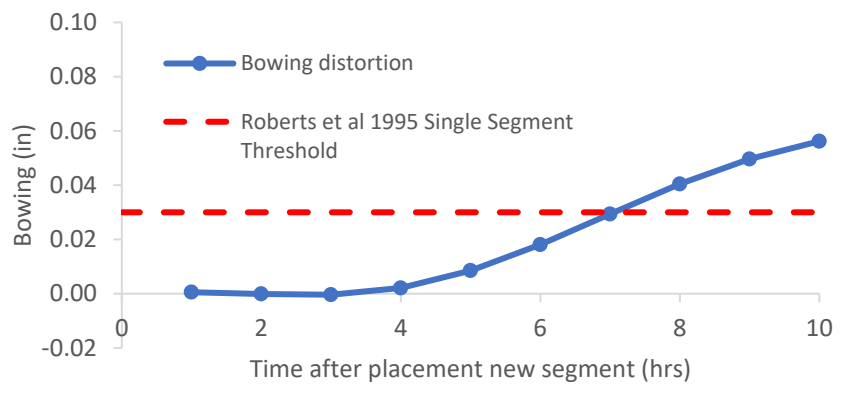

Figure B-467: Simulation 156 - Bowing distortion progression of match-cast segment from time of placement of new segment to 10 hours
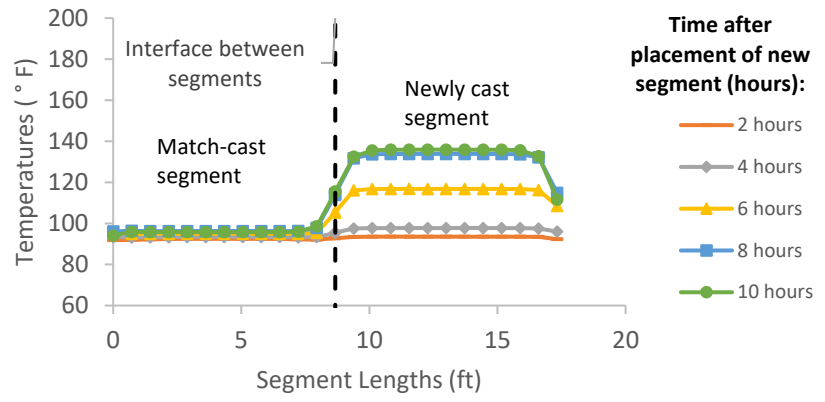

Figure B-468: Simulation 156 - Internal temperatures along the wing of segments

Simulation 157 -Results Summary

Table B-157: Model input parameters simulation 157

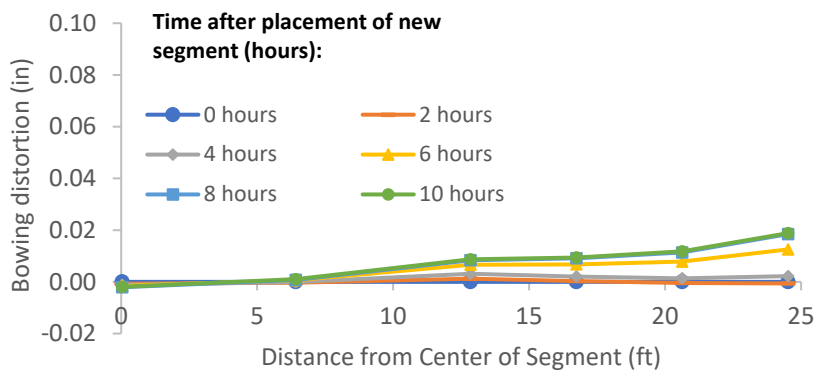| Model details		
Permutation number	157	
Geometry	Florida Bridge C - w/l=10.89	
Max. Mesh Size	3.54	in
Time Step	1	hrs
Placement Temperature	95	°F
Match-cast segment Time of Simulation at Casting	0	hrs
New Segment Time of Simulation at Casting	24	hrs
Concrete Properties		
Cement Content	950.11	lb/yd³
Activation Energy	28.43	BTU/mol
Heat of Hydration Parameters		
Total Heat Development, $Q_{ult} = \alpha_u \cdot H_u$	124.95	BTU/lb
Time Parameter, τ	10.50	hrs
Curvature Parameter, β	1.60	
Density	3034.390	lb/yd³
Specific Heat	0.21	BTU/(lb·°F)
Thermal Conductivity	1.084	BTU/(ft·h·°F)
Match-cast segment Elastic Modulus Dev. Parameters		
Final Value	3100.00	ksi
Time Parameter	12.420	hrs
Curvature Parameter	1.068	
New Segment Elastic Modulus Dev. Parameters		
Final Value	14.50	ksi
Time Parameter	n/a	hrs
Curvature Parameter	n/a	
Poisson Ratio	0.17	
Coefficient of Thermal Expansion	5.10	με/°F
Thermal Boundary Conditions (Applied to Appropriate Faces)		
Ambient Temp	Miami - Summer - Morning - Placement	
Wind	Medium-Wind	7.50	mph
Formwork	Steel Formwork	34.60	BTU/(ft·h·°F)
	Thickness	0.118	in
Curing	Burlap	0.18	BTU/(ft·h·°F)
	Thickness	0.39	in

Figure B-469: Simulation 157 - Bowing distortion of match-cast segment after placement of the new segment
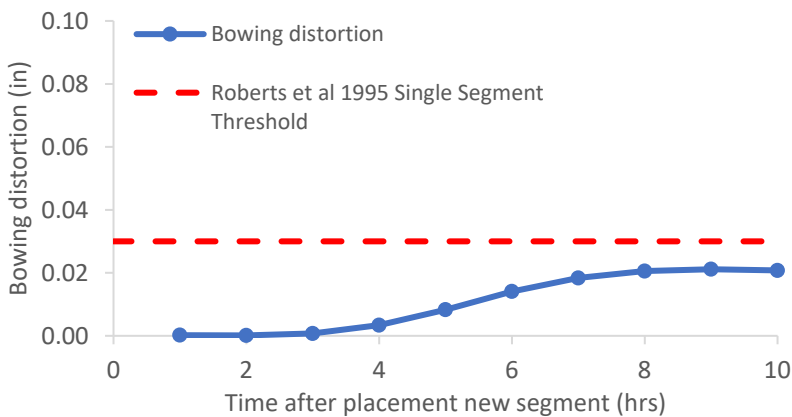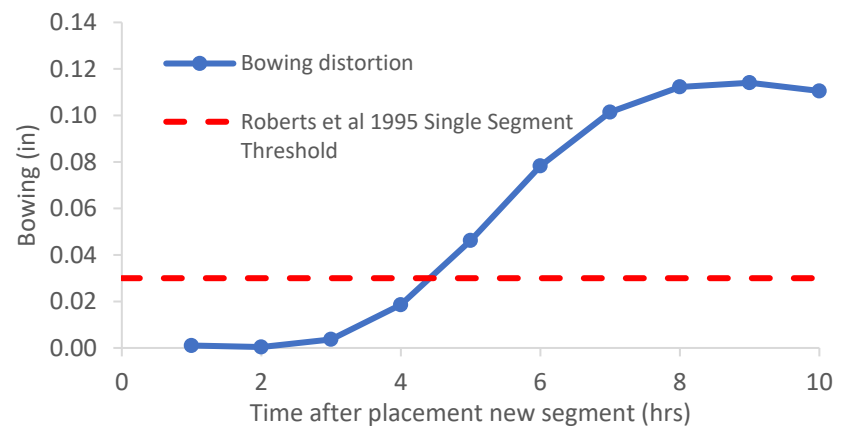

Figure B-470: Simulation 157 - Bowing distortion progression of match-cast segment from time of placement of new segment to 10 hours
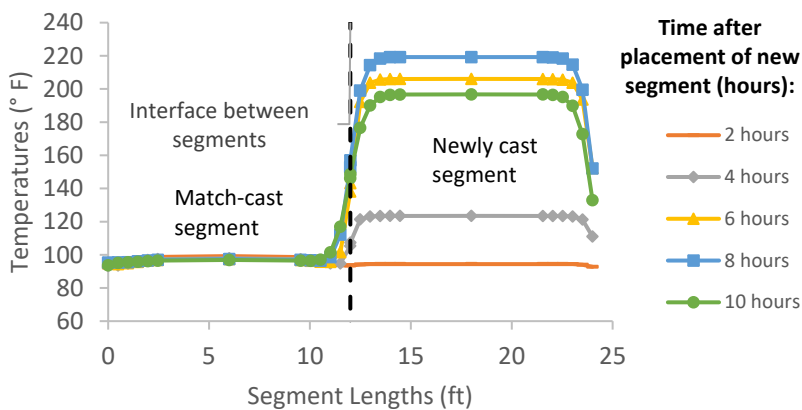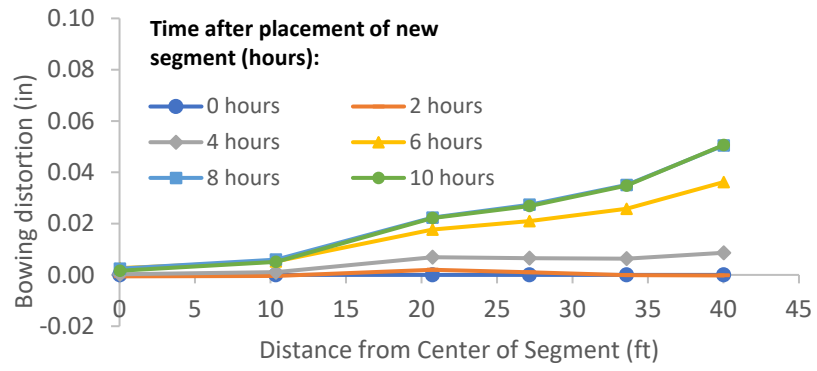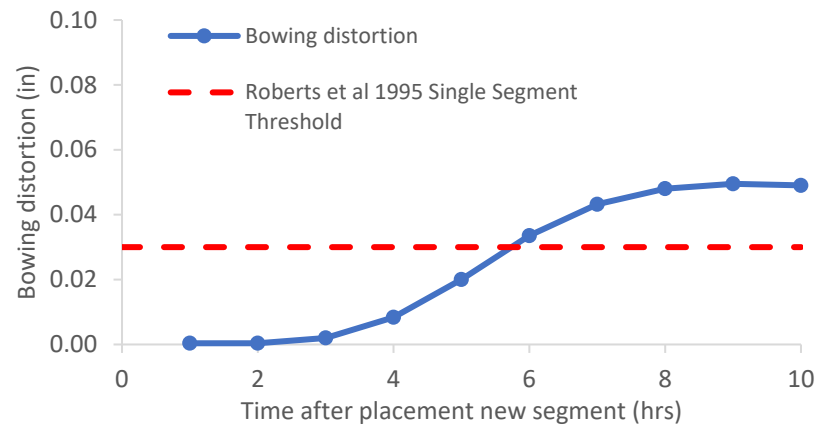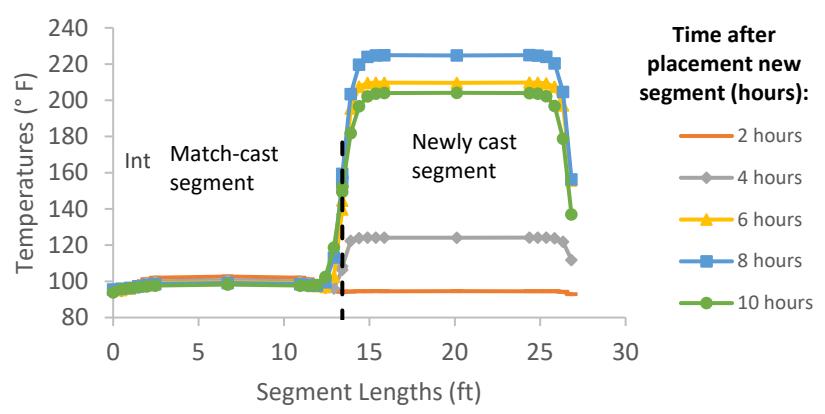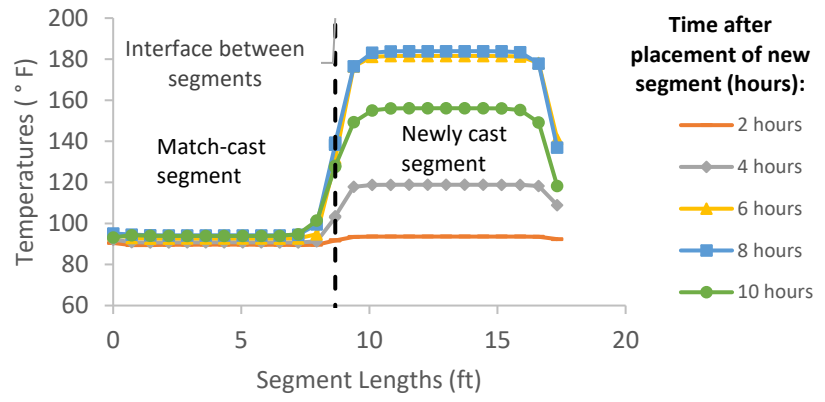

Figure B-471: Simulation 157 - Internal temperatures along the wing of segments

Appendix C. Simulation Factors in Mitigation Decision Tree and Simulated Bowing Amount

Table C-1: Simulation factors used in mitigation decision tree

#	Bridge Geometry	w/l	Equivalent cement content (ECC) (lb/yd^3)	Coefficient of Thermal Expansion (CTE) of Concrete (1/°F)	Concrete Placement Temperature + Ambient Temp at Placement (°F)	FEM Bowing distortion of match-cast segment 10 hrs after placement newly cast segment (in)	No analysis or mitigation needed (✓) or Analysis - mitigation needed (X)
1	Florida Bridge E, w/l=4.08	4.08	552.57	4.55E-06	185.0	0.006	✓
2	Florida Bridge B, w/l=5.97	5.97	552.57	4.55E-06	185.0	0.013	✓
3	Florida Bridge C, w/l=10.90	10.90	552.57	4.55E-06	185.0	0.029	✓
4	Florida Bridge E, w/l=4.08	4.08	552.57	4.55E-06	185.0	0.006	✓
5	Florida Bridge B, w/l=5.97	5.97	552.57	4.55E-06	185.0	0.013	✓
6	Florida Bridge C, w/l=10.90	10.90	552.57	4.55E-06	185.0	0.031	✓
7	Florida Bridge E, w/l=4.08	4.08	552.57	4.55E-06	185.0	0.003	✓
8	Florida Bridge B, w/l=5.97	5.97	552.57	4.55E-06	185.0	0.007	✓
9	Florida Bridge C, w/l=10.90	10.90	552.57	4.55E-06	185.0	0.017	✓
10	Florida Bridge E, w/l=4.08	4.08	705.83	4.54E-06	185.0	0.008	✓
11	Florida Bridge B, w/l=5.97	5.97	705.83	4.54E-06	185.0	0.019	✓
12	Florida Bridge C, w/l=10.90	10.90	705.83	4.54E-06	185.0	0.046	X
13	Florida Bridge E, w/l=4.08	4.08	705.83	4.54E-06	185.0	0.008	✓
14	Florida Bridge B, w/l=5.97	5.97	705.83	4.54E-06	185.0	0.019	✓
15	Florida Bridge C, w/l=10.90	10.90	705.83	4.54E-06	185.0	0.045	X
16	Florida Bridge E, w/l=4.08	4.08	705.83	4.54E-06	185.0	0.006	✓
17	Florida Bridge B, w/l=5.97	5.97	705.83	4.54E-06	185.0	0.014	✓
18	Florida Bridge C, w/l=10.90	10.90	705.83	4.54E-06	185.0	0.033	X
19	Florida Bridge E, w/l=4.08	4.08	950.11	4.54E-06	185.0	0.013	✓
20	Florida Bridge B, w/l=5.97	5.97	950.11	4.54E-06	185.0	0.030	✓
21	Florida Bridge C, w/l=10.90	10.90	950.11	4.54E-06	185.0	0.070	X
22	Florida Bridge E, w/l=4.08	4.08	950.11	4.54E-06	185.0	0.013	✓
23	Florida Bridge B, w/l=5.97	5.97	950.11	4.54E-06	185.0	0.030	✓
24	Florida Bridge C, w/l=10.90	10.90	950.11	4.54E-06	185.0	0.070	X

Table C-1, continued

#	Bridge Geometry	w/l	Equivalent cement content (ECC) (lb/yd^3)	Coefficient of Thermal Expansion (CTE) of Concrete (1/°F)	Concrete Placement Temperature + Ambient Temp at Placement (°F)	FEM Bowing distortion of match-cast segment 10 hrs after placement newly cast segment (in)	No analysis or mitigation needed (✓) or Analysis - mitigation needed (X)
25	Florida Bridge E, w/l=4.08	4.08	950.11	4.54E-06	185.0	0.012	✓
26	Florida Bridge B, w/l=5.97	5.97	950.11	4.54E-06	185.0	0.028	✓
27	Florida Bridge C, w/l=10.90	10.90	950.11	4.54E-06	185.0	0.067	X
28	Florida Bridge E, w/l=4.08	4.08	552.57	4.55E-06	185.0	0.002	✓
29	Florida Bridge B, w/l=5.97	5.97	552.57	4.55E-06	185.0	0.005	✓
30	Florida Bridge C, w/l=10.90	10.90	552.57	4.55E-06	185.0	0.013	✓
31	Florida Bridge E, w/l=4.08	4.08	705.83	4.54E-06	185.0	0.002	✓
32	Florida Bridge B, w/l=5.97	5.97	705.83	4.54E-06	185.0	0.013	✓
33	Florida Bridge C, w/l=10.90	10.90	705.83	4.54E-06	185.0	0.035	X
34	Florida Bridge E, w/l=4.08	4.08	950.11	4.54E-06	185.0	0.014	✓
35	Florida Bridge B, w/l=5.97	5.97	950.11	4.54E-06	185.0	0.030	✓
36	Florida Bridge C, w/l=10.90	10.90	950.11	4.54E-06	185.0	0.082	X
37	Florida Bridge E, w/l=4.08	4.08	552.57	6.08E-06	185.0	0.004	✓
38	Florida Bridge B, w/l=5.97	5.97	552.57	6.08E-06	185.0	0.009	✓
39	Florida Bridge C, w/l=10.90	10.90	552.57	6.08E-06	185.0	0.021	✓
40	Florida Bridge E, w/l=4.08	4.08	705.83	6.08E-06	185.0	0.007	✓
41	Florida Bridge B, w/l=5.97	5.97	705.83	6.08E-06	185.0	0.017	✓
42	Florida Bridge C, w/l=10.90	10.90	705.83	6.08E-06	185.0	0.042	X
43	Florida Bridge E, w/l=4.08	4.08	950.11	6.07E-06	185.0	0.015	✓
44	Florida Bridge B, w/l=5.97	5.97	950.11	6.07E-06	185.0	0.035	✓
45	Florida Bridge C, w/l=10.90	10.90	950.11	6.07E-06	185.0	0.086	X
46	Florida Bridge E, w/l=4.08	4.08	552.57	3.12E-06	185.0	0.002	✓
47	Florida Bridge B, w/l=5.97	5.97	552.57	3.12E-06	185.0	0.005	✓
48	Florida Bridge C, w/l=10.90	10.90	552.57	3.12E-06	185.0	0.013	✓
49	Florida Bridge E, w/l=4.08	4.08	705.83	3.30E-06	185.0	0.004	✓

Table C-1, continued

#	Bridge Geometry	w/l	Equivalent cement content (ECC) (lb/yd^3)	Coefficient of Thermal Expansion (CTE) of Concrete (1/°F)	Concrete Placement Temperature + Ambient Temp at Placement (°F)	FEM Bowing distortion of match-cast segment 10 hrs after placement newly cast segment (in)	No analysis or mitigation needed (✓) or Analysis - mitigation needed (X)
50	Florida Bridge B, w/l=5.97	5.97	705.83	3.30E-06	185.0	0.011	✓
51	Florida Bridge C, w/l=10.90	10.90	705.83	3.30E-06	185.0	0.025	✓
52	Florida Bridge E, w/l=4.08	4.08	950.11	3.40E-06	185.0	0.009	✓
53	Florida Bridge B, w/l=5.97	5.97	950.11	3.40E-06	185.0	0.021	✓
54	Florida Bridge C, w/l=10.90	10.90	950.11	3.40E-06	185.0	0.052	X
55	Florida Bridge E, w/l=4.08	4.08	552.57	4.55E-06	149.0	0.001	✓
56	Florida Bridge B, w/l=5.97	5.97	552.57	4.55E-06	149.0	0.003	✓
57	Florida Bridge C, w/l=10.90	10.90	552.57	4.55E-06	149.0	0.016	✓
58	Florida Bridge E, w/l=4.08	4.08	705.83	4.54E-06	149.0	0.003	✓
59	Florida Bridge B, w/l=5.97	5.97	705.83	4.54E-06	149.0	0.008	✓
60	Florida Bridge C, w/l=10.90	10.90	705.83	4.54E-06	149.0	0.020	✓
61	Florida Bridge E, w/l=4.08	4.08	950.11	4.54E-06	149.0	0.009	✓
62	Florida Bridge B, w/l=5.97	5.97	950.11	4.54E-06	149.0	0.021	✓
63	Florida Bridge C, w/l=10.90	10.90	950.11	4.54E-06	149.0	0.050	X
64	Florida Bridge E, w/l=4.08	4.08	552.57	4.55E-06	116.0	-0.001	✓
65	Florida Bridge B, w/l=5.97	5.97	552.57	4.55E-06	116.0	-0.002	✓
66	Florida Bridge C, w/l=10.90	10.90	552.57	4.55E-06	116.0	-0.005	✓
67	Florida Bridge E, w/l=4.08	4.08	705.83	4.54E-06	116.0	0.001	✓
68	Florida Bridge B, w/l=5.97	5.97	705.83	4.54E-06	116.0	0.002	✓
69	Florida Bridge C, w/l=10.90	10.90	705.83	4.54E-06	116.0	0.005	✓
70	Florida Bridge E, w/l=4.08	4.08	950.11	4.54E-06	116.0	0.003	✓
71	Florida Bridge B, w/l=5.97	5.97	950.11	4.54E-06	116.0	0.009	✓
72	Florida Bridge C, w/l=10.90	10.90	950.11	4.54E-06	116.0	0.020	X
73	Florida Bridge E, w/l=4.08	4.08	552.57	4.55E-06	185.0	0.003	✓
74	Florida Bridge B, w/l=5.97	5.97	552.57	4.55E-06	185.0	0.006	✓
75	Florida Bridge C, w/l=10.90	10.90	552.57	4.55E-06	185.0	0.018	✓

Table C-1, continued

#	Bridge Geometry	w/l	Equivalent cement content (ECC) (lb/yd^3)	Coefficient of Thermal Expansion (CTE) of Concrete (1/°F)	Concrete Placement Temperature + Ambient Temp at Placement (°F)	FEM Bowing distortion of match-cast segment 10 hrs after placement newly cast segment (in)	No analysis or mitigation needed (✓) or Analysis - mitigation needed (X)
76	Florida Bridge E, w/l=4.08	4.08	705.83	4.54E-06	185.0	0.007	✓
77	Florida Bridge B, w/l=5.97	5.97	705.83	4.54E-06	185.0	0.015	✓
78	Florida Bridge C, w/l=10.90	10.90	705.83	4.54E-06	185.0	0.041	X
79	Florida Bridge E, w/l=4.08	4.08	950.11	4.54E-06	185.0	0.015	✓
80	Florida Bridge B, w/l=5.97	5.97	950.11	4.54E-06	185.0	0.033	✓
81	Florida Bridge C, w/l=10.90	10.90	950.11	4.54E-06	185.0	0.090	X
82	Florida Bridge E, w/l=4.08	4.08	552.57	4.55E-06	185.0	0.003	✓
83	Florida Bridge B, w/l=5.97	5.97	552.57	4.55E-06	185.0	0.007	✓
84	Florida Bridge C, w/l=10.90	10.90	552.57	4.55E-06	185.0	0.015	✓
85	Florida Bridge E, w/l=4.08	4.08	705.83	4.54E-06	185.0	0.005	✓
86	Florida Bridge B, w/l=5.97	5.97	705.83	4.54E-06	185.0	0.012	✓
87	Florida Bridge C, w/l=10.90	10.90	705.83	4.54E-06	185.0	0.028	X
88	Florida Bridge E, w/l=4.08	4.08	950.11	4.54E-06	185.0	0.010	✓
89	Florida Bridge B, w/l=5.97	5.97	950.11	4.54E-06	185.0	0.024	✓
90	Florida Bridge C, w/l=10.90	10.90	950.11	4.54E-06	185.0	0.055	X
91	Florida Bridge E, w/l=4.08	4.08	552.57	4.55E-06	170.0	-0.003	✓
92	Florida Bridge B, w/l=5.97	5.97	552.57	4.55E-06	170.0	-0.006	✓
93	Florida Bridge C, w/l=10.90	10.90	552.57	4.55E-06	170.0	-0.017	✓
94	Florida Bridge E, w/l=4.08	4.08	705.83	4.54E-06	170.0	0.001	✓
95	Florida Bridge B, w/l=5.97	5.97	705.83	4.54E-06	170.0	0.002	✓
96	Florida Bridge C, w/l=10.90	10.90	705.83	4.54E-06	170.0	0.008	X
97	Florida Bridge E, w/l=4.08	4.08	950.11	4.54E-06	170.0	0.009	✓
98	Florida Bridge B, w/l=5.97	5.97	950.11	4.54E-06	170.0	0.021	✓
99	Florida Bridge C, w/l=10.90	10.90	950.11	4.54E-06	170.0	0.058	X
100	Florida Bridge E, w/l=4.08	4.08	552.57	4.55E-06	170.0	-0.005	✓
101	Florida Bridge B, w/l=5.97	5.97	552.57	4.55E-06	170.0	-0.010	✓

Table C-1, continued

#	Bridge Geometry	w/l	Equivalent cement content (ECC) (lb/yd^3)	Coefficient of Thermal Expansion (CTE) of Concrete (1/°F)	Concrete Placement Temperature + Ambient Temp at Placement (°F)	FEM Bowing distortion of match-cast segment 10 hrs after placement newly cast segment (in)	No analysis or mitigation needed (✓) or Analysis - mitigation needed (X)
102	Florida Bridge C, w/l=10.90	10.90	552.57	4.55E-06	170.0	-0.026	✓
103	Florida Bridge E, w/l=4.08	4.08	705.83	4.54E-06	170.0	-0.001	✓
104	Florida Bridge B, w/l=5.97	5.97	705.83	4.54E-06	170.0	0.000	✓
105	Florida Bridge C, w/l=10.90	10.90	705.83	4.54E-06	170.0	0.000	X
106	Florida Bridge E, w/l=4.08	4.08	950.11	4.54E-06	170.0	0.007	✓
107	Florida Bridge B, w/l=5.97	5.97	950.11	4.54E-06	170.0	0.018	✓
108	Florida Bridge C, w/l=10.90	10.90	950.11	4.54E-06	170.0	0.050	X
109	Florida Bridge A, w/l=2.15	2.15	950.11	4.54E-06	185.0	0.005	✓
110	Florida Bridge F, w/l=5.91	5.91	950.11	4.54E-06	185.0	0.024	✓
111	Florida Bridge D, w/l=9.39	9.39	950.11	4.54E-06	185.0	0.053	X
112	Bang Na, w/l=21.76	21.76	950.11	4.54E-06	185.0	0.216	X
113	Florida Bridge A, w/l=2.15	2.15	950.11	4.54E-06	185.0	0.006	✓
114	Florida Bridge F, w/l=5.91	5.91	950.11	4.54E-06	185.0	0.028	✓
115	Florida Bridge D, w/l=9.39	9.39	950.11	4.54E-06	185.0	0.059	X
116	Bang Na, w/l=21.76	21.76	950.11	4.54E-06	185.0	0.258	X
117	Florida Bridge A, w/l=2.15	2.15	950.11	6.07E-06	185.0	0.006	✓
118	Florida Bridge F, w/l=5.91	5.91	950.11	6.07E-06	185.0	0.030	✓
119	Florida Bridge D, w/l=9.39	9.39	950.11	6.07E-06	185.0	0.067	X
120	Bang Na, w/l=21.76	21.76	950.11	6.07E-06	185.0	0.286	X
121	Florida Bridge A, w/l=2.15	2.15	950.11	3.40E-06	185.0	0.004	✓
122	Florida Bridge F, w/l=5.91	5.91	950.11	3.40E-06	185.0	0.018	✓
123	Florida Bridge D, w/l=9.39	9.39	950.11	3.40E-06	185.0	0.041	X
124	Bang Na, w/l=21.76	21.76	950.11	3.40E-06	185.0	0.166	X
125	Florida Bridge A, w/l=2.15	2.15	950.11	4.54E-06	149.0	0.004	✓
126	Florida Bridge F, w/l=5.91	5.91	950.11	4.54E-06	149.0	0.018	✓
127	Florida Bridge D, w/l=9.39	9.39	950.11	4.54E-06	149.0	0.038	X

Table C-1, continued

#	Bridge Geometry	w/l	Equivalent cement content (ECC) (lb/yd^3)	Coefficient of Thermal Expansion (CTE) of Concrete (1/°F)	Concrete Placement Temperature + Ambient Temp at Placement (°F)	FEM Bowing distortion of match-cast segment 10 hrs after placement newly cast segment (in)	No analysis or mitigation needed (✓) or Analysis - mitigation needed (X)
128	Bang Na, w/l=21.76	21.76	950.11	4.54E-06	149.0	0.159	X
129	Florida Bridge A, w/l=2.15	2.15	950.11	4.54E-06	96.4	0.001	✓
130	Florida Bridge F, w/l=5.91	5.91	950.11	4.54E-06	96.4	0.003	✓
131	Florida Bridge D, w/l=9.39	9.39	950.11	4.54E-06	96.4	0.007	X
132	Bang Na, w/l=21.76	21.76	950.11	4.54E-06	96.4	0.047	X
133	Florida Bridge A, w/l=2.15	2.15	950.11	4.54E-06	185.0	0.007	✓
134	Florida Bridge F, w/l=5.91	5.91	950.11	4.54E-06	185.0	0.030	✓
135	Florida Bridge D, w/l=9.39	9.39	950.11	4.54E-06	185.0	0.063	X
136	Bang Na, w/l=21.76	21.76	950.11	4.54E-06	185.0	0.286	X
137	Florida Bridge A, w/l=2.15	2.15	950.11	4.54E-06	185.0	0.004	✓
138	Florida Bridge F, w/l=5.91	5.91	950.11	4.54E-06	185.0	0.020	✓
139	Florida Bridge D, w/l=9.39	9.39	950.11	4.54E-06	185.0	0.045	X
140	Bang Na, w/l=21.76	21.76	950.11	4.54E-06	185.0	0.176	X
141	Florida Bridge A, w/l=2.15	2.15	950.11	4.54E-06	170.0	0.004	✓
142	Florida Bridge F, w/l=5.91	5.91	950.11	4.54E-06	170.0	0.020	✓
143	Florida Bridge D, w/l=9.39	9.39	950.11	4.54E-06	170.0	0.039	X
144	Bang Na, w/l=21.76	21.76	950.11	4.54E-06	170.0	0.185	X
145	Florida Bridge A, w/l=2.15	2.15	950.11	4.54E-06	170.0	0.003	✓
146	Florida Bridge F, w/l=5.91	5.91	950.11	4.54E-06	170.0	0.018	✓
147	Florida Bridge D, w/l=9.39	9.39	950.11	4.54E-06	170.0	0.033	X
148	Bang Na, w/l=21.76	21.76	950.11	4.54E-06	170.0	0.160	X
149	Florida Bridge E, w/l=4.08	4.08	552.57	5.10E-06	185.0	0.006	✓
150	Florida Bridge B, w/l=5.97	5.97	552.57	5.10E-06	185.0	0.014	✓
151	Florida Bridge C, w/l=10.90	10.90	552.57	5.10E-06	185.0	0.031	✓
152	Florida Bridge E, w/l=4.08	4.08	705.83	5.10E-06	185.0	0.011	✓
153	Florida Bridge B, w/l=5.97	5.97	705.83	5.10E-06	185.0	0.025	✓

Table C-1, continued

#	Bridge Geometry	w/l	Equivalent cement content (ECC) (lb/yd^3)	Coefficient of Thermal Expansion (CTE) of Concrete (1/°F)	Concrete Placement Temperature + Ambient Temp at Placement (°F)	FEM Bowing distortion of match-cast segment 10 hrs after placement newly cast segment (in)	No analysis or mitigation needed (✓) or Analysis - mitigation needed (X)
154	Florida Bridge C, w/l=10.90	10.90	705.83	5.10E-06	185.0	0.056	X
155	Florida Bridge E, w/l=4.08	4.08	950.11	5.10E-06	185.0	0.021	✓
156	Florida Bridge B, w/l=5.97	5.97	950.11	5.10E-06	185.0	0.049	✓
157	Florida Bridge C, w/l=10.90	10.90	950.11	5.10E-06	185.0	0.111	X